Neutrinoless ββ decay: physics that matters (… but doesn't antimatter)

Cheryl Patrick, University College London

International Neutrino Summer School 2019, Fermilab

In the beginning was…

In the beginning was...

In the beginning was…

2 matter particles

No antimatter particles

In the beginning was…

2 matter particles

No antimatter particles

- How did we get this imbalance?

In the beginning was…

2 matter particles

No antimatter particles

- How did we get this imbalance?
- Neutrinoless double-beta decay would CREATE matter…

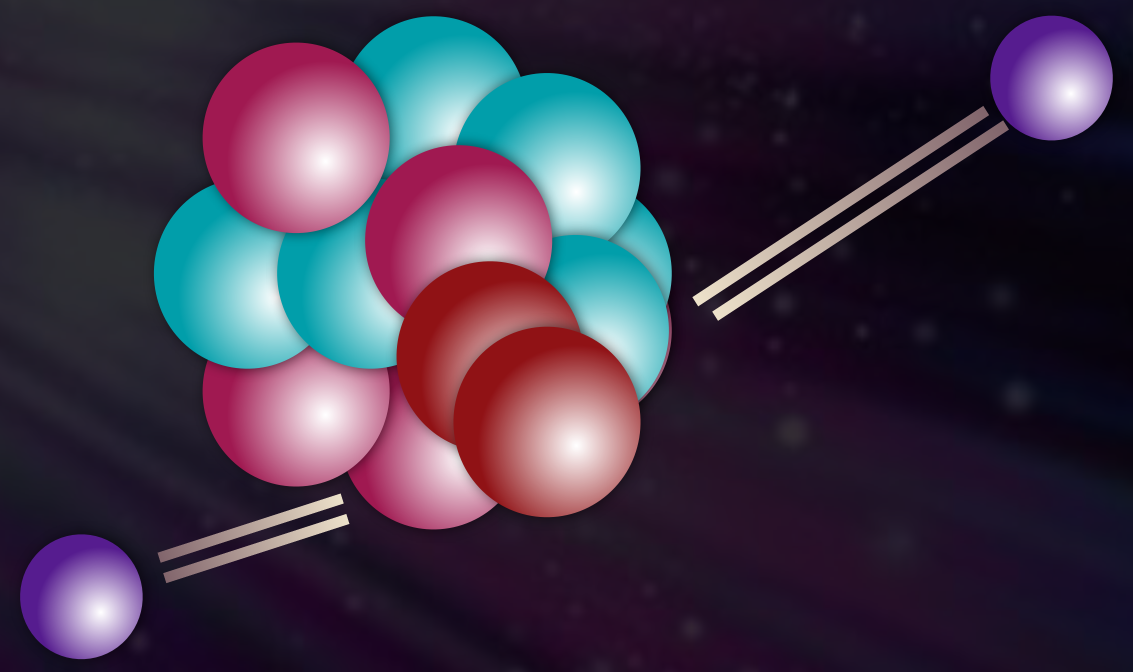

In the beginning was…

2 matter particles

No antimatter particles

- How did we get this imbalance?
- Neutrinoless double-beta decay would CREATE matter…
- … tells us about the nature of the neutrino (that isn't there)…

In the beginning was…

2 matter particles

No antimatter particles

- How did we get this imbalance?
- Neutrinoless double-beta decay would CREATE matter…
- … tells us about the nature of the neutrino (that isn't there)…
- … and could help us measure its mass

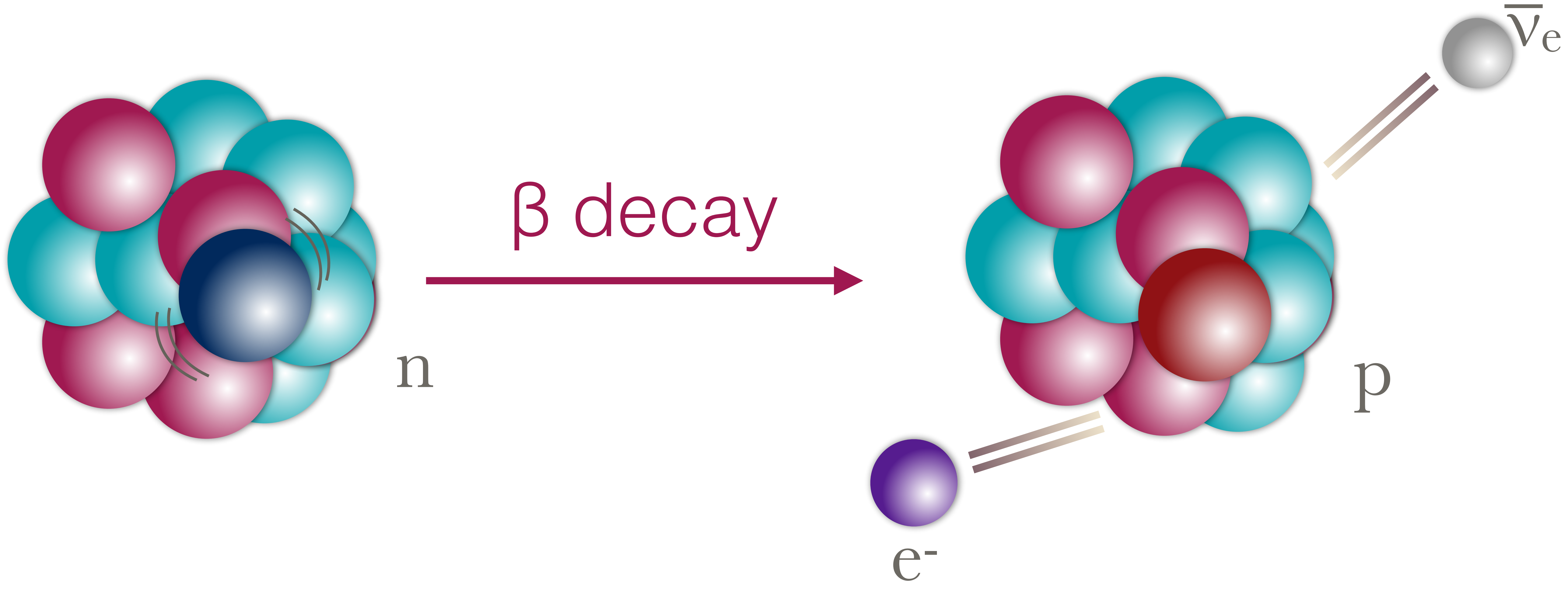
β decay
n
p
$\bar{\nu}_e$
e^-

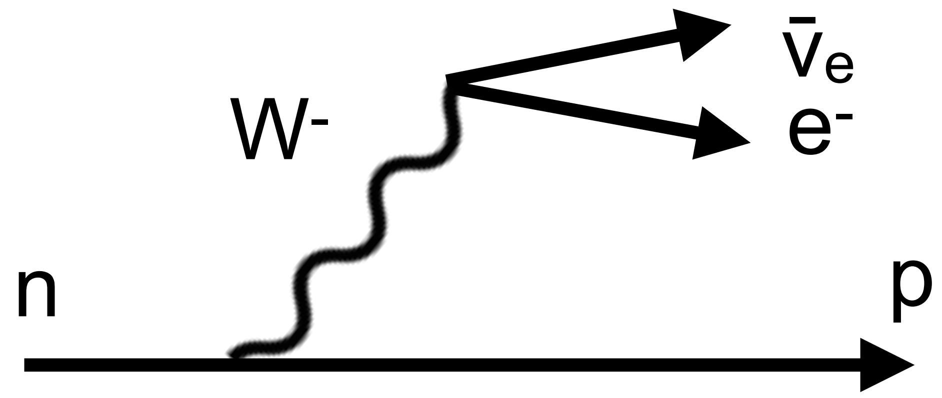
W-
$\bar{\nu}_e$
e^-
n
p

double-beta decay

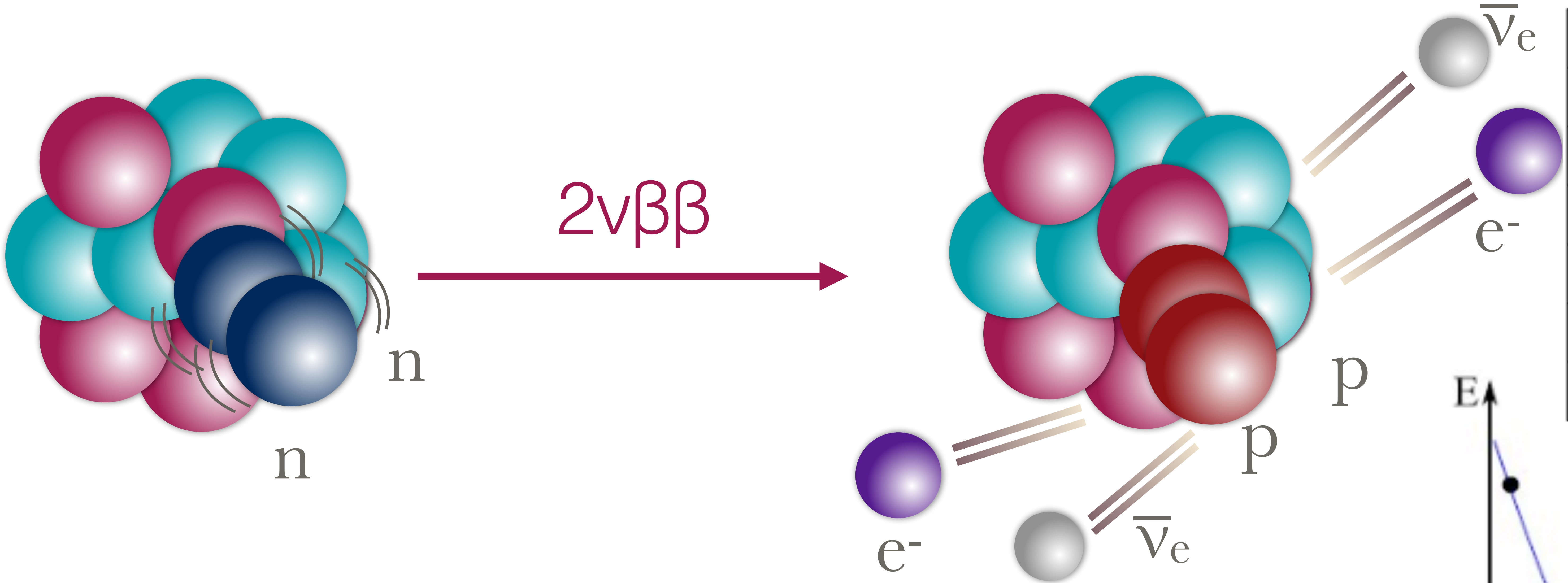

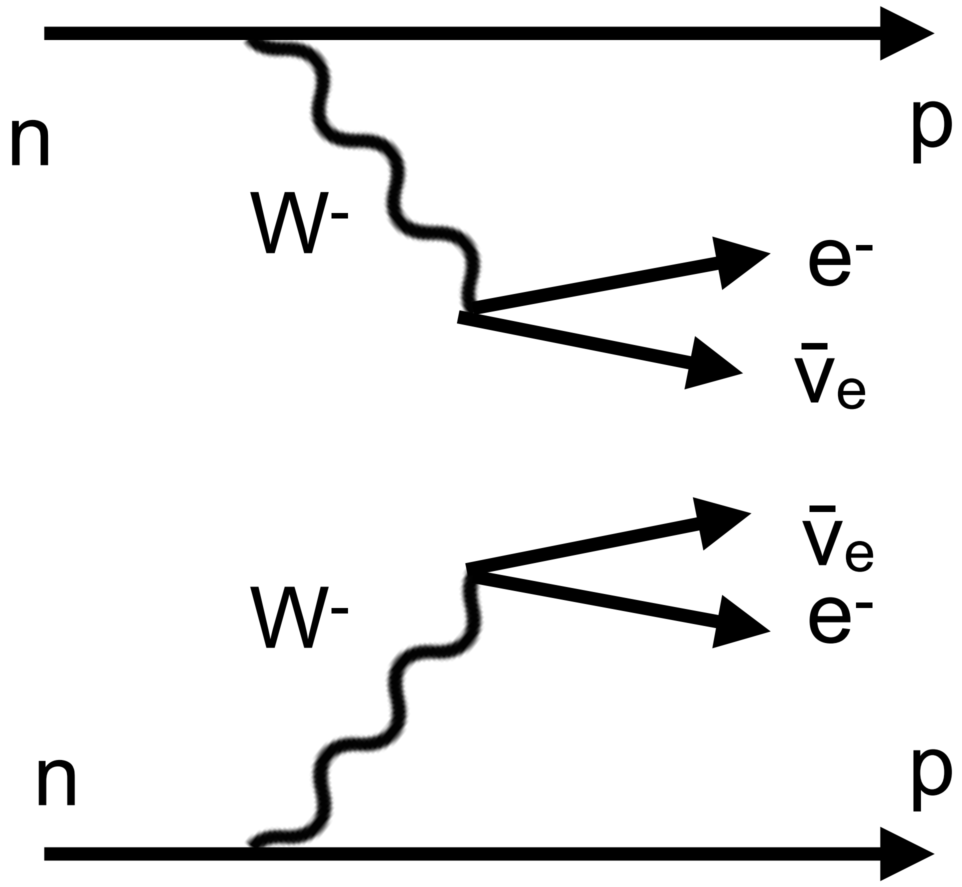

Lepton number conserved

$\Delta L = 0$

$T_{1/2} \sim 10^{20}$ years

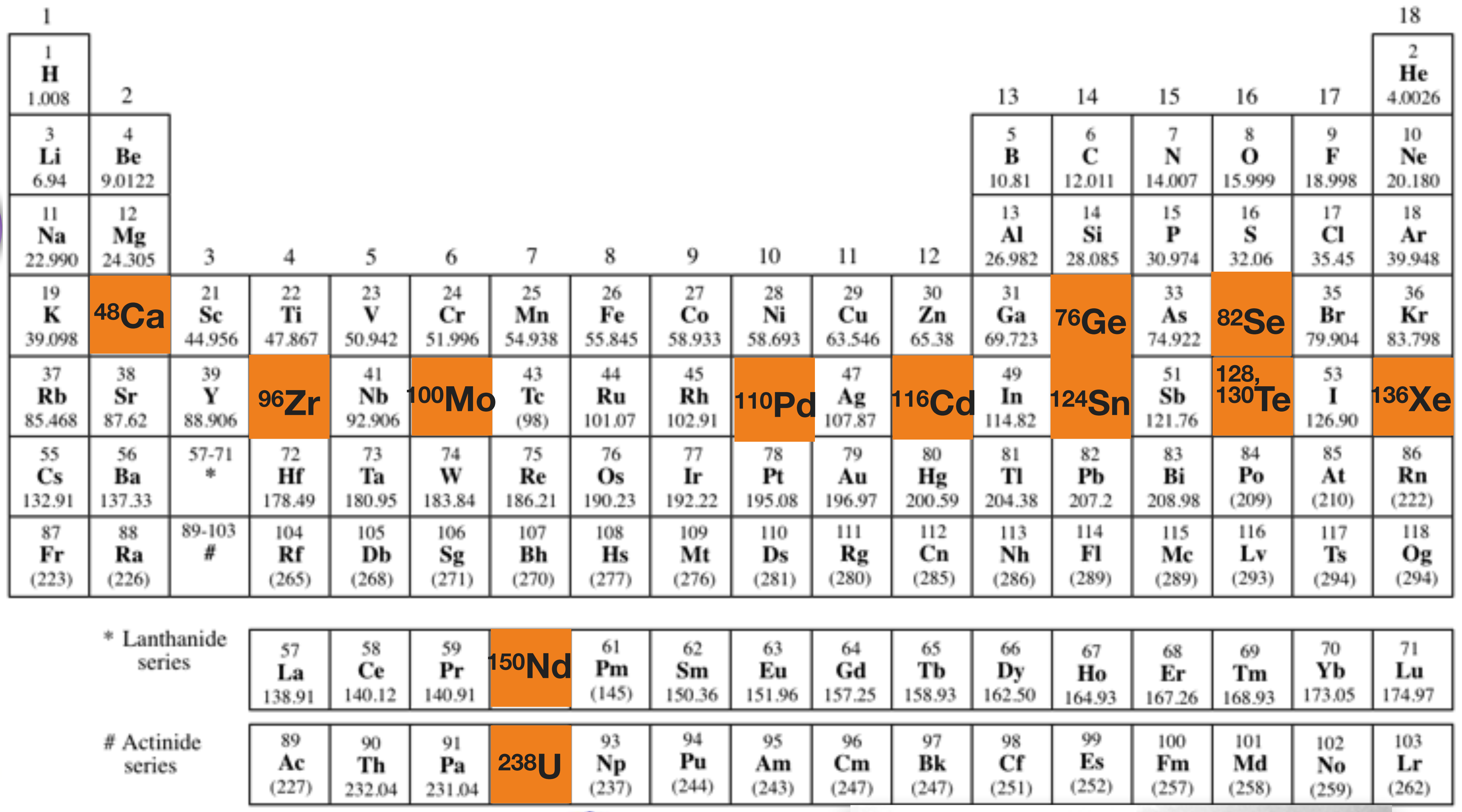

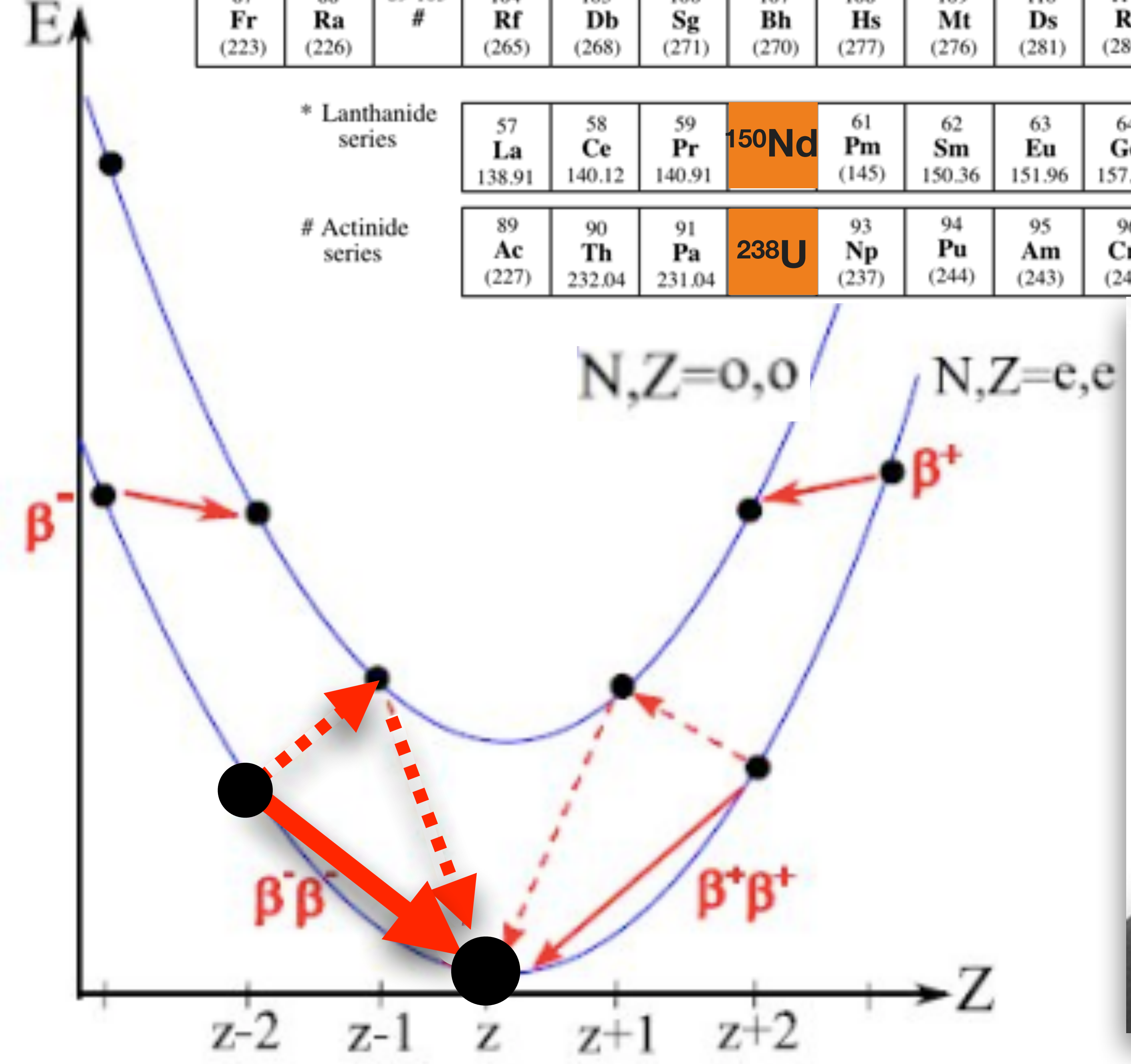

Diagram - E. Falk

Maria Göppert Mayer

Neutrinoless double-beta decay : the smoking gun for Majorana

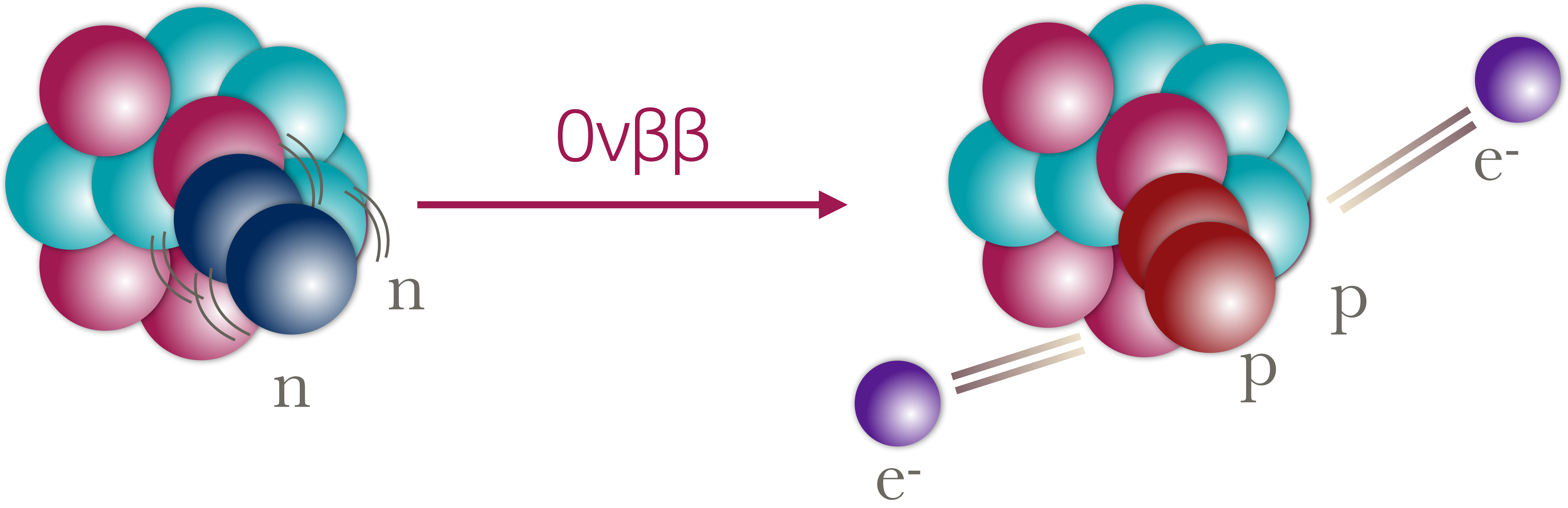

Wendell Furry

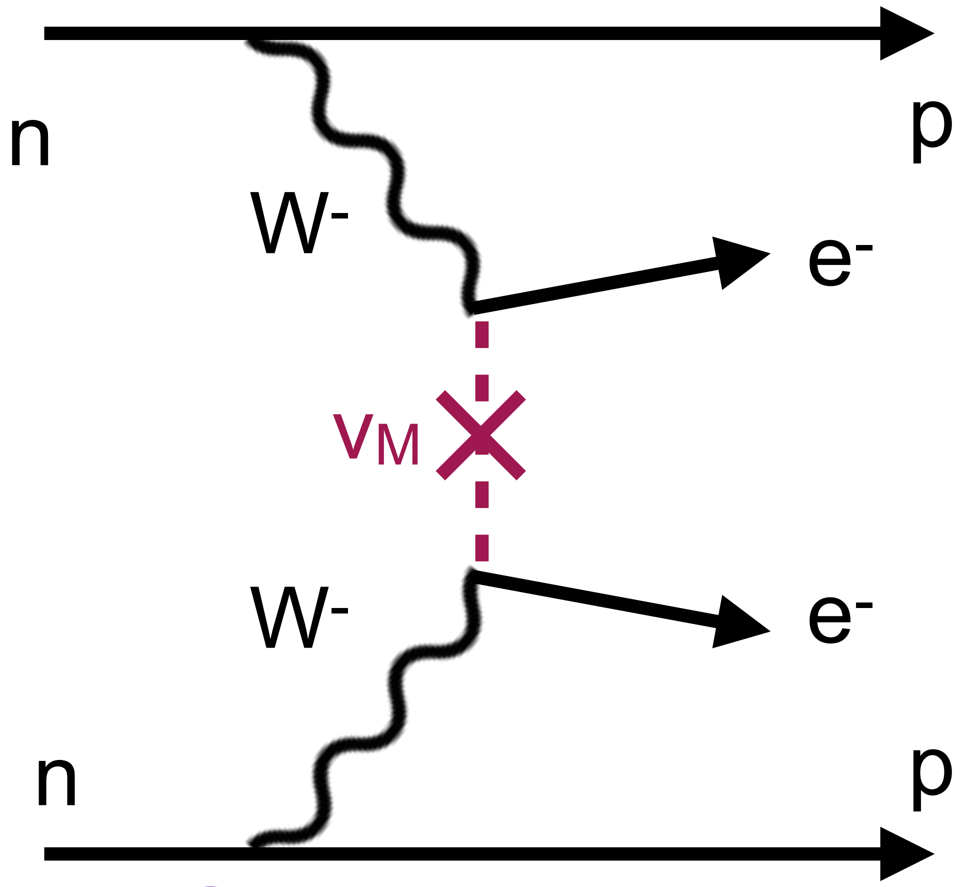

Lepton number violated

$\Delta L = 2$

$T_{1/2} > 10^{24} - 10^{26}$ years

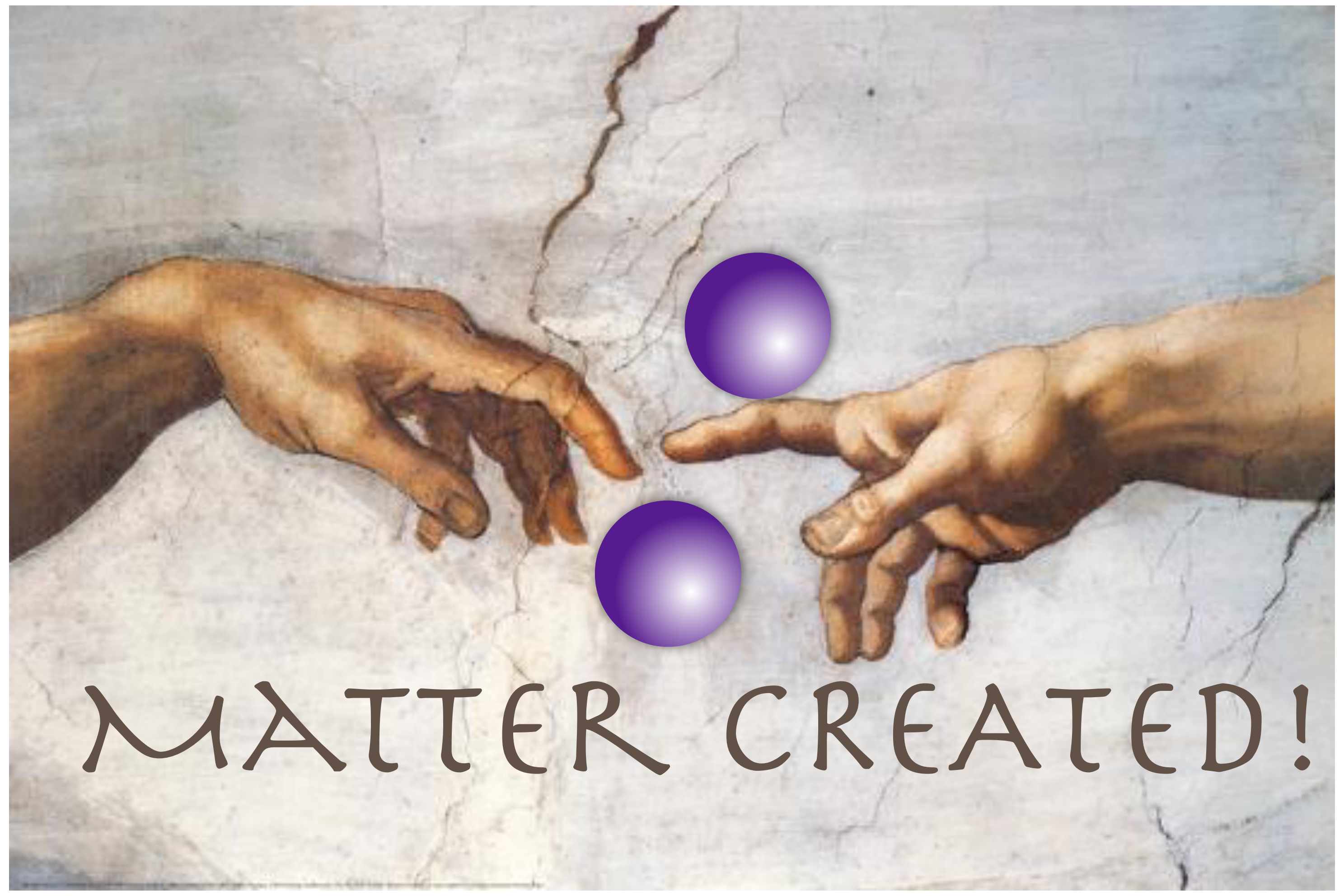

Only if $\nu=\bar{\nu}$: **Majorana** neutrino

0νββ could tell us about neutrino mass

0νββ rate

$$\frac{1}{T_{1/2}^{0\nu\beta\beta}} = G_{0\nu}(Q_{\beta\beta}, Z) g_A^4 |M_{0\nu}|^2 \frac{\langle m_{\beta\beta} \rangle^2}{m_e^2}$$

← **Neutrino mass**

0νββ could tell us about neutrino mass

0νββ rate

$$\frac{1}{T_{1/2}^{0\nu\beta\beta}} = G_{0\nu}(Q_{\beta\beta}, Z) g_A^4 |M_{0\nu}|^2 \frac{\langle m_{\beta\beta} \rangle^2}{m_e^2}$$

Neutrino mass

$$m_{\beta\beta} = \left| \sum_{i=1}^{3} |U_{ei}|^2 m_i e^{i\alpha_i} \right|$$

0νββ could tell us about neutrino mass

0νββ rate $$\frac{1}{T_{1/2}^{0\nu\beta\beta}} = G_{0\nu}(Q_{\beta\beta}, Z)g_A^4|M_{0\nu}|^2 \frac{\langle m_{\beta\beta}\rangle^2}{m_e^2}$$

Neutrino mass

PMNS mixing angles

$$m_{\beta\beta} = \left| \sum_{i=1}^{3} |U_{ei}|^2 m_i e^{i\alpha_i} \right|$$

0νββ could tell us about neutrino mass

0νββ rate $$\frac{1}{T_{1/2}^{0\nu\beta\beta}} = G_{0\nu}(Q_{\beta\beta}, Z) g_A^4 |M_{0\nu}|^2 \frac{\langle m_{\beta\beta} \rangle^2}{m_e^2}$$

Neutrino mass

PMNS mixing angles

$$m_{\beta\beta} = \left| \sum_{i=1}^{3} |U_{ei}|^2 m_i e^{i\alpha_i} \right|$$

Individual neutrino masses

0νββ could tell us about neutrino mass

0νββ rate

$$\frac{1}{T_{1/2}^{0\nu\beta\beta}} = G_{0\nu}(Q_{\beta\beta}, Z) g_A^4 |M_{0\nu}|^2 \frac{\langle m_{\beta\beta}\rangle^2}{m_e^2}$$

← **Neutrino mass**

PMNS mixing angles

Majorana phases

$$m_{\beta\beta} = \left| \sum_{i=1}^{3} |U_{ei}|^2 m_i e^{i\alpha_i} \right|$$

Individual neutrino masses

0νββ could tell us about neutrino mass

0νββ rate $$\frac{1}{T_{1/2}^{0\nu\beta\beta}} = G_{0\nu}(Q_{\beta\beta}, Z) g_A^4 |M_{0\nu}|^2 \frac{\langle m_{\beta\beta}\rangle^2}{m_e^2}$$

← **Neutrino mass**

$$U = \begin{bmatrix} U_{e1} & U_{e2} & U_{e3} \\ U_{\mu 1} & U_{\mu 2} & U_{\mu 3} \\ U_{\tau 1} & U_{\tau 2} & U_{\tau 3} \end{bmatrix} = \begin{bmatrix} 1 & 0 & 0 \\ 0 & c_{23} & s_{23} \\ 0 & -s_{23} & c_{23} \end{bmatrix} \begin{bmatrix} c_{13} & 0 & s_{13}e^{-i\delta} \\ 0 & 1 & 0 \\ -s_{13}e^{i\delta} & 0 & c_{13} \end{bmatrix} \begin{bmatrix} c_{12} & s_{12} & 0 \\ -s_{12} & c_{12} & 0 \\ 0 & 0 & 1 \end{bmatrix} \begin{bmatrix} 1 & 0 & 0 \\ 0 & e^{i\alpha_1/2} & 0 \\ 0 & 0 & e^{i\alpha_2/2} \end{bmatrix}$$

PMNS mixing angles

Majorana phases

$$m_{\beta\beta} = \left| \sum_{i=1}^{3} |U_{ei}|^2 m_i e^{i\alpha_i} \right|$$

Individual neutrino masses

0νββ could tell us about neutrino mass

UCL

0νββ rate
$$\frac{1}{T_{1/2}^{0\nu\beta\beta}} = G_{0\nu}(Q_{\beta\beta}, Z) g_A^4 |M_{0\nu}|^2 \frac{\langle m_{\beta\beta}\rangle^2}{m_e^2}$$
← Neutrino mass

$$U = \begin{bmatrix} U_{e1} & U_{e2} & U_{e3} \\ U_{\mu1} & U_{\mu2} & U_{\mu3} \\ U_{\tau1} & U_{\tau2} & U_{\tau3} \end{bmatrix}$$
$$= \begin{bmatrix} 1 & 0 & 0 \\ 0 & c_{23} & s_{23} \\ 0 & -s_{23} & c_{23} \end{bmatrix} \begin{bmatrix} c_{13} & 0 & s_{13}e^{-i\delta} \\ 0 & 1 & 0 \\ -s_{13}e^{i\delta} & 0 & c_{13} \end{bmatrix} \begin{bmatrix} c_{12} & s_{12} & 0 \\ -s_{12} & c_{12} & 0 \\ 0 & 0 & 1 \end{bmatrix} \begin{bmatrix} 1 & 0 & 0 \\ 0 & e^{i\alpha_1/2} & 0 \\ 0 & 0 & e^{i\alpha_2/2} \end{bmatrix}$$

PMNS mixing angles

Majorana phases

$$m_{\beta\beta} = \left| \sum_{i=1}^{3} |U_{ei}|^2 m_i e^{i\alpha_i} \right|$$

Individual neutrino masses

$$m_{\beta\beta} = c_{12}^2 c_{13}^2 m_{\nu_1} + s_{12}^2 c_{13}^2 m_{\nu_2} e^{i\alpha_1} + s_{13}^2 m_{\nu_3} e^{i\alpha_3}$$

0.68 0.30 0.02

0νββ could tell us about neutrino mass

0νββ rate $\frac{1}{T_{1/2}^{0\nu\beta\beta}} = G_{0\nu}(Q_{\beta\beta}, Z) g_A^4 |M_{0\nu}|^2 \frac{\langle m_{\beta\beta}\rangle^2}{m_e^2}$ ← **Neutrino mass**

Beta decay endpoint

$$m_{\bar{\nu}_e} =$$

Neutrinoless double beta decay

$$m_{\beta\beta} = \left| \sum_{i=1}^{3} |U_{ei}|^2 m_i e^{i\alpha_i} \right|$$

$$m_{\beta\beta} = c_{12}^2 c_{13}^2 m_{\nu_1} + s_{12}^2 c_{13}^2 m_{\nu_2} e^{i\alpha_1} + s_{13}^2 m_{\nu_3} e^{i\alpha_3}$$

0.68 **0.30** **0.02**

0νββ could tell us about neutrino mass

0νββ rate $$\frac{1}{T_{1/2}^{0\nu\beta\beta}} = G_{0\nu}(Q_{\beta\beta}, Z) g_A^4 |M_{0\nu}|^2 \frac{\langle m_{\beta\beta} \rangle^2}{m_e^2}$$ ← **Neutrino mass**

Beta decay endpoint

$$m_{\bar{\nu}_e} = \sqrt{\sum_{i=1}^{3} |U_{ei}|^2 m_i^2}$$

Neutrinoless double beta decay

$$m_{\beta\beta} = \left| \sum_{i=1}^{3} |U_{ei}|^2 m_i e^{i\alpha_i} \right|$$

$$m_{\beta\beta} = c_{12}^2 c_{13}^2 m_{\nu_1} + s_{12}^2 c_{13}^2 m_{\nu_2} e^{i\alpha_1} + s_{13}^2 m_{\nu_3} e^{i\alpha_3}$$

0.68 **0.30** **0.02**

0νββ could tell us about neutrino mass

0νββ rate $$\frac{1}{T_{1/2}^{0\nu\beta\beta}} = G_{0\nu}(Q_{\beta\beta}, Z) g_A^4 |M_{0\nu}|^2 \frac{\langle m_{\beta\beta}\rangle^2}{m_e^2}$$ ← **Neutrino mass**

Beta decay endpoint

Incoherent sum

$$m_{\bar{\nu}_e} = \sqrt{\sum_{i=1}^{3} |U_{ei}|^2 m_i^2}$$

Neutrinoless double beta decay

Coherent sum

$$m_{\beta\beta} = \left| \sum_{i=1}^{3} |U_{ei}|^2 m_i e^{i\alpha_i} \right|$$

$$m_{\beta\beta} = c_{12}^2 c_{13}^2 m_{\nu_1} + s_{12}^2 c_{13}^2 m_{\nu_2} e^{i\alpha_1} + s_{13}^2 m_{\nu_3} e^{i\alpha_3}$$

0.68 0.30 0.02

0νββ could tell us about neutrino mass

UCL

0νββ rate $$\frac{1}{T_{1/2}^{0\nu\beta\beta}} = G_{0\nu}(Q_{\beta\beta}, Z) g_A^4 |M_{0\nu}|^2 \frac{\langle m_{\beta\beta}\rangle^2}{m_e^2}$$

← Neutrino mass

Beta decay endpoint

$$m_{\bar{\nu}_e} = \sqrt{\sum_{i=1}^{3} |U_{ei}|^2 m_i^2}$$

Is there a lower bound?

Neutrinoless double beta decay

$$m_{\beta\beta} = \left| \sum_{i=1}^{3} |U_{ei}|^2 m_i e^{i\alpha_i} \right|$$

$$m_{\beta\beta} = c_{12}^2 c_{13}^2 m_{\nu_1} + s_{12}^2 c_{13}^2 m_{\nu_2} e^{i\alpha_1} + s_{13}^2 m_{\nu_3} e^{i\alpha_3}$$

0.68 0.30 0.02

0νββ could tell us about neutrino mass

0νββ rate $$\frac{1}{T_{1/2}^{0\nu\beta\beta}} = G_{0\nu}(Q_{\beta\beta}, Z) g_A^4 |M_{0\nu}|^2 \frac{\langle m_{\beta\beta}\rangle^2}{m_e^2}$$

Neutrino mass

Beta decay endpoint

$$m_{\bar{\nu}_e} = \sqrt{\sum_{i=1}^{3} |U_{ei}|^2 m_i^2}$$

Neutrinoless double beta decay

$$m_{\beta\beta} = \left| \sum_{i=1}^{3} |U_{ei}|^2 m_i e^{i\alpha_i} \right|$$

Is there a lower bound?

$$m_{\beta\beta} = c_{12}^2 c_{13}^2 m_{\nu_1} + s_{12}^2 c_{13}^2 m_{\nu_2} e^{i\alpha_1} + s_{13}^2 m_{\nu_3} e^{i\alpha_3}$$

0.68 0.30 0.02

0νββ could tell us about neutrino mass

0νββ rate

$$\frac{1}{T_{1/2}^{0\nu\beta\beta}} = G_{0\nu}(Q_{\beta\beta}, Z) g_A^4 |M_{0\nu}|^2 \frac{\langle m_{\beta\beta}\rangle^2}{m_e^2}$$

← **Neutrino mass**

Beta decay endpoint

$$m_{\bar{\nu}_e} = \sqrt{\sum_{i=1}^{3} |U_{ei}|^2 m_i^2}$$

Neutrinoless double beta decay

$$m_{\beta\beta} = \left| \sum_{i=1}^{3} |U_{ei}|^2 m_i e^{i\alpha_i} \right|$$

Is there a lower bound?

It's complicated…

$$m_{\beta\beta} = c_{12}^2 c_{13}^2 m_{\nu_1} + s_{12}^2 c_{13}^2 m_{\nu_2} e^{i\alpha_1} + s_{13}^2 m_{\nu_3} e^{i\alpha_3}$$

0.68 **0.30** **0.02**

0νββ could tell us about neutrino mass

0νββ rate $$\frac{1}{T_{1/2}^{0\nu\beta\beta}} = G_{0\nu}(Q_{\beta\beta}, Z) g_A^4 |M_{0\nu}|^2 \frac{\langle m_{\beta\beta}\rangle^2}{m_e^2}$$ ← **Neutrino mass**

Beta decay endpoint

$$m_{\bar{\nu}_e} = \sqrt{\sum_{i=1}^{3} |U_{ei}|^2 m_i^2}$$

Neutrinoless double beta decay

$$m_{\beta\beta} = \left| \sum_{i=1}^{3} |U_{ei}|^2 m_i e^{i\alpha_i} \right|$$

Is there a lower bound?

It's ~~complicated…~~ complex

$$m_{\beta\beta} = c_{12}^2 c_{13}^2 m_{\nu_1} + s_{12}^2 c_{13}^2 m_{\nu_2} e^{i\alpha_1} + s_{13}^2 m_{\nu_3} e^{i\alpha_3}$$

0.68 **0.30** **0.02**

All about $m_{\beta\beta}$ featuring: the double-beta decay lobster!

$$m_{\beta\beta} = \left| \sum_{i=1}^{3} |U_{ei}|^2 m_i e^{i\alpha_i} \right|$$

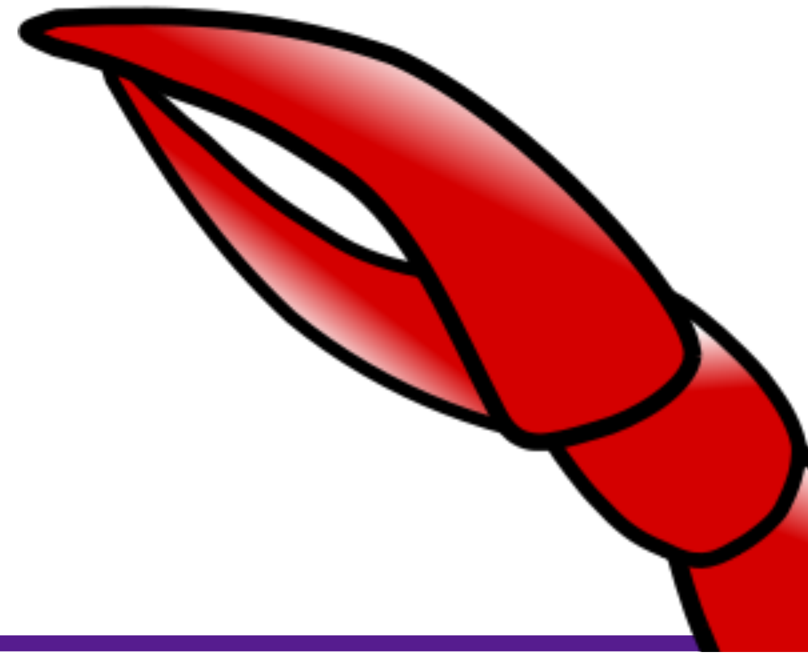

All about $m_{\beta\beta}$ featuring: the double-beta decay lobster!

$$m_{\beta\beta} = \left| \sum_{i=1}^{3} |U_{ei}|^2 m_i e^{i\alpha_i} \right|$$

Real number between 0 and 1

All about $m_{\beta\beta}$ featuring: the double-beta decay lobster!

$$m_{\beta\beta} = \left| \sum_{i=1}^{3} |U_{ei}|^2 m_i e^{i\alpha_i} \right|$$

Complex phases

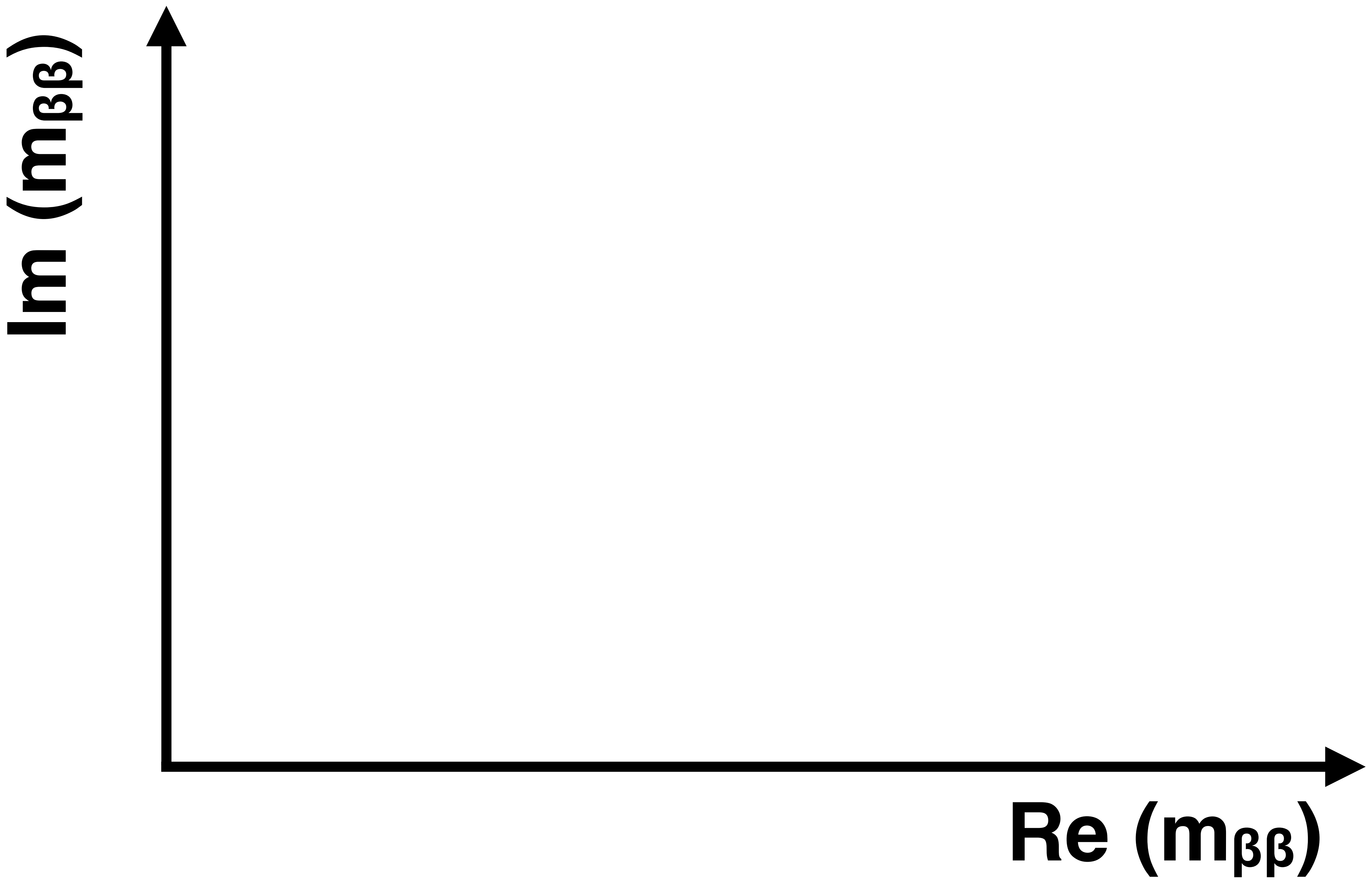

All about $m_{\beta\beta}$ featuring: the double-beta decay lobster!

$$m_{\beta\beta} = \left| \sum_{i=1}^{3} |U_{ei}|^2 m_i e^{i\alpha_i} \right|$$

Complex phases

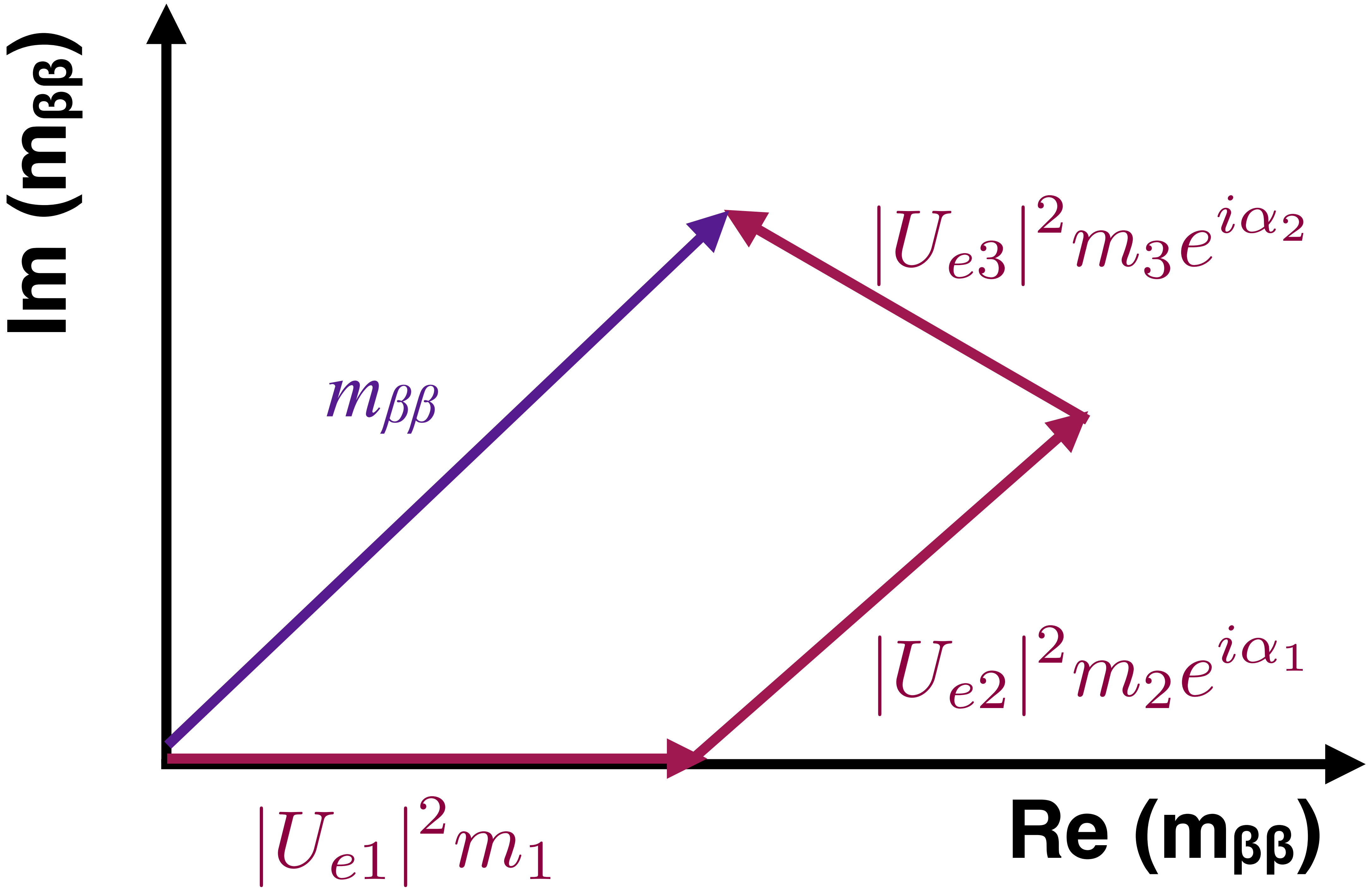

No Majorana phase for m_1 component (choice in PMNS matrix)

$$U = \begin{bmatrix} U_{e1} & U_{e2} & U_{e3} \\ U_{\mu 1} & U_{\mu 2} & U_{\mu 3} \\ U_{\tau 1} & U_{\tau 2} & U_{\tau 3} \end{bmatrix}$$
$$= \begin{bmatrix} 1 & 0 & 0 \\ 0 & c_{23} & s_{23} \\ 0 & -s_{23} & c_{23} \end{bmatrix} \begin{bmatrix} c_{13} & 0 & s_{13}e^{-i\delta} \\ 0 & 1 & 0 \\ -s_{13}e^{i\delta} & 0 & c_{13} \end{bmatrix} \begin{bmatrix} c_{12} & s_{12} & 0 \\ -s_{12} & c_{12} & 0 \\ 0 & 0 & 1 \end{bmatrix} \begin{bmatrix} 1 & 0 & 0 \\ 0 & e^{i\alpha_1/2} & 0 \\ 0 & 0 & e^{i\alpha_2/2} \end{bmatrix}$$

$$\begin{bmatrix} 1 & 0 & 0 \\ 0 & e^{i\alpha_1/2} & 0 \\ 0 & 0 & e^{i\alpha_2/2} \end{bmatrix}$$

All about $m_{\beta\beta}$ featuring: the double-beta decay lobster!

$$m_{\beta\beta} = \left| \sum_{i=1}^{3} |U_{ei}|^2 m_i e^{i\alpha_i} \right|$$

Complex phases

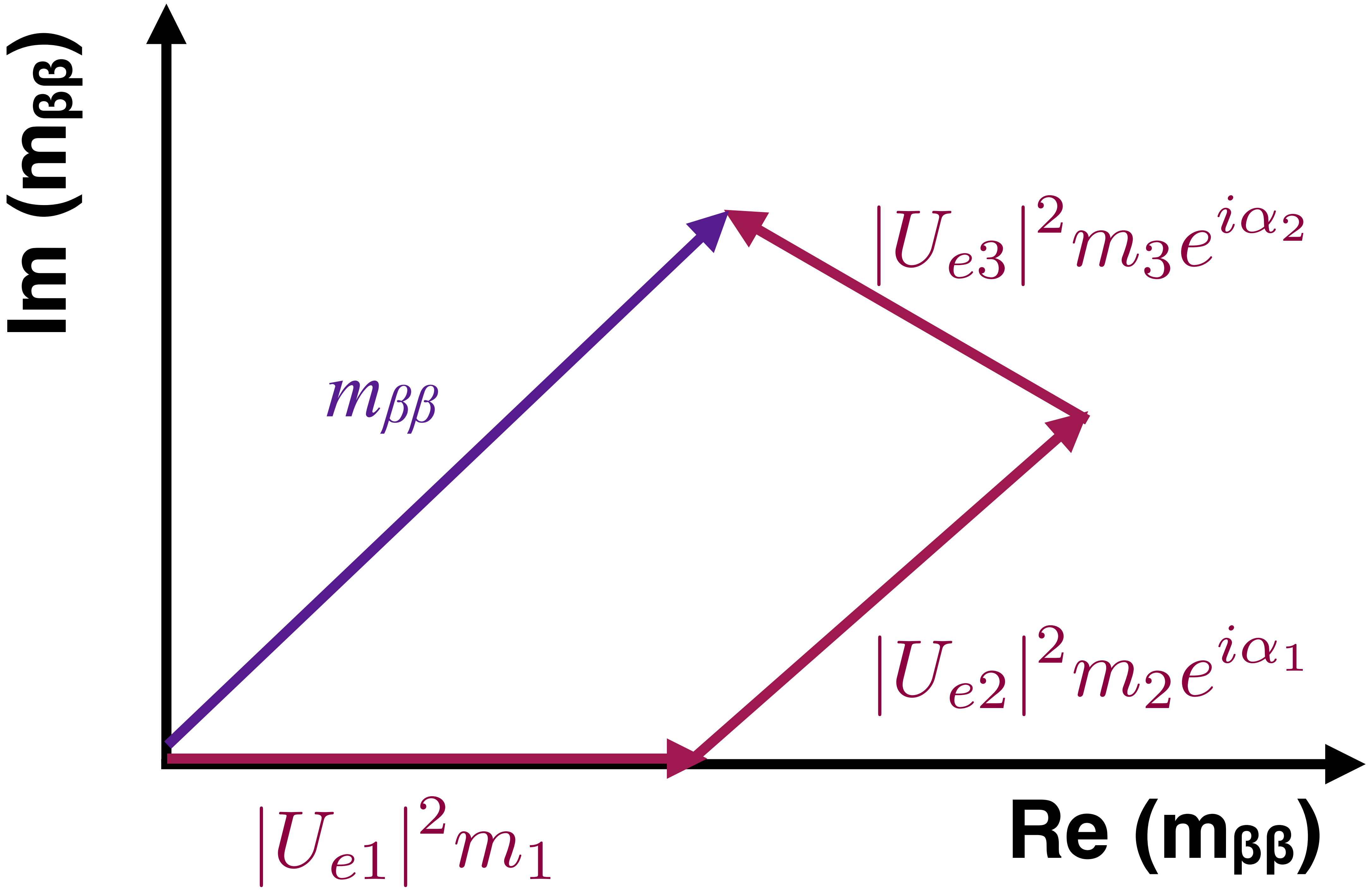

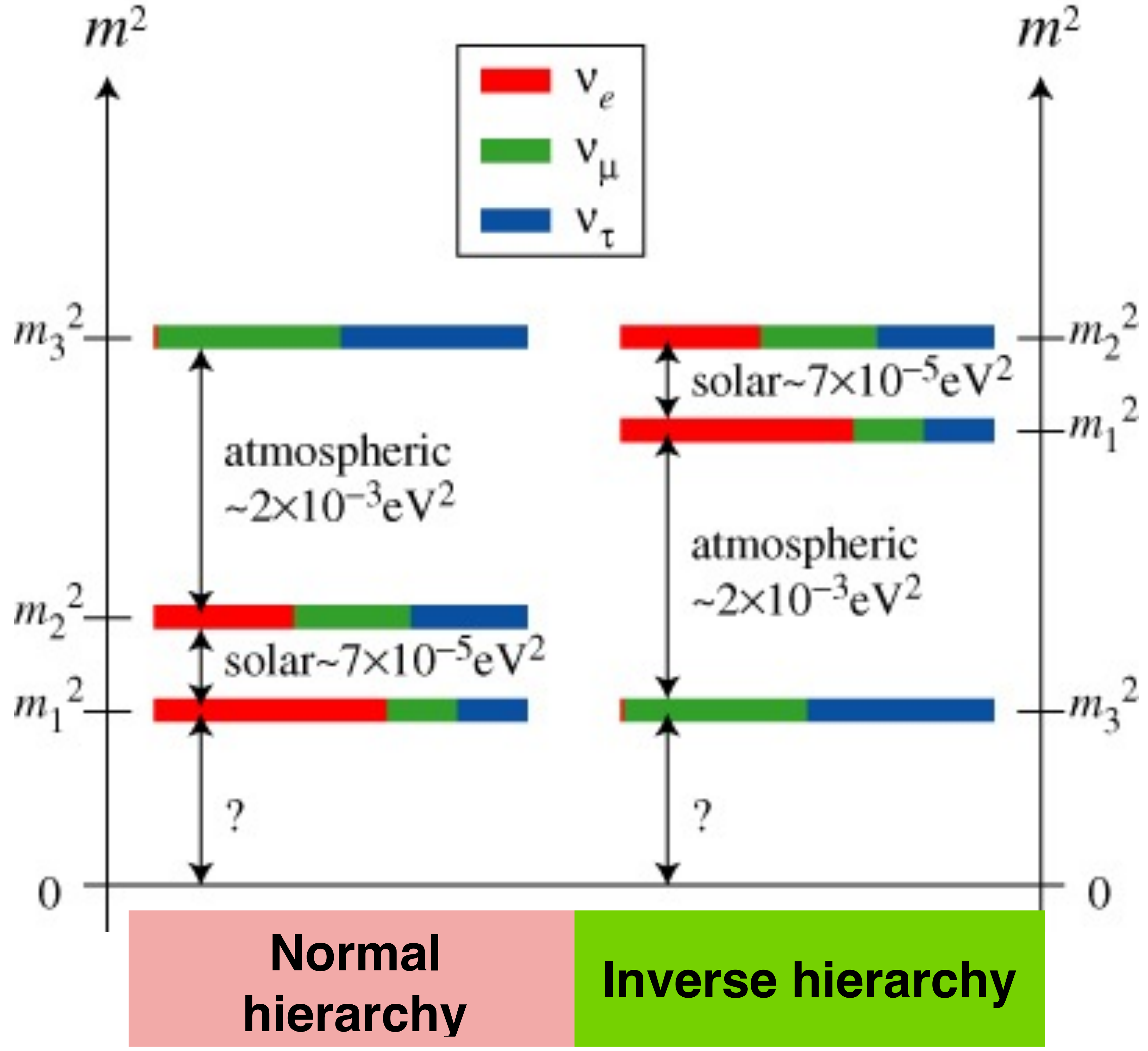

All about $m_{\beta\beta}$ featuring: the double-beta decay lobster!

$$m_{\beta\beta} = \left| \sum_{i=1}^{3} |U_{ei}|^2 m_i e^{i\alpha_i} \right|$$

Complex phases

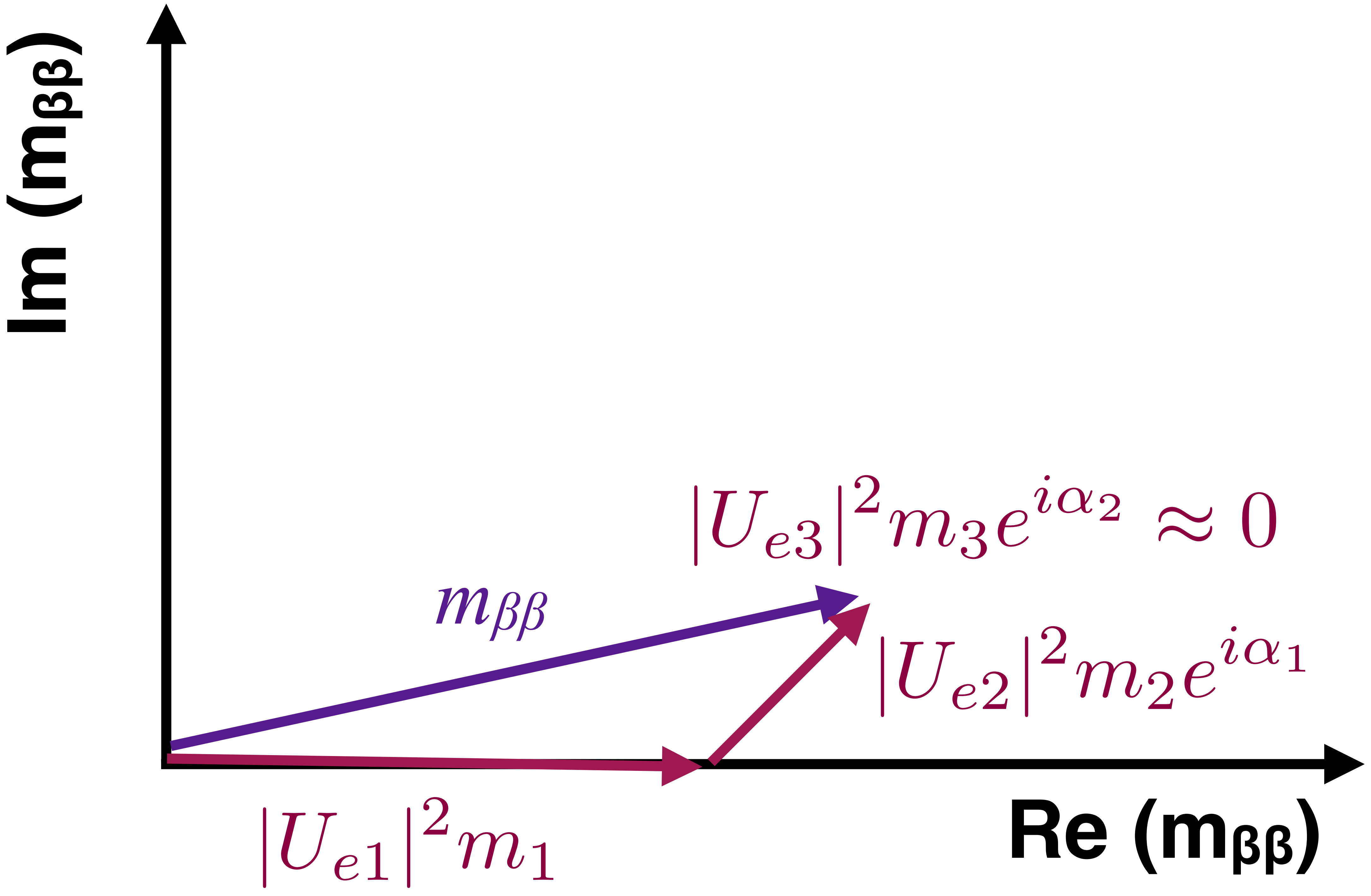

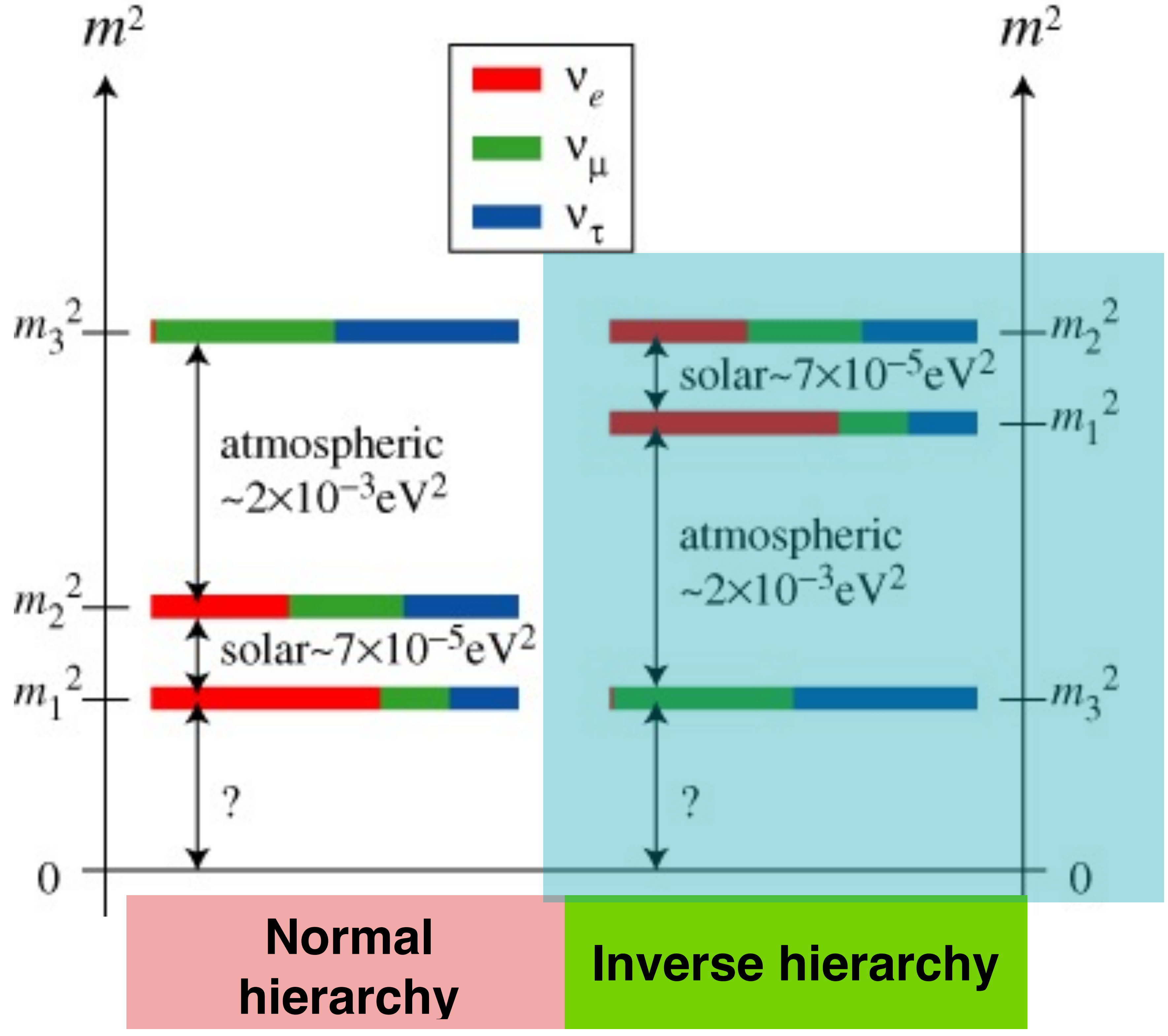

Scenario 1: Inverse hierarchy: $m_2 \sim m_1 >> m_3$

$$m_{\beta\beta} = c_{12}^2 c_{13}^2 m_{\nu_1} + s_{12}^2 c_{13}^2 m_{\nu_2} e^{i\alpha_1} + s_{13}^2 m_{\nu_3} e^{i\alpha_3}$$

0.68   0.30   0.02

All about $m_{\beta\beta}$ featuring: the double-beta decay lobster!

$$m_{\beta\beta} = \left| \sum_{i=1}^{3} |U_{ei}|^2 m_i e^{i\alpha_i} \right|$$

Complex phases

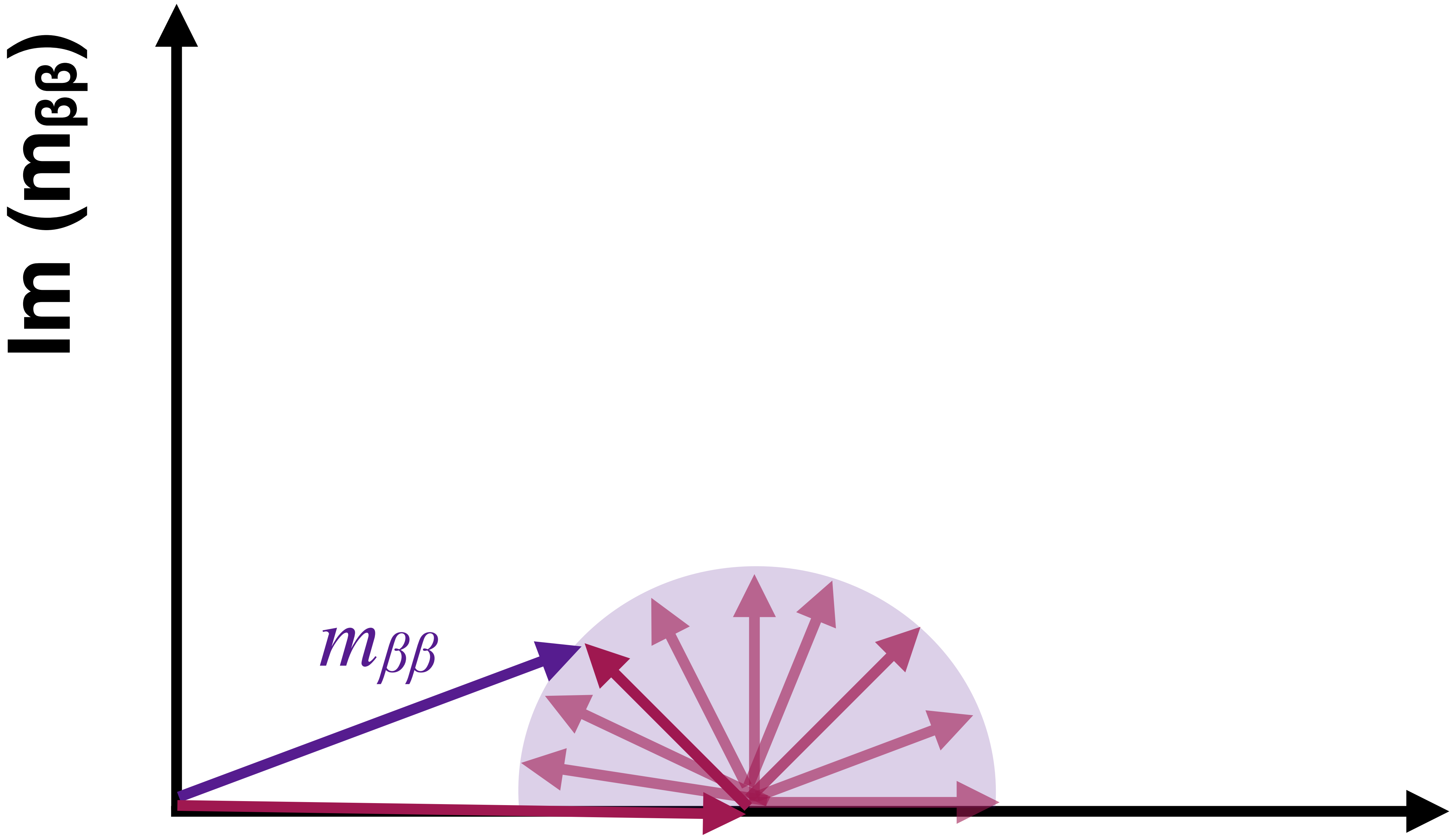

We know length (mixing angles) but not direction (Majorana phase) of m_2 vector

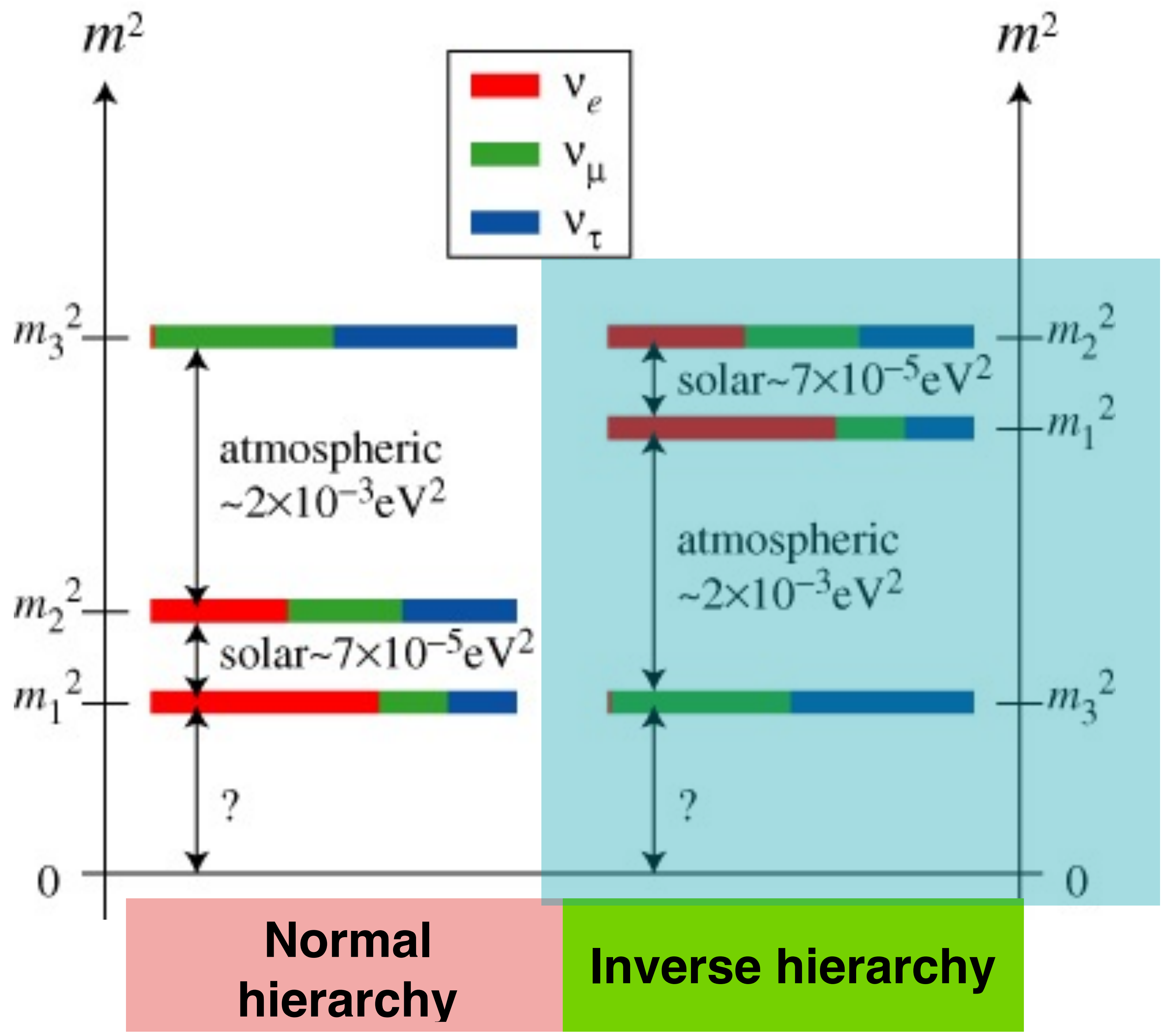

$$m_{\beta\beta} = c_{12}^2 c_{13}^2 m_{\nu_1} + s_{12}^2 c_{13}^2 m_{\nu_2} e^{i\alpha_1} + s_{13}^2 m_{\nu_3} e^{i\alpha_3}$$

0.68 0.30 0.02

All about $m_{\beta\beta}$ featuring: the double-beta decay lobster!

UCL

$$m_{\beta\beta} = \left| \sum_{i=1}^{3} |U_{ei}|^2 m_i e^{i\alpha_i} \right|$$

Complex phases

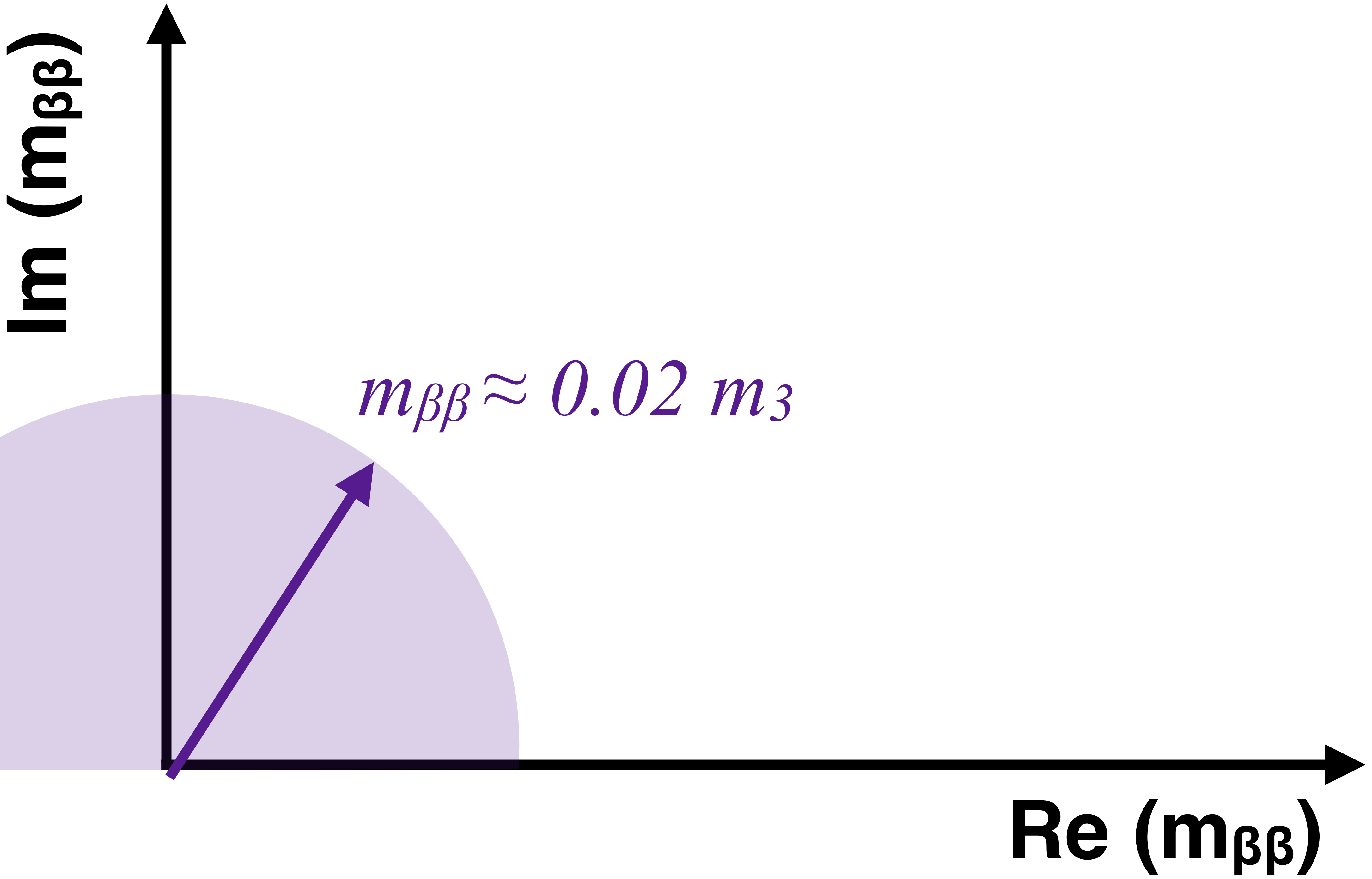

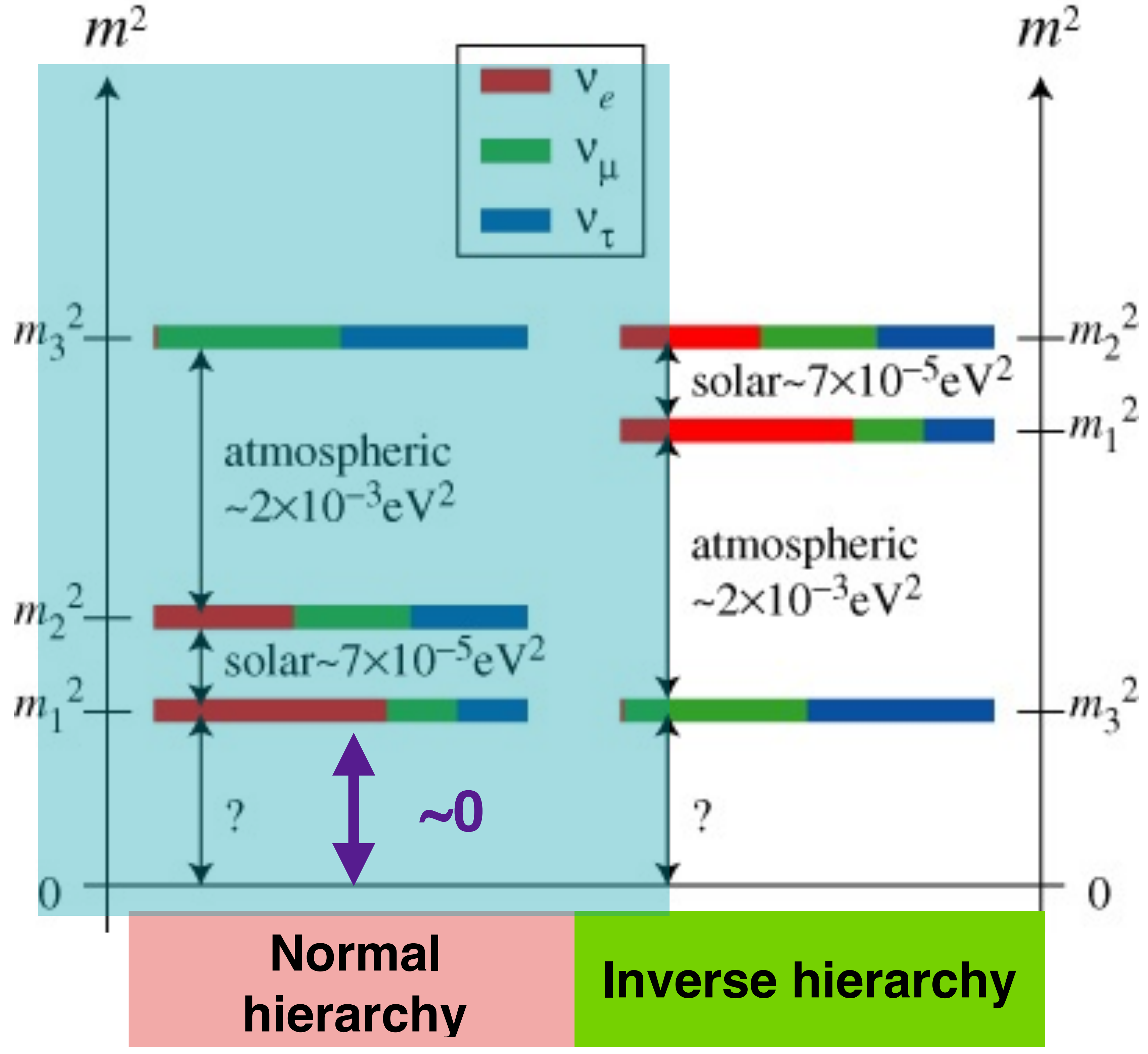

Scenario 2: Normal hierarchy: $m_3 >> m_2 > m_1$

$$m_{\beta\beta} = c_{12}^2 c_{13}^2 m_{\nu_1} + s_{12}^2 c_{13}^2 m_{\nu_2} e^{i\alpha_1} + s_{13}^2 m_{\nu_3} e^{i\alpha_3}$$

0.68 | 0.30 | 0.02

All about $m_{\beta\beta}$ featuring: the double-beta decay lobster!

UCL

$$m_{\beta\beta} = \left| \sum_{i=1}^{3} |U_{ei}|^2 m_i e^{i\alpha_i} \right|$$

Complex phases

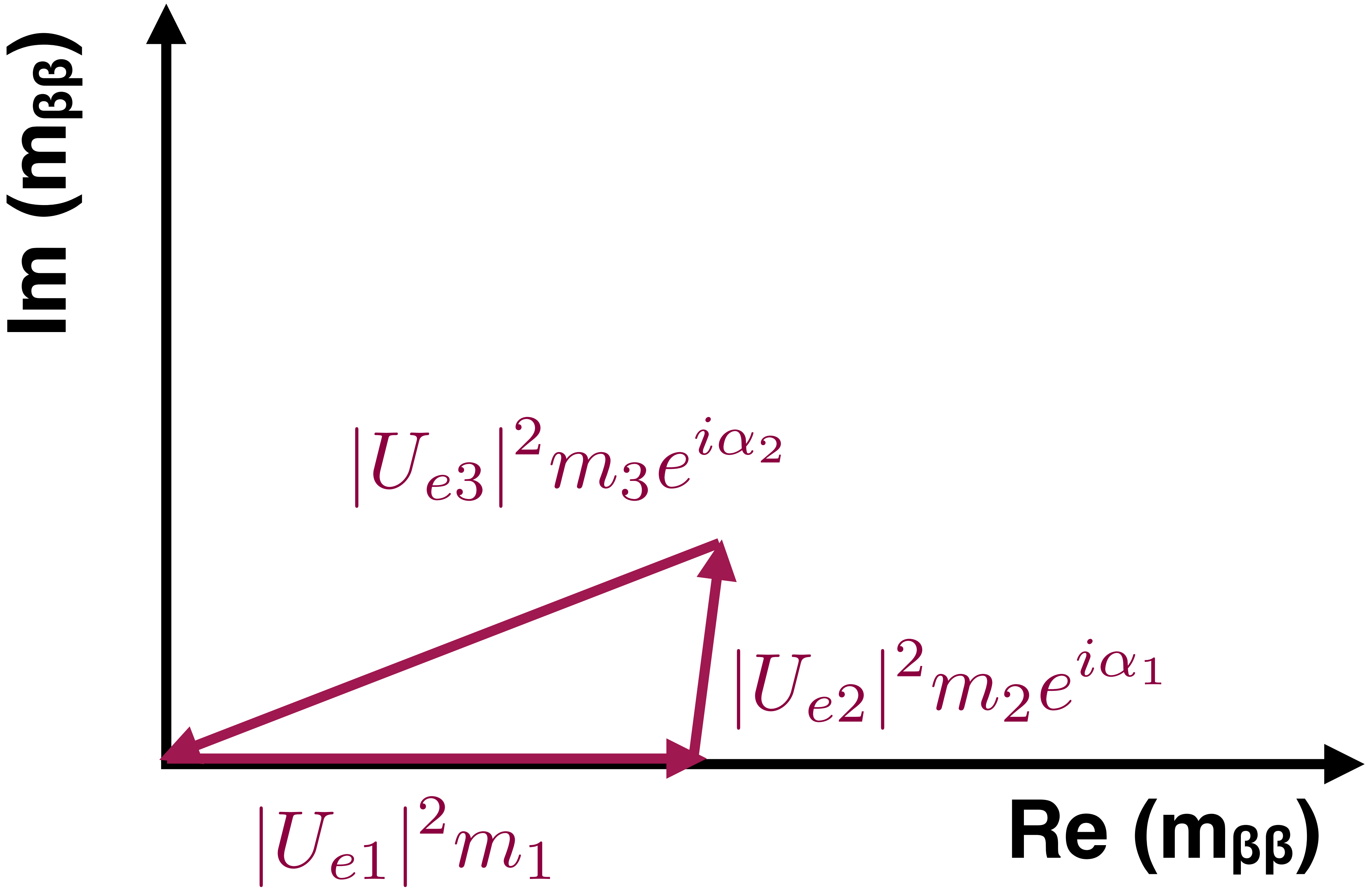

$m_{\beta\beta}$ = 0 is possible for the some masses / phases!

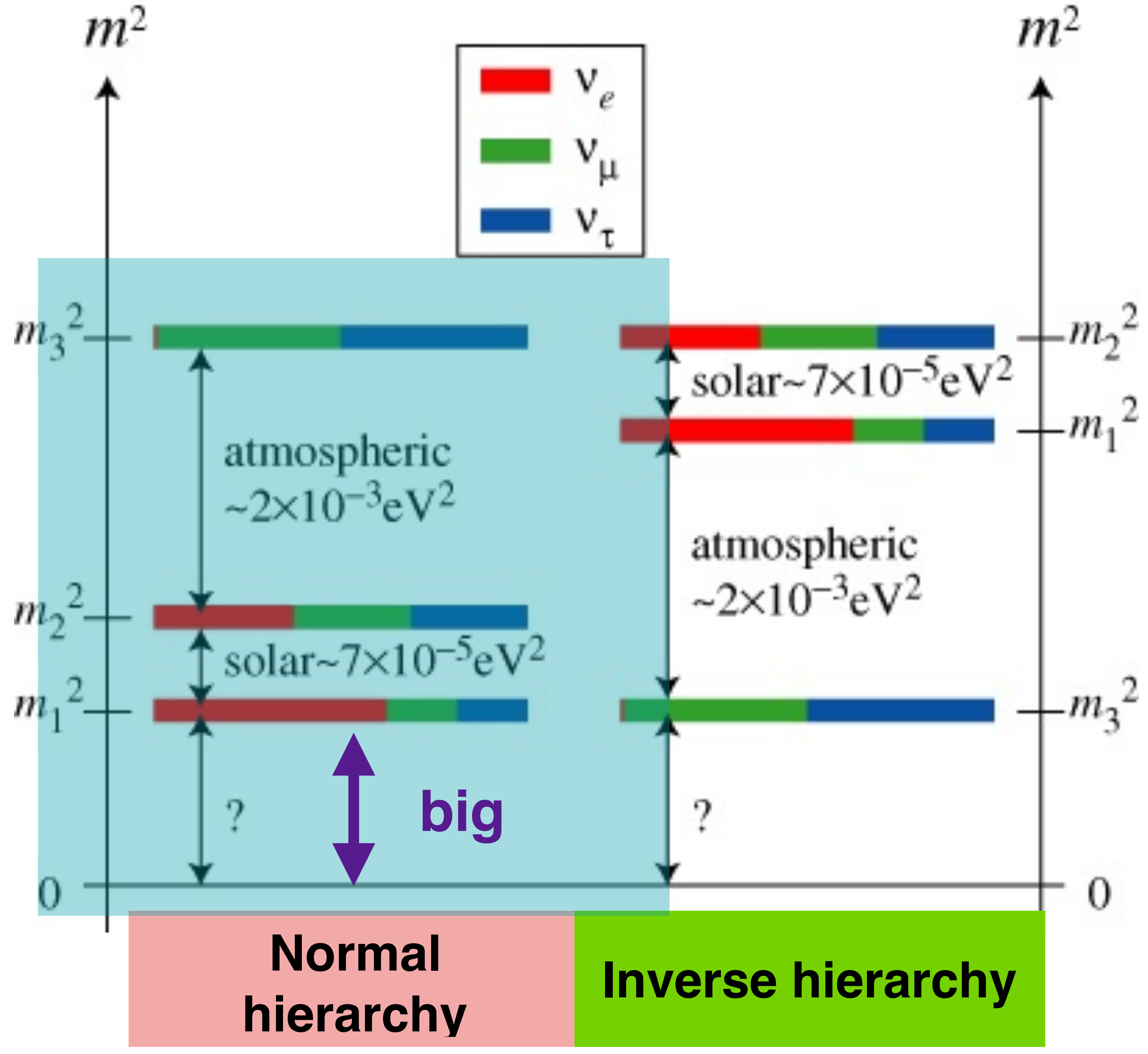

Scenario 3: Normal hierarchy: $m_3 > m_2 > m_1$

$$m_{\beta\beta} = c_{12}^2 c_{13}^2 m_{\nu_1} + s_{12}^2 c_{13}^2 m_{\nu_2} e^{i\alpha_1} + s_{13}^2 m_{\nu_3} e^{i\alpha_3}$$

0.68 | 0.30 | 0.02

Introducing the lobster!

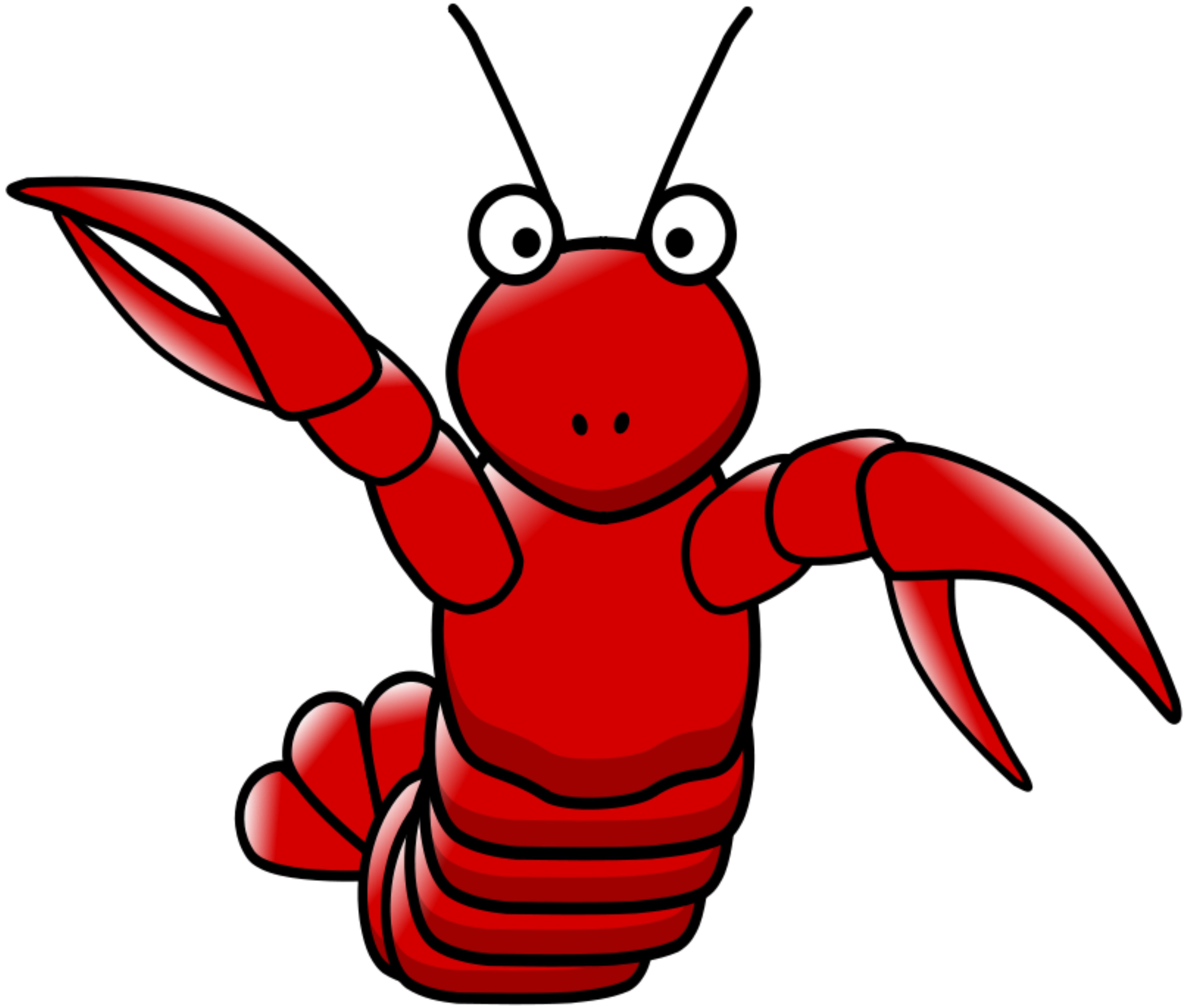

Adapted from PRL 117, 082503 (2016)

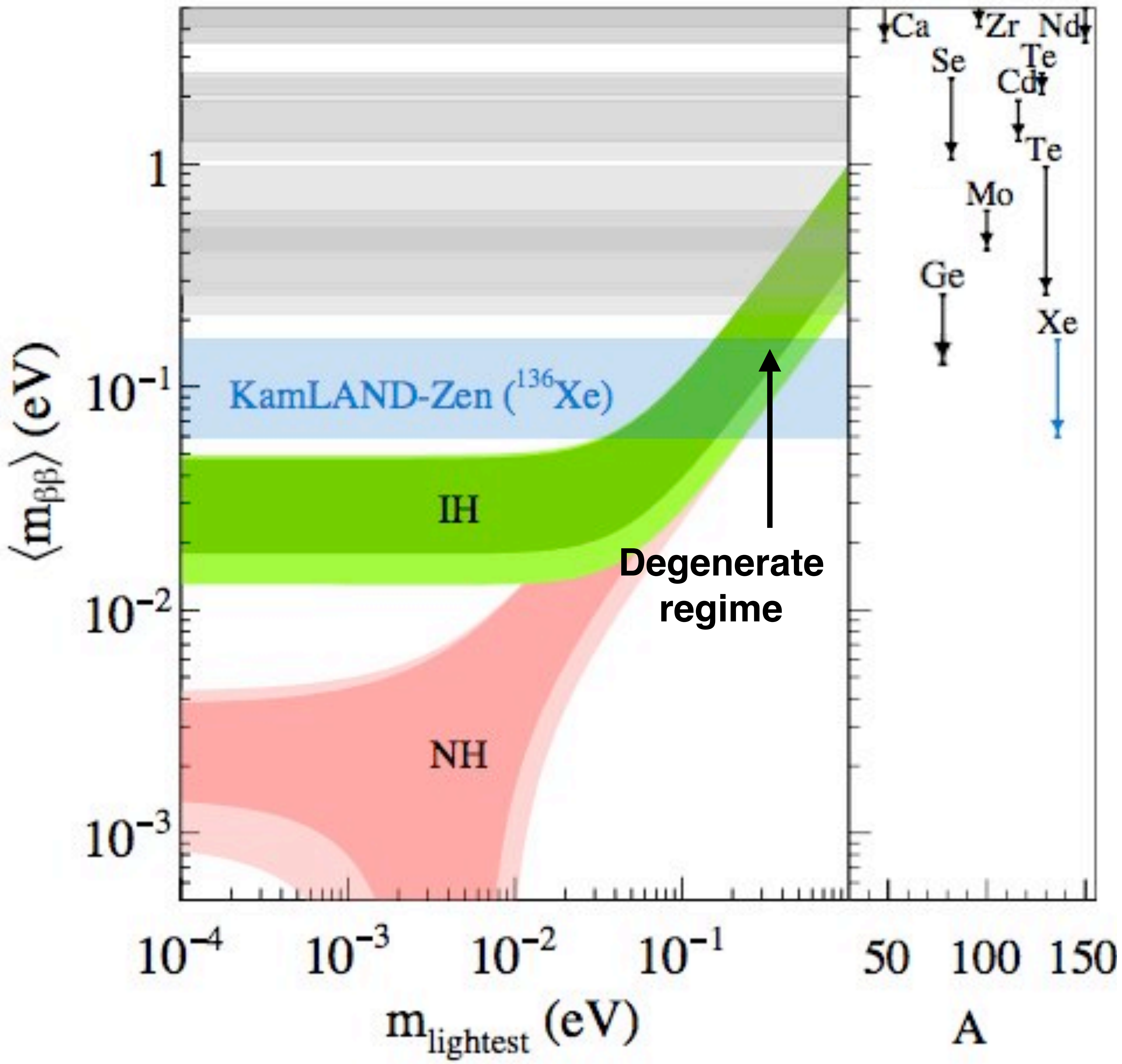

Introducing the lobster!

Nuclear effects

0νββ rate $$\frac{1}{T_{1/2}^{0\nu\beta\beta}} = G_{0\nu}(Q_{\beta\beta}, Z) g_A^4 |M_{0\nu}|^2 \frac{\langle m_{\beta\beta}\rangle^2}{m_e^2}$$

- **Best** current limit on the **0νββ rate**

$T_{1/2} >$ 1.07 x 10^{26} years

- Corresponds to **lowest $m_{\beta\beta}$ limit**

$\langle m_{\beta\beta}\rangle$ < 61-165 meV

- **Range** due to model uncertainty on **nuclear effects**

Adapted from PRL 117, 082503 (2016)

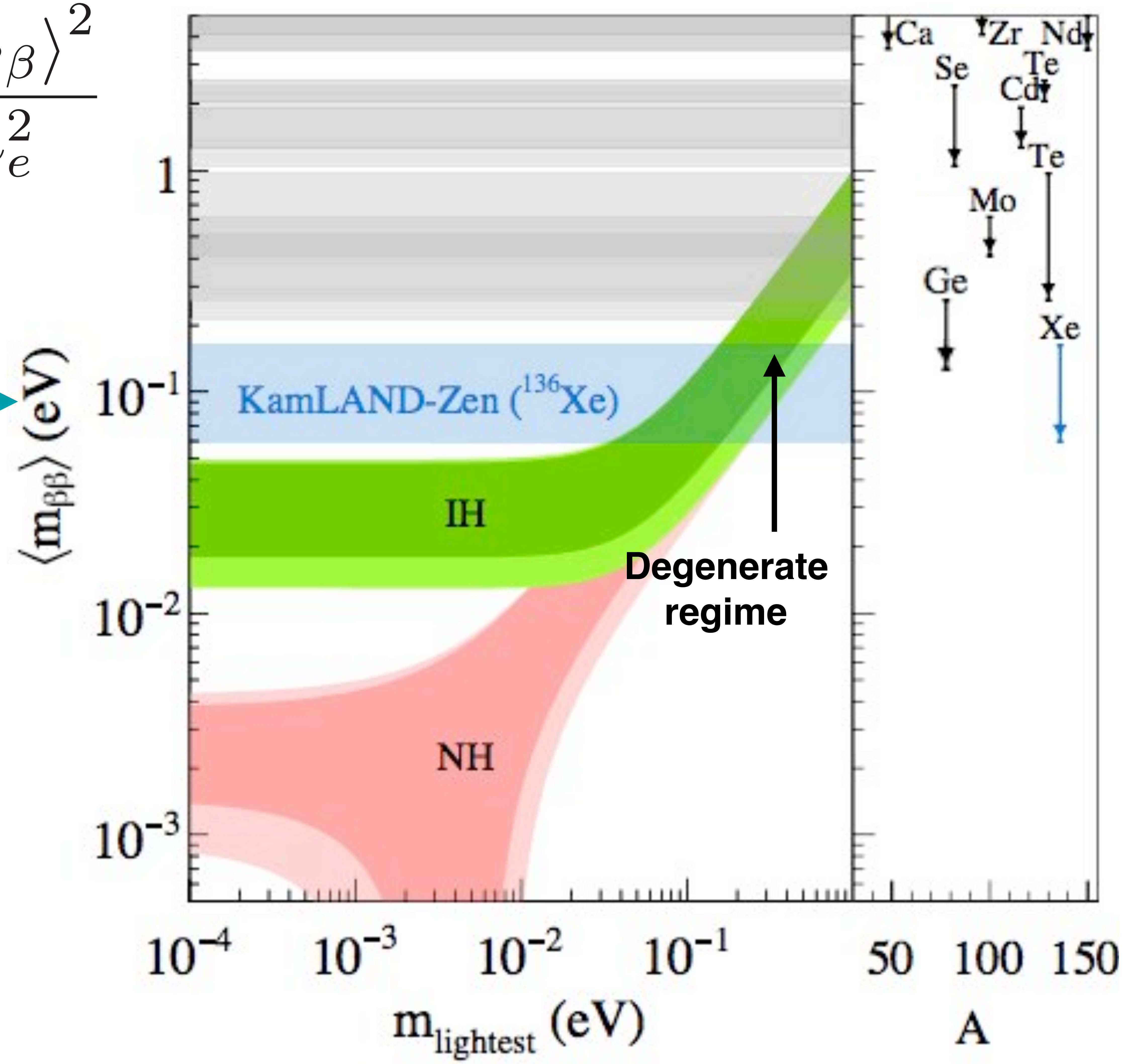

Double-beta decay and the nucleus

0νββ rate

$$\frac{1}{T_{1/2}^{0\nu\beta\beta}} = G_{0\nu}(Q_{\beta\beta}, Z) g_A^4 |M_{0\nu}|^2 \frac{\langle m_{\beta\beta}\rangle^2}{m_e^2}$$

Double-beta decay and the nucleus

0νββ rate $$\frac{1}{T_{1/2}^{0\nu\beta\beta}} = G_{0\nu}(Q_{\beta\beta}, Z) g_A^4 |M_{0\nu}|^2 \frac{\langle m_{\beta\beta} \rangle^2}{m_e^2}$$

Phase space factor

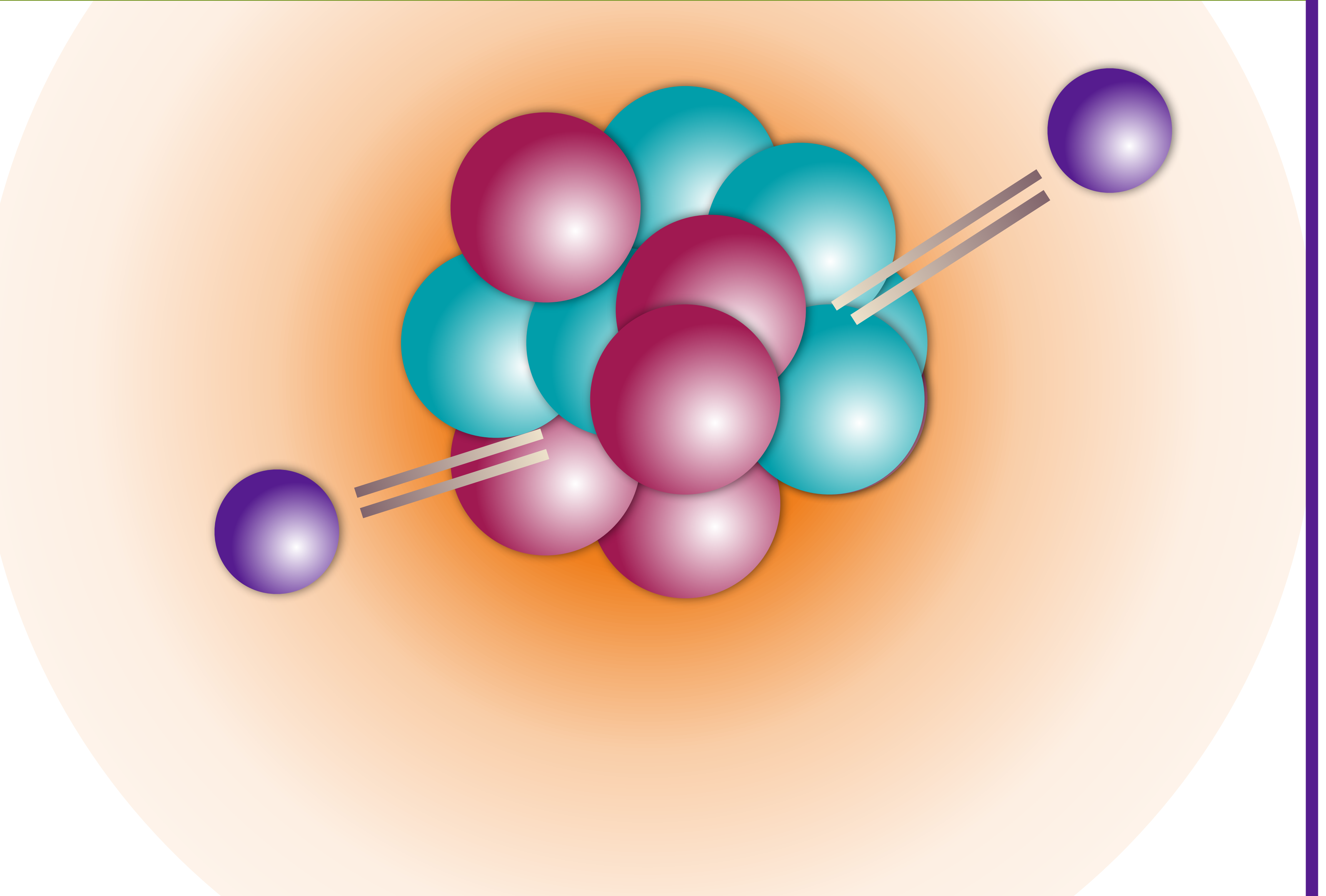

Coulomb effects of the nucleus on the emitted electrons

Double-beta decay and the nucleus

0νββ rate $$\frac{1}{T_{1/2}^{0\nu\beta\beta}} = G_{0\nu}(Q_{\beta\beta}, Z) g_A^4 |M_{0\nu}|^2 \frac{\langle m_{\beta\beta}\rangle^2}{m_e^2}$$

Phase space factor

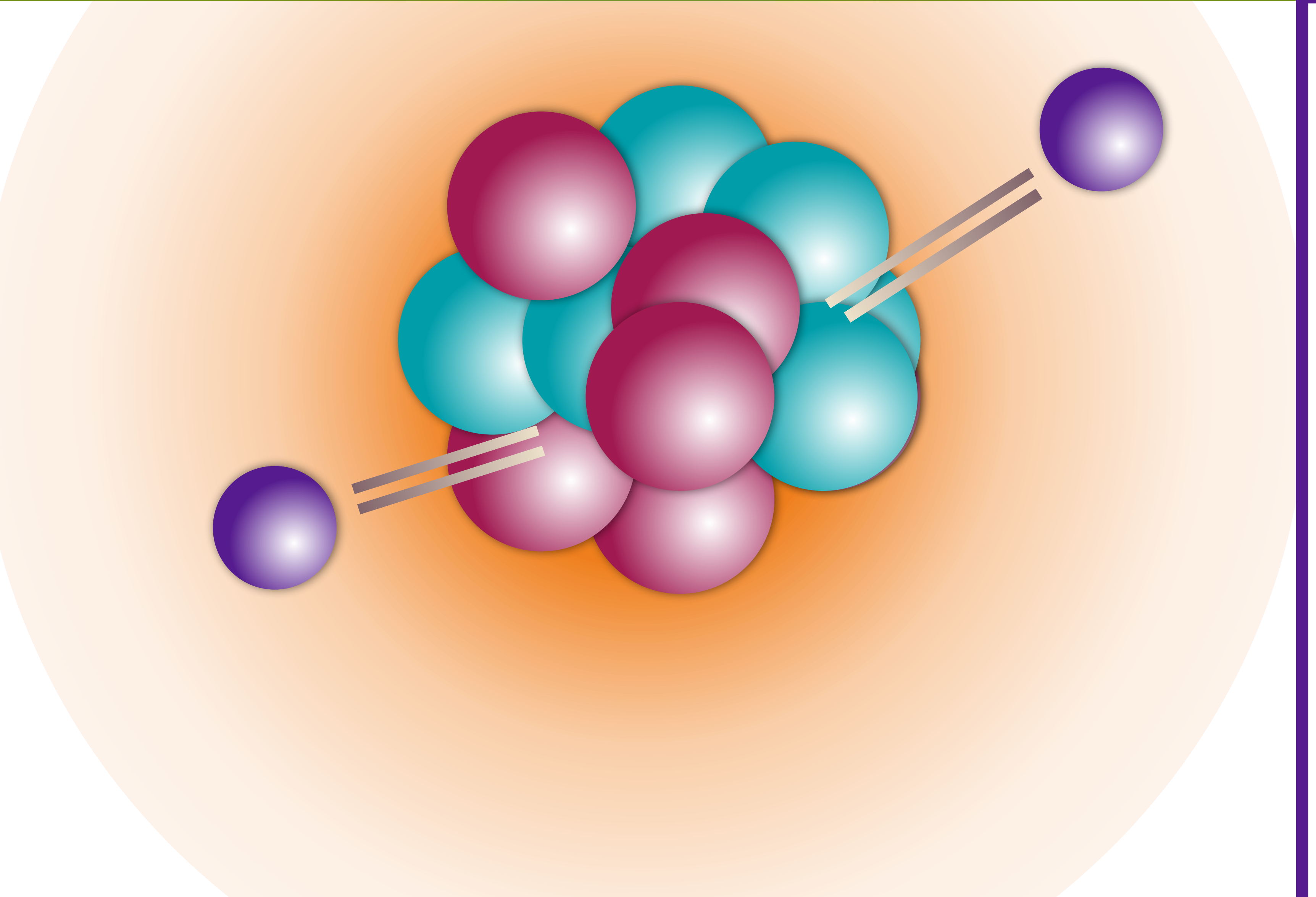

Coulomb effects of the nucleus on the emitted electrons

Axial coupling constant

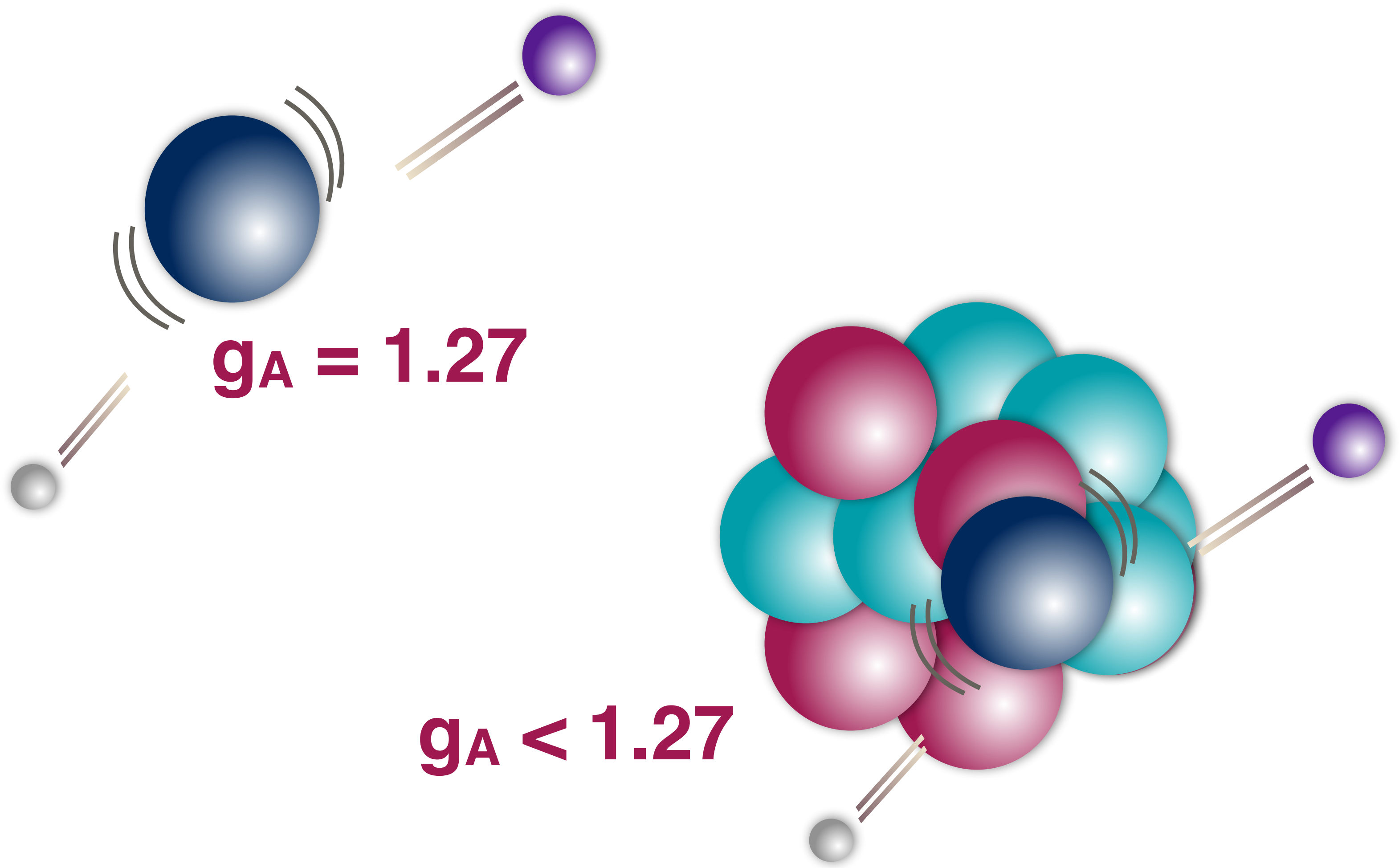

Axial vector coupling constant appears quenched in heavy nuclei

Double-beta decay and the nucleus

0νββ rate

$$\frac{1}{T^{0\nu\beta\beta}_{1/2}} = G_{0\nu}(Q_{\beta\beta}, Z)\, g_A^4\, |M_{0\nu}|^2 \frac{\langle m_{\beta\beta}\rangle^2}{m_e^2}$$

Phase space factor

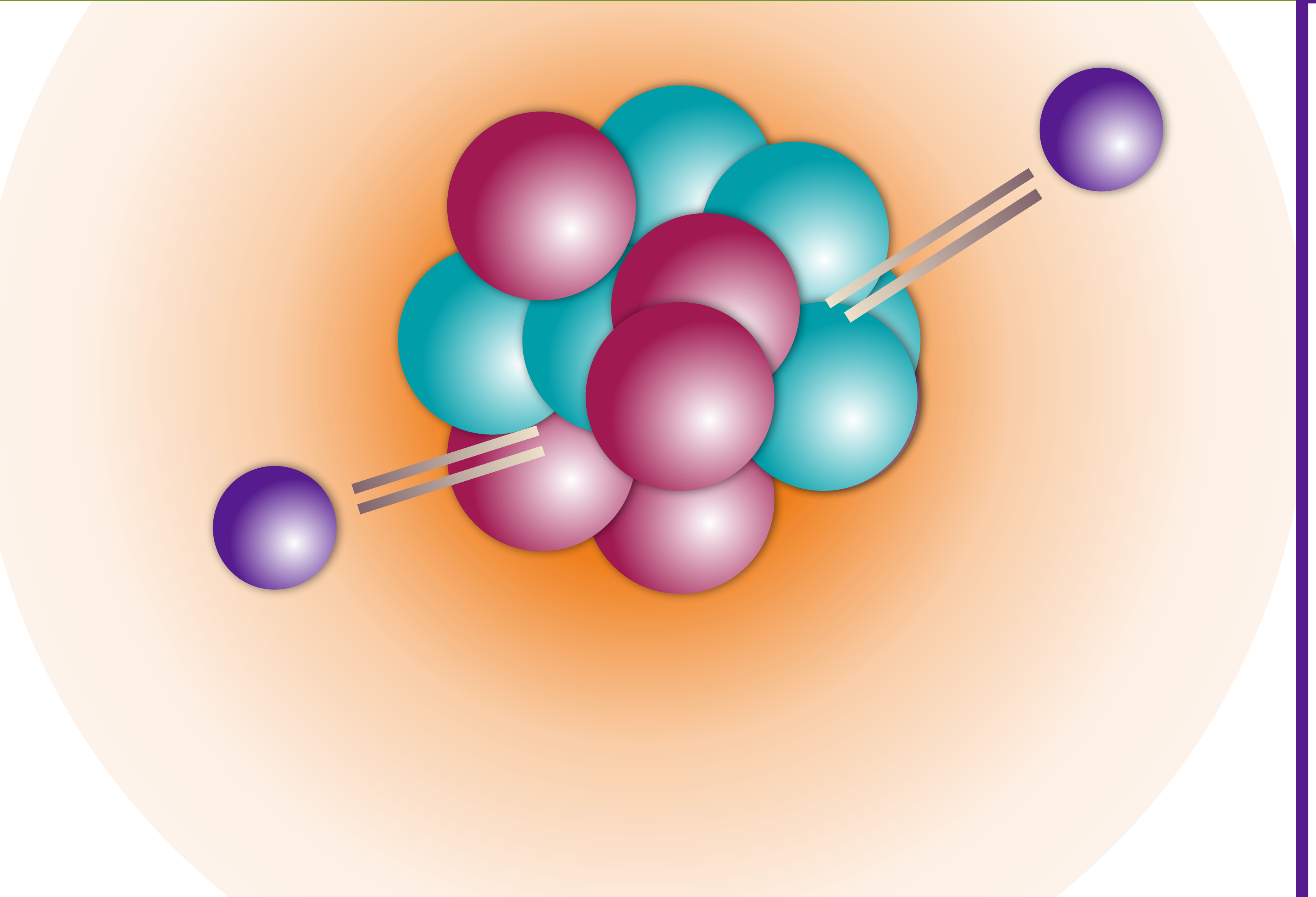

Coulomb effects of the nucleus on the emitted electrons

Axial coupling constant

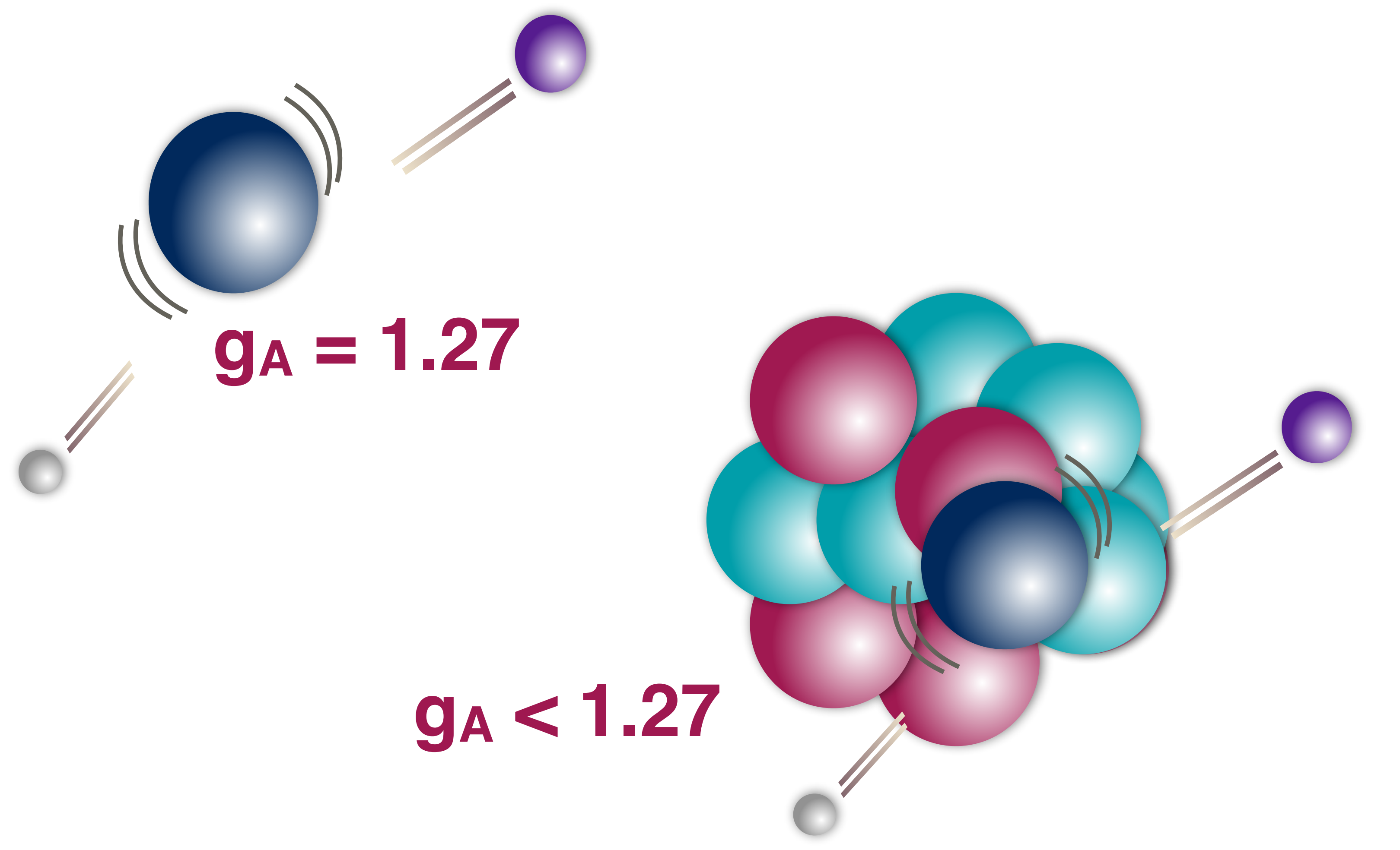

Axial vector coupling constant appears quenched in heavy nuclei

Nuclear matrix element

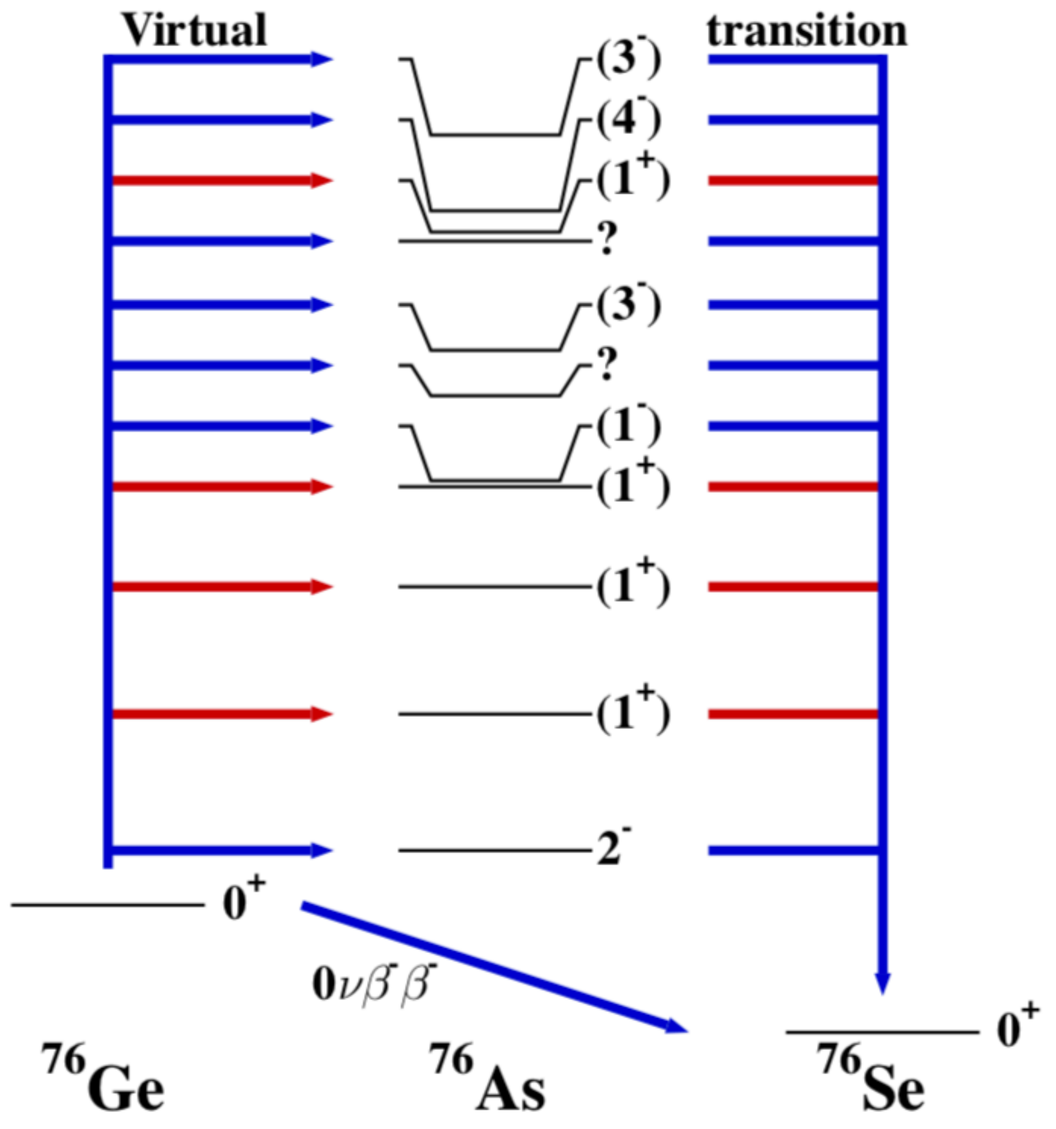

Nuclear structure effects of the parent, daughter, and intermediate nuclei

IPPP/05/56, DCPT/05/114

Phase space factors

0νββ rate $$\frac{1}{T_{1/2}^{0\nu\beta\beta}} = G_{0\nu}(Q_{\beta\beta}, Z) g_A^4 |M_{0\nu}|^2 \frac{\langle m_{\beta\beta}\rangle^2}{m_e^2}$$

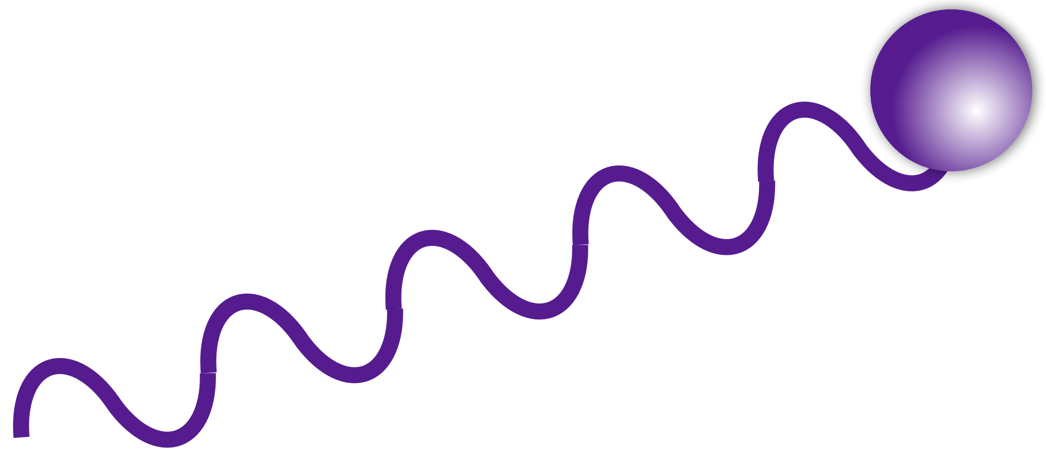

DOI: 10.3389/fphy.2019.00012

Phase space factors

0νββ rate $$\frac{1}{T_{1/2}^{0\nu\beta\beta}} = G_{0\nu}(Q_{\beta\beta}, Z) g_A^4 |M_{0\nu}|^2 \frac{\langle m_{\beta\beta} \rangle^2}{m_e^2}$$

- The wave function for a free electron: a **plane wave**

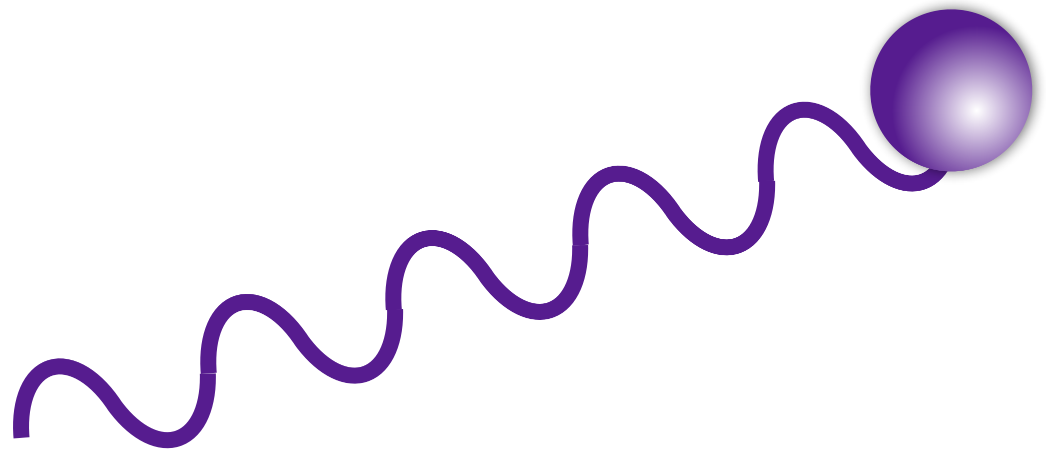

DOI: 10.3389/fphy.2019.00012

Phase space factors

0νββ rate $$\frac{1}{T_{1/2}^{0\nu\beta\beta}} = G_{0\nu}(Q_{\beta\beta}, Z) g_A^4 |M_{0\nu}|^2 \frac{\langle m_{\beta\beta}\rangle^2}{m_e^2}$$

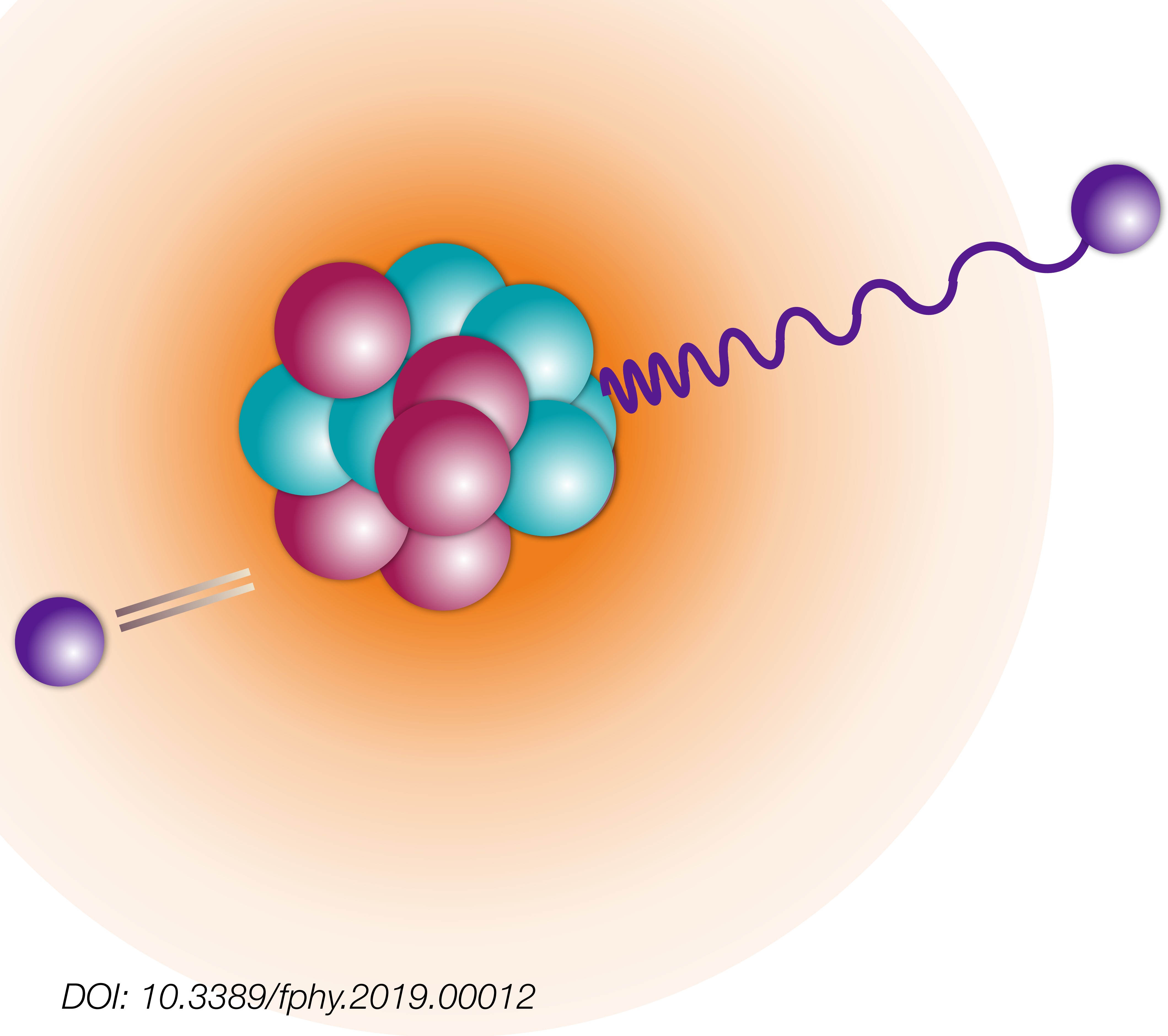

- The wave function for a free electron: a **plane wave**
- … is distorted by the **Coulomb field** of the nucleus

DOI: 10.3389/fphy.2019.00012

Phase space factors

0νββ rate $\frac{1}{T_{1/2}^{0\nu\beta\beta}} = G_{0\nu}(Q_{\beta\beta}, Z) g_A^4 |M_{0\nu}|^2 \frac{\langle m_{\beta\beta} \rangle^2}{m_e^2}$

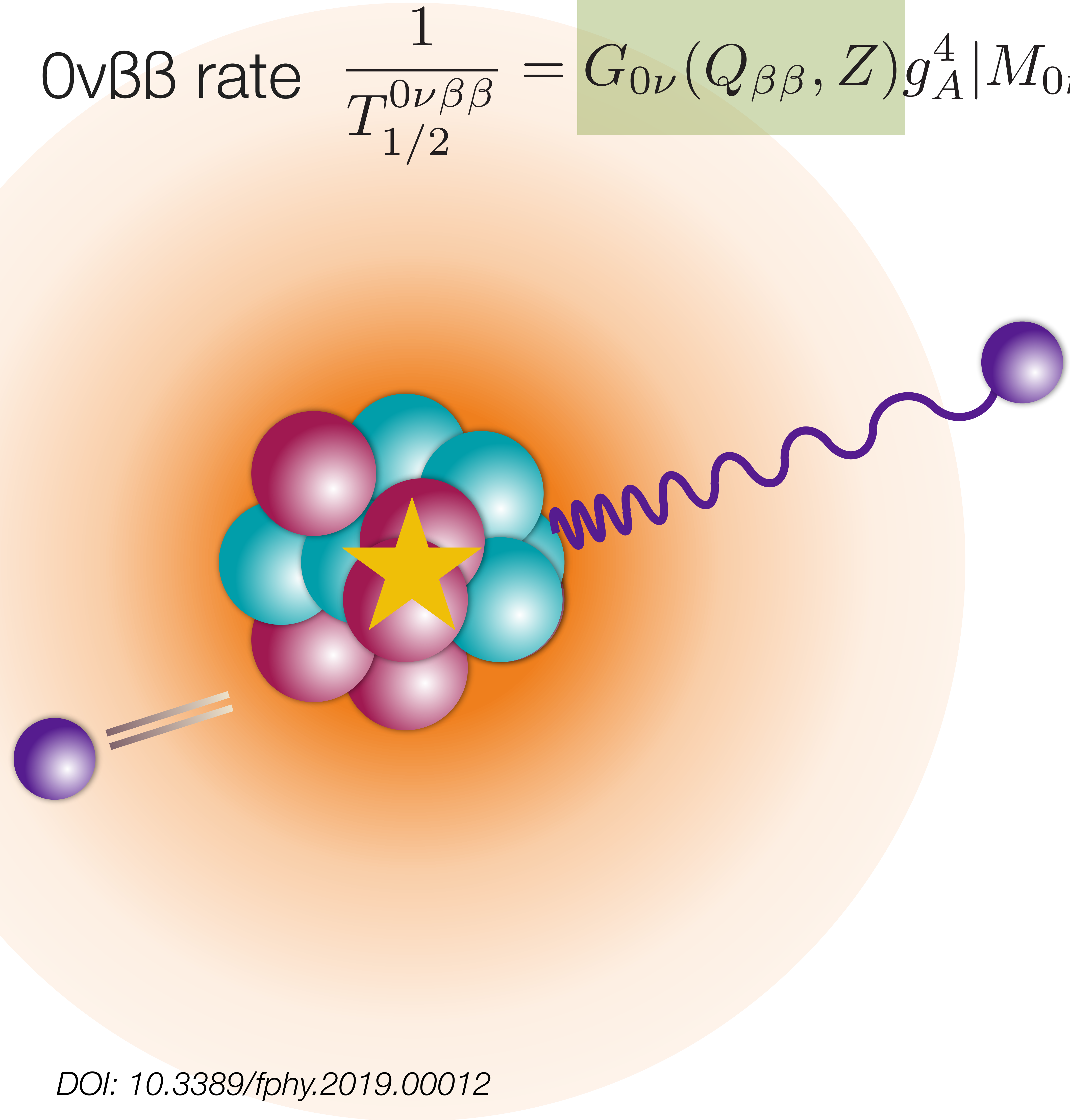

- The wave function for a free electron: a **plane wave**
- … is distorted by the **Coulomb field** of the nucleus
- **Nonrelativistic** model - multiply electron wave function by a **Fermi factor**
  - Solve Schrödinger equation for a Coulomb potential of **point charge** equal to nuclear charge Z
  - Divide by **plane wave** solution
  - Evaluate at the **origin**

DOI: 10.3389/fphy.2019.00012

Phase space factors

0νββ rate $$\frac{1}{T_{1/2}^{0\nu\beta\beta}} = G_{0\nu}(Q_{\beta\beta}, Z) g_A^4 |M_{0\nu}|^2 \frac{\langle m_{\beta\beta}\rangle^2}{m_e^2}$$

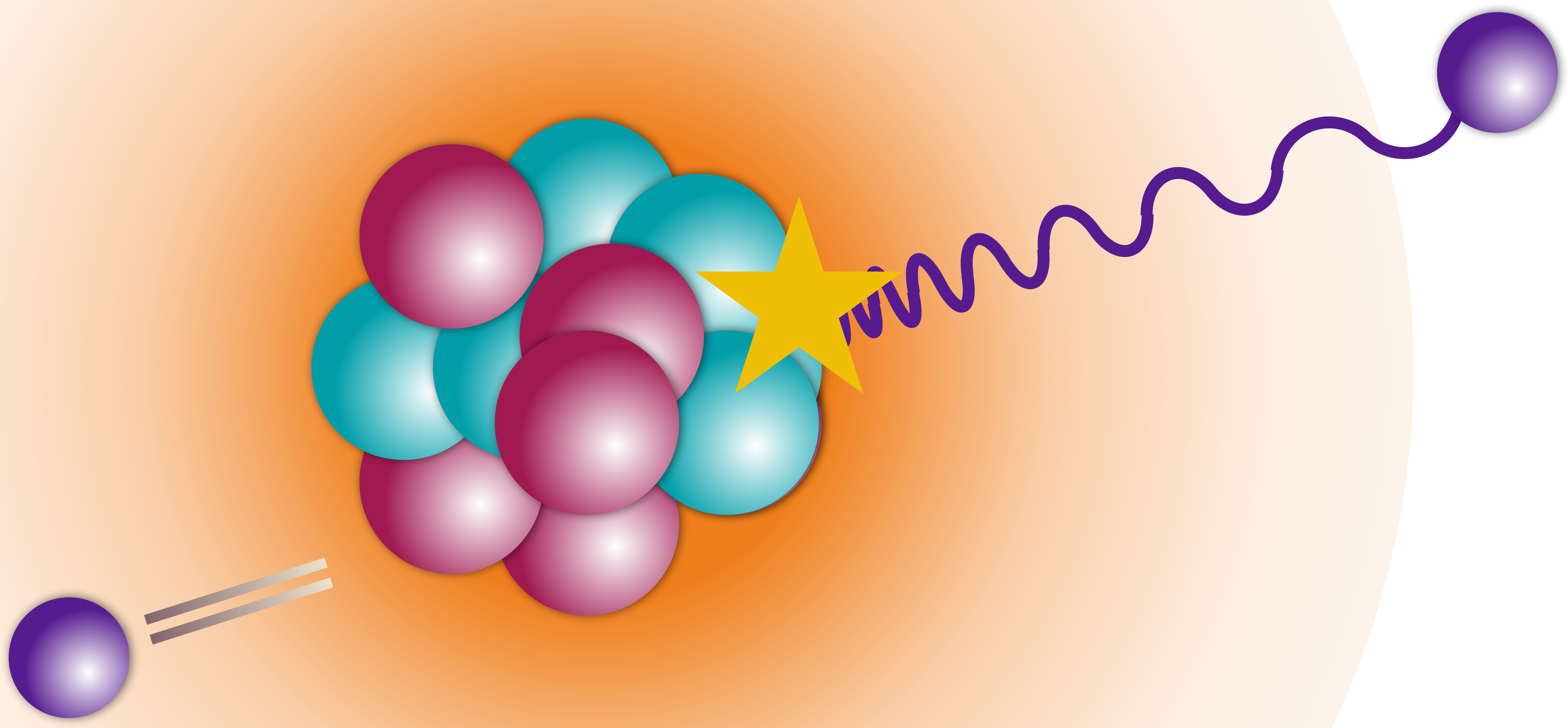

- The wave function for a free electron: a **plane wave**
- … is distorted by the **Coulomb field** of the nucleus
- **Nonrelativistic** model - multiply electron wave function by a **Fermi factor**
  - Solve Schrödinger equation for a Coulomb potential of **point charge** equal to nuclear charge Z
  - Divide by **plane wave** solution
  - Evaluate at the **origin**
- **Relativistic** model:
  - Solve **Dirac equation** in point charge potential
  - Divide by plane wave at **nuclear surface**

DOI: 10.3389/fphy.2019.00012

Phase space factors

$0\nu\beta\beta$ rate $$\frac{1}{T^{0\nu\beta\beta}_{1/2}} = G_{0\nu}(Q_{\beta\beta}, Z) g_A^4 |M_{0\nu}|^2 \frac{\langle m_{\beta\beta}\rangle^2}{m_e^2}$$

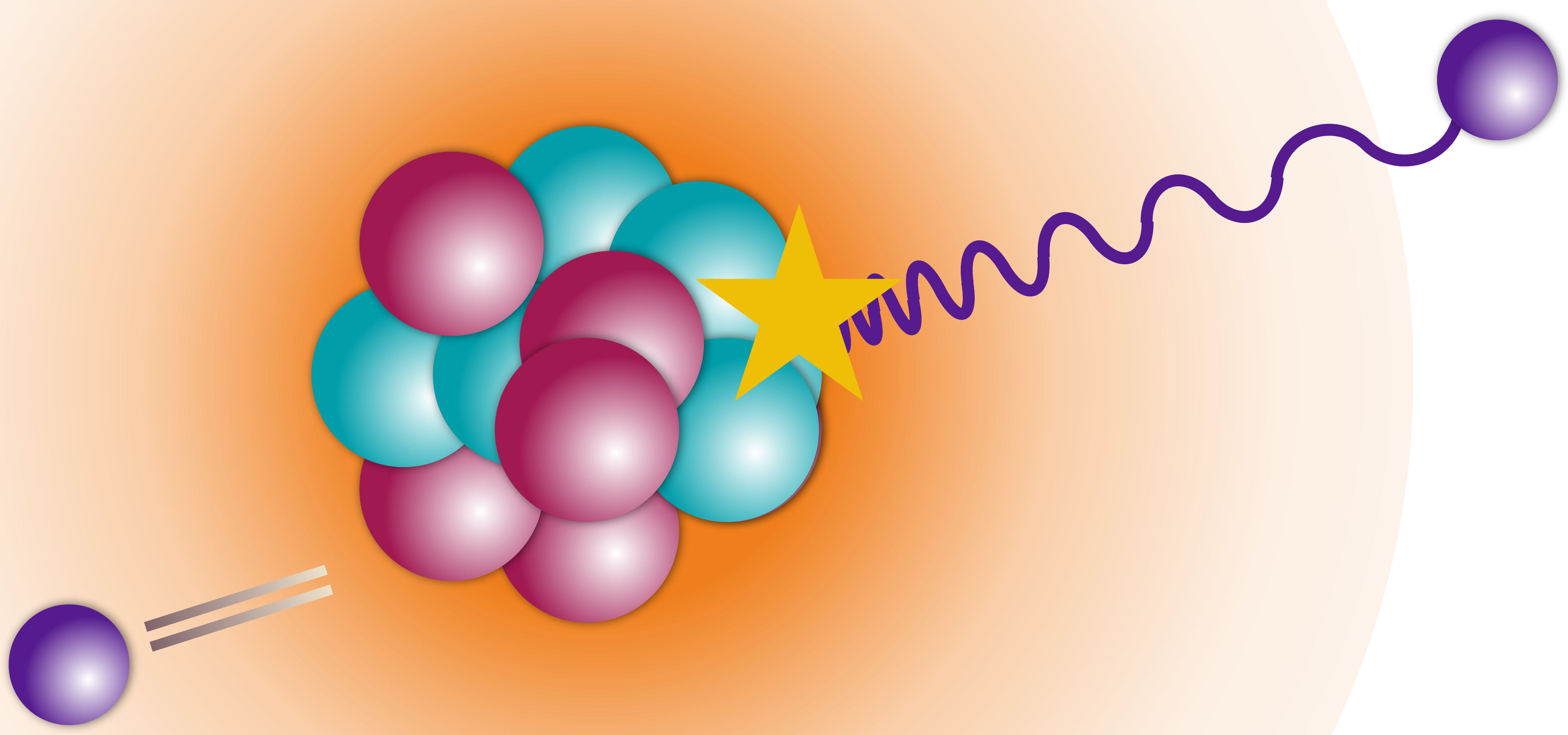

- The wave function for a free electron: a **plane wave**
- … is distorted by the **Coulomb field** of the nucleus
- **Nonrelativistic** model - multiply electron wave function by a **Fermi factor**
  - Solve Schrödinger equation for a Coulomb potential of **point charge** equal to nuclear charge Z
  - Divide by **plane wave** solution
  - Evaluate at the **origin**
- **Relativistic** model:
  - Solve **Dirac equation** in point charge potential
  - Divide by plane wave at **nuclear surface**
- Recent **enhancements** include
  - **Screening**
  - Realistic **proton density** functions
  - Including transitions to **excited nuclear states**

DOI: 10.3389/fphy.2019.00012

Phase space factor cheat sheet

Nucleus	Z	$Q_{\beta\beta}$	$G_{0\nu}$ (10^{-15} yr^{-1}): various models					
^{48}Ca	20	4.267	24.65	24.81	26.1	26	24.83	24.55
^{150}Nd	60	3.371	61.94	63.03	85.9	78.4	63.16	66
^{100}Mo	42	3.034	15.84	15.92	18.7	45.6	15.95	15.74
^{82}Se	34	2.996	10.14	10.16	11.4	11.1	10.18	9.96
^{130}Te	52	2.528	14.24	14.22	19.4	16.7	14.25	14.1
^{136}Xe	54	2.458	14.54	14.58	19.4	17.7	14.62	14.49
^{76}Ge	32	2.039	2.372	2.363	2.62	2.55	2.37	2.28

Adapted from DOI: 10.3389/fphy.2019.00012

Phase space factor cheat sheet

Nucleus	Z	$Q_{\beta\beta}$	$G_{0\nu}$ (10^{-15} yr^{-1}): various models					
^{48}Ca	20	4.267	24.65	24.81	26.1	26	24.83	24.55
^{150}Nd	60	3.371	61.94	63.03	85.9	78.4	63.16	66
^{100}Mo	42	3.034	15.84	15.92	18.7	45.6	15.95	15.74
^{82}Se	34	2.996	10.14	10.16	11.4	11.1	10.18	9.96
^{130}Te	52	2.528	14.24	14.22	19.4	16.7	14.25	14.1
^{136}Xe	54	2.458	14.54	14.58	19.4	17.7	14.62	14.49
^{76}Ge	32	2.039	2.372	2.363	2.62	2.55	2.37	2.28

Adapted from DOI: 10.3389/fphy.2019.00012

$G_{0\nu}$ increases strongly with $Q_{\beta\beta}$

$$T_{1/2}^{0\nu} \propto Q_{\beta\beta}^{-5}$$

Phase space factor cheat sheet

Nucleus	Z	$Q_{\beta\beta}$	$G_{0\nu}$ (10^{-15} yr^{-1}): various models					
^{48}Ca	20	4.267	24.65	24.81	26.1	26	24.83	24.55
^{150}Nd	60	3.371	61.94	63.03	85.9	78.4	63.16	66
^{100}Mo	42	3.034	15.84	15.92	18.7	45.6	15.95	15.74
^{82}Se	34	2.996	10.14	10.16	11.4	11.1	10.18	9.96
^{130}Te	52	2.528	14.24	14.22	19.4	16.7	14.25	14.1
^{136}Xe	54	2.458	14.54	14.58	19.4	17.7	14.62	14.49
^{76}Ge	32	2.039	2.372	2.363	2.62	2.55	2.37	2.28

Adapted from DOI: 10.3389/fphy.2019.00012

$G_{0\nu}$ increases strongly with $Q_{\beta\beta}$

$$T^{0\nu}_{1/2} \propto Q^{-5}_{\beta\beta}$$

Also depends on Z, nuclear radius (~$A^{1/3}$), charge density

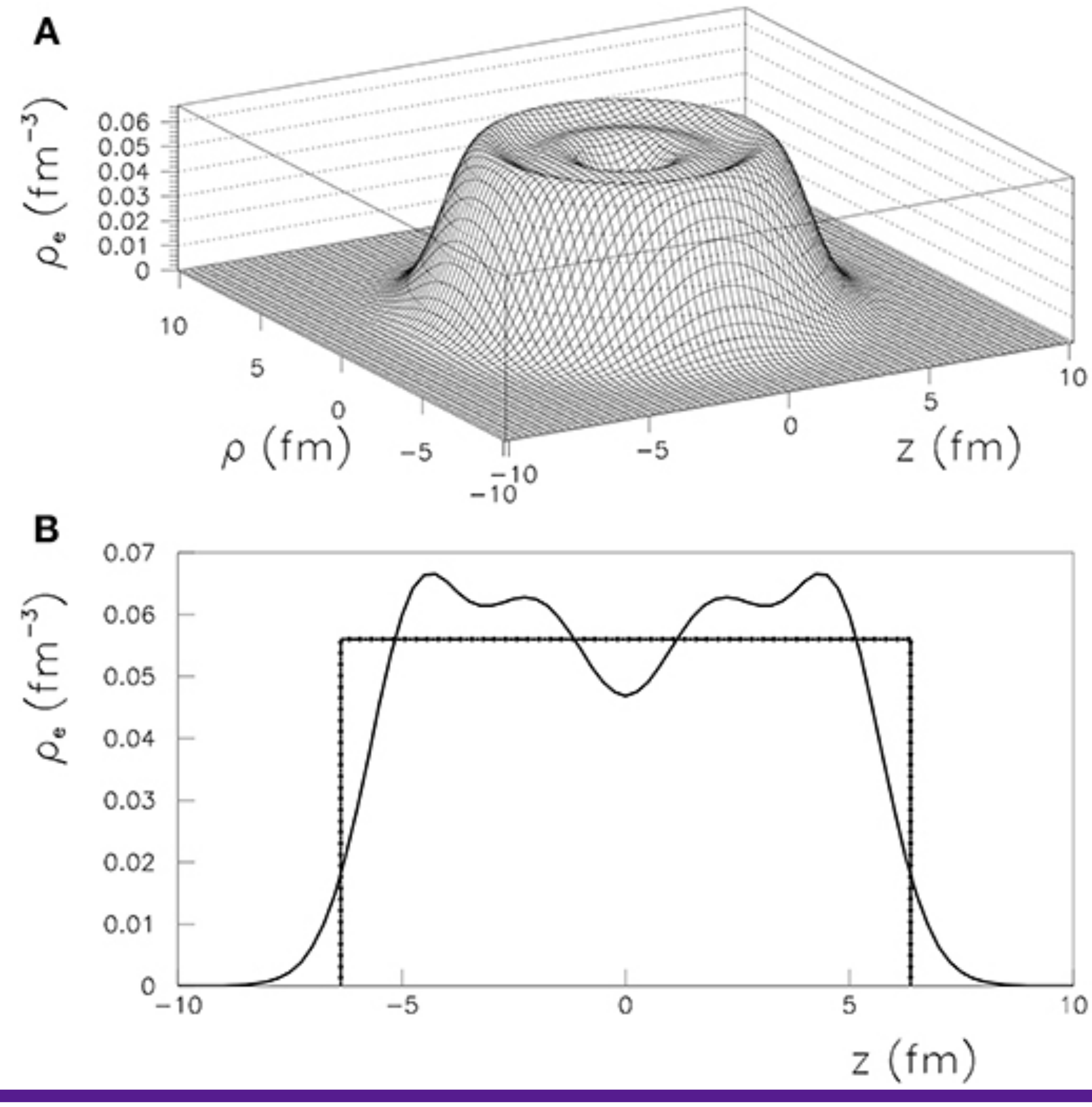

Phase space factor cheat sheet

Nucleus	Z	$Q_{\beta\beta}$	$G_{0\nu}$ (10^{-15} yr^{-1}): various models					
^{48}Ca	20	4.267	24.65	24.81	26.1	26	24.83	24.55
^{150}Nd	60	3.371	61.94	63.03	85.9	78.4	63.16	66
^{100}Mo	42	3.034	15.84	15.92	18.7	? 45.6 ?	15.95	15.74
^{82}Se	34	2.996	10.14	10.16	11.4	11.1	10.18	9.96
^{130}Te	52	2.528	14.24	14.22	19.4	16.7	14.25	14.1
^{136}Xe	54	2.458	14.54	14.58	19.4	17.7	14.62	14.49
^{76}Ge	32	2.039	2.372	2.363	2.62	2.55	2.37	2.28

Adapted from DOI: 10.3389/fphy.2019.00012

$G_{0\nu}$ increases strongly with $Q_{\beta\beta}$

$$T^{0\nu}_{1/2} \propto Q^{-5}_{\beta\beta}$$

Also depends on Z, nuclear radius (~$A^{1/3}$), charge density

Relatively little variation between models

g_A quenching

0vββ rate $$\frac{1}{T_{1/2}^{0\nu\beta\beta}} = G_{0\nu}(Q_{\beta\beta}, Z) g_A^4 |M_{0\nu}|^2 \frac{\langle m_{\beta\beta}\rangle^2}{m_e^2}$$

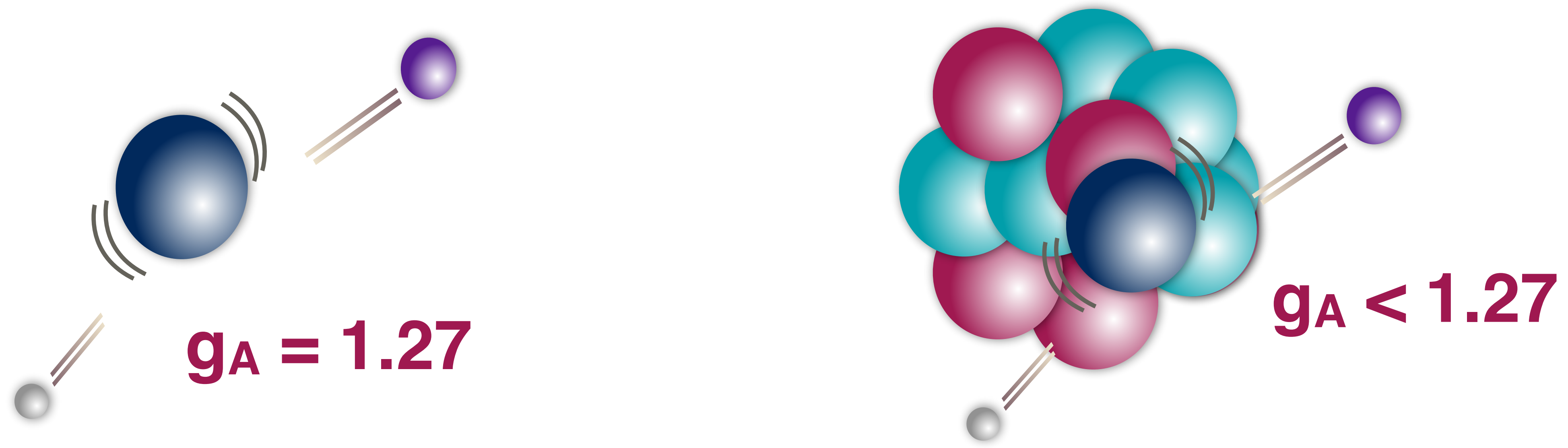

Quenching effect of the **axial vector coupling** for heavy nuclei has been observed for 2νββ and β-decay…

g_A quenching

0νββ rate $\frac{1}{T^{0\nu\beta\beta}_{1/2}} = G_{0\nu}(Q_{\beta\beta}, Z) g_A^4 |M_{0\nu}|^2 \frac{\langle m_{\beta\beta}\rangle^2}{m_e^2}$

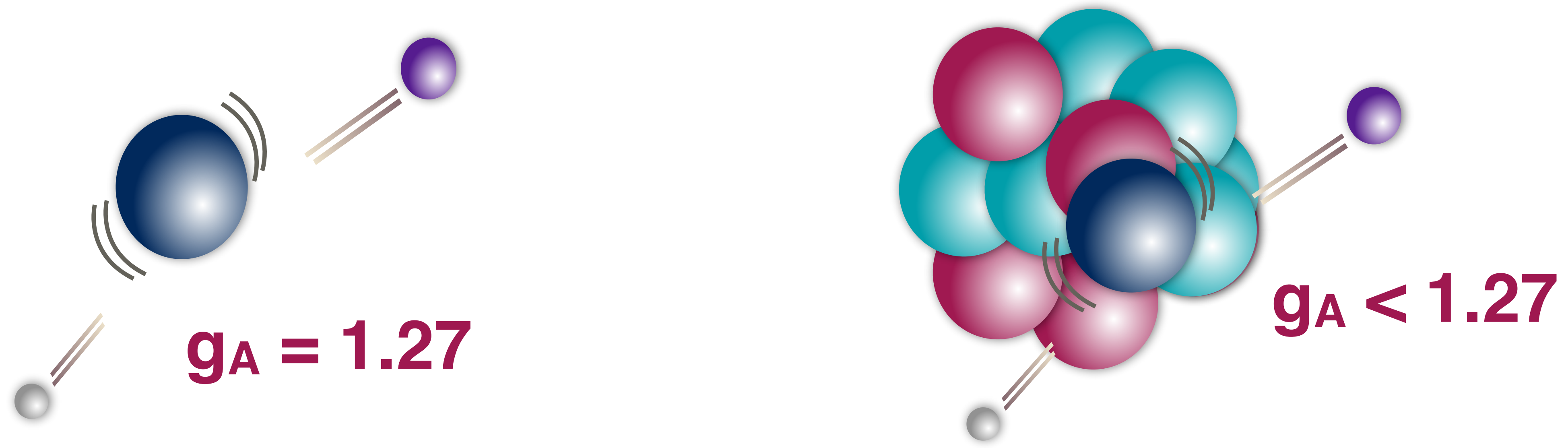

Quenching effect of the **axial vector coupling** for heavy nuclei has been observed for 2νββ and β-decay…

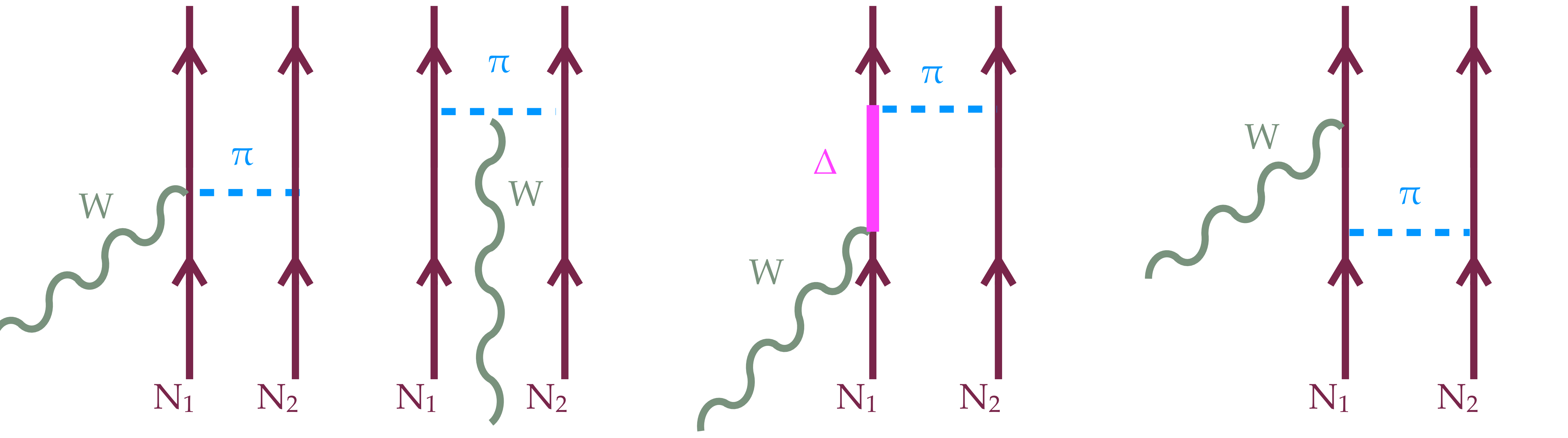

Contact/pion-in-flight *Δ-meson exchange current* *Correlation*

...due to **multi-nucleon effects** like meson-exchange currents

g_A quenching

0νββ rate $\frac{1}{T_{1/2}^{0\nu\beta\beta}} = G_{0\nu}(Q_{\beta\beta}, Z) g_A^4 |M_{0\nu}|^2 \frac{\langle m_{\beta\beta}\rangle^2}{m_e^2}$

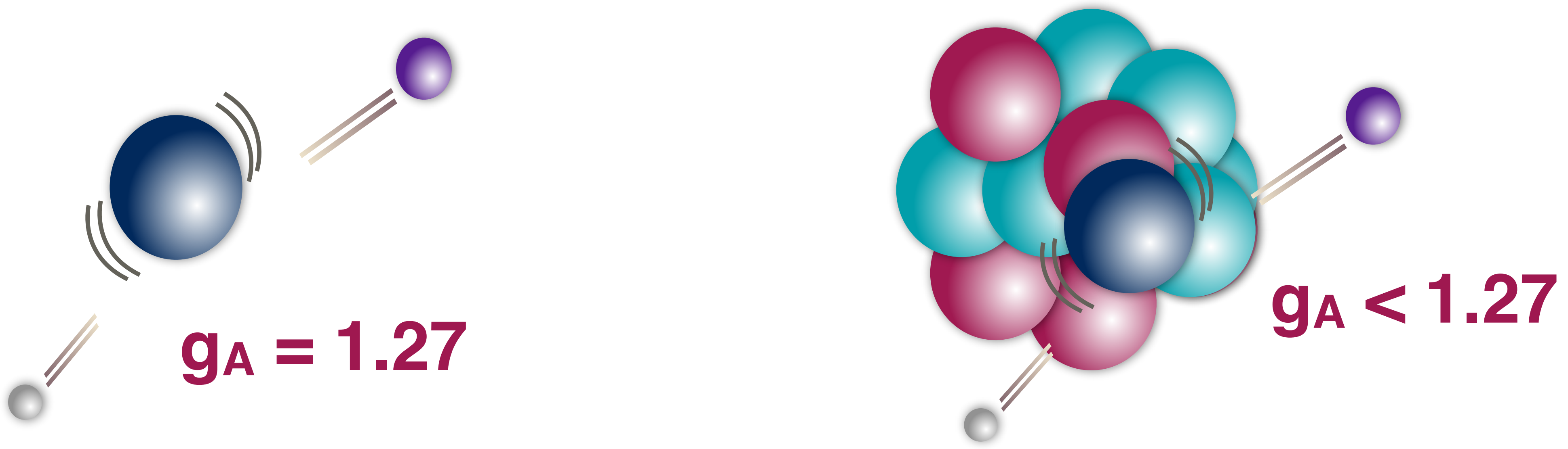

Quenching effect of the **axial vector coupling** for heavy nuclei has been observed for 2νββ and β-decay…

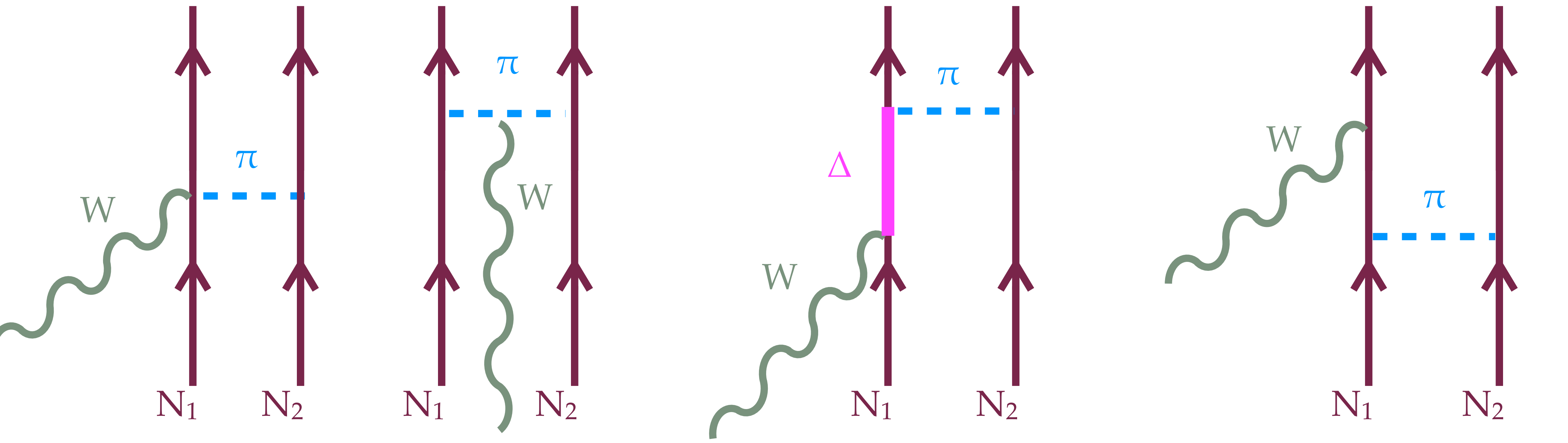

Contact/pion-in-flight *Δ-meson exchange current* *Correlation*

...due to **multi-nucleon effects** like meson-exchange currents

2νββ experiments can help set **limits**

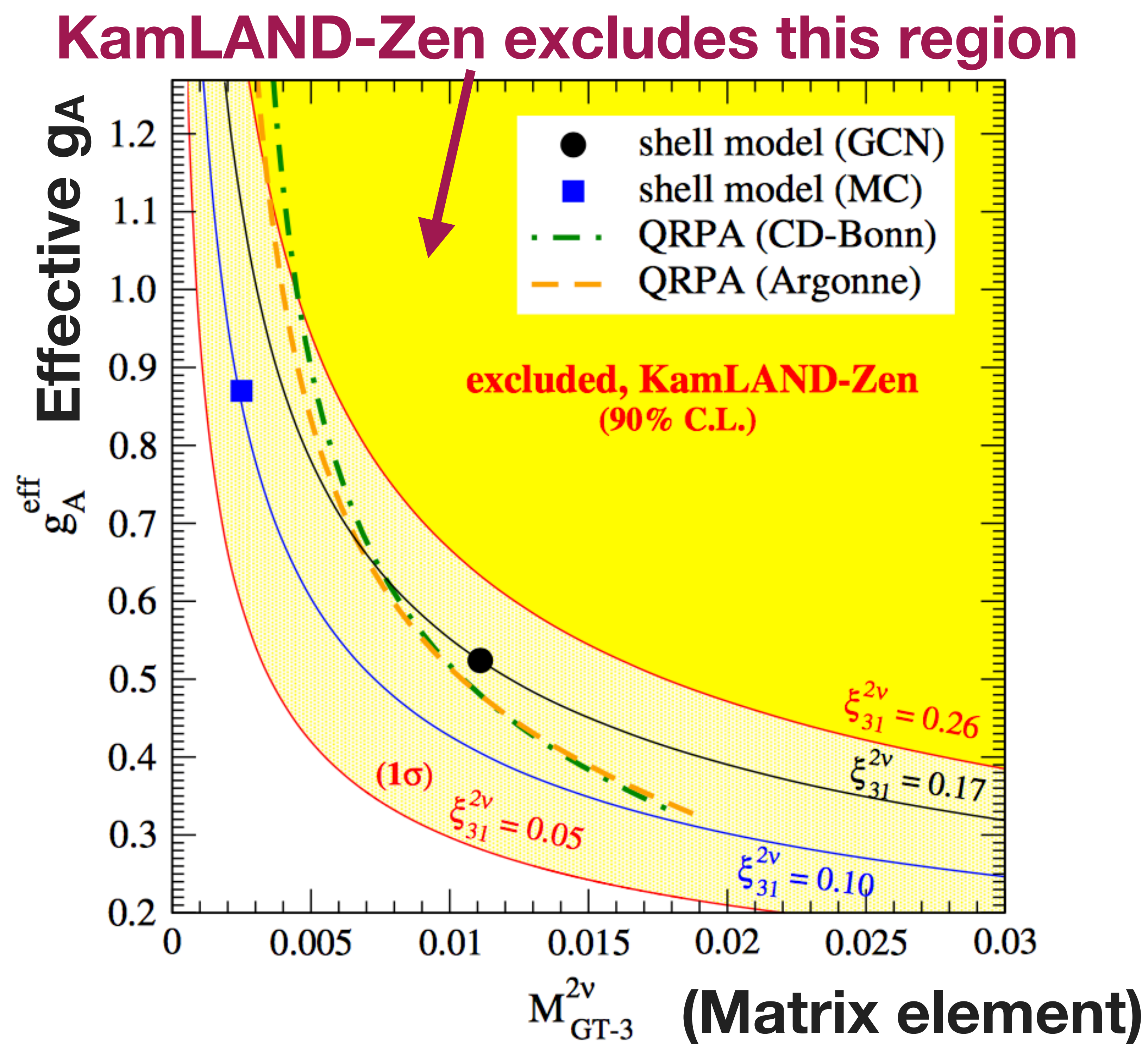

gA quenching

0νββ rate $\frac{1}{T_{1/2}^{0\nu\beta\beta}} = G_{0\nu}(Q_{\beta\beta}, Z) g_A^4 |M_{0\nu}|^2 \frac{\langle m_{\beta\beta}\rangle^2}{m_e^2}$

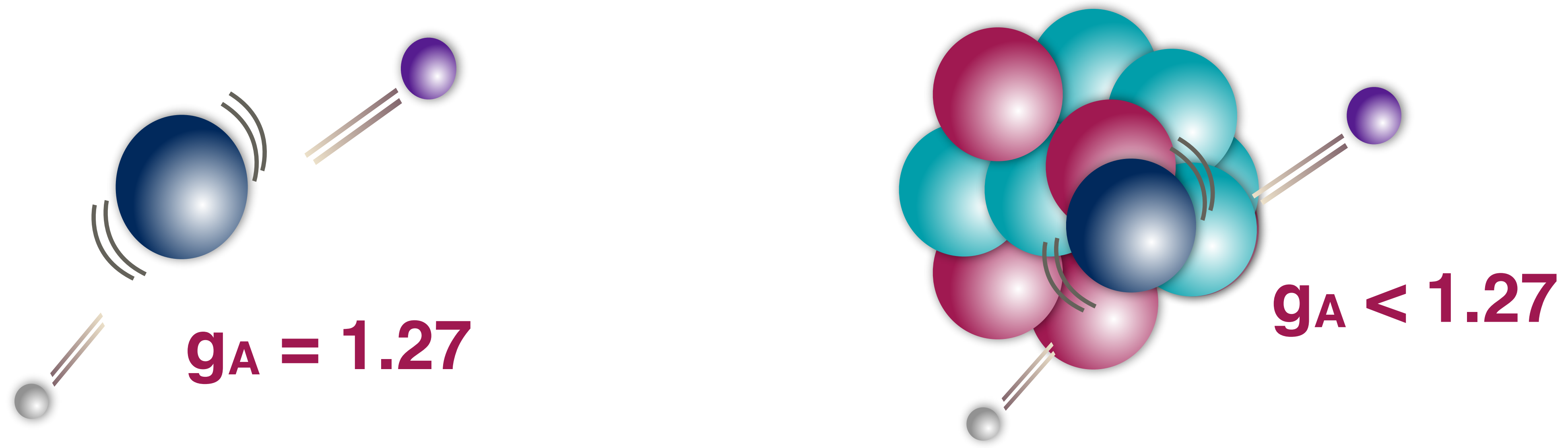

Quenching effect of the **axial vector coupling** for heavy nuclei has been observed for 2νββ and β-decay…

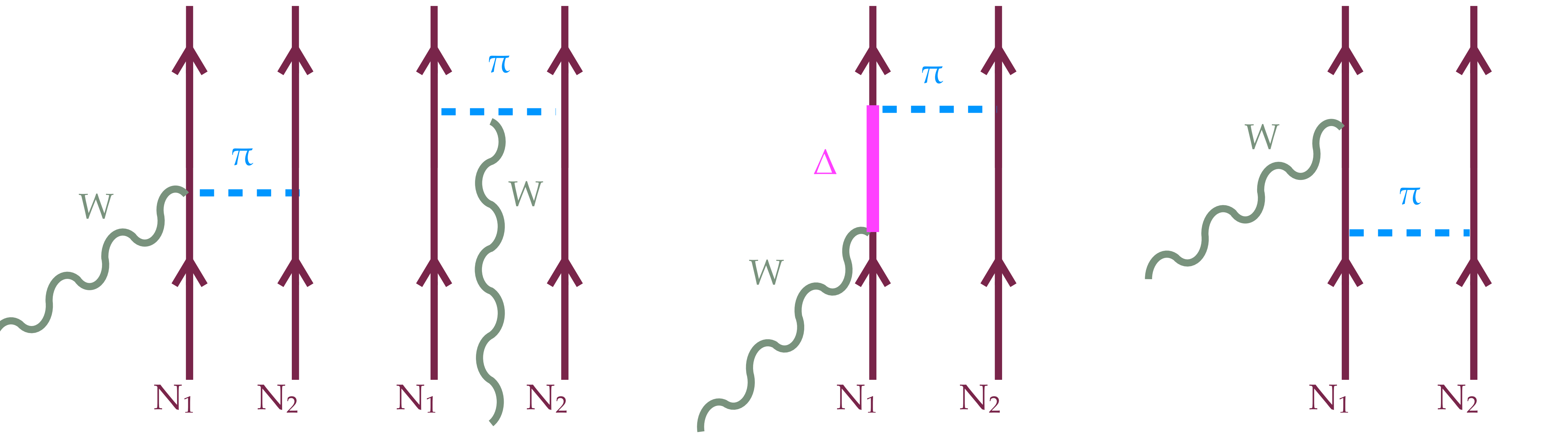

Contact/pion-in-flight *Δ-meson exchange current* *Correlation*

...due to **multi-nucleon effects** like meson-exchange currents

2νββ experiments can help set **limits**

KamLAND-Zen excludes this region

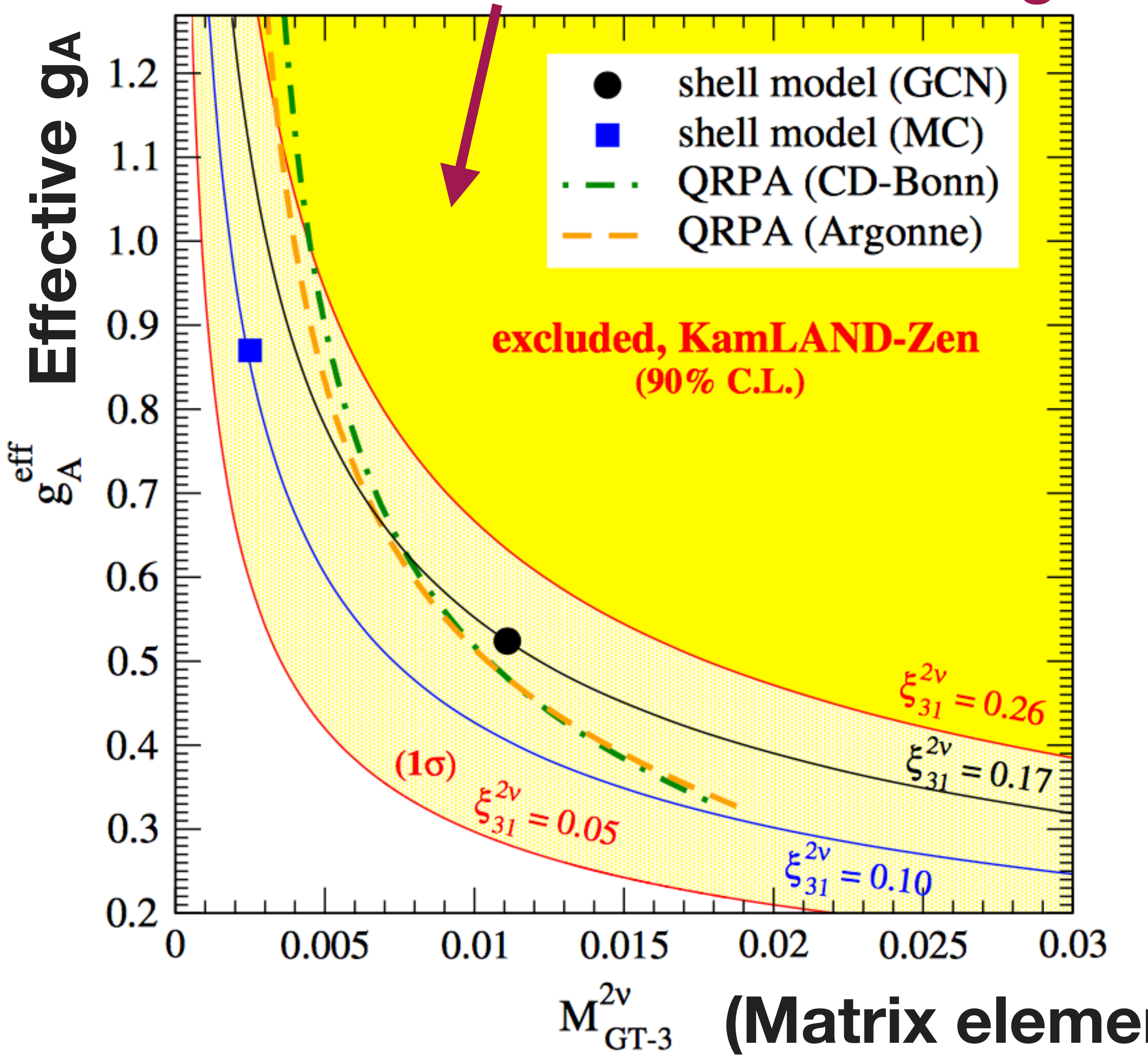

nature physics

Discrepancy between experimental and theoretical β-decay rates resolved from first principles

New *ab initio* calculations can **model** these effects in the **nuclear matrix element**

Nature Physics volume 15, pages 428–431 (2019)

Nuclear matrix elements in very little detail

0νββ rate $$\frac{1}{T_{1/2}^{0\nu\beta\beta}} = G_{0\nu}(Q_{\beta\beta}, Z) g_A^4 |M_{0\nu}|^2 \frac{\langle m_{\beta\beta}\rangle^2}{m_e^2}$$

- Describe the **nuclear structure effects** of the parent, daughter and intermediate nuclei
- Different NMEs correspond to **2νββ (testable)** and each **0νββ mechanism**
- Some prescriptions include **g_A** dependence in the NME calculation
- **Biggest uncertainty in $m_{\beta\beta}$ calculation**

Rept.Prog. Phys. 80, 046301 (2017)

Nuclear matrix elements in very little detail

UCL

0νββ rate $$\frac{1}{T_{1/2}^{0\nu\beta\beta}} = G_{0\nu}(Q_{\beta\beta}, Z) g_A^4 |M_{0\nu}|^2 \frac{\langle m_{\beta\beta} \rangle^2}{m_e^2}$$

- Describe the **nuclear structure effects** of the parent, daughter and intermediate nuclei
- Different NMEs correspond to **2vββ (testable)** and each **0vββ mechanism**
- Some prescriptions include **g_A** dependence in the NME calculation
- **Biggest uncertainty in $m_{\beta\beta}$ calculation**

$$M_{0\nu} = M_{0\nu}^{GT} - \frac{g_V^2}{g_A^2} M_{0\nu}^{F} + M_{0\nu}^{T}$$

Gamow-Teller **Fermi** **Tensor**

g_A again!

electron spins parallel

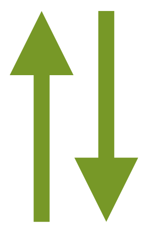

electron spins anti-parallel

Rept.Prog. Phys. 80, 046301 (2017)

Nuclear matrix elements in very little detail

0νββ rate $\frac{1}{T^{0\nu\beta\beta}_{1/2}} = G_{0\nu}(Q_{\beta\beta}, Z) g_A^4 |M_{0\nu}|^2 \frac{\langle m_{\beta\beta}\rangle^2}{m_e^2}$

- Describe the **nuclear structure effects** of the parent, daughter and intermediate nuclei
- Different NMEs correspond to **2νββ (testable)** and each **0νββ mechanism**
- Some prescriptions include **g_A** dependence in the NME calculation
- **Biggest uncertainty in $m_{\beta\beta}$ calculation**

$$M_{0\nu} = M^{GT}_{0\nu} - \frac{g_V^2}{g_A^2} M^F_{0\nu} + M^T_{0\nu}$$

Gamow-Teller — electron spins parallel

g_A again!

Fermi — electron spins anti-parallel

Tensor

Spherical Bessel functions

Inter-nucleon position

Neutrino potential

Operators act on nuclear states

$$M^{GT}_{0\nu} = \frac{2R}{\pi g_A^2} \int_0^\infty |\boldsymbol{q}|\, d|\boldsymbol{q}|\, \langle f| \sum_{a,b} \frac{j_0(|\boldsymbol{q}|r_{ab}) h_{GT}(|\boldsymbol{q}|) \boldsymbol{\sigma}_a \cdot \boldsymbol{\sigma}_b}{|\boldsymbol{q}| + \overline{E} - (E_i + E_f)/2} \tau_a^+ \tau_b^+ |i\rangle\,,$$

$$M^{F}_{0\nu} = \frac{2R}{\pi g_A^2} \int_0^\infty |\boldsymbol{q}|\, d|\boldsymbol{q}|\, \langle f| \sum_{a,b} \frac{j_0(|\boldsymbol{q}|r_{ab}) h_{F}(|\boldsymbol{q}|)}{|\boldsymbol{q}| + \overline{E} - (E_i + E_f)/2} \tau_a^+ \tau_b^+ |i\rangle\,,$$

$$M^{T}_{0\nu} = \frac{2R}{\pi g_A^2} \int_0^\infty |\boldsymbol{q}|\, d|\boldsymbol{q}|\, \langle f| \sum_{a,b} \frac{j_2(|\boldsymbol{q}|r_{ab}) h_{T}(|\boldsymbol{q}|)\, [3\boldsymbol{\sigma}_j \cdot \hat{\boldsymbol{r}}_{ab} \boldsymbol{\sigma}_k \cdot \hat{\boldsymbol{r}}_{ab} - \boldsymbol{\sigma}_a \cdot \boldsymbol{\sigma}_b]}{|\boldsymbol{q}| + \overline{E} - (E_i + E_f)/2} \tau_a^+ \tau_b^+ |i\rangle$$

Rept.Prog. Phys. 80, 046301 (2017)

Nuclear matrix elements in very little detail

0νββ rate $\frac{1}{T_{1/2}^{0\nu\beta\beta}} = G_{0\nu}(Q_{\beta\beta}, Z) g_A^4 |M_{0\nu}|^2 \frac{\langle m_{\beta\beta}\rangle^2}{m_e^2}$

- Describe the **nuclear structure effects** of the parent, daughter and intermediate nuclei
- Different NMEs correspond to **2vββ (testable)** and each **0vββ mechanism**
- Some prescriptions include **g_A** dependence in the NME calculation
- **Biggest uncertainty in $m_{\beta\beta}$ calculation**

$$M_{0\nu} = M_{0\nu}^{GT} - \frac{g_V^2}{g_A^2} M_{0\nu}^F + M_{0\nu}^T$$

Gamow-Teller — electron spins parallel

g_A again!

Fermi — electron spins anti-parallel

Tensor

Spherical Bessel functions

Inter-nucleon position

Neutrino potential

Operators act on nuclear states

$$M_{0\nu}^{GT} = \frac{2R}{\pi g_A^2}\int_0^\infty |\boldsymbol{q}|\, d|\boldsymbol{q}|\, \langle f| \sum_{a,b} \frac{j_0(|\boldsymbol{q}|r_{ab}) h_{GT}(|\boldsymbol{q}|)\boldsymbol{\sigma}_a \cdot \boldsymbol{\sigma}_b}{|\boldsymbol{q}| + \overline{E} - (E_i + E_f)/2} \tau_a^+ \tau_b^+ |i\rangle ,$$

$$M_{0\nu}^{F} = \frac{2R}{\pi g_A^2}\int_0^\infty |\boldsymbol{q}|\, d|\boldsymbol{q}|\, \langle f| \sum_{a,b} \frac{j_0(|\boldsymbol{q}|r_{ab}) h_{F}(|\boldsymbol{q}|)}{|\boldsymbol{q}| + \overline{E} - (E_i + E_f)/2} \tau_a^+ \tau_b^+ \ldots$$

$$M_{0\nu}^{T} = \frac{2R}{\pi g_A^2}\int_0^\infty |\boldsymbol{q}|\, d|\boldsymbol{q}|\, \langle f| \sum_{a,b} \frac{j_2(|\boldsymbol{q}|r_{ab}) h_{T}(|\boldsymbol{q}|)\,[3\boldsymbol{\sigma}_j \cdot \hat{\boldsymbol{r}}_{ab} \ldots}{|\boldsymbol{q}| + \overline{E} - (E \ldots} \ldots \tau_a^+ \tau_b^+ |i\rangle$$

Rept.Prog. Phys. 80, 046301 (2017)

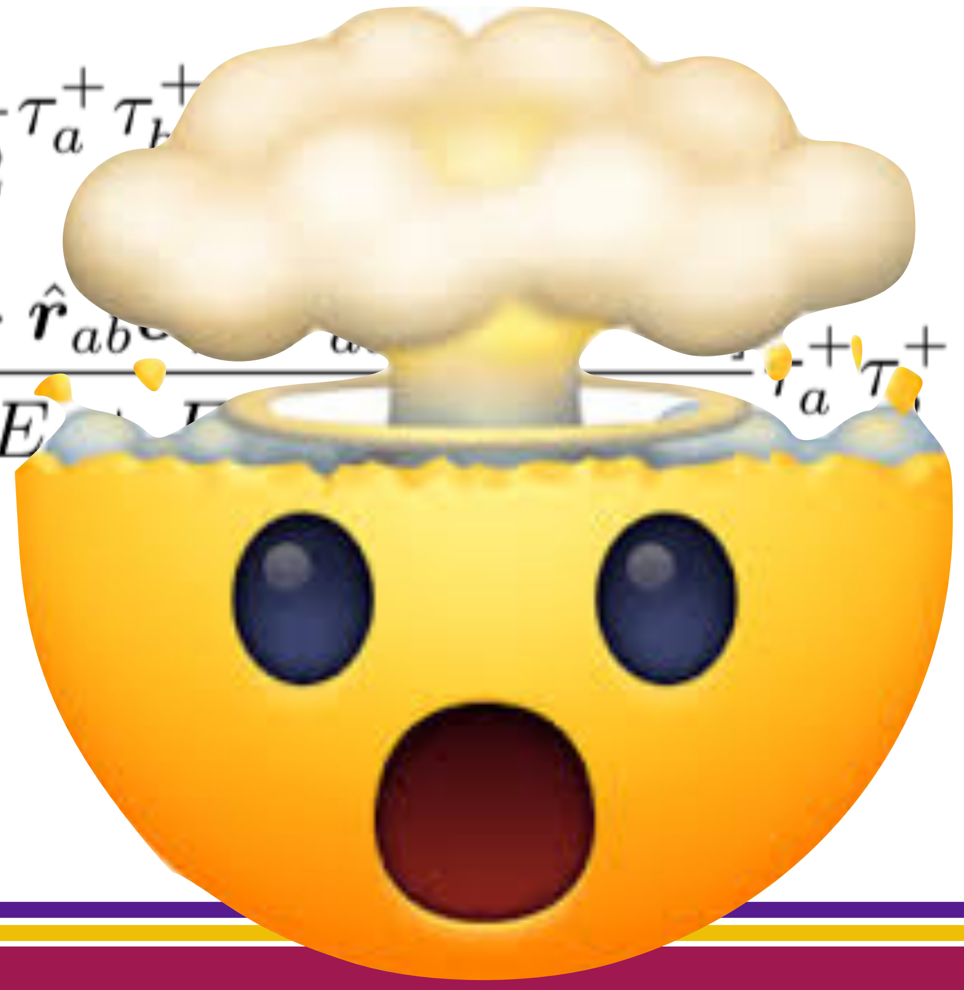

Two approaches: both difficult

QRPA: Quasi-particle Random Phase Approximation	NSM: Nuclear Shell Model

Ann.Rev.Nucl.Part.Sci.52:115-151,2002

Two approaches: both difficult

QRPA: Quasi-particle Random Phase Approximation

Most popular method, relying on **small deviations** from ground state, and modeling two main ingredients:

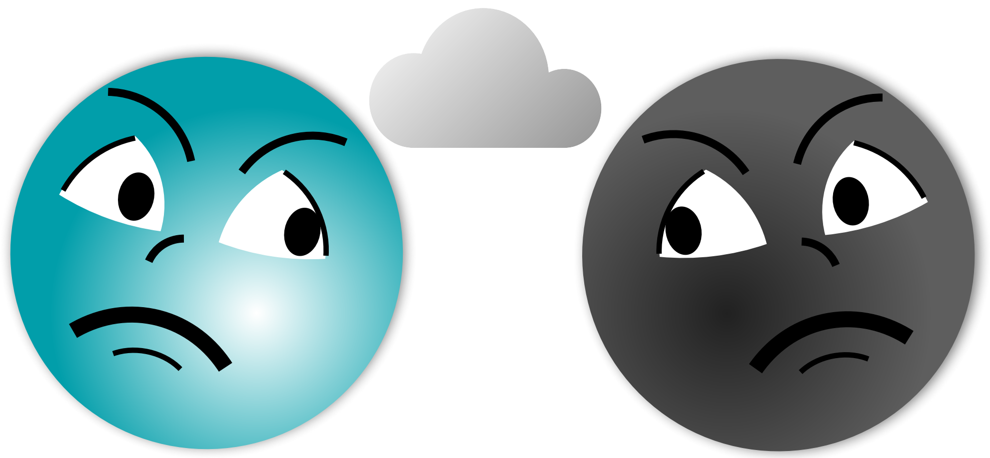

Repulsive particle-hole spin-isospin interaction

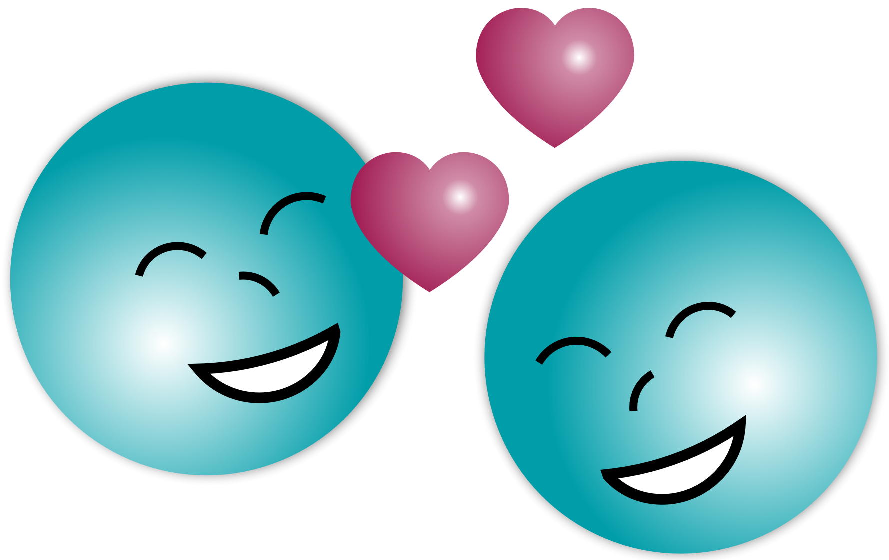

Attractive particle-particle interaction

NSM: Nuclear Shell Model

Ann.Rev.Nucl.Part.Sci.52:115-151,2002

Two approaches: both difficult

QRPA: Quasi-particle Random Phase Approximation

Most popular method, relying on **small deviations** from ground state, and modeling two main ingredients:

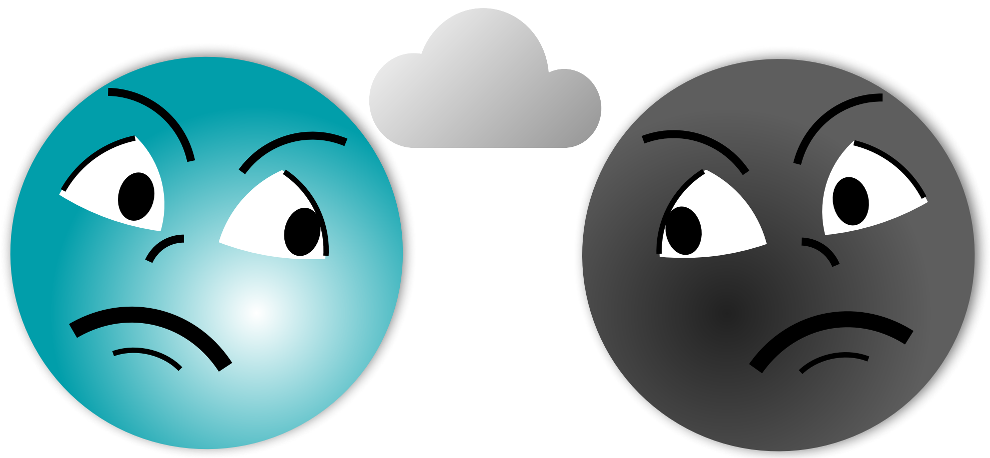

Repulsive particle-hole spin-isospin interaction

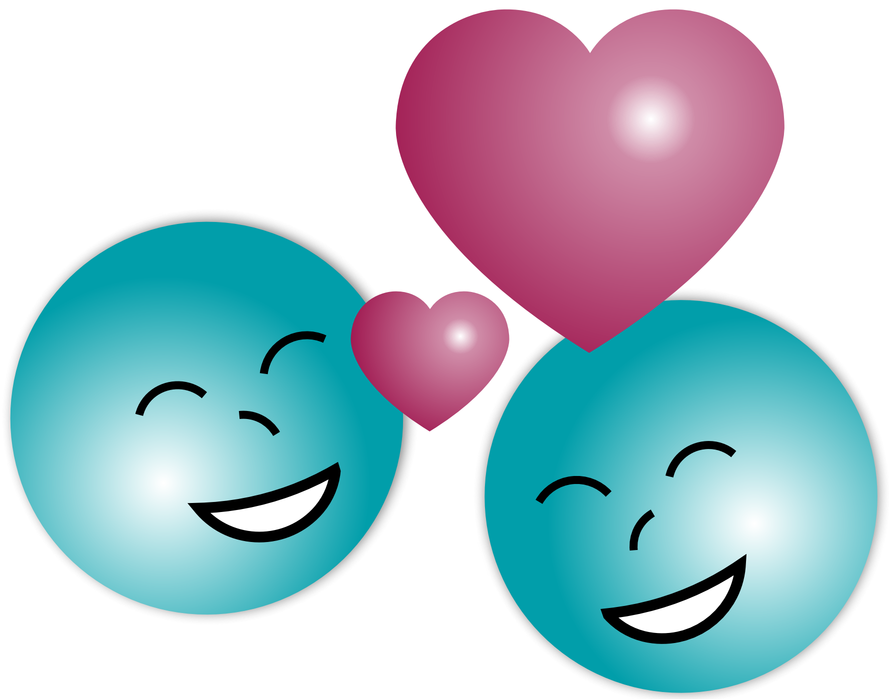

Attractive particle-particle interaction

But requires adjusting **strength** of particle-particle interaction (measurable in 2νββ):

NSM: Nuclear Shell Model

Ann.Rev.Nucl.Part.Sci.52:115-151,2002

Two approaches: both difficult

QRPA: Quasi-particle Random Phase Approximation	NSM: Nuclear Shell Model

Most popular method, relying on **small deviations** from ground state, and modeling two main ingredients:

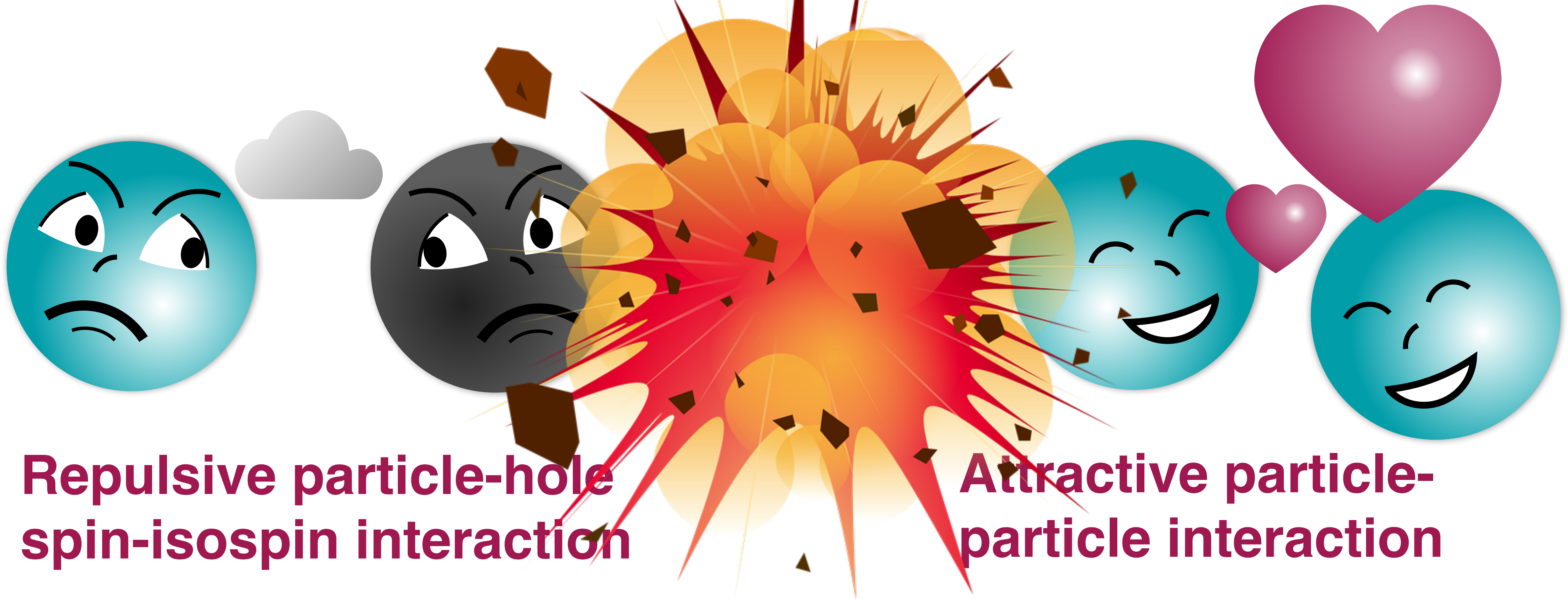

Repulsive particle-hole spin-isospin interaction

Attractive particle-particle interaction

But requires adjusting **strength** of particle-particle interaction (measurable in 2νββ): realistic values close to **collapse** of validity

Ann.Rev.Nucl.Part.Sci.52:115-151,2002

Two approaches: both difficult

QRPA: Quasi-particle Random Phase Approximation

NSM: Nuclear Shell Model

Most popular method, relying on **small deviations** from ground state, and modeling two main ingredients:

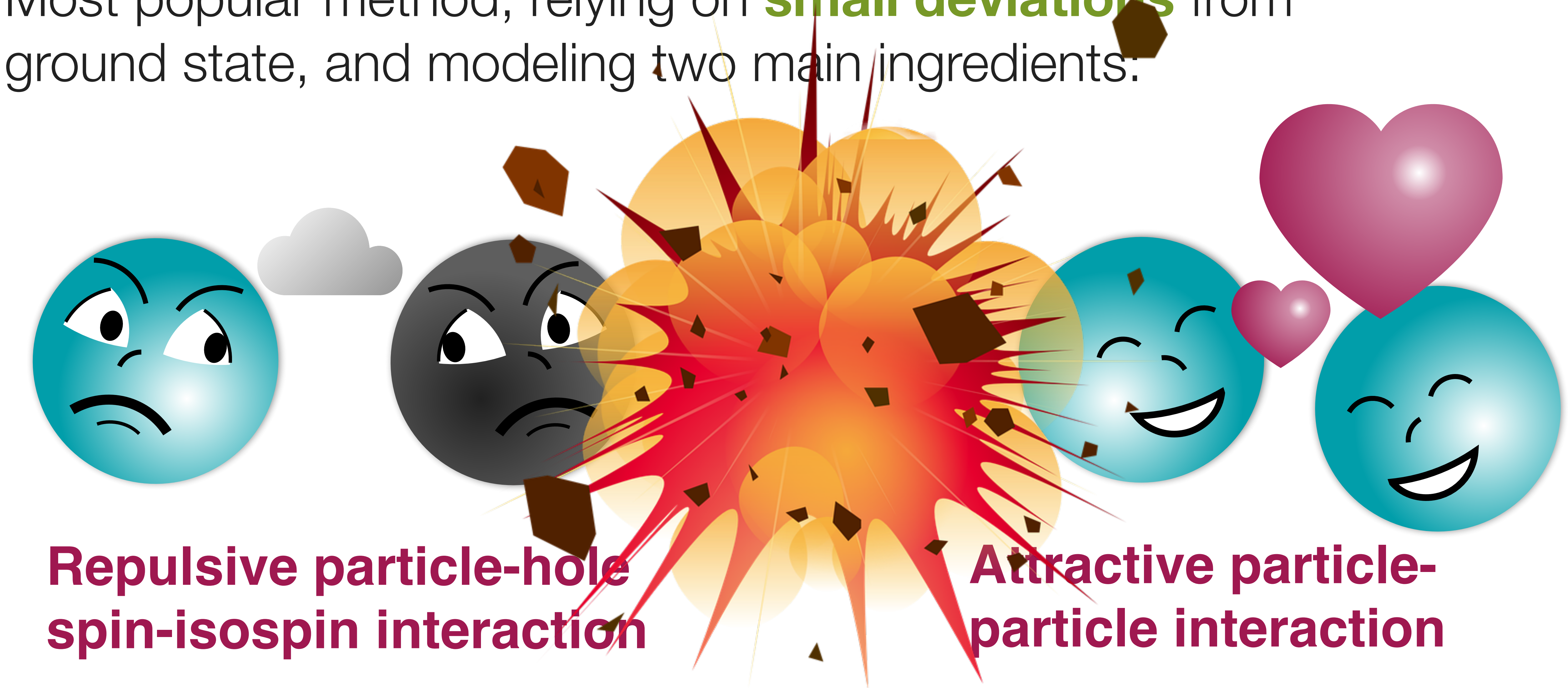

Repulsive particle-hole spin-isospin interaction

Attractive particle-particle interaction

But requires adjusting **strength** of particle-particle interaction (measurable in $2\nu\beta\beta$): realistic values close to **collapse** of validity

Basic versions don't include **multi-particle** states

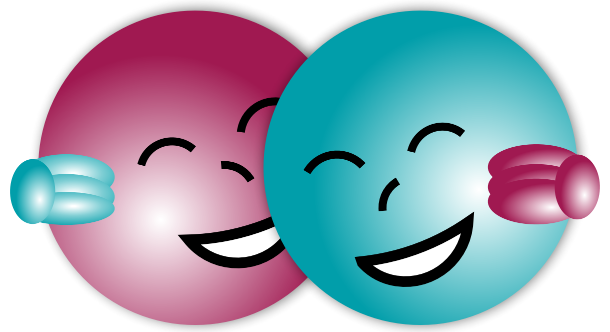

Ann.Rev.Nucl.Part.Sci.52:115-151,2002

Two approaches: both difficult

QRPA: Quasi-particle Random Phase Approximation

Most popular method, relying on **small deviations** from ground state, and modeling two main ingredients:

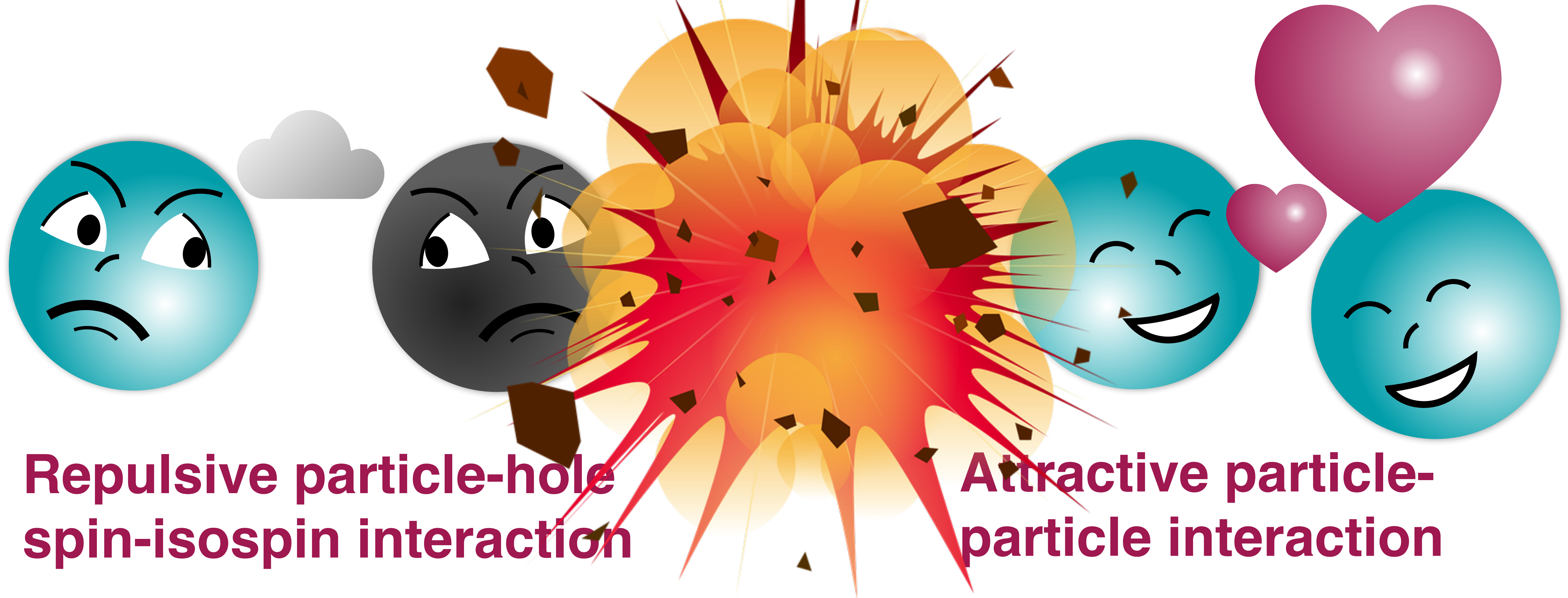

Repulsive particle-hole spin-isospin interaction

Attractive particle-particle interaction

But requires adjusting **strength** of particle-particle interaction (measurable in $2\nu\beta\beta$): realistic values close to **collapse** of validity

Basic versions don't include **multi-particle** states

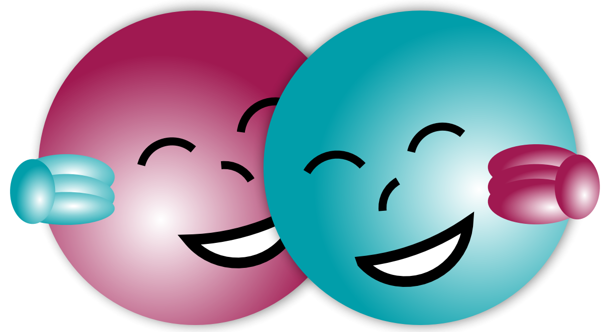

NSM: Nuclear Shell Model

Theoretically **better** method but limited by computing power for all but **lighter isotopes** (up to ^{48}Ca)

- Start from set of all **single-particle states**
- Find **effective Hamiltonian** based on modified nucleon-nucleon interaction to describe them
- Use all configurations, including **correlations** to diagonalize Hamiltonian and **extract NME**

Ann.Rev.Nucl.Part.Sci.52:115-151,2002

Two approaches: both difficult

QRPA: Quasi-particle Random Phase Approximation

Most popular method, relying on **small deviations** from ground state, and modeling two main ingredients:

Repulsive particle-hole spin-isospin interaction

Attractive particle-particle interaction

But requires adjusting **strength** of particle-particle interaction (measurable in 2νββ): realistic values close to **collapse** of validity

Basic versions don't include **multi-particle** states

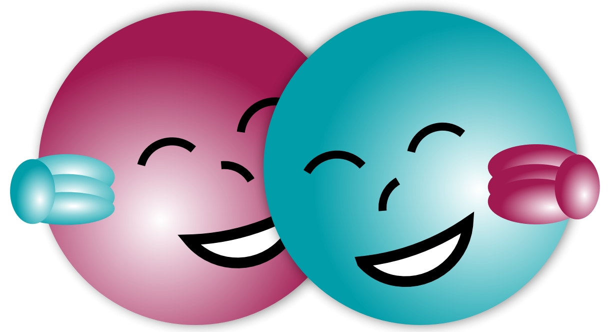

NSM: Nuclear Shell Model

Theoretically **better** method but limited by computing power for all but **lighter isotopes** (up to ^{48}Ca)

Computationally impossible - have to use a subset

- Start from set of ~~all~~ **single-particle states**
- Find **effective Hamiltonian** based on modified nucleon-nucleon interaction to describe them
- Use all configurations, including **correlations** to diagonalize Hamiltonian and **extract NME**

Ann.Rev.Nucl.Part.Sci.52:115-151,2002

Two approaches: both difficult

QRPA: Quasi-particle Random Phase Approximation

Most popular method, relying on **small deviations** from ground state, and modeling two main ingredients:

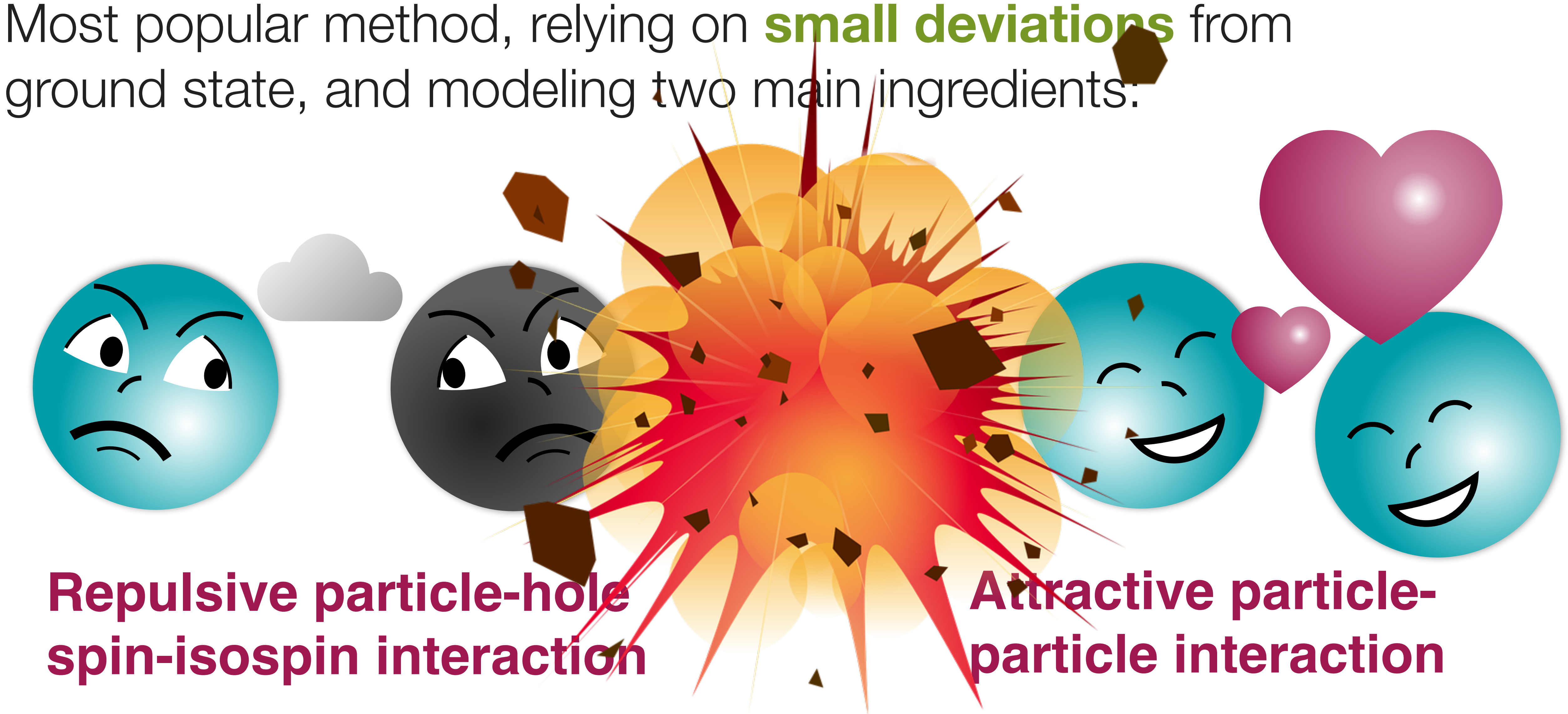

Repulsive particle-hole spin-isospin interaction

Attractive particle-particle interaction

But requires adjusting **strength** of particle-particle interaction (measurable in 2νββ): realistic values close to **collapse** of validity

Basic versions don't include **multi-particle** states

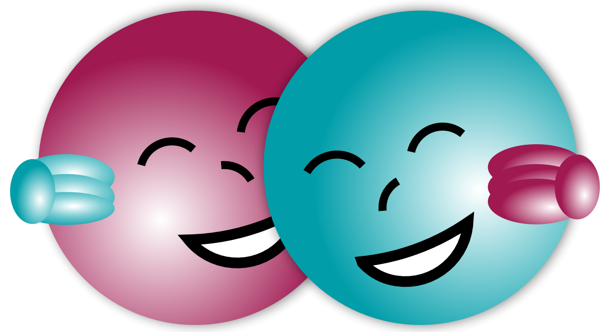

NSM: Nuclear Shell Model

Theoretically **better** method but limited by computing power for all but **lighter isotopes** (up to ^{48}Ca)

Computationally impossible - have to use a subset

- Start from set of ~~all~~ **single-particle states**
- Find **effective Hamiltonian** based on modified nucleon-nucleon interaction to describe them
- Use all configurations, including **correlations** to diagonalize Hamiltonian and **extract NME**

Not clear what effective operators will simulate the excluded states

Ann.Rev.Nucl.Part.Sci.52:115-151,2002

Different calculations give very different results

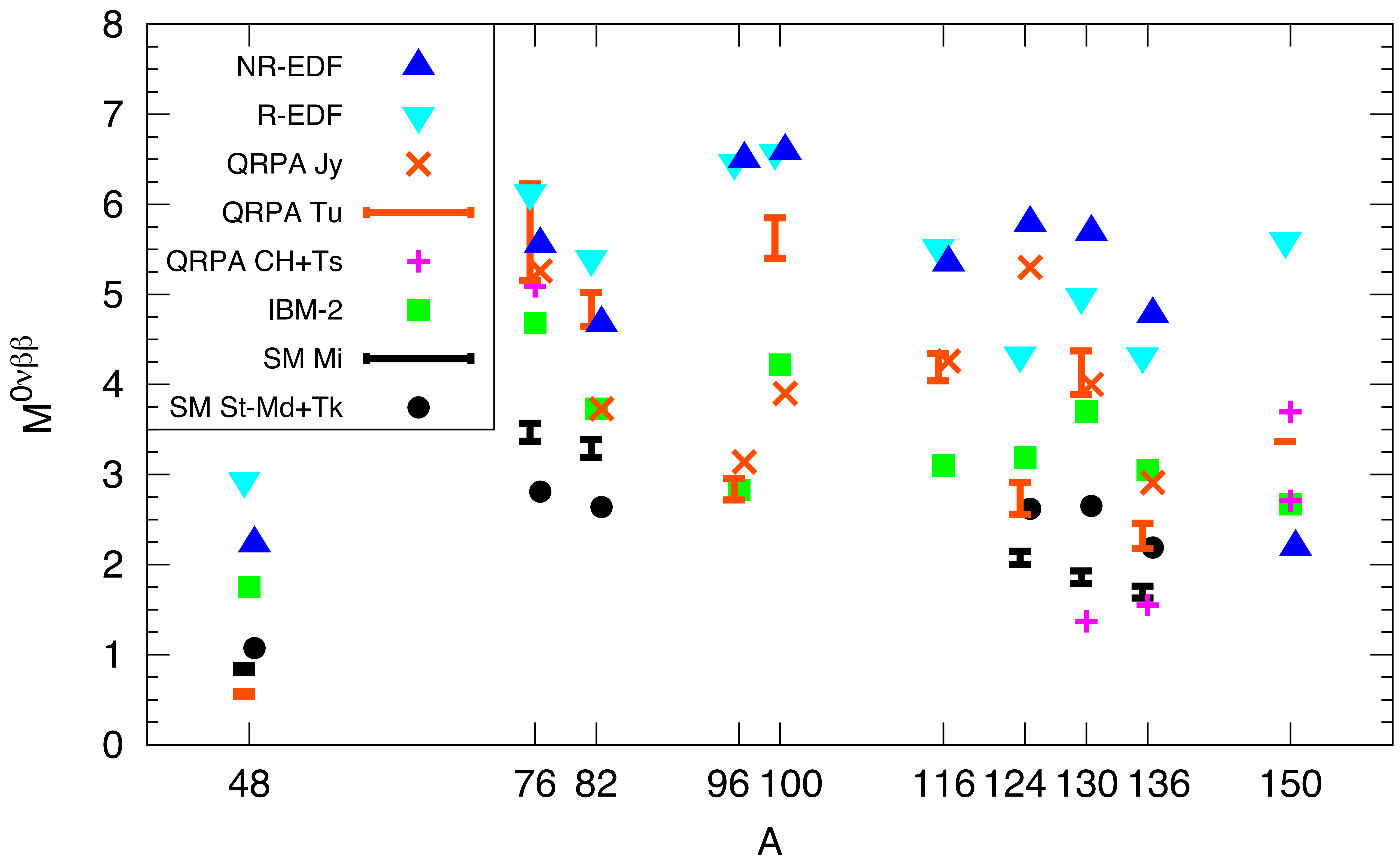

Rept.Prog. Phys. 80, 046301 (2017)

NME's calculated by various groups using:

Different calculations give very different results

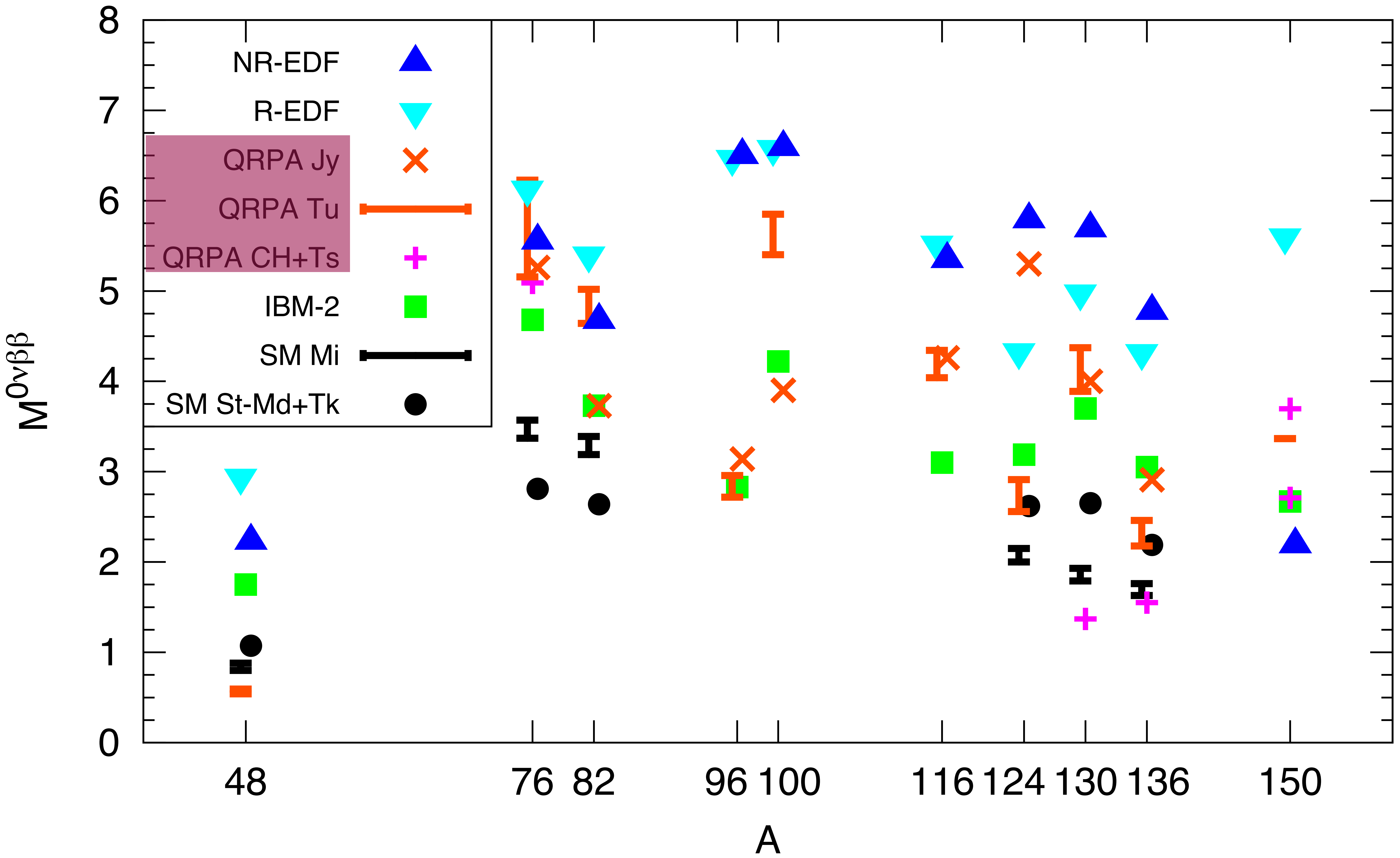

Rept.Prog. Phys. 80, 046301 (2017)

NME's calculated by various groups using:

QRPA

Different calculations give very different results

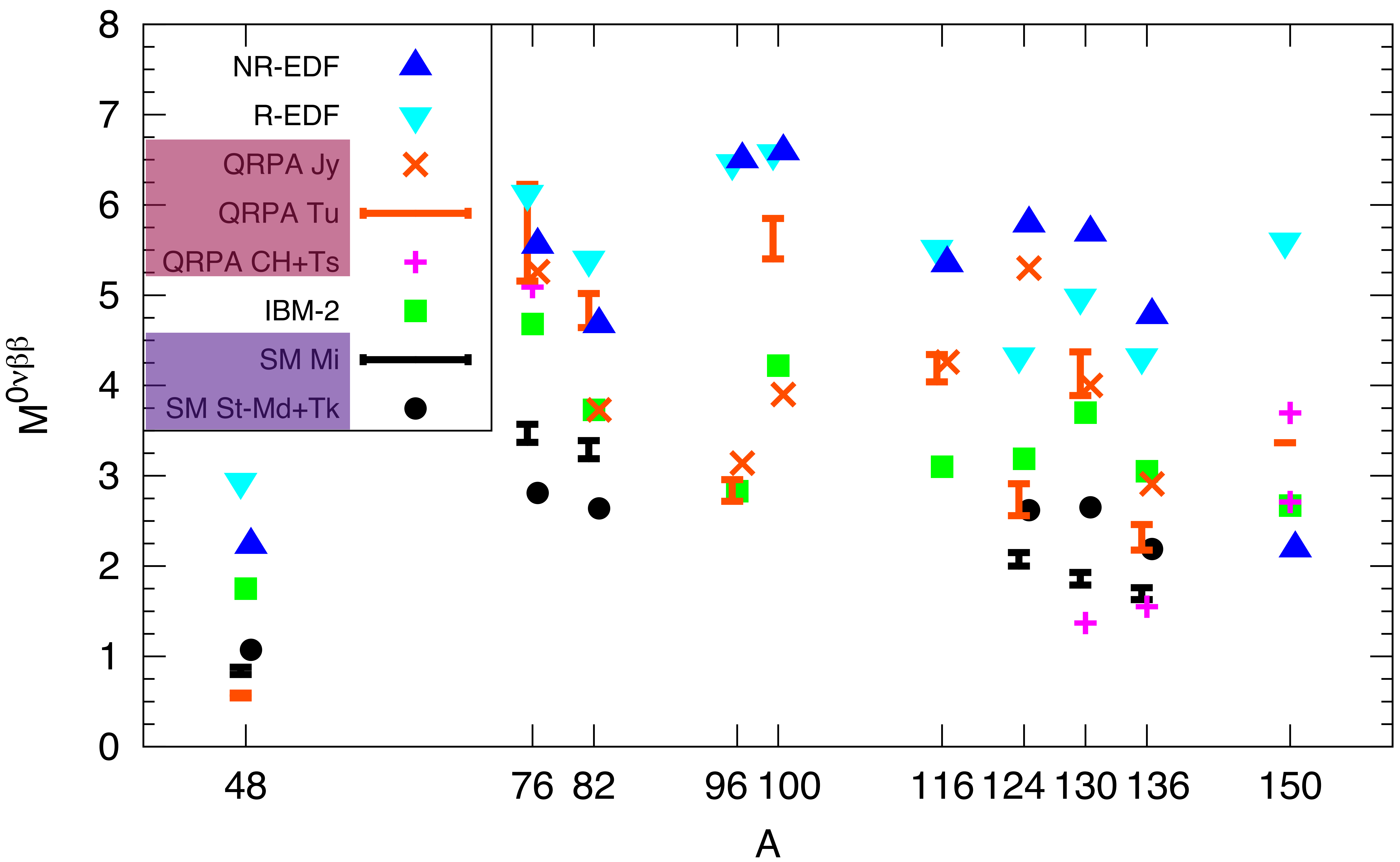

Rept.Prog. Phys. 80, 046301 (2017)

NME's calculated by various groups using:

QRPA

Shell Model

Different calculations give very different results

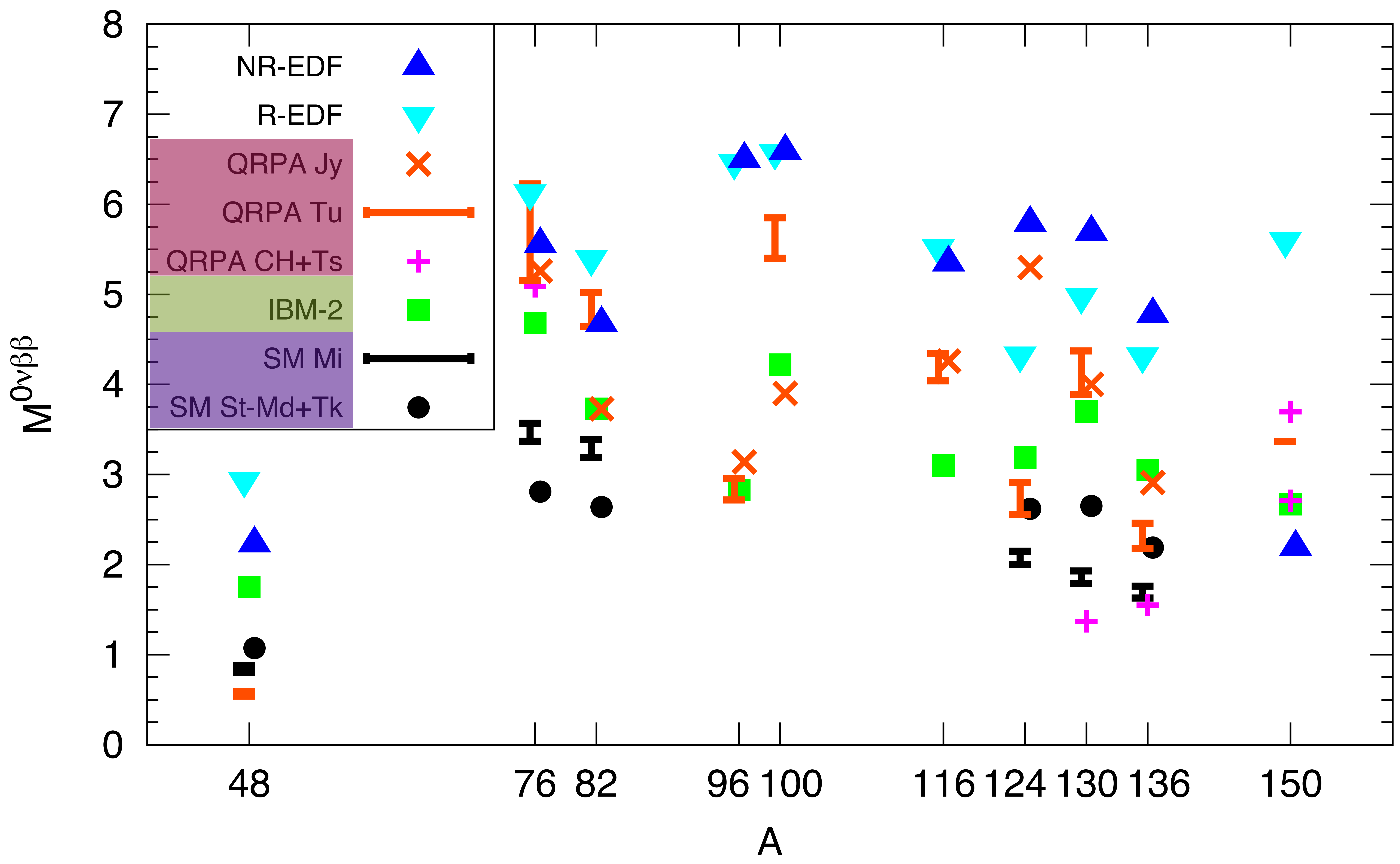

Rept.Prog. Phys. 80, 046301 (2017)

NME's calculated by various groups using:

QRPA

Shell Model

Interacting boson model

Variation on shell model that aims to describe collective excitations up to heavy nuclei, modelling low-energy states as bosons

Different calculations give very different results

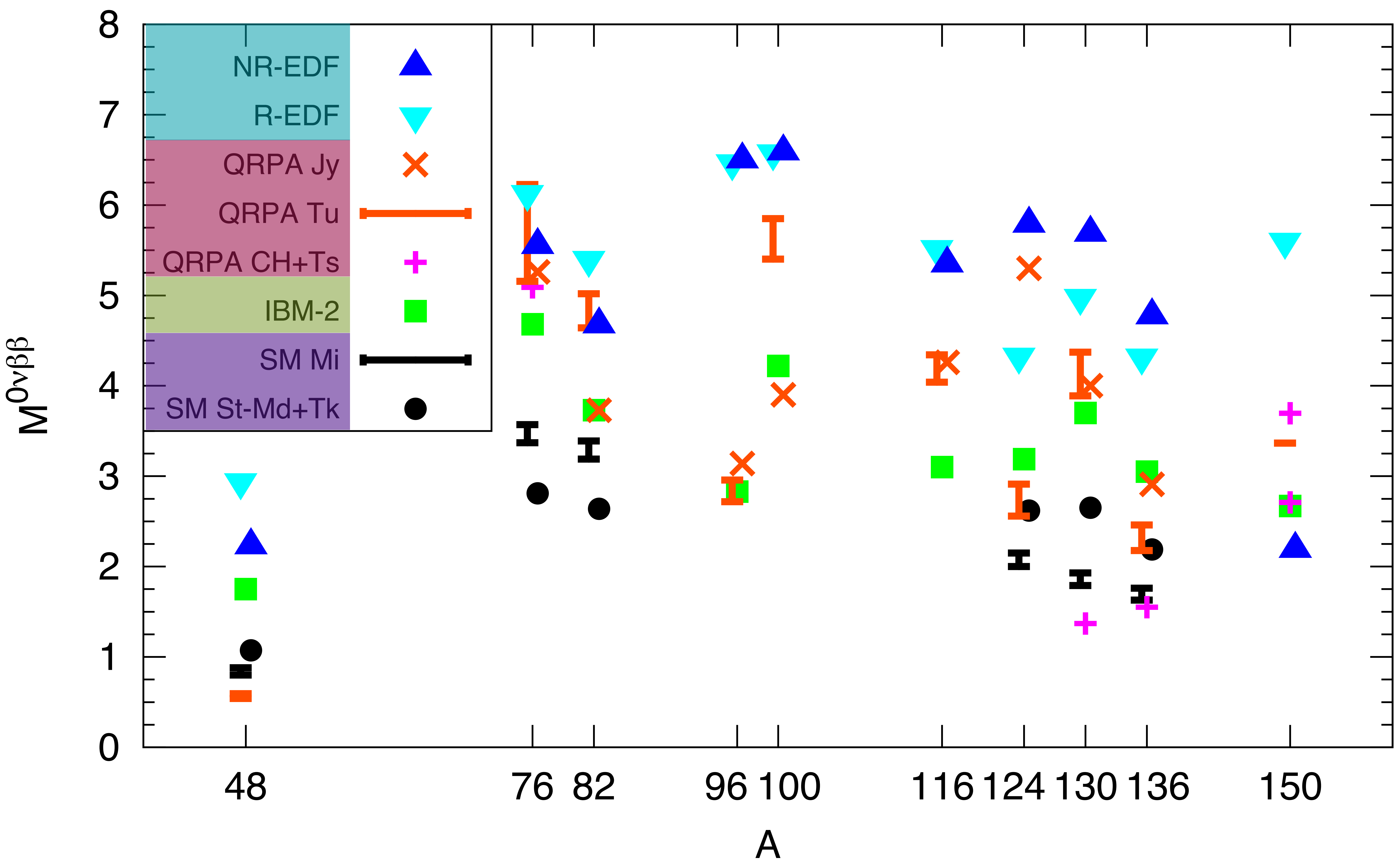

Rept.Prog. Phys. 80, 046301 (2017)

NME's calculated by various groups using:

QRPA

Shell Model

Interacting boson model

Energy density functional theory

Can be used when QRPA breaks down

Different calculations give very different results

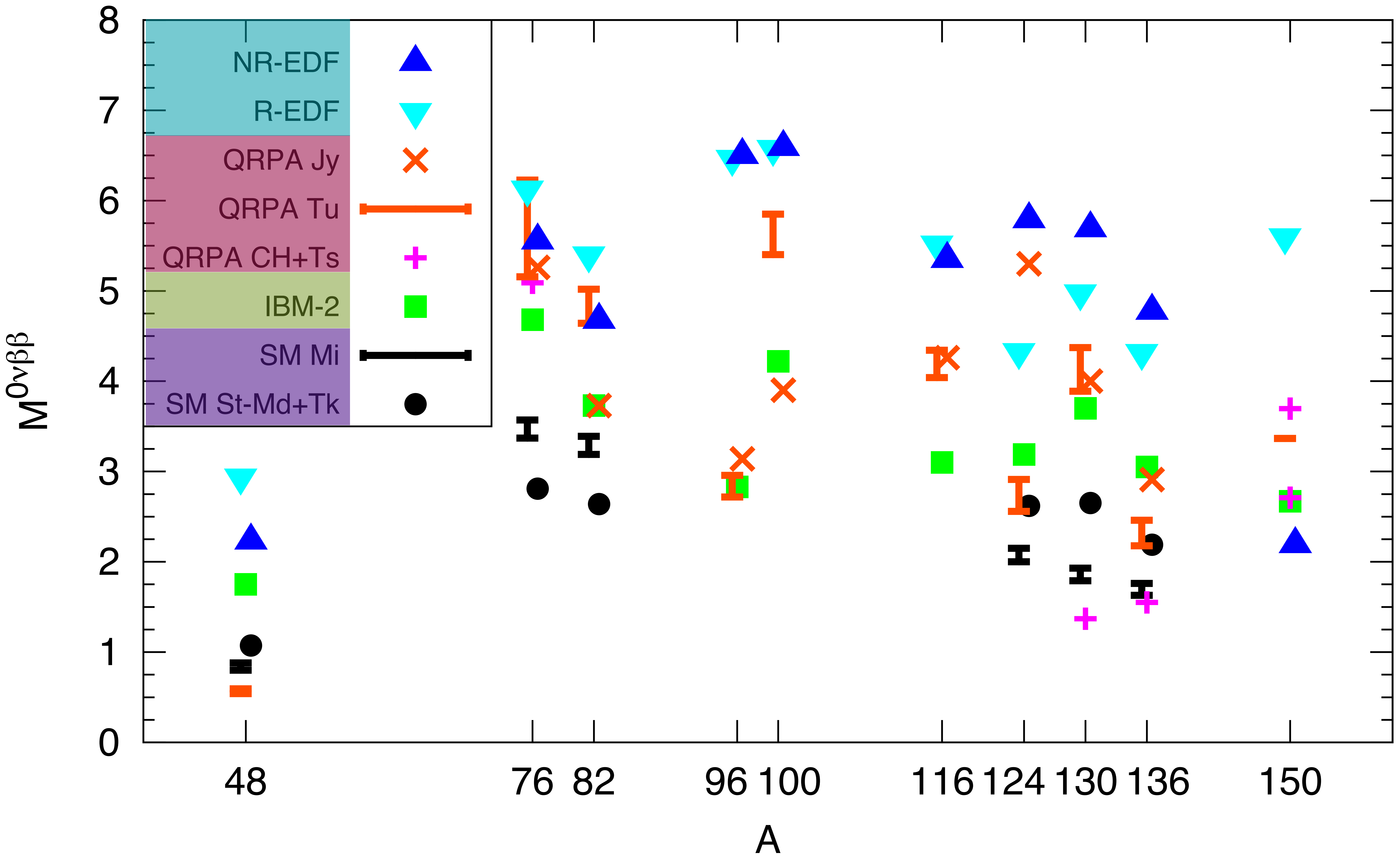

Rept.Prog. Phys. 80, 046301 (2017)

NME's calculated by various groups using:

QRPA

Shell Model

Interacting boson model

Energy density functional theory

Calculated results can vary by a factor of 3 or more

Looking for 0νββ

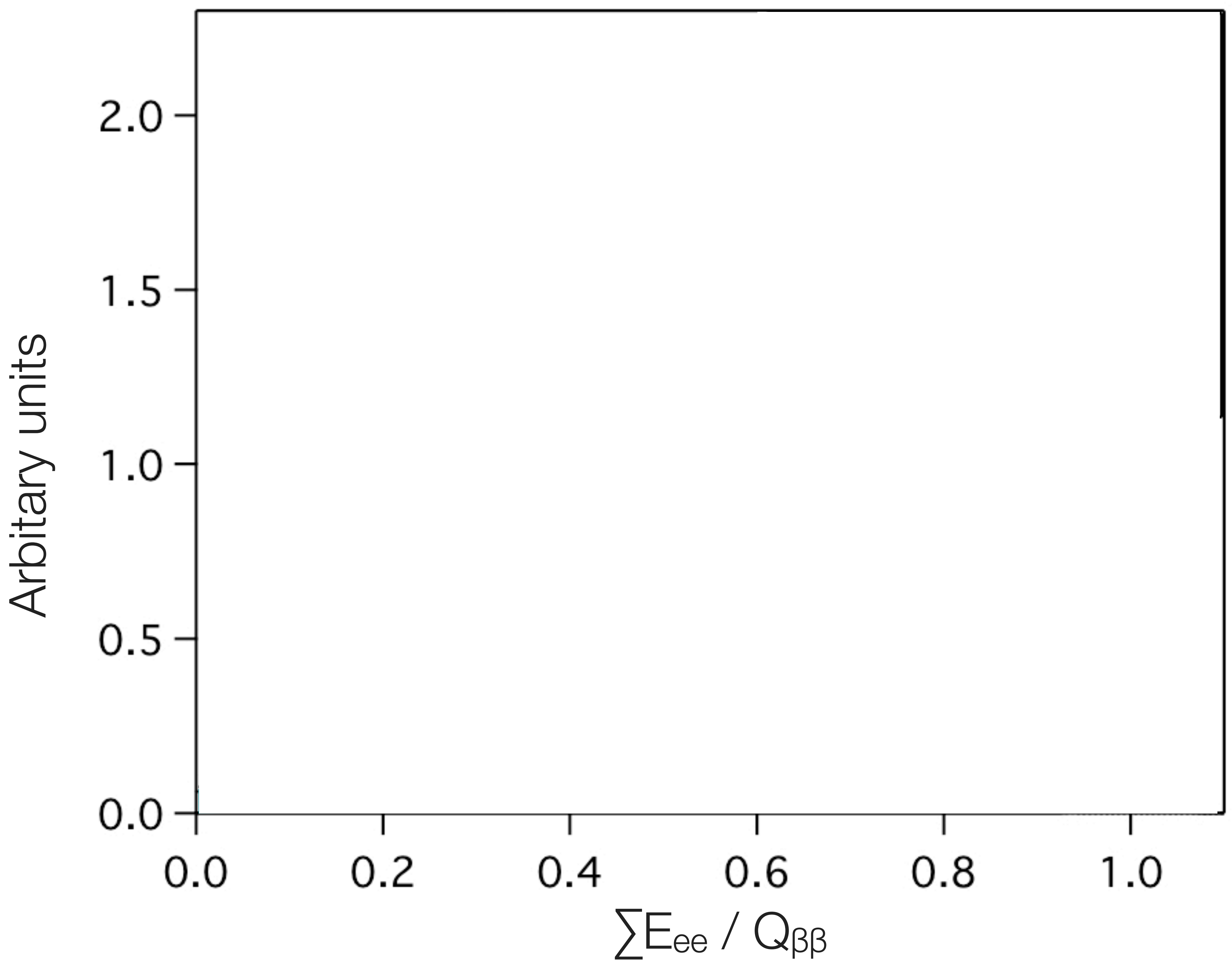

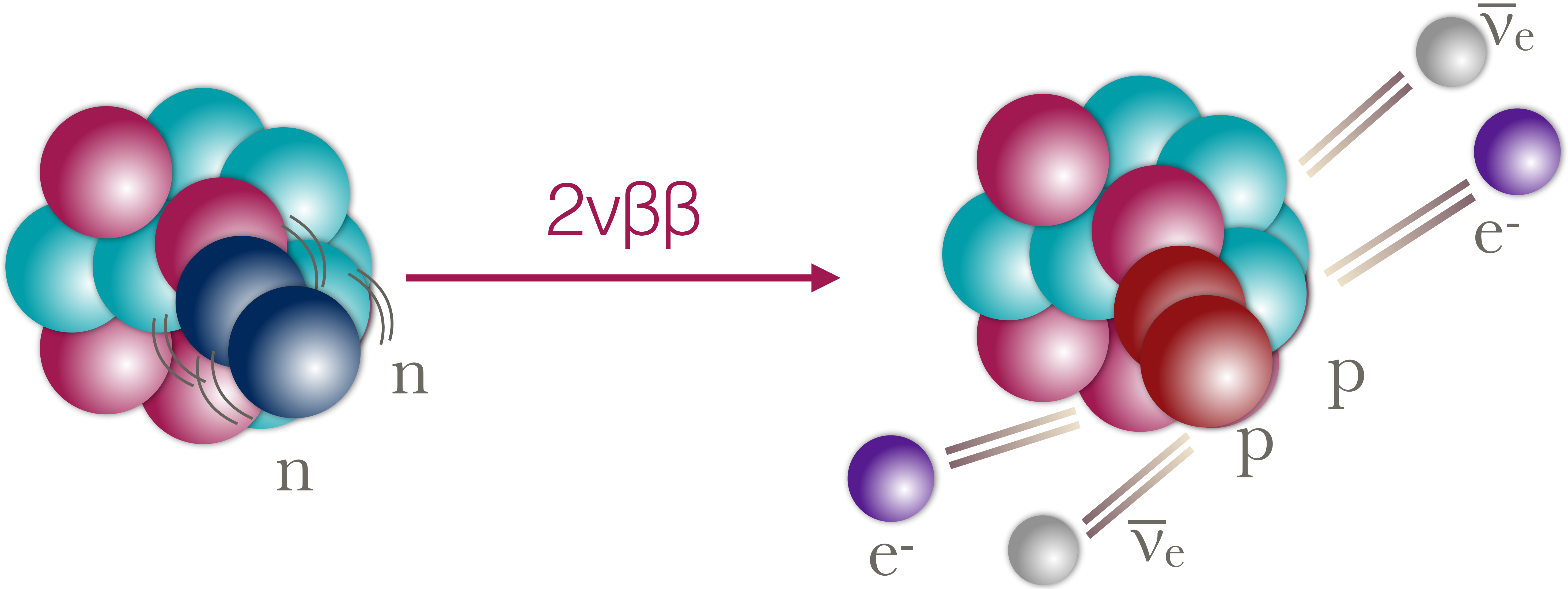

Sum of the **2 electron energies**, as fraction of ββ decay energy

Looking for 0νββ

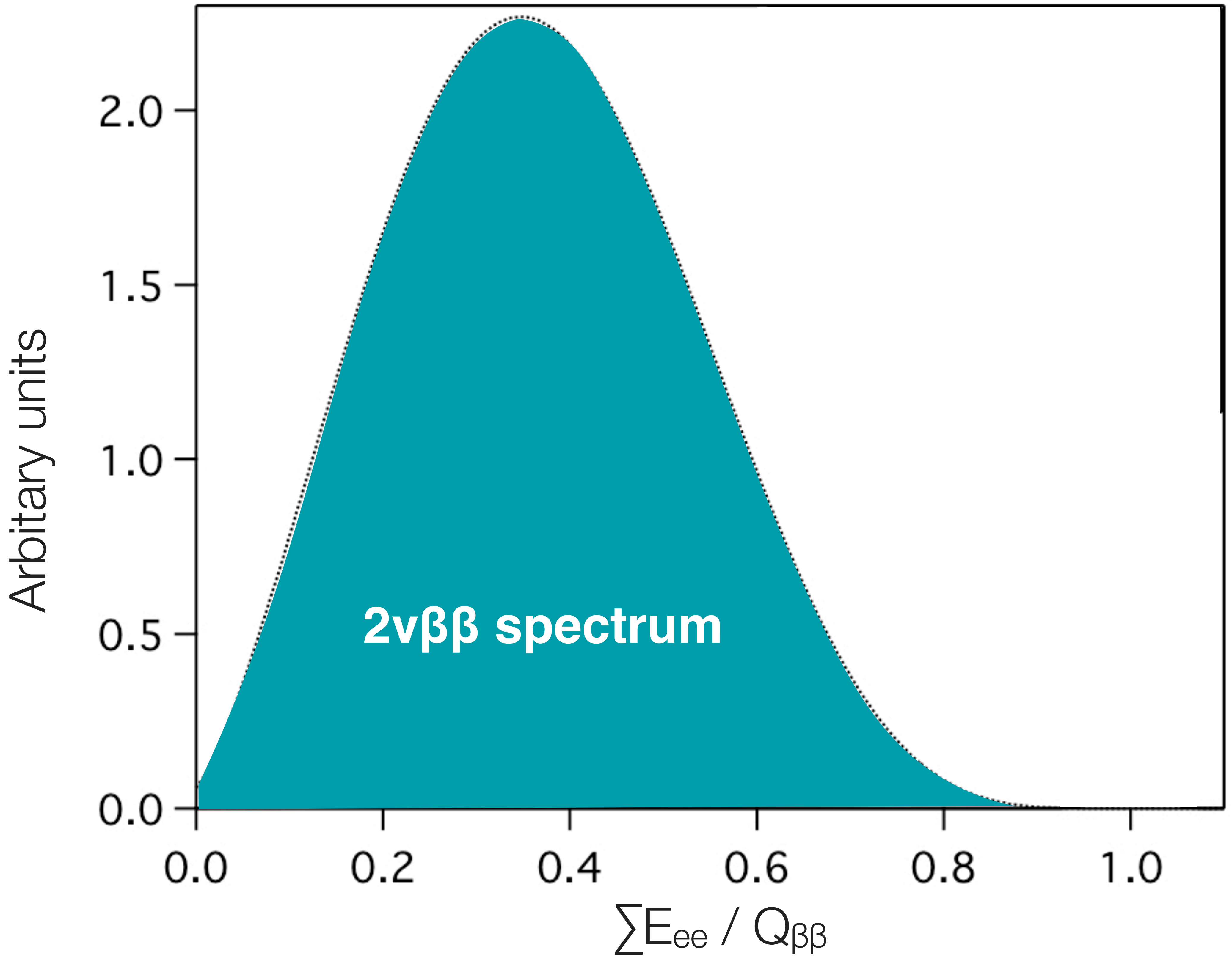

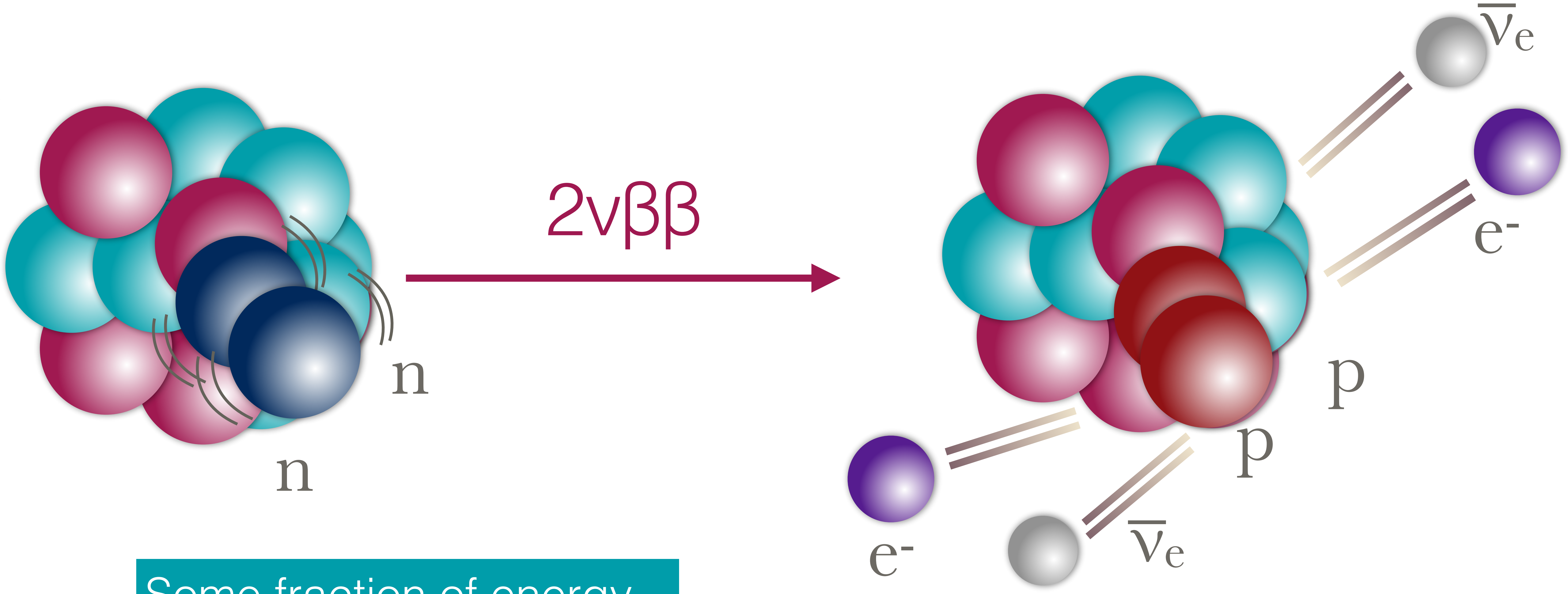

Some fraction of energy goes to neutrinos

Sum of the **2 electron energies**, as fraction of ββ decay energy

Looking for 0νββ

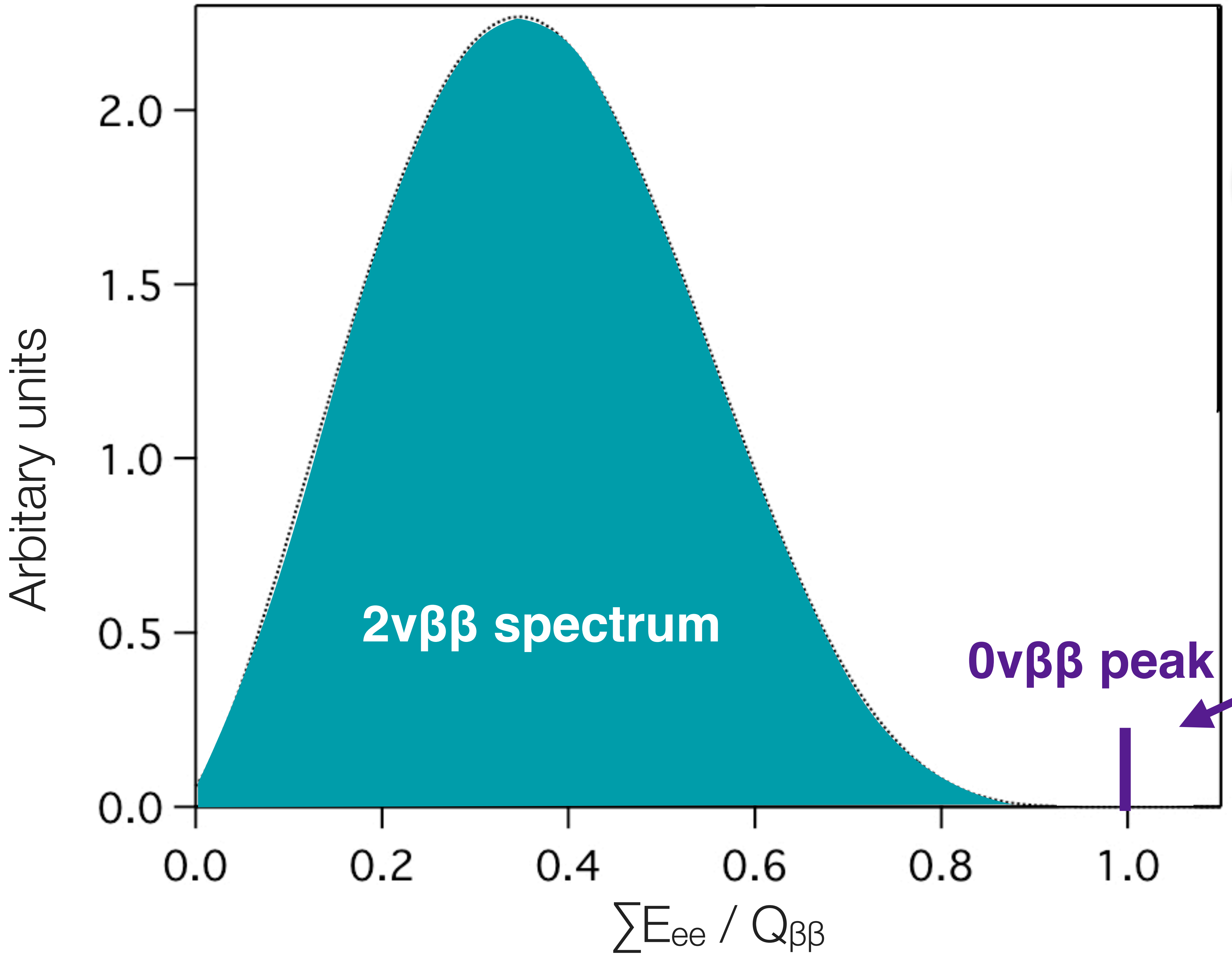

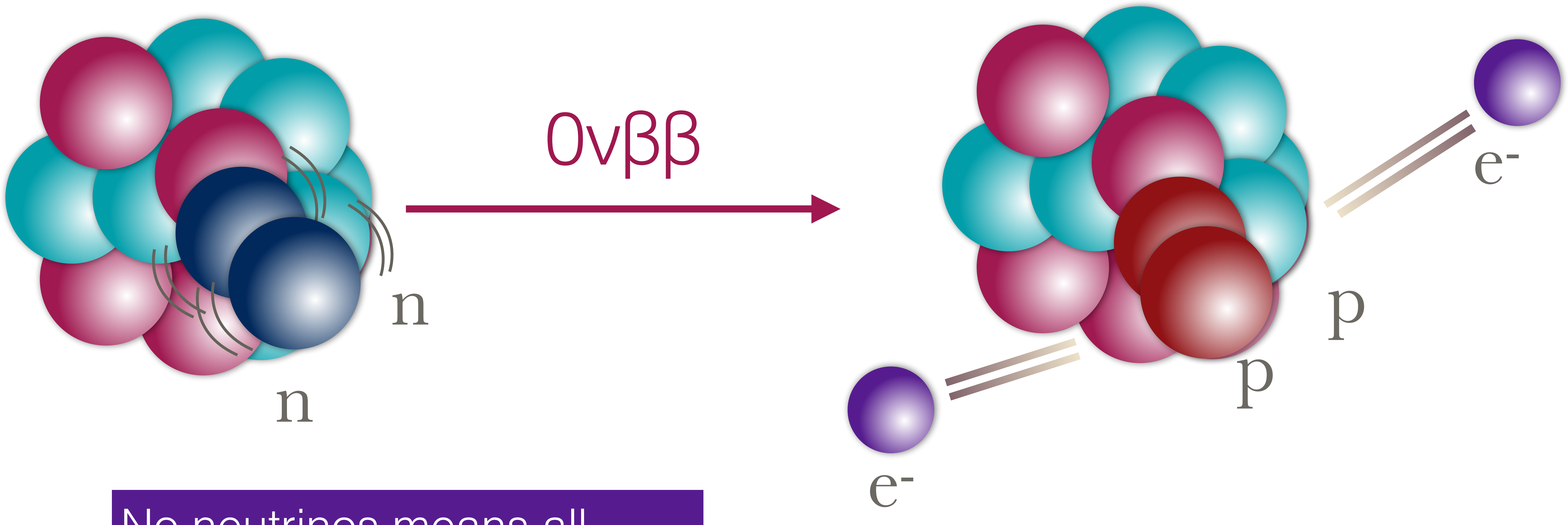

No neutrinos means all energy goes to electrons

Sum of the **2 electron energies**, as fraction of ββ decay energy

Looking for 0νββ

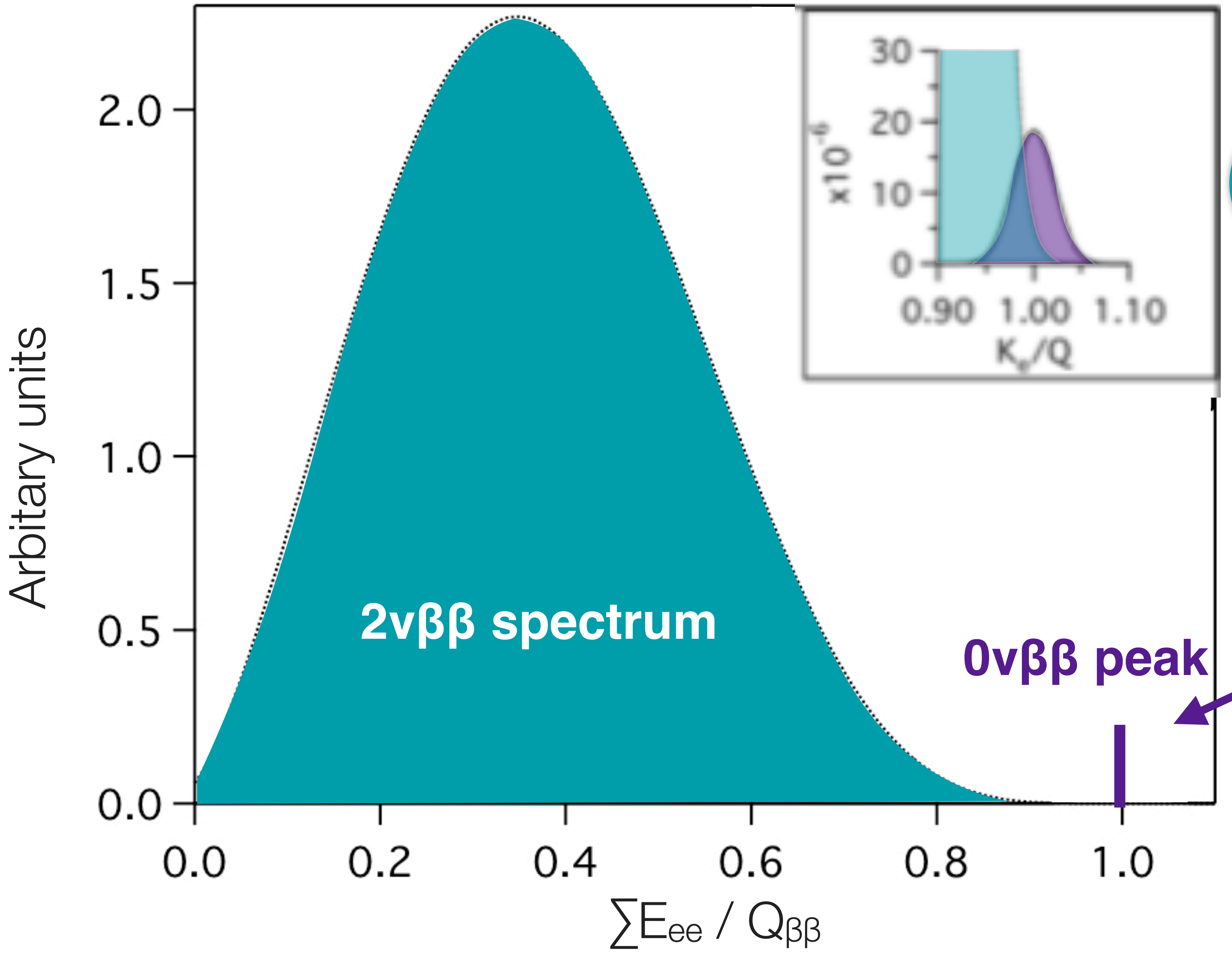

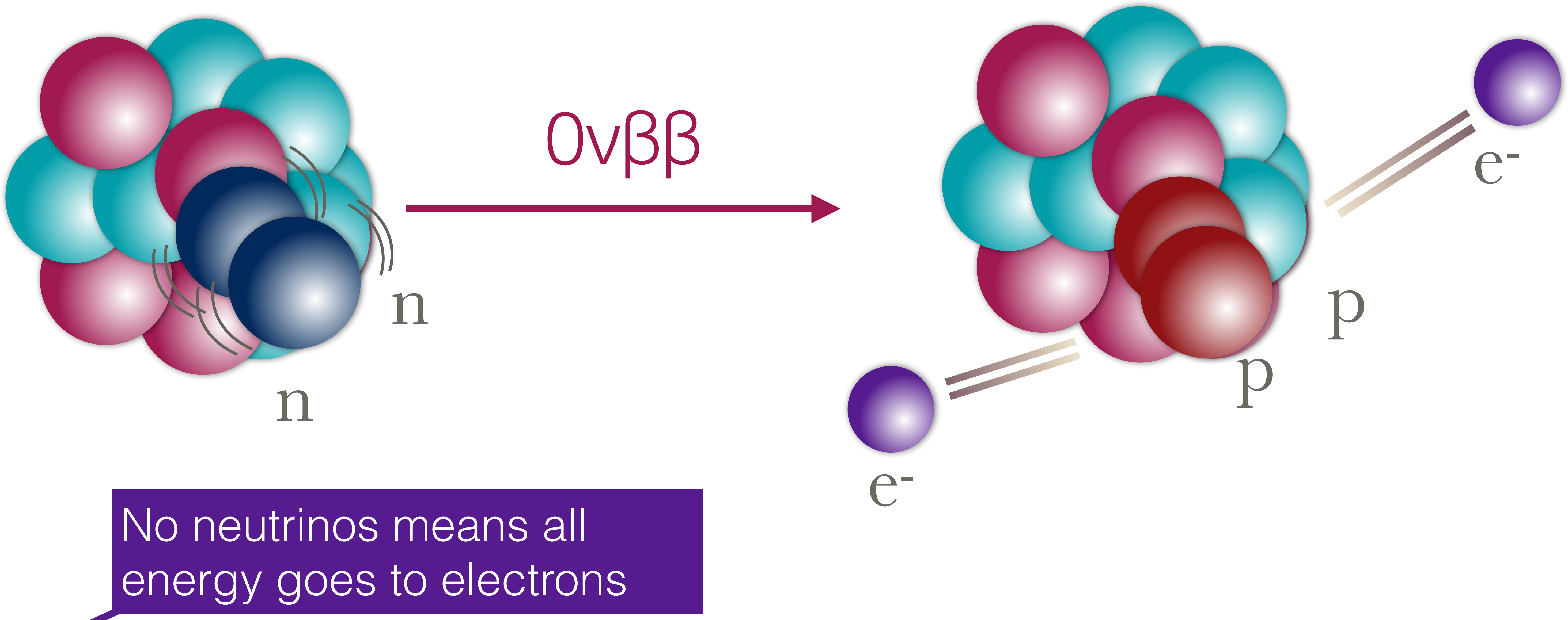

Sum of the **2 electron energies**, as fraction of ββ decay energy

Choosing an isotope

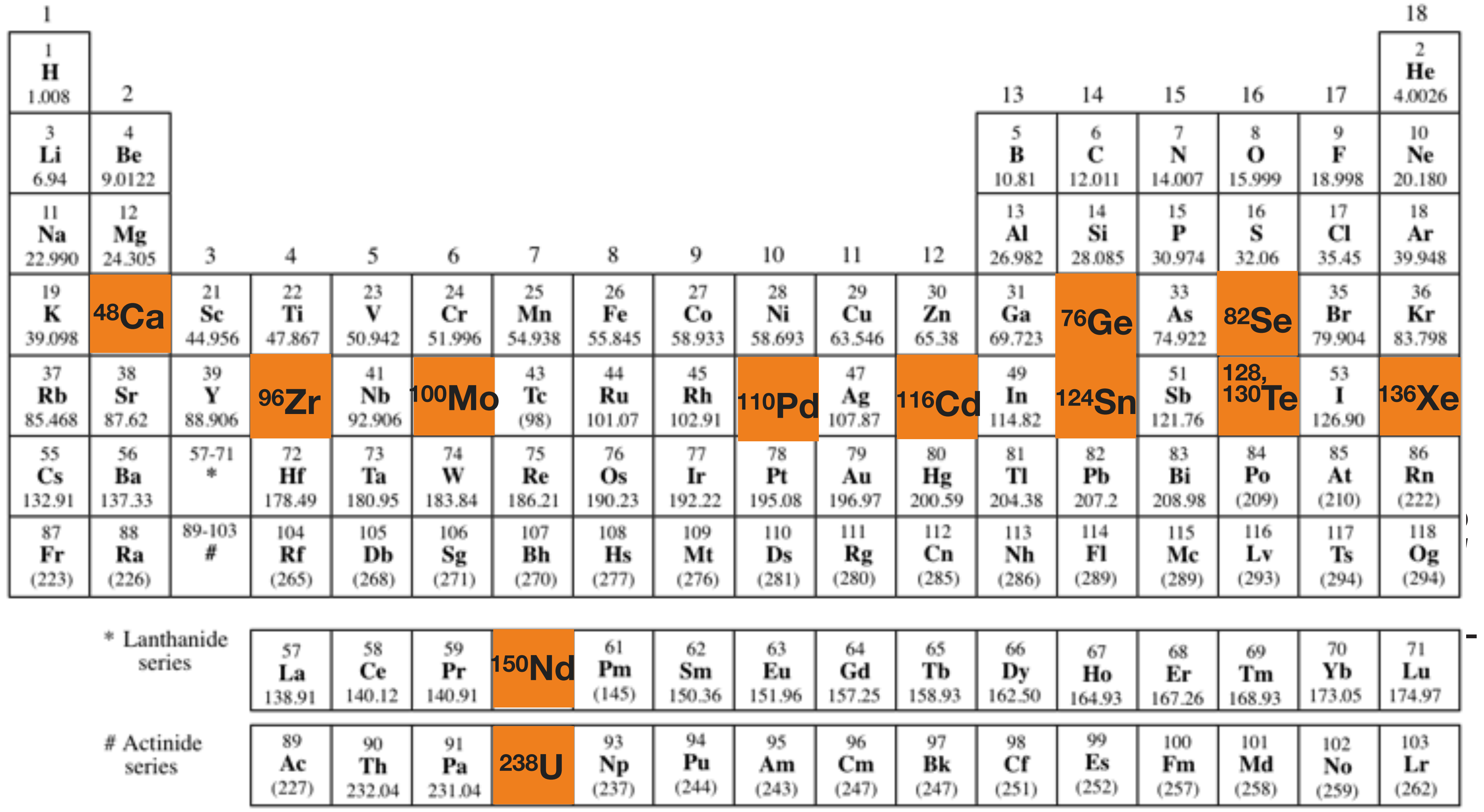

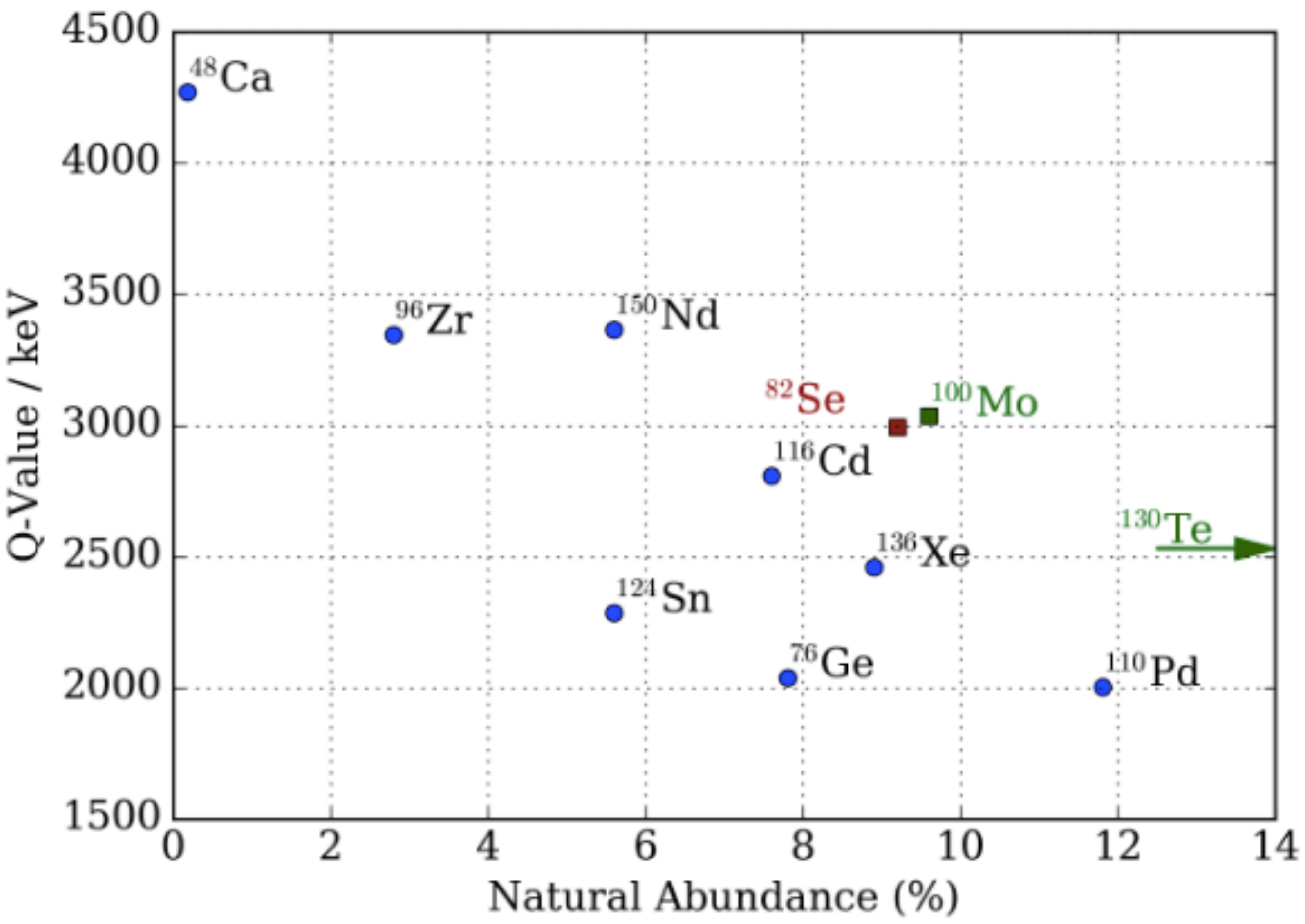

JINST 13 (2018) no.03, P03015

Choosing an isotope

- **"Short" half-life**

$$\frac{1}{T_{1/2}^{0\nu\beta\beta}} = G_{0\nu}(Q_{\beta\beta}, Z)|M_{0\nu}|^2 \frac{\langle m_{\beta\beta}\rangle^2}{m_e{}^2}$$

Better

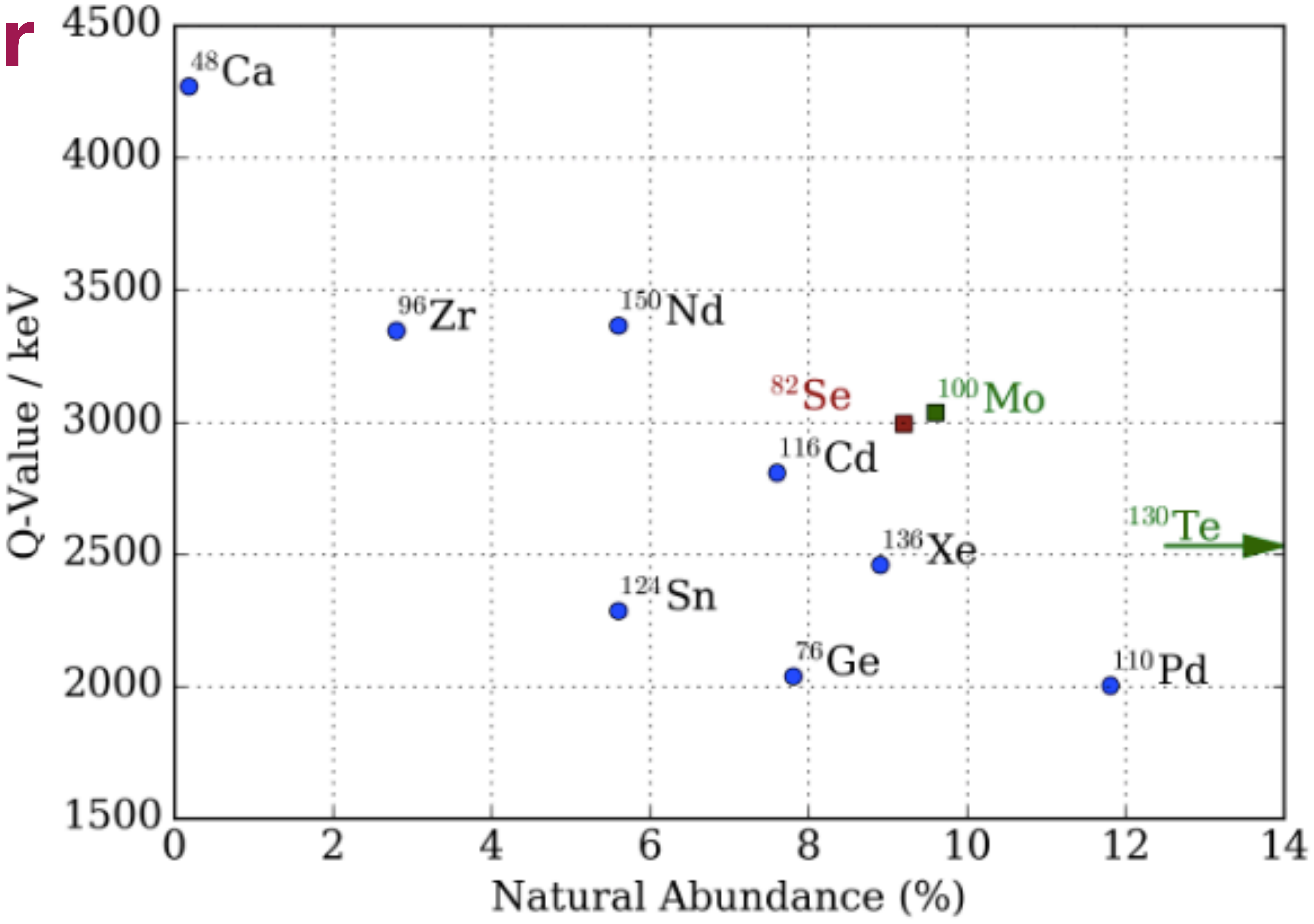

$T_{1/2}^{0\nu} \propto Q^{-5}$

JINST 13 (2018) no.03, P03015

Choosing an isotope

- “Short” half-life
- Lots of isotope

total mass of isotope

ββ isotopic abundance | mass of source material ← **$$**

$$T_{1/2}^{0\nu\beta\beta} \text{limit} \propto a\epsilon m t$$

efficiency | run time

effective run time

(If no backgrounds)

Better ↑

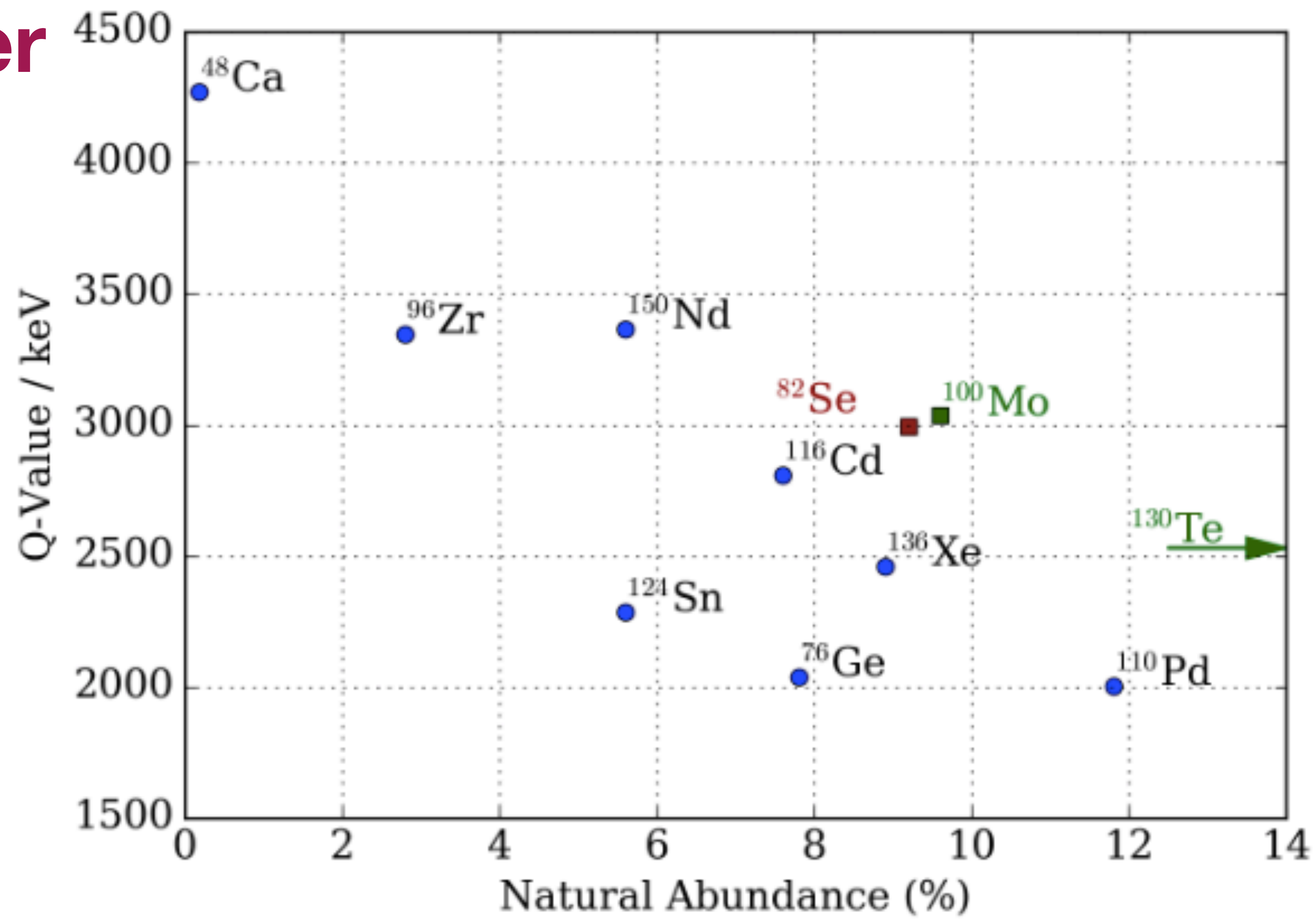

Better →

JINST 13 (2018) no.03, P03015

Choosing an isotope

- “Short” half-life
- Lots of isotope
- (Ultra-) Low backgrounds

Better

less “value” for increasing exposure

$$T_{1/2}^{0\nu}\ \text{limit} \propto a\epsilon\sqrt{\frac{mt}{b\Delta E}}$$

background events

energy resolution

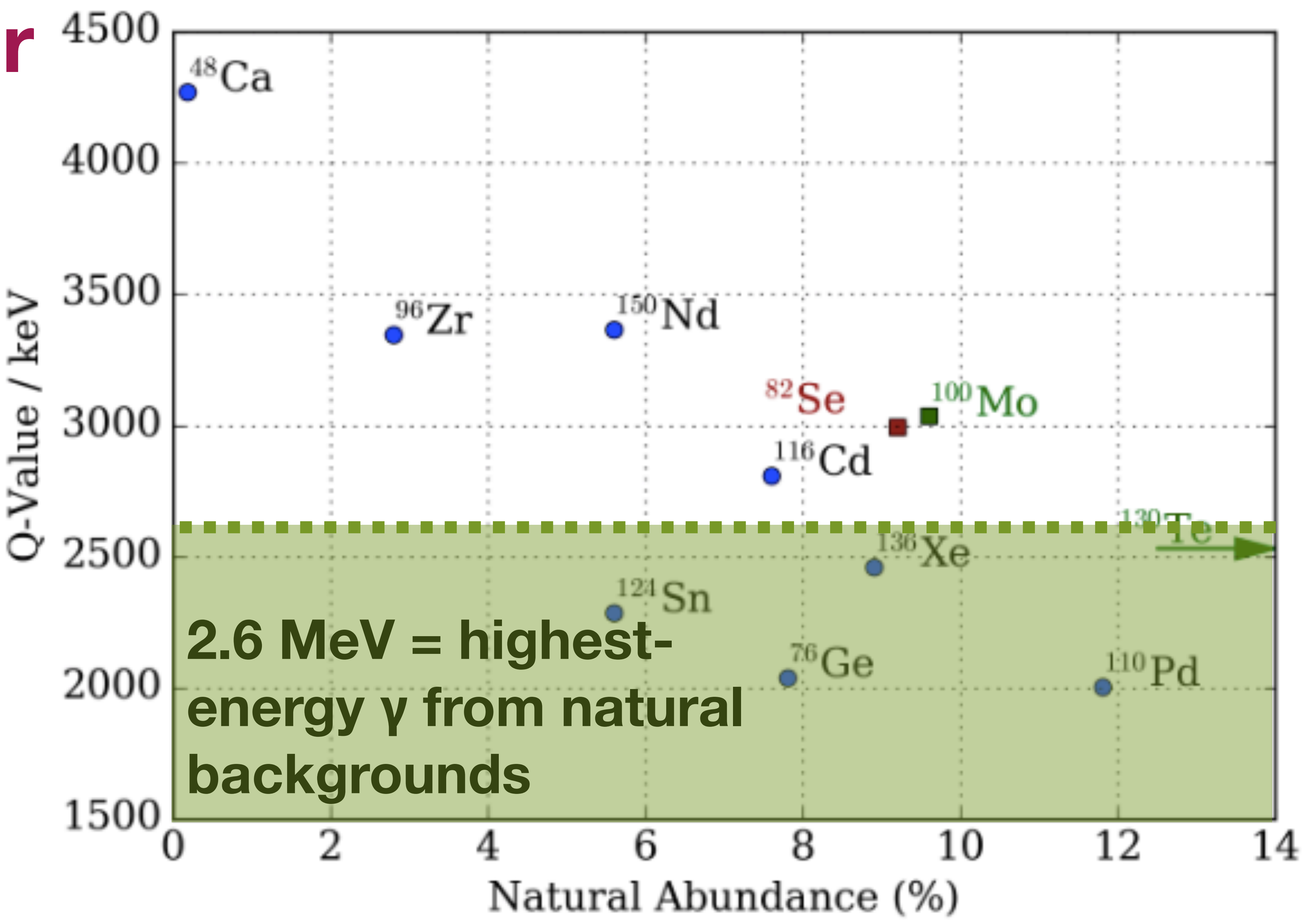

Better

JINST 13 (2018) no.03, P03015

Choosing an isotope

- “Short” half-life
- Lots of isotope
- (Ultra-) Low backgrounds
- Nuclear matrix element

$$\frac{1}{T_{1/2}^{0\nu\beta\beta}} = G_{0\nu}(Q_{\beta\beta}, Z) g_A^4 |M_{0\nu}|^2 \frac{\langle m_{\beta\beta} \rangle^2}{m_e^2}$$

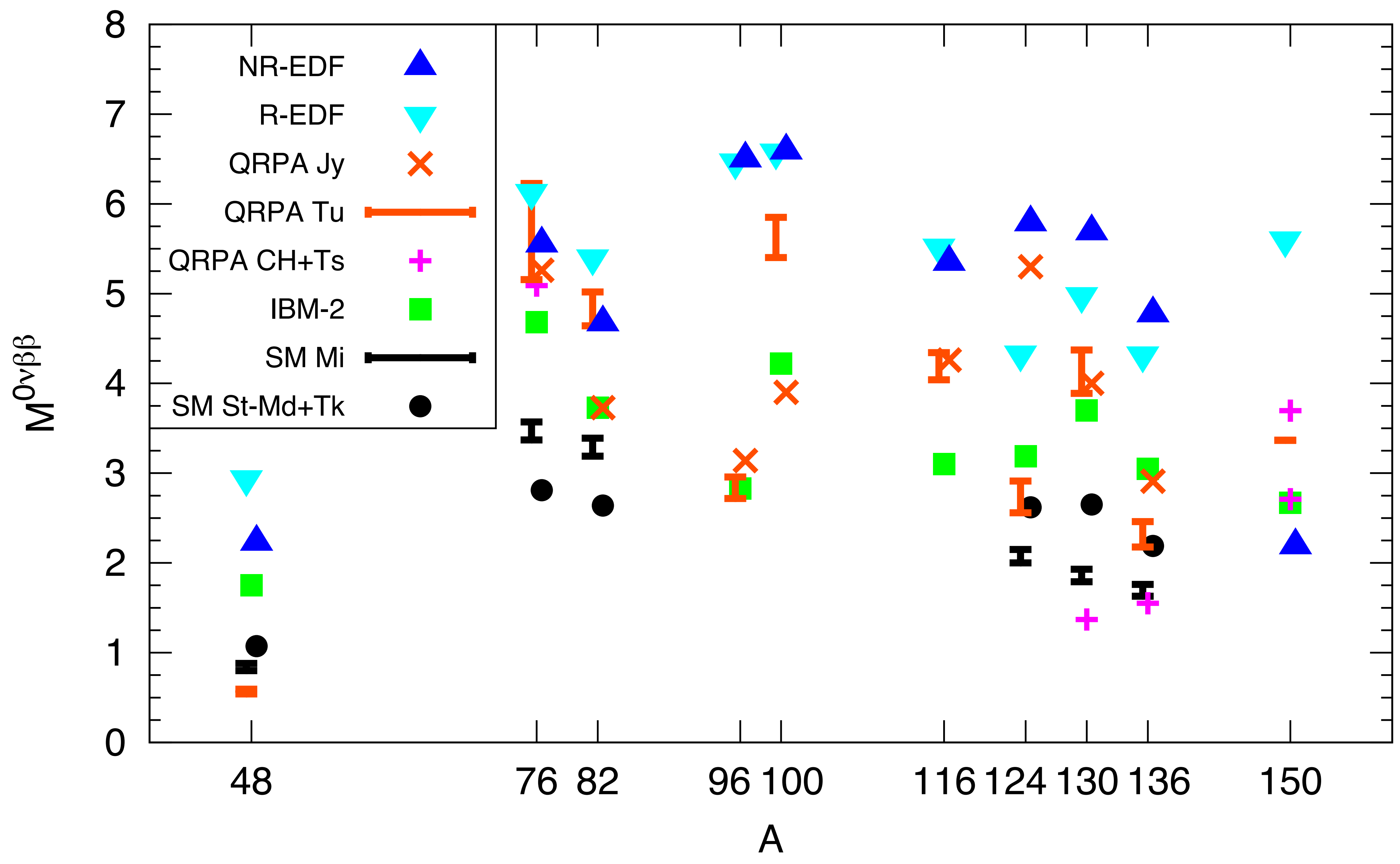

JINST 13 (2018) no.03, P03015

Backgrounds to double-beta experiments

2νββ high-energy tail

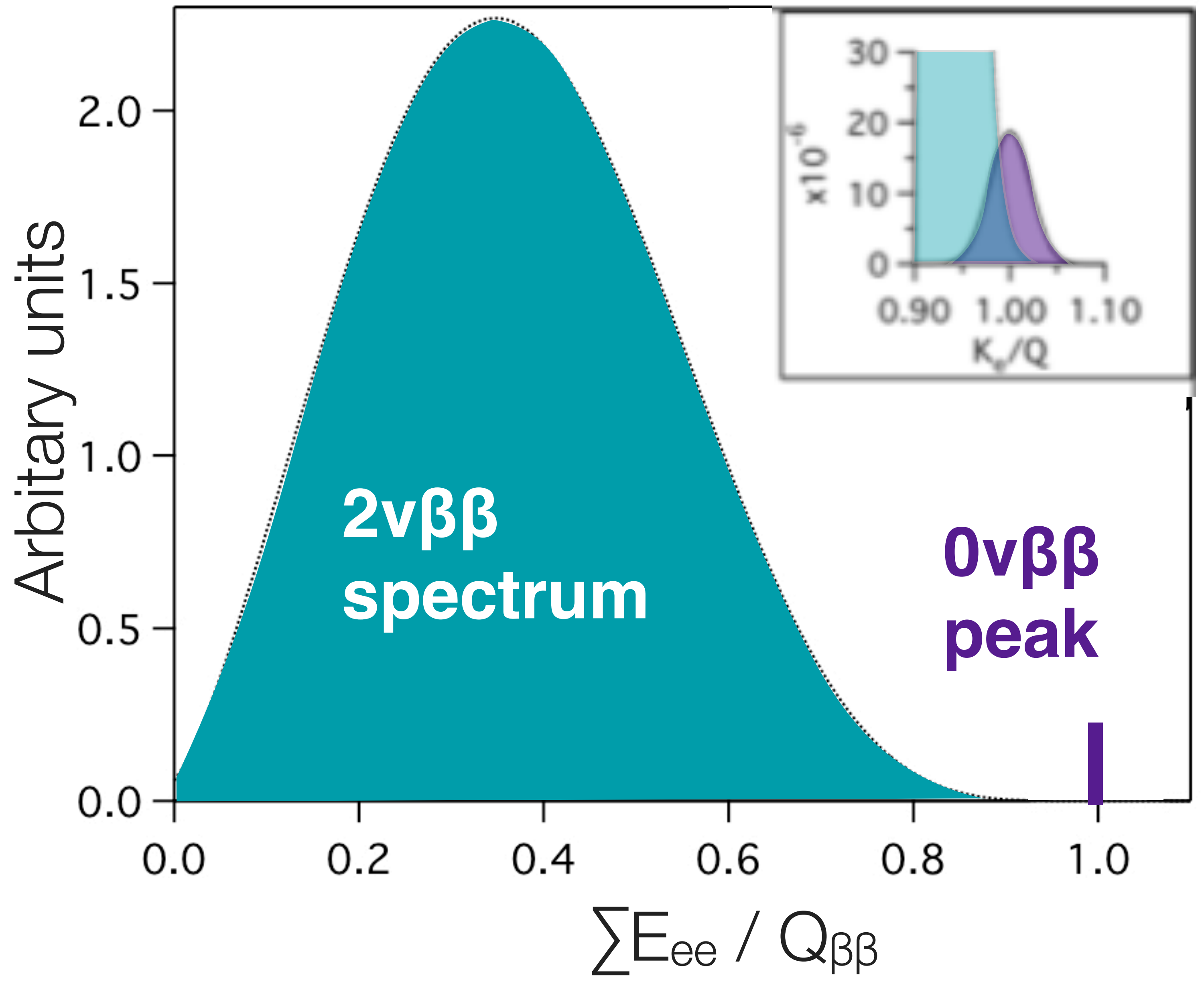

- **Irreducible** - all 2νββ isotopes also exhibit 2νββ
- Exactly the **same signature** apart from energy difference
- Excellent **energy resolution** is the only way to mitigate

Backgrounds to double-beta experiments

2νββ high-energy tail

Cosmic rays

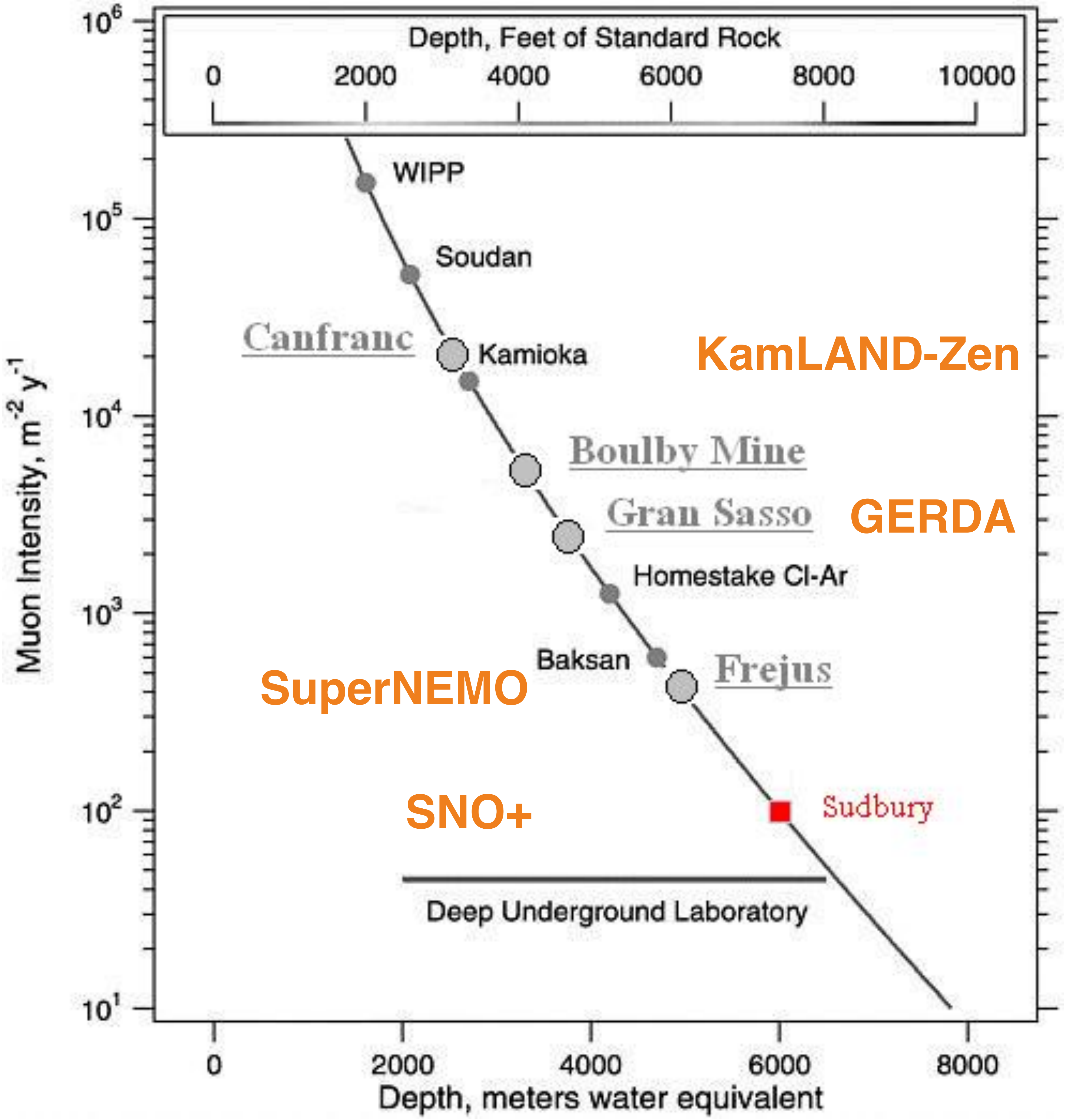

Alps at Modane (SuperNEMO)

Sudbury nickel mine (SNO+)

Backgrounds to double-beta experiments

2νββ high-energy tail

Cosmic rays

β-decaying isotopes

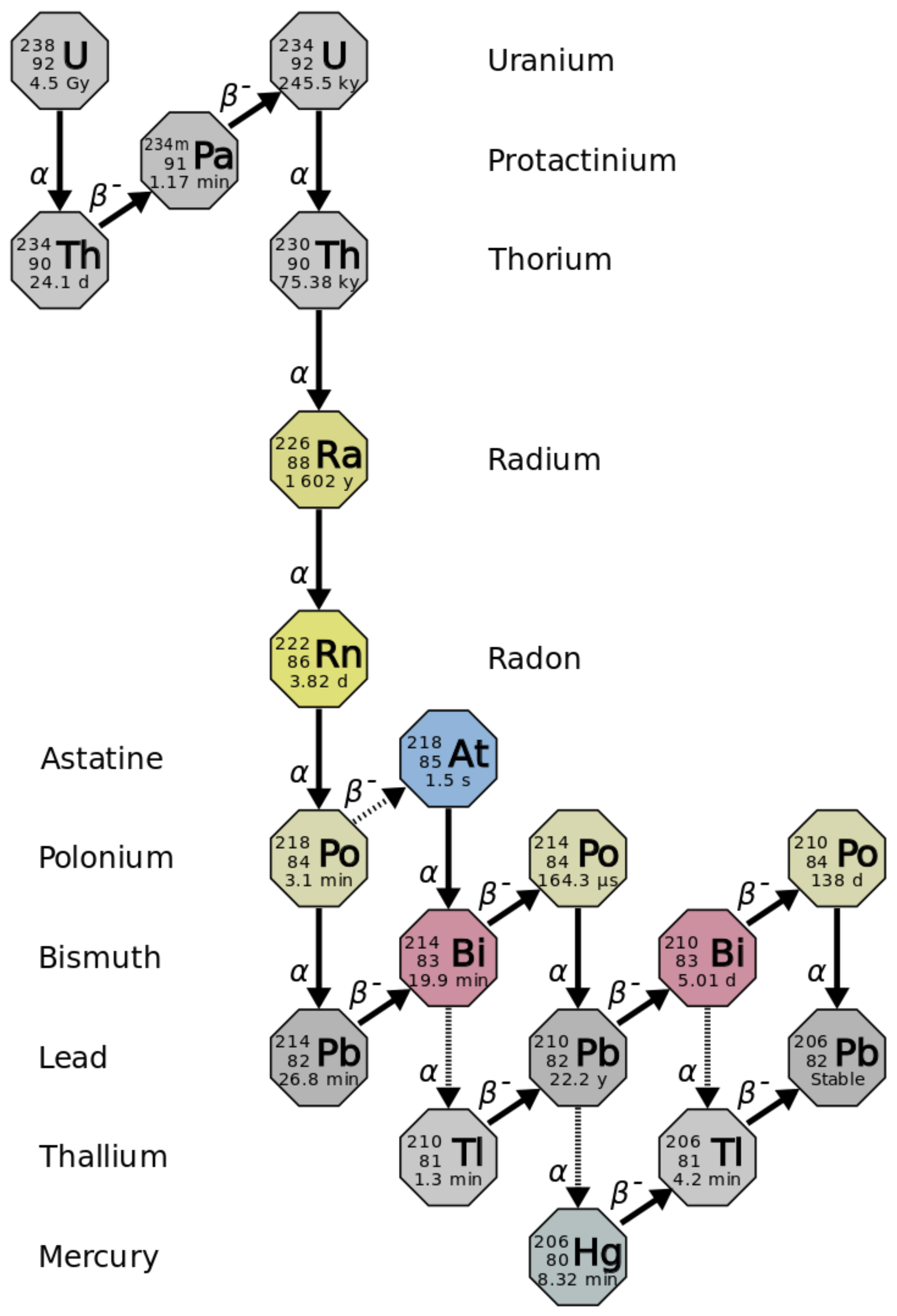

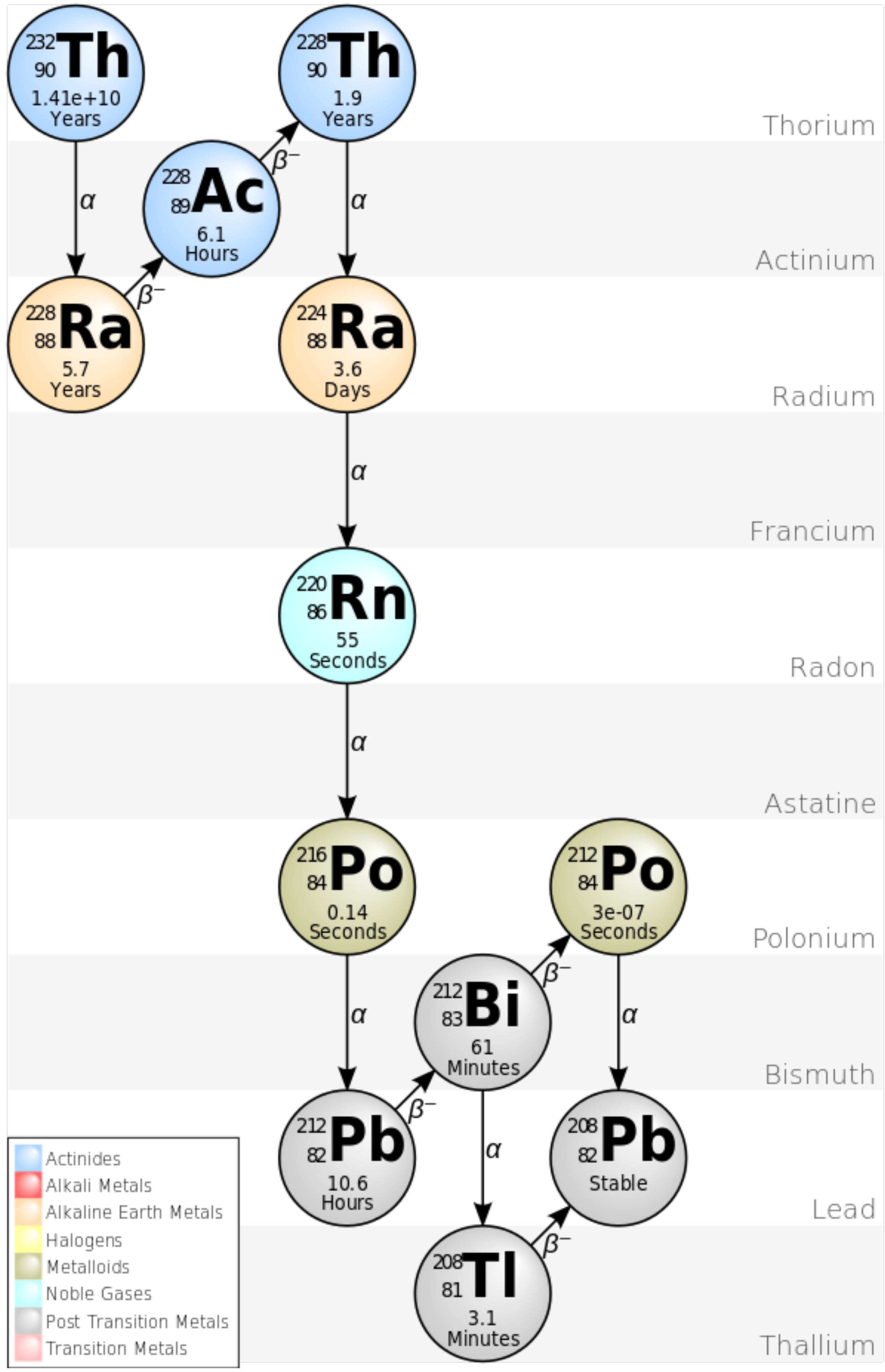

Backgrounds to double-beta experiments

2νββ high-energy tail

Cosmic rays

β-decaying isotopes

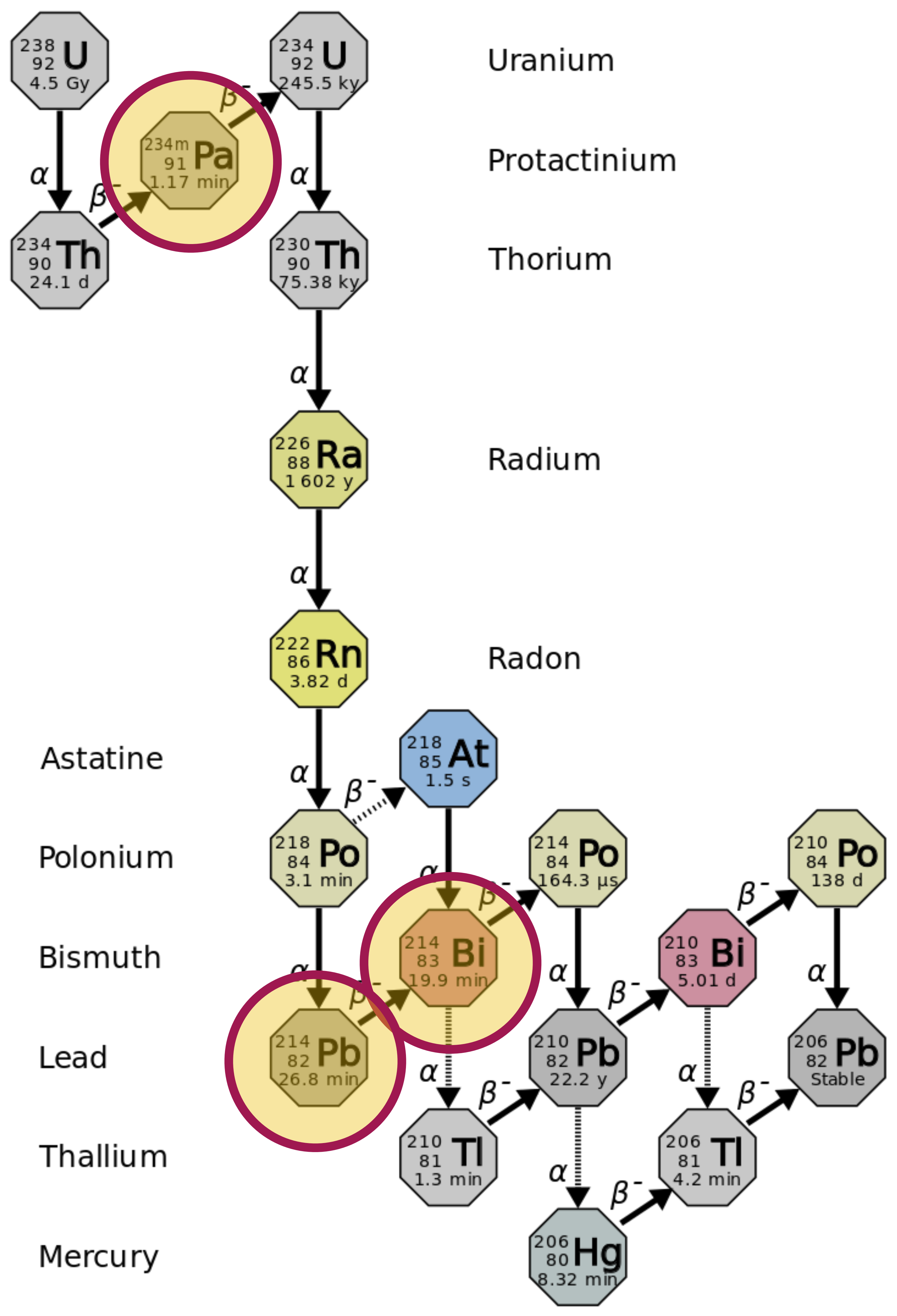

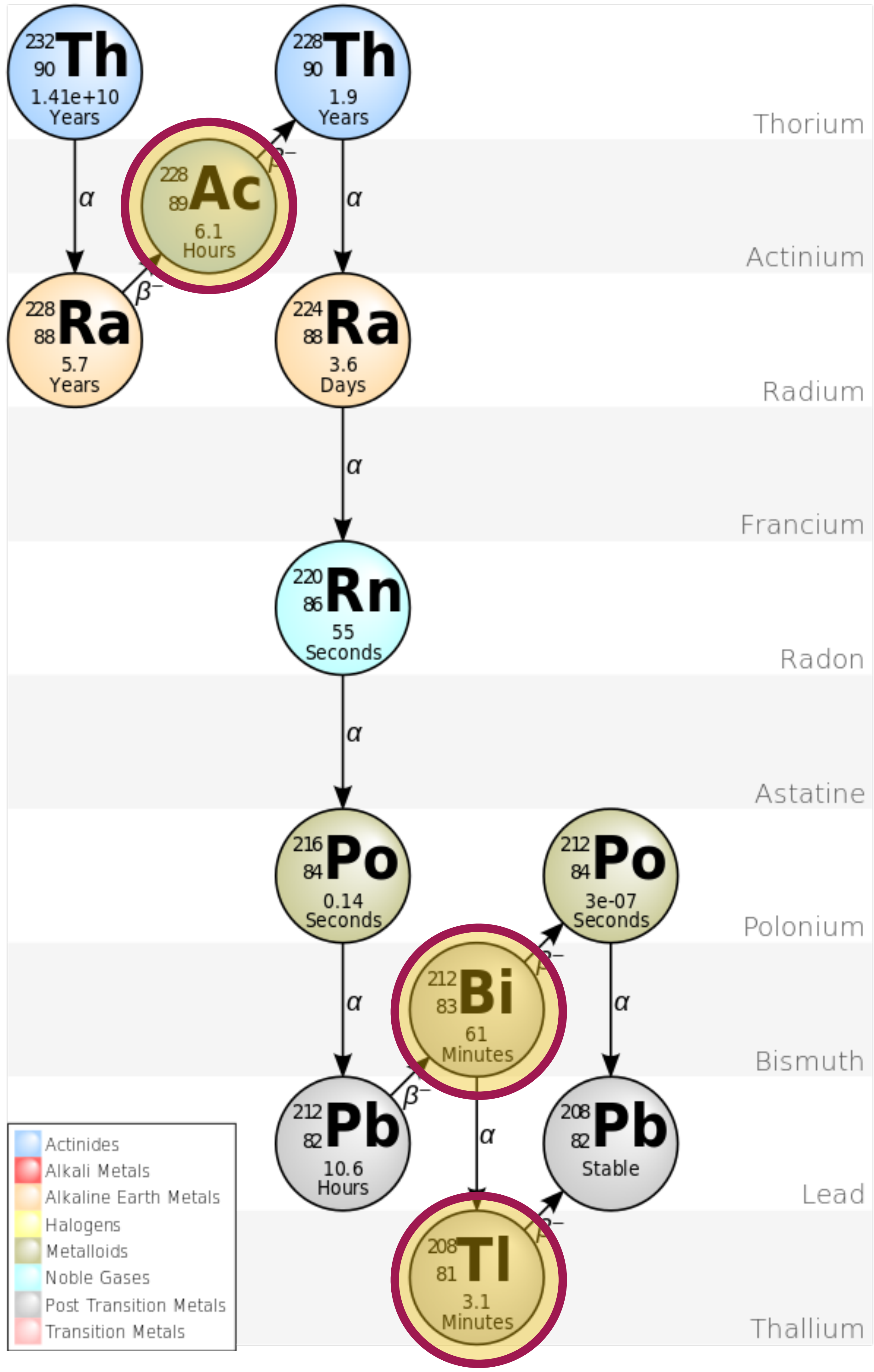

Backgrounds to double-beta experiments

2νββ high-energy tail

Cosmic rays

β-decaying isotopes

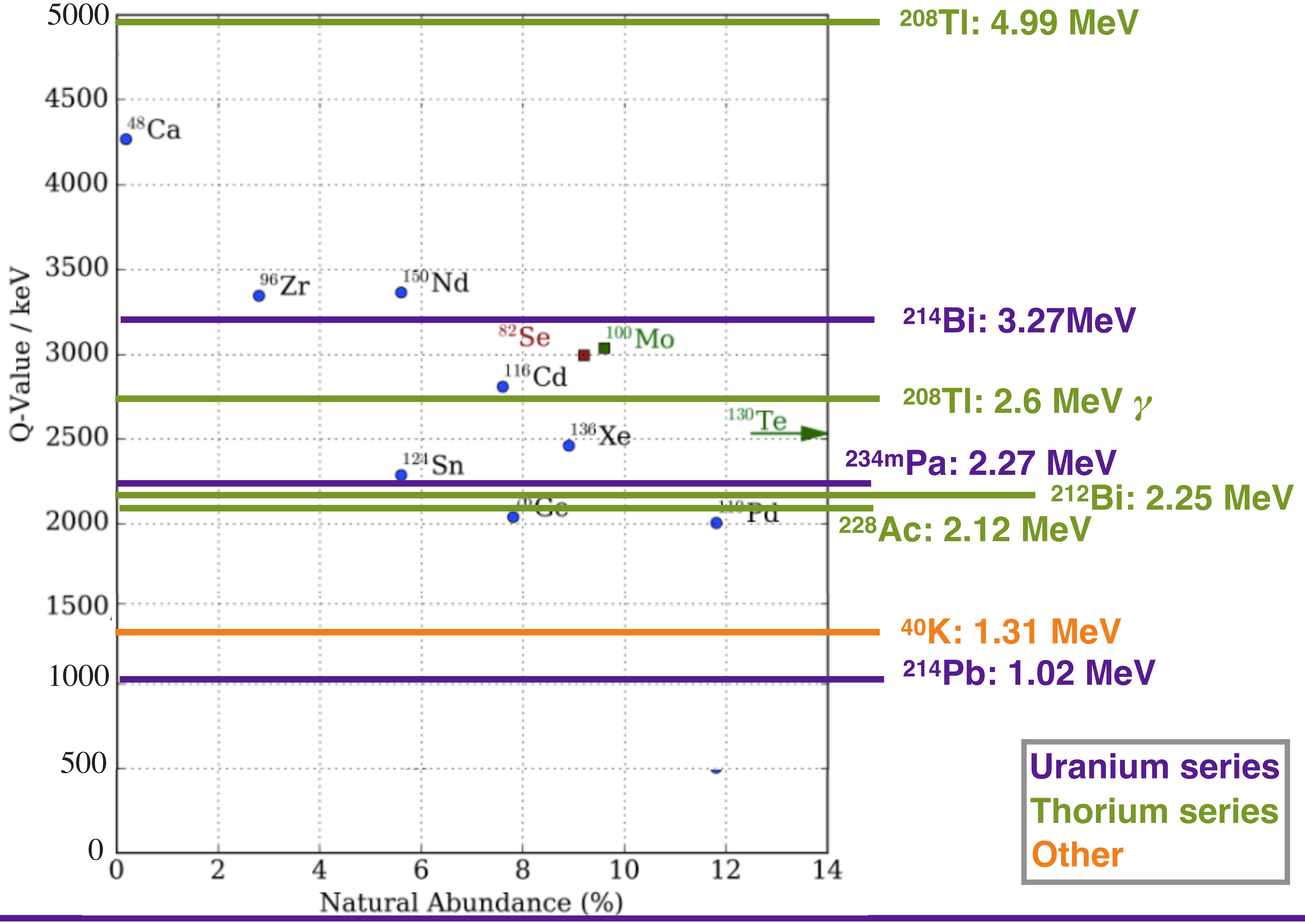

Backgrounds to double-beta experiments

2νββ high-energy tail

Cosmic rays

β-decaying isotopes

External contamination

Building the GERDA detector array in the glovebox © J. Suvorov, GERDA collaboration

Working in the SuperNEMO cleanroom

Backgrounds to double-beta experiments

2νββ high-energy tail

Cosmic rays

β-decaying isotopes

External contamination

Detector components

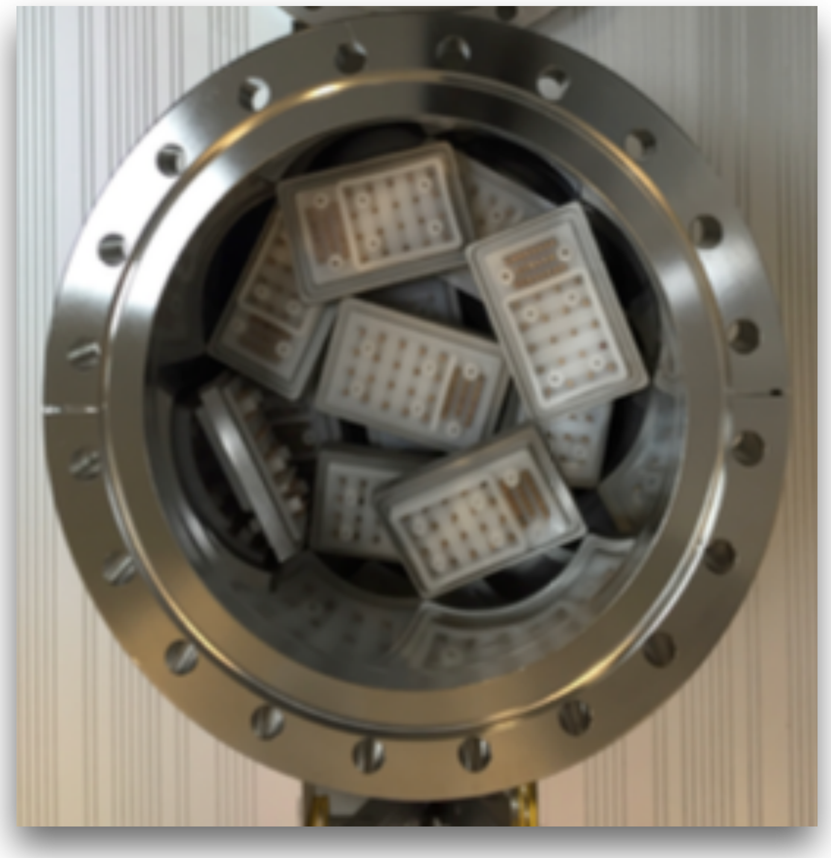

Radiopure components selected & allowed to **emanate radon**. Activity is measured with an **electrostatic detector** (SuperNEMO)

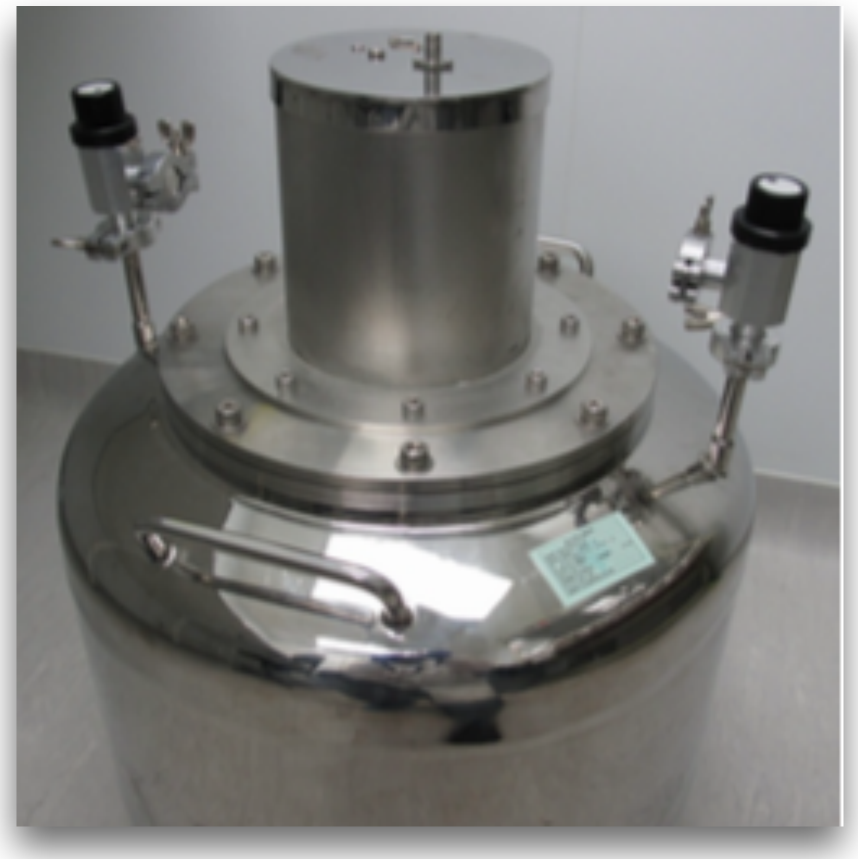

Components machined and cleaned in underground cleanroom (MAJORANA)

Backgrounds to double-beta experiments

- 2vββ high-energy tail
- Cosmic rays
- β-decaying isotopes
- External contamination
- Detector components
- BiPo events

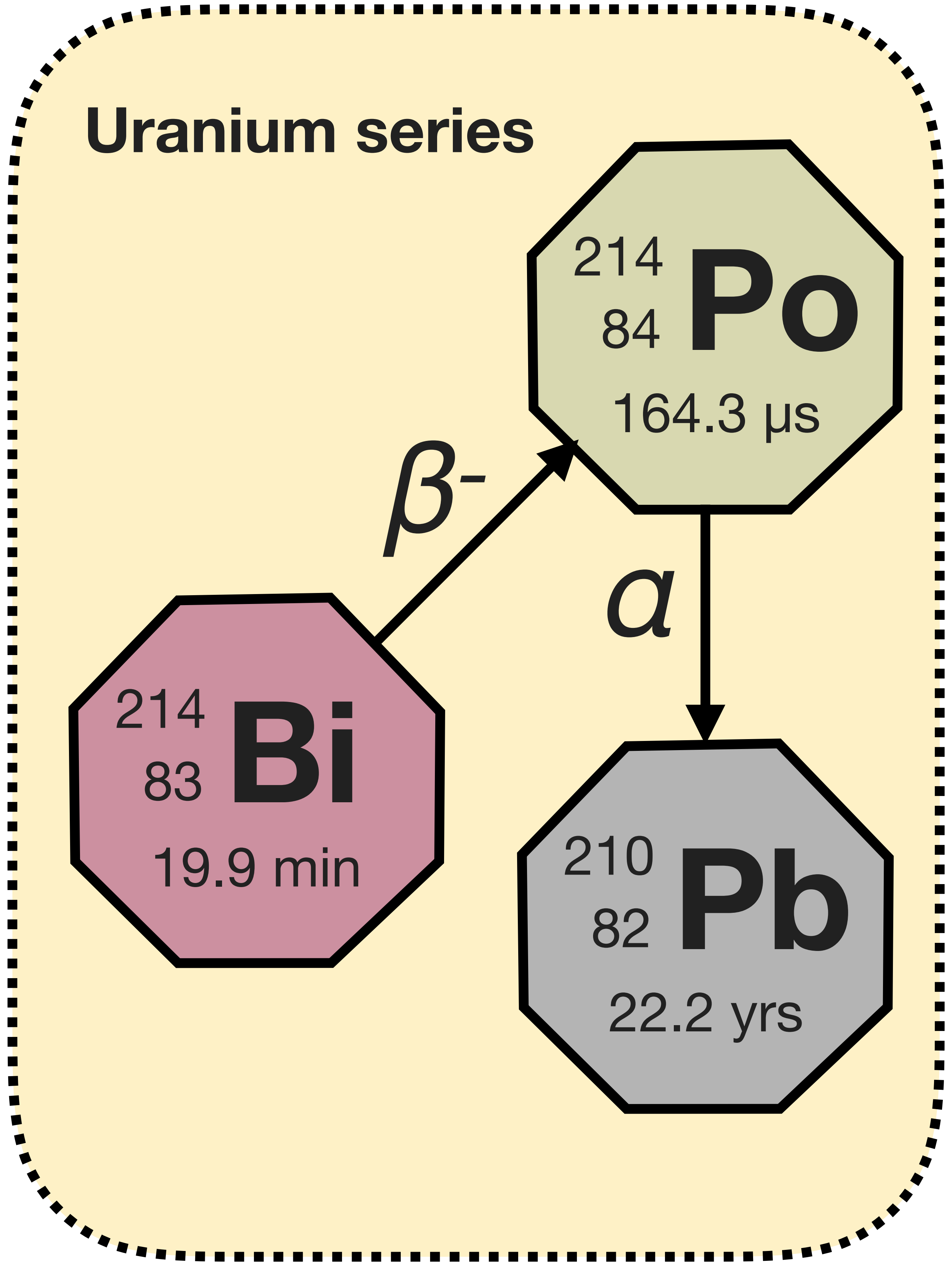

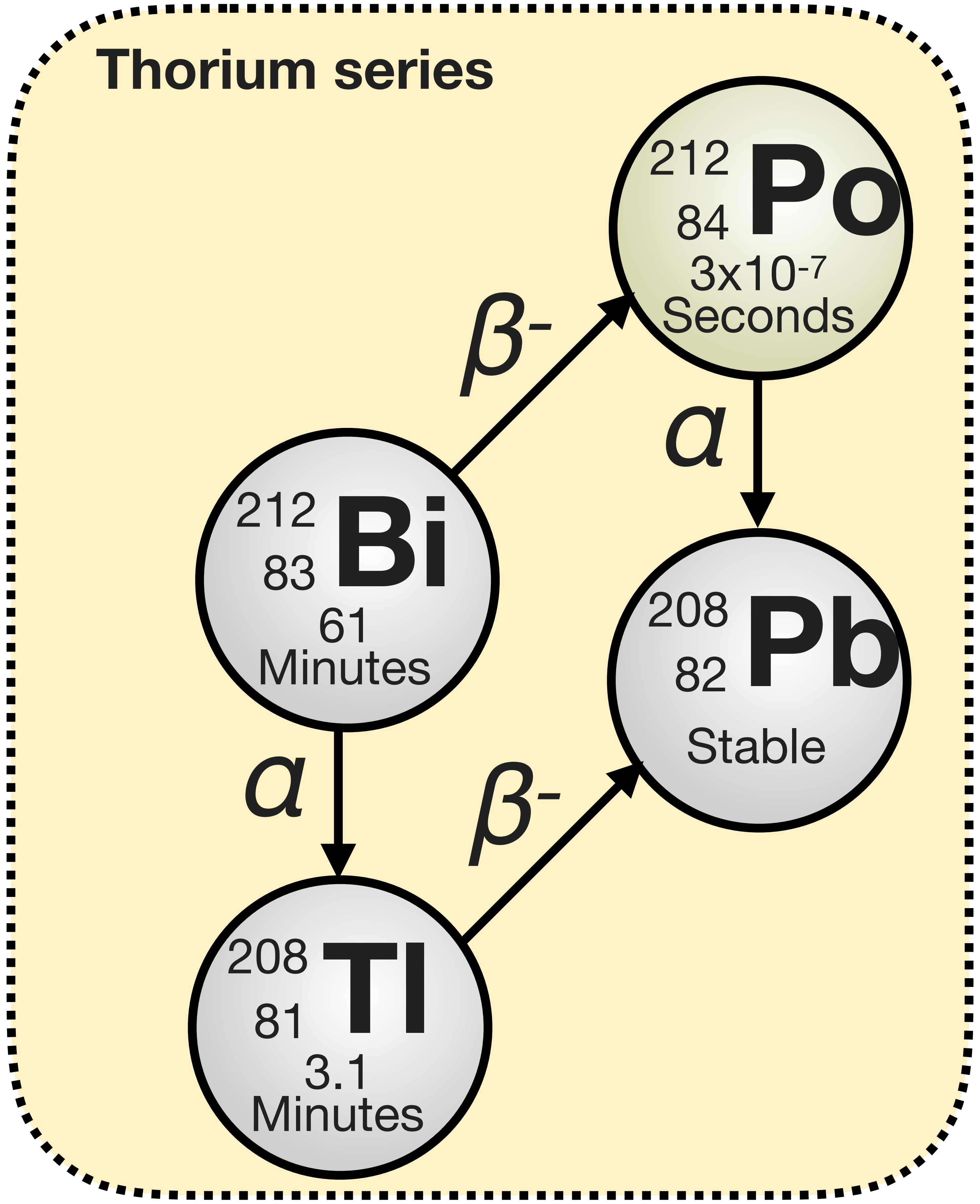

Backgrounds to double-beta experiments

- 2νββ high-energy tail
- Cosmic rays
- β-decaying isotopes
- External contamination
- Detector components
- BiPo events

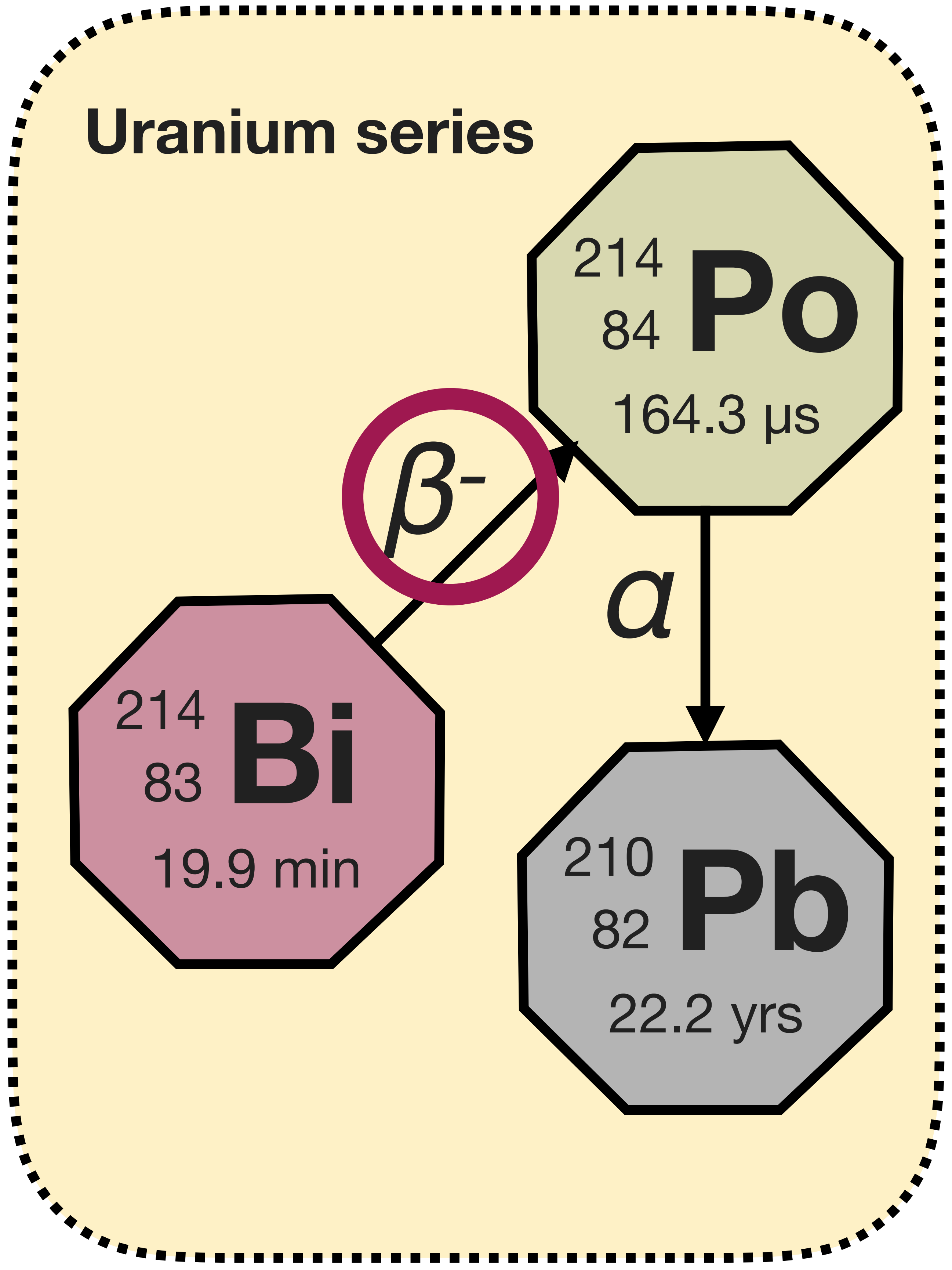

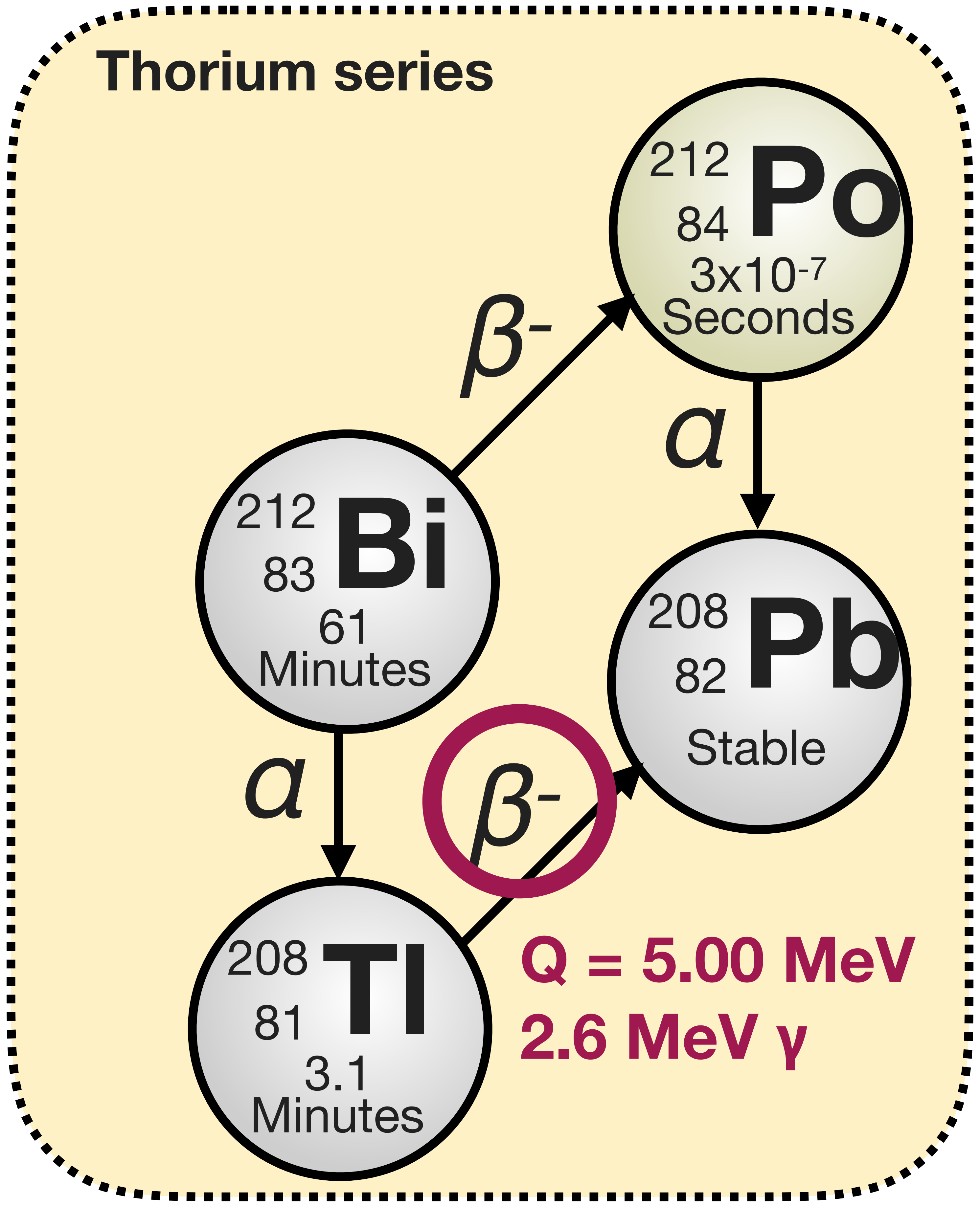

UCL

- $2\nu\beta\beta$ high-energy tail
- Cosmic rays
- β-decaying isotopes
- External contamination
- Detector components
- BiPo events

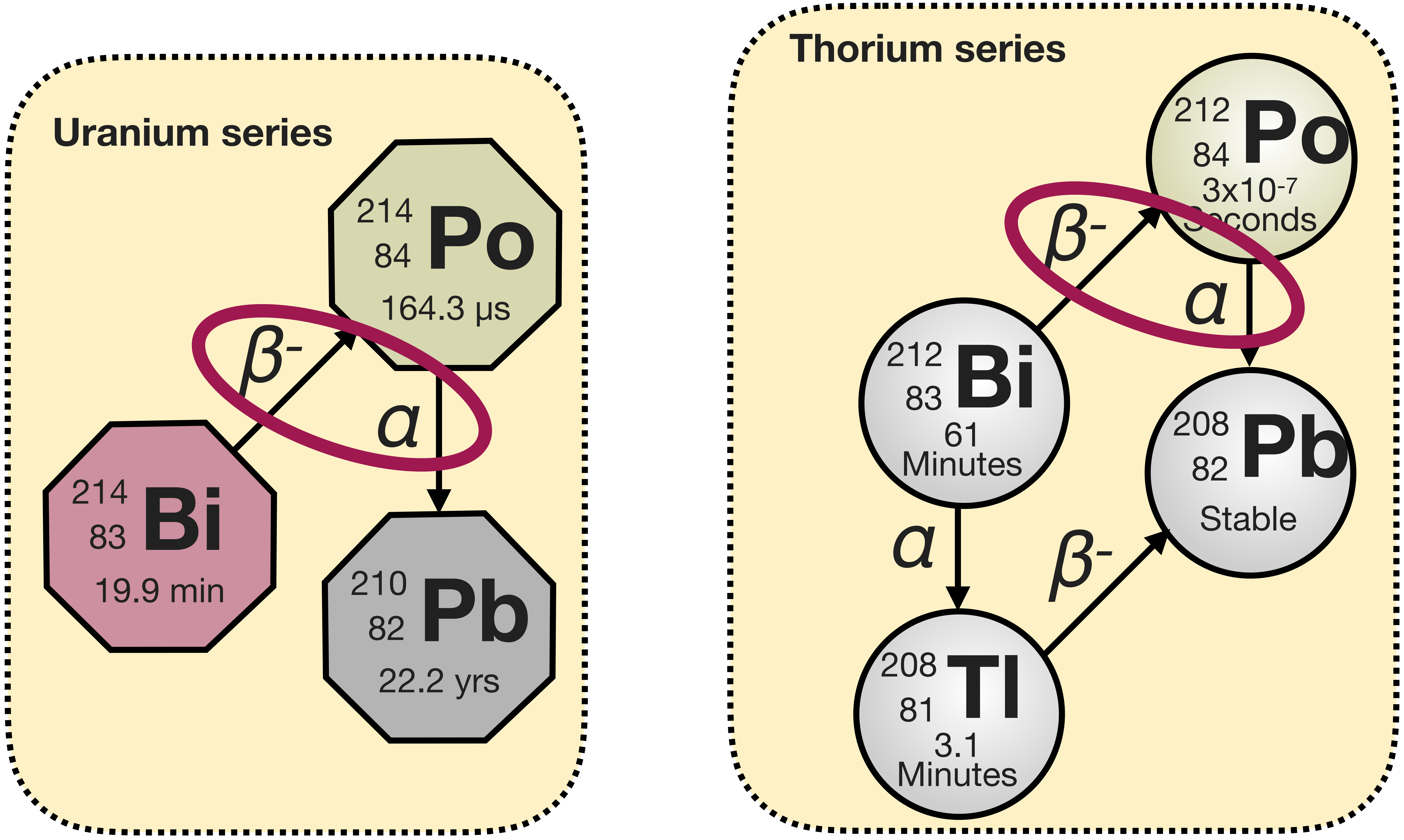

Backgrounds to double-beta experiments

- 2νββ high-energy tail
- Cosmic rays
- β-decaying isotopes
- External contamination
- Detector components
- BiPo events

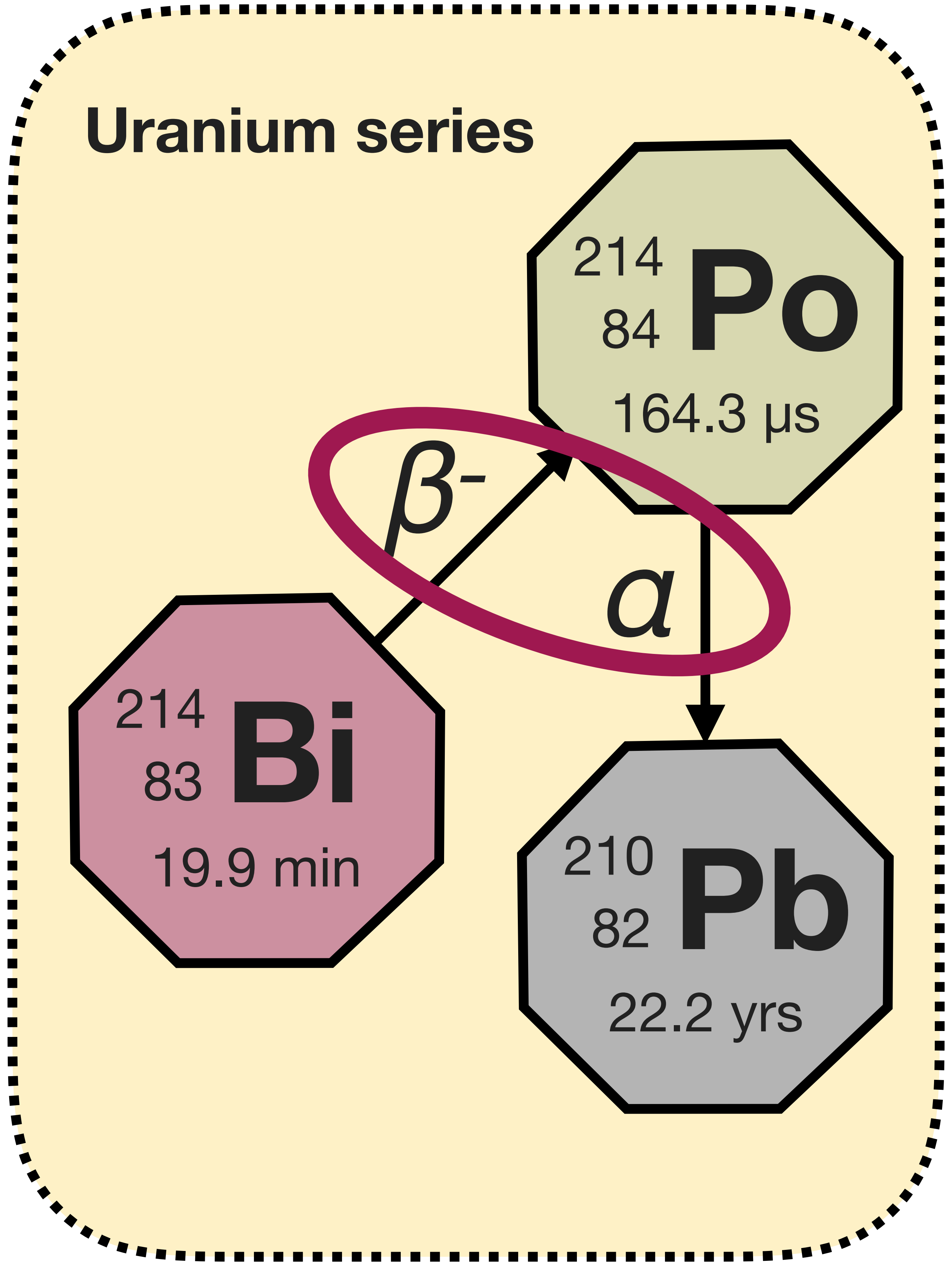

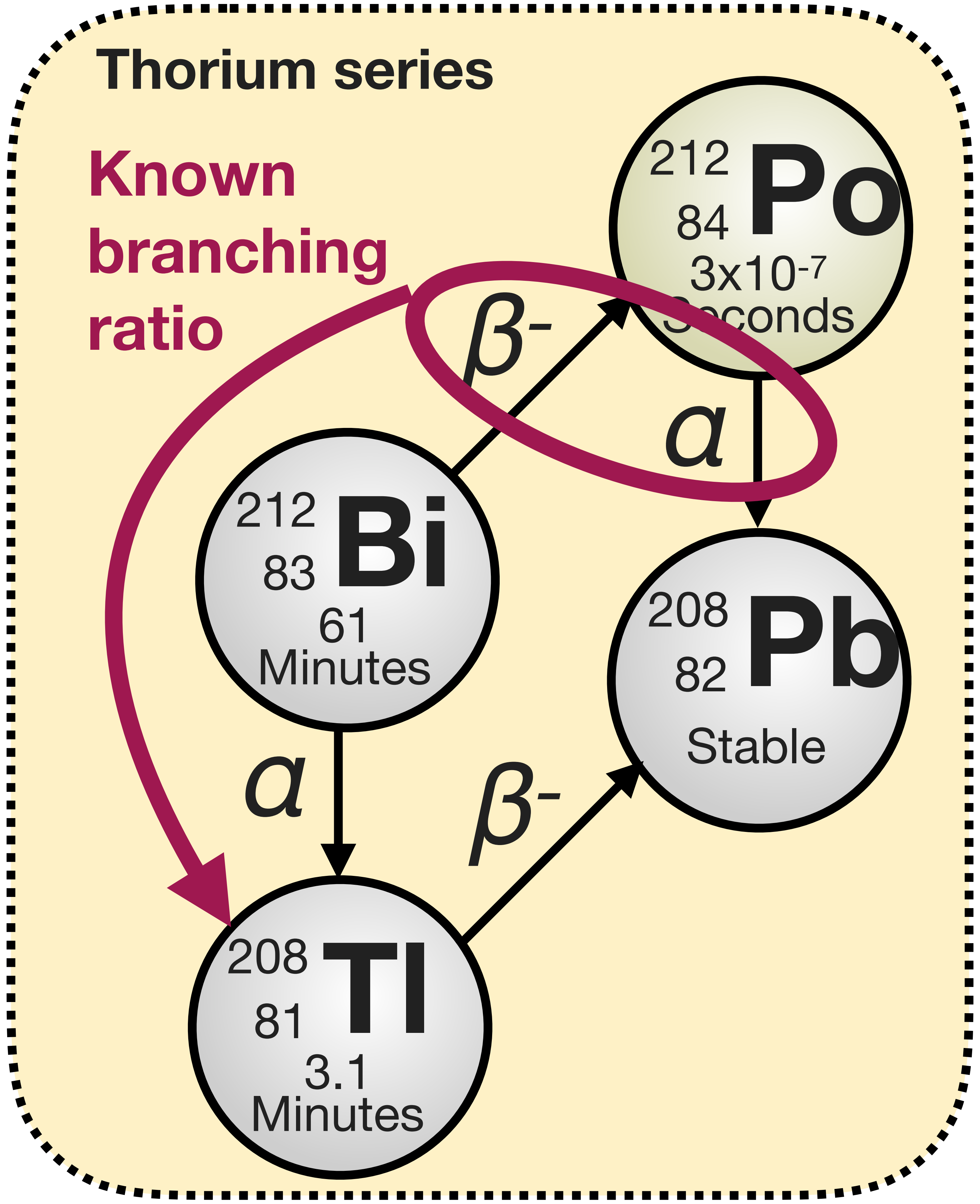

Backgrounds to double-beta experiments

- 2νββ high-energy tail
- Cosmic rays
- β-decaying isotopes
- External contamination
- Detector components
- BiPo events

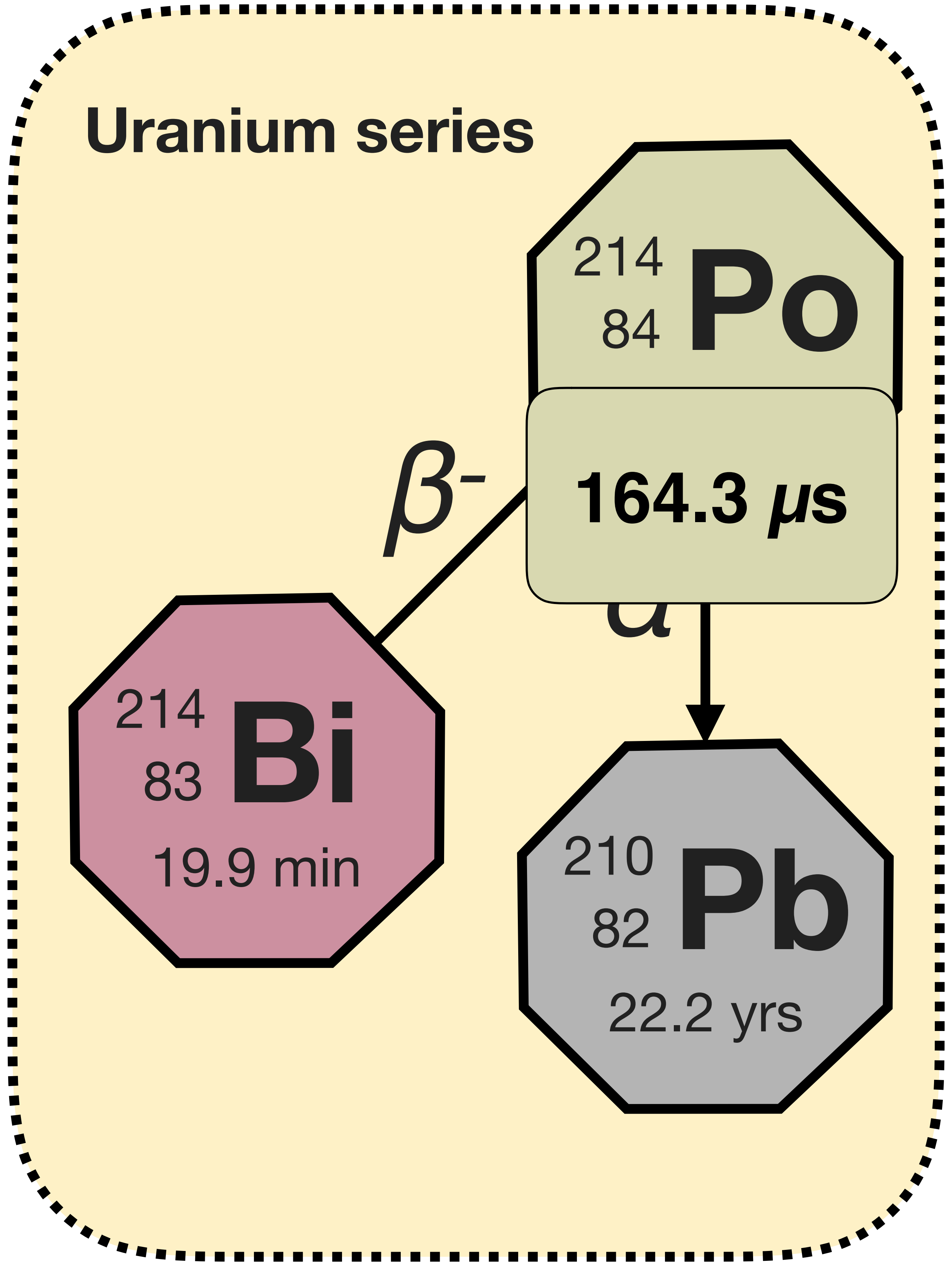

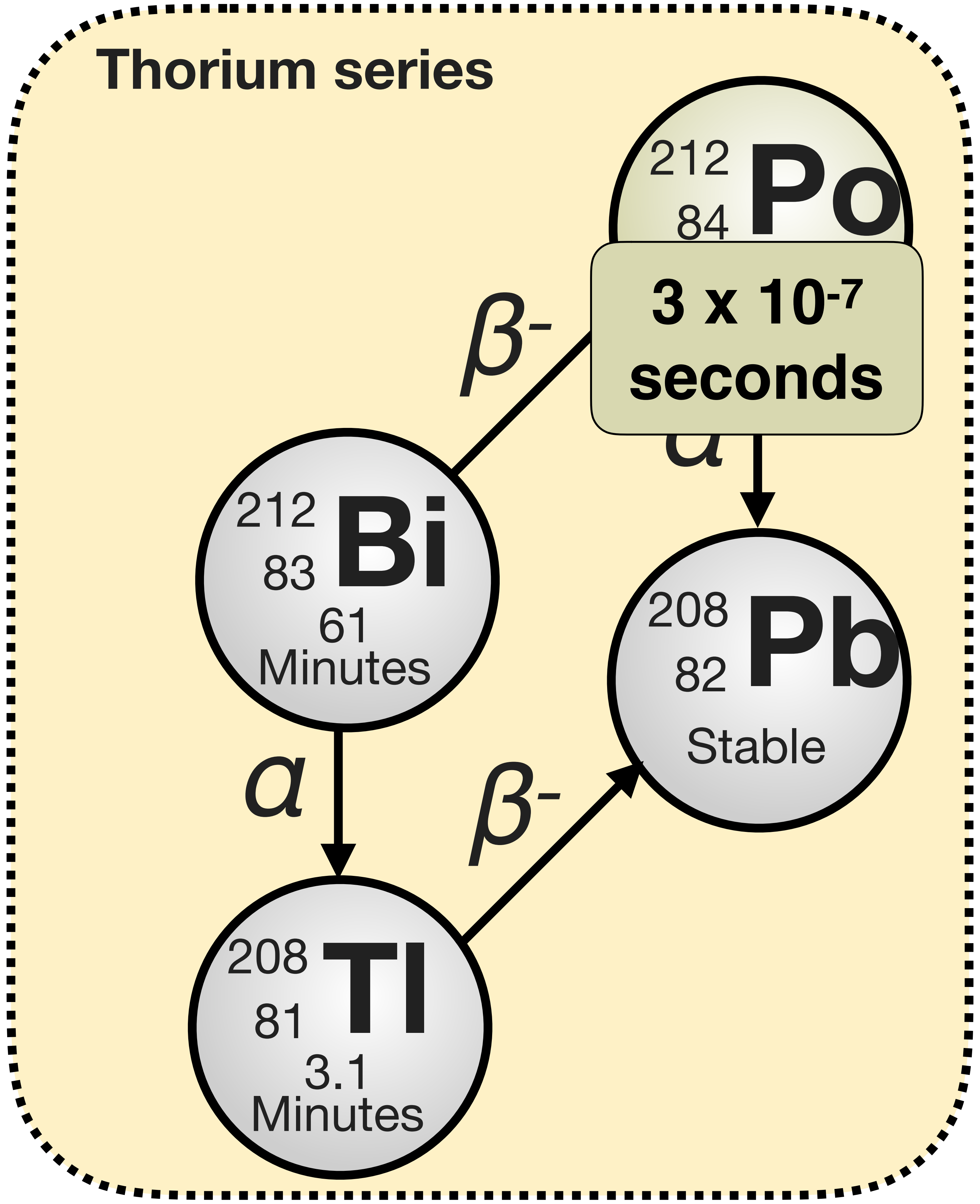

Backgrounds to double-beta experiments

- **2νββ high-energy tail**
- **Cosmic rays**
- **β-decaying isotopes**
- **External contamination**
- **Detector components**
- **BiPo events**

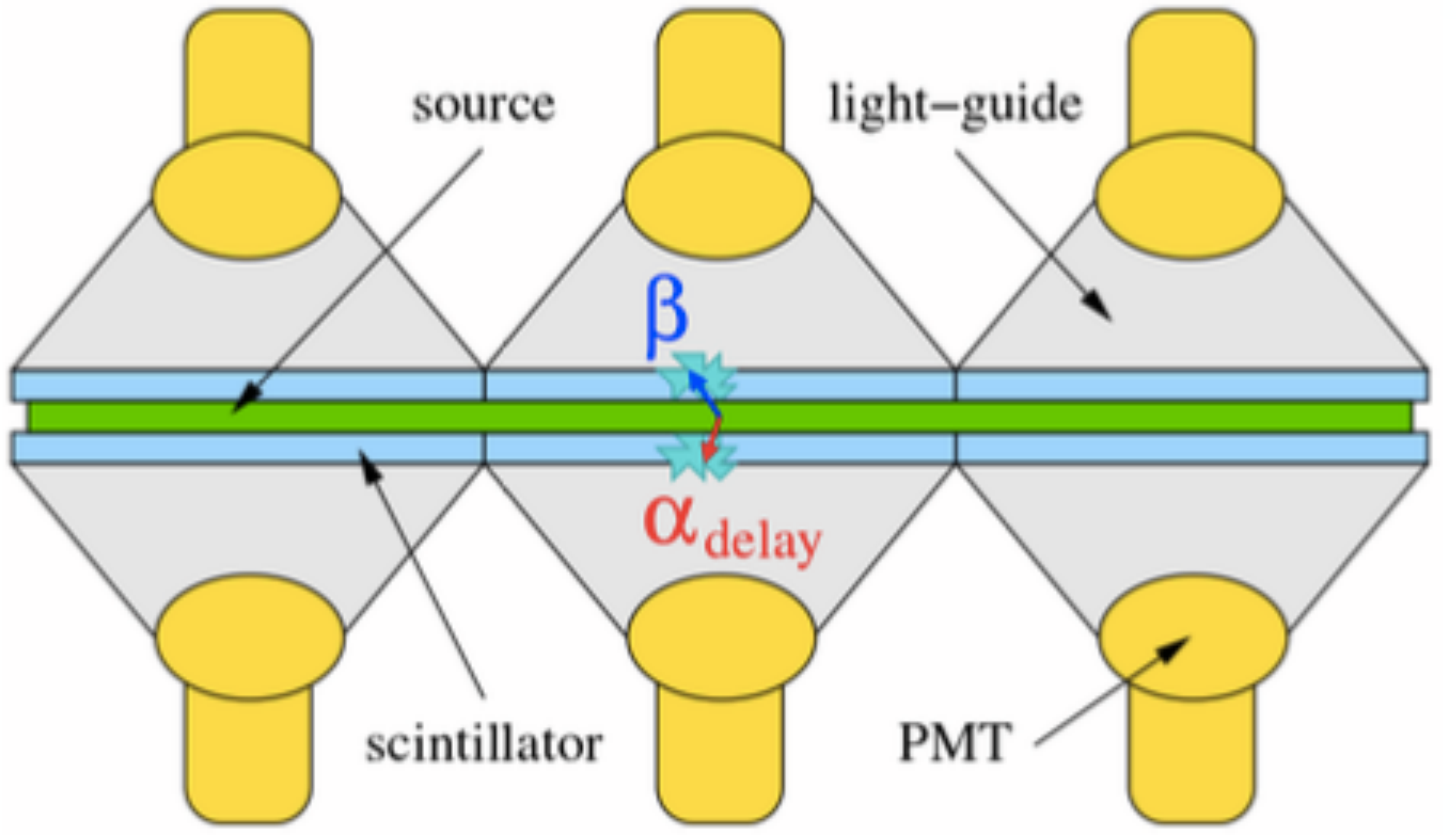

BiPo-3 detector looks for this topology

Canfranc underground lab was formerly Europe's biggest train station

Double-beta decay experiments

Better

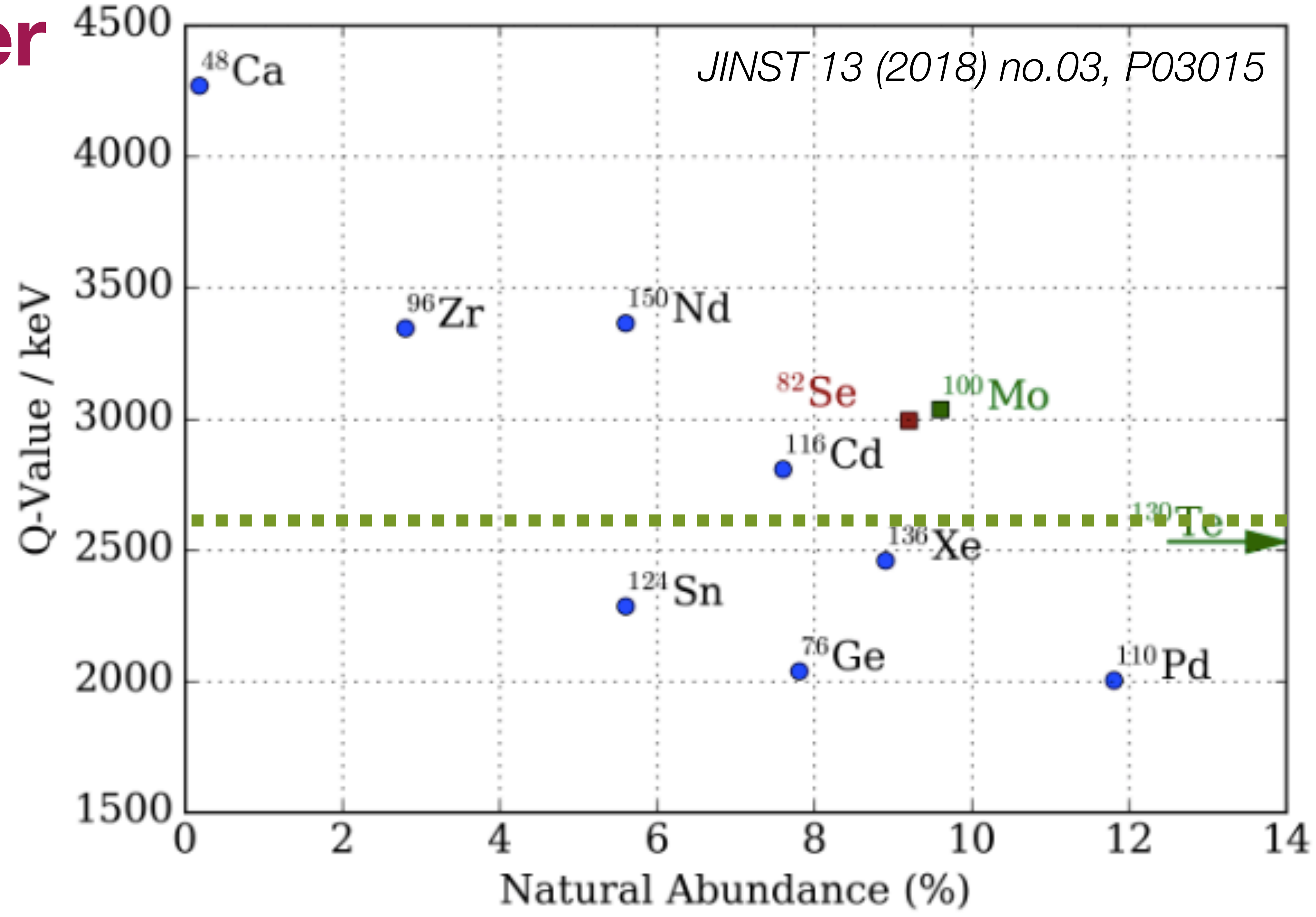

Better

Double-beta decay experiments

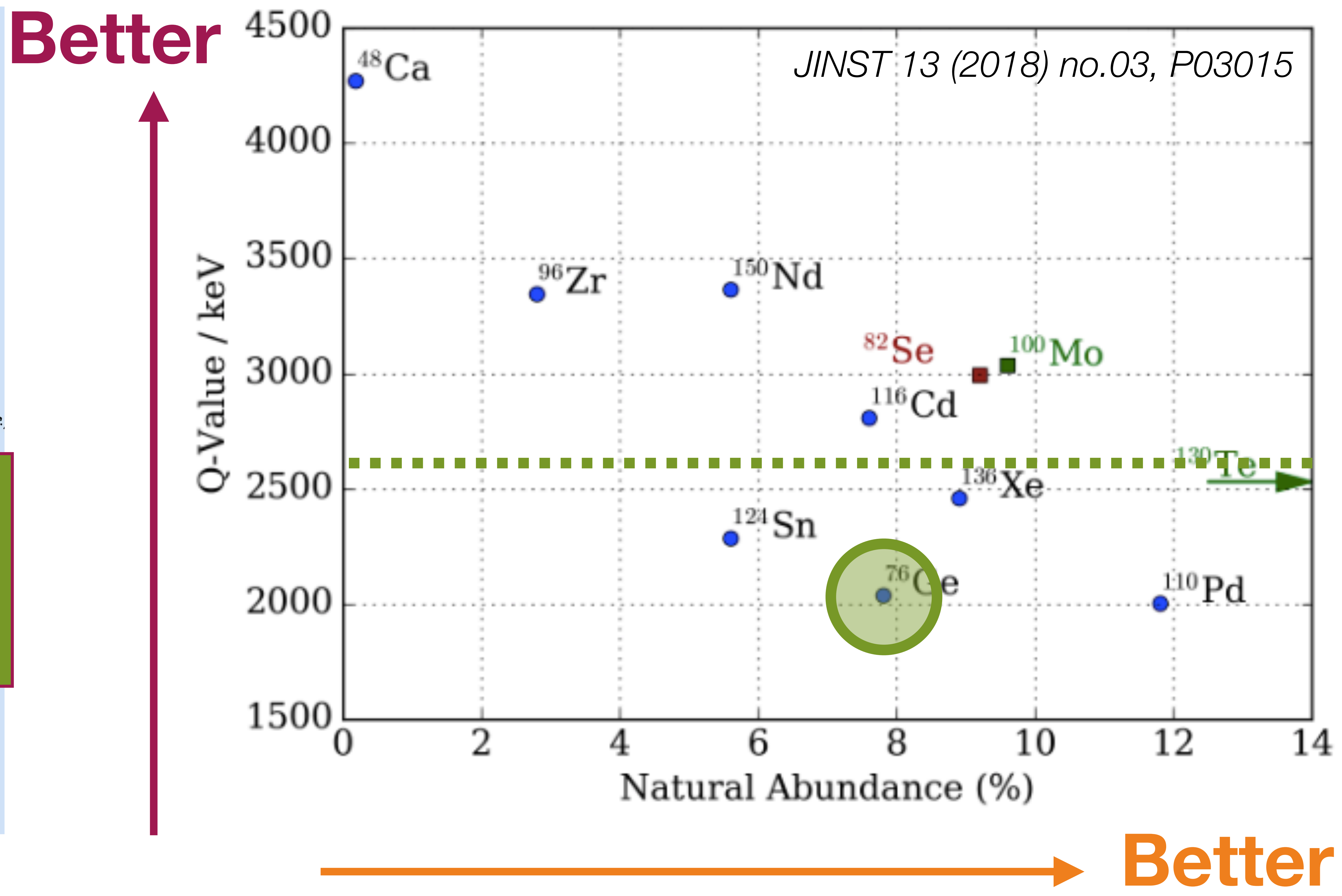

- **ββ source = detector** (^{76}Ge)
- Excellent **efficiency** and **resolution**
- Future : **LEGEND**

LEGEND

Double-beta decay experiments

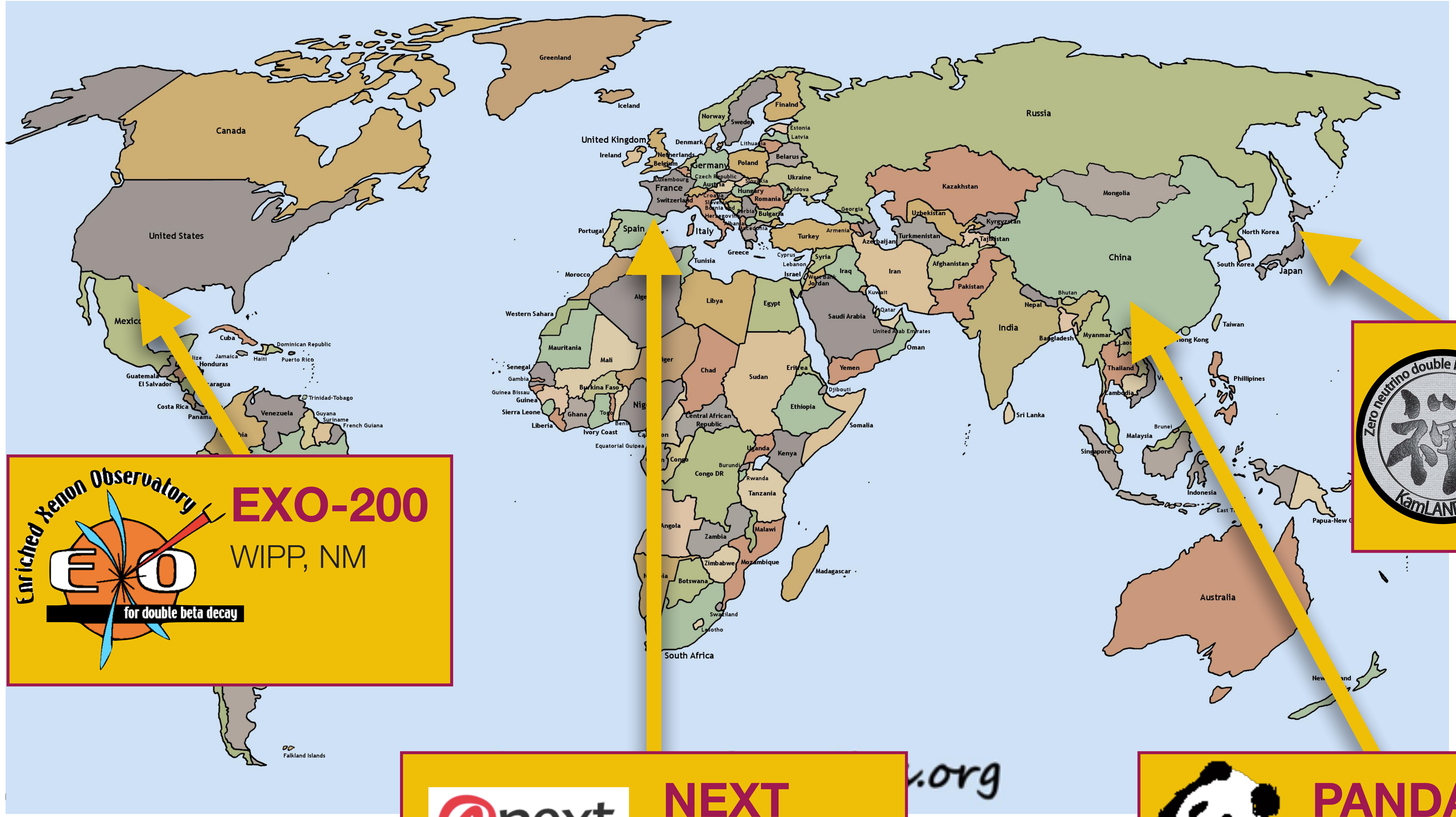

EXO-200
WIPP, NM

NEXT
Canfranc, Spain

PANDA-X III
Sichuan, China

KamLAND-Zen
Kamioka, Japan

Better ↑

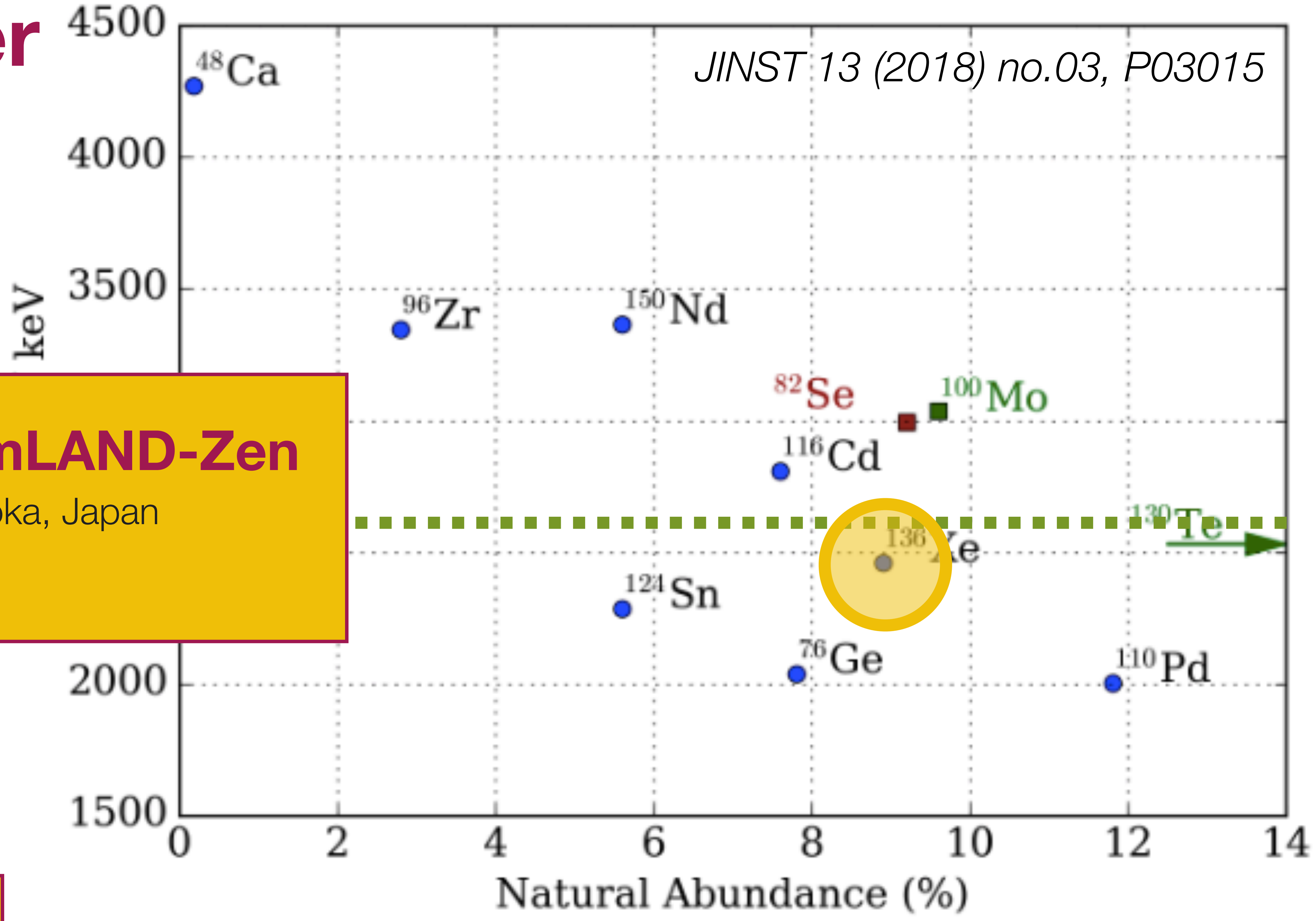

Better →

- Large detectors : **hundreds of kg** of isotope
- KamLAND-Zen has current best 0νββ half-life /$m_{\beta\beta}$ mass limit (**⟨$m_{\beta\beta}$⟩ < 61-165 meV**)
- Future detectors - **nEXO, KamLAND2 Zen**

Double-beta decay experiments

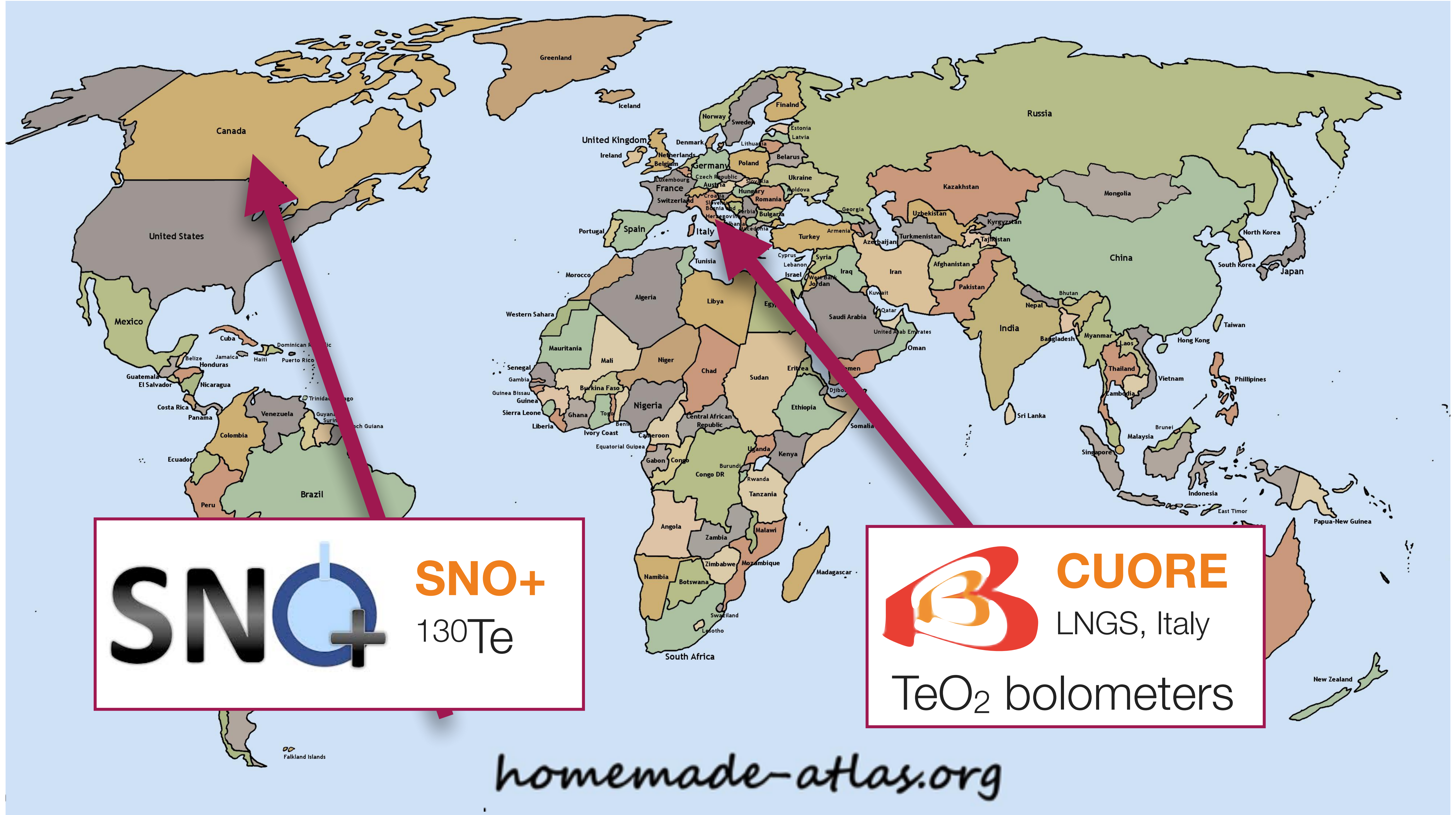

Better

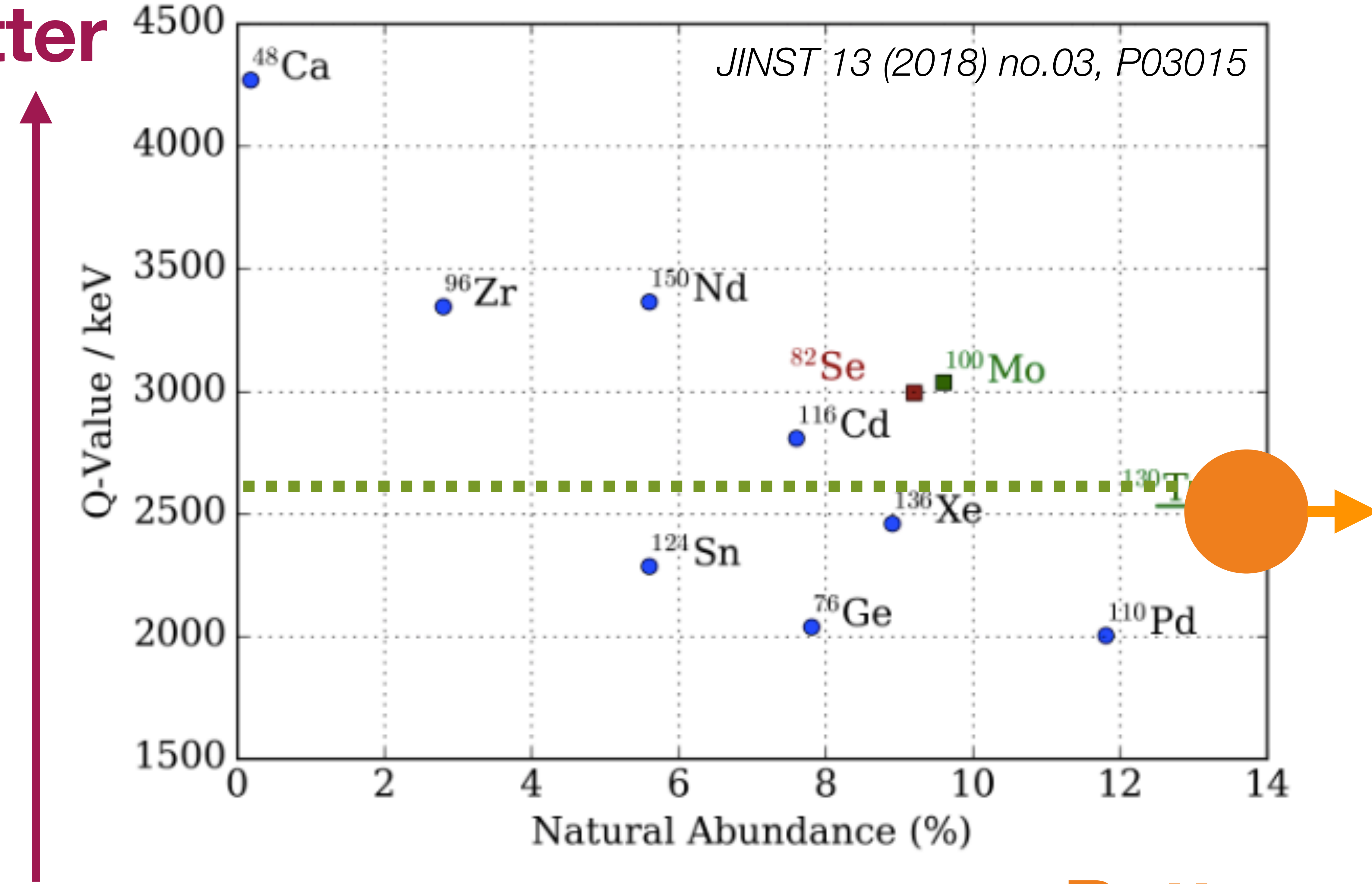

Better

- ^{130}Te has 34% natural **abundance**

Double-beta decay experiments

CANDLES
Kamioka, Japan

Better

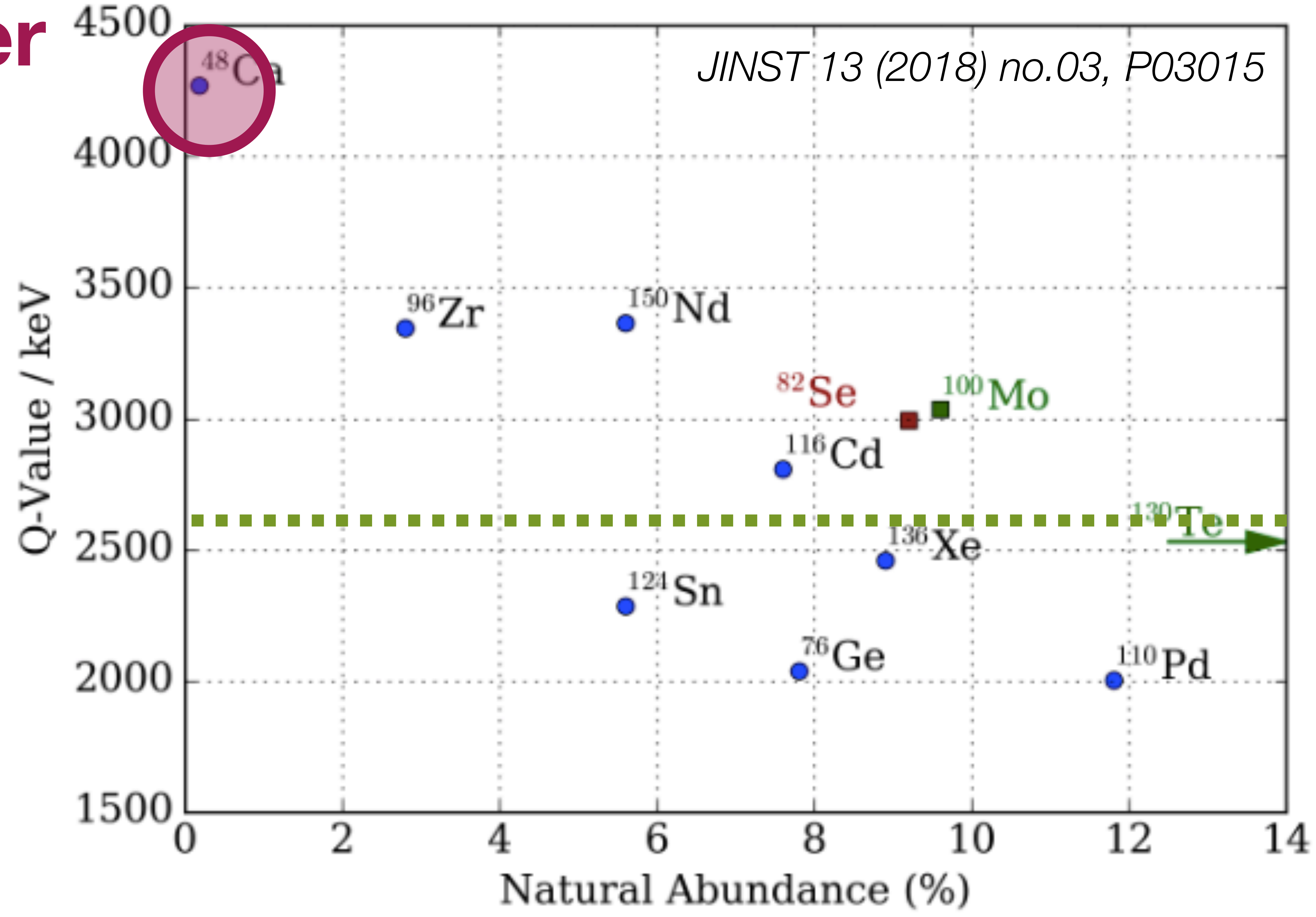

Better

- High **Q-value** makes this an attractive isotope
- Low abundance makes **enrichment** a challenge

Double-beta decay experiments

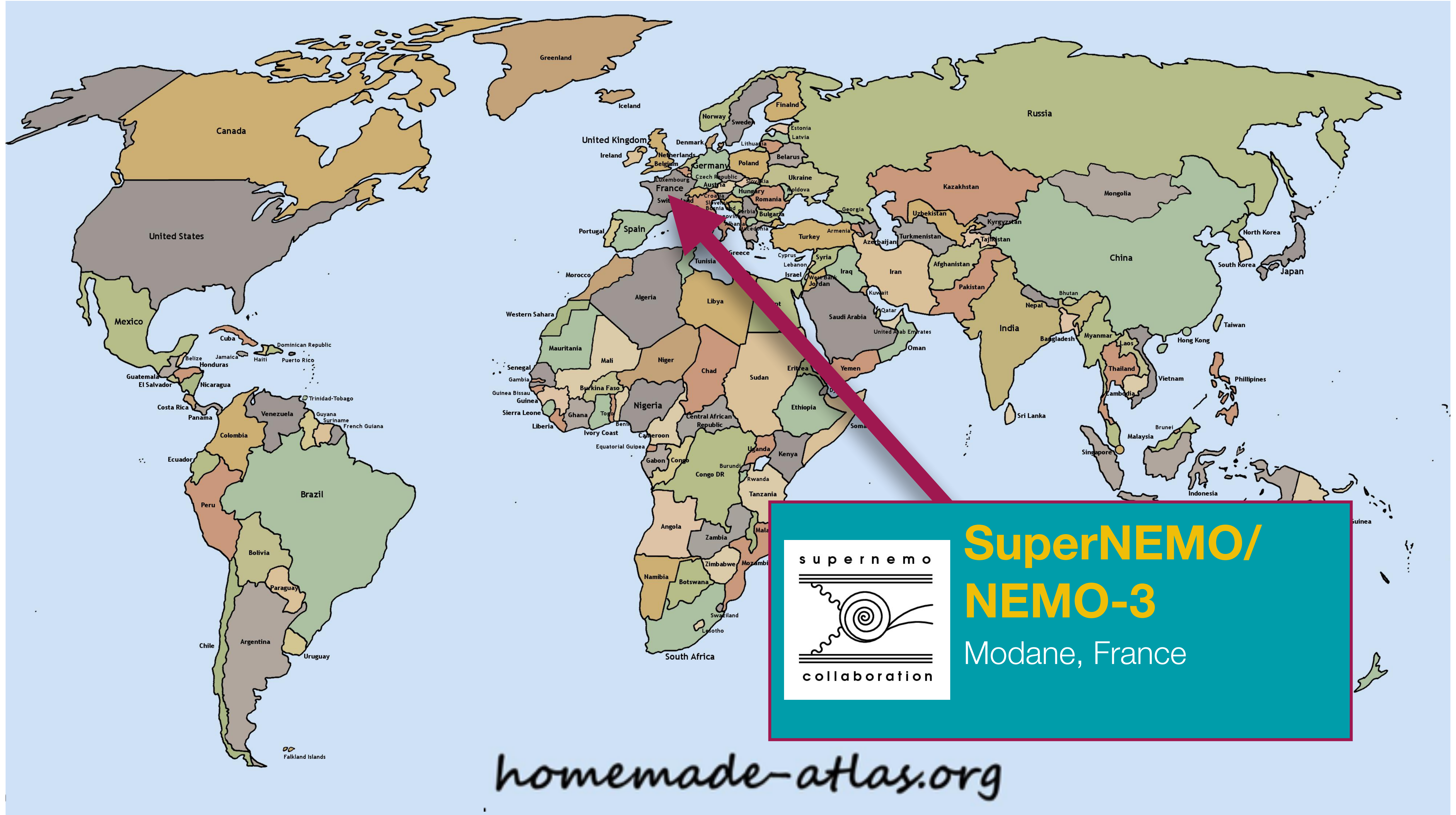

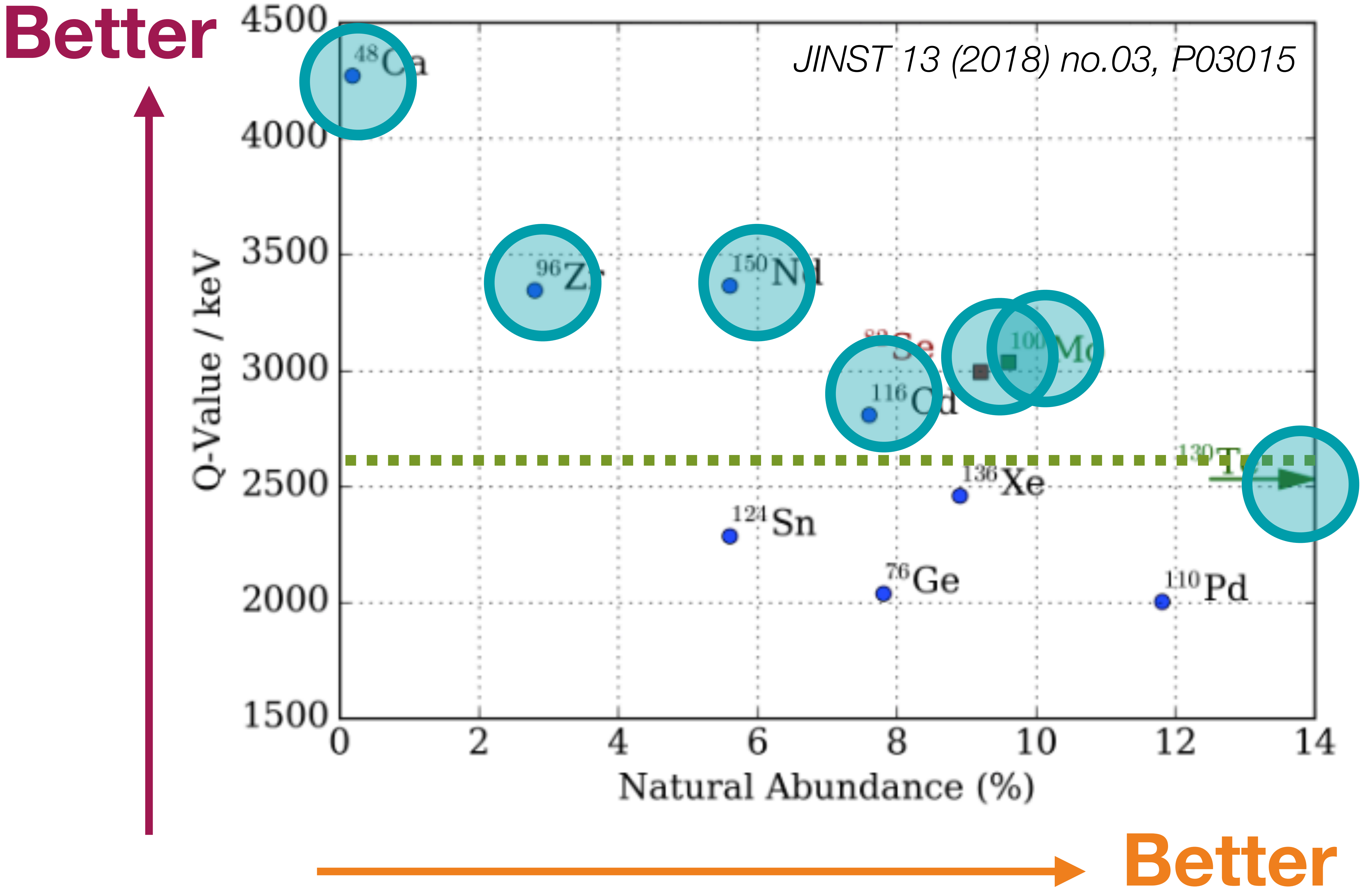

- Source separated from detector - use **any solid isotope**
- SuperNEMO - ^{82}**Se**, NEMO-3 mostly ^{100}**Mo**
- High-granularity tracker-calorimeter design gives **individual electron** energies and trajectories

^{76}Ge experiments

Better

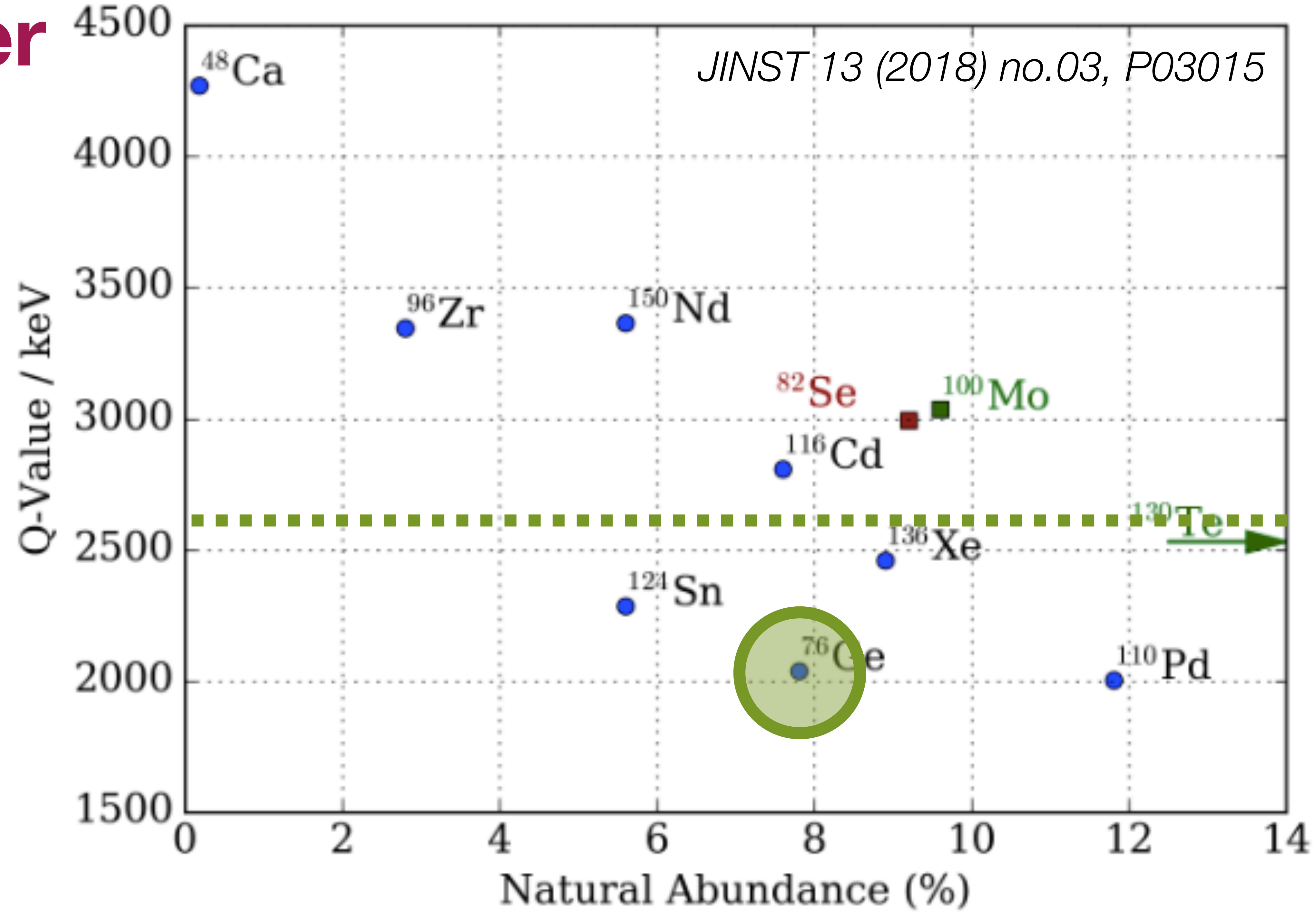

- **ββ source = detector** (^{76}Ge)
- Excellent **efficiency** and **resolution**
- Future : **LEGEND**

GERDA: HPGe detector at Gran Sasso, Italy

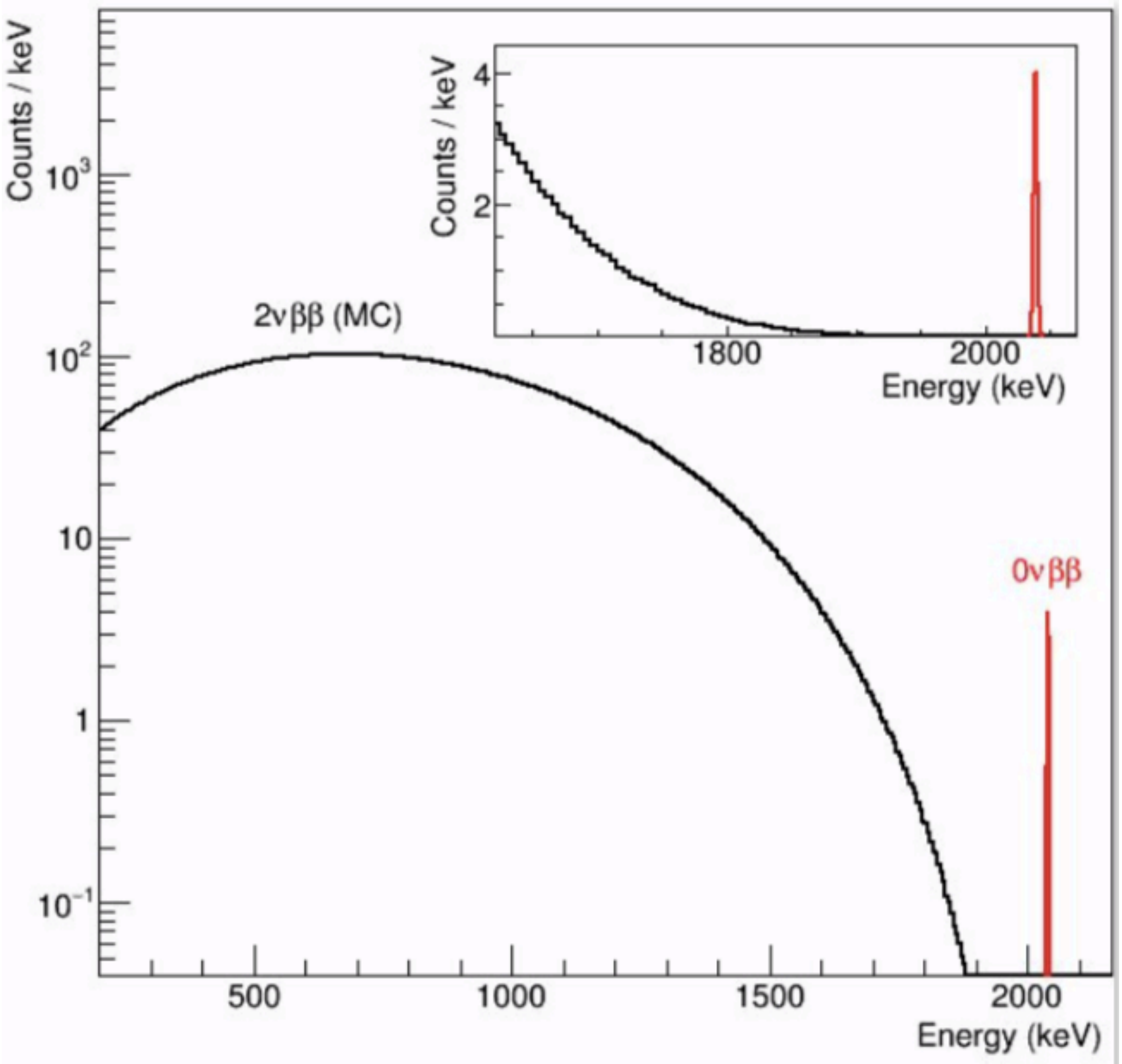

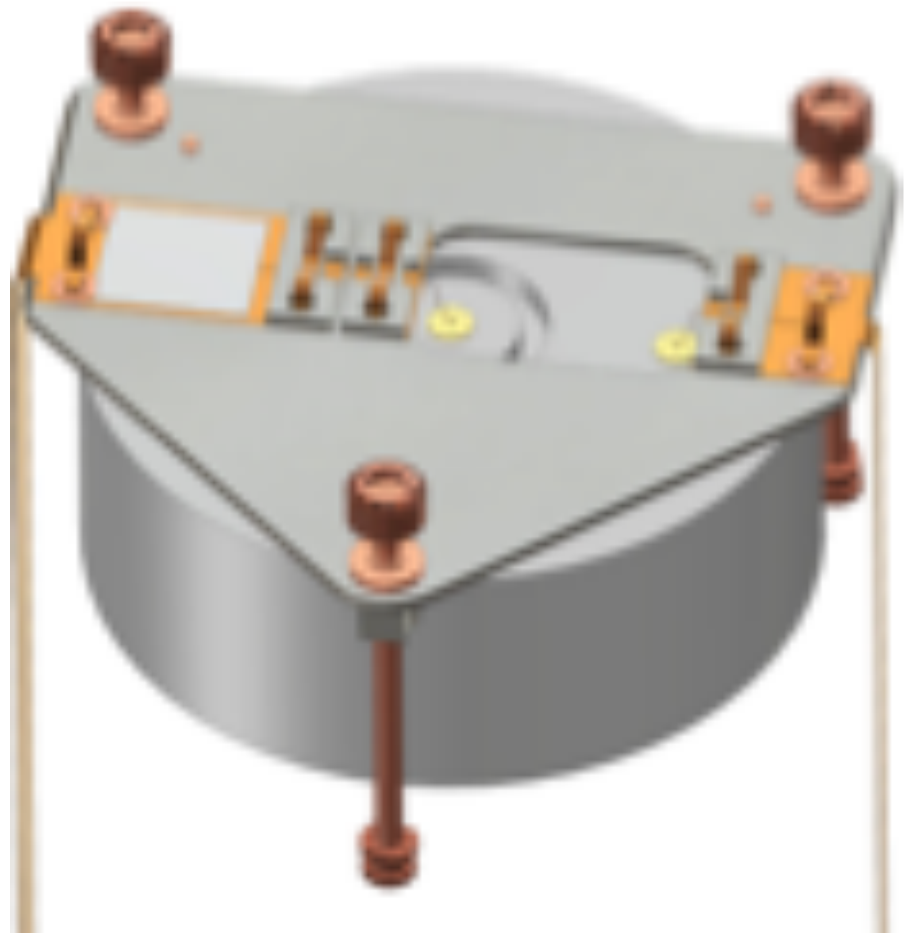

- Germanium detector, enriched to **88% ^{76}Ge** ($Q_{\beta\beta}$ = 2039 keV)
- Intrinsically **pure material** reduces **backgrounds**
- Source = detector: high detection **efficiency**
- Excellent **energy resolution** ($\sigma_E/E \approx 0.2\%$) **zero 2νββ background** in region of interest (3-4 keV)
- Electron range in Ge~1mm: ββ events are **point-like** (vs. multisite gamma backgrounds)

M Agostini, Neutrino 2016

A Zsigmond, Neutrino 2018

*Nature **544** (2017) 47*

GERDA: HPGe detector at Gran Sasso, Italy

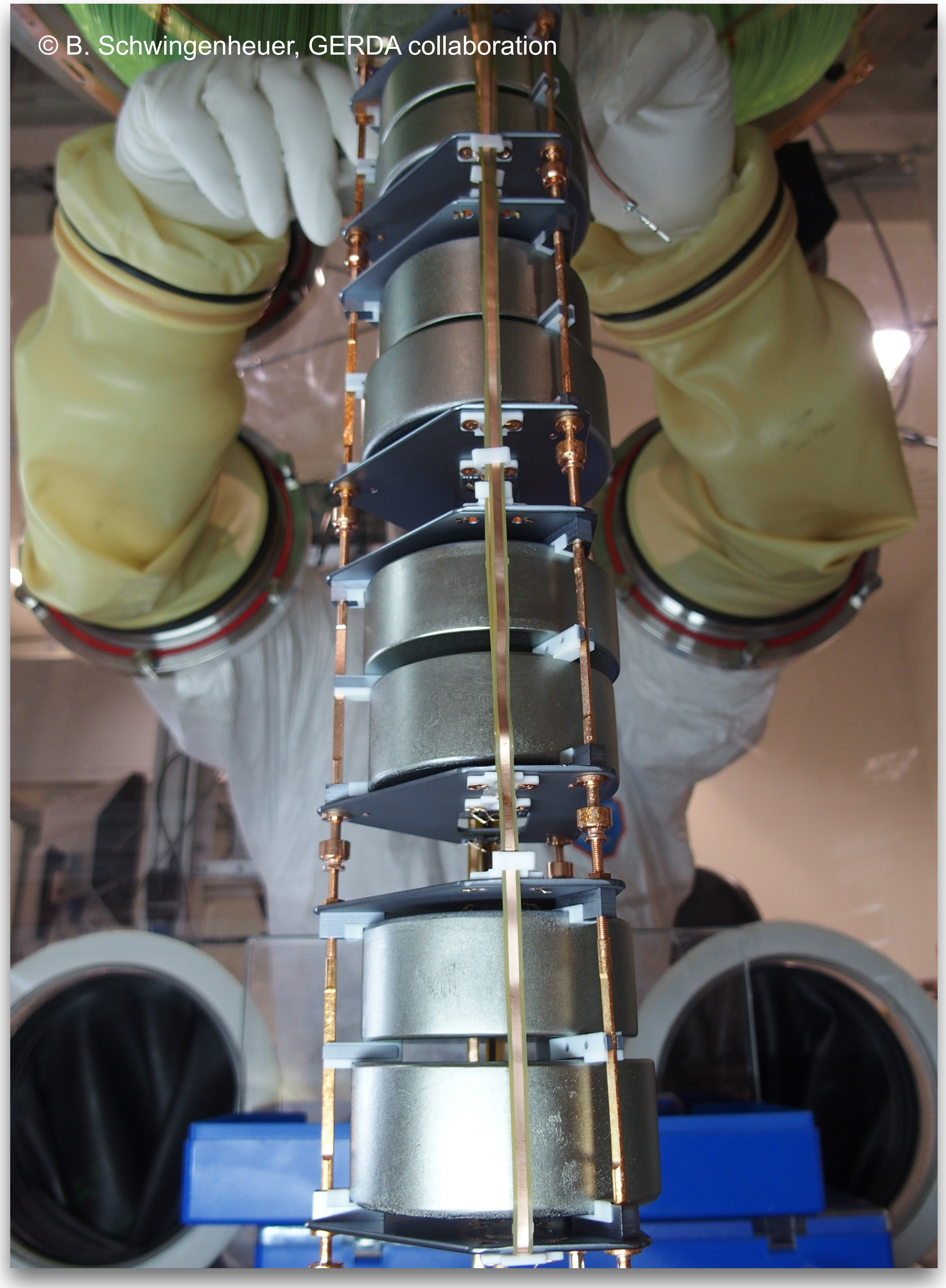

7 strings with **40 detectors** in total (**43.2kg**)

- 7 enriched semi-coaxial (15.6 kg)
- 30 enriched thick window Broad Energy germanium detectors (BEGe) (20.0 kg)
- 3 natural semi-coaxial (7.6 kg)

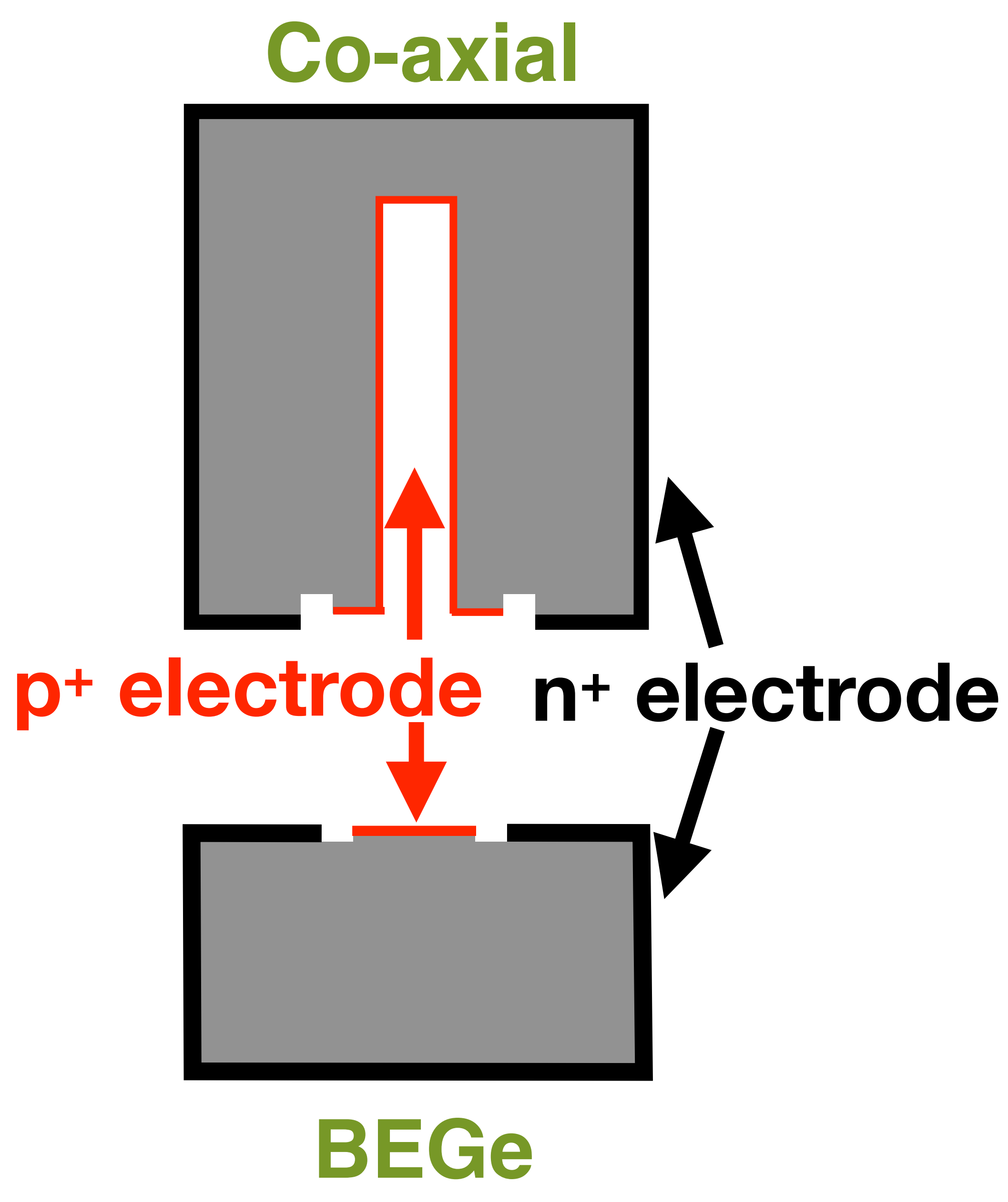

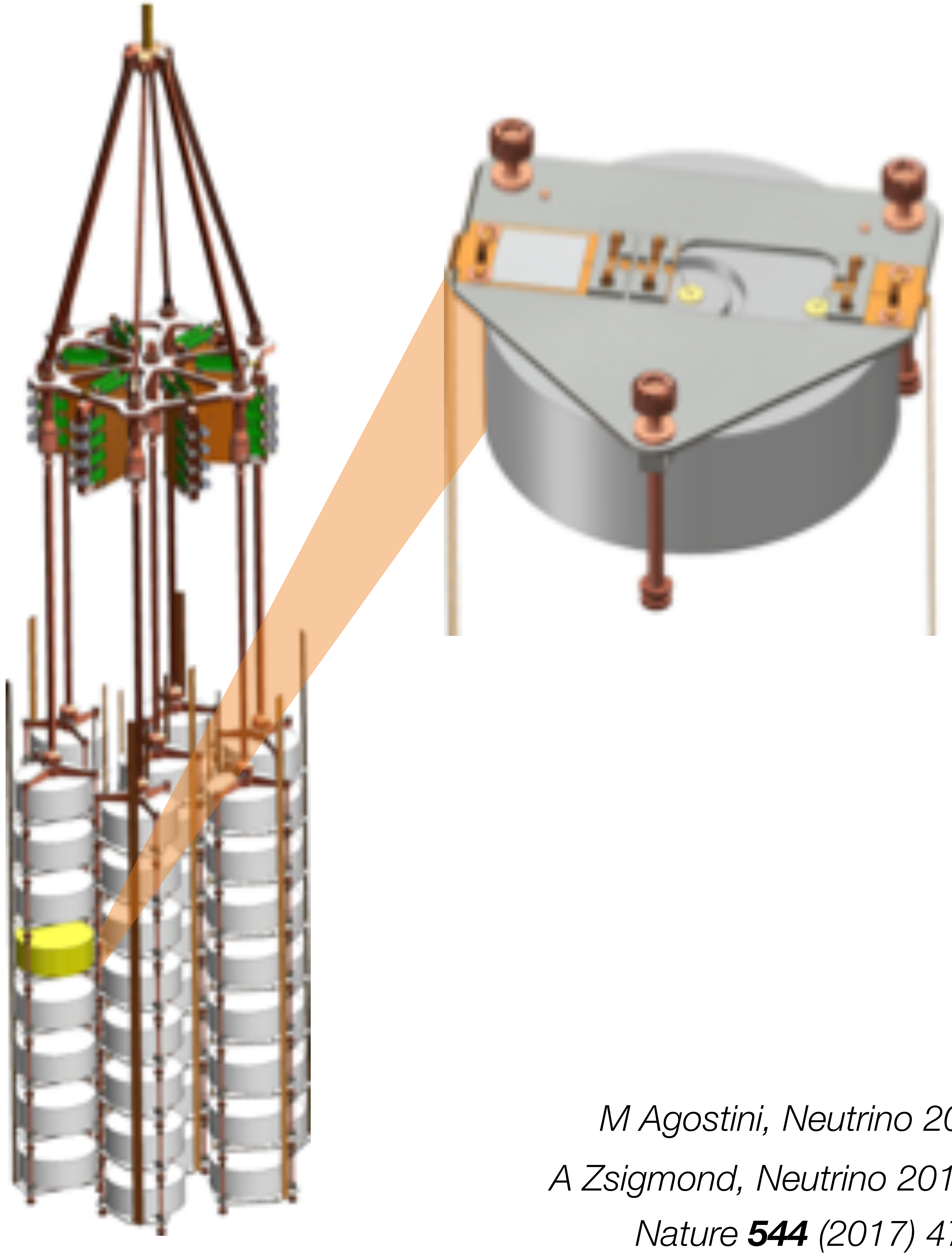

M Agostini, Neutrino 2016

A Zsigmond, Neutrino 2018

*Nature **544** (2017) 47*

GERDA: HPGe detector at Gran Sasso, Italy

LAr electronics

Wavelength-shifting fibres deliver LAr scintillation light to SiPMs for γ and β veto

Low-activity PMTs

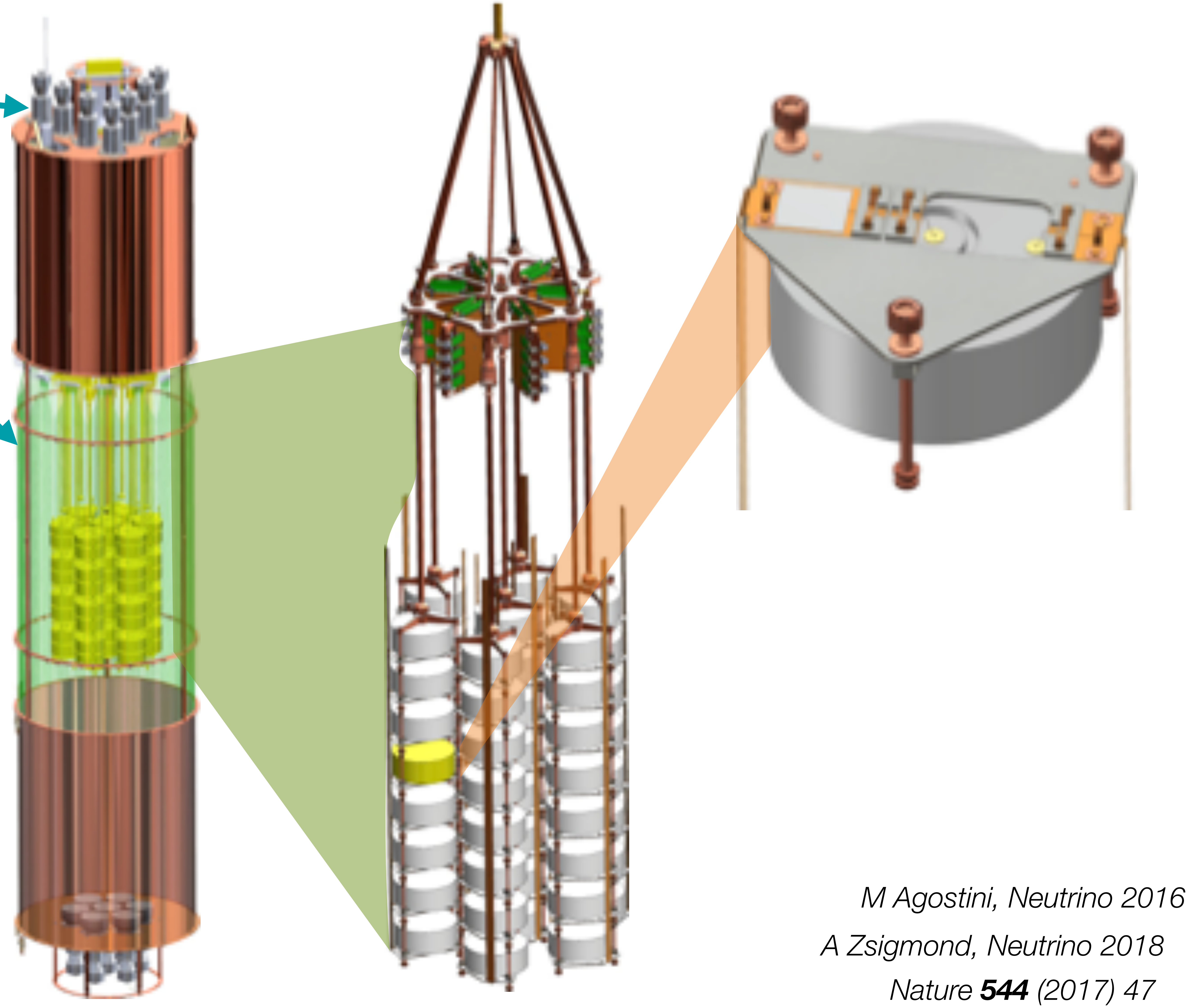

M Agostini, Neutrino 2016

A Zsigmond, Neutrino 2018

*Nature **544** (2017) 47*

GERDA: HPGe detector at Gran Sasso, Italy

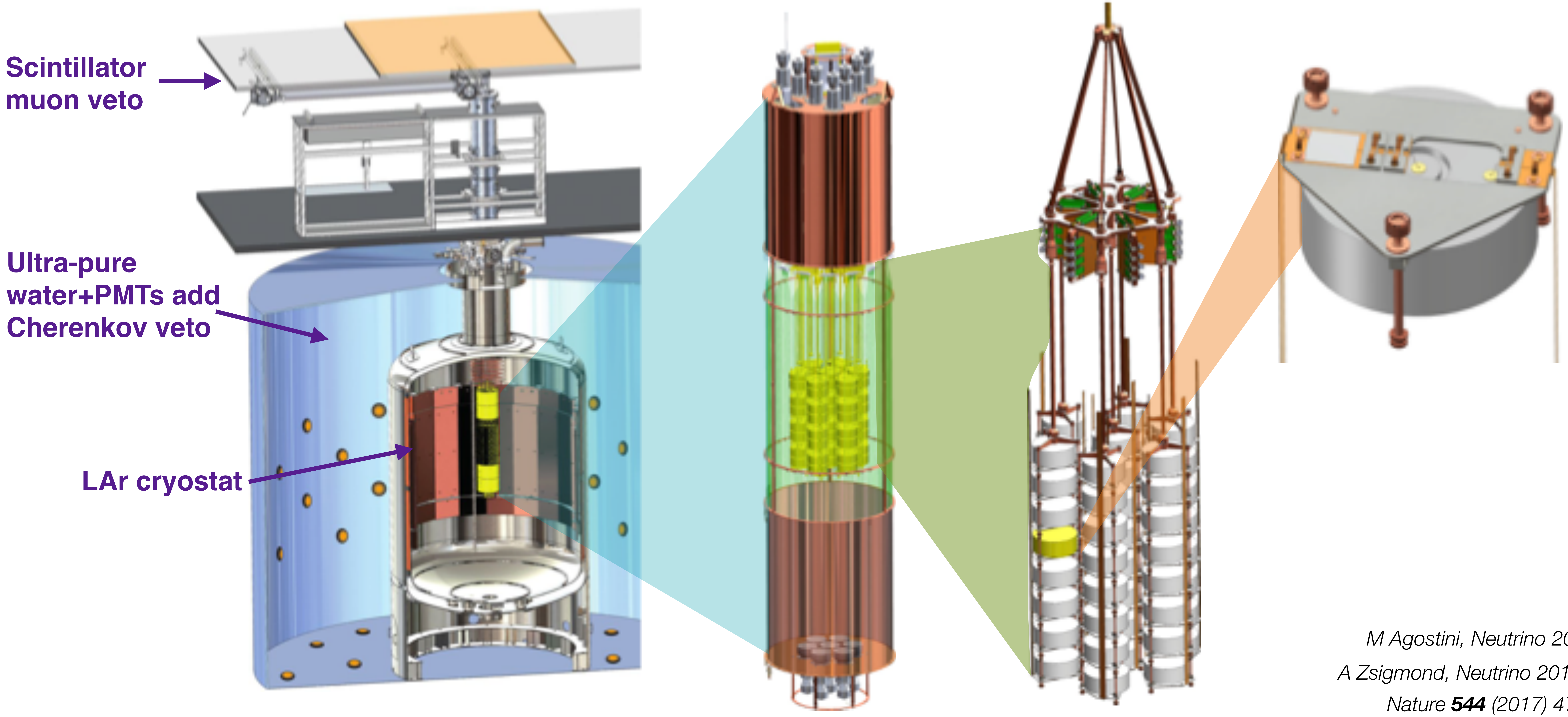

M Agostini, Neutrino 2016

A Zsigmond, Neutrino 2018

Nature ***544*** *(2017) 47*

GERDA: HPGe detector at Gran Sasso, Italy

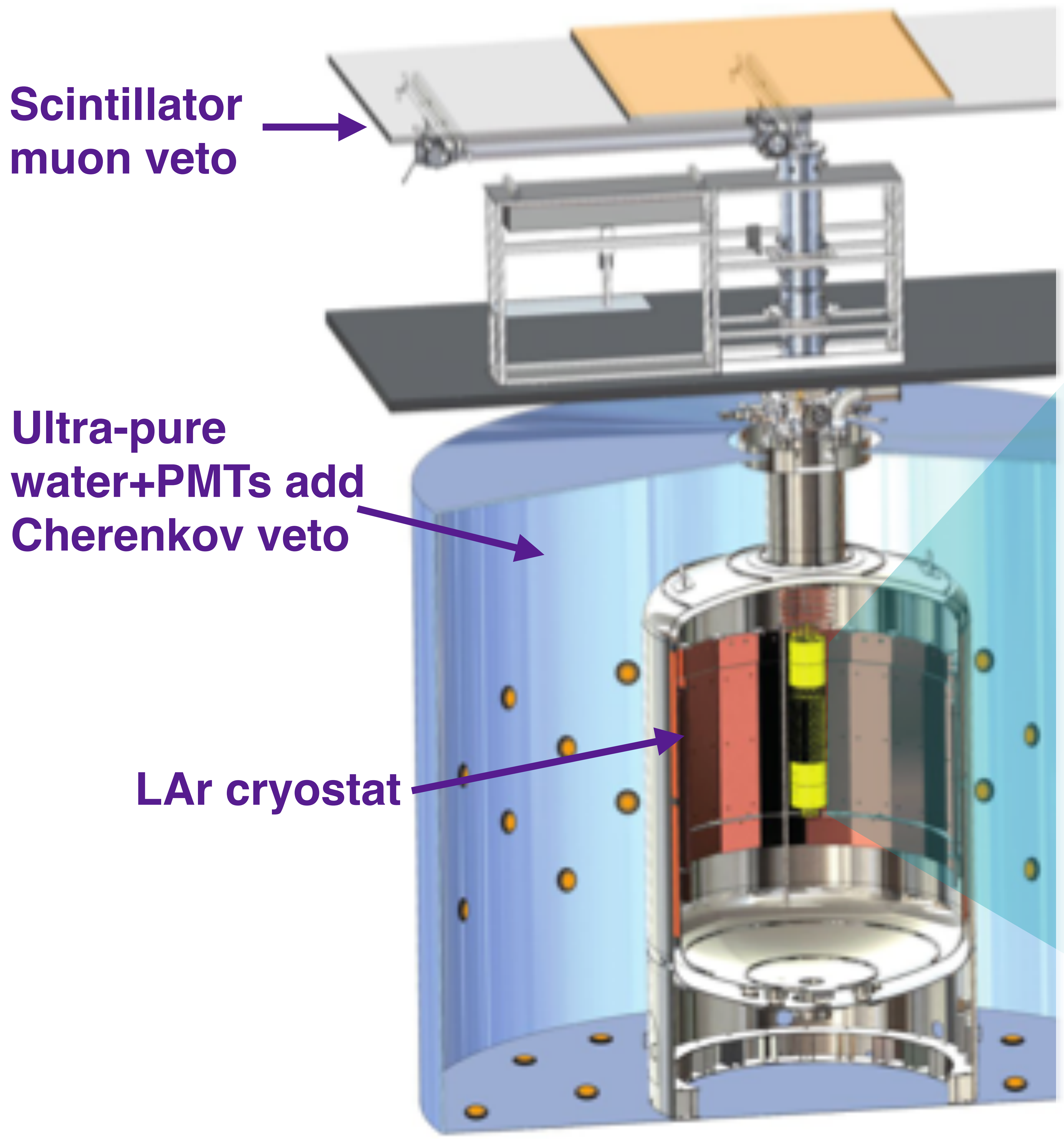

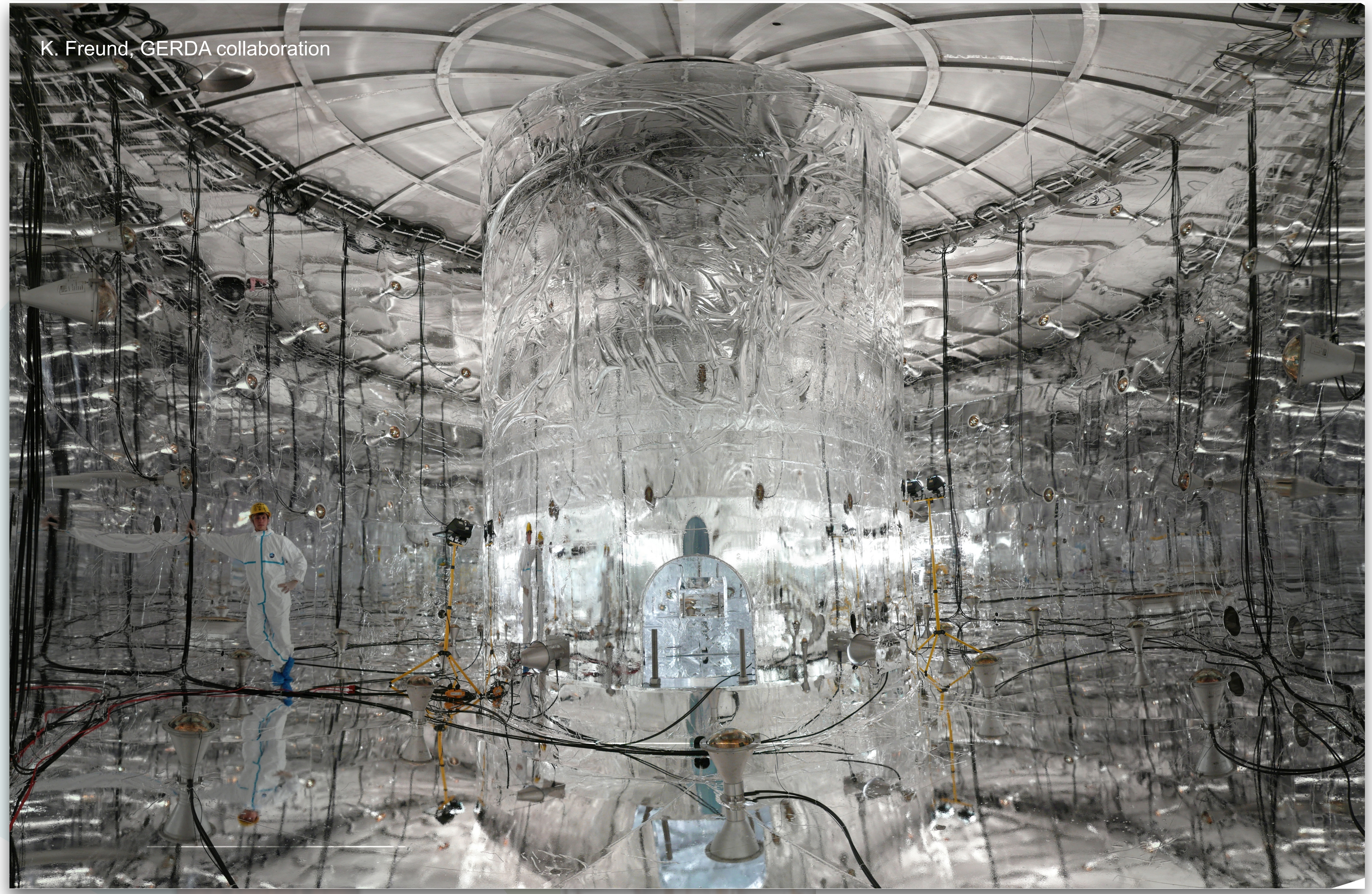

M Agostini, Neutrino 2016

A Zsigmond, Neutrino 2018

*Nature **544** (2017) 47*

How GERDA got background-free

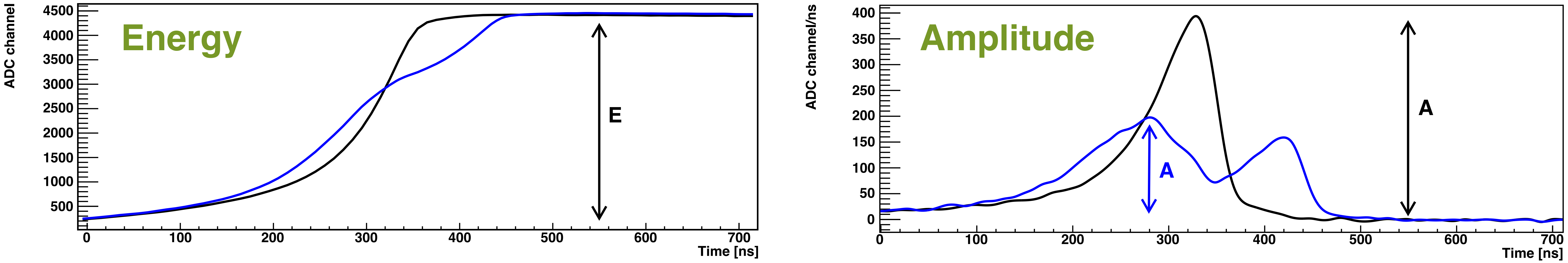

Pulse shape (energy and amplitude) distinguishes **single (ββ)** vs **multi-site (background)** events. Plots for BEGe detector.

2011 JINST 6 P04005

How GERDA got background-free

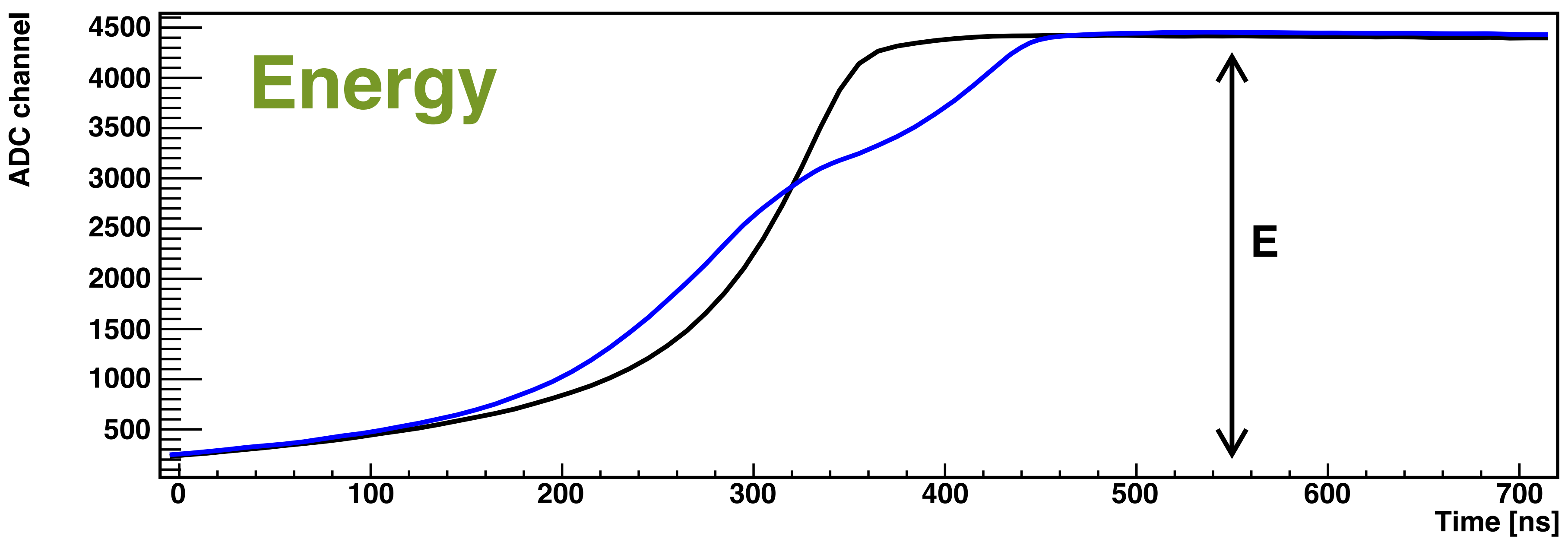

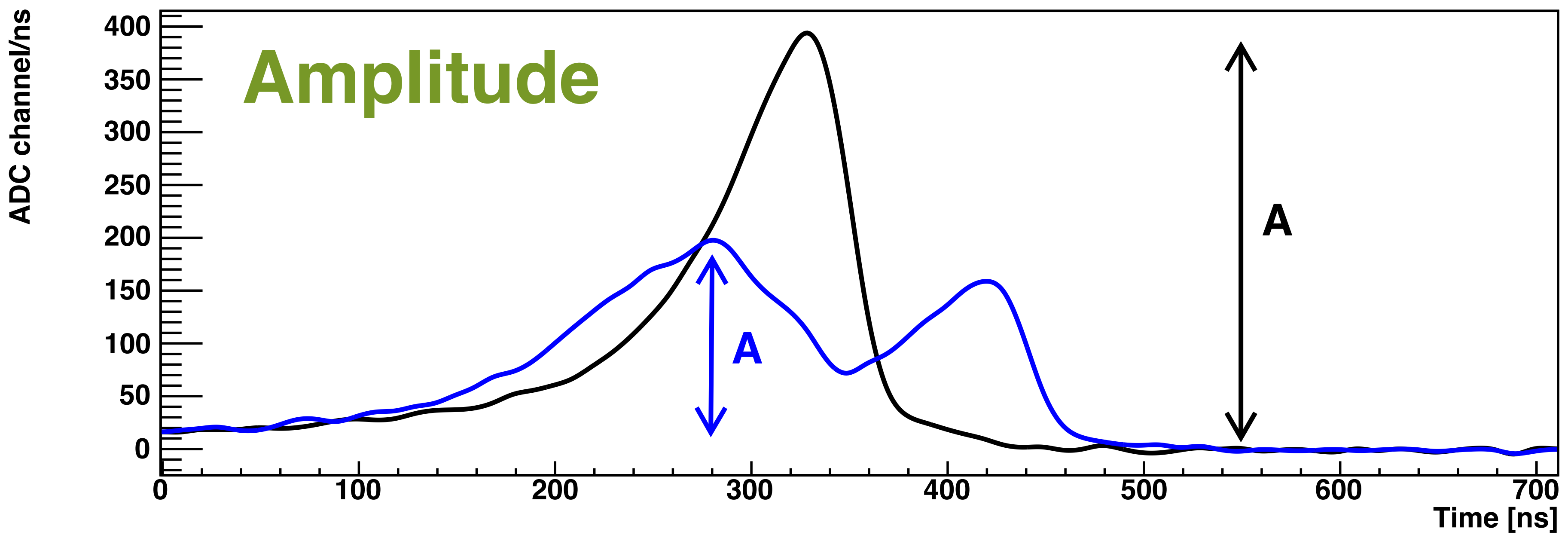

Pulse shape (energy and amplitude) distinguishes **single (ββ)** vs **multi-site (background)** events. Plots for BEGe detector.

2011 JINST 6 P04005

Muon veto from plastic scintillator and Cherenkov light in water: **> 99% rejection efficiency**

EPJ C, 2016, Vol 76, Number 5, Page 1

How GERDA got background-free

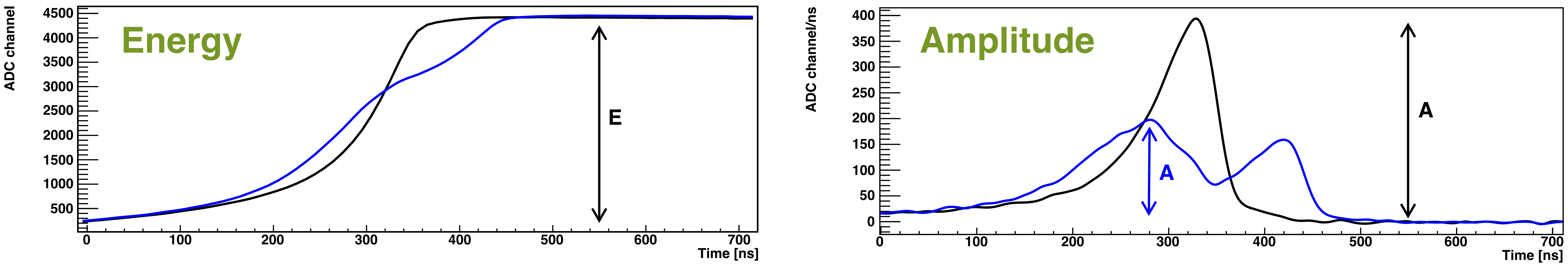

Pulse shape (energy and amplitude) distinguishes **single (ββ)** vs **multi-site (background)** events. Plots for BEGe detector.

2011 JINST 6 P04005

Muon veto from plastic scintillator and Cherenkov light in water: **> 99% rejection efficiency**

EPJ C, 2016, Vol 76, Number 5, Page 1

before veto **after veto**

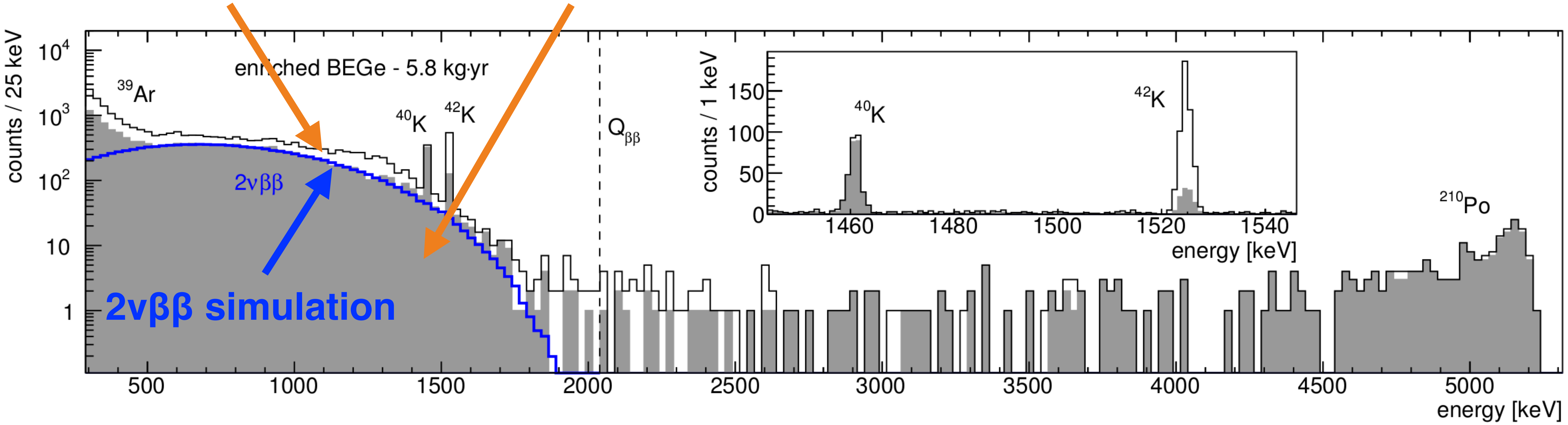

Liquid argon veto removes external backgrounds to give clean **2νββ spectrum** (98% efficiency. Plot for BEGe detectors.

*Nature **544** (2017) 47-52*

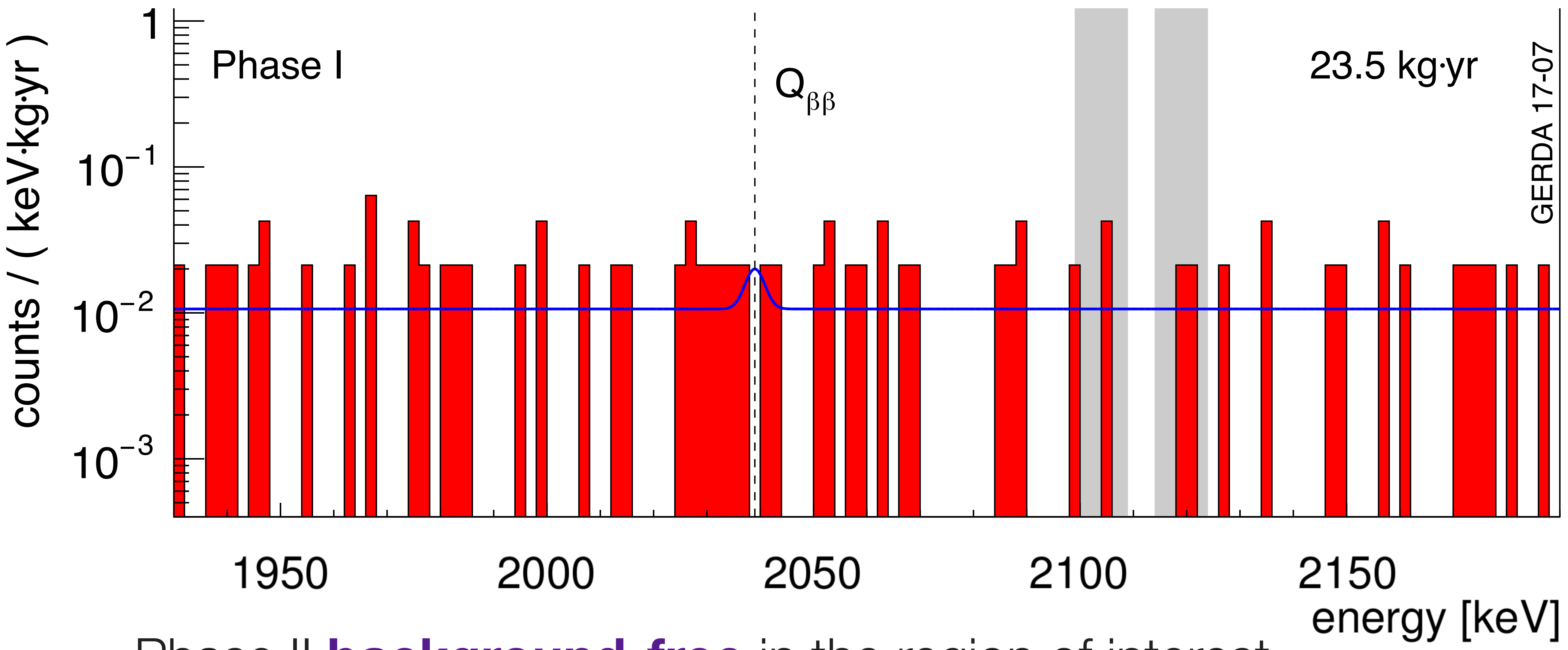

- Phase II **background-free** in the region of interest

$$1.0^{+0.6}_{-0.4} \times 10^{-3} \text{cts} \ / \ (\text{keV} \cdot \text{kg} \cdot \text{yr})$$

- **Limit** set at 90% confidence level: 2 events in 34.4 kg·yr, or

$$T^{0\nu}_{1/2} > 8.0 \times 10^{25} \text{yr}$$

for light Majorana neutrino exchange:

$$m_{\beta\beta} < 0.12 - 0.26 \text{eV}$$

- At **design exposure** of 100 kg.yr, **sensitivity > 10^{26} yr**

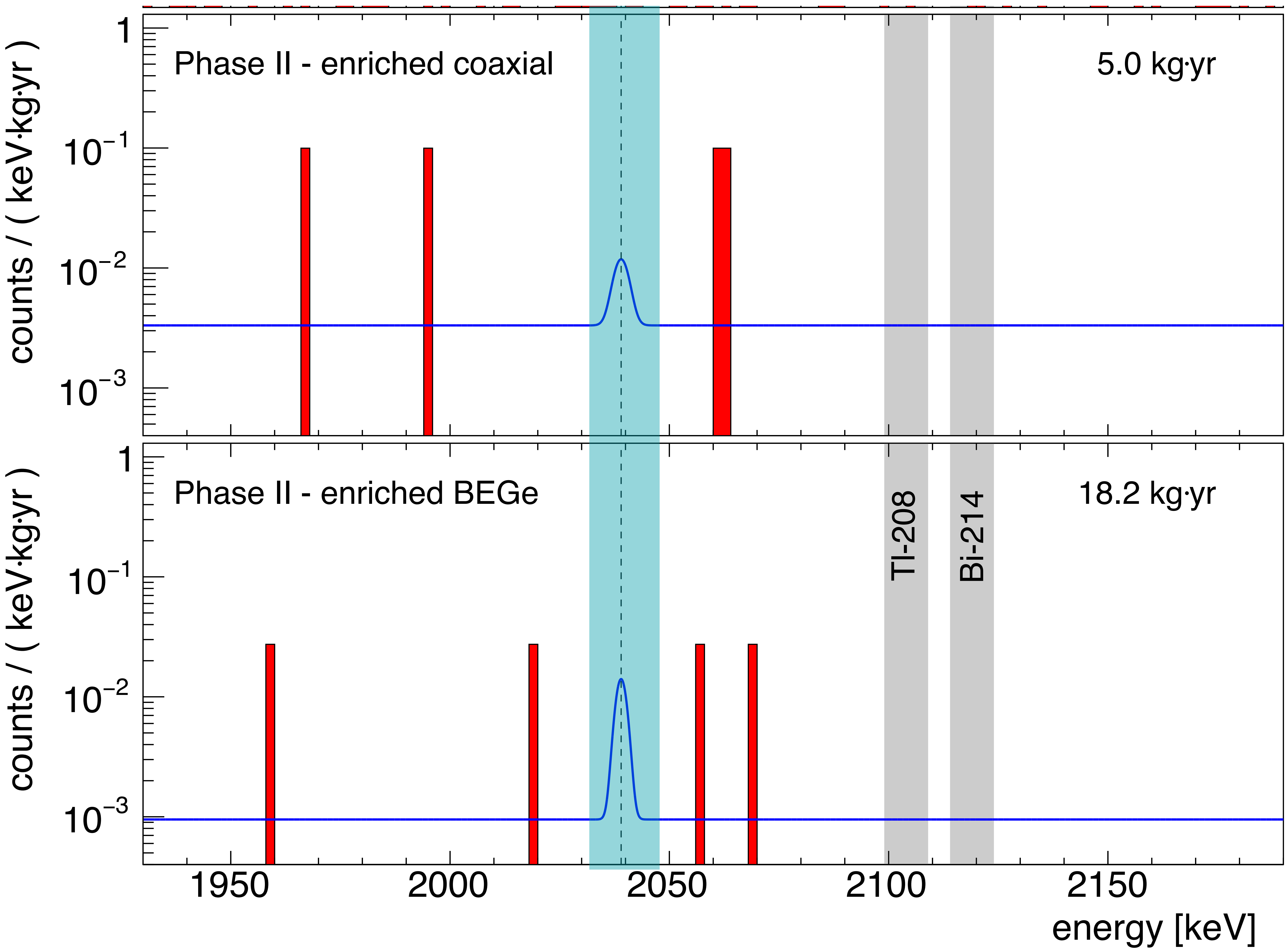

GERDA cryostat can hold 200kg of detectors

Phys. Rev. Lett. 120 (2018) 132503

More ^{76}Ge: MAJORANA Demonstrator at Sanford, SD

- Enriched **p-type point-contact HPGe detectors** have
  - Excellent **pulse-shape discrimination**
  - Benefits of standard **coaxial HPGe** detectors
  - Low capacitance (~1pF): excellent low-energy resolution

Small, dimple-like central contact

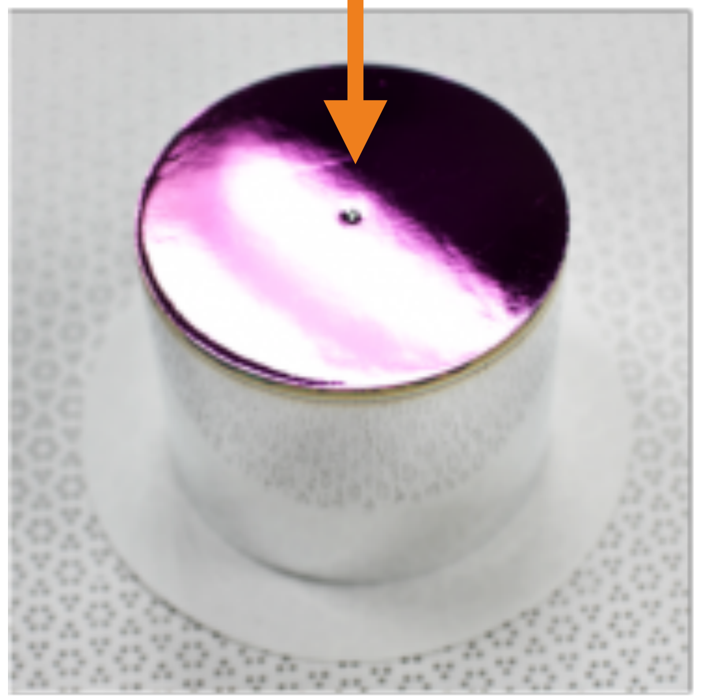

PPC HPGe Detector

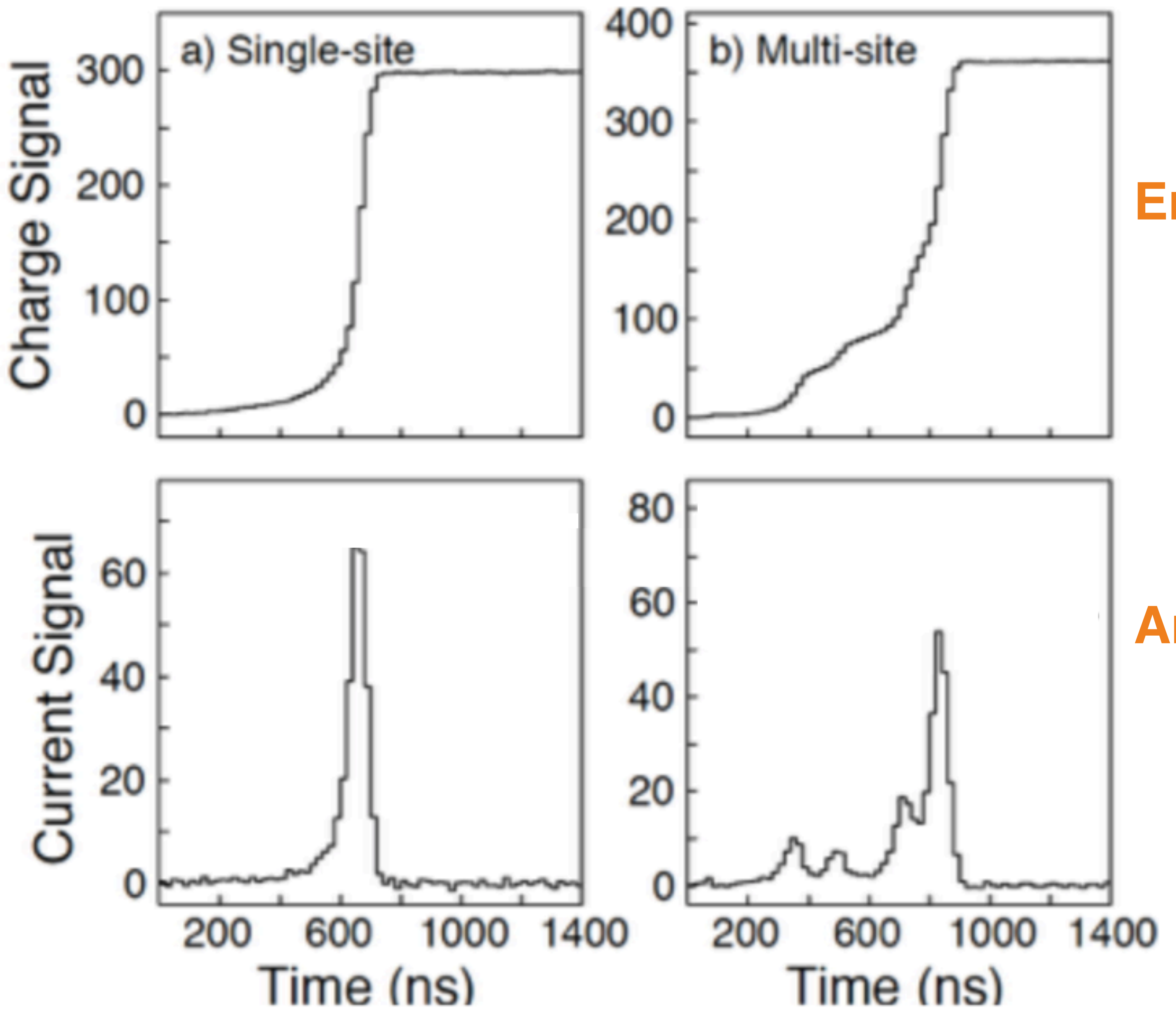

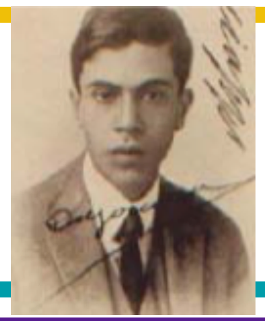

More ^{76}Ge: MAJORANA Demonstrator at Sanford, SD

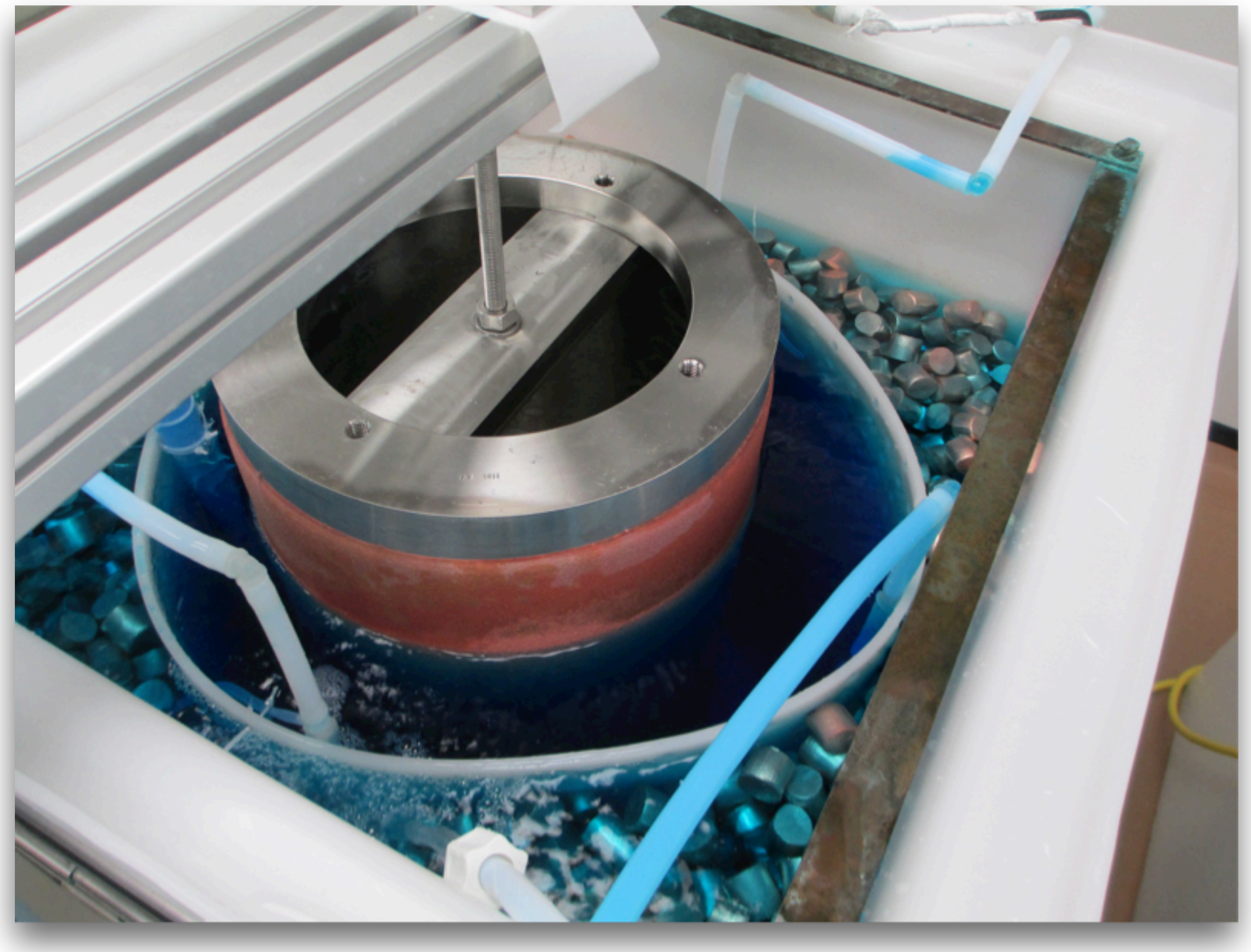

- All components made from highly **radiopure materials**
  - **Underground electroformed copper**
  - **NXT-85** cleanroom-manufactured Teflon

10x less radioactive than commercial copper

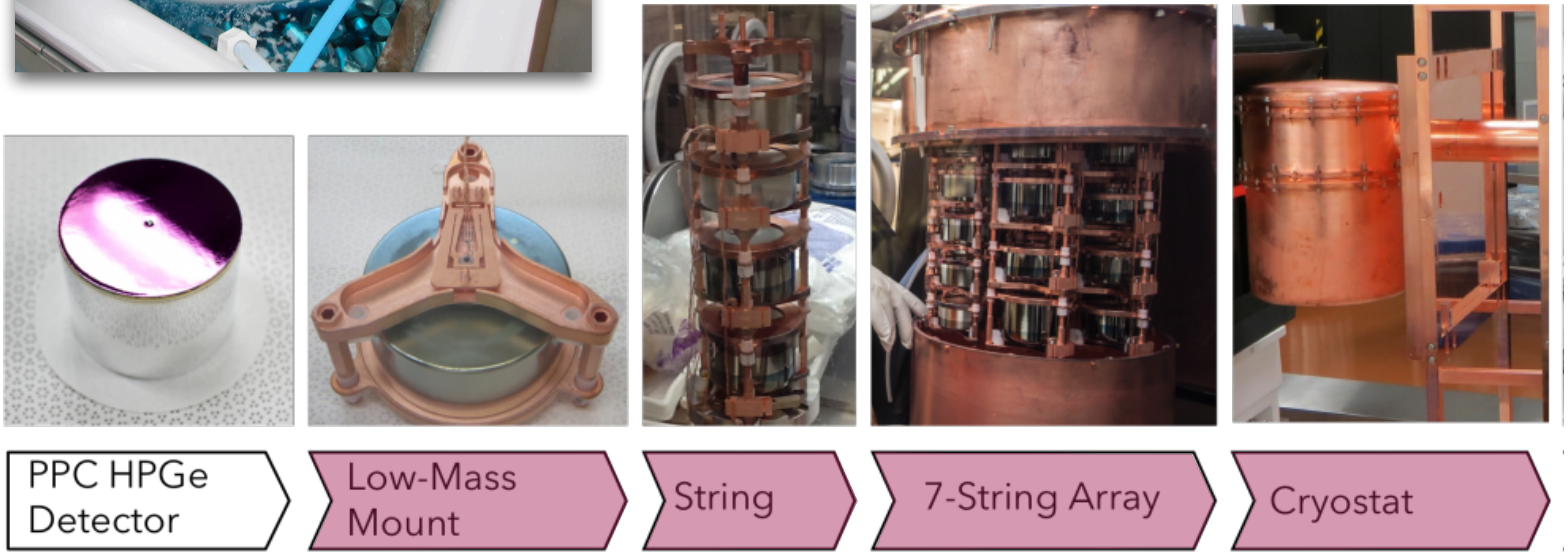

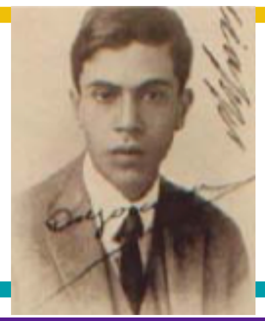

More ^{76}Ge: MAJORANA Demonstrator at Sanford, SD

- **Modular** design:
  - 2 **independent cryostats** with their own vacuum, electronics, and cooling
  - Each with **7 strings of 4-5 detectors**
- Total **44.1 kg** of germanium detectors
- Assembled in glove box with **purged N_2 environment**

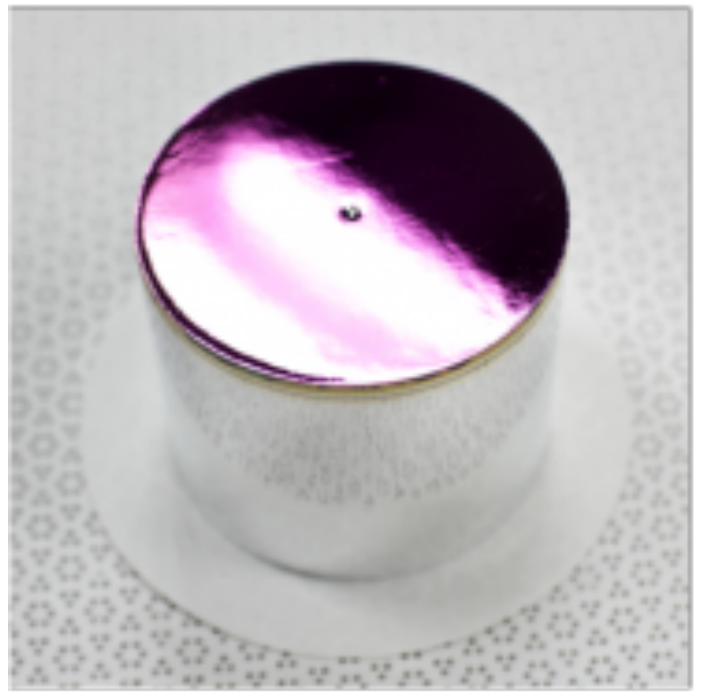



PPC HPGe Detector → Low-Mass Mount → String → 7-String Array → Cryostat

More ^{76}Ge: MAJORANA Demonstrator at Sanford, SD

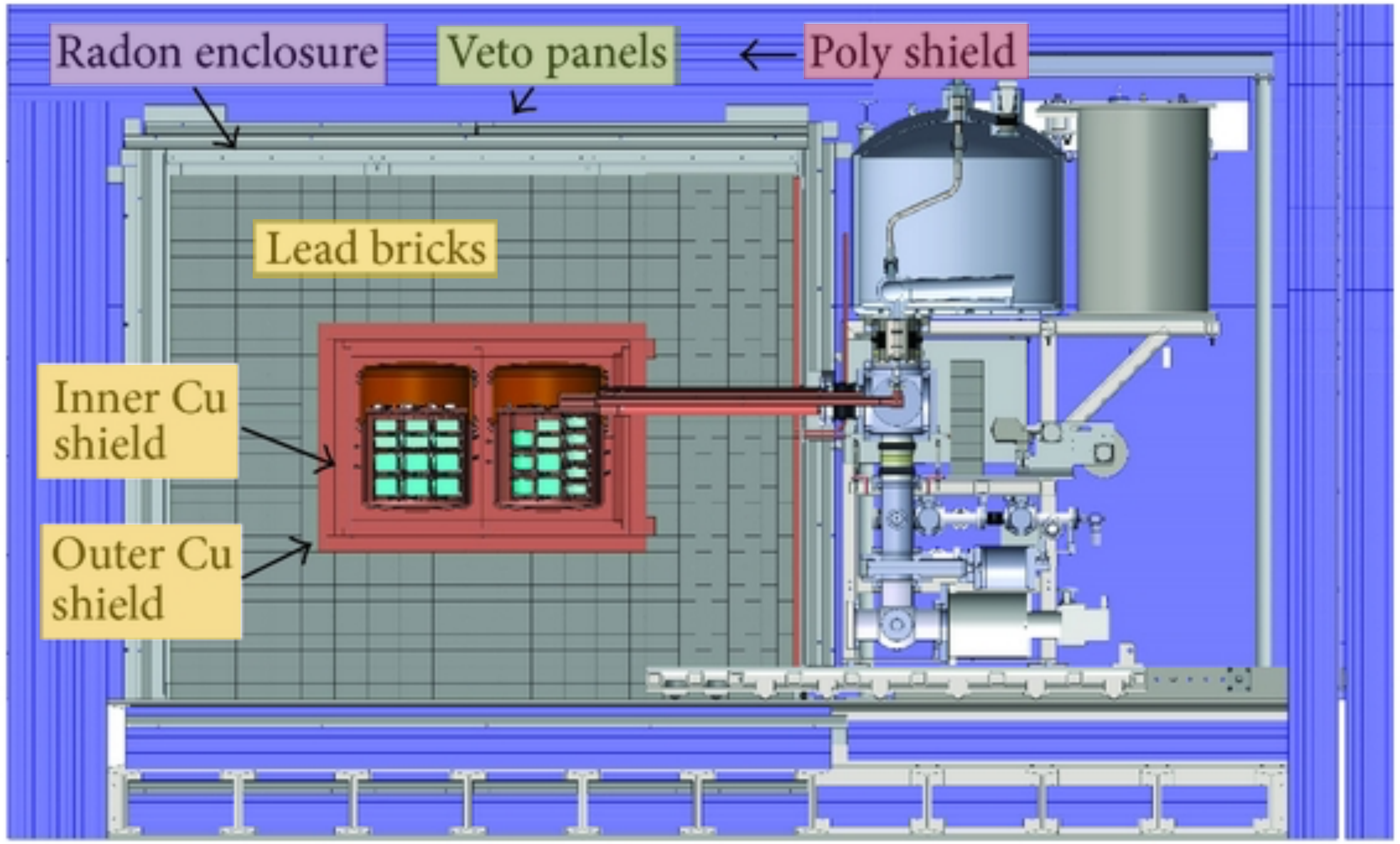

- External **gammas** blocked by **copper and lead** shielding
- **Neutron** background reduced by borated **poly shield**
- Active **muon** veto panels made of plastic **scintillator**
- Ultra-low **radon** N_2 **purge** gas

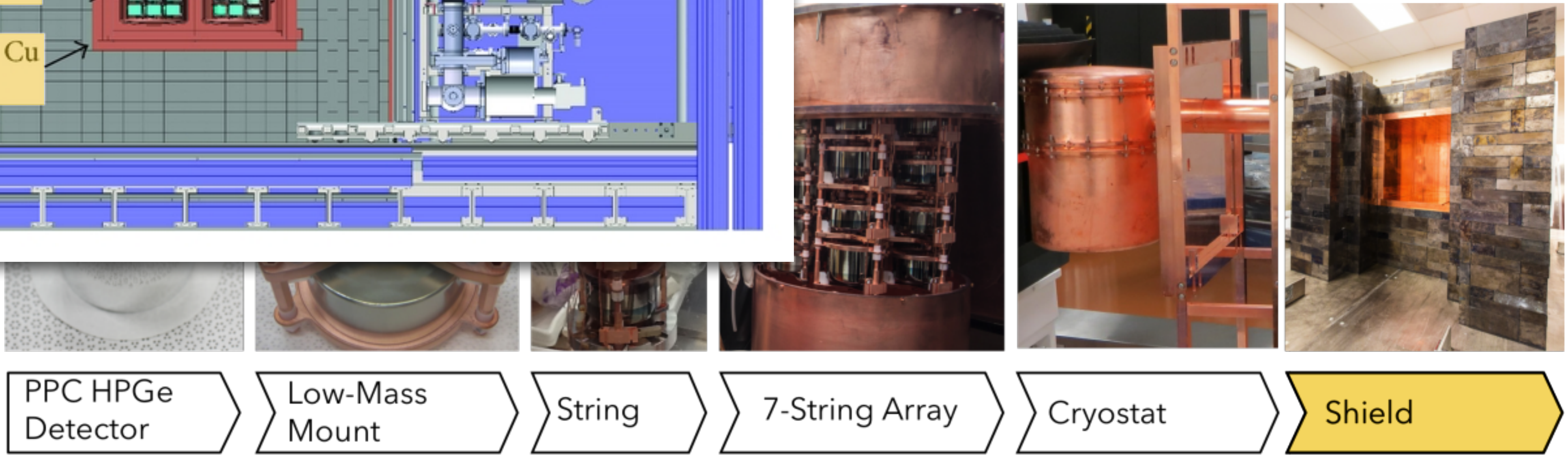

GERDA + MAJORANA = LEGEND

GERDA

- Liquid argon veto
- Low-A shield

- Low-noise electronics
- Radio-pure parts (mounts, cables etc)

Underground argon

New inverted coaxial point-contact HPGe detectors

Reduce passive materials

LEGEND

Large Enriched Germanium Experiment for Neutrinoless ββ Decay

LEGEND Sensitivity

LEGEND-200

- **200 kg** upgrade of GERDA at LNGS
- Background goal **0.6 cts / (FWHM t yr)**
- Data start ~2021

LEGEND-1000

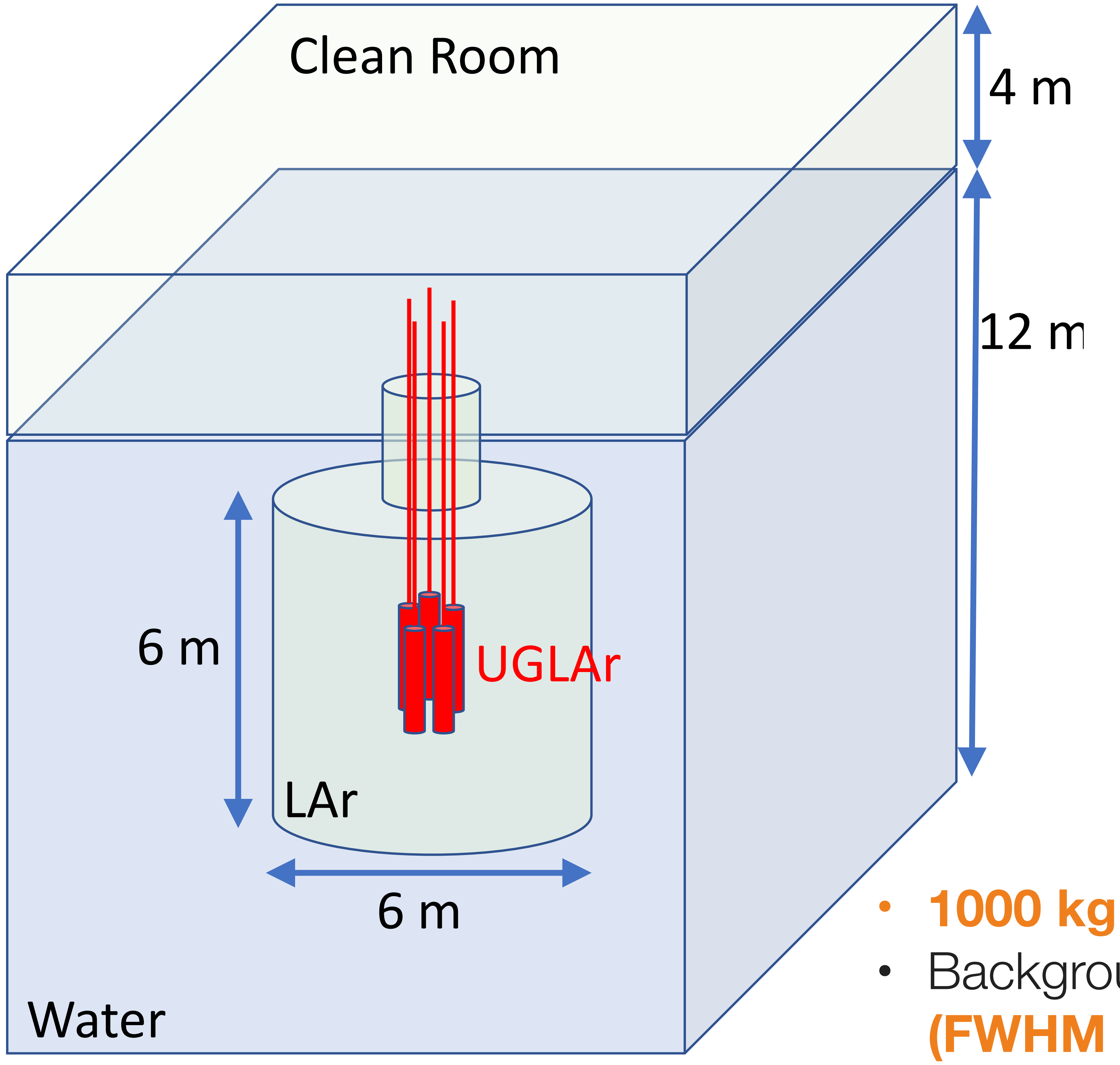

- **1000 kg**
- Background target **0.1 / (FWHM t yr)**
- Location not yet chosen

LEGEND Sensitivity

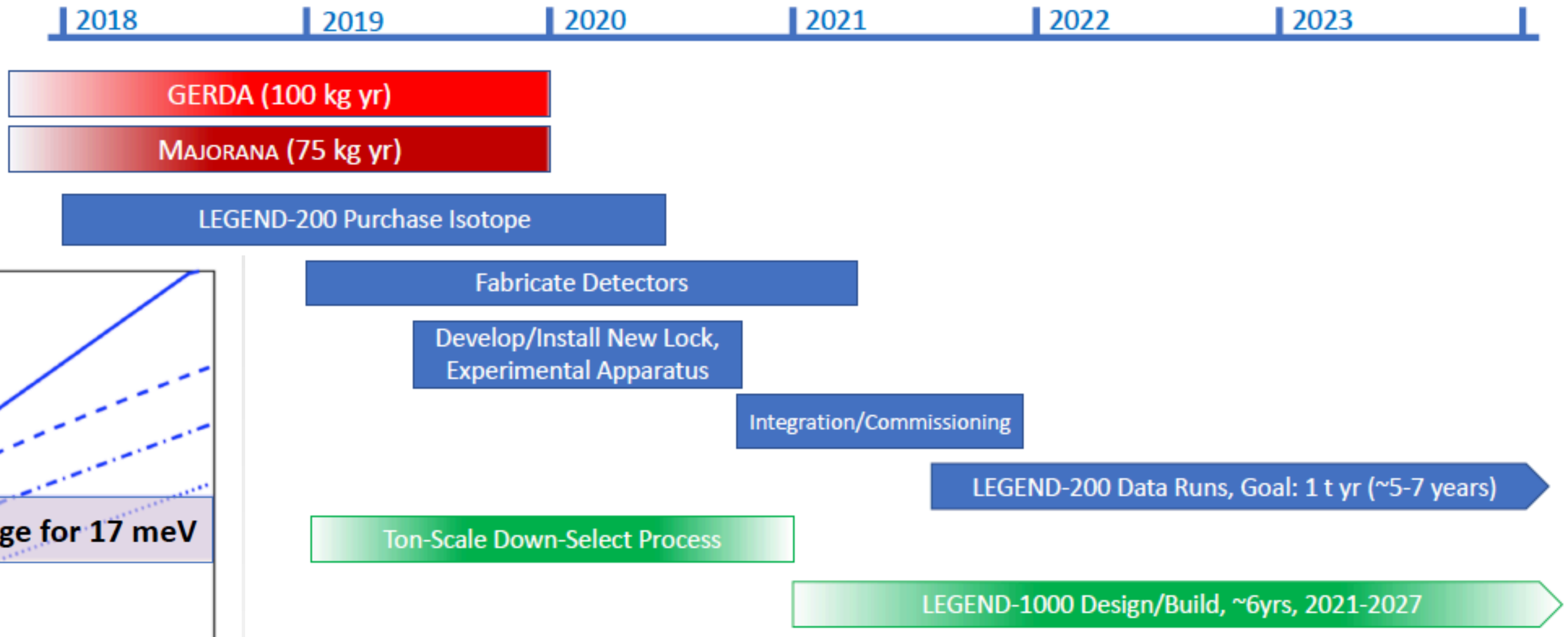

Earliest LEGEND-1000 Data Start 2025/6

^{76}Ge (88% enriched)

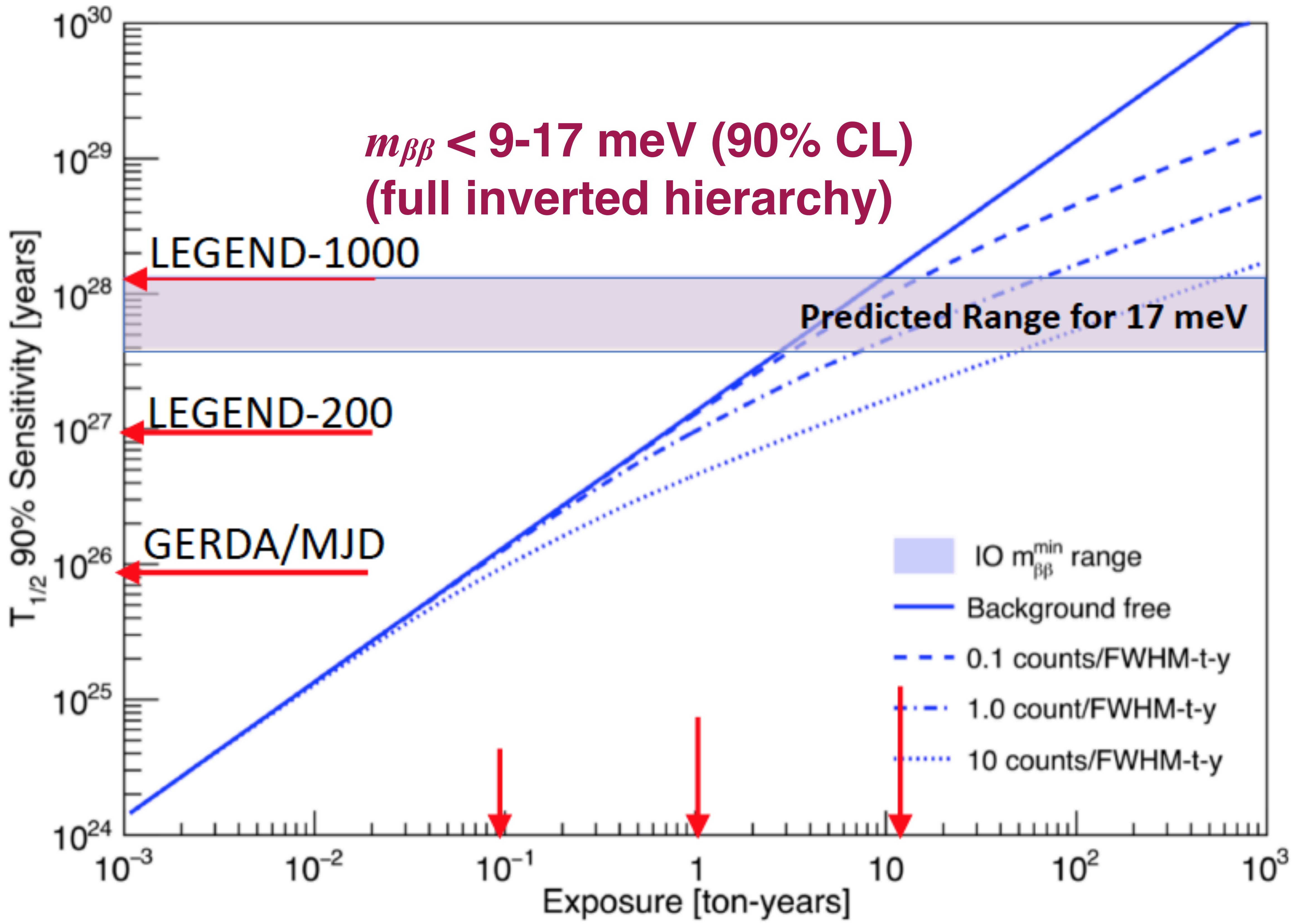

R Saakyan, UK Double-beta meeting 2019

^{136}Xe experiments

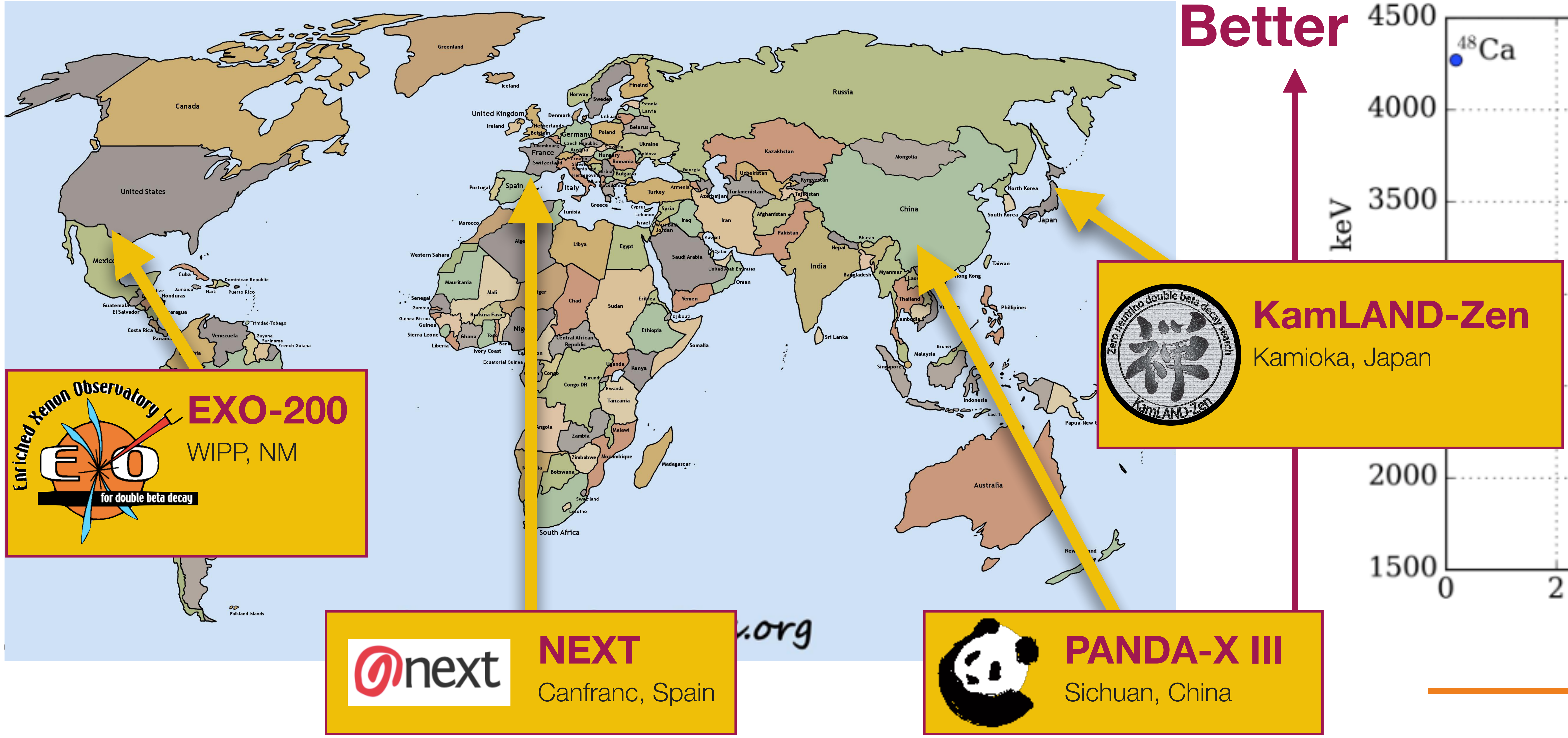

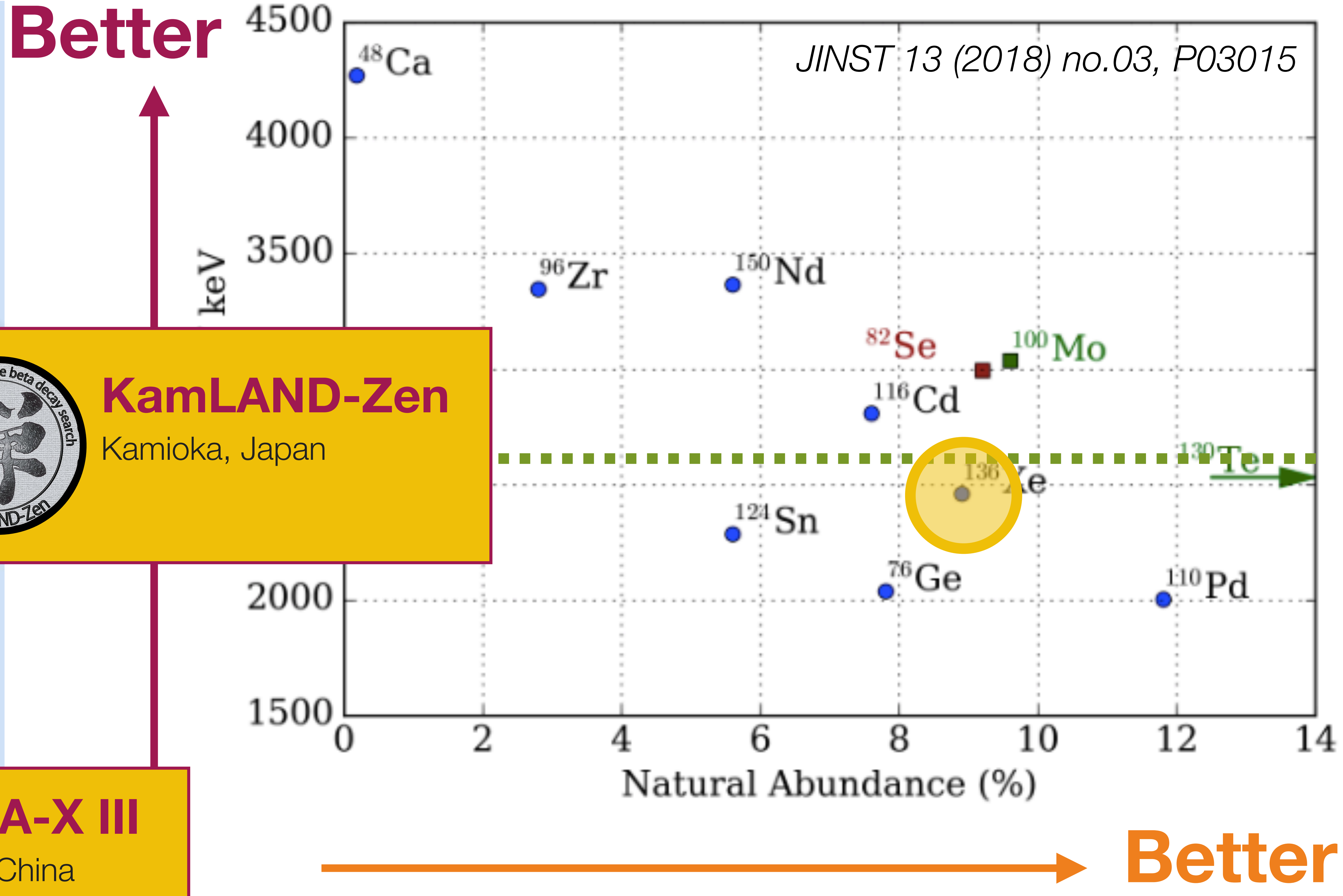

- Large detectors : **hundreds of kg** of isotope
- KamLAND-Zen has current best 0νββ half-life /$m_{\beta\beta}$ mass limit (**⟨$m_{\beta\beta}$⟩ < 61-165 meV**)
- Future detectors - **nEXO, KamLAND2 Zen**

EXO-200: Liquid xenon TPC at WIPP, New Mexico

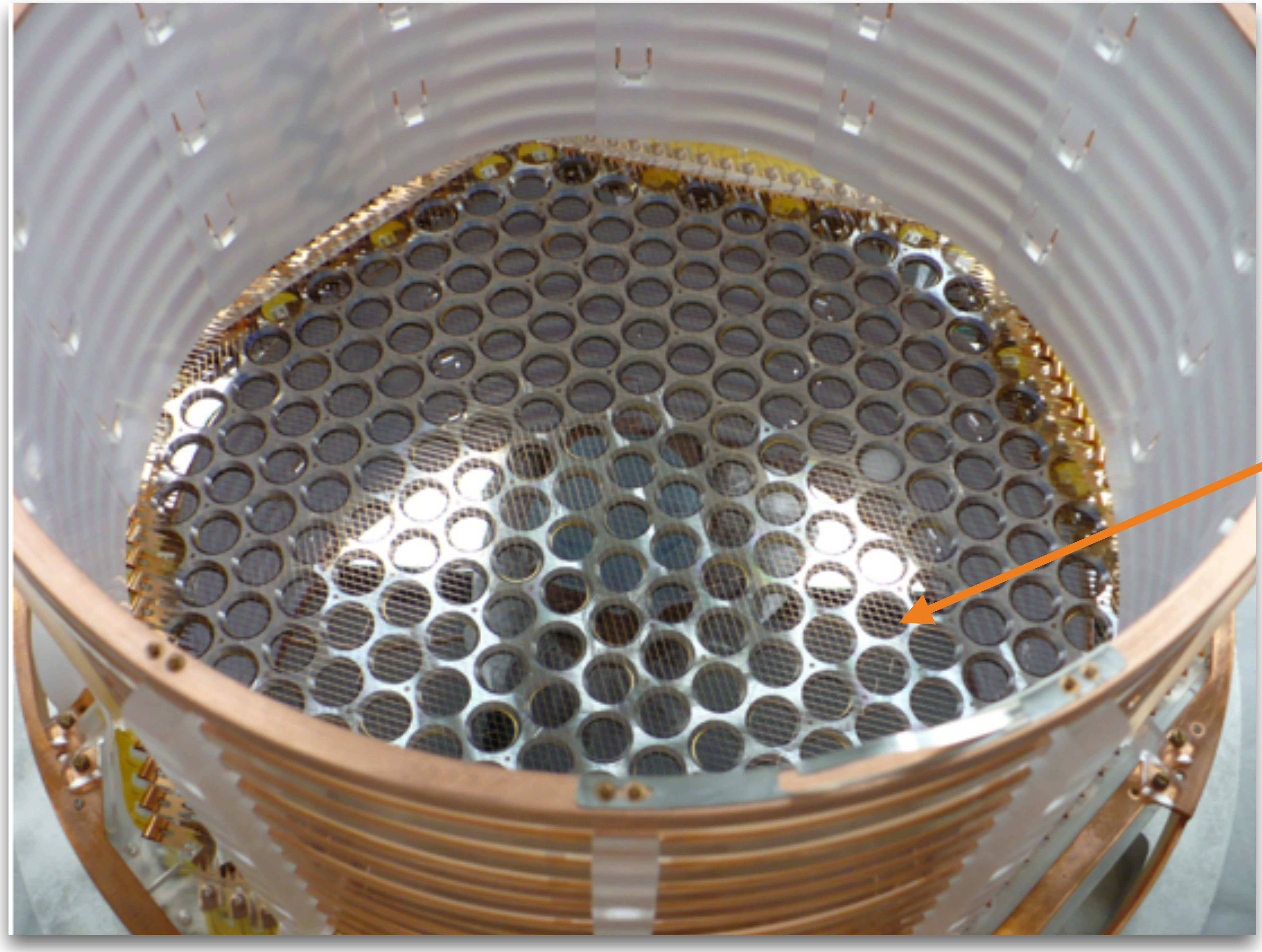

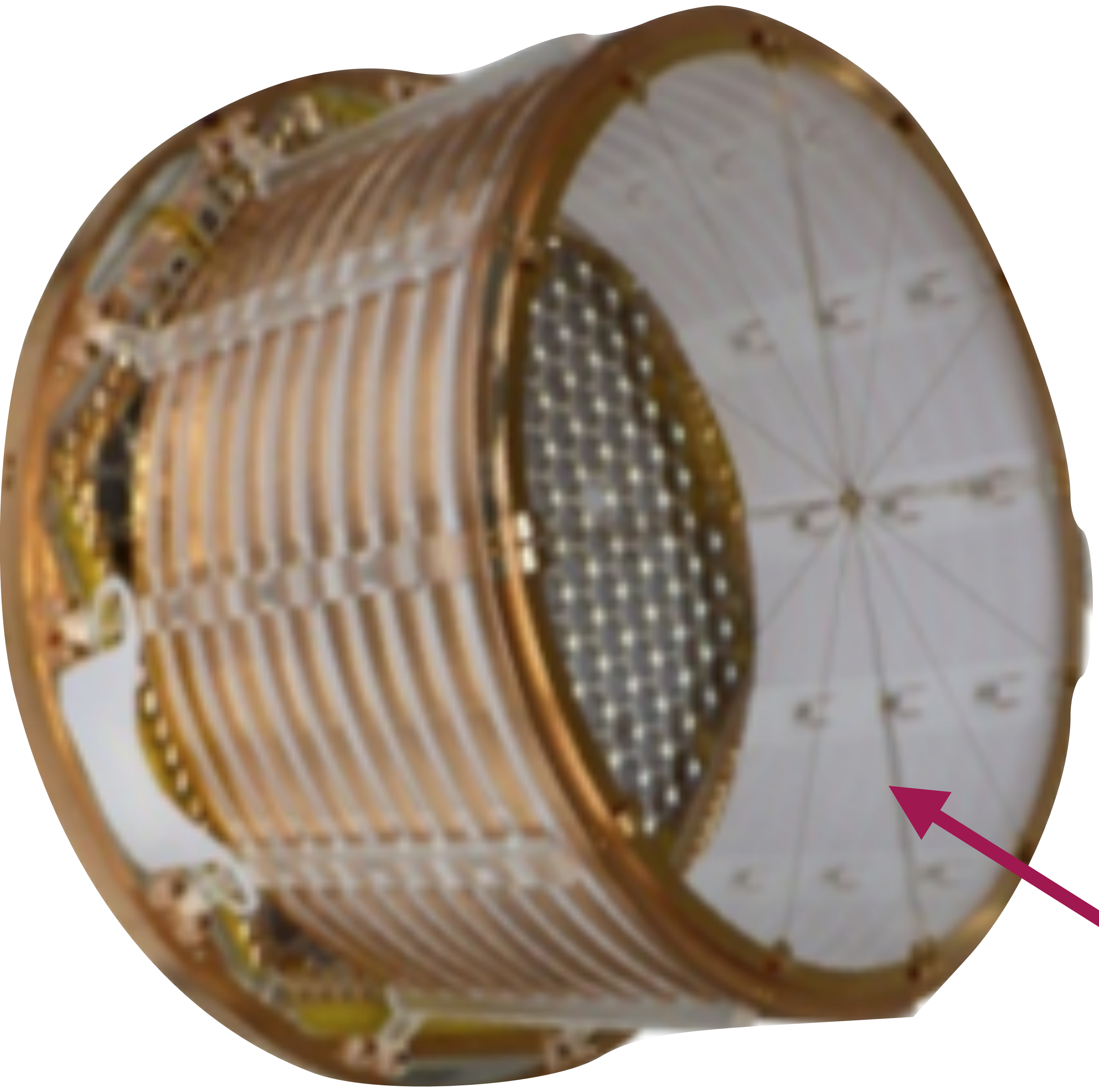

Charge collection grid

40cm

Central cathode held at high negative voltage (-8 to-12 kV)

EXO-200: Liquid xenon TPC at WIPP, New Mexico

Liquid xenon (80.6% ^{136}Xe) has 3 roles
- TPC ionizer
- ββ emitter
- Scintillator

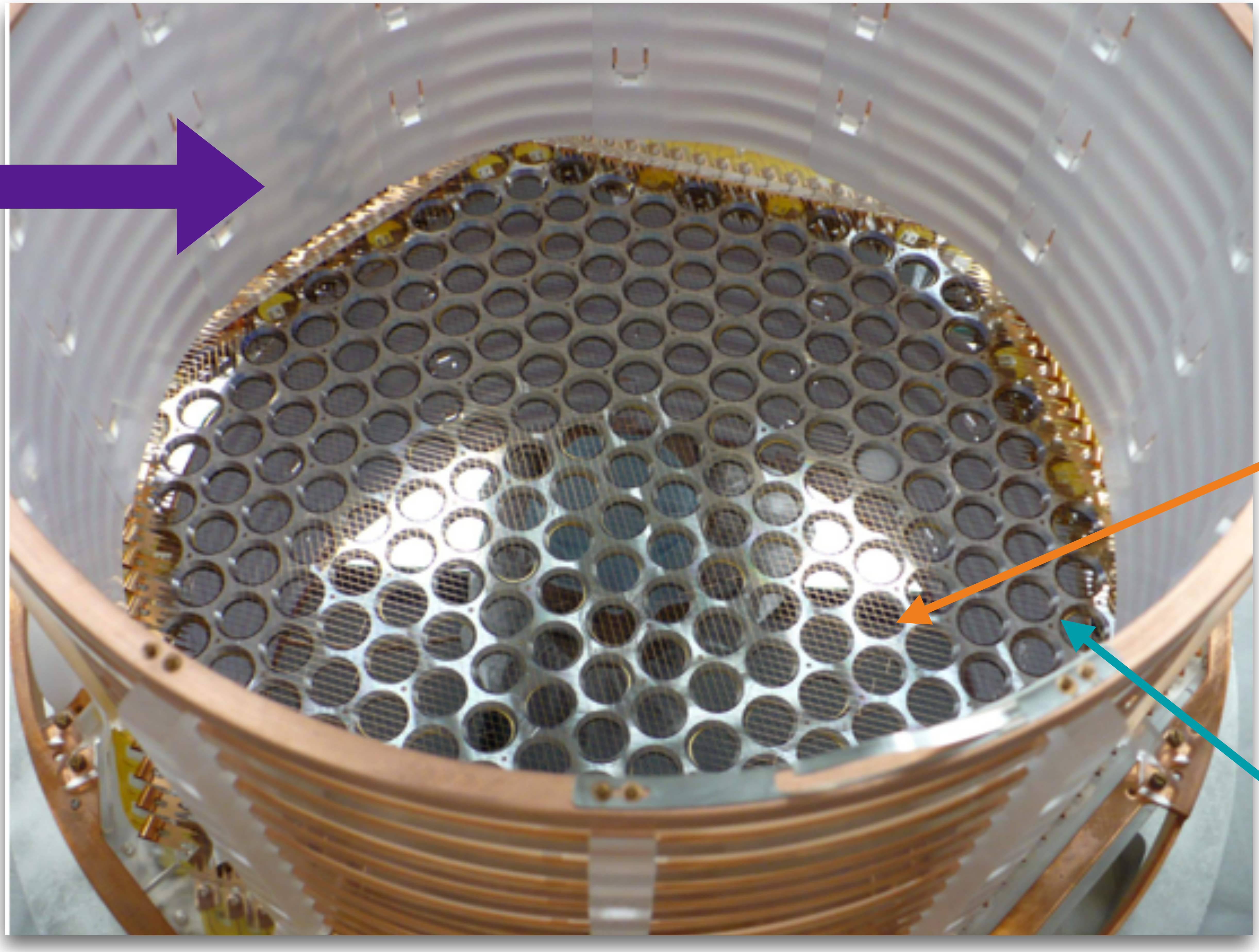

Charge collection grid

Avalanche photodiodes collect 175nm scintillation light

40cm

EXO-200: Reconstruction

L Yang, Neutrino 2016

TPC wire signals give x-y position

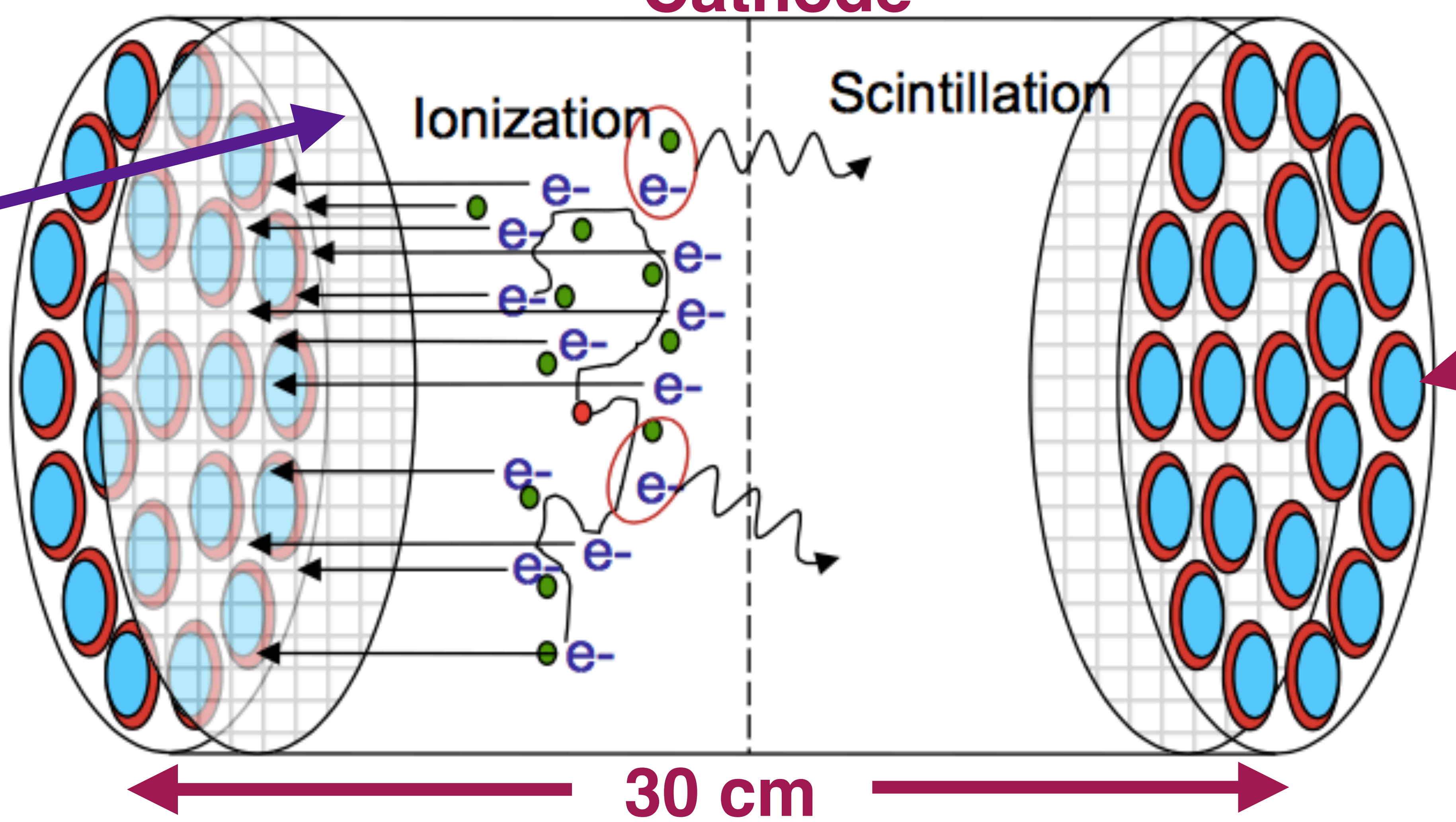

Time delay between scintillation light and wire signals gives longitudinal position

3-D reconstruction distinguishes between **single-site (ββ)** and **multi-site (γ background)** events

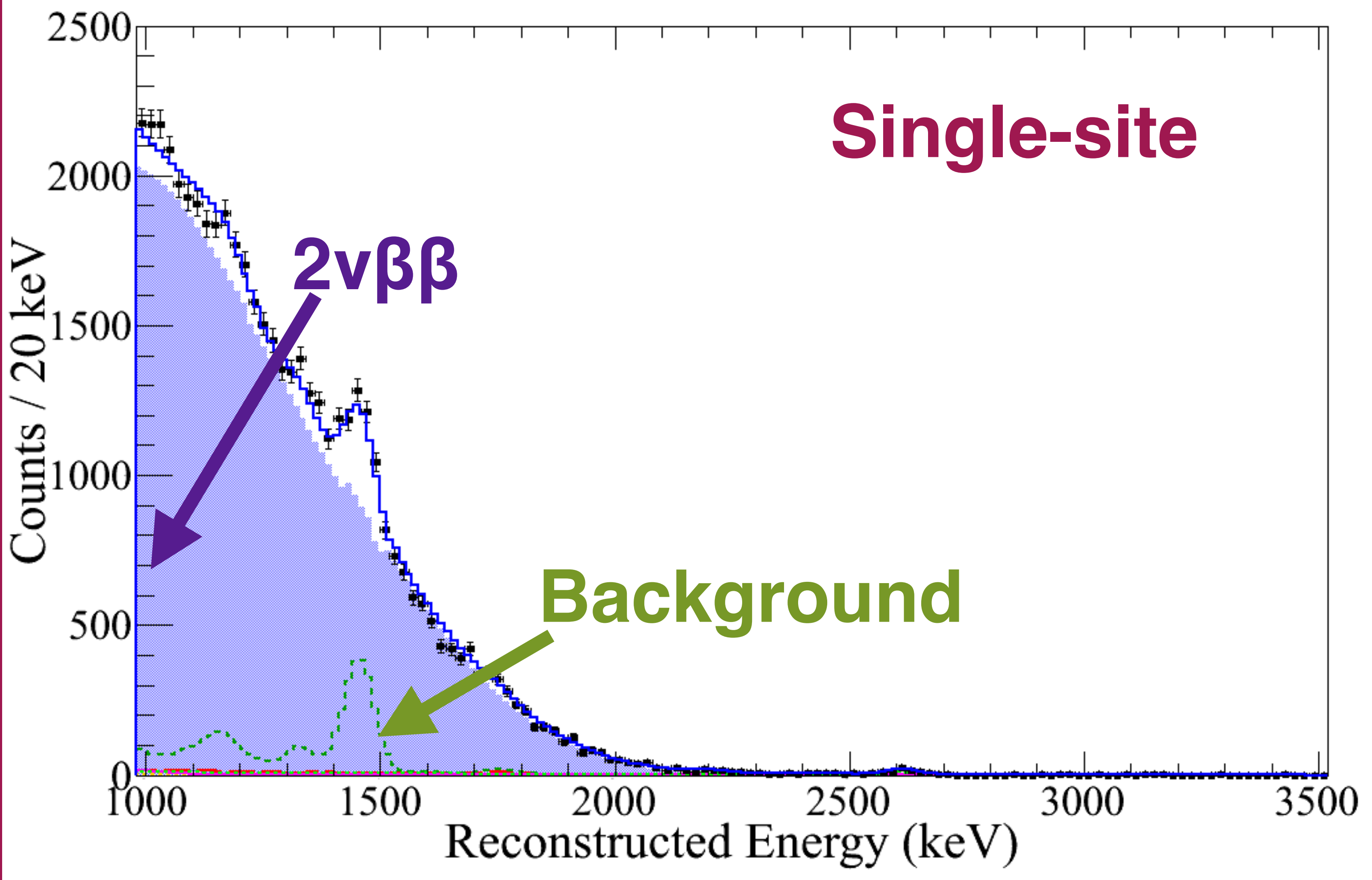

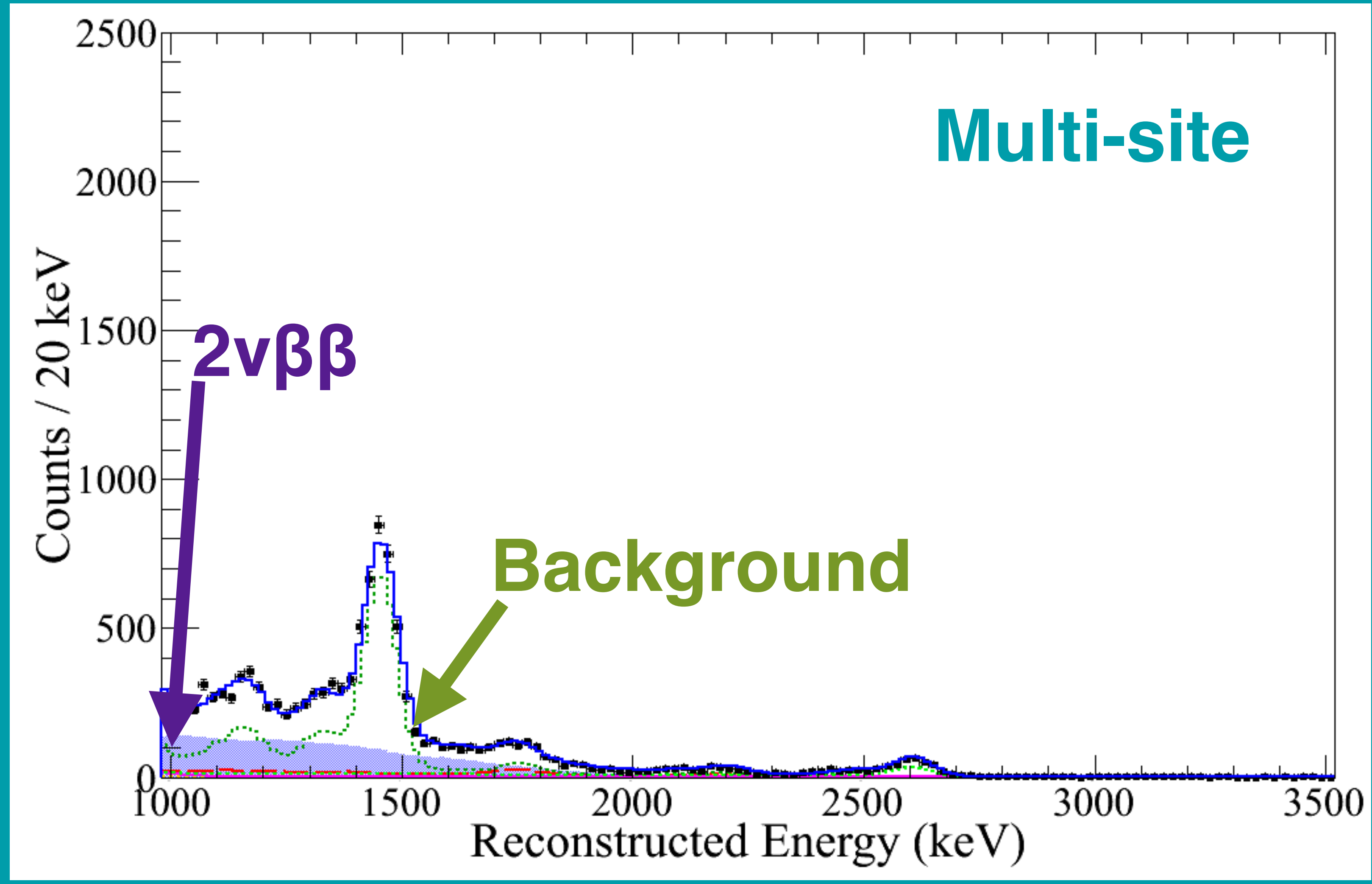

EXO-200: Identifying 0νββ

Single-site cut

Energy cut
($\sigma_E / E = 1.23\%$)

Boosted decision tree

Phys. Rev. Lett. 120, 072701 (2018)

EXO-200: Identifying 0νββ

Single-site cut → **Energy cut** ($\sigma_E / E = 1.23\%$) → **Boosted decision tree**

Time between 5 and 95% of charge being collected

Backgrounds tend to fire neighbouring channels

External backgrounds generate clusters near TPC surface

15% sensitivity improvement

Phys. Rev. Lett. 120, 072701 (2018)

EXO-200: Latest results

Phys. Rev. Lett. 120, 072701 (2018)

Phase I vs Phase II - 2014 accident at WIPP; 2 year pause and upgrades

$T_{1/2}$ > 1.8 x 10^{25} years
(90% C.L)
($\langle m_{\beta\beta} \rangle$ < *147 – 398* meV)
177.6 kg.years

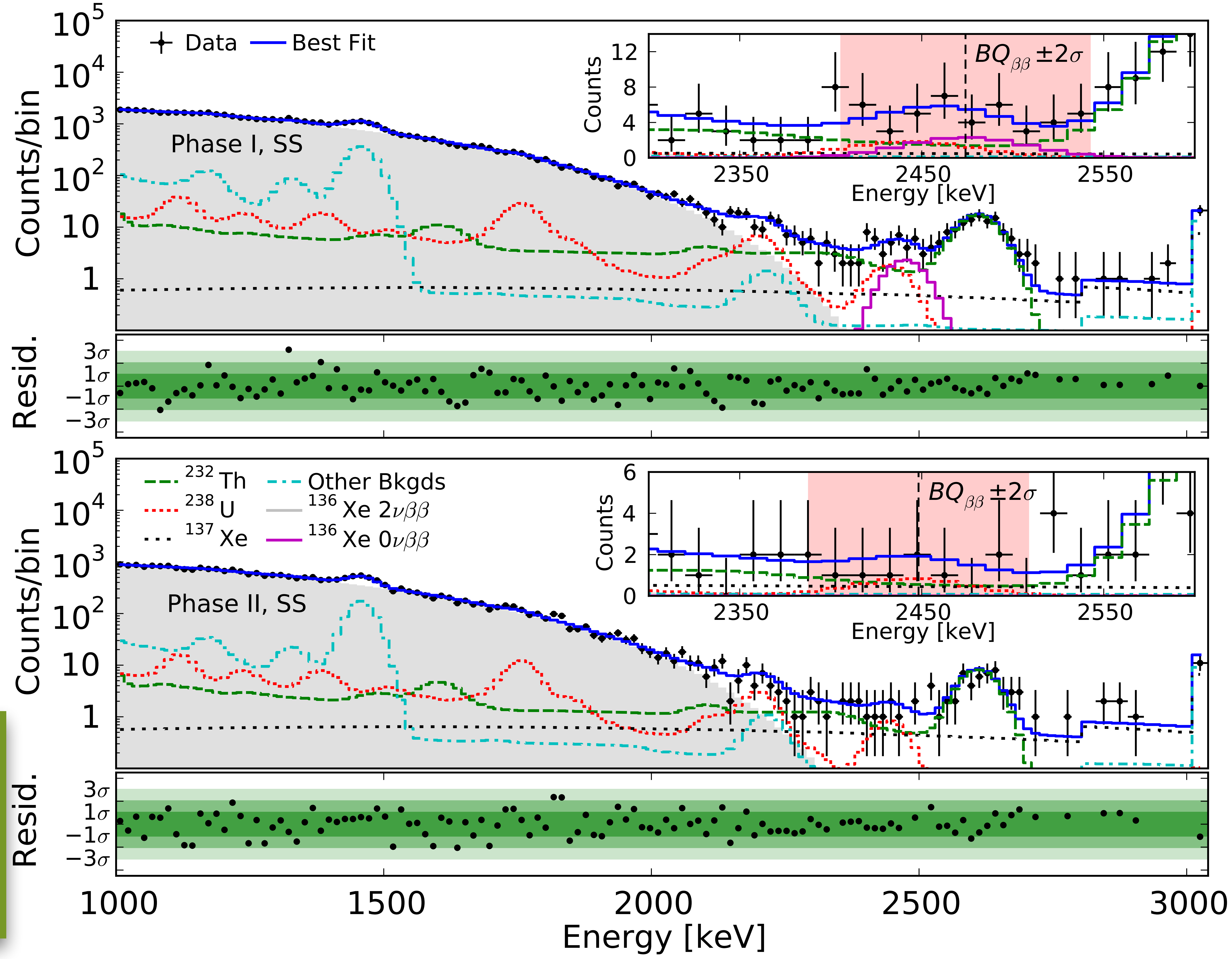

Single-site

BDT discriminator

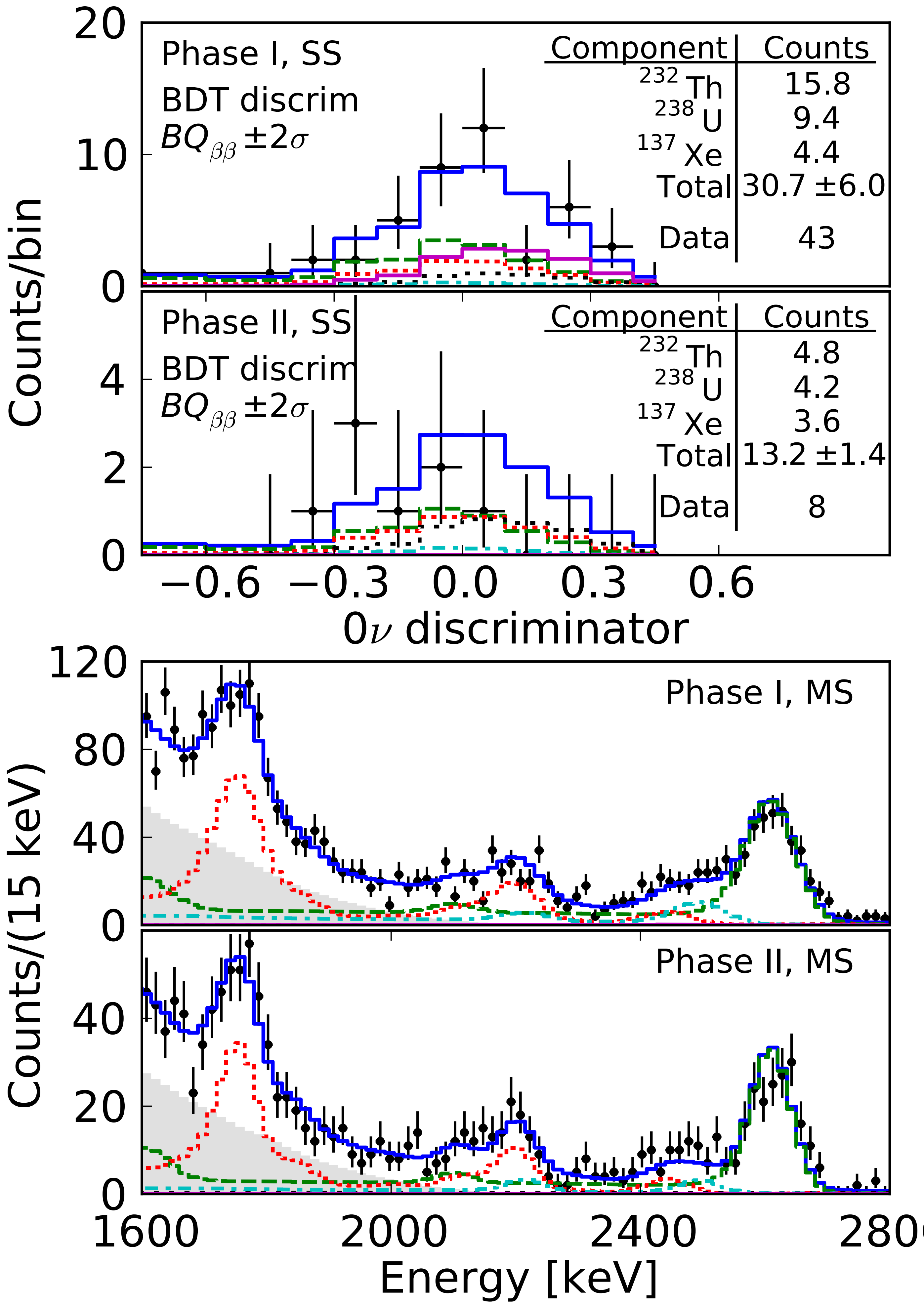

Multi-site

The future: nEXO

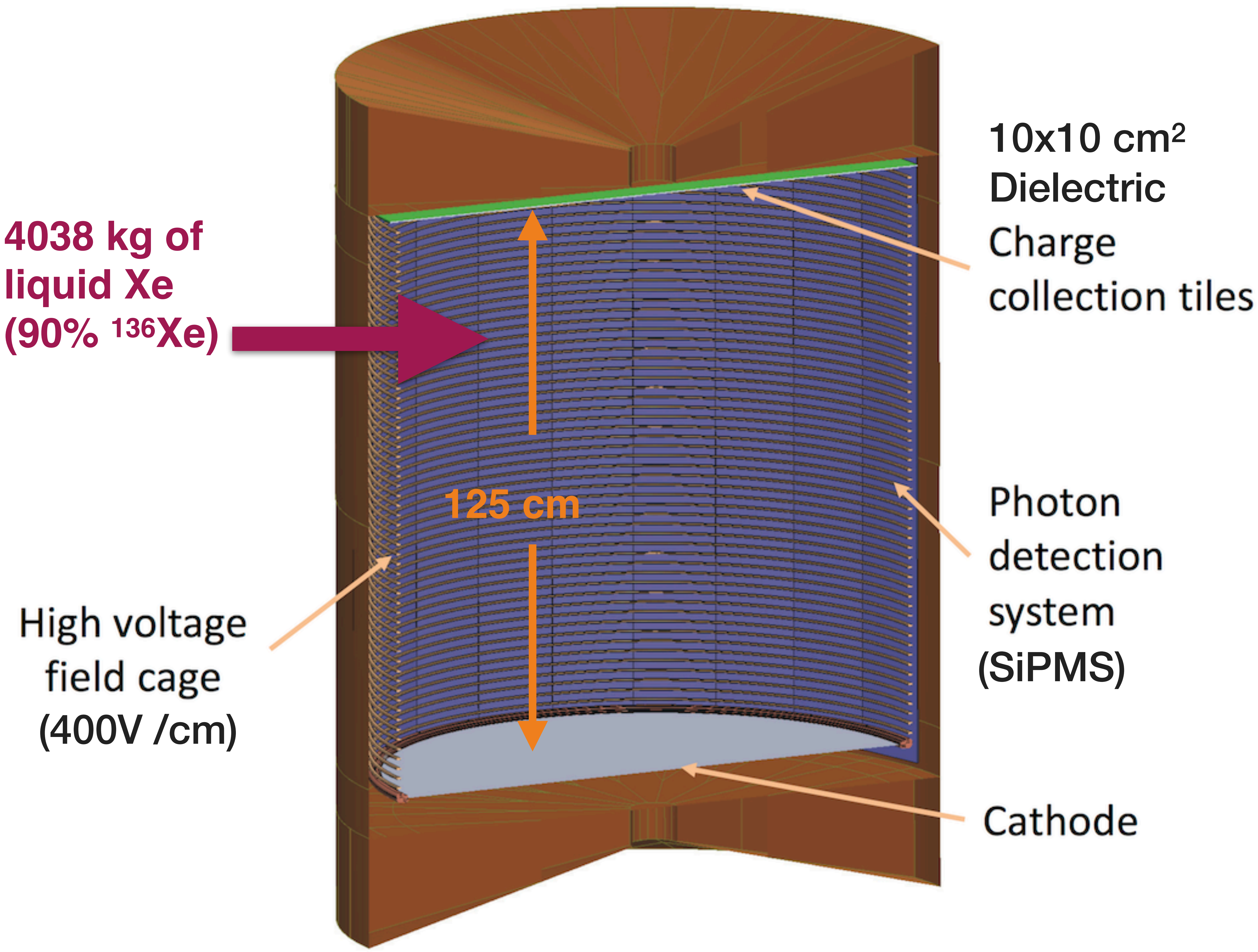

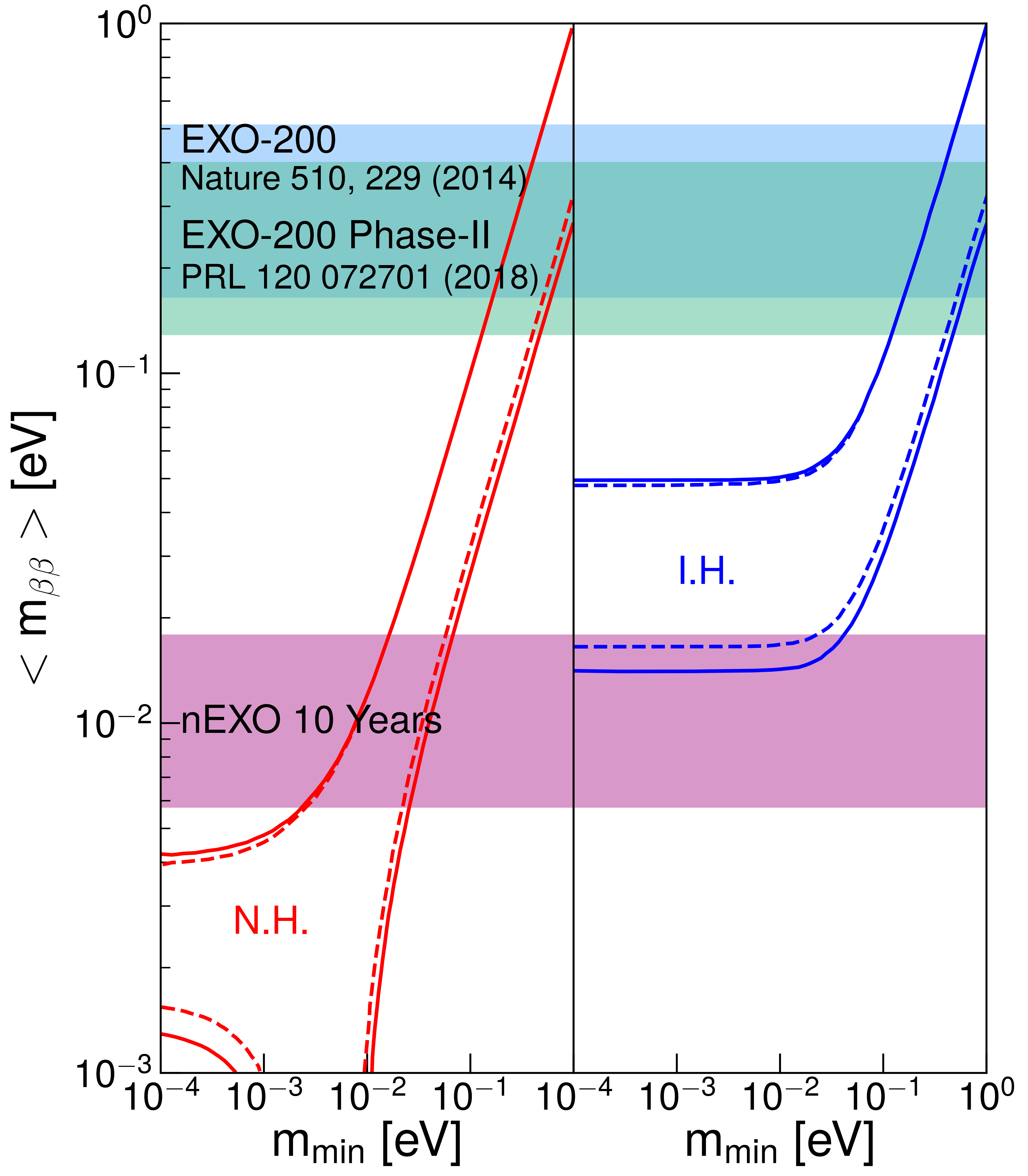

Phys. Rev. C 97, 065503 (2018)

NEXT: high-pressure gas xenon TPC at Canfranc, Spain

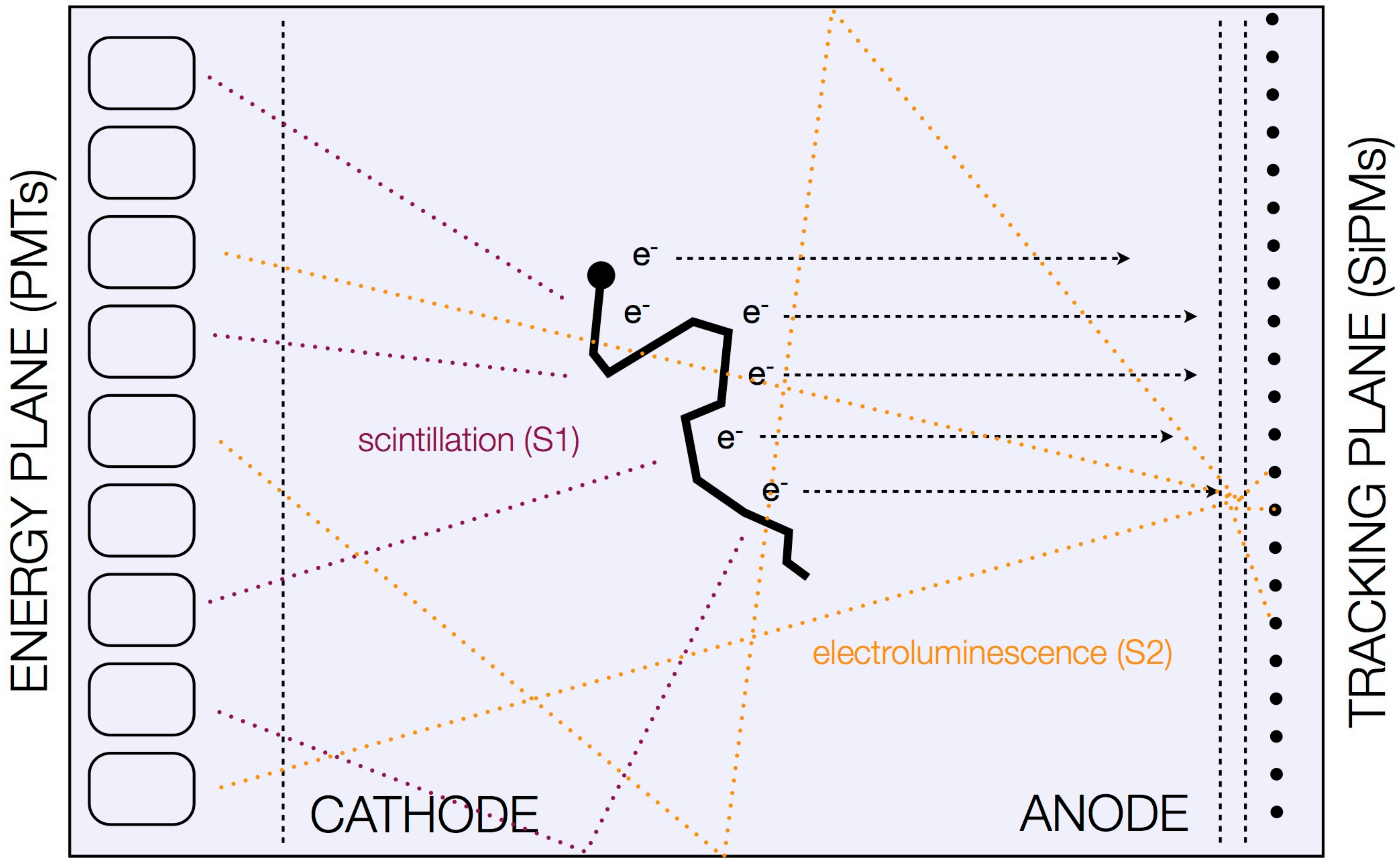

SOFT TPC
Separated Optimized FuncTion

Charged particle travels through TPC

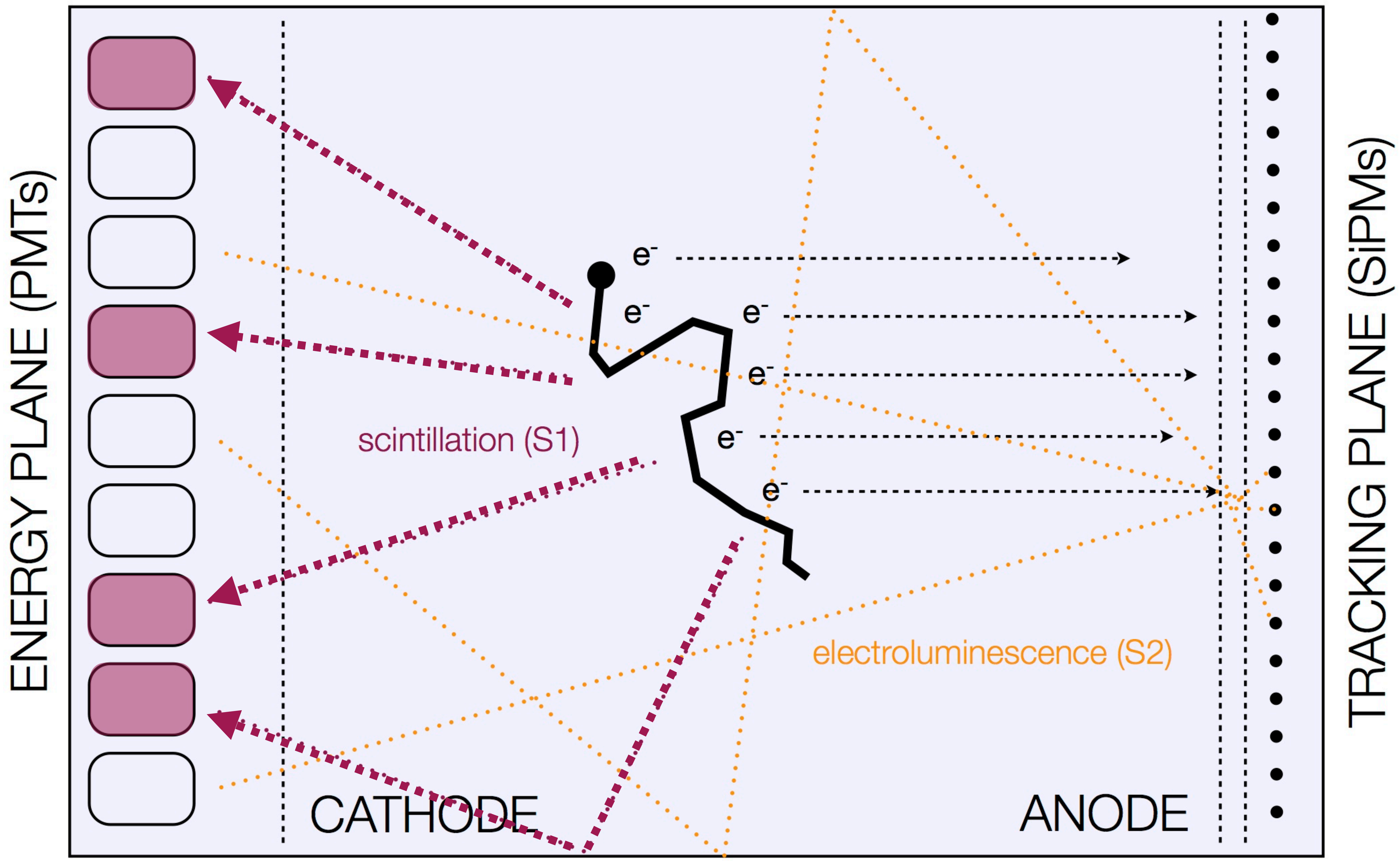

SOFT TPC
Separated Optimized FuncTion

Charged particle travels through TPC

Primary scintillation light gives event trigger time

NEXT: high-pressure gas xenon TPC at Canfranc, Spain

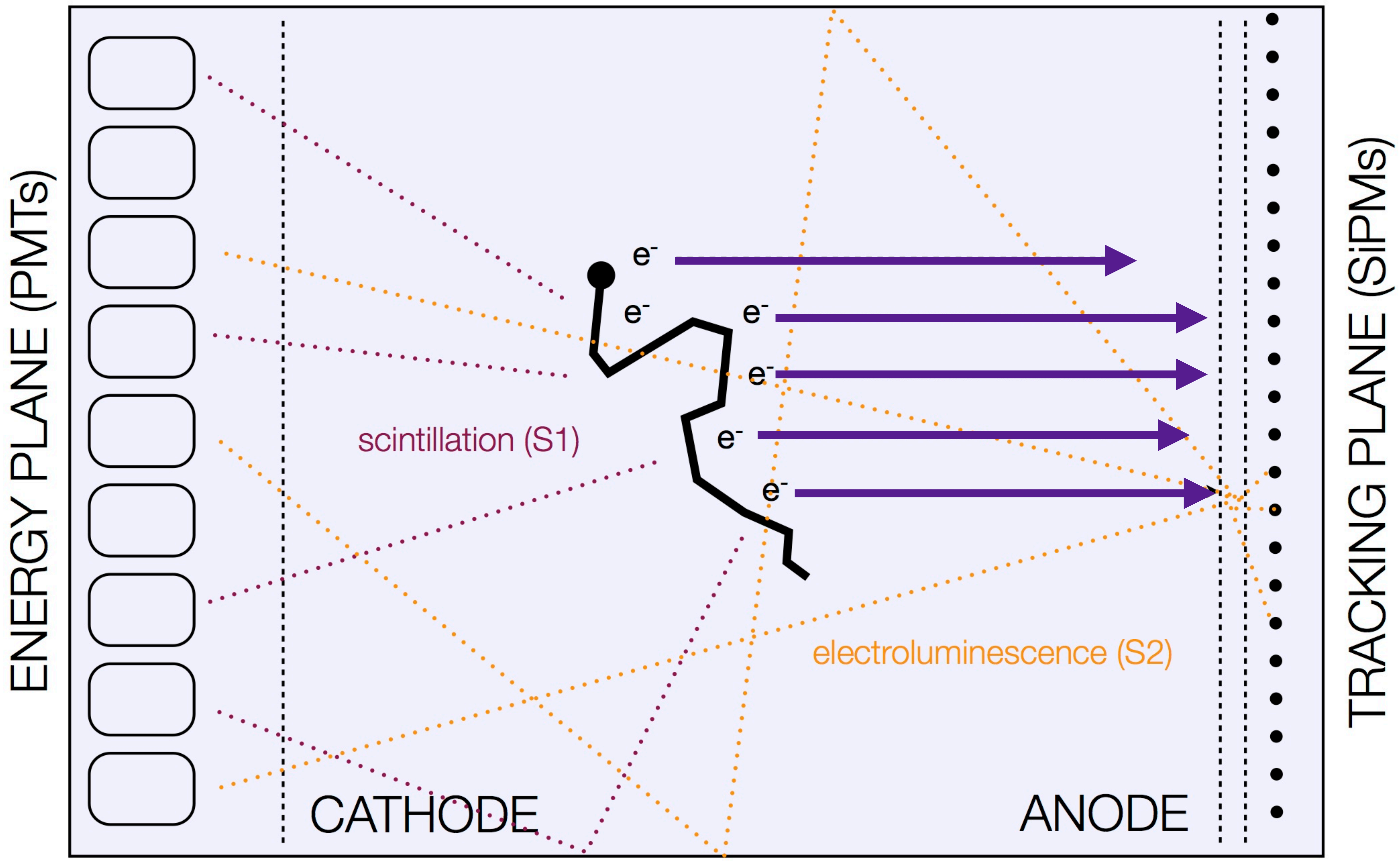

SOFT TPC

Separated Optimized FuncTion

Charged particle travels through TPC

Primary scintillation light gives event trigger time

Ionization electrons drift to anode

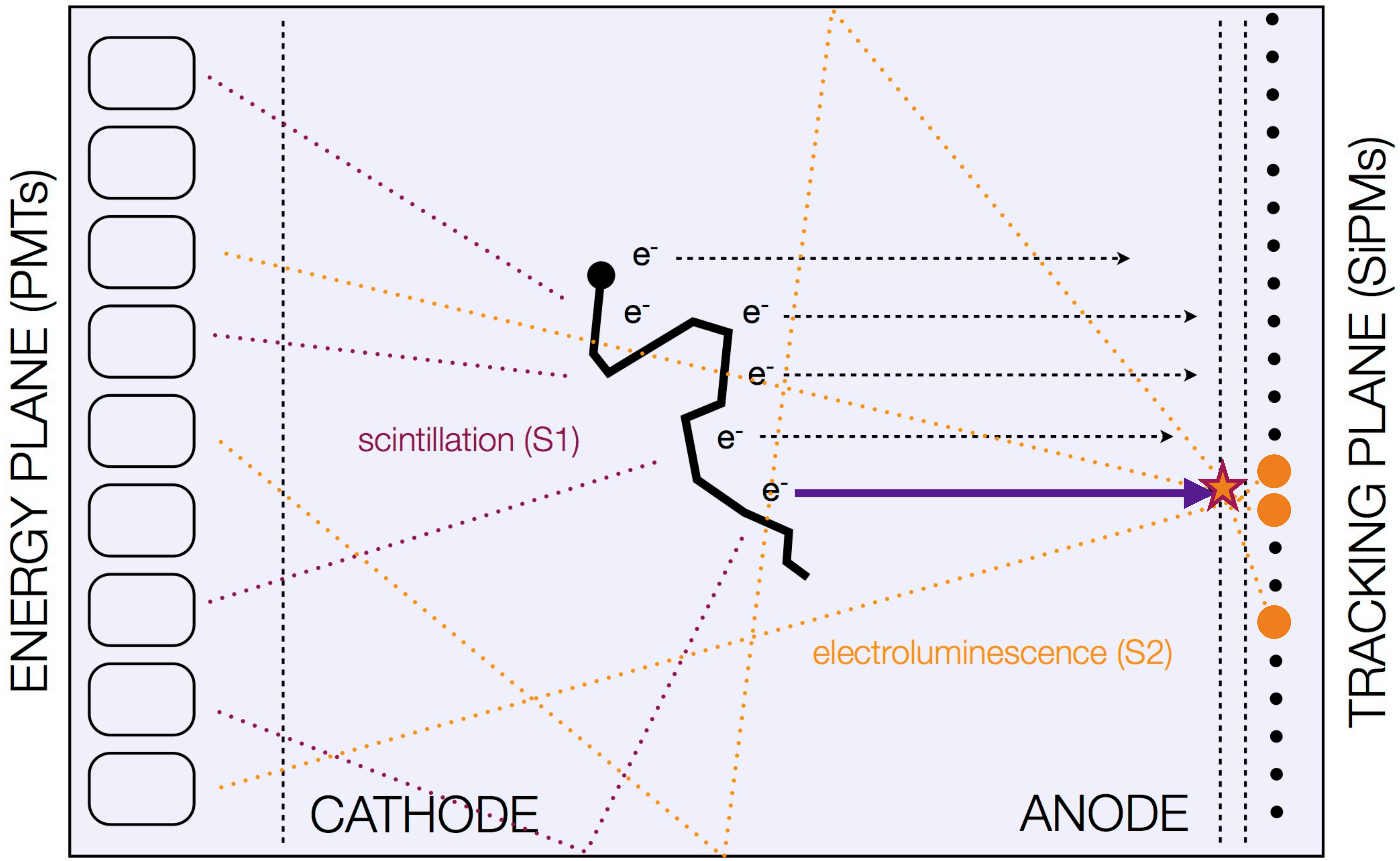

SOFT TPC

Separated Optimized FuncTion

Charged particle travels through TPC

Primary scintillation light gives event trigger time

Ionization electrons drift to anode

Electroluminescent light generated at anode is recorded in SiPMs and used for tracking

NEXT: high-pressure gas xenon TPC at Canfranc, Spain

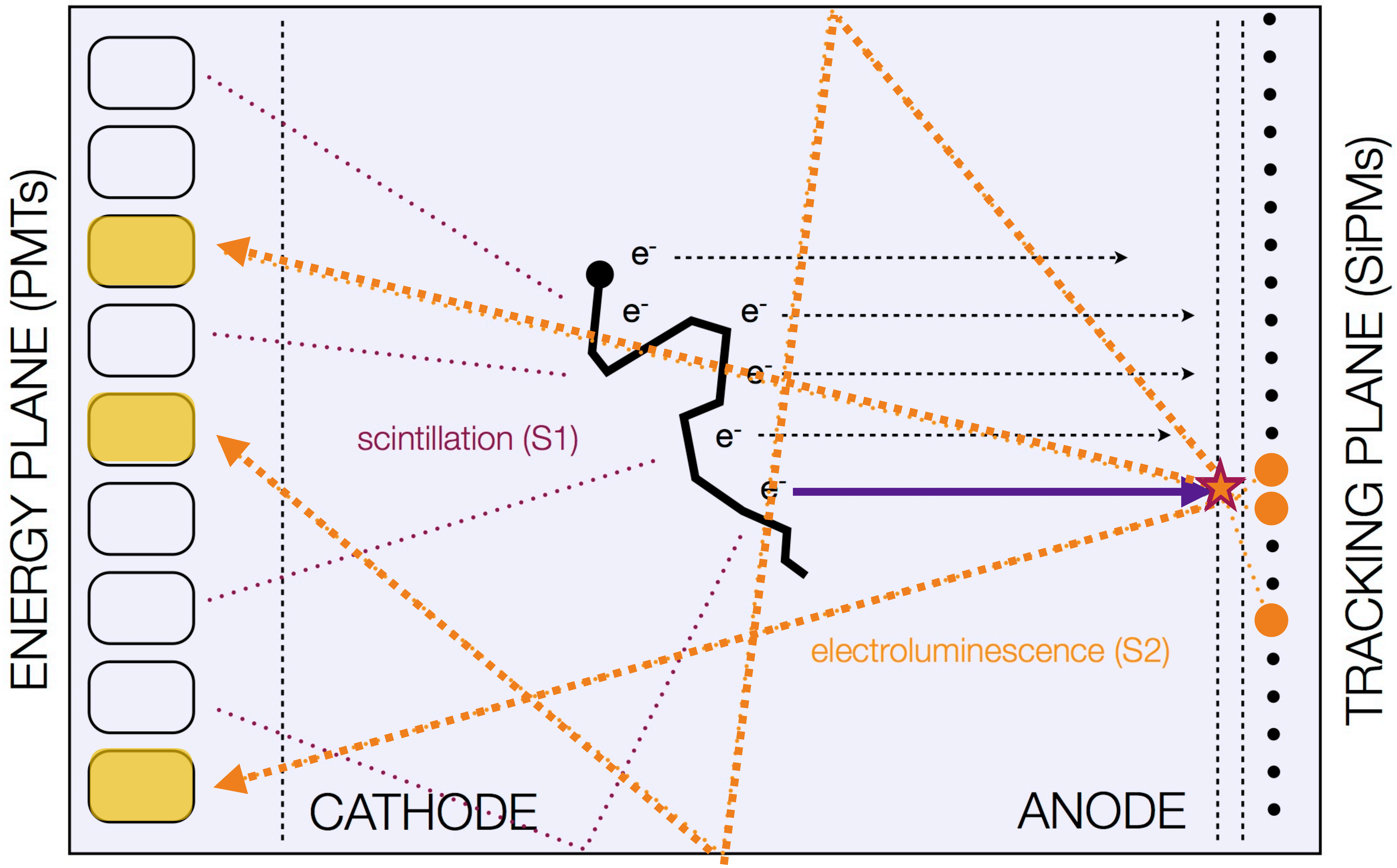

SOFT TPC

Separated Optimized FuncTion

Charged particle travels through TPC

Primary scintillation light gives event trigger time

Ionization electrons drift to anode

Electroluminescent light generated at anode is recorded in SiPMs and used for tracking

Electroluminescent light also recorded in PMTs and used for energy measurement

NEXT: high-pressure gas xenon TPC at Canfranc, Spain

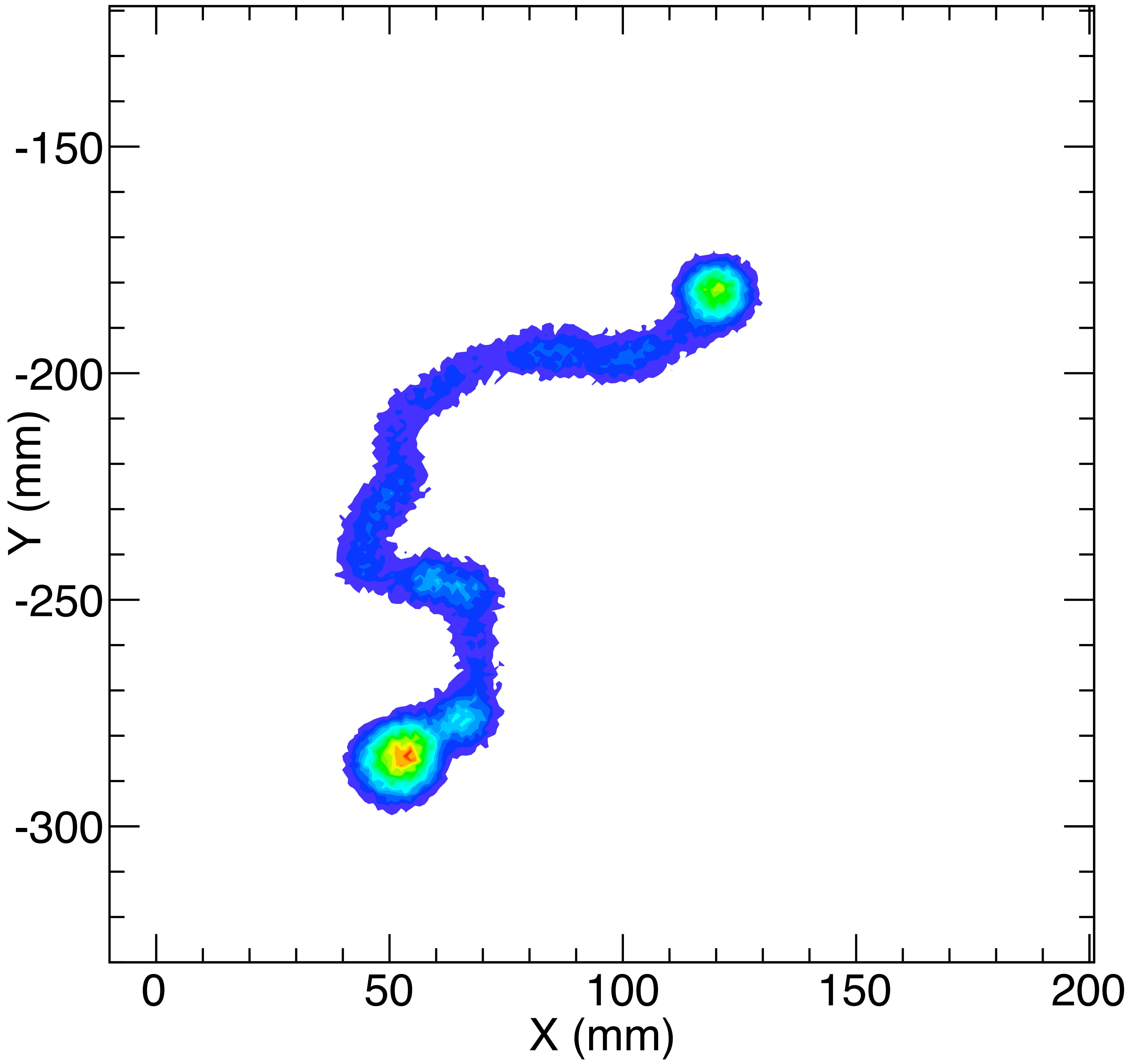

SOFT TPC

Separated Optimized FuncTion

Charged particle travels through TPC

Primary scintillation light gives event trigger time

Ionization electrons drift to anode

Electroluminescent light generated at anode is recorded in SiPMs and used for tracking

Electroluminescent light also recorded in PMTs and used for energy measurement

Each electron generates a constant deposition, followed by a “blob” of energy at the end - count blobs to separate signal from background

NEXT-White (NEW) - current 10kg detector

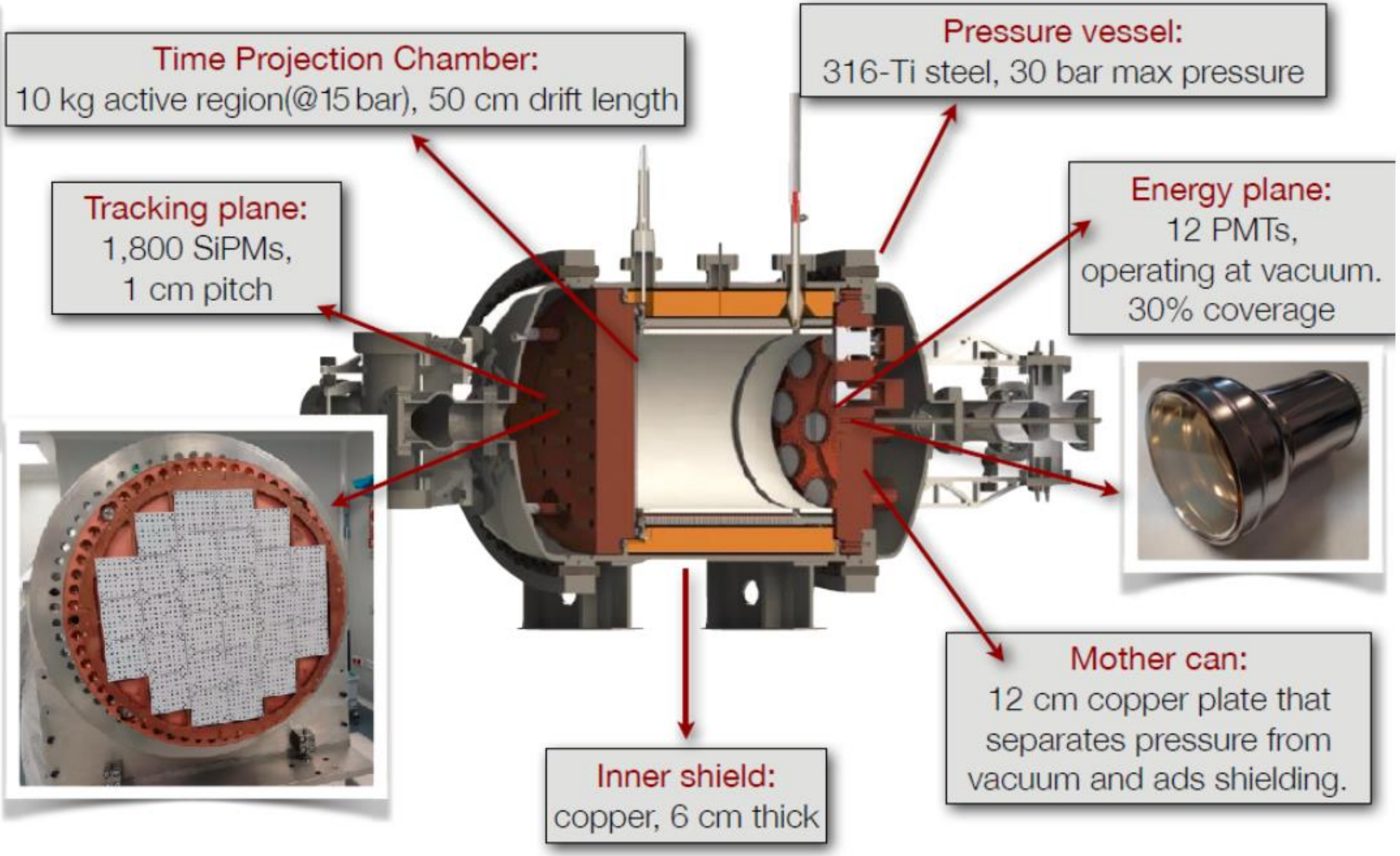

Ran with depleted Xe in 2018 - now running with enriched Xe

arXiv:1804.02409

NEXT-100 (starts next year)

L Arazi

JHEP 2016 159

TPC: 100 kg active region, 130 cm drift length

Pressure vessel: St-St, rated for 15 bar

Energy plane: 60 radio-pure PMTs, 30% coverage

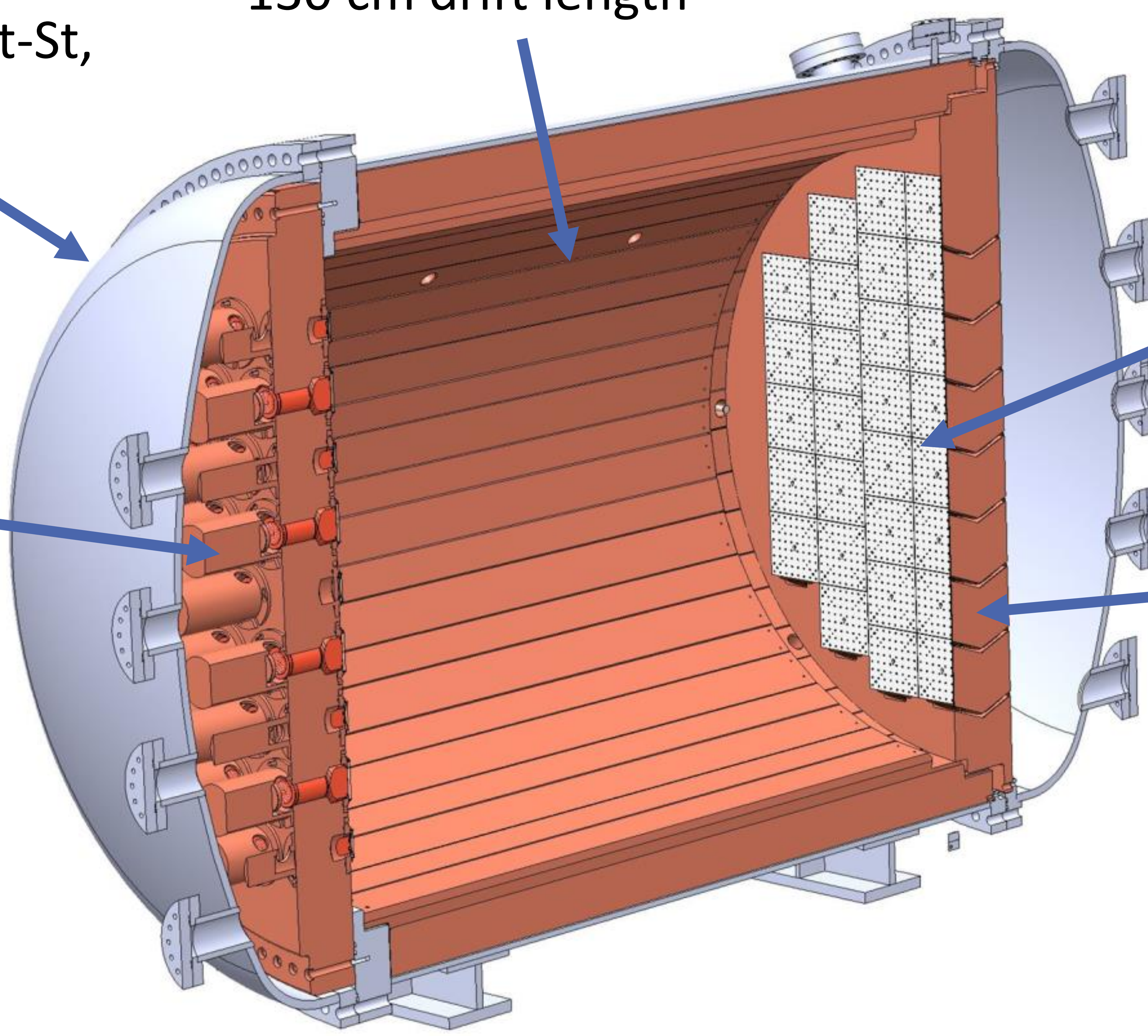

Tracking plane: 3000 SiPMs, 15 mm pitch

Inner shield: 12 cm Cu

Outer shield: lead castle with Rn-free air

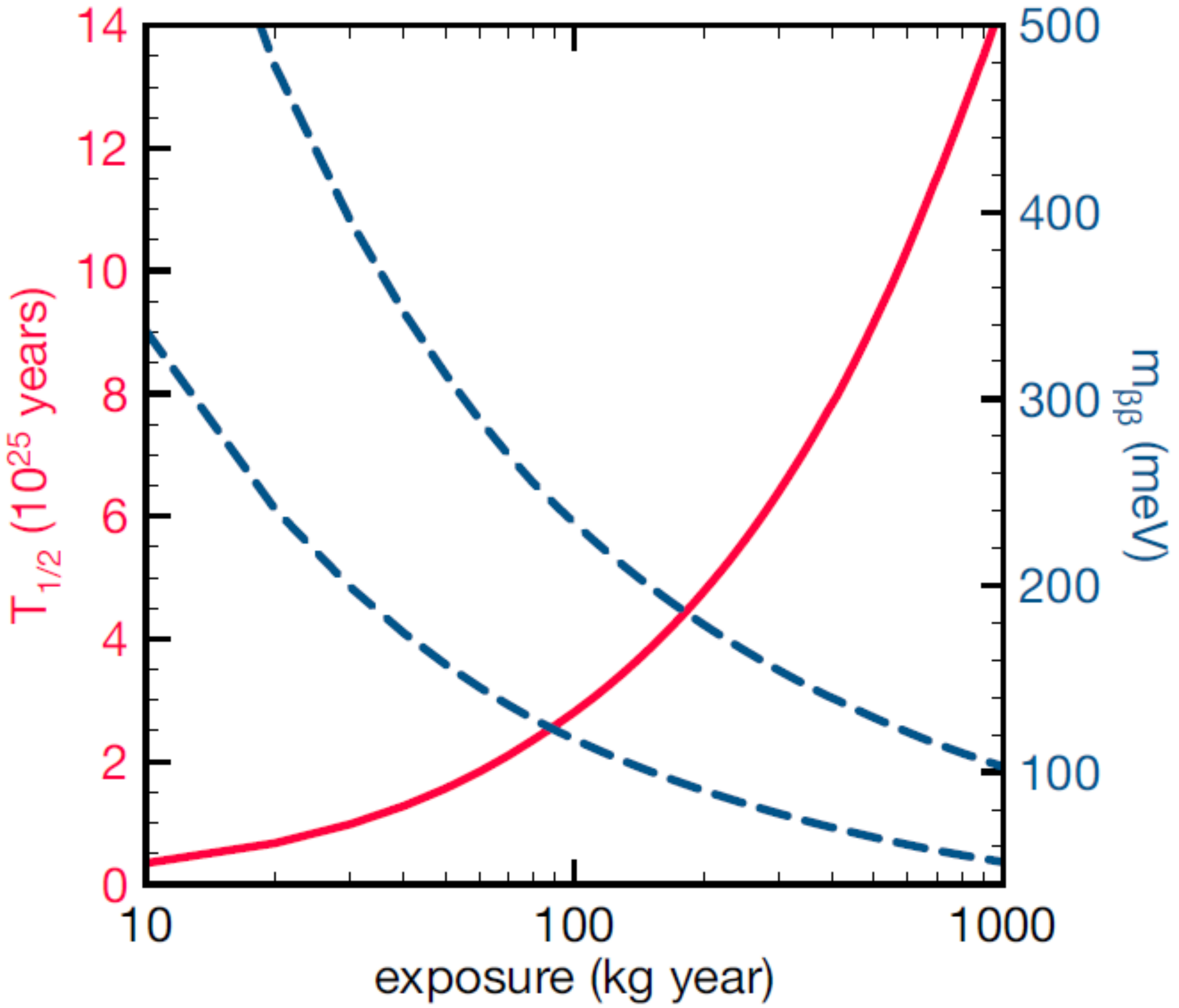

Resolution 1% FWHM

1 background count / 100 kg / year

Demonstrator for ton-scale experiment

PandaX-III at China Jinping Underground Laboratory

PandaX-II

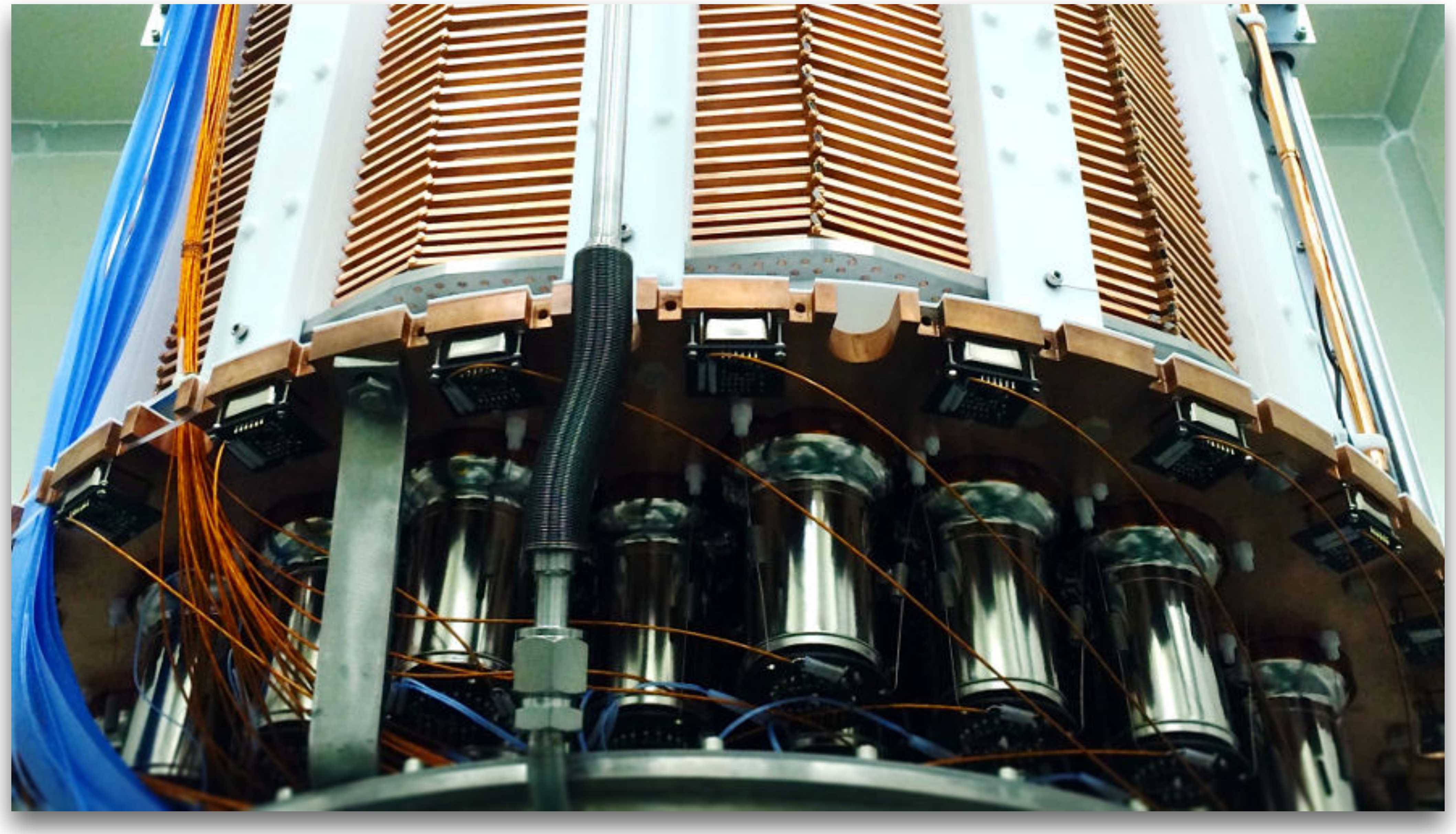

- **PandaX-II** is a **dark matter** direct detection experiment equipped with a half-ton scale **dual-phase TPC**
- **PandaX-III** will enrich with 200kg- 1 ton of 90% ^{136}Xe

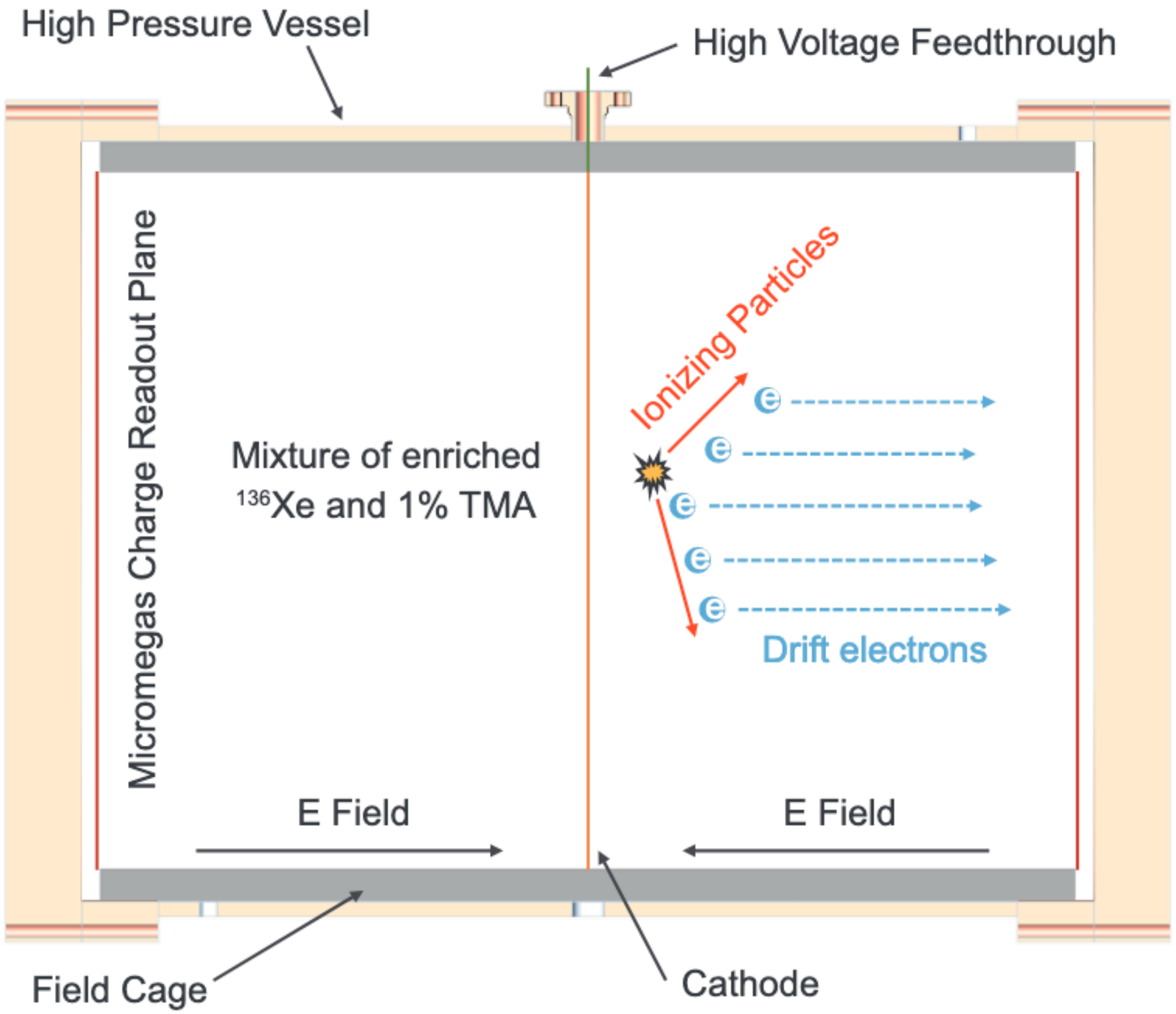

Microbulk Micromegas readout at both ends (no PMTs)

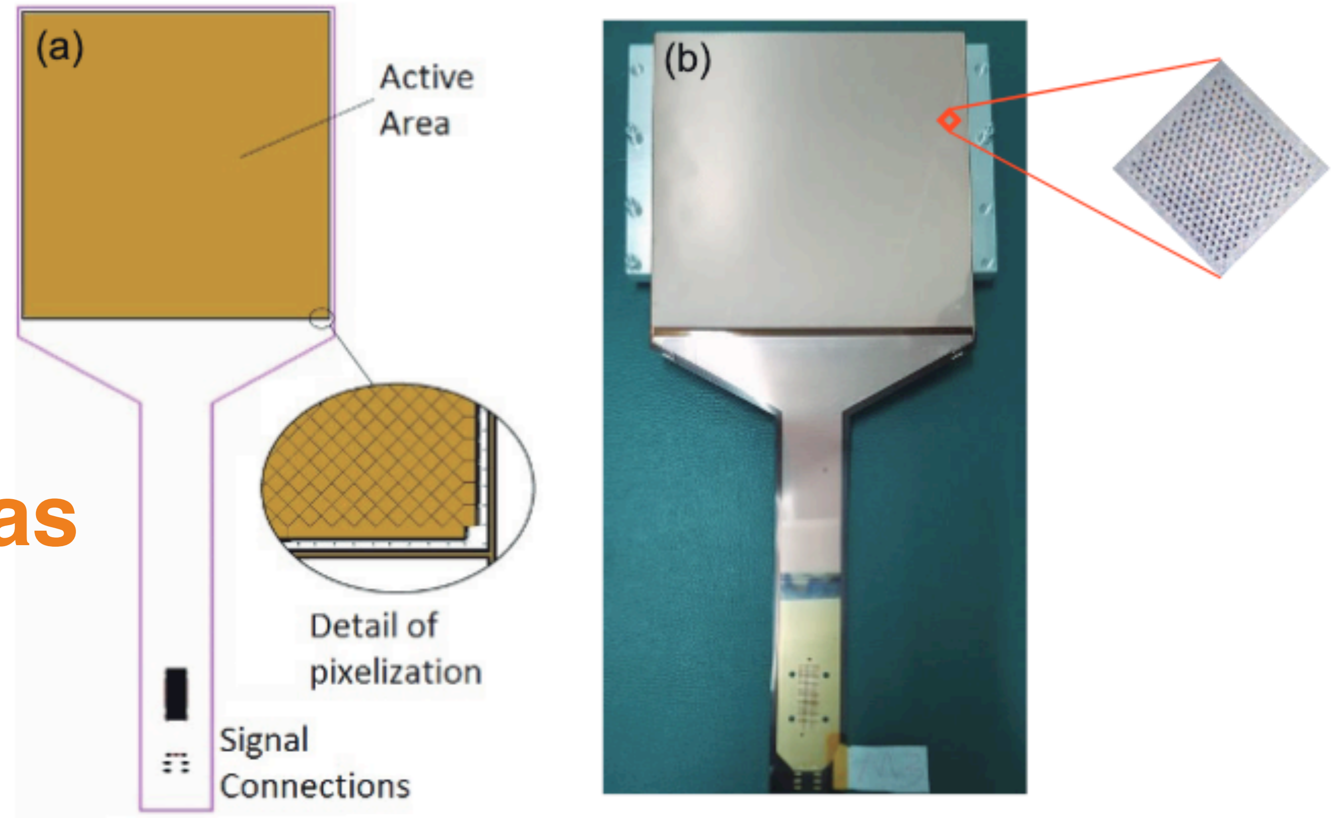

KamLAND

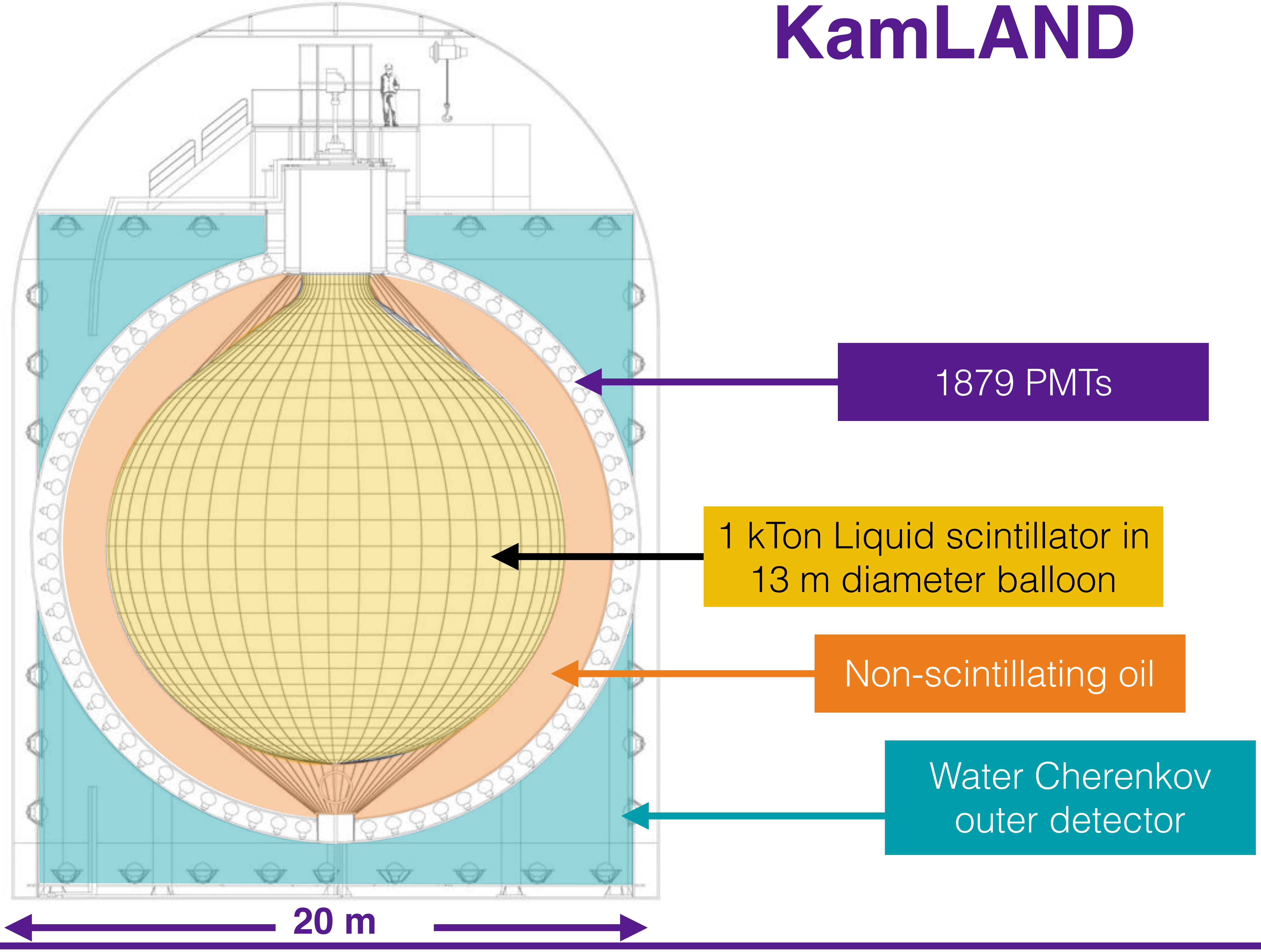
1879 PMTs
1 kTon Liquid scintillator in 13 m diameter balloon
Non-scintillating oil
Water Cherenkov outer detector
20 m

KamLAND - Zen

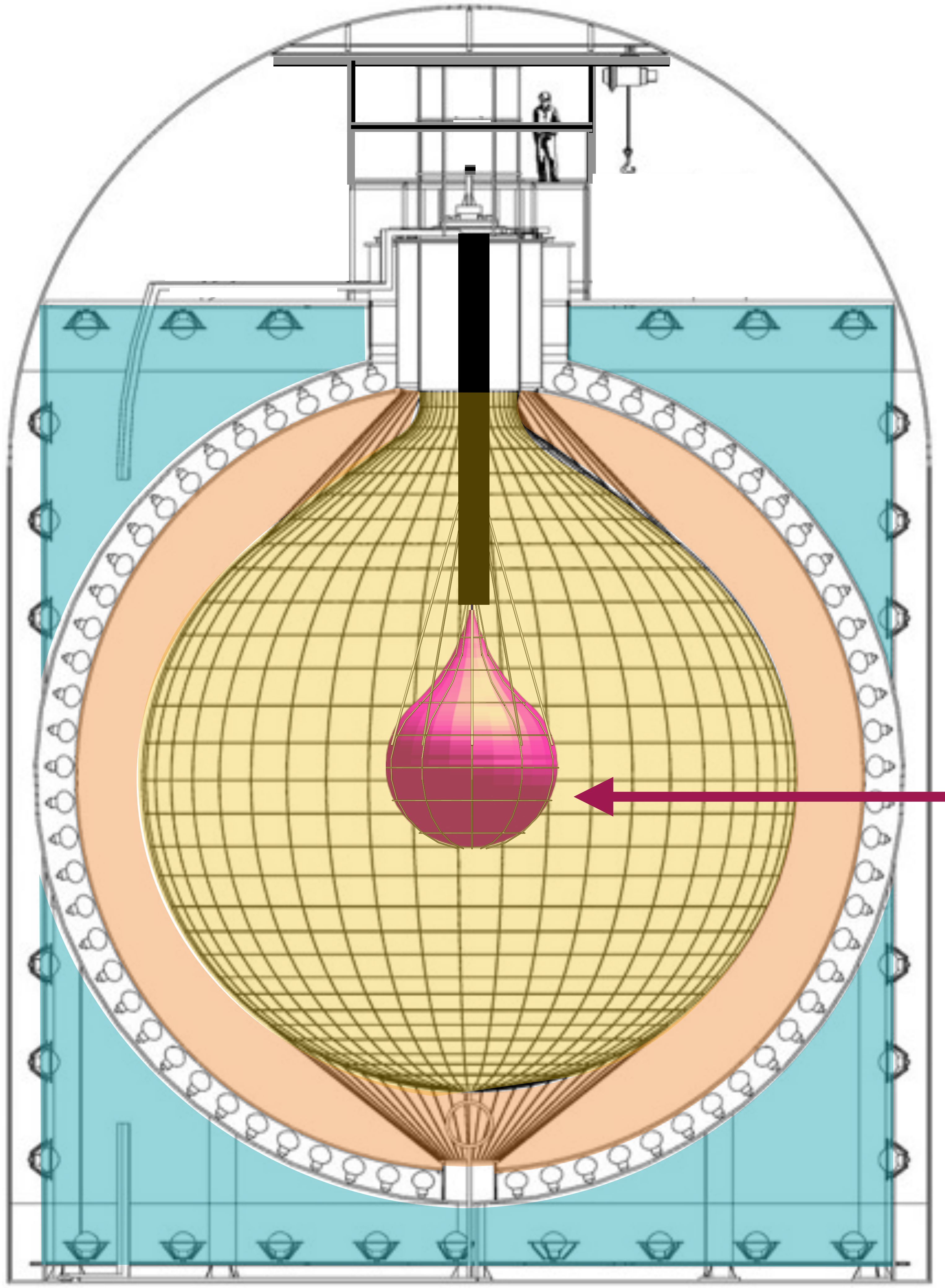

^{136}Xe-loaded liquid scintillator in inner balloon

KamLAND-Zen: ^{136}Xe in scintillator in Kamioka, Japan

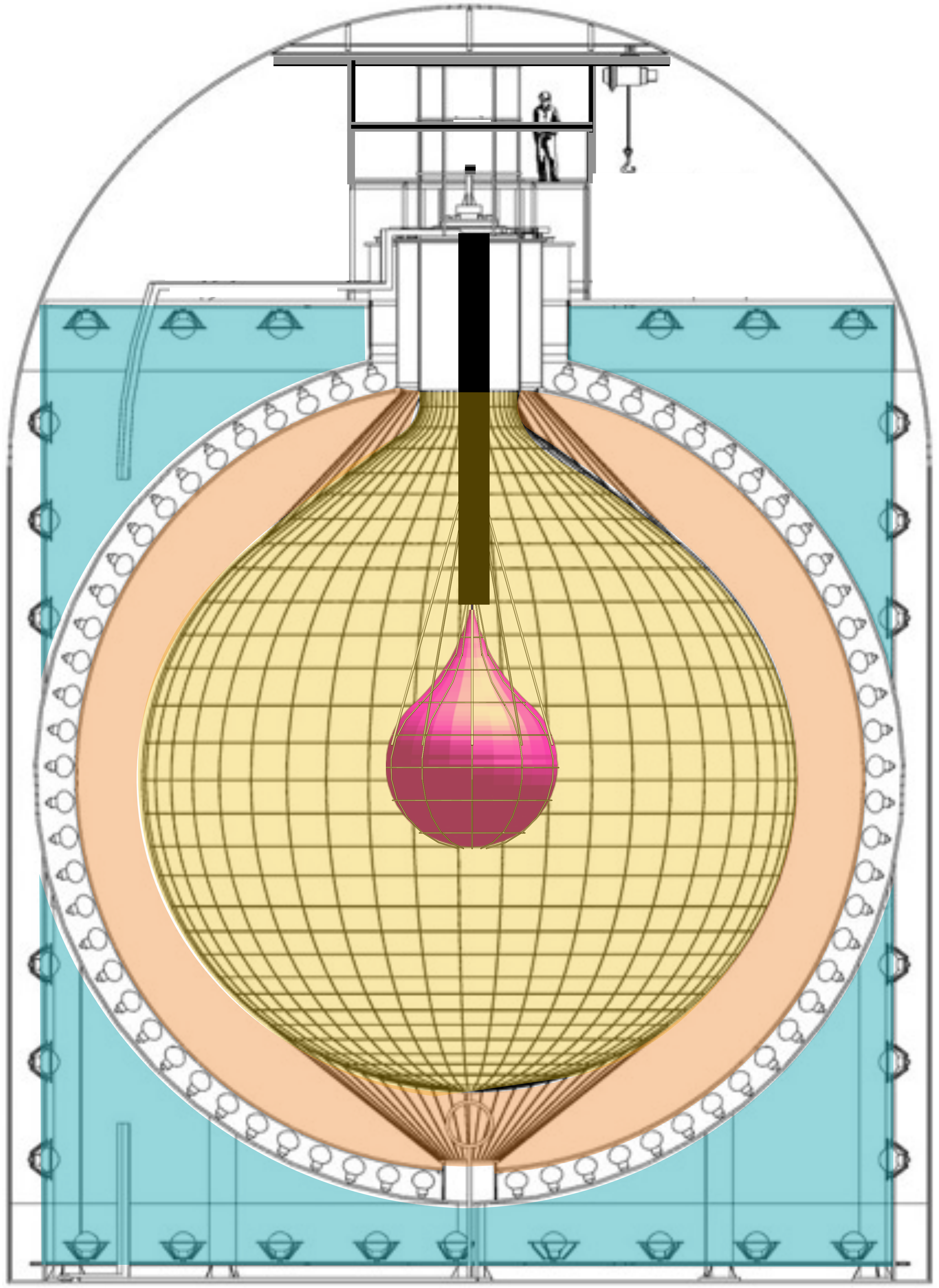

KamLAND - Zen

2011-2015	2018-	Future
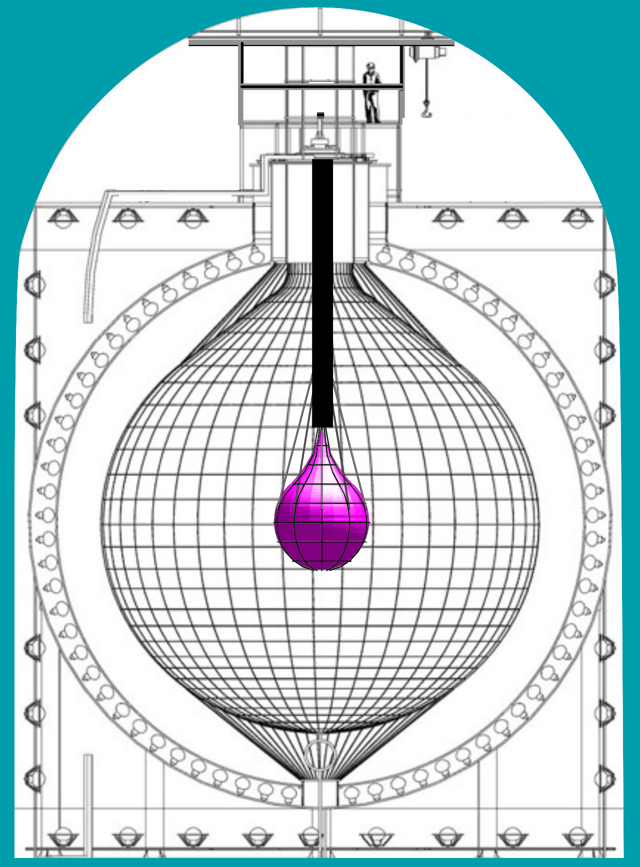	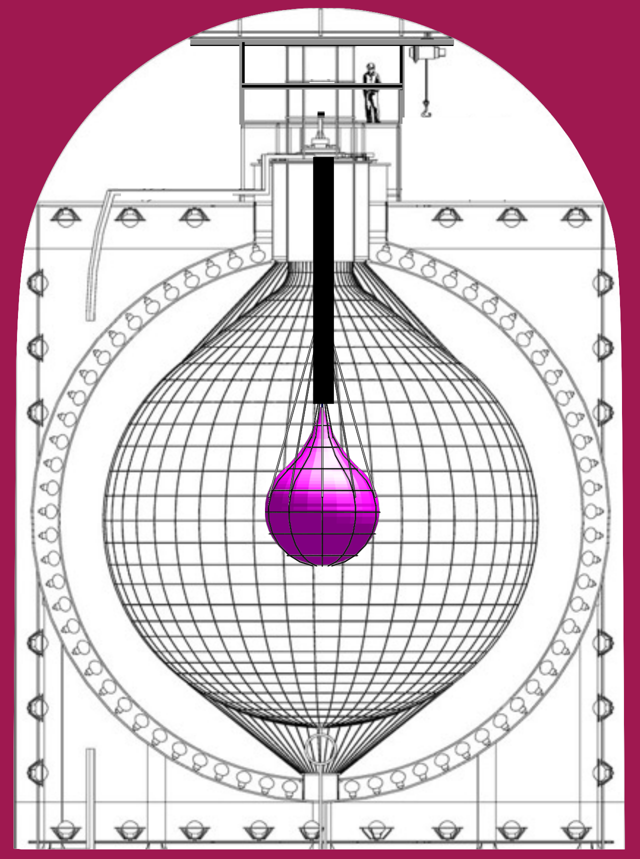	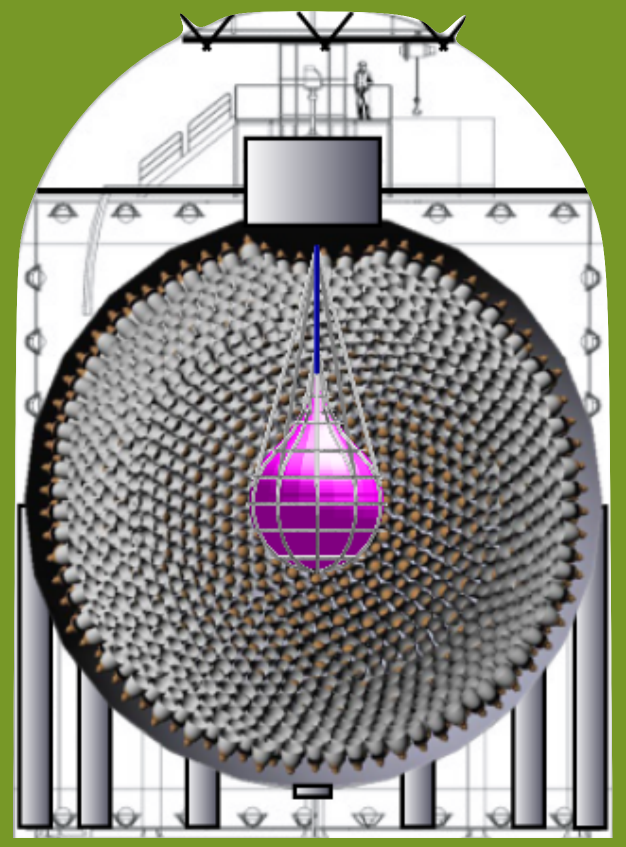
KamLAND-Zen 400	KamLAND-Zen 800	KamLAND2-Zen
320-380 kg of Xe	750 kg of Xe	1 ton of Xe
91% enriched		Better energy resolution

KamLAND-Zen: Backgrounds

^{110m}**Ag** (β emitter) in XeLS from Fukushima fallout: scintillator cleaned for Phase II

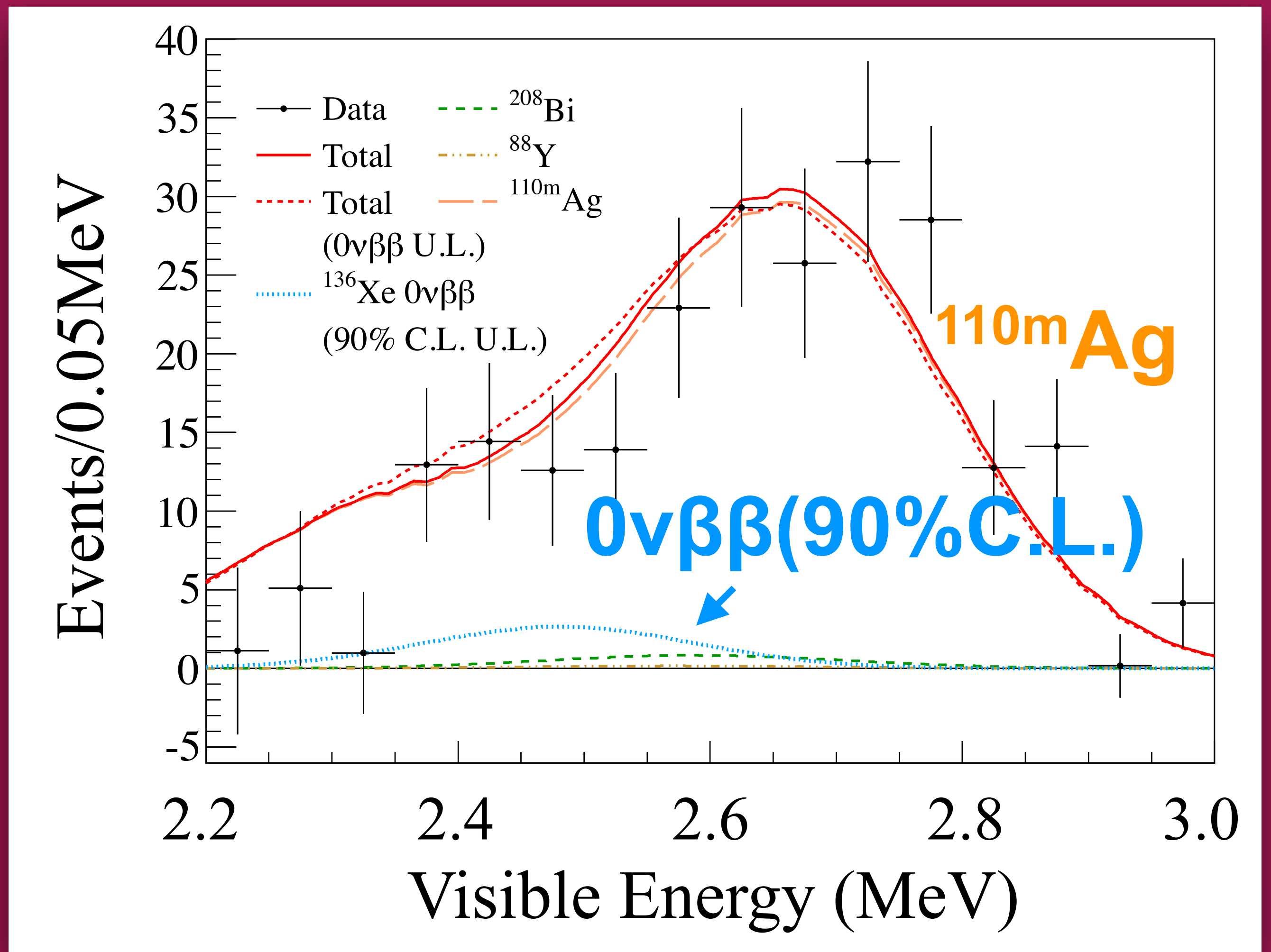

Inner balloon contamination from mine air

Large, monolithic detector lets you limit fiducial volume

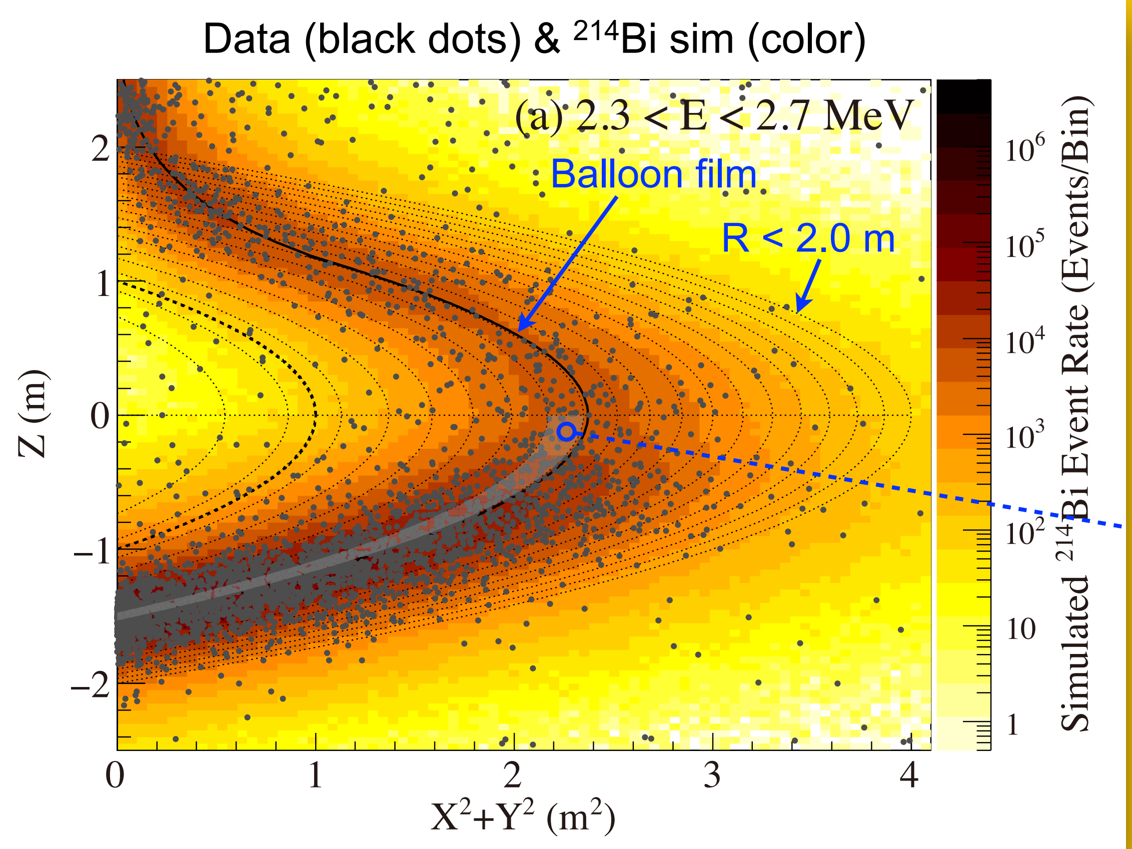

Muon-induced spallation product ^{10}C: triple coincidence muon + neutron + ^{10}C β^+ decay

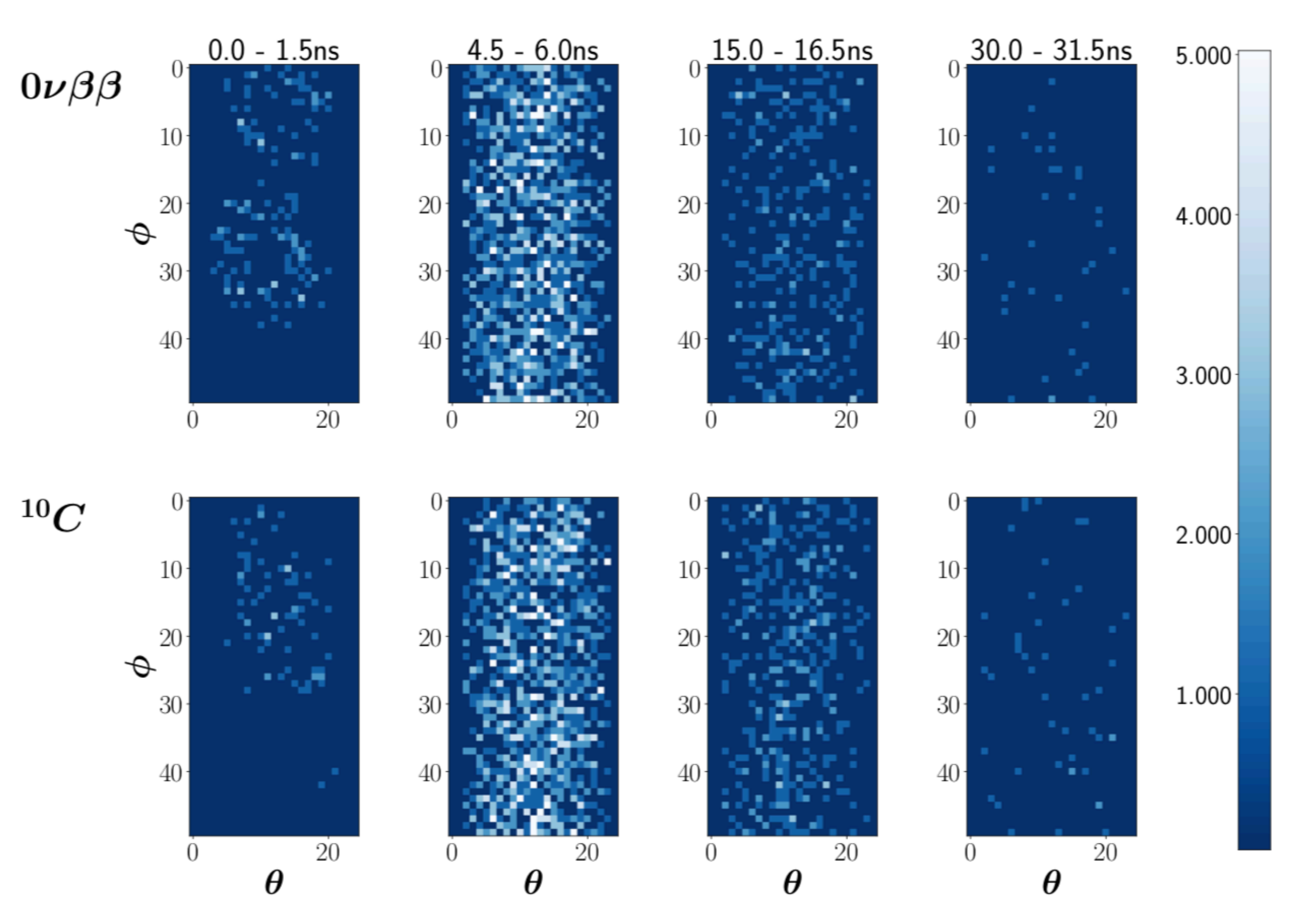

Separation with computer-vision algorithm

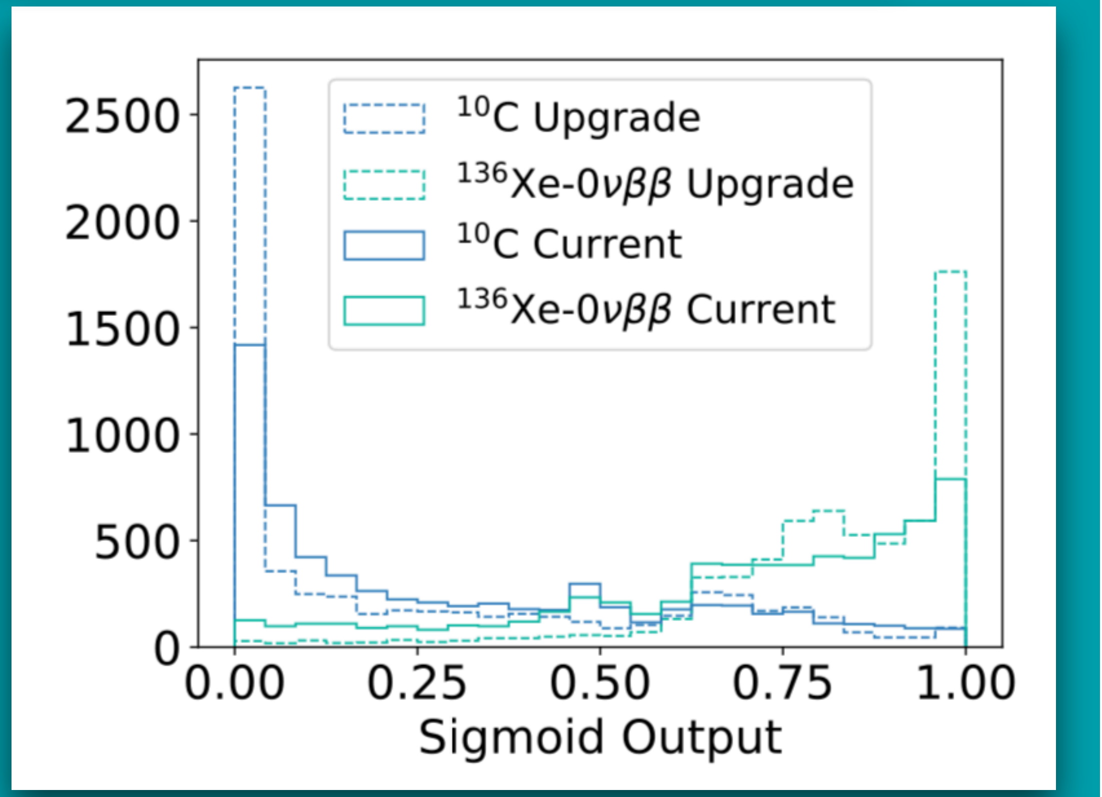

arXiv:1812.02906 [physics.ins-det]

KamLAND-Zen in pictures

Inner balloon being prepared…

… and installed into the detector…

…ready to be filled with scintillator and ^{136}Xe

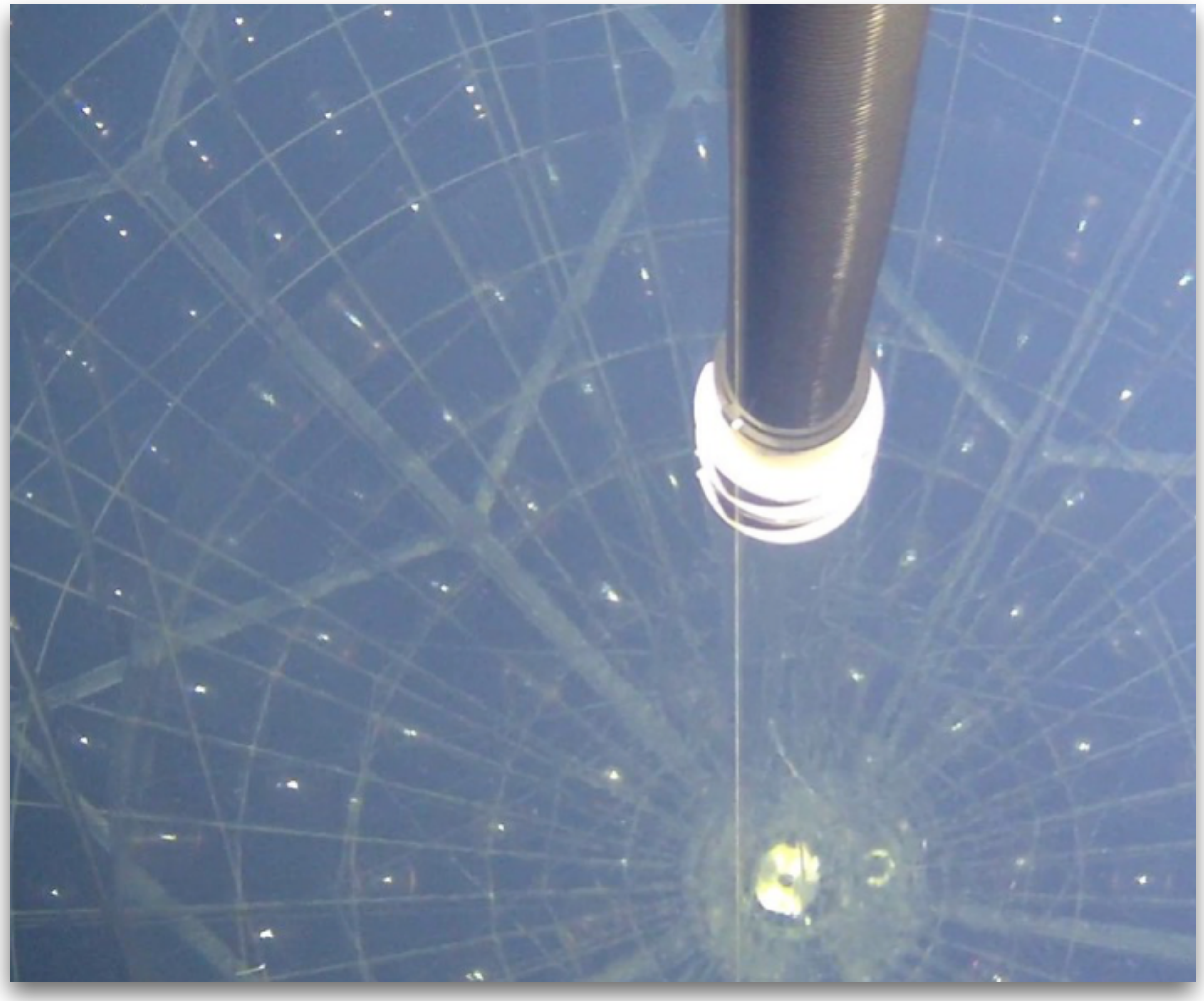

KamLAND-Zen: results

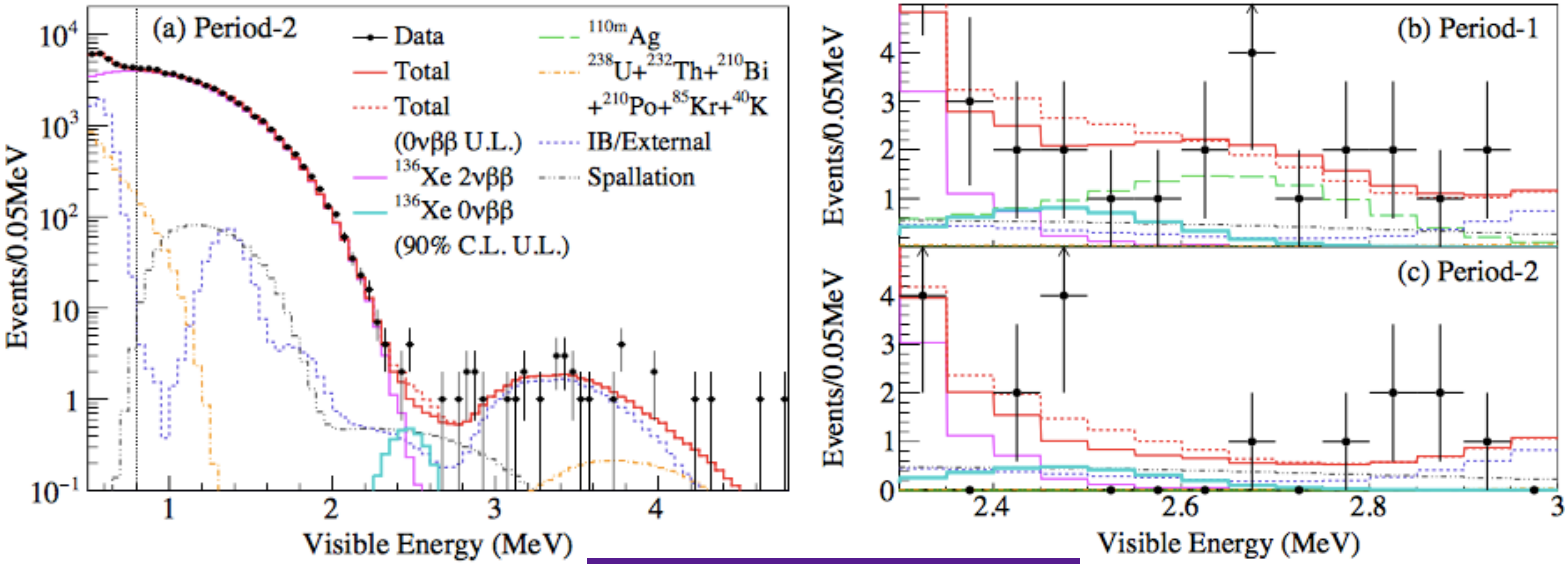

$T_{1/2} > 1.07 \times 10^{26}$ years
(〈$m_{\beta\beta}$〉 < 61-165 meV)
504 kg.years

Phys Rev Lett 117, 082503 (2016)

^{130}Te experiments

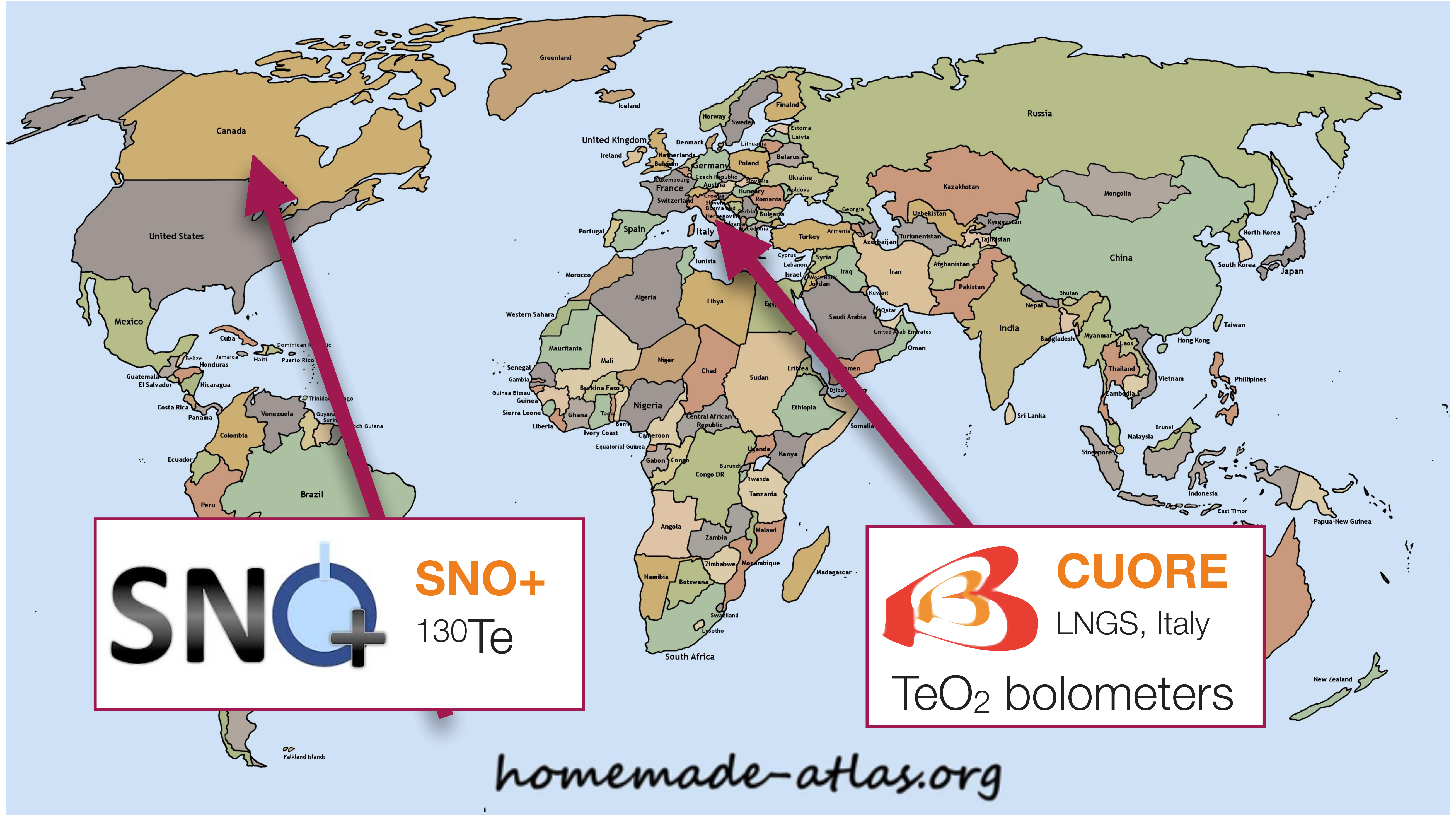

Better

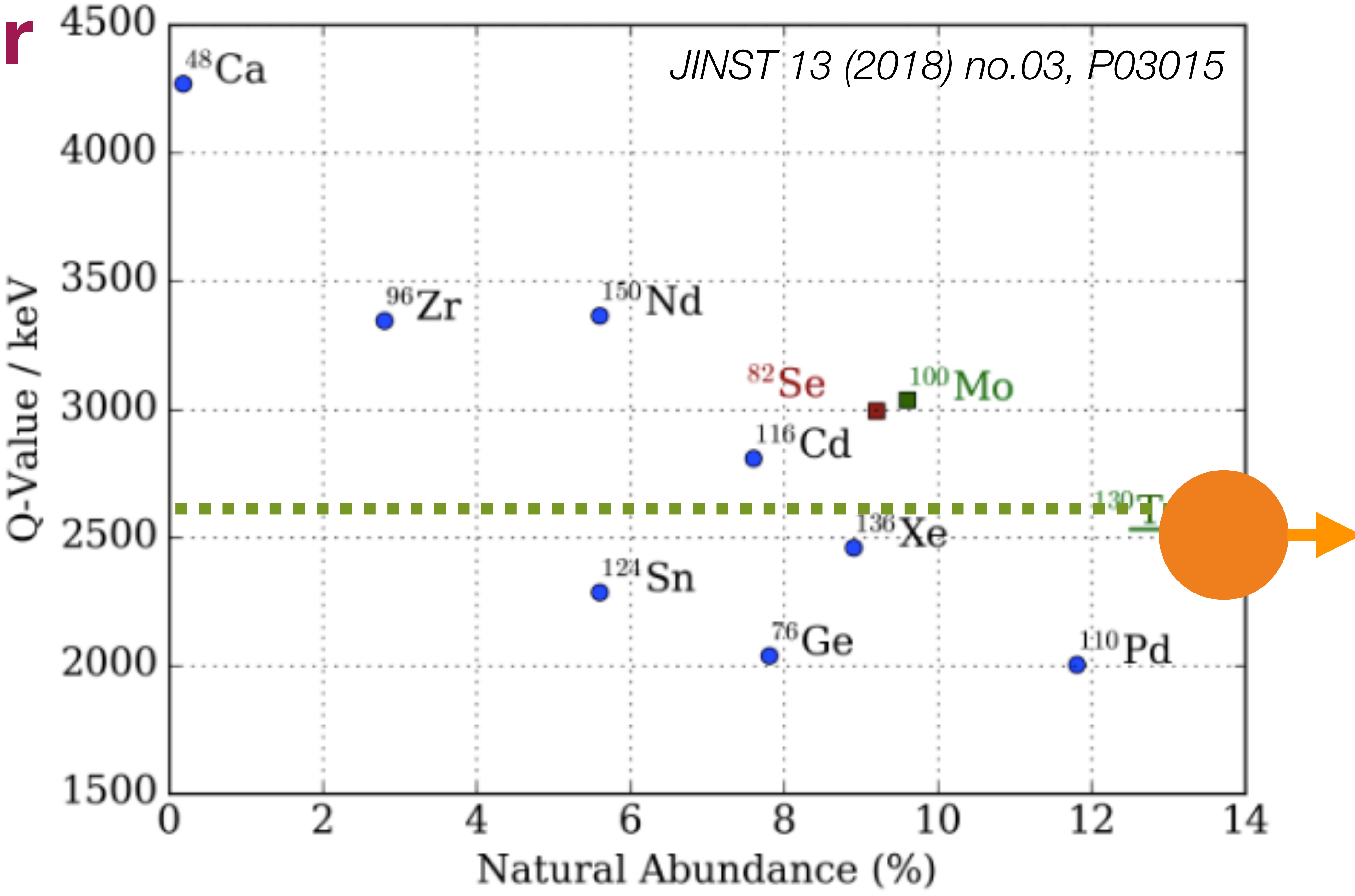

Better

- ^{130}Te has 34% natural **abundance**

SNO+ - Tellurium in liquid scintillator

SNO+ - Tellurium in liquid scintillator

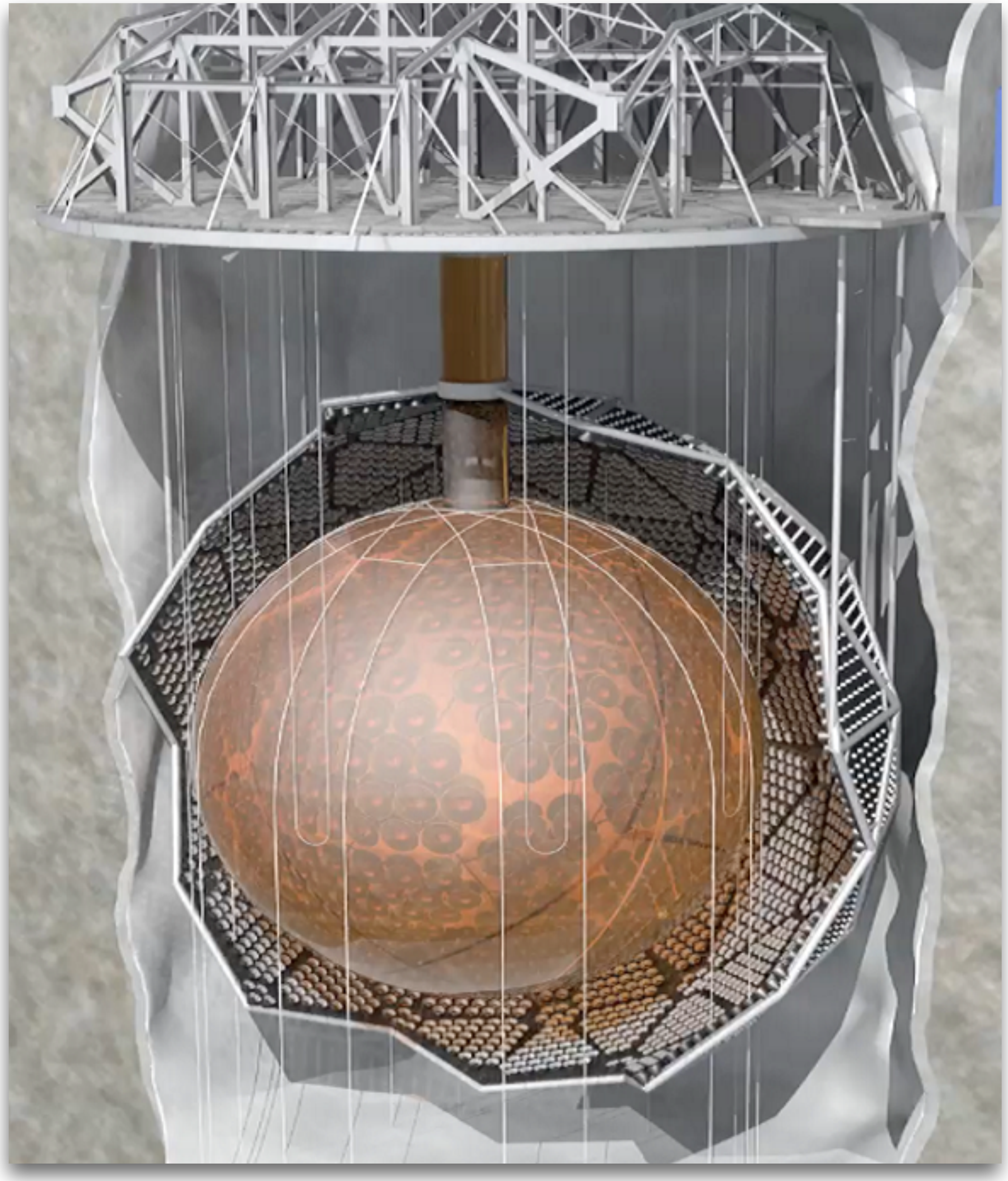

Thanks to Steve Biller & Esther Turner for slide content

- Highly **economical**
  - ^{130}Te is the most economically scalable **isotope** (high natural abundance);
  - Liquid scintillator also very economically scalable **detector technology**!
- Potential for dramatic **scale-up**

SNO+ - Tellurium in liquid scintillator

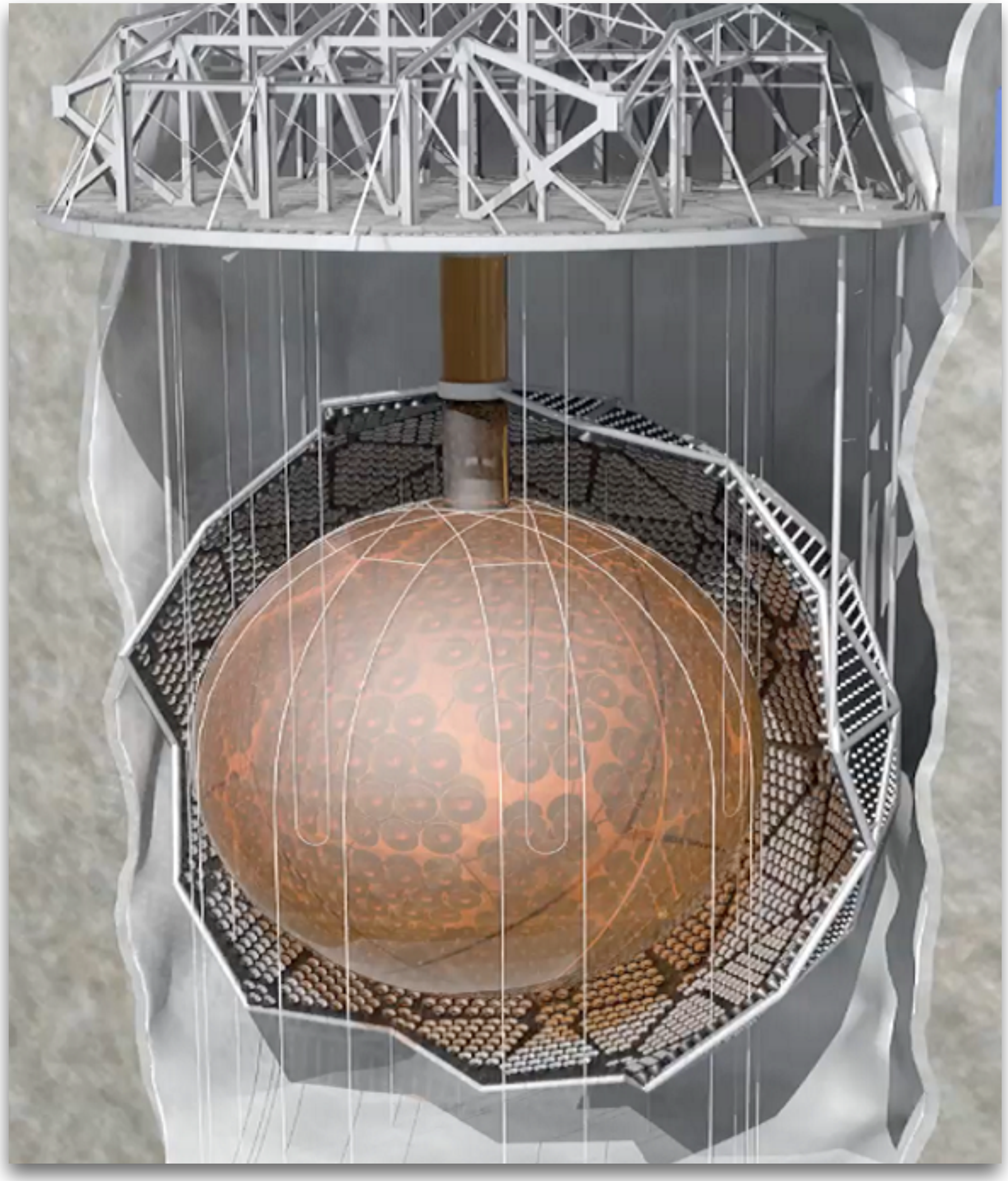

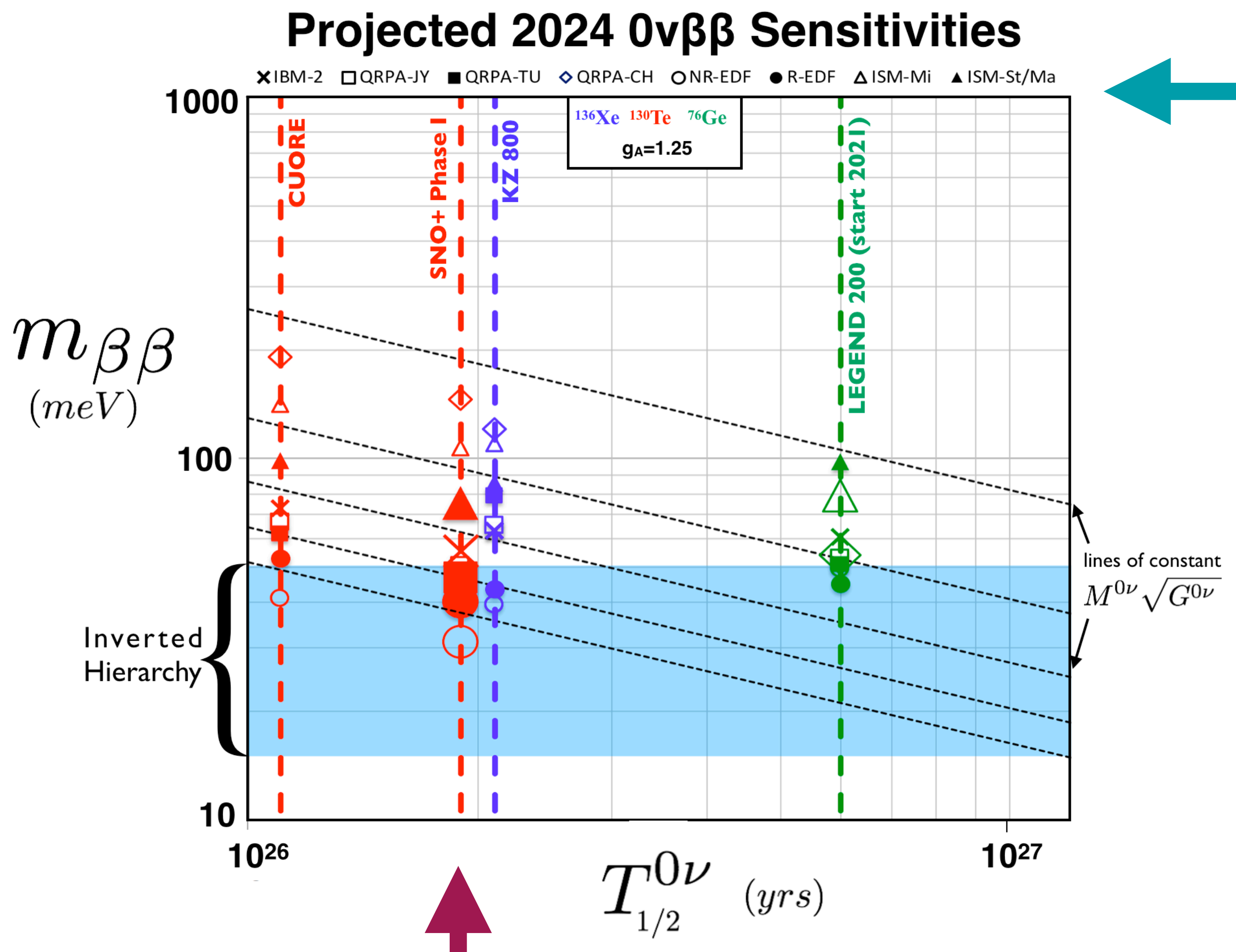

Different matrix element calculations give different masses for the same half-life

- Highly **economical**
  - ^{130}Te is the most economically scalable **isotope** (high natural abundance);
  - Liquid scintillator also very economically scalable **detector technology**!
- Potential for dramatic **scale-up**
- Allows **sensitivity** above current leading measurement:
  - $T_{1/2}^{0\nu\beta\beta} > 2.1e^{26}$ years (**$m_{\beta\beta}$ < 37- 89 meV**) after 5 years of running

SNO+ - Tellurium in liquid scintillator

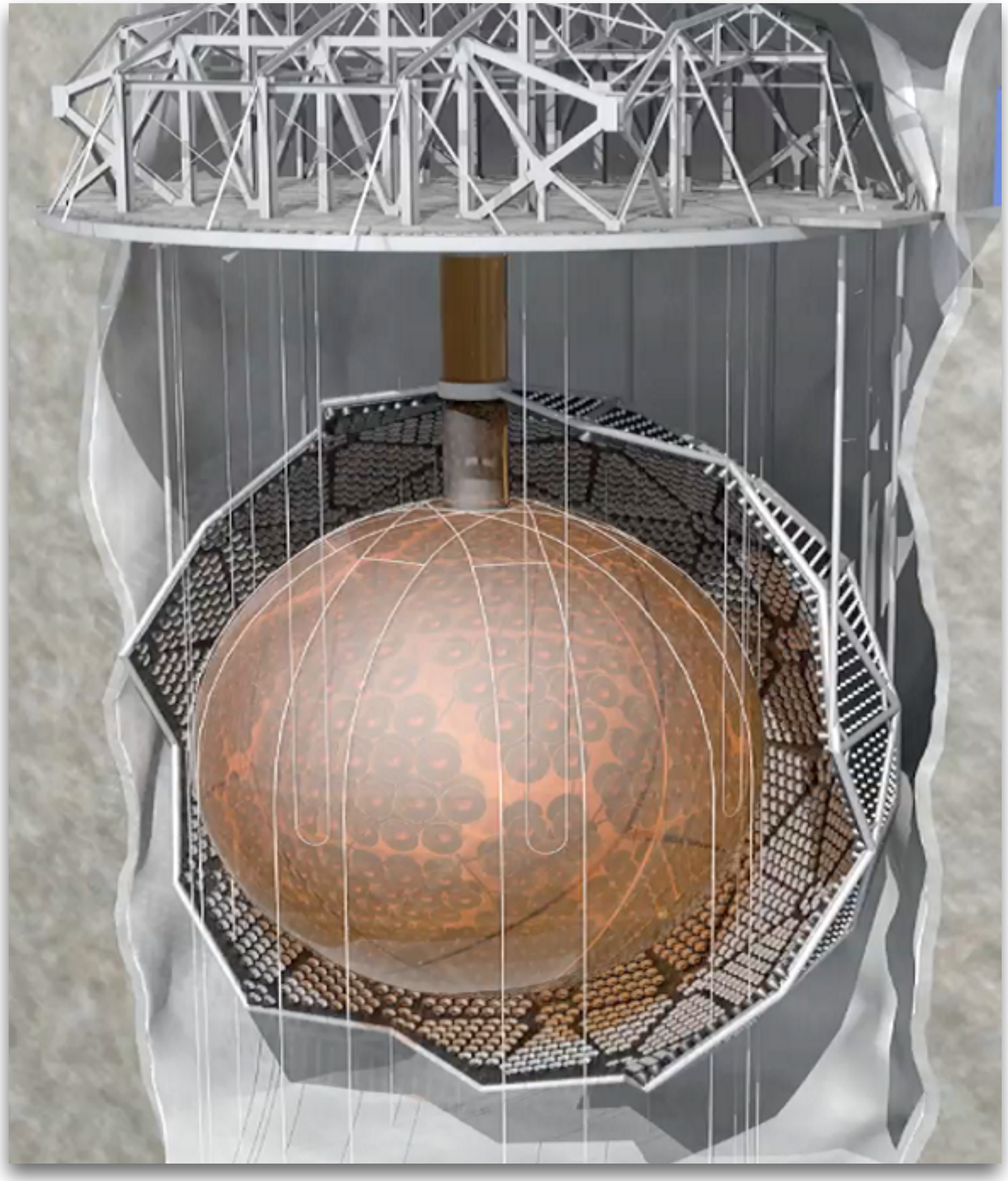

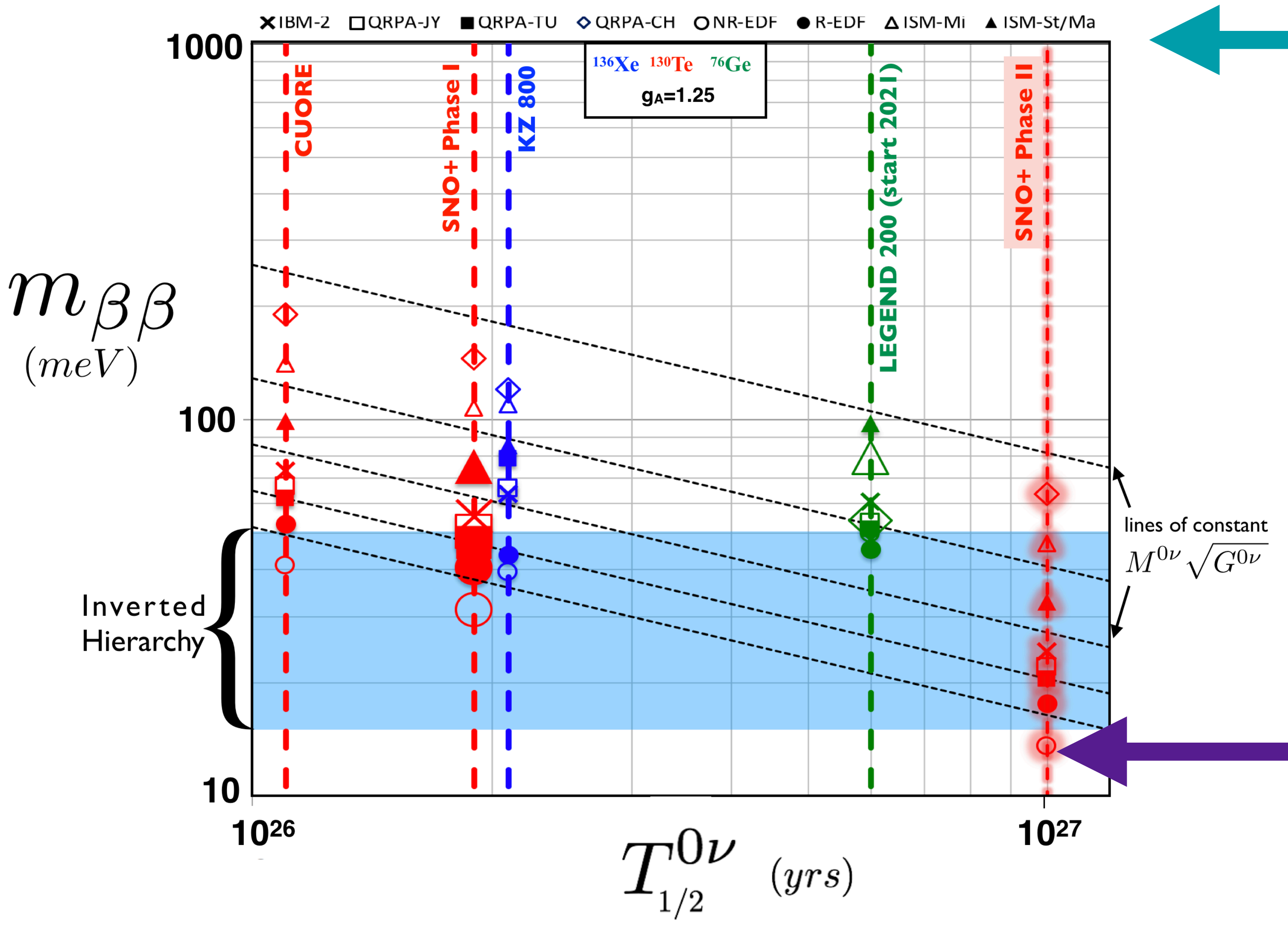

Different matrix element calculations give different masses for the same half-life

New chemistry developments may make it possible to simply increase the loading in the current instrument to achieve this

- Highly **economical**
  - ^{130}Te is the most economically scalable **isotope** (high natural abundance);
  - Liquid scintillator also very economically scalable **detector technology**!
- Potential for dramatic **scale-up**
- Allows **sensitivity** above current leading measurement:
  - $T_{1/2}^{0\nu\beta\beta} > 2.1e^{26}$ years (**$m_{\beta\beta}$ < 37- 89 meV**) after 5 years of running
- **Phase II** could reach **10^{27}** years with the same detector but **higher loading**

SNO+ tellurium loading

New loading method:
Te-butanediol complex dissolved in liquid scintillator

- Simple **synthesis**
- Single **safe**, distillable chemical
- Low **radioactivity** levels
- Minimal optical **absorption**
- High **light levels** at 0.5% ^{nat}Te loading

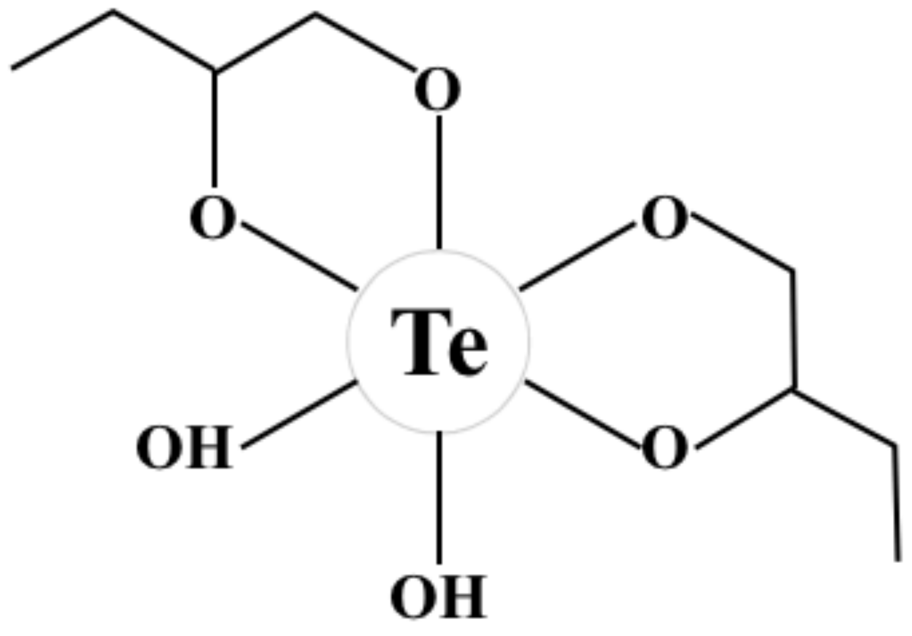

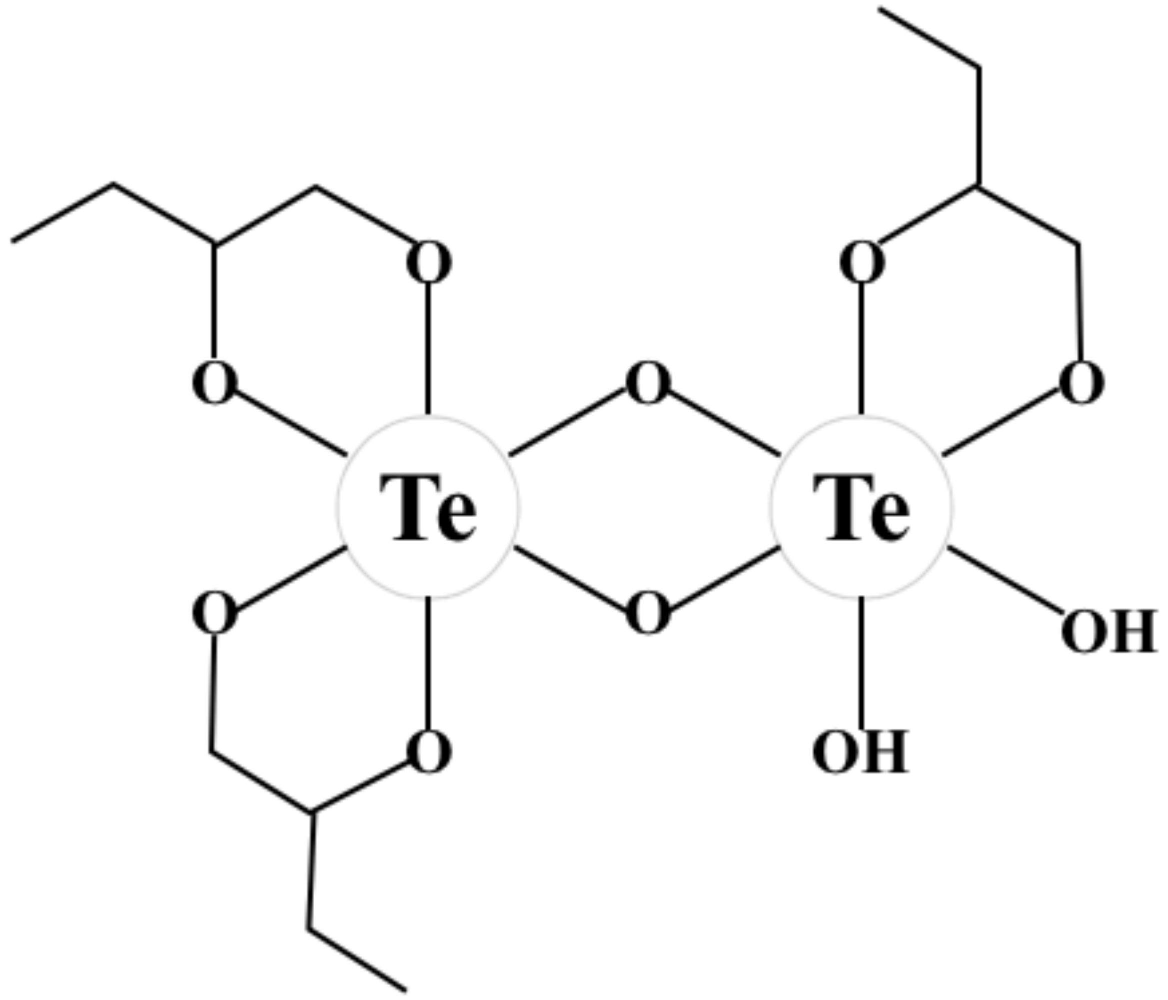

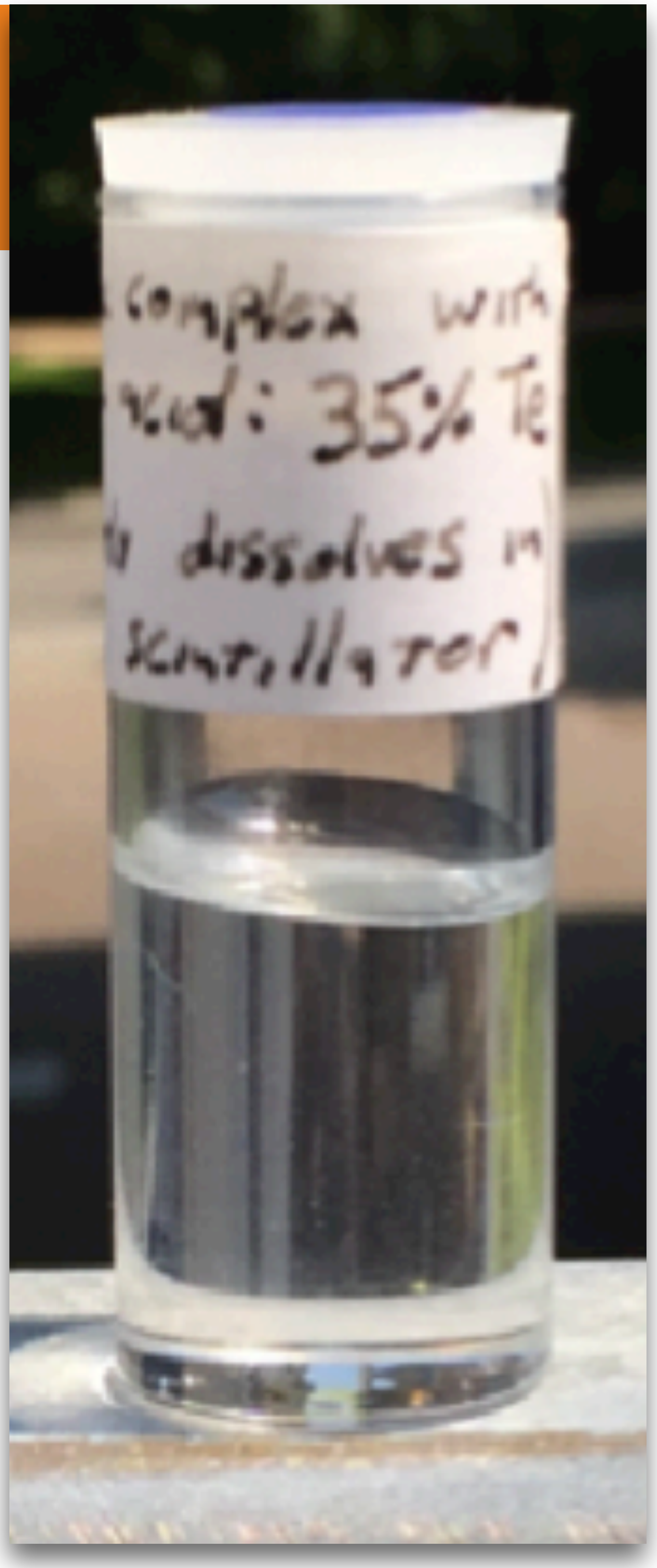

Natural tellurium is 34% ^{130}Te

Detector progress

- Operating with **water** from 2017

PHYSICAL REVIEW D **99,** 012012 (2019)

Measurement of the ^{8}B solar neutrino flux in SNO+ with very low backgrounds

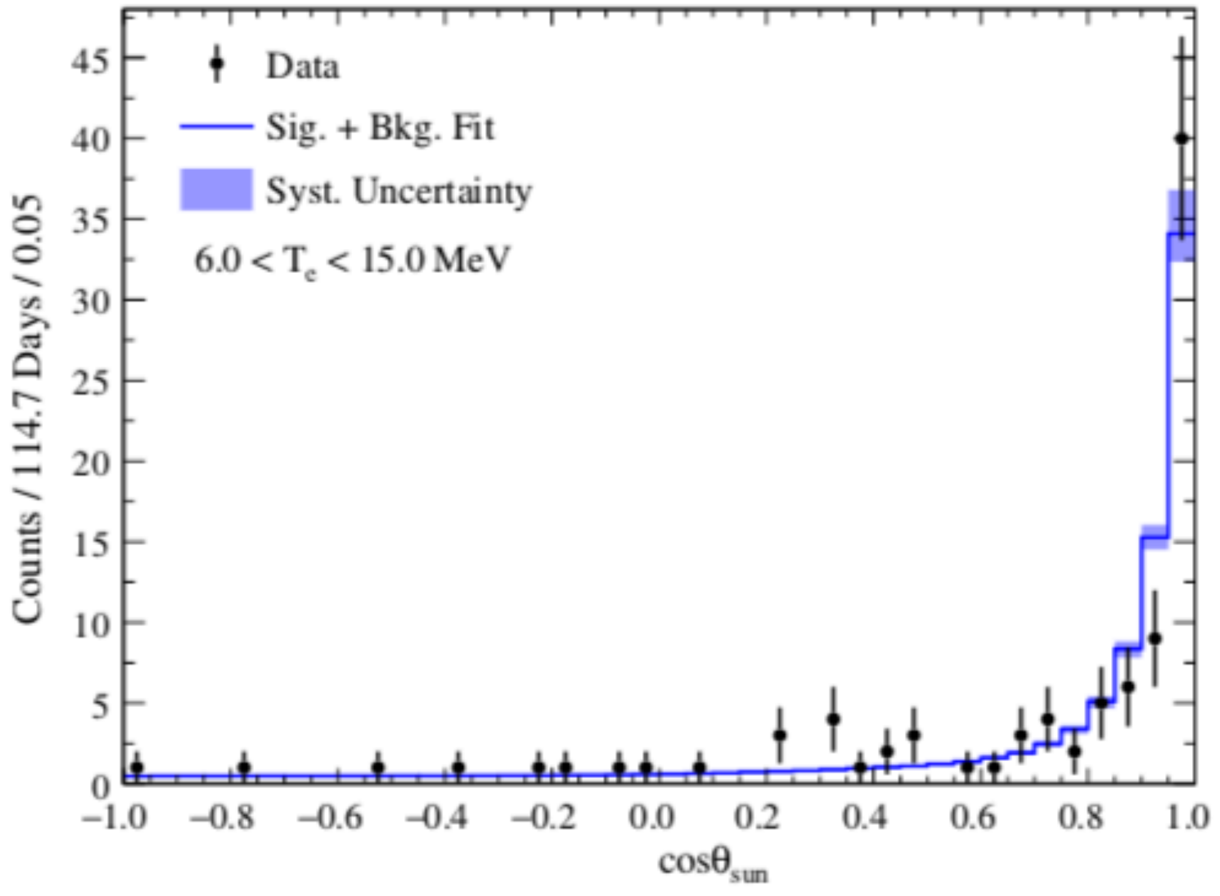

FIG. 4. Distribution of event directions with respect to solar direction for events with energy in the range 6.0–15.0 MeV.

↑ Largest background to 0νββ

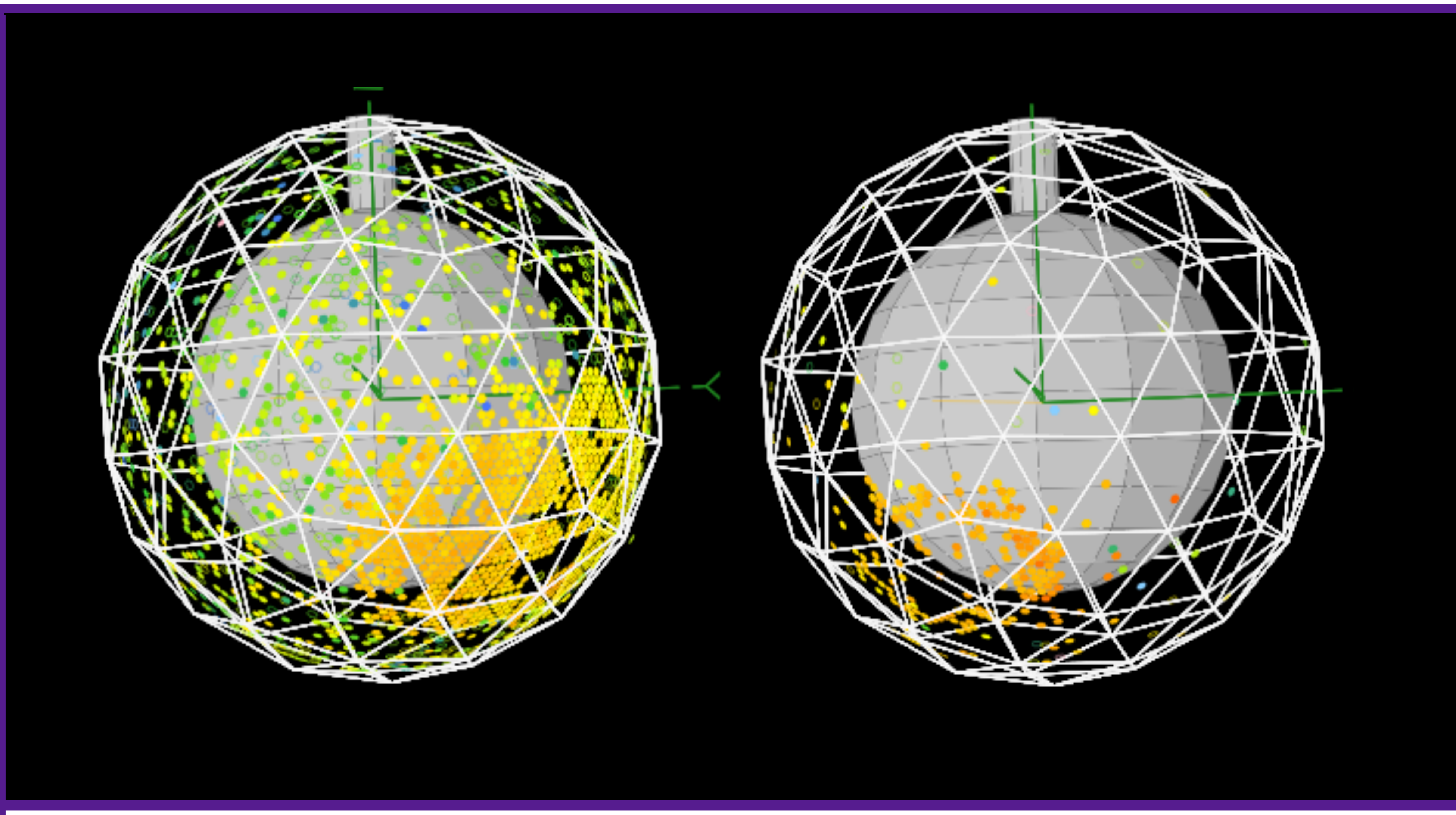

PHYSICAL REVIEW D **99,** 032008 (2019)

Search for invisible modes of nucleon decay in water with the SNO+ detector

TABLE VI. Lifetime limits at 90% C.I. for the spectral and counting analysis, including statistical and systematic uncertainties alongside the existing limits.

	Spectral analysis	Counting analysis	Existing limits
n	2.5×10^{29} y	2.6×10^{29} y	5.8×10^{29} y [9]
p	3.6×10^{29} y	3.4×10^{29} y	2.1×10^{29} y [10]
pp	4.7×10^{28} y	4.1×10^{28} y	5.0×10^{25} y [11]
pn	2.6×10^{28} y	2.3×10^{28} y	2.1×10^{25} y [13]
nn	1.3×10^{28} y	0.6×10^{28} y	1.4×10^{30} y [9]

- **Invisible nucleon decay**
- **Solar neutrinos**
- **Supernova neutrinos**

Plus neutron capture, muon-induced neutrons (in progress)

Detector progress

- Operating with **water** from 2017
- Transition to **scintillator** happening now

- Invisible nucleon decay
- Solar neutrinos
- Supernova neutrinos
- **Reactor antineutrinos (Δm^2_{12})**
- **Geo-neutrinos**

- Scintillator purification plant commissioned
- **LAB solvent** successfully distilled underground
- **PPO fluor** prep underway
- N_2/steam stripping tested

Detector progress

- Operating with **water** from 2017
- Transition to **scintillator** happening now
- **Tellurium** loading for ββ due in 2019-20 (1330 kg ^{130}Te)

- Invisible nucleon decay
- Solar neutrinos
- Supernova neutrinos
- Reactor neutrinos (Δm^2_{12})
- Geo-neutrinos
- **Neutrinoless double-beta decay**

Te needed for Phase I **all underground**

Te **purification system** almost complete

Te-diol synthesis plant construction is well advanced (synthesised from telluric acid)

SNO+ Sensitivity and backgrounds

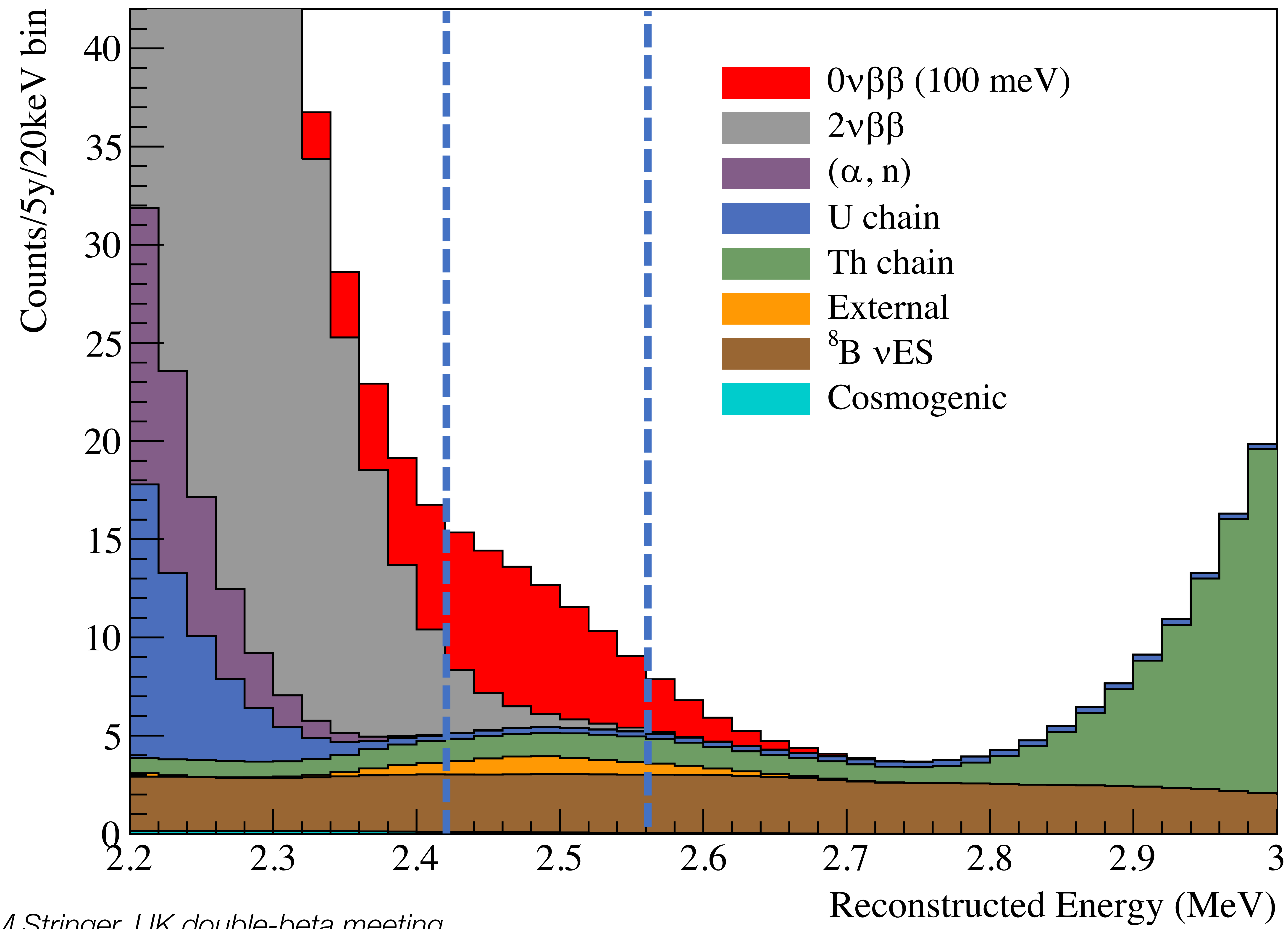

M Stringer, UK double-beta meeting

ROI: 2.42 - 2.56 MeV [-0.5σ - 1.5σ]
Counts/Year: 9.47

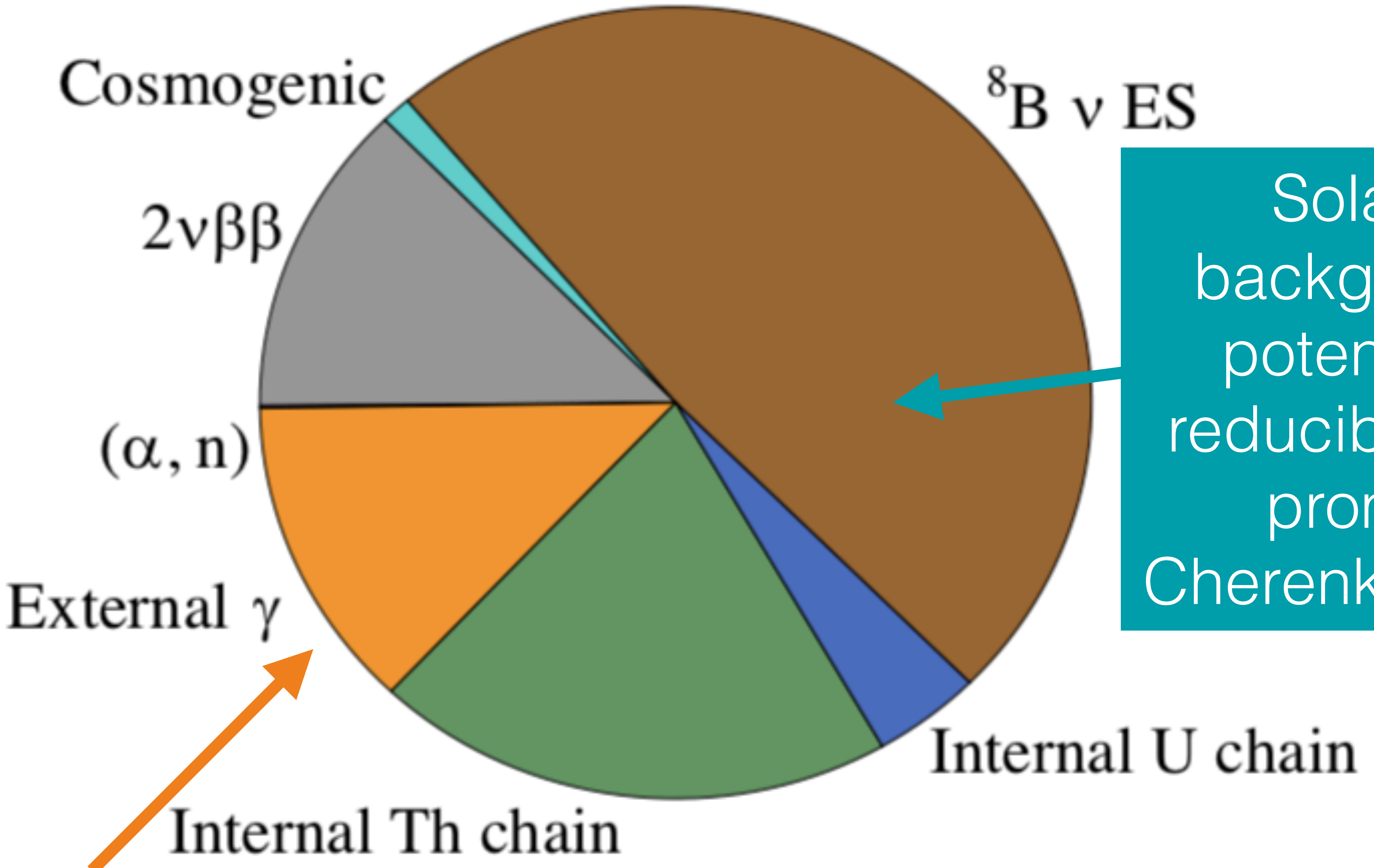

Solar ν background potentially reducible with prompt Cherenkov light

Fiducial volume cut reduces externals

$T_{1/2} > 2.1 \times 10^{26}$ years
Predicted for 5 years of running

CUORE: TeO_2 bolometers at LNGS, Italy

988 natural TeO_2 crystals (206 kg of ^{130}Te)

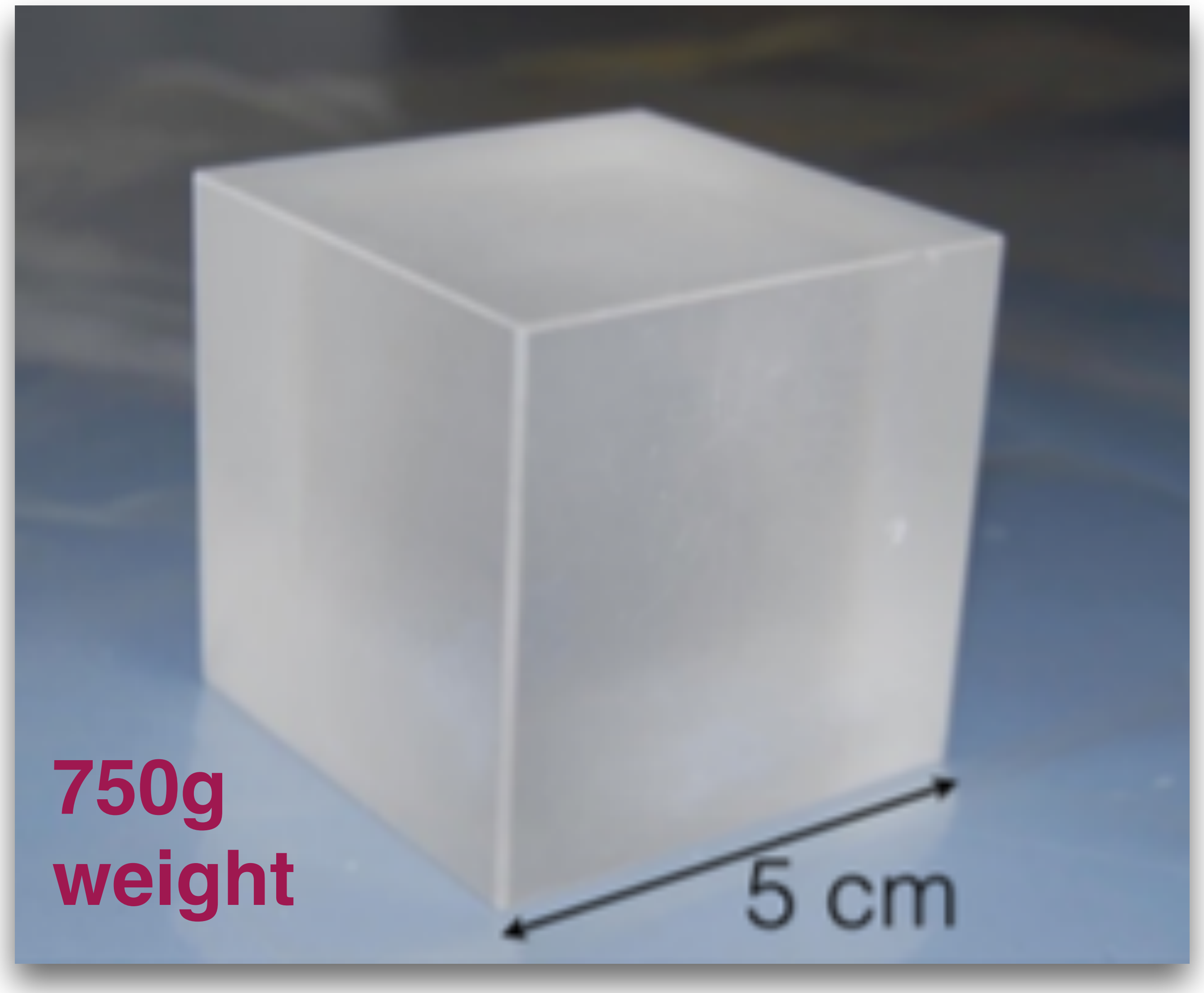

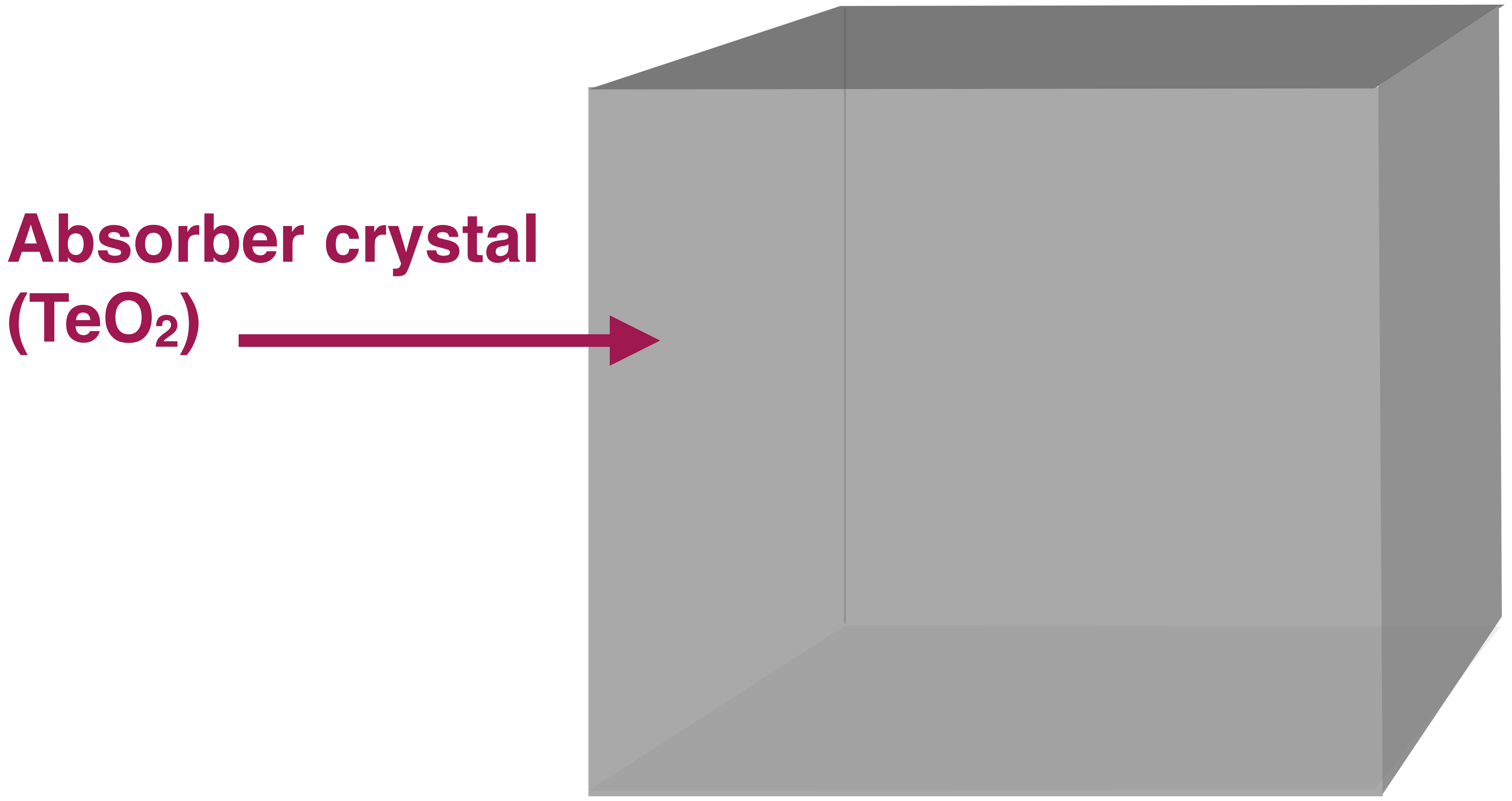

- Crystal is **source and detector** (solid-state bolometer)
- Future plans to use **other isotopes** (^{82}Se)

CUORE: TeO_2 bolometers at LNGS, Italy

- Crystals at low temperature: **10 mK**

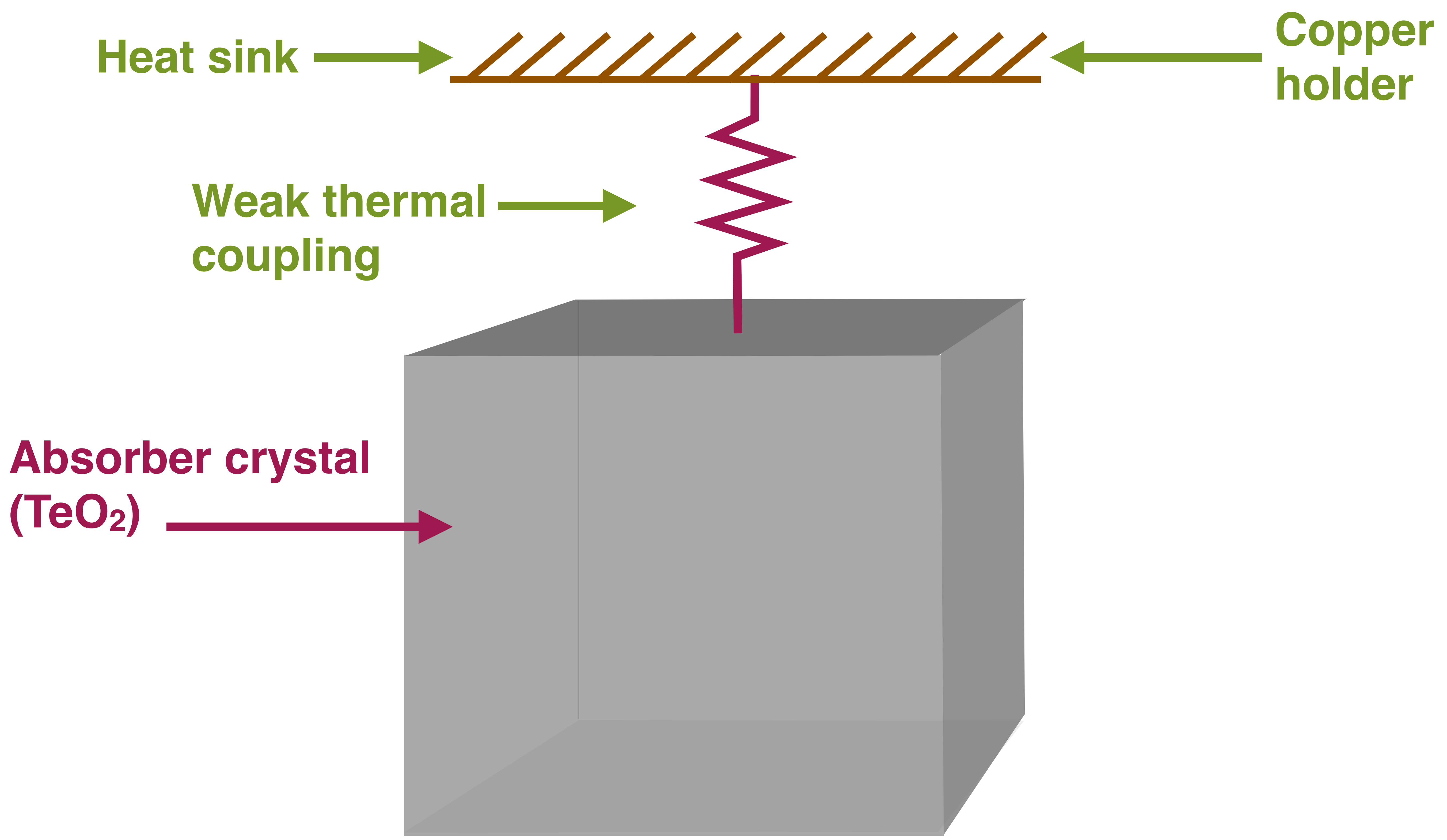

CUORE: TeO_2 bolometers at LNGS, Italy

- Crystals at low temperature: **10 mK**
- Energy deposition (e.g. ββ decay) **raises temperature** by ~ **100 μK / MeV**

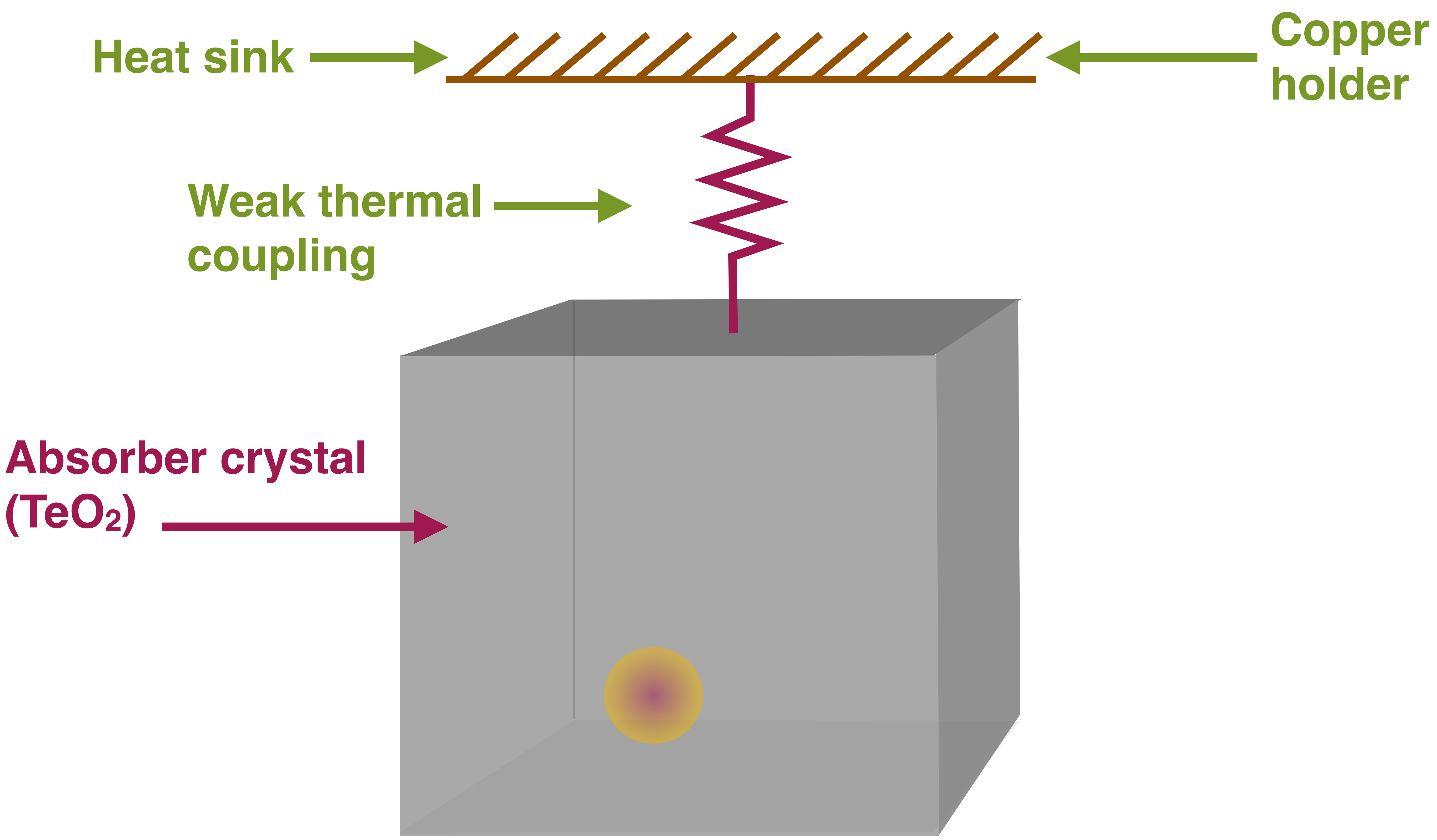

CUORE: TeO_2 bolometers at LNGS, Italy

- Crystals at low temperature: **10 mK**
- Energy deposition (e.g. ββ decay) **raises temperature** by ~ **100 μK / MeV**
- Read out by a germanium neutron transmutation doped **thermometer**

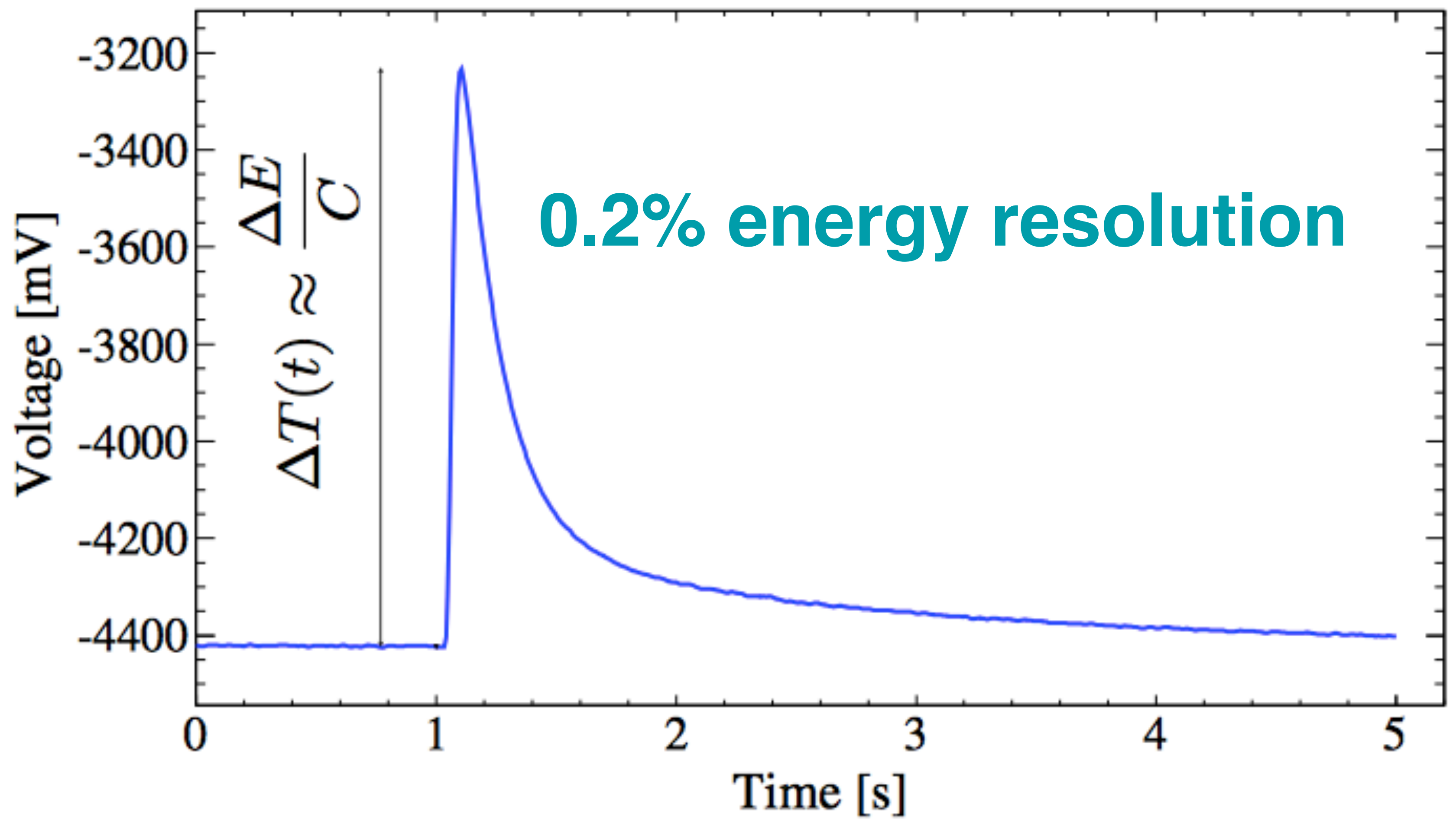

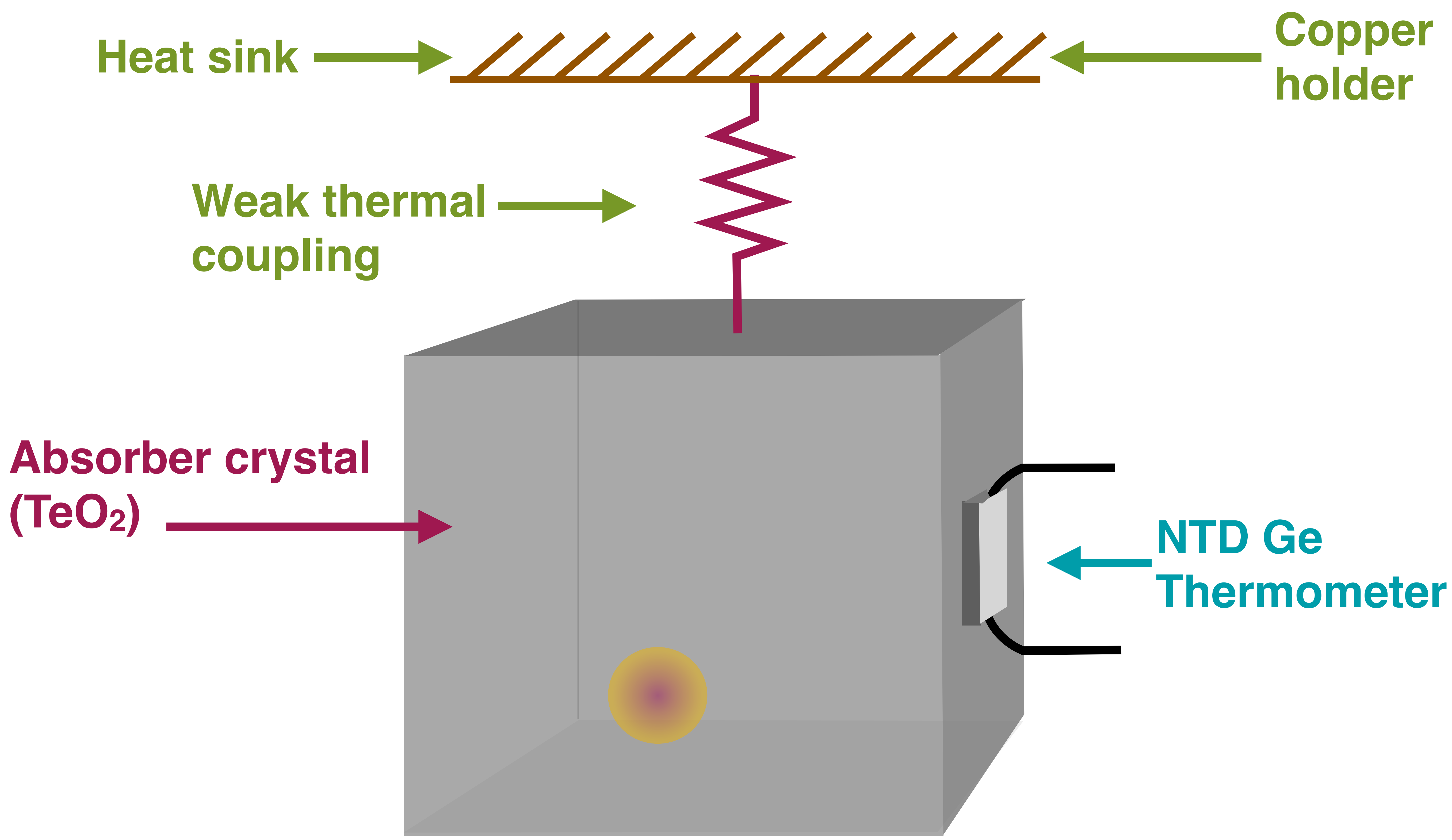

CUORE: TeO_2 bolometers at LNGS, Italy

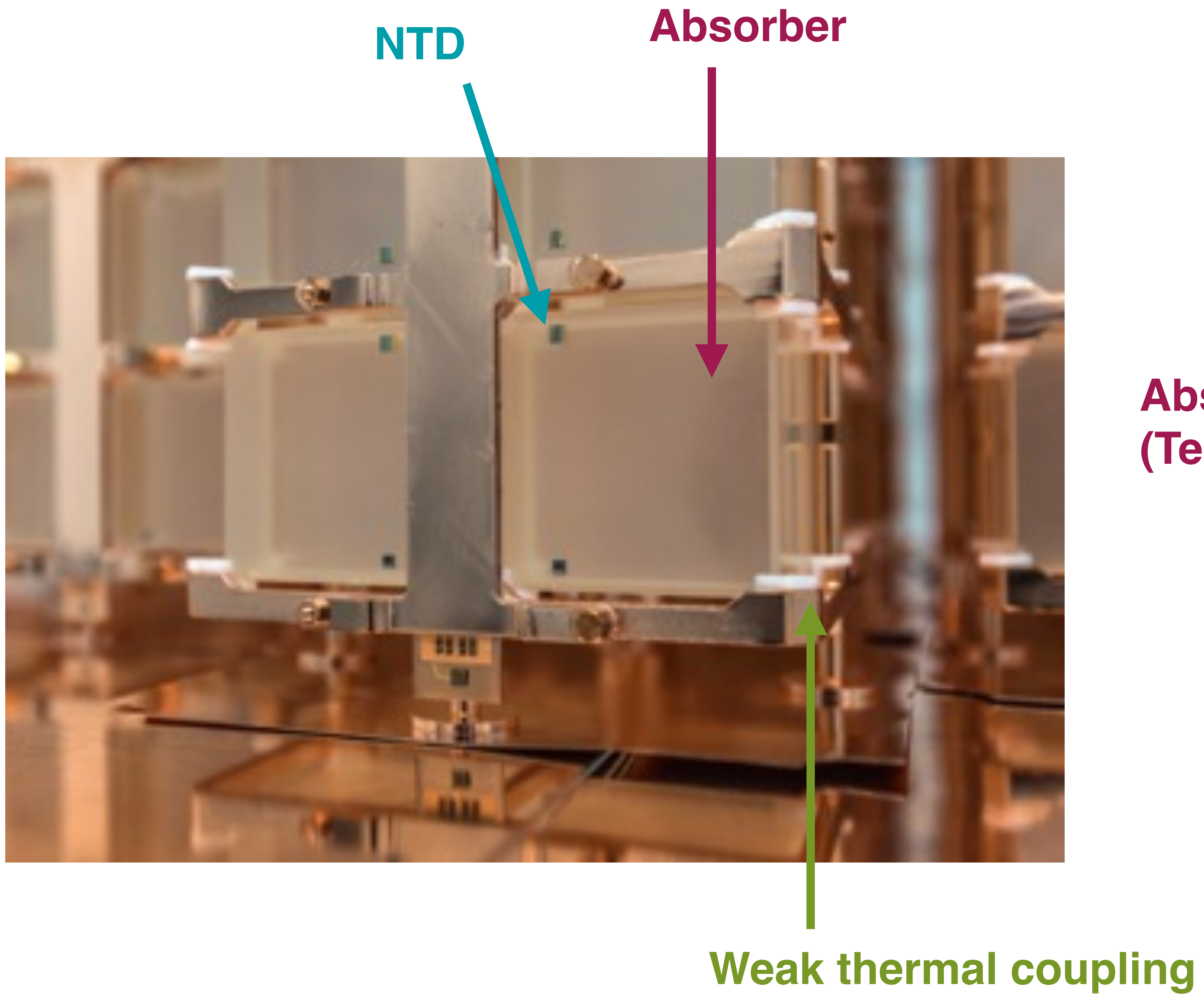

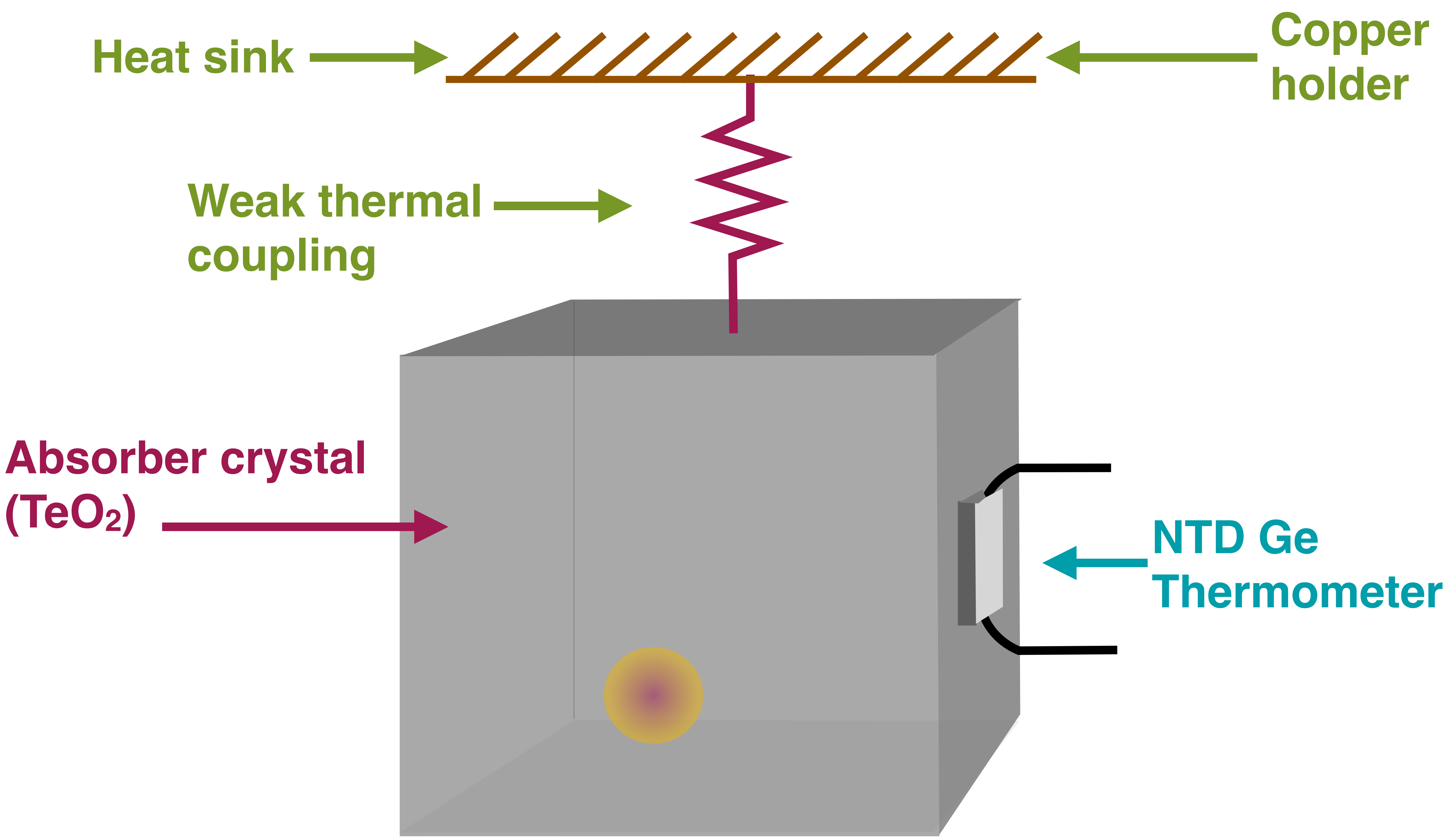

CUORE detector

Cooling

- Detectors cooled to 10 mK
- Long-term **stable** base temperature **6.3 mK**

Coldest cubic metre in the known universe

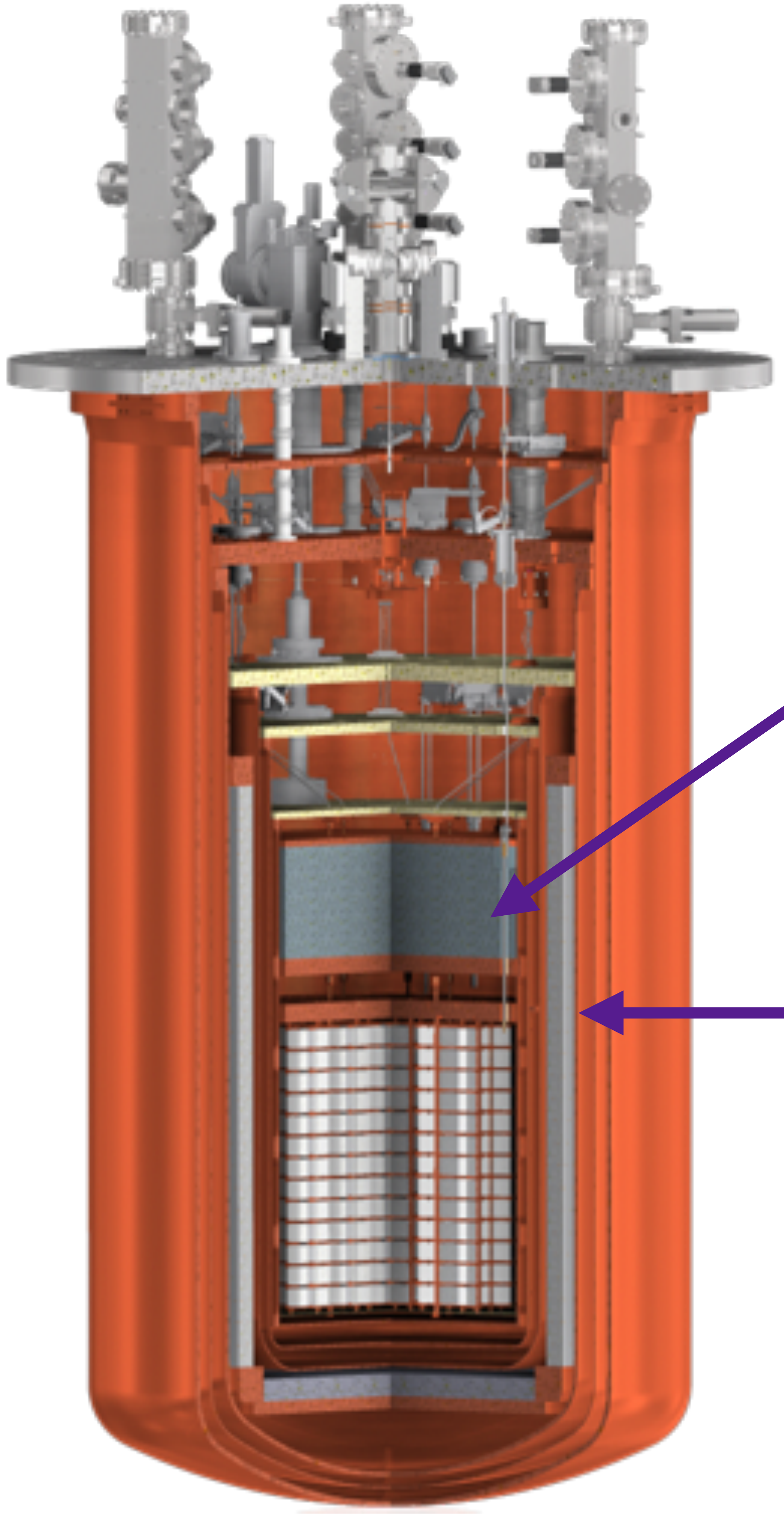

Shielding

- Radiopure copper
- 70 tons of lead including 4 of **Roman lead**

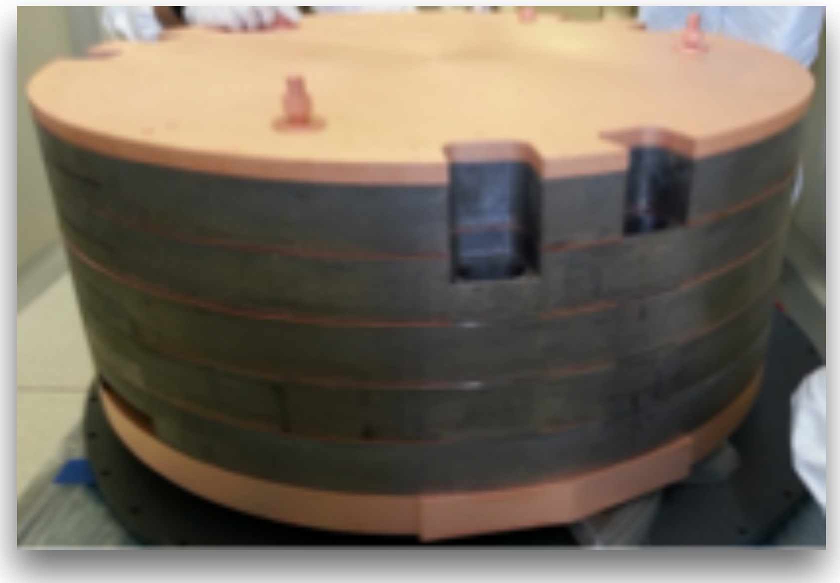

CUORE detector

- Detectors
- Long-term
  mK

n lead

- Found off Sardinia coast in 1988
- Shipwreck from 80-50 B.C.E
- 120 lead ingots have lost their natural radioactivity

- Ingots originated in Spain
- Used for ammunition
- Inscriptions preserved for archaeology

https://www.nature.com/news/2010/100415/full/news.2010.186.html

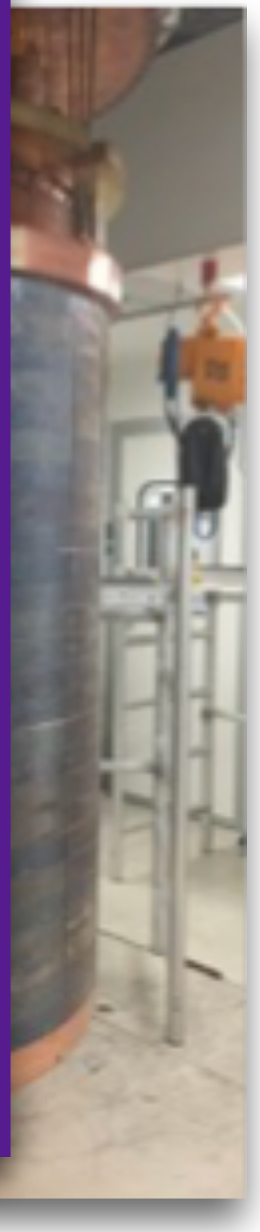

CUORE photo gallery

J Ouellet, Neutrino 2018

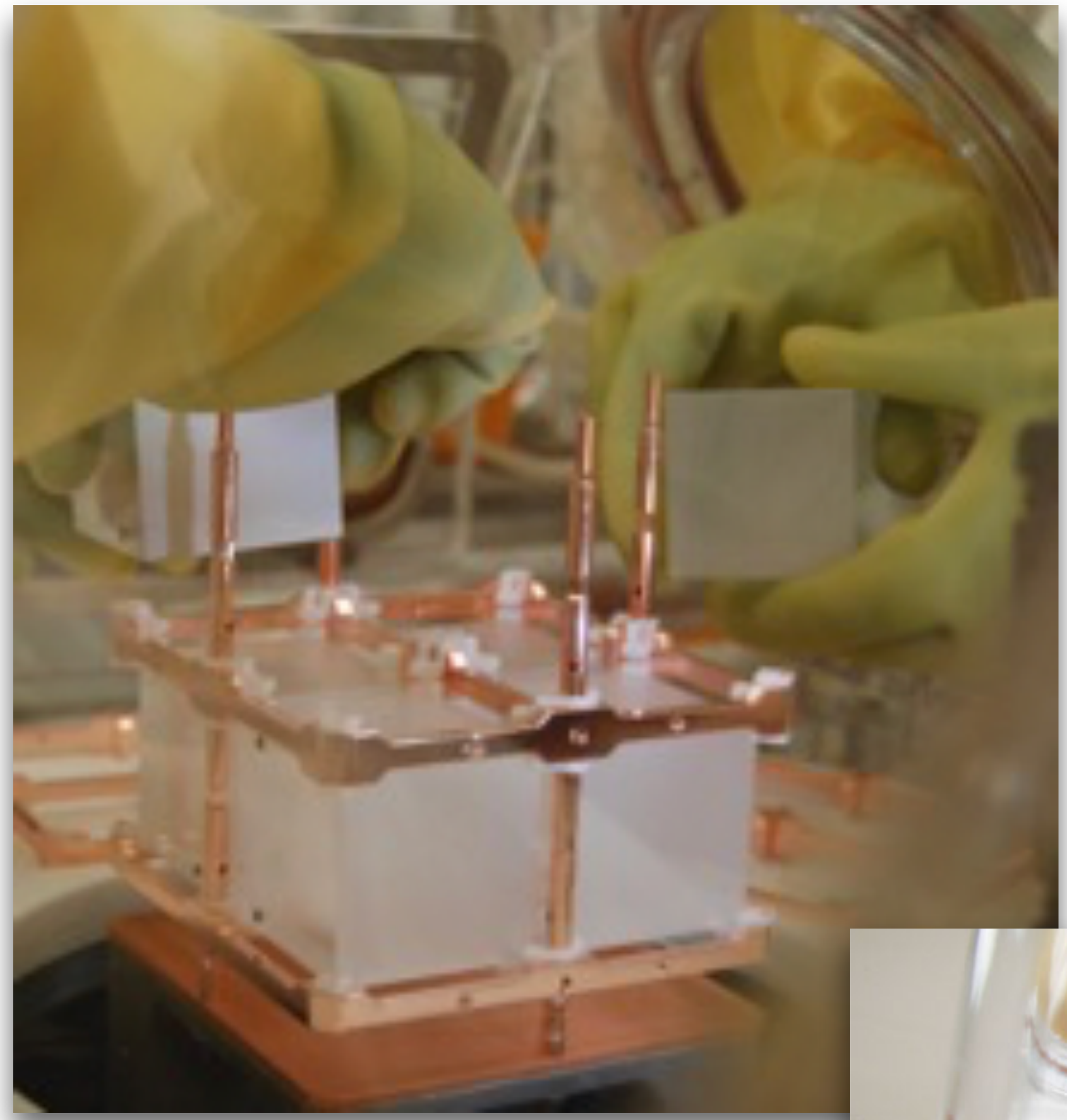

Installing the detector tower

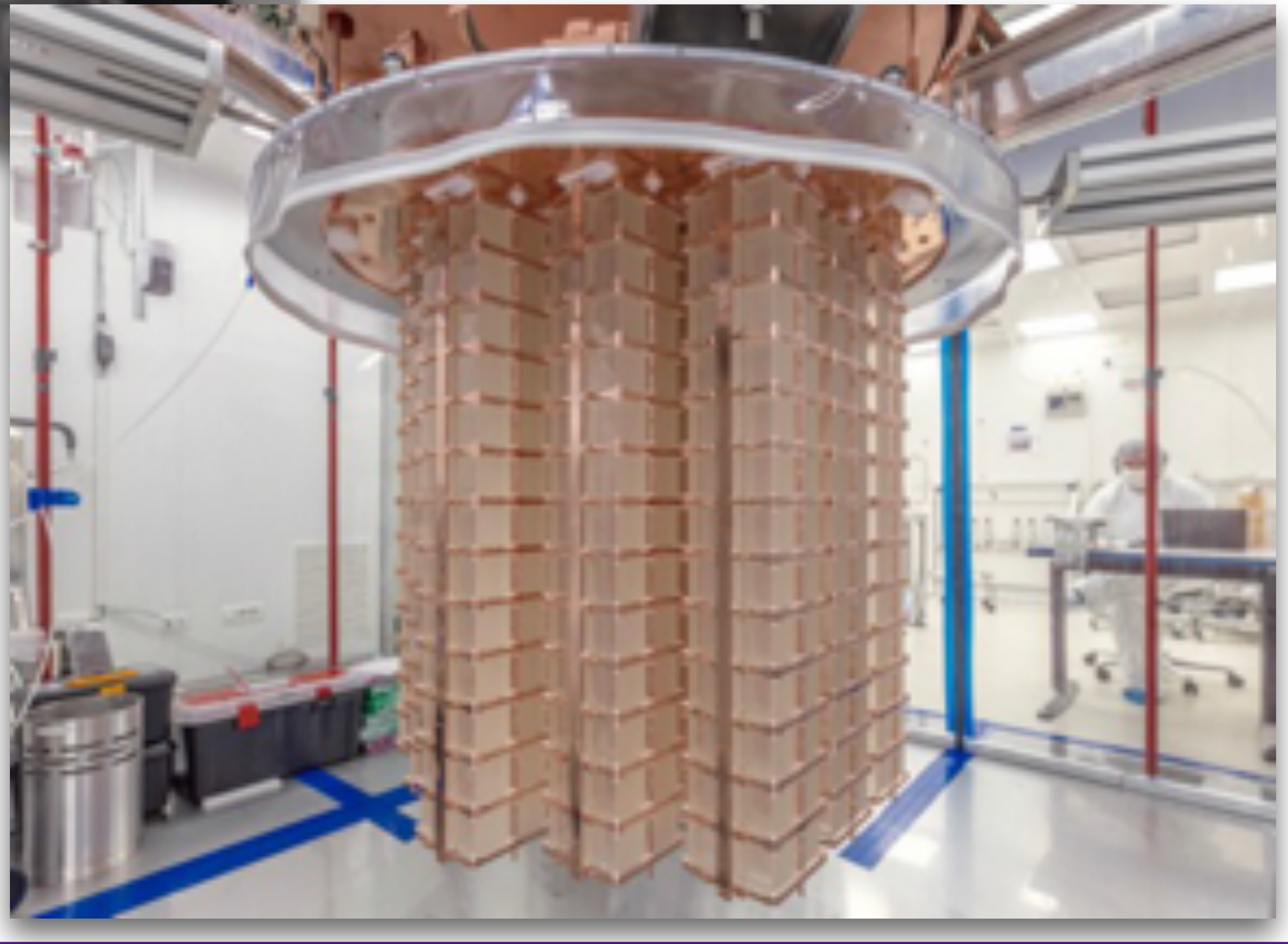

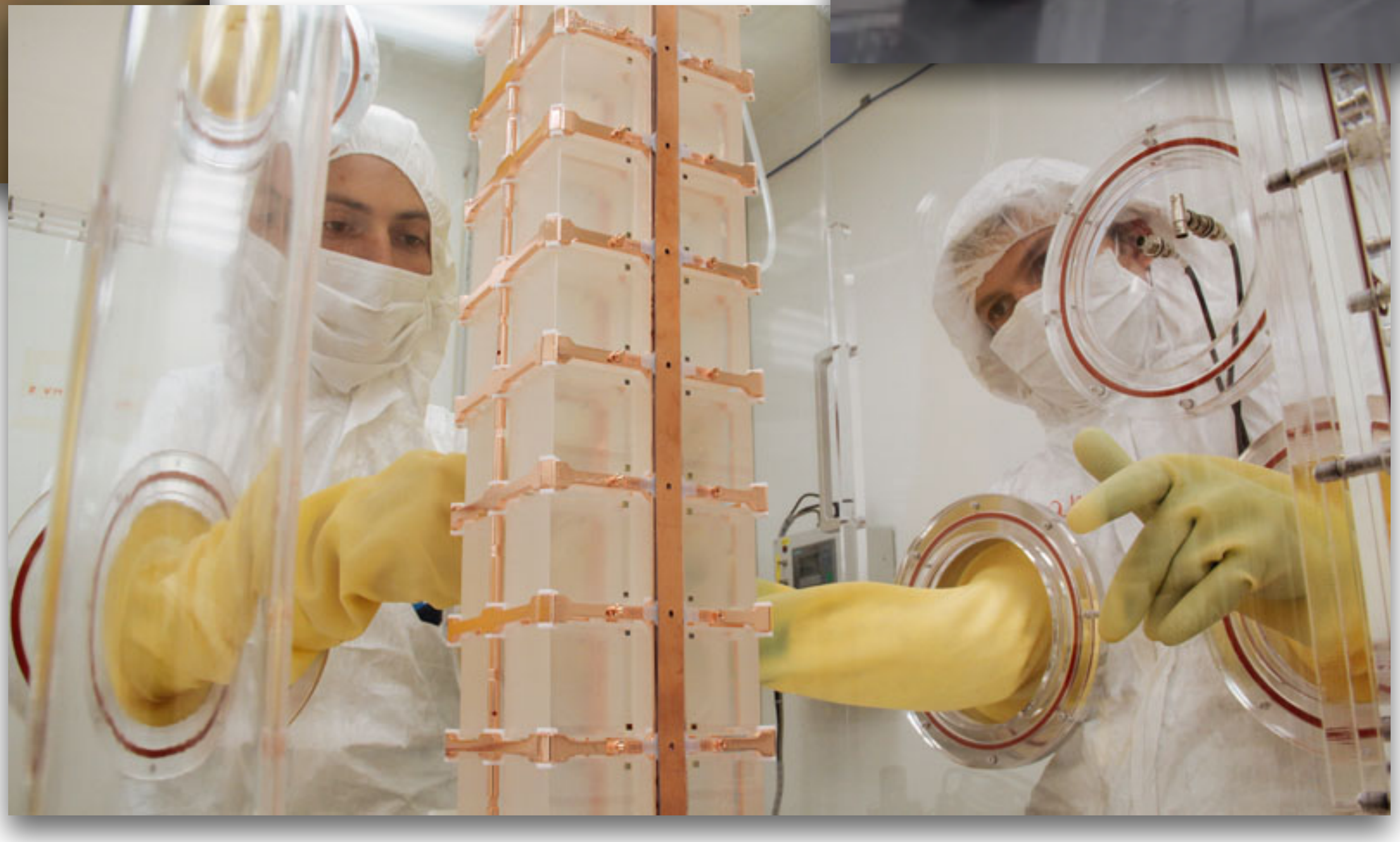

Assembling in N_2 environment

CUORE results

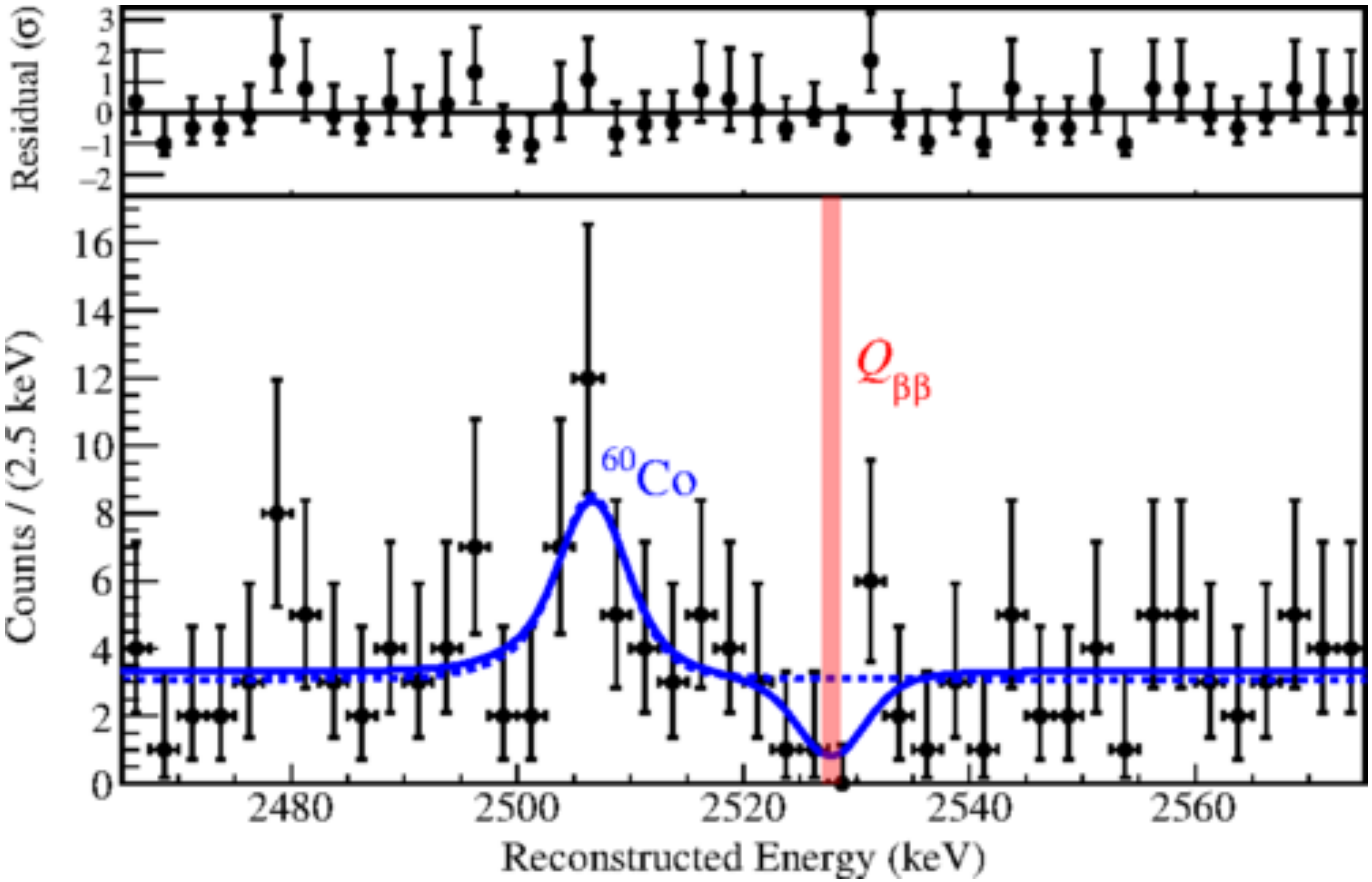

Phys. Rev. Lett. ***120****, 132501 (2018)*

$T_{1/2} > 1.5 \times 10^{25}$ years
($\langle m_{\beta\beta} \rangle$ < 110-520 meV)
86.3 kg.years
5 years: 9.5×10^{25} years

Eur. Phys. J. C ***77****, 13 (2017)*

CUPID - adding particle ID (at LNGS and LSM)

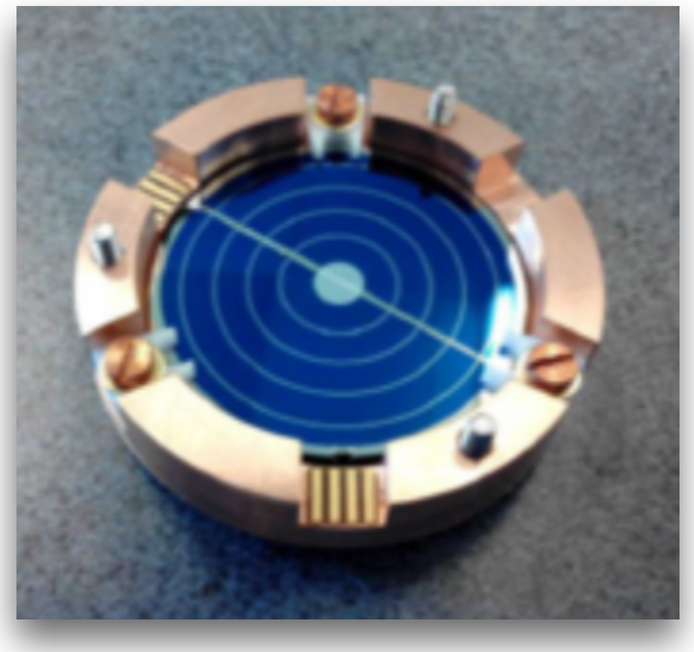

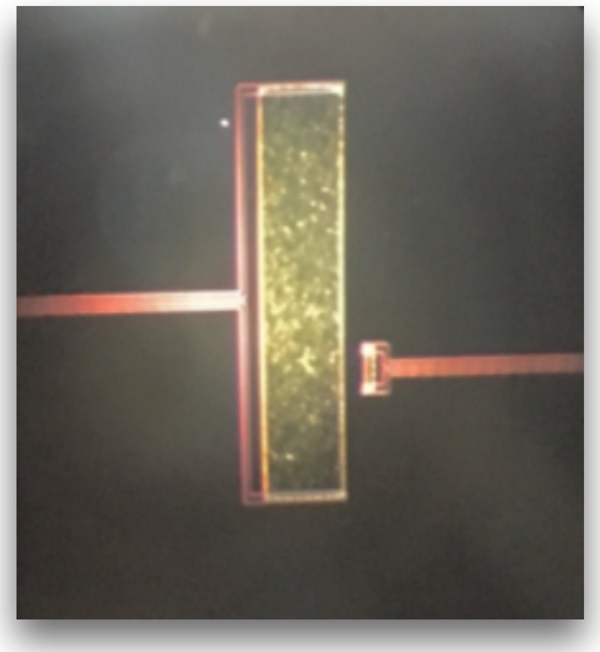

Light-emitting bolometers allow particle ID

CUPID - adding particle ID (at LNGS and LSM)

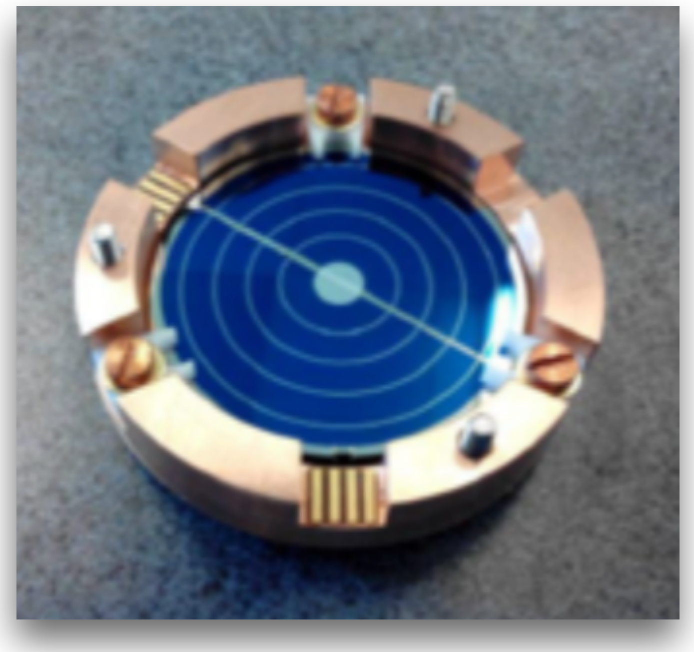

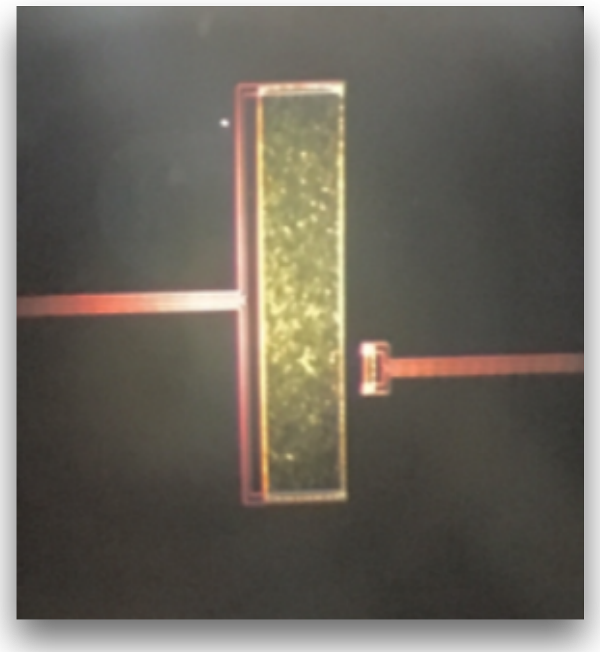

Light-emitting bolometers allow particle ID

Light shape parameter separates **α events** from β and γ decays

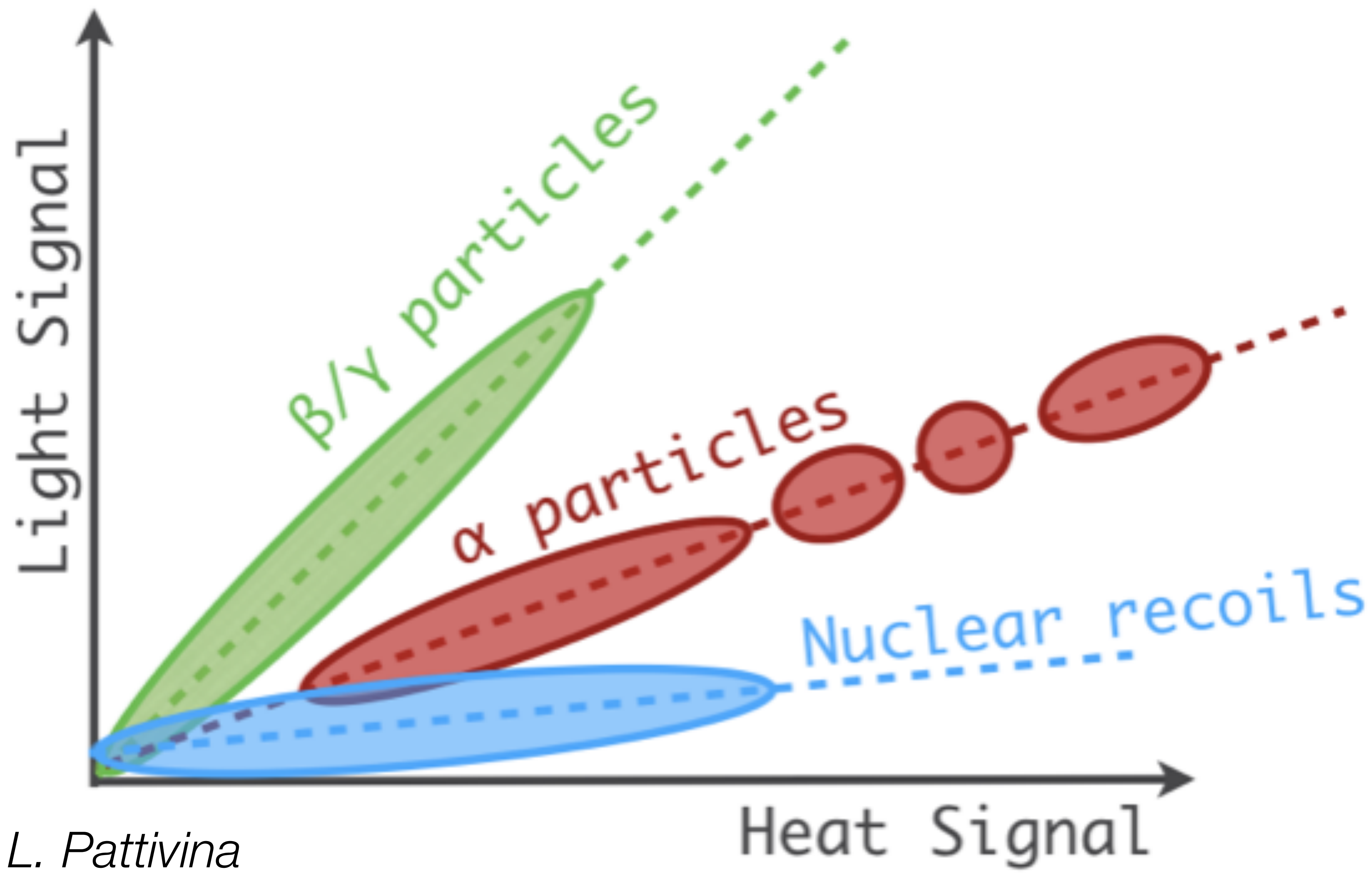

L. Pattivina

CUPID - adding particle ID (at LNGS and LSM)

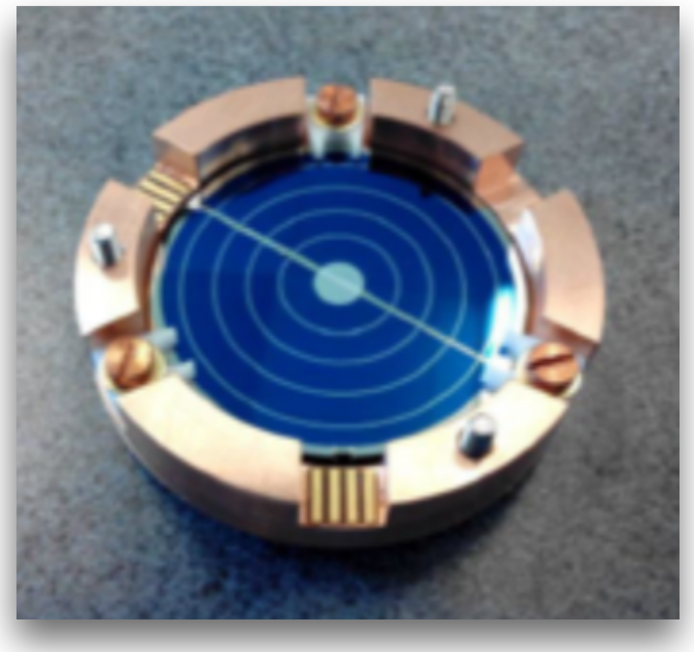

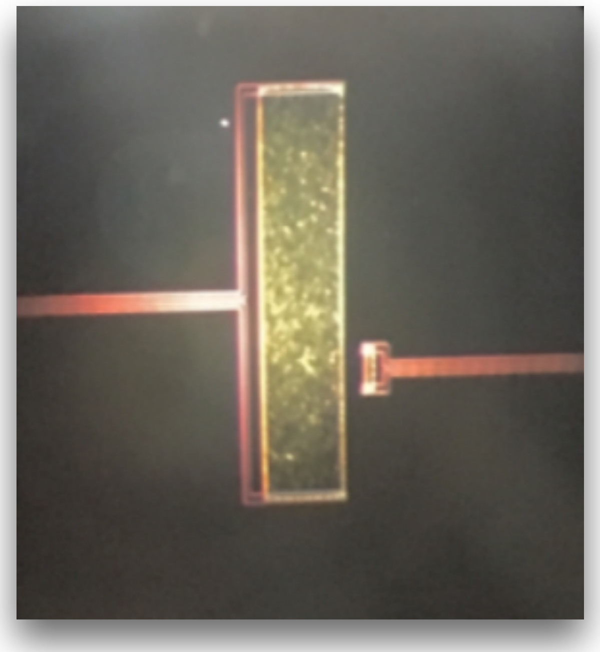

Light-emitting bolometers allow particle ID

Light shape parameter separates **α events** from β and γ decays

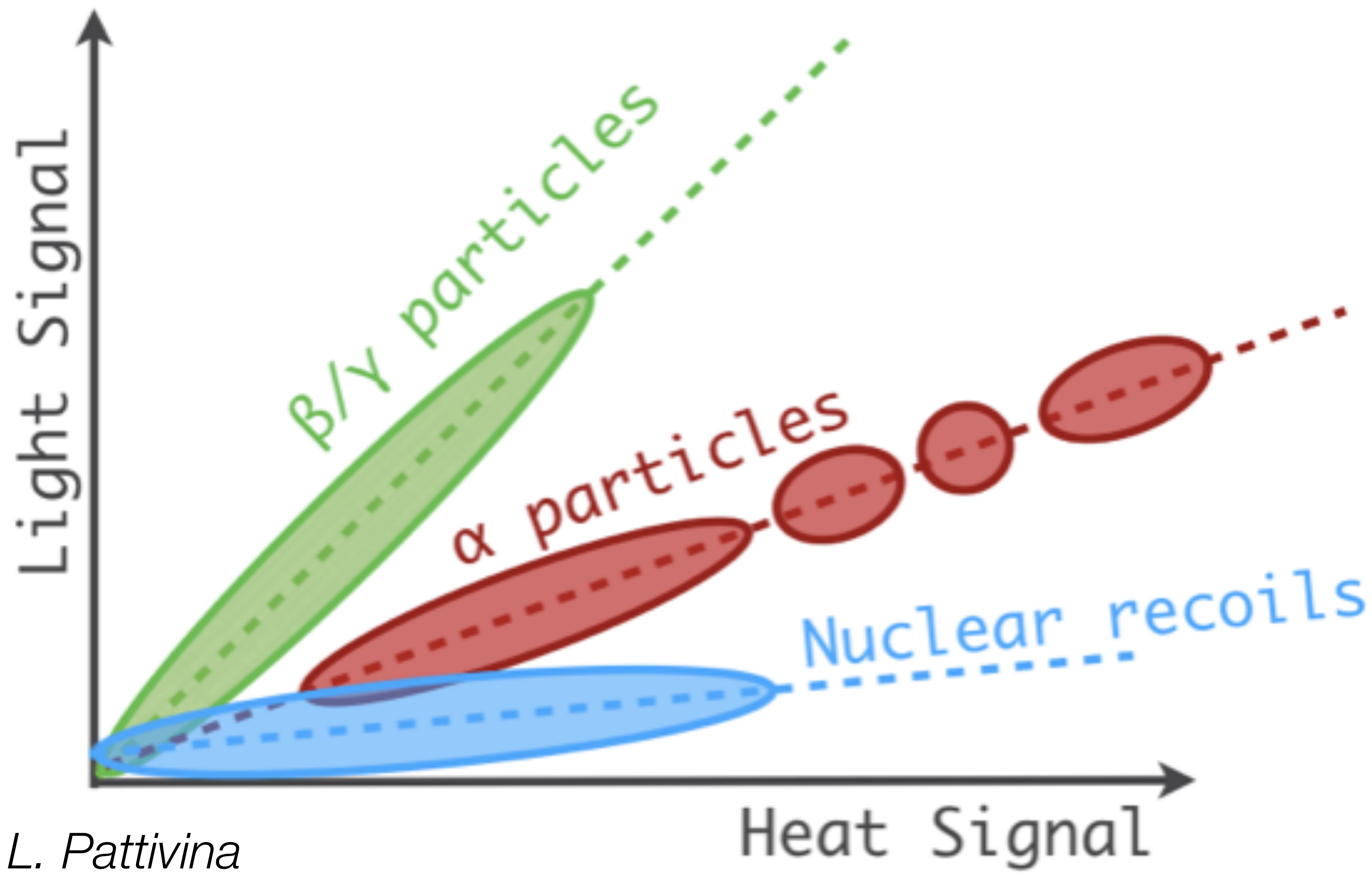

L. Pattivina

CUPID-0: $Zn^{82}Se$ bolometers (5.28 kg ^{82}Se)

CUPID-Mo uses $Li_2{}^{100}MoO_4$ crystals

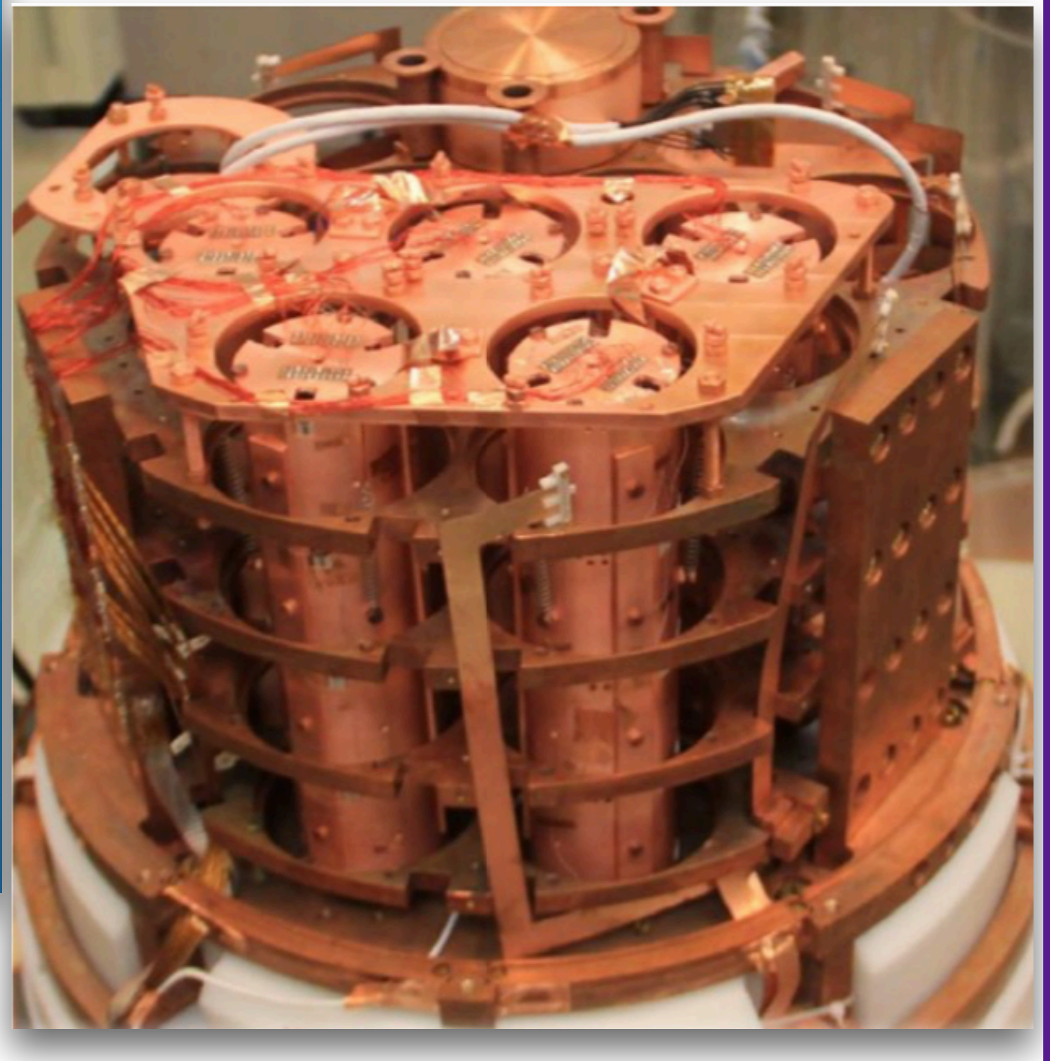

TeO_2 scintillating bolometers under R&D

CUPID - adding particle ID (at LNGS and LSM)

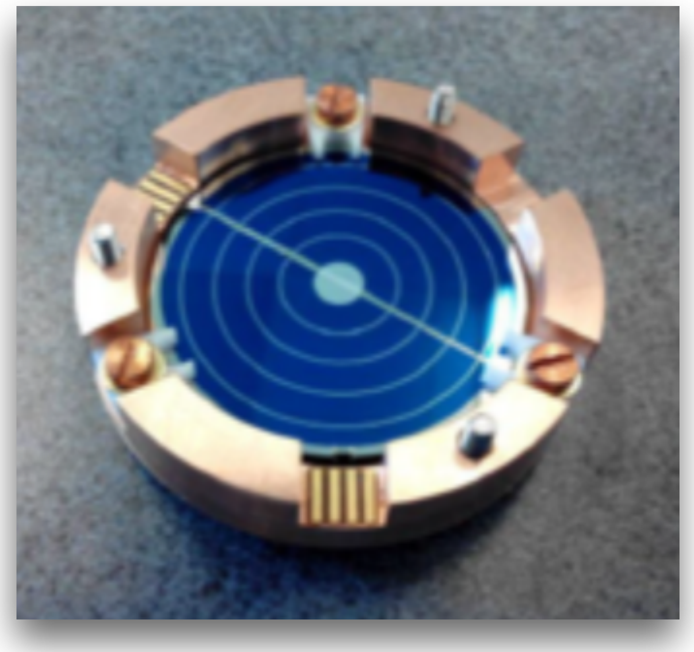

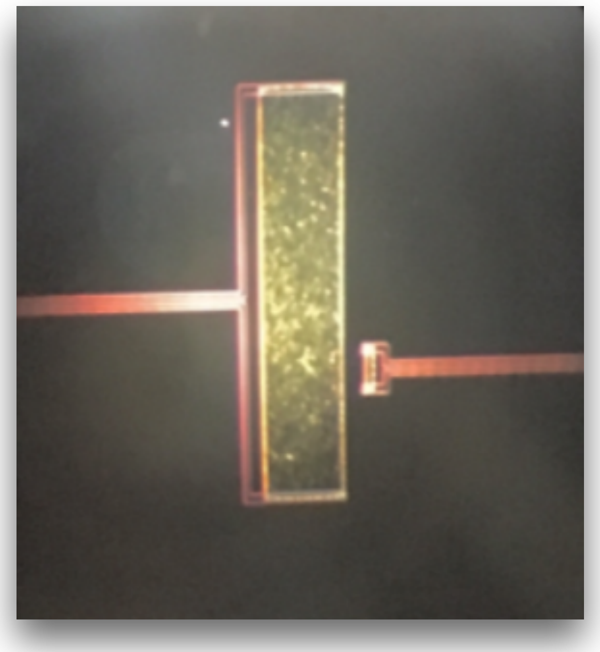

Light-emitting bolometers allow particle ID

Light shape parameter separates **α events** from β and γ decays

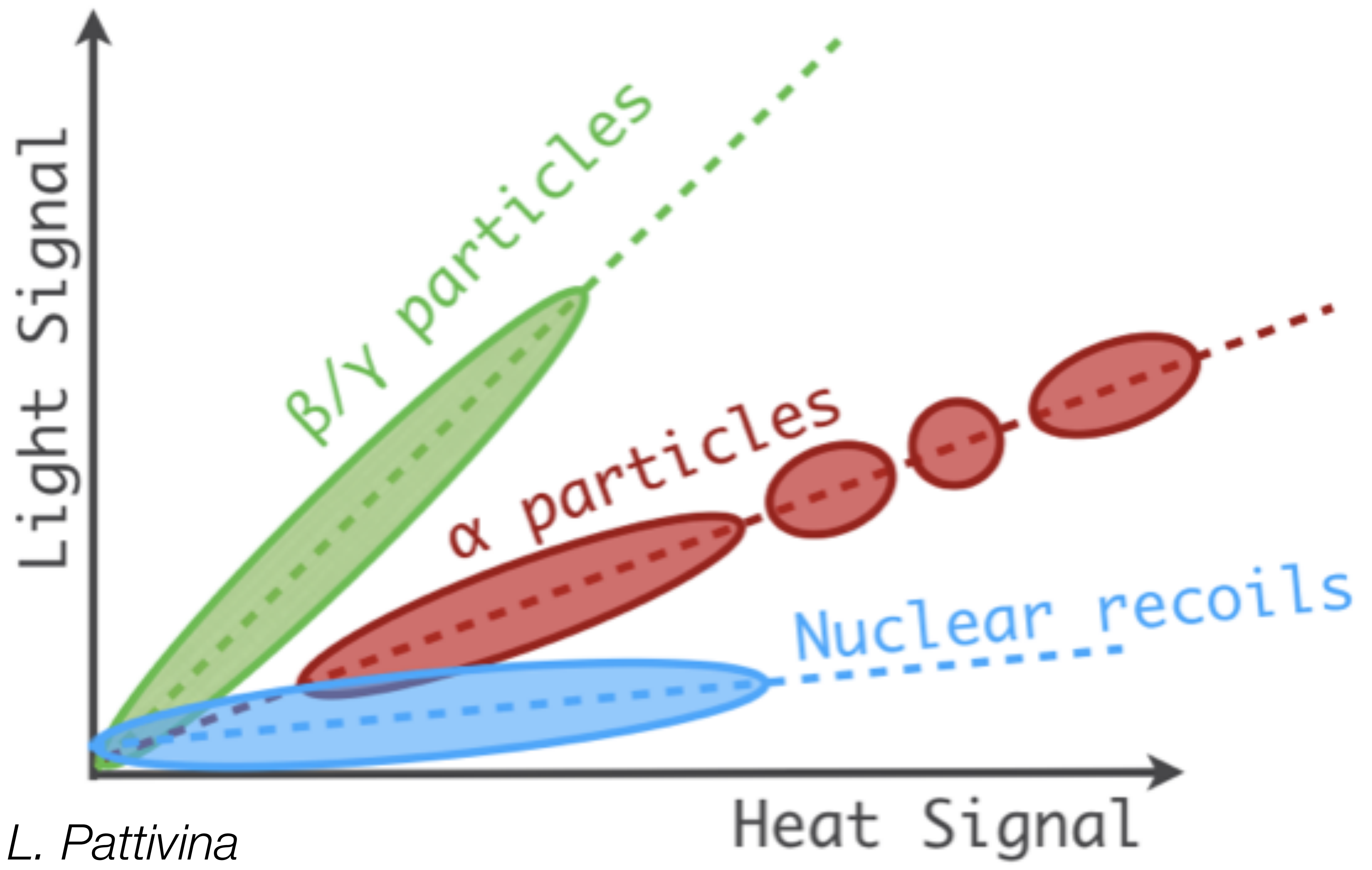

L. Pattivina

CUPID-0: **$Zn^{82}Se$** bolometers (5.28 kg ^{82}Se)

CUPID-Mo uses $Li_2{}^{100}MoO_4$ crystals

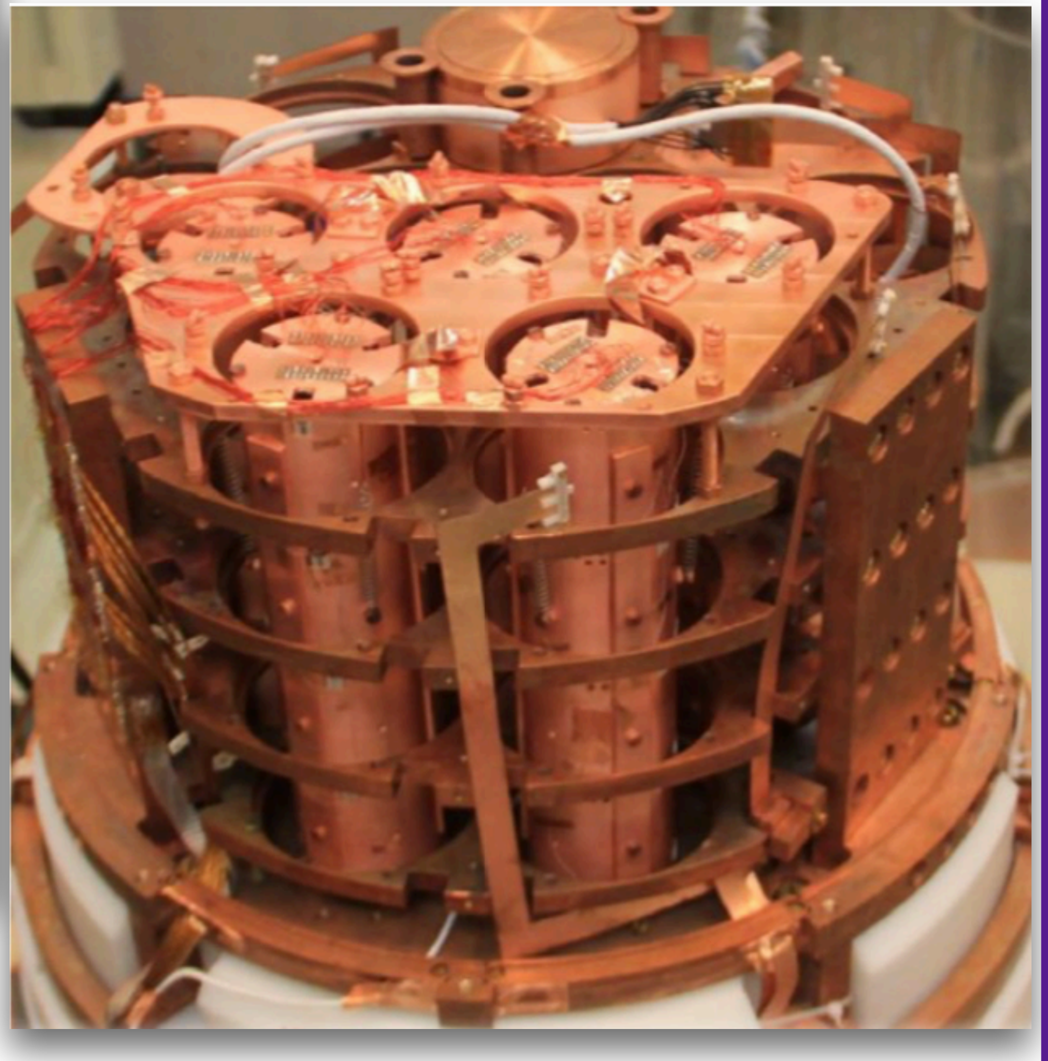

TeO_2 scintillating bolometers under R&D

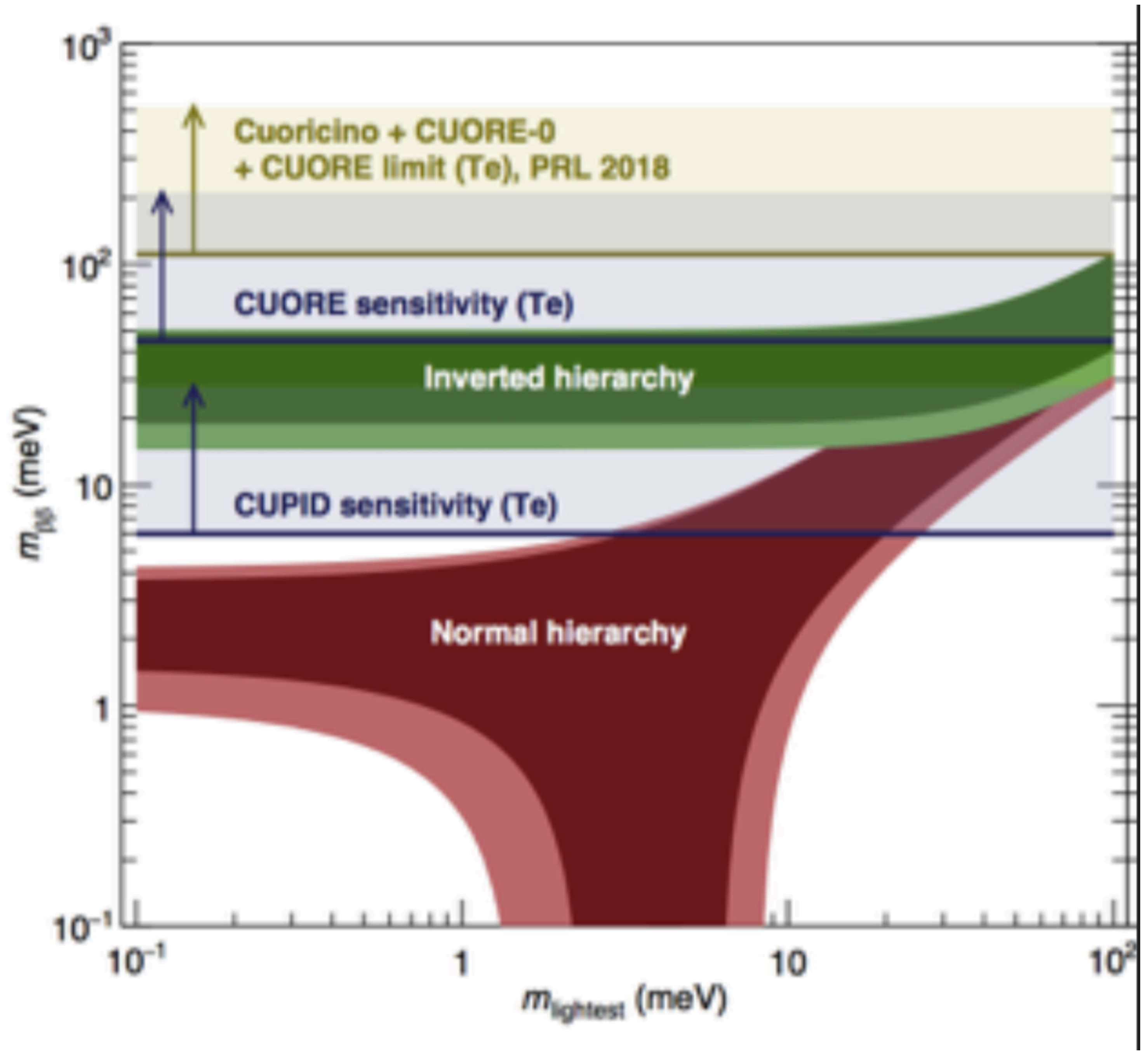

Target CUPID sensitivity covers whole **inverted hierarchy** ($m_{\beta\beta}$ ~ 6 - 20 meV, $T_{1/2}$ ~ 10^{27} yr)

… and the rest

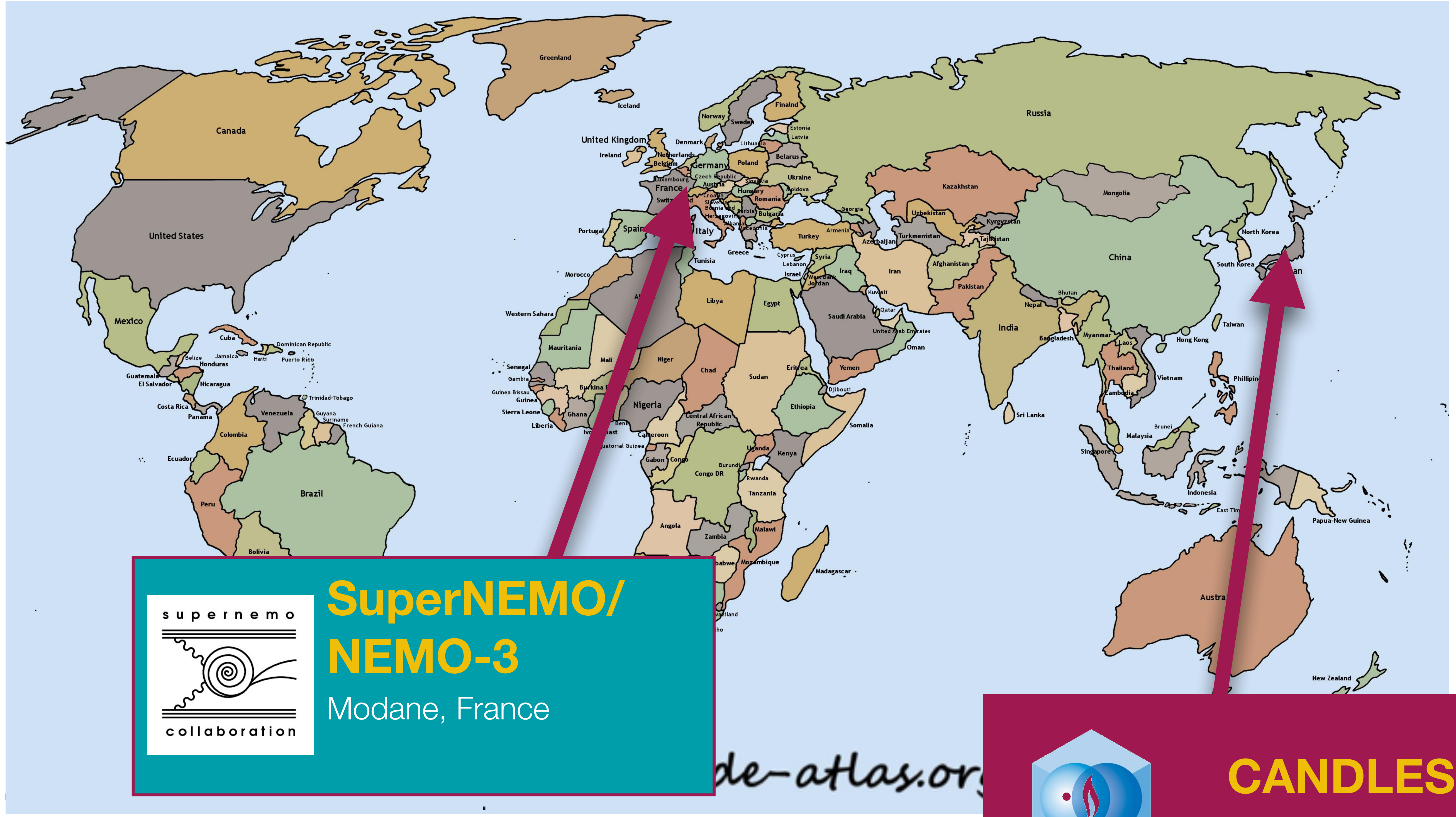

SuperNEMO/ NEMO-3
Modane, France

CANDLES
Kamioka, Japan

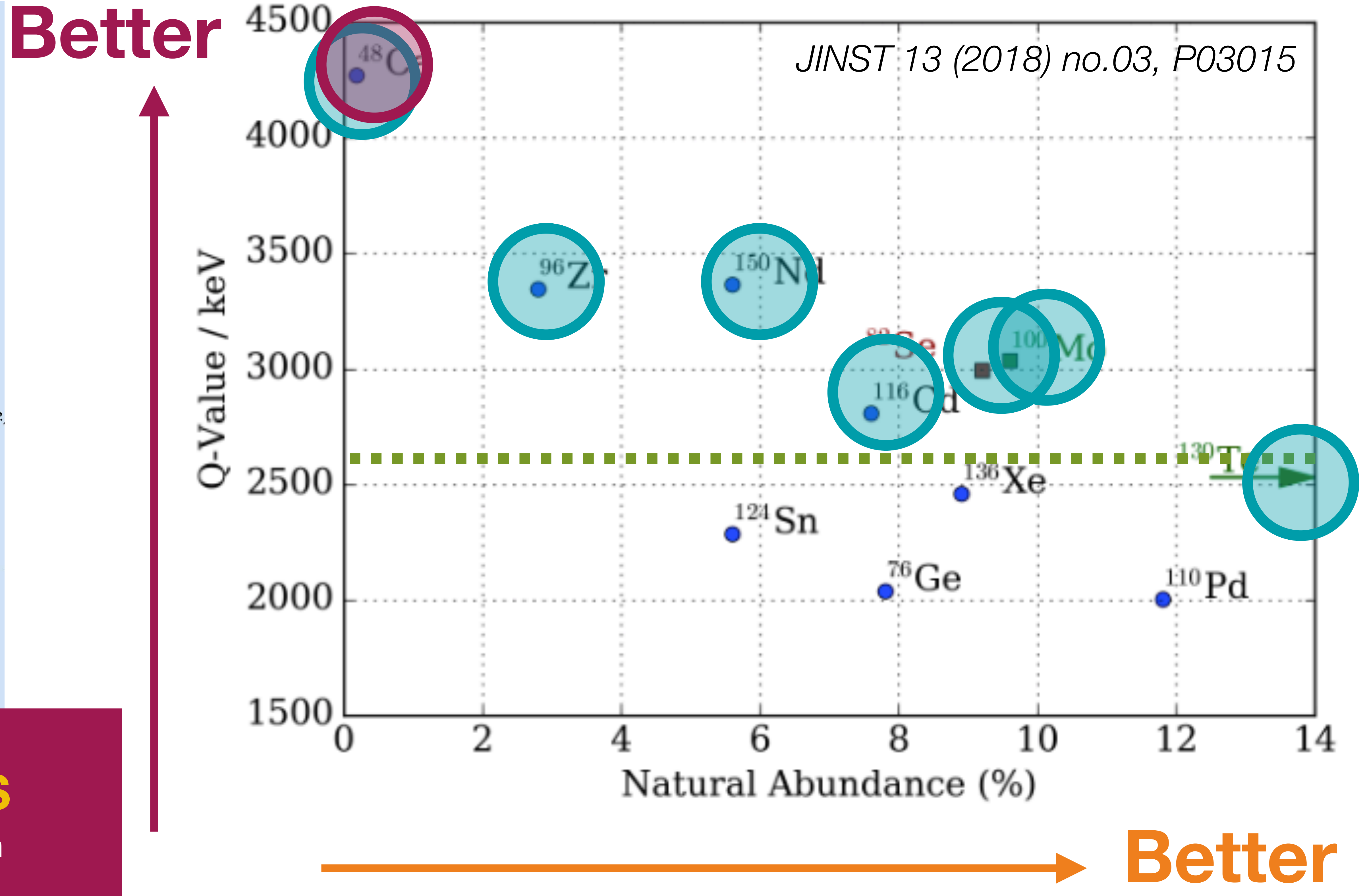

CANDLES: Ca^{48} at Kamioka

Highest Q-value
- low backgrounds
- big phase space factor = high rate

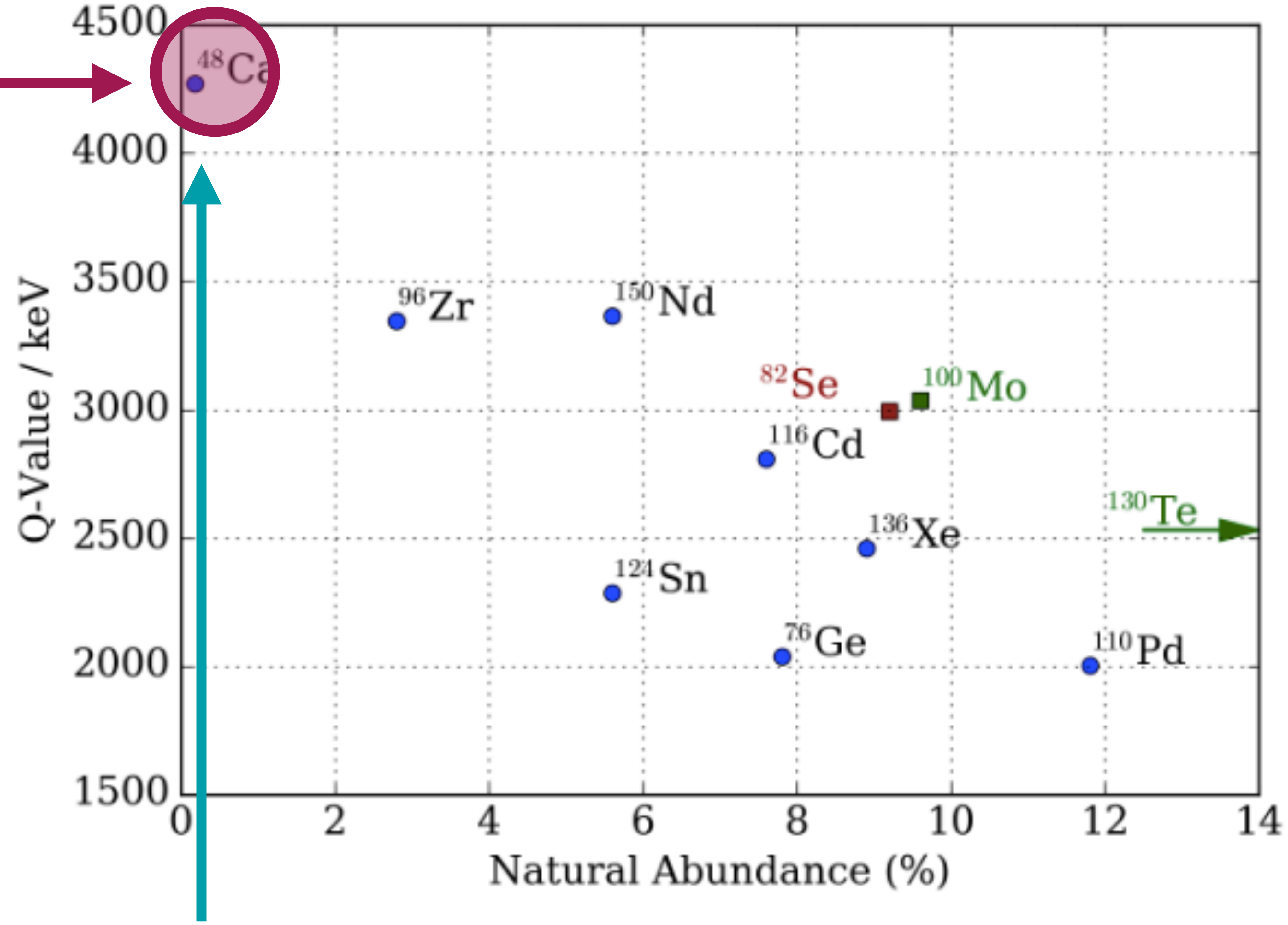

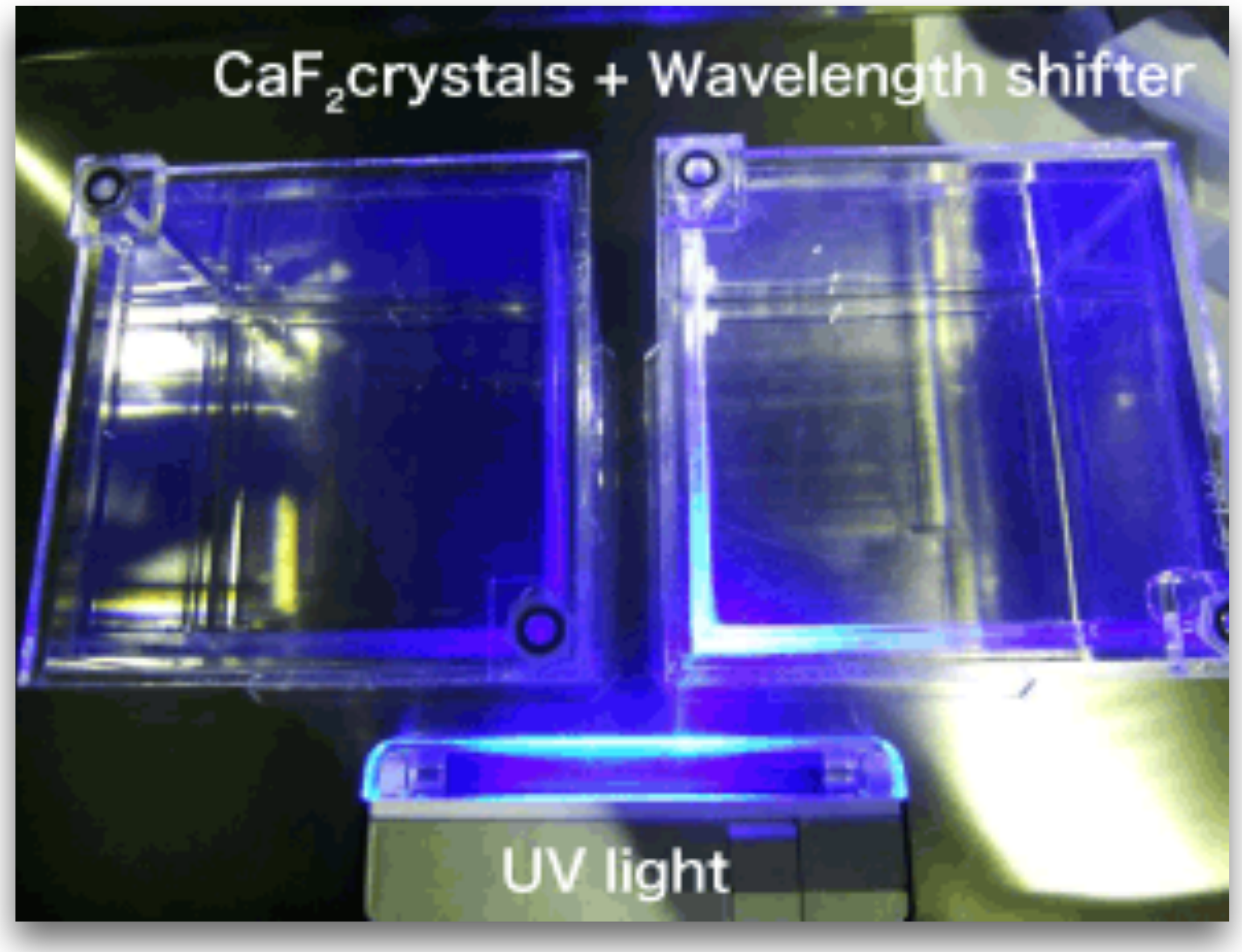

Image: Osaka University

lowest abundance (< 0.2%)
- **zero background** (i.e. high resolution) vital
- CANDLES working on **enrichment** techniques & scintillating bolometers

CANDLES III detector

T Kishimoto, DBD18

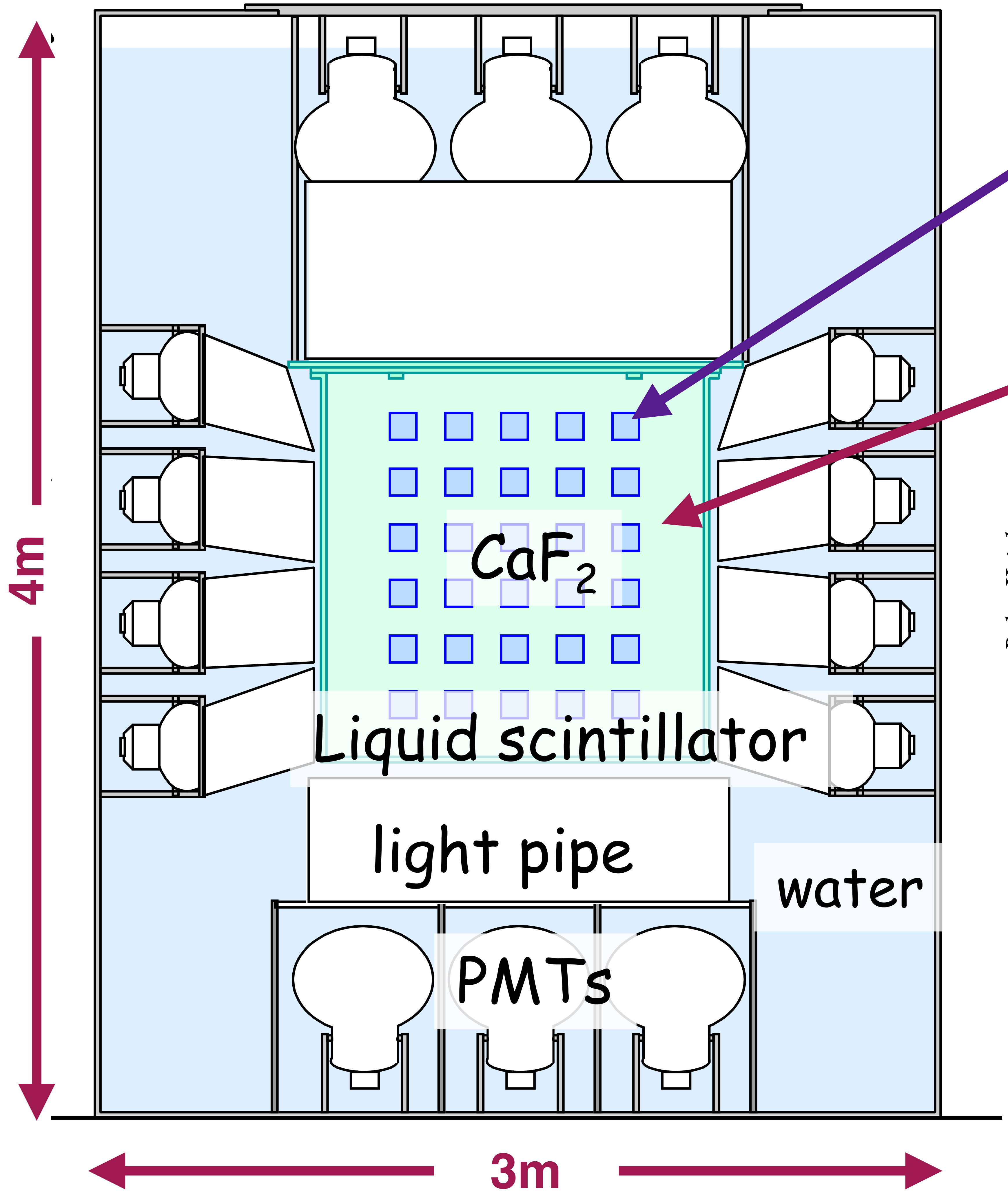

96 x 3.2 kg of unenriched CaF_2 scintillator crystals

LS response time ~ 100x faster than CaF_2: background rejection

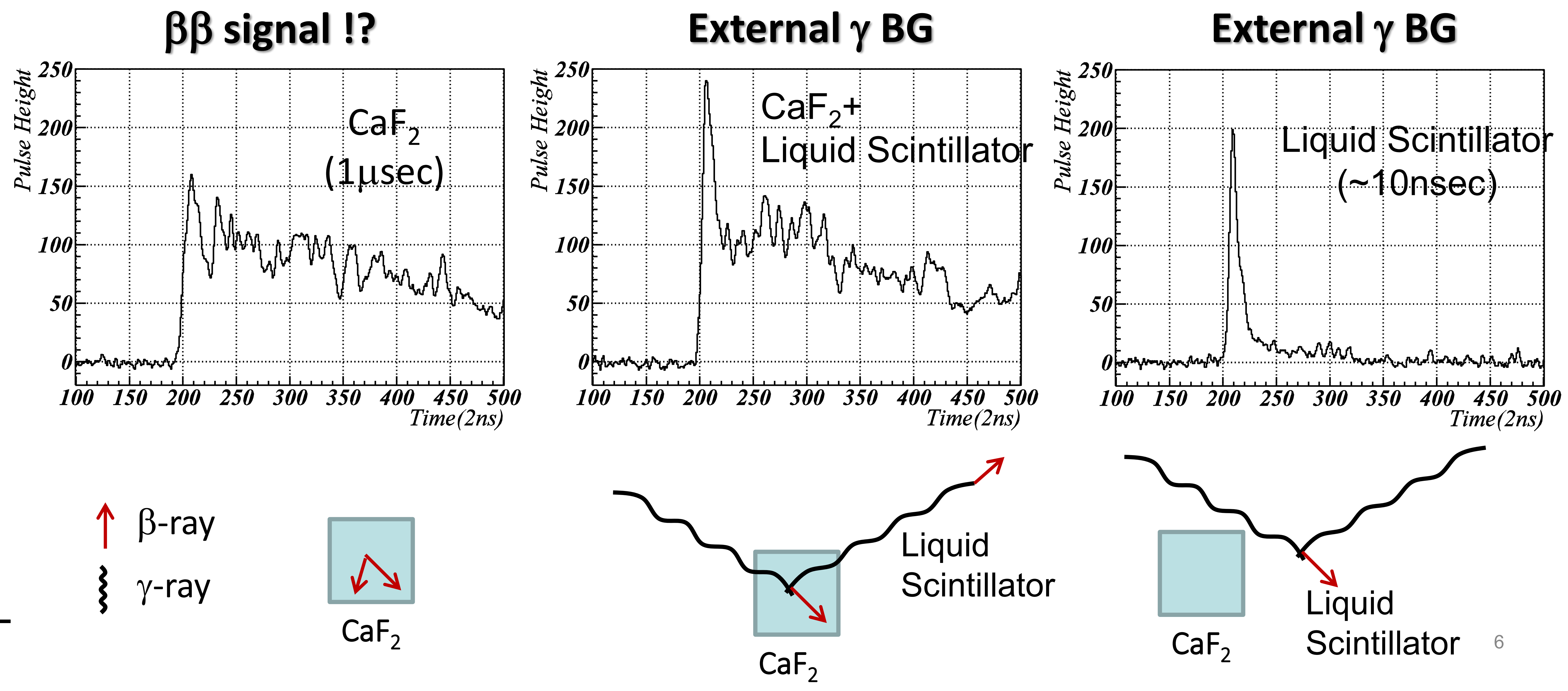

6

CANDLES III detector

T Kishimoto, DBD18

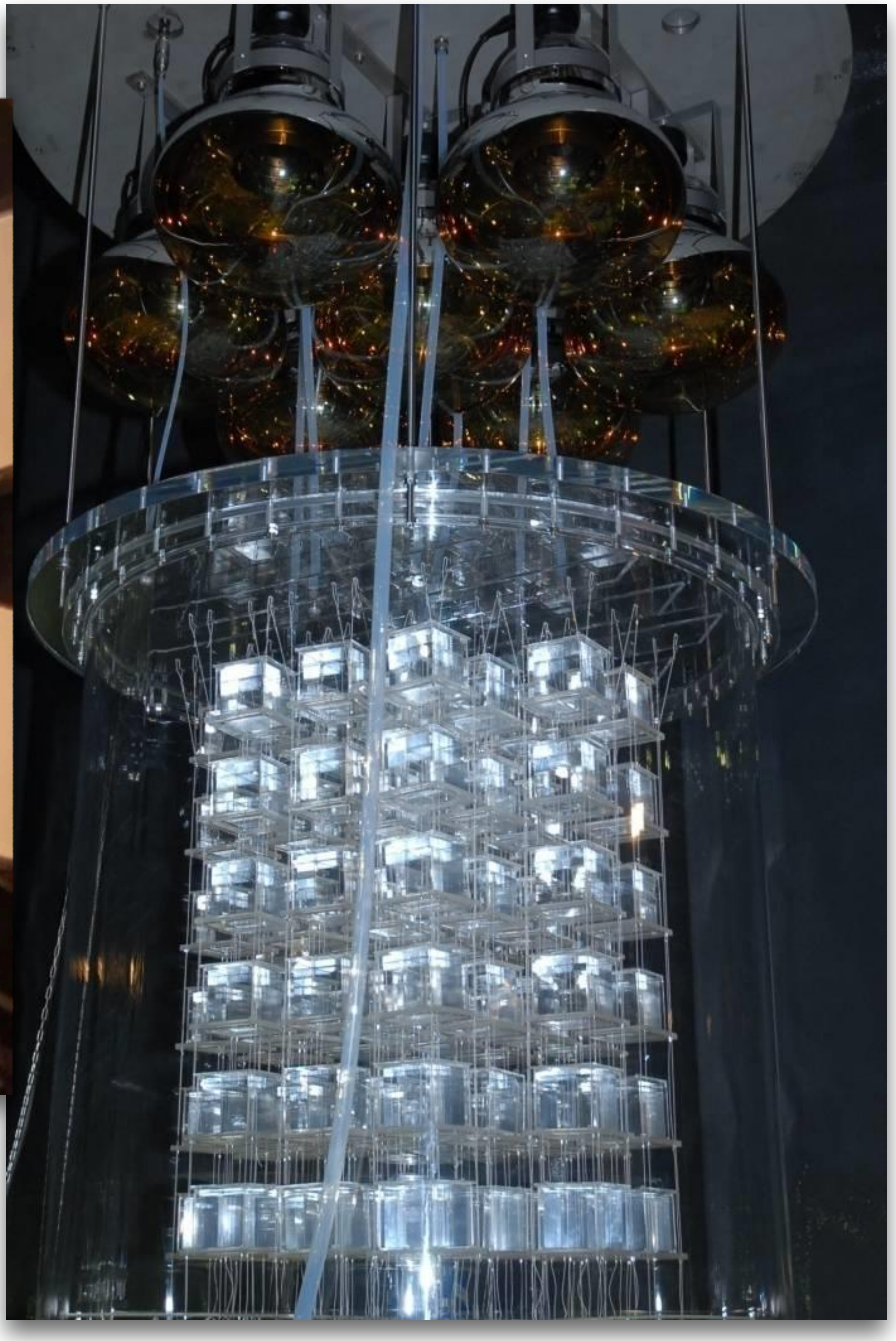

$T_{1/2}^{0\nu} > 6.2 \times 10^{22}$ years
(world's best)

But enrichment needed…

The NEMO principle

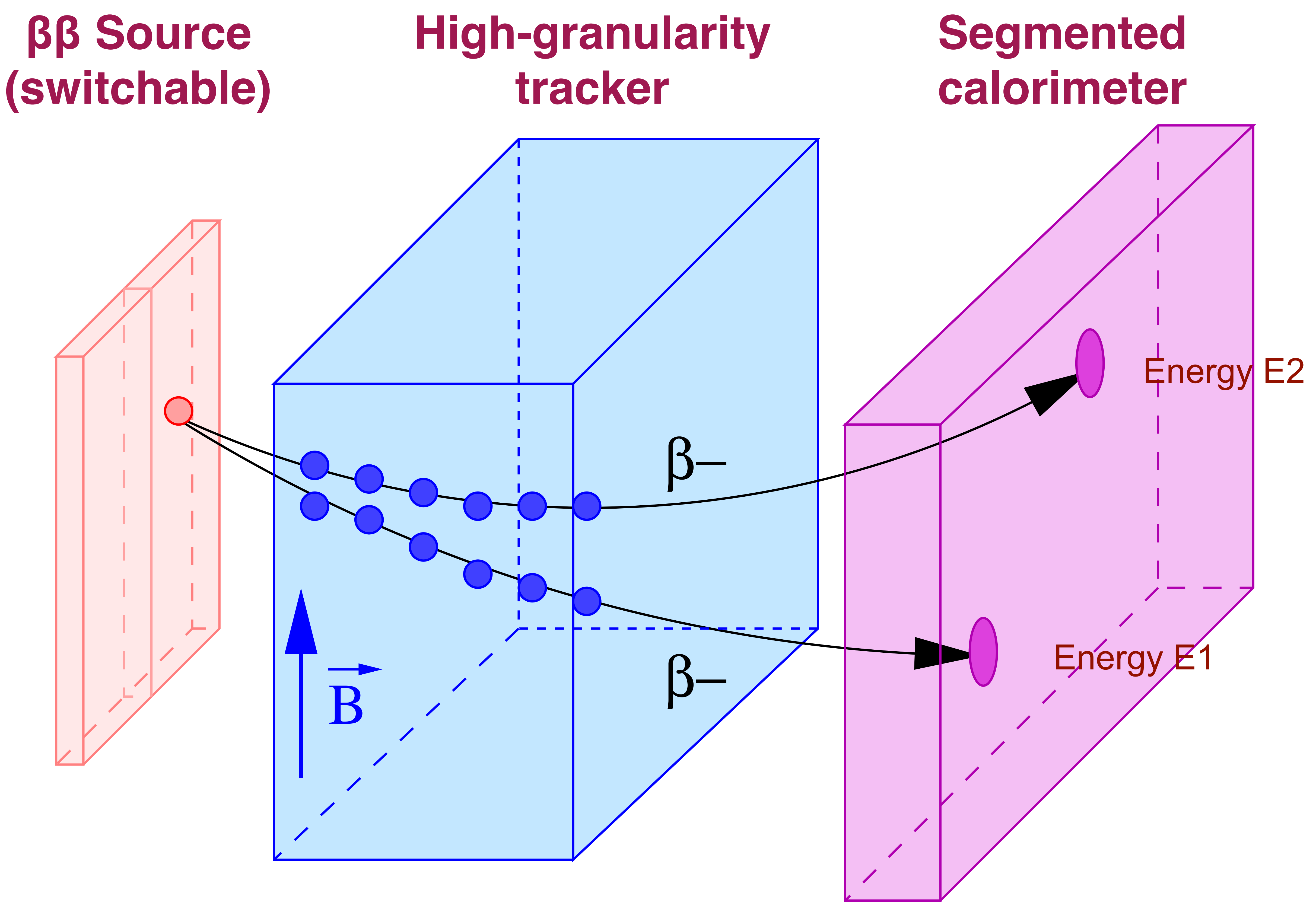

Strengths

- Source decoupled from detector - use **any solid ββ source** isotope
- Track reconstruction gives **particle identification**
- Combine with timings to identify topologies for ultra-high **background rejection**
- Tracking info (angle between tracks) & individual energy distributions can distinguish between **ββ mechanisms**

Weaknesses

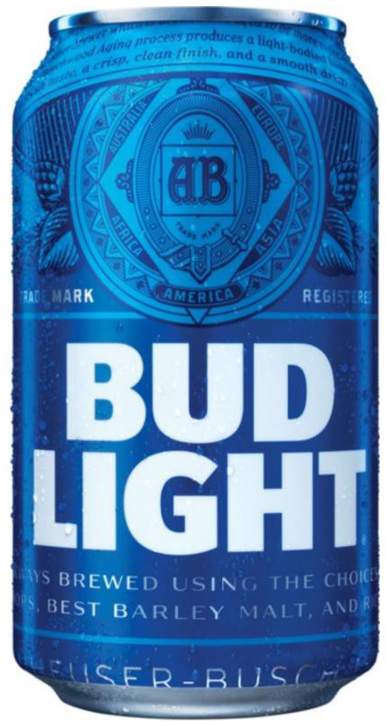

- **Energy resolution** poorer than for most homogenous detectors
- Doesn't scale as well as some other designs

The NEMO tracker

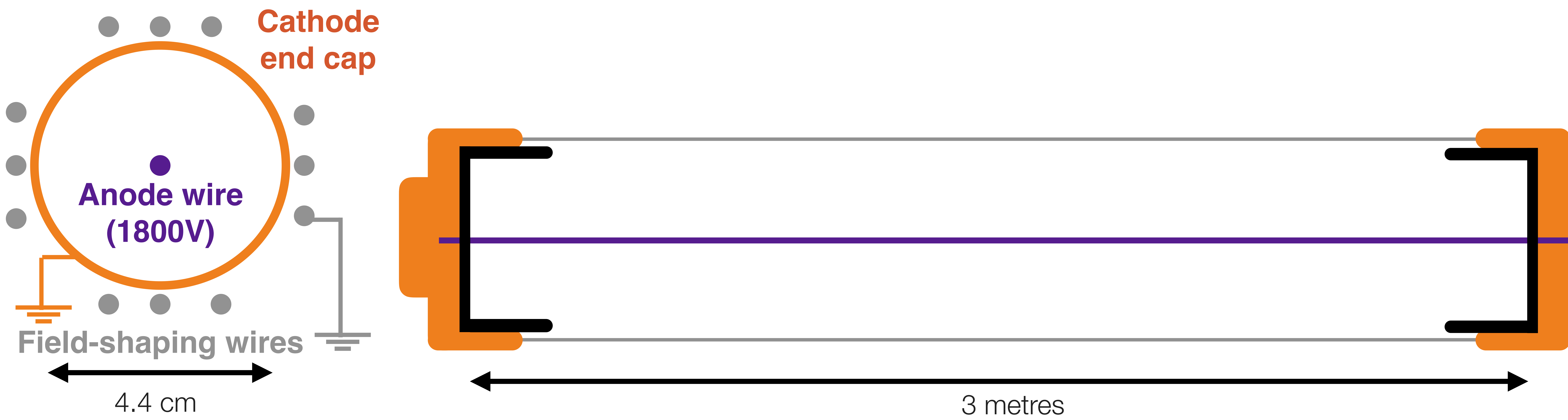

The NEMO tracker

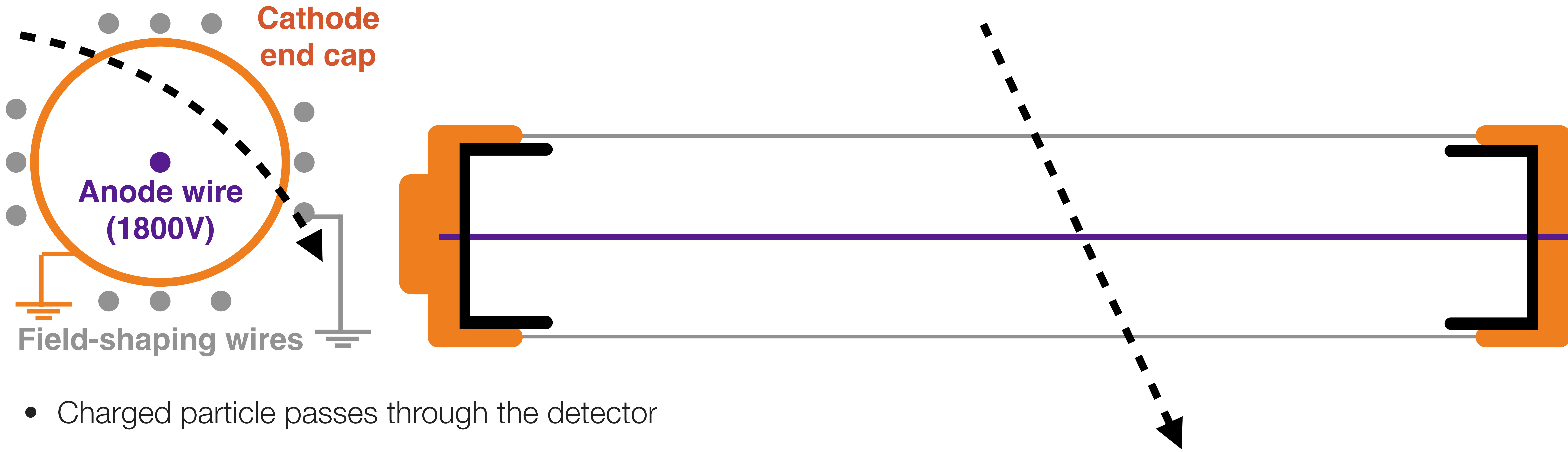

- Charged particle passes through the detector

The NEMO tracker

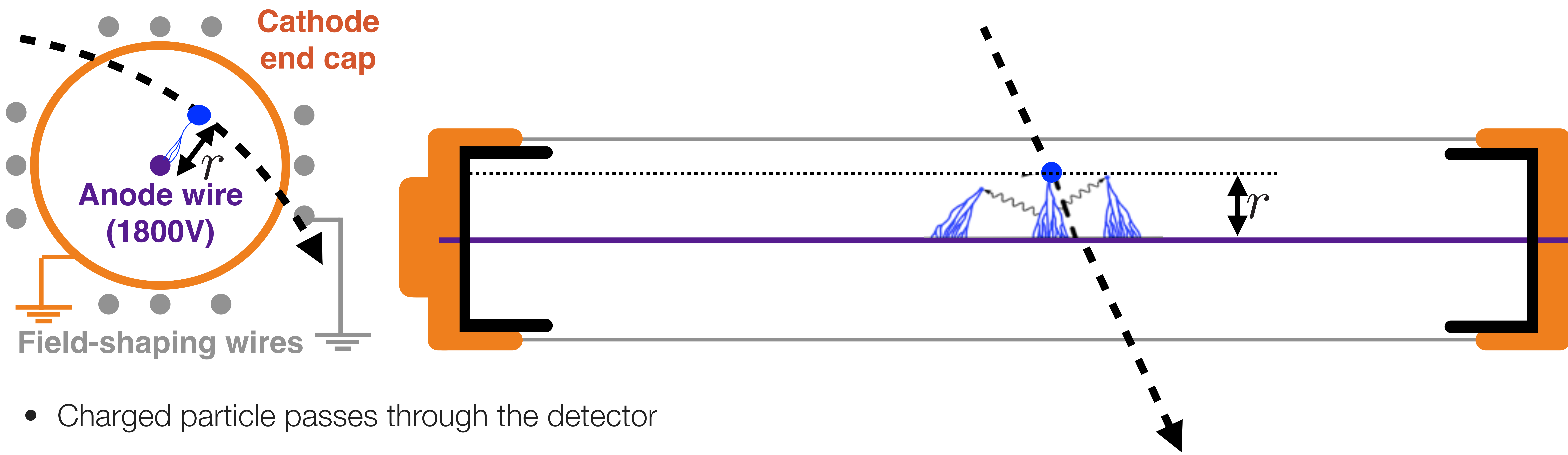

- Charged particle passes through the detector
- Electron avalanche drifts to anode (Geiger mode)
  - Drift time gives radius of closest approach r

The NEMO tracker

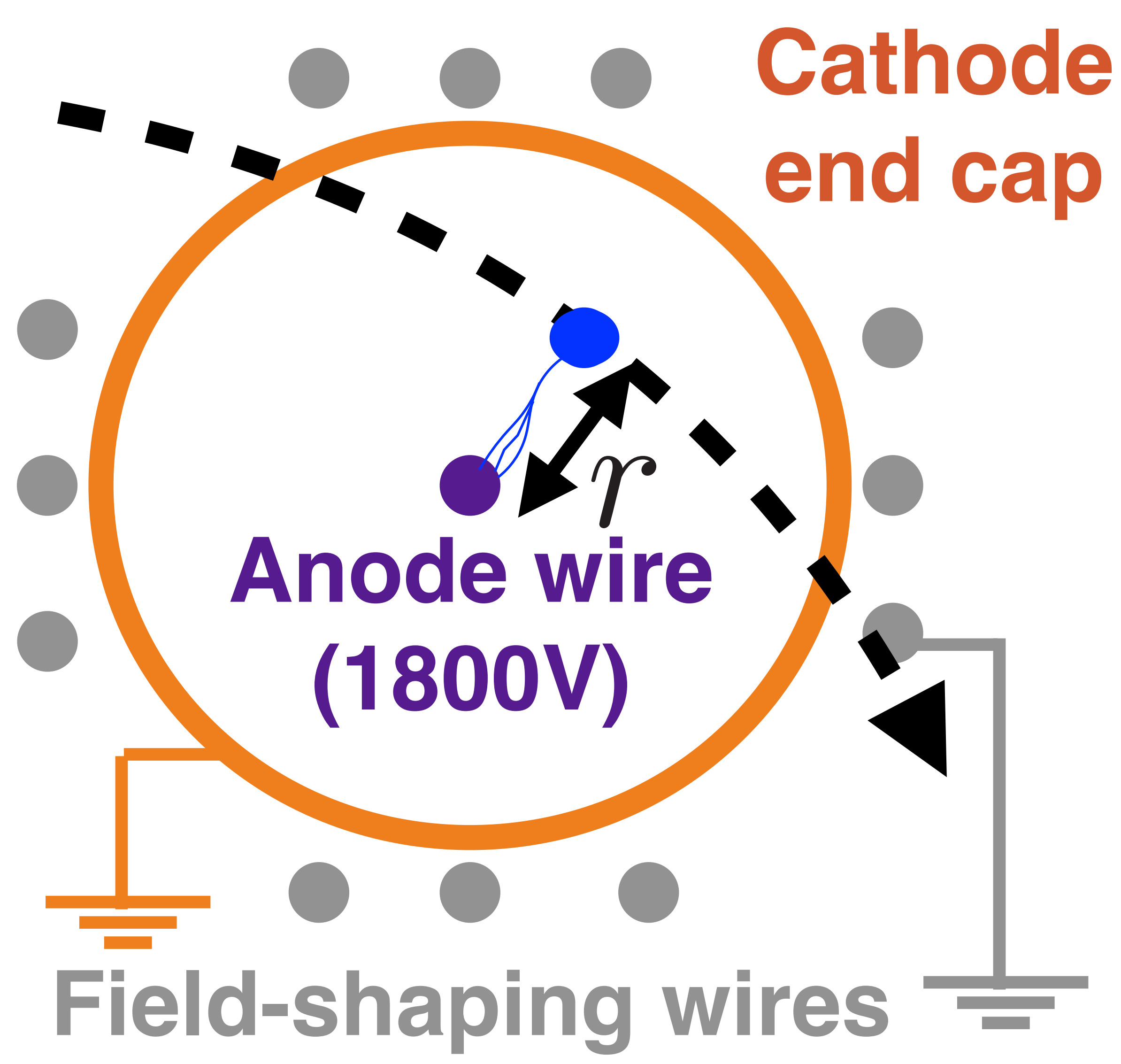

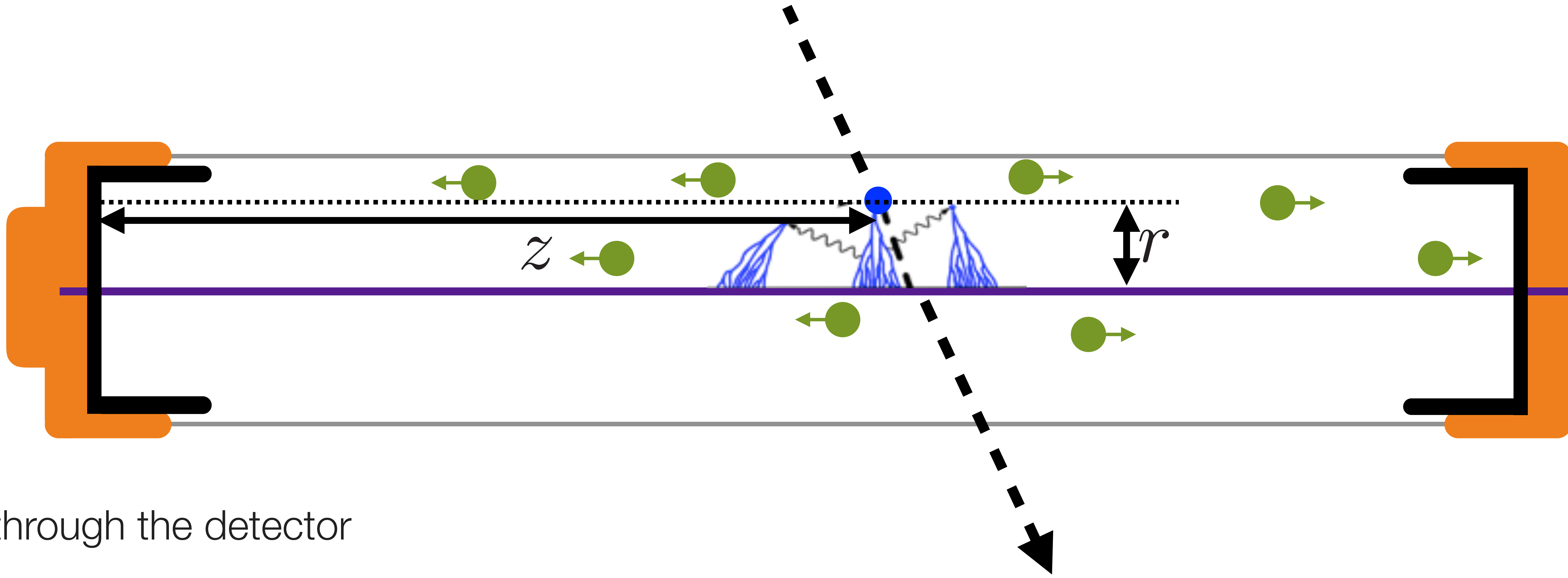

- Charged particle passes through the detector
- Electron avalanche drifts to anode (Geiger mode)
  - Drift time gives radius of closest approach r
- Plasma propagates towards the two cathode end caps
  - Difference in drift times gives distance along wire z

Allows 3-d track reconstruction

NEMO-3 (2003-11)

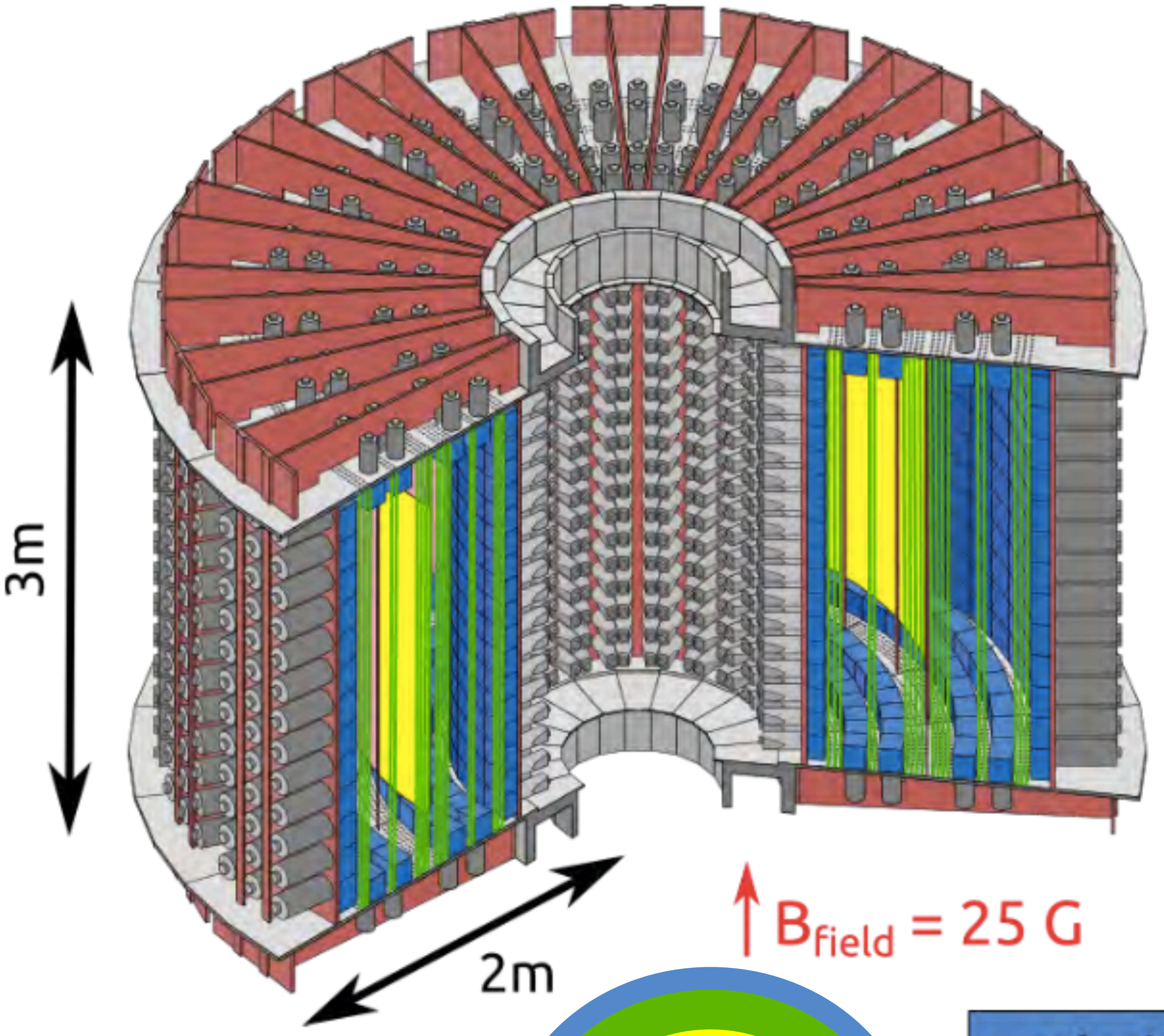

$\uparrow B_{field} = 25$ G

NEMO-3 "camembert" (source top view)

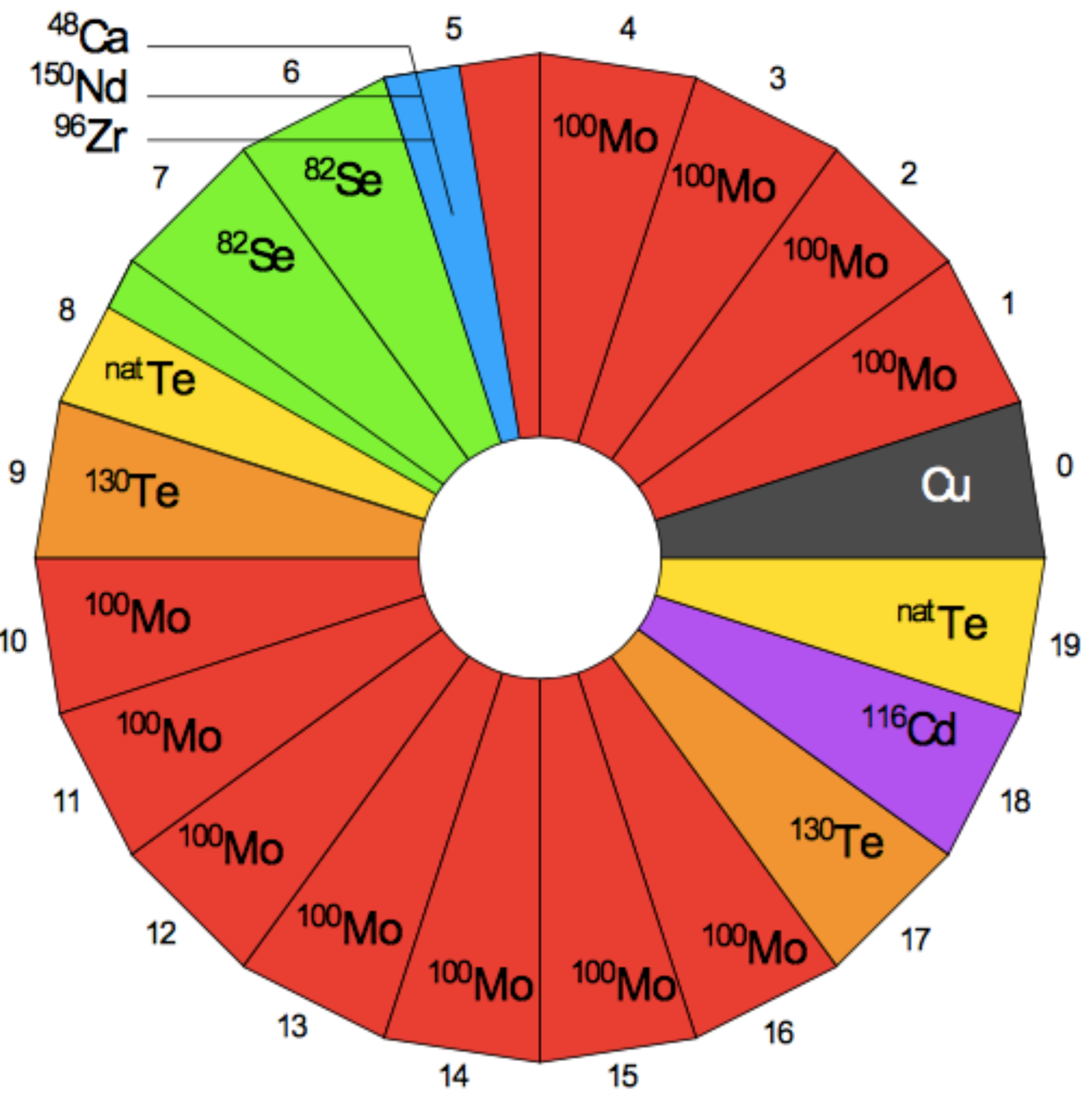

- ^{100}Mo 6,9 kg
- ^{82}Se 0,93 kg
- ^{130}Te 0,45 kg
- ^{116}Cd 0,40 kg
- ^{150}Nd 36,5 g
- ^{96}Zr 9,43 g
- ^{48}Ca 6,99 g

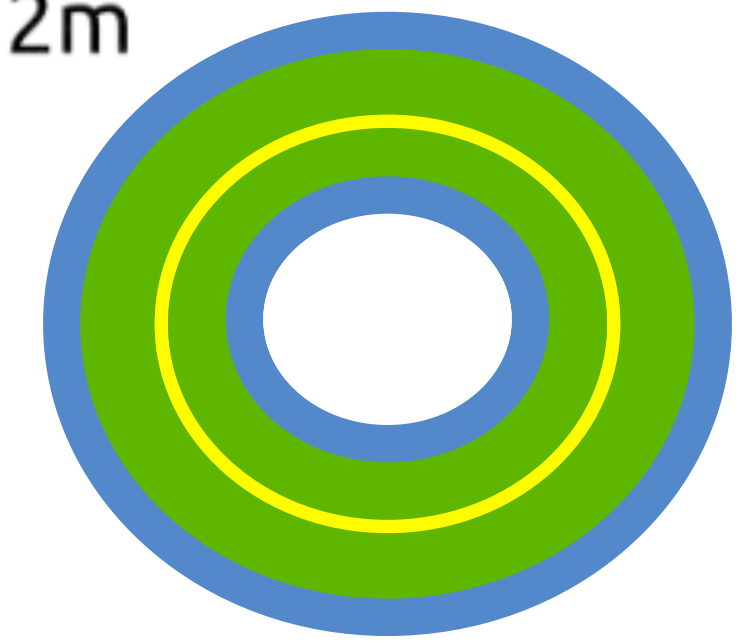

calorimeter
1940 optical modules :
polystyren scintillators
+ 3" and 5" PMTs
$FWHM_E \sim 15\% / \sqrt{E_{MeV}}$
$\sigma_t \sim 250$ ps

tracker
6180 Geiger cells
vertex resolution :
$\sigma_{xy} \sim 3$ mm $\sigma_z \sim 10$ mm

sources
60 mg/cm² foils
10 kg of ββ isotopes

NEMO-3 results highlights

2νββ measurements and 0νββ limit

- ^{100}Mo (Eur. Phys. J. C (2019) 79: 440)

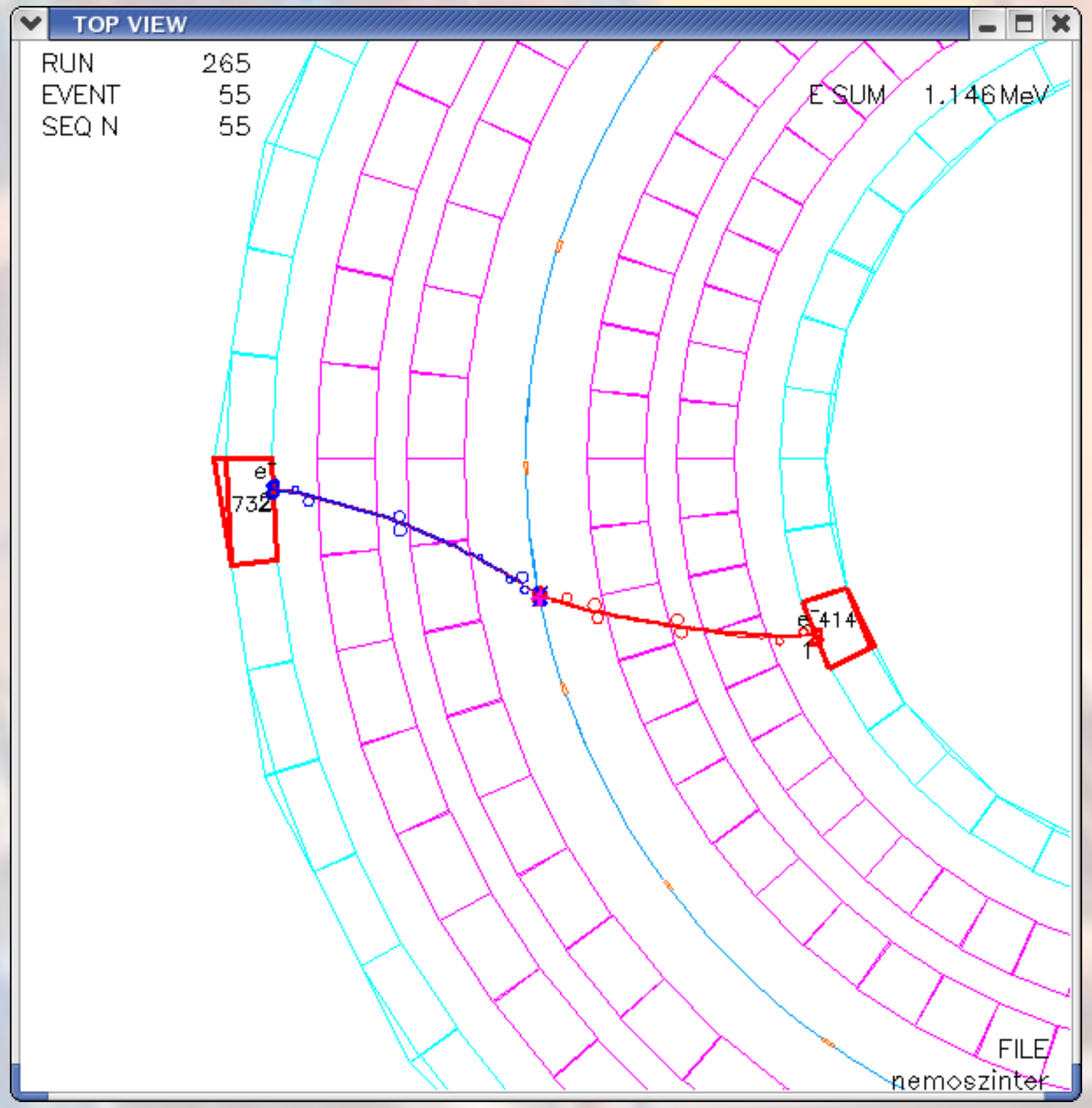

Individual electron track angles and energies give extra information

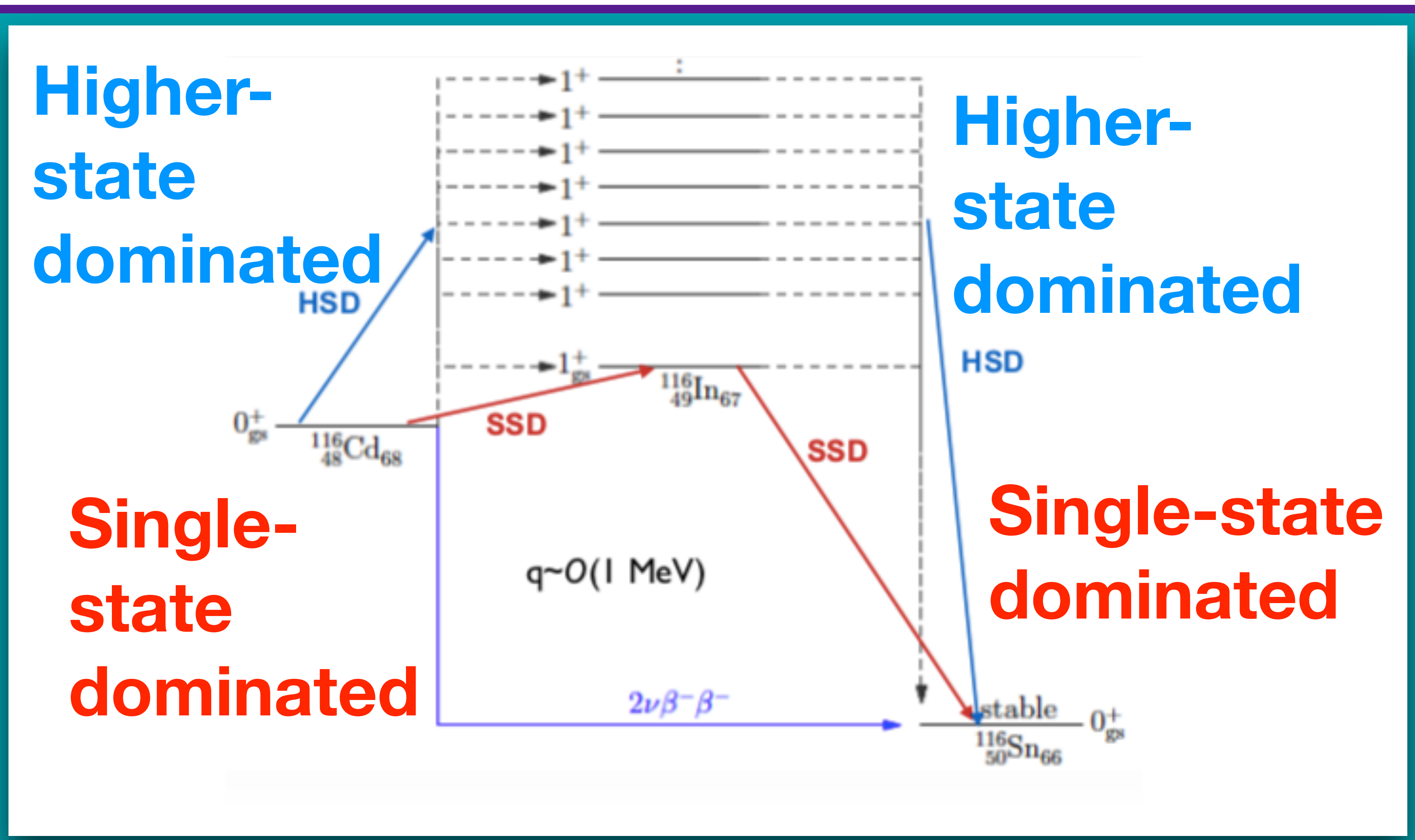

5 x 10^5 events
Signal / bkgd ~ 80

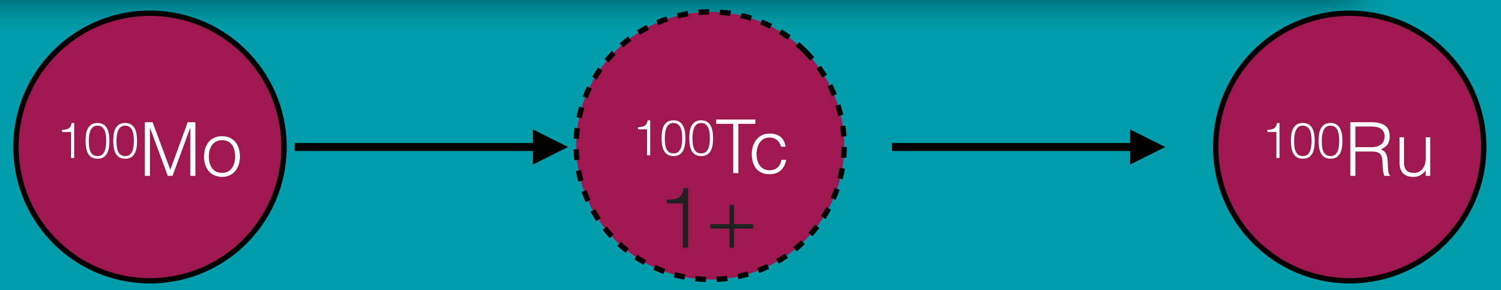

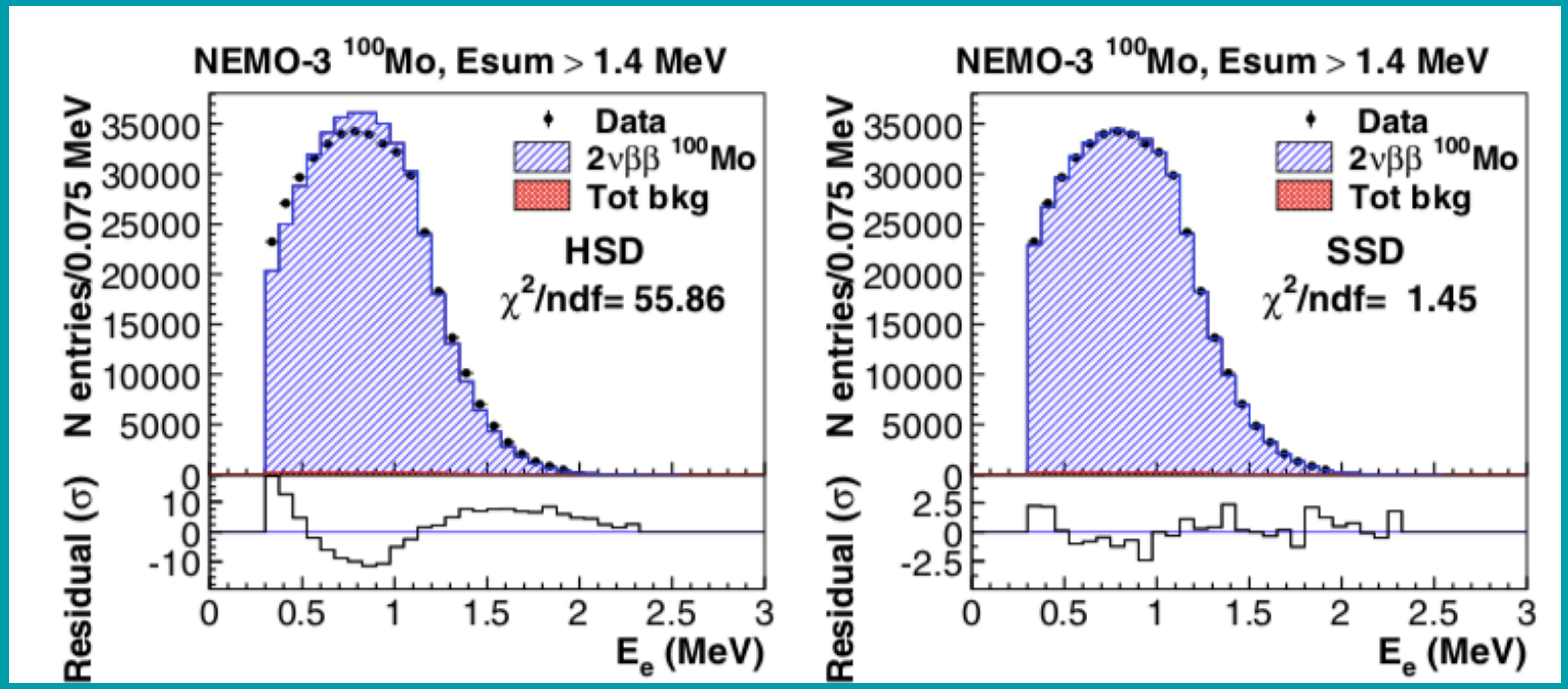

NEMO-3 results highlights

2νββ measurements and 0νββ limit

- ^{100}Mo (Eur. Phys. J. C (2019) 79: 440)
- ^{82}Se (Eur. Phys. J. C (2018) 78: 821)
- ^{48}Ca (Phys. Rev. D 93, 112008)
- ^{150}Nd (Phys. Rev. D 94, 072003)
- ^{116}Cd (Phys. Rev. D 95, 012007)
- ^{130}Te (Phys. Rev. Lett. 107, 062504)
- ^{96}Zr (Nucl.Phys.A847:168-179)

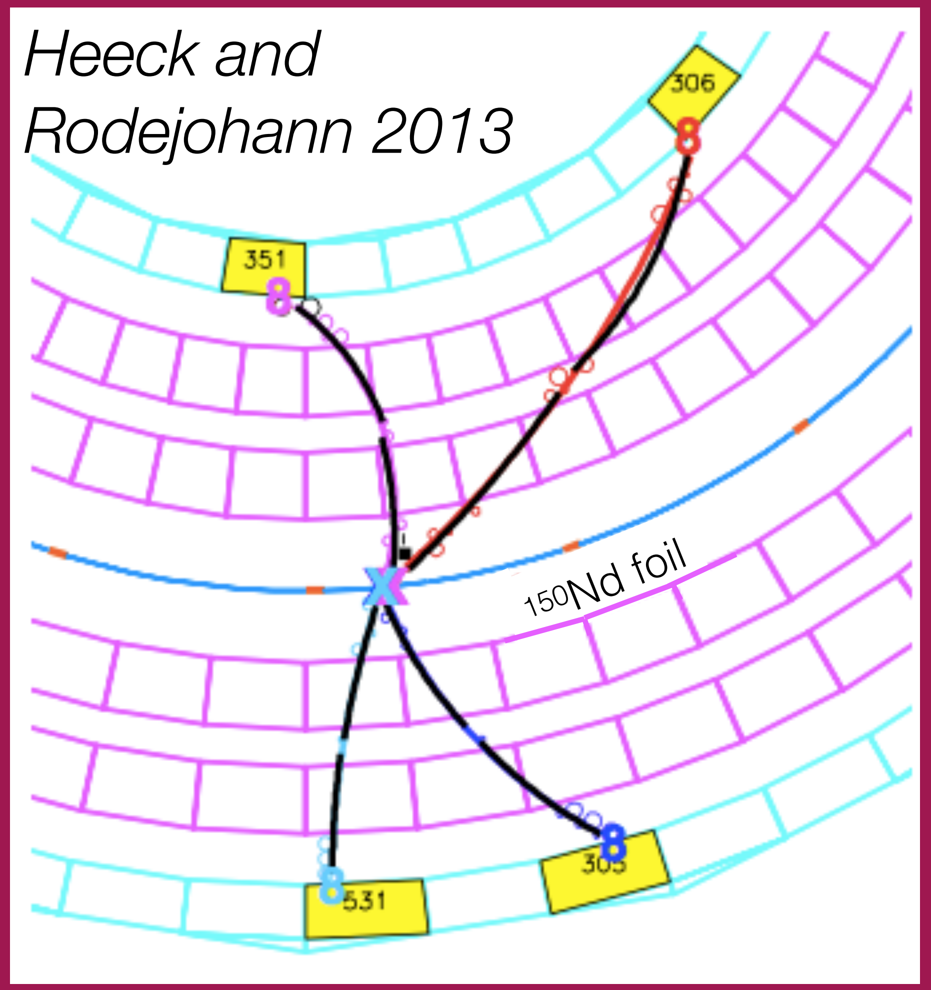

0ν4β decays would violate lepton number, but could occur even if neutrinos are Dirac

Allowed for **3 isotopes**, including ^{150}Nd

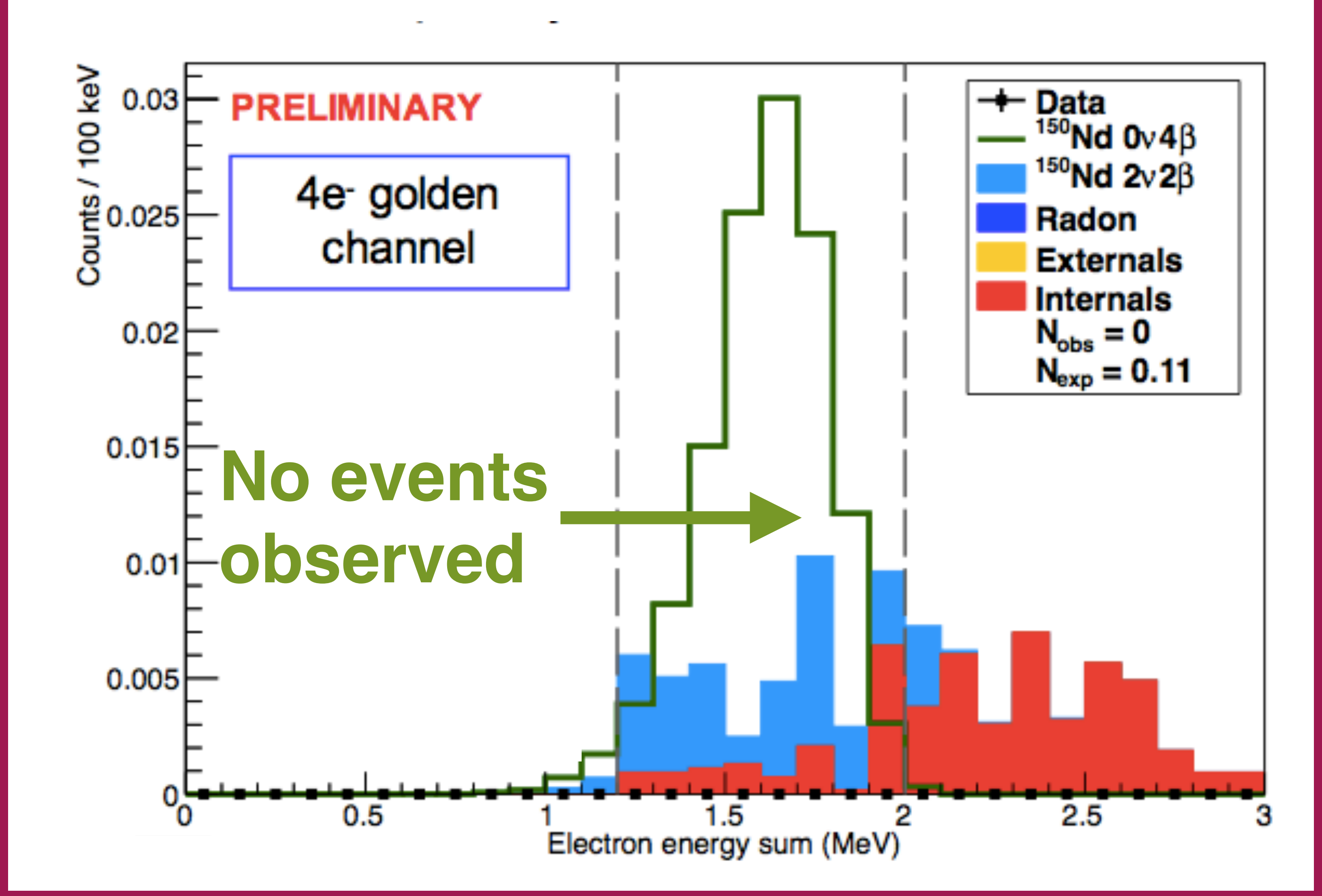

$T_{1/2}$ **> 2.6 x 10^{21} yr** (90%CL)

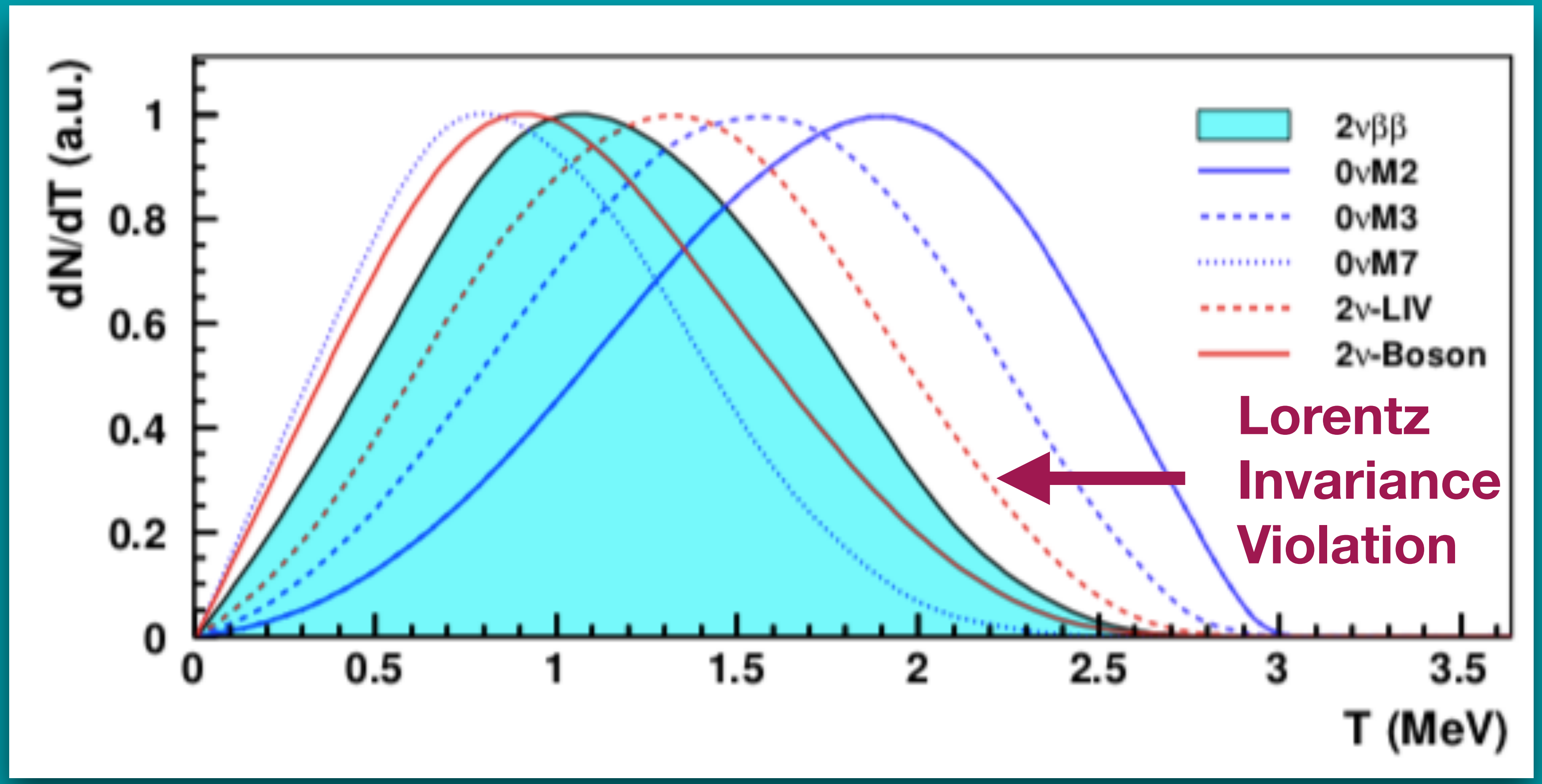

Lorentz Invariance Violation and exotic 0νββ **mechanisms** would modify energy spectrum

Limit set on contribution from Lorentz-Invariance violating events

$$-4.2 \times 10^{-7}\ \mathrm{GeV} < \mathring{a}^{(3)}_{of} < 3.5 \times 10^{-7}\ \mathrm{GeV}$$

(90% C.L.).

Now at LSM: SuperNEMO Demonstrator

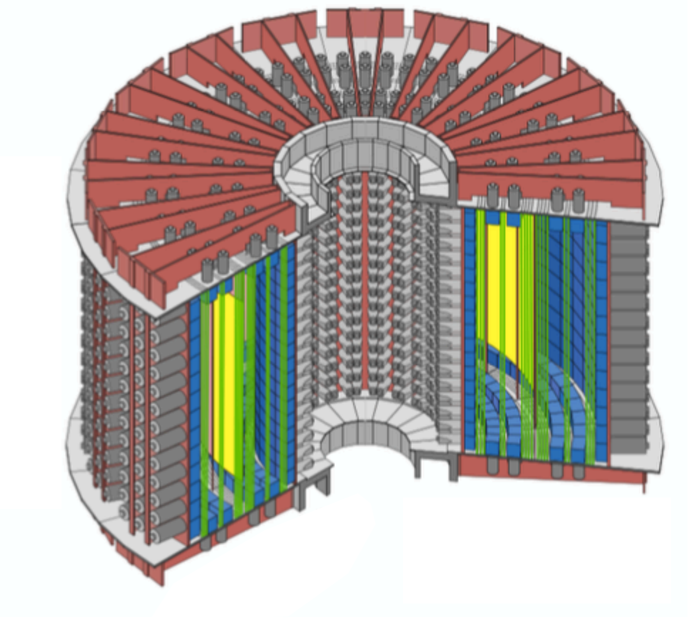

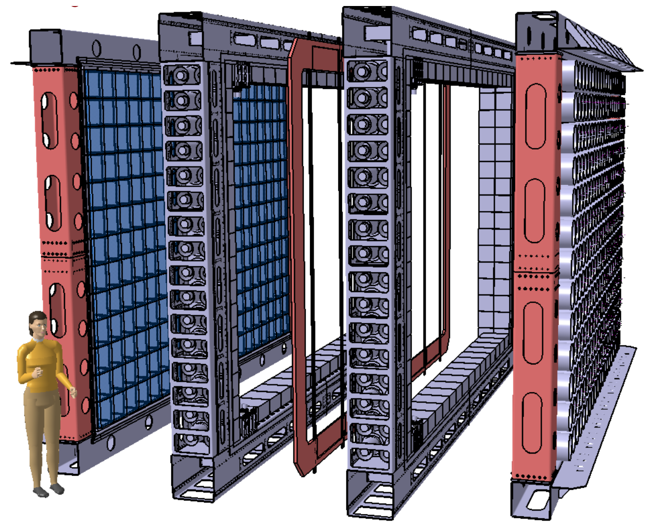

Magnetic field

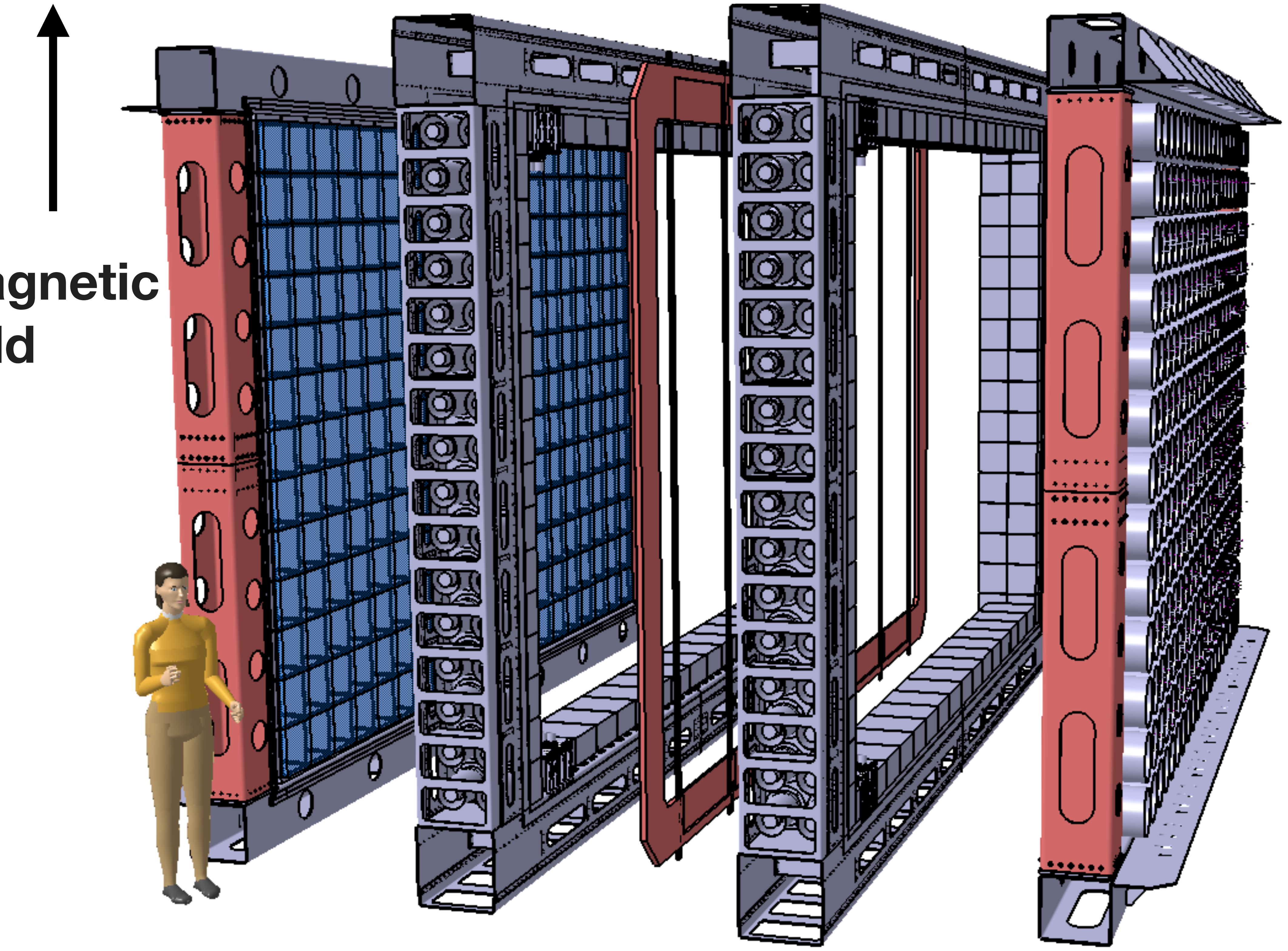

	NEMO-3	SuperNEMO demonstrator
Mass [kg] (main isotopes)	7 (^{100}Mo)	6.3 (^{82}Se)
$T^{2\nu}_{1/2}$ [y]	6.8 x 10^{18}	9.4 x 10^{19}
Energy resolution		
FWHM at 1 MeV	15 %	8 %
FWHM at 3 MeV	8 %	4 %
Source radiopurity		
A(^{208}Tl)	$\sim 100\ \mu$Bq/kg	$< 2\ \mu$Bq/kg
A(^{214}Bi)	$< 300\ \mu$Bq/kg	$< 10\ \mu$Bq/kg
Level of radon A(^{222}Rn)	~ 5.0 mBq/m^3	< 0.15 mBq/m^3
Sensitivity after 5 (2.5) y data taking	$T^{0\nu}_{1/2} > 10^{24}$ y	$T^{0\nu}_{1/2} > 6 \times 10^{24}$ y

Now at LSM: SuperNEMO Demonstrator

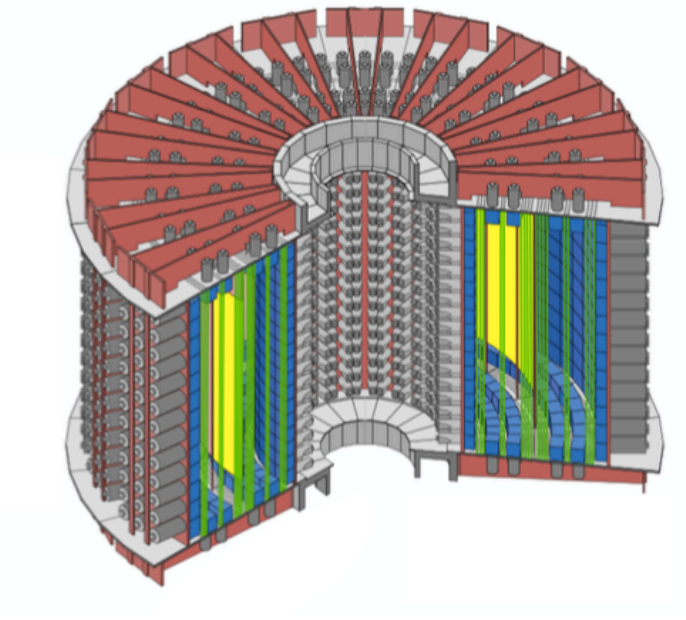

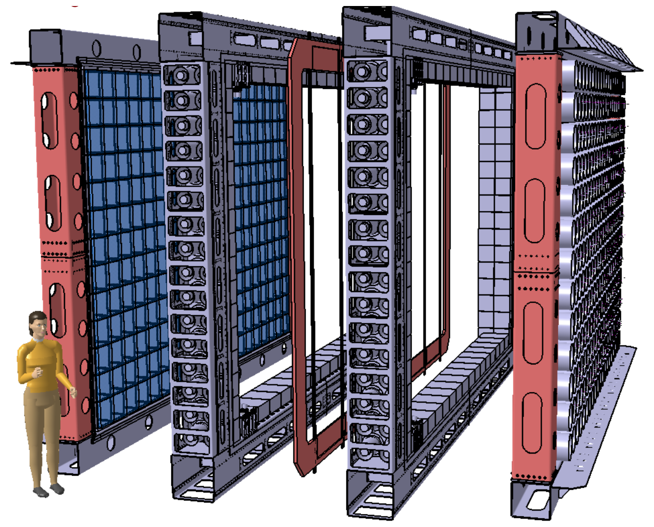

	NEMO-3	SuperNEMO demonstrator
Mass [kg] (main isotopes)	7 (^{100}Mo)	6.3 (^{82}Se)
$T^{2\nu}_{1/2}$ [y]	6.8 x 10^{18}	9.4 x 10^{19}
Energy resolution FWHM at 1 MeV FWHM at 3 MeV	 15 % 8 %	 8 % 4 %
Source radiopurity A(^{208}Tl) A(^{214}Bi)	 $\sim 100\ \mu$Bq/kg $< 300\ \mu$Bq/kg	 $< 2\ \mu$Bq/kg $< 10\ \mu$Bq/kg
Level of radon A(^{222}Rn)	~ 5.0 mBq/m^3	< 0.15 mBq/m^3
Sensitivity after 5 (2.5) y data taking	$T^{0\nu}_{1/2} > 10^{24}$ y	$T^{0\nu}_{1/2} > 6 \times 10^{24}$ y

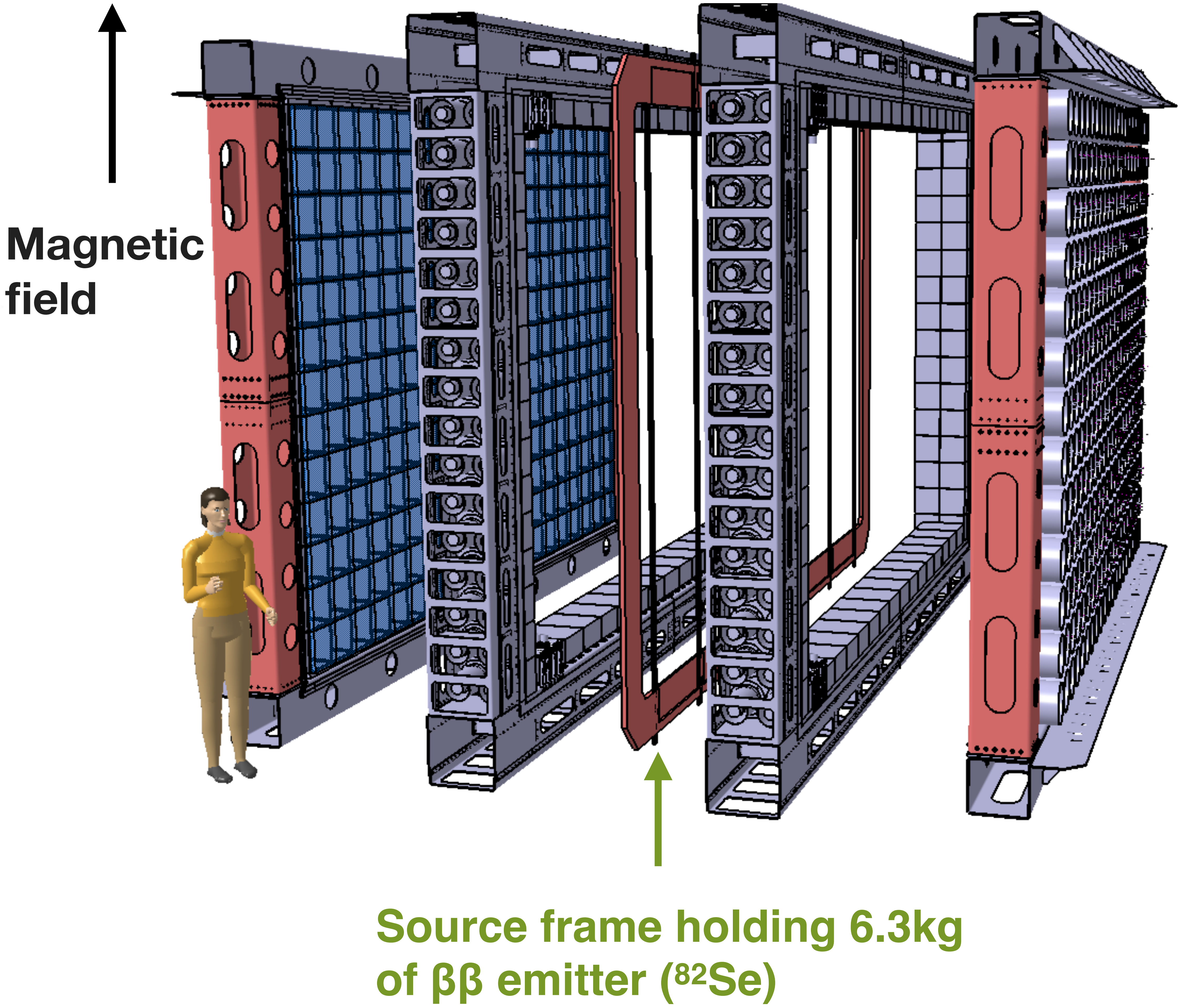

Now at LSM: SuperNEMO Demonstrator

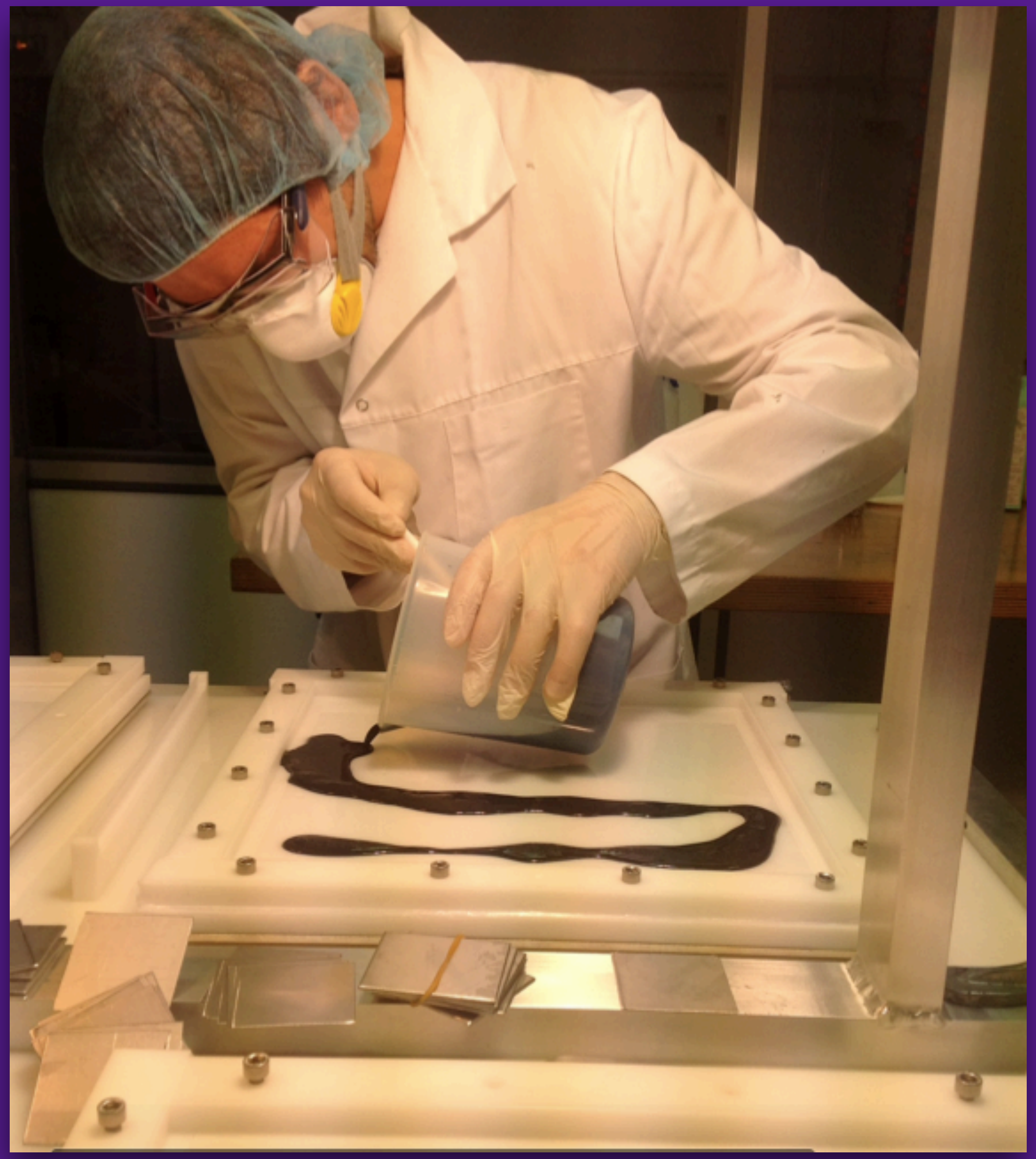

- 34 foils
- Enriched Se powder mixed with PVA
- Increased radio purity through distillation / chromatography / chemical precipitation

Se

gnetic
d

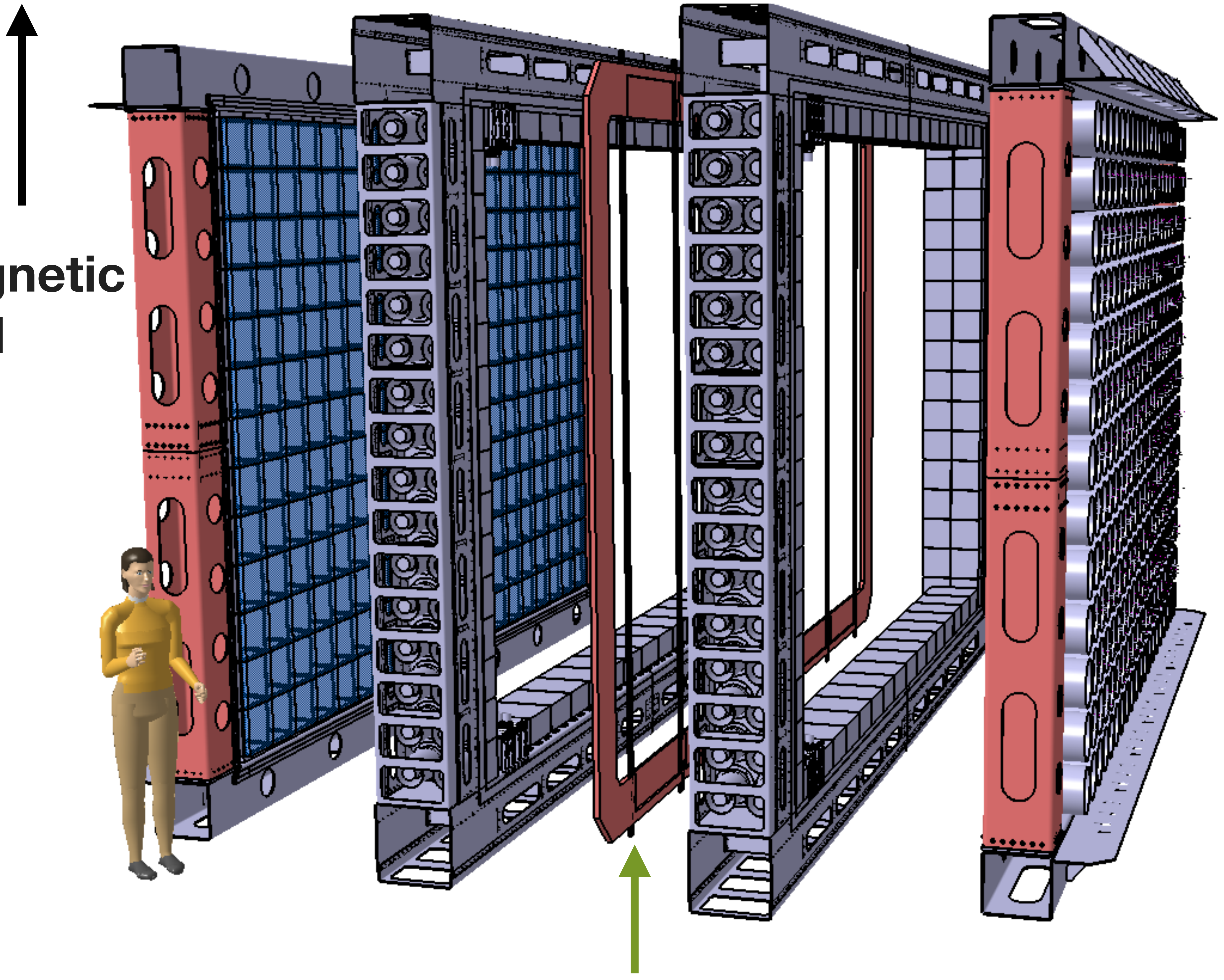

Source frame holding 6.3kg of ββ emitter (^{82}Se)

Now at LSM: SuperNEMO Demonstrator

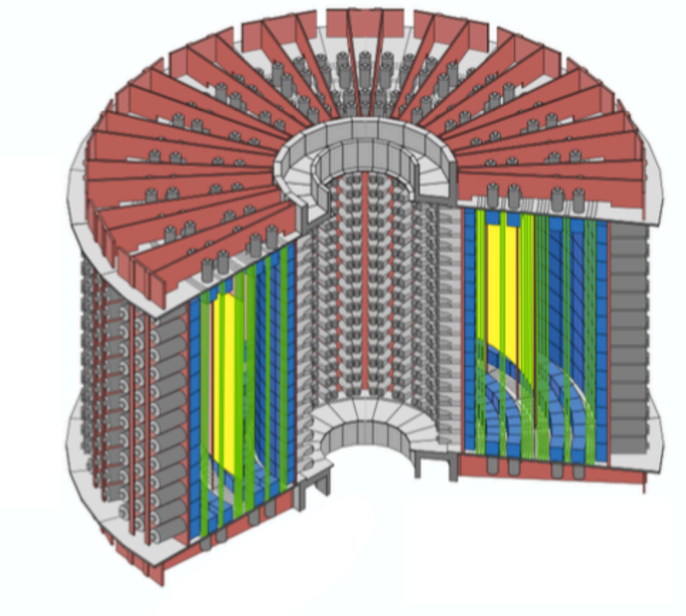

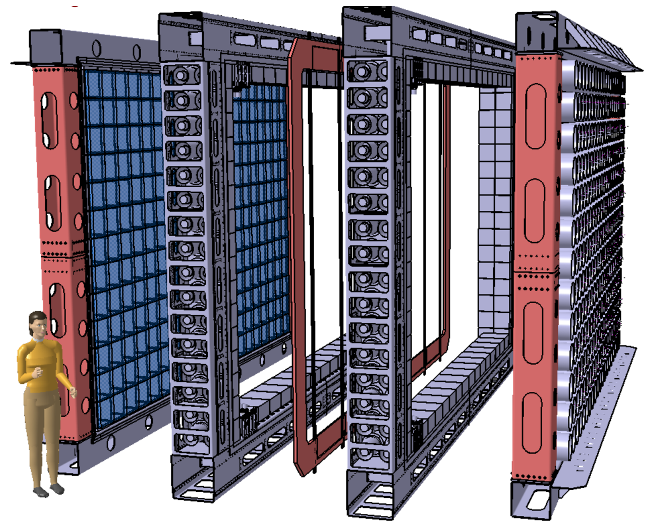

	NEMO-3	SuperNEMO demonstrator
Mass [kg] (main isotopes)	7 (^{100}Mo)	6.3 (^{82}Se)
$T^{2\nu}_{1/2}$ [y]	6.8 x 10^{18}	9.4 x 10^{19}
Energy resolution		
FWHM at 1 MeV	15 %	8 %
FWHM at 3 MeV	8 %	4 %
Source radiopurity		
A(^{208}Tl)	$\sim 100\ \mu$Bq/kg	$< 2\ \mu$Bq/kg
A(^{214}Bi)	$< 300\ \mu$Bq/kg	$< 10\ \mu$Bq/kg
Level of radon A(^{222}Rn)	~ 5.0 mBq/m^3	< 0.15 mBq/m^3
Sensitivity after 5 (2.5) y data taking	$T^{0\nu}_{1/2} > 10^{24}$ y	$T^{0\nu}_{1/2} > 6 \times 10^{24}$ y

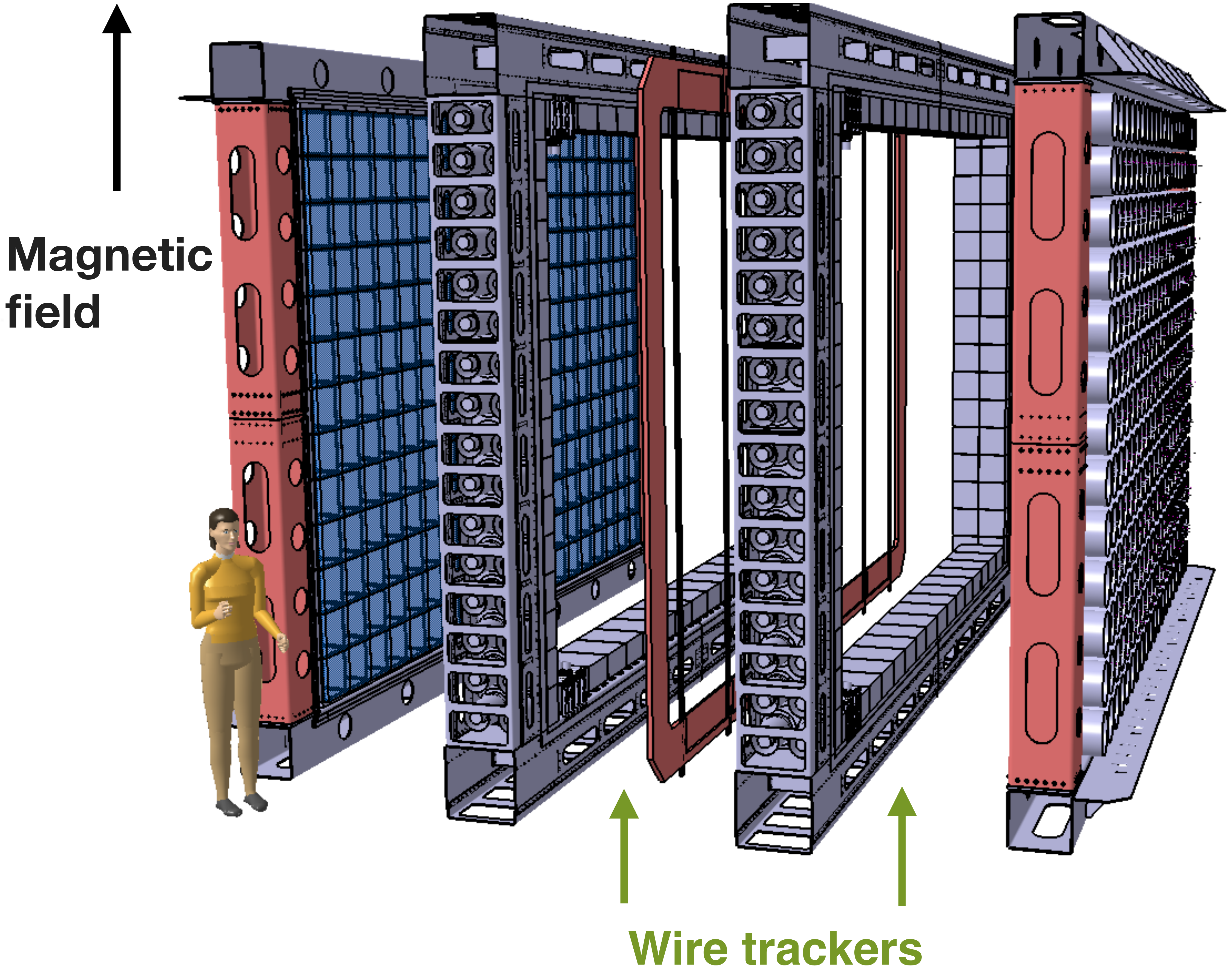

Now at LSM: SuperNEMO Demonstrator

- 2034 drift cells (13,000 wires!)
- He/Ar/Ethanol gas mixture with advanced radon reduction program

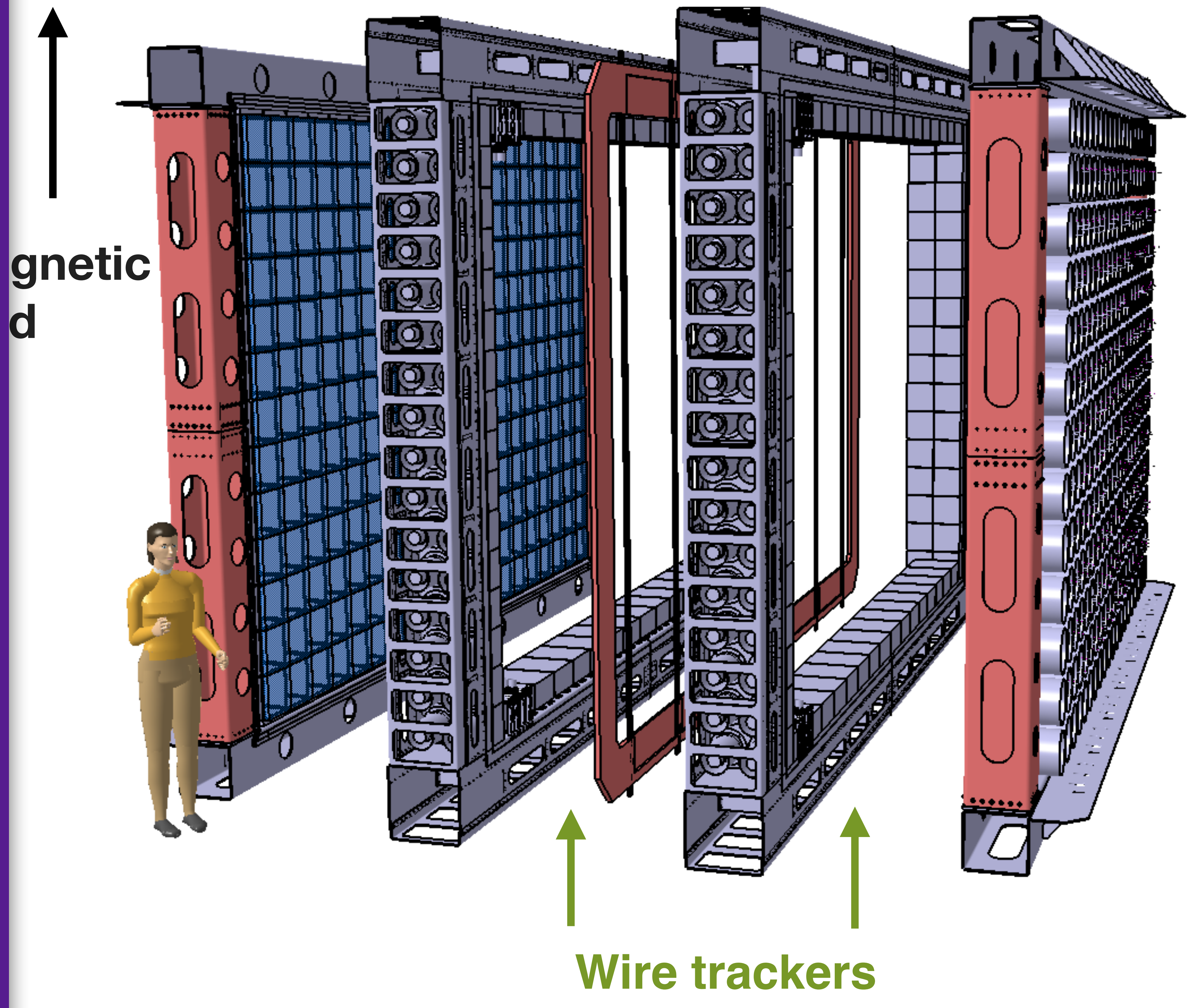

Se

Now at LSM: SuperNEMO Demonstrator

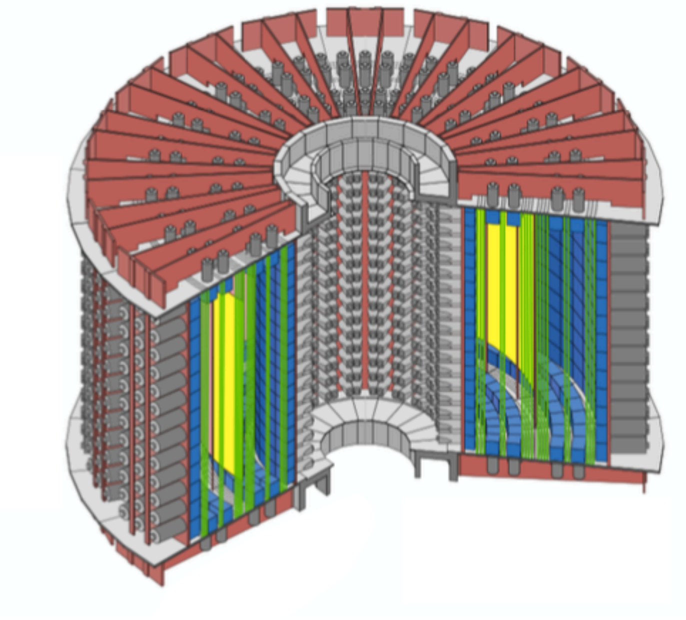

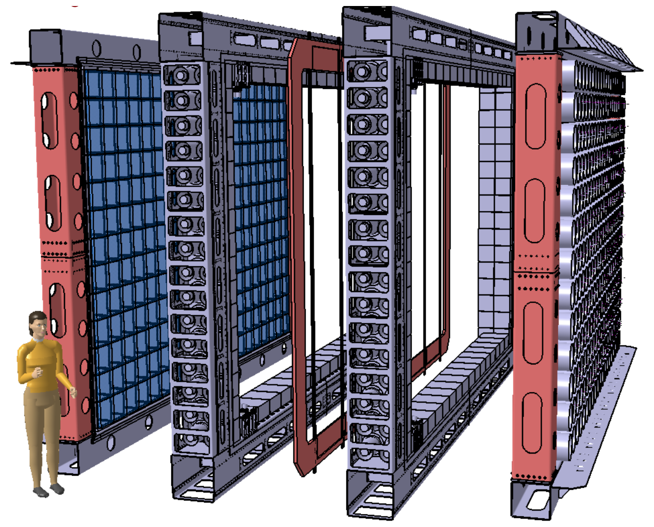

	NEMO-3	SuperNEMO demonstrator
Mass [kg] (main isotopes)	7 (^{100}Mo)	6.3 (^{82}Se)
$T^{2\nu}_{1/2}$ [y]	6.8 x 10^{18}	9.4 x 10^{19}
Energy resolution		
FWHM at 1 MeV	15 %	8 %
FWHM at 3 MeV	8 %	4 %
Source radiopurity		
A(^{208}Tl)	$\sim 100\ \mu$Bq/kg	$< 2\ \mu$Bq/kg
A(^{214}Bi)	$< 300\ \mu$Bq/kg	$< 10\ \mu$Bq/kg
Level of radon A(^{222}Rn)	~ 5.0 mBq/m^3	< 0.15 mBq/m^3
Sensitivity after 5 (2.5) y data taking	$T^{0\nu}_{1/2} > 10^{24}$ y	$T^{0\nu}_{1/2} > 6 \times 10^{24}$ y

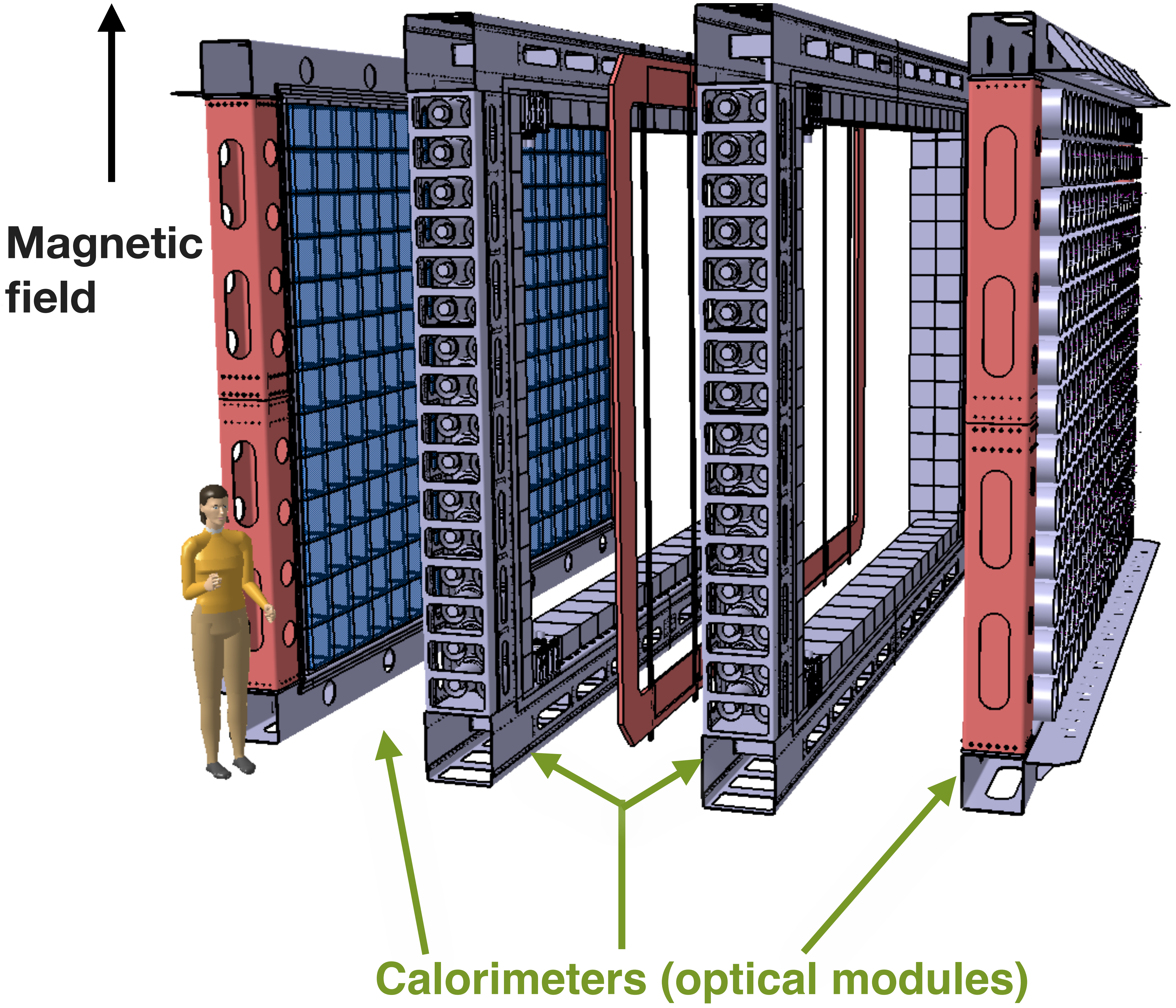

Now at LSM: SuperNEMO Demonstrator

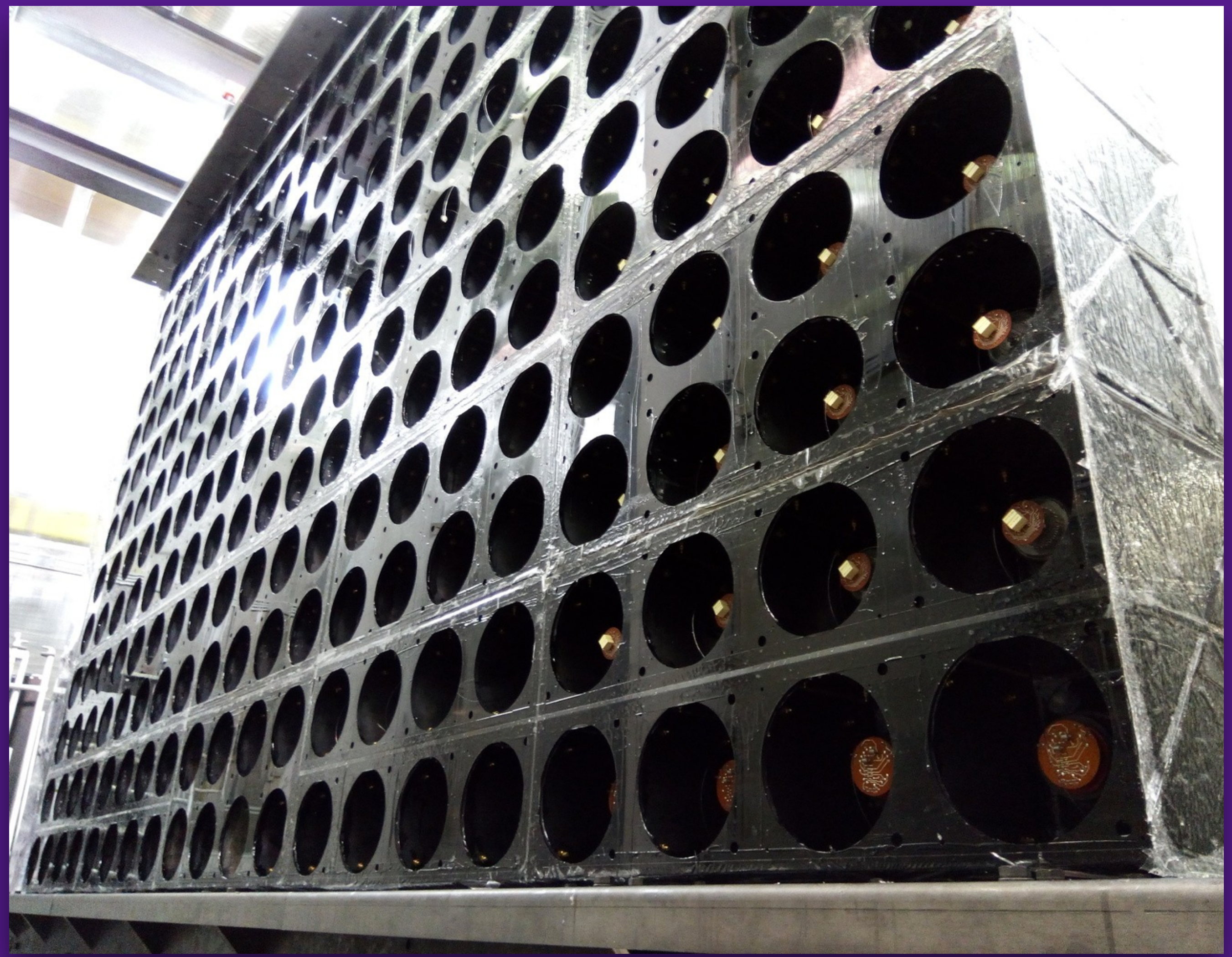

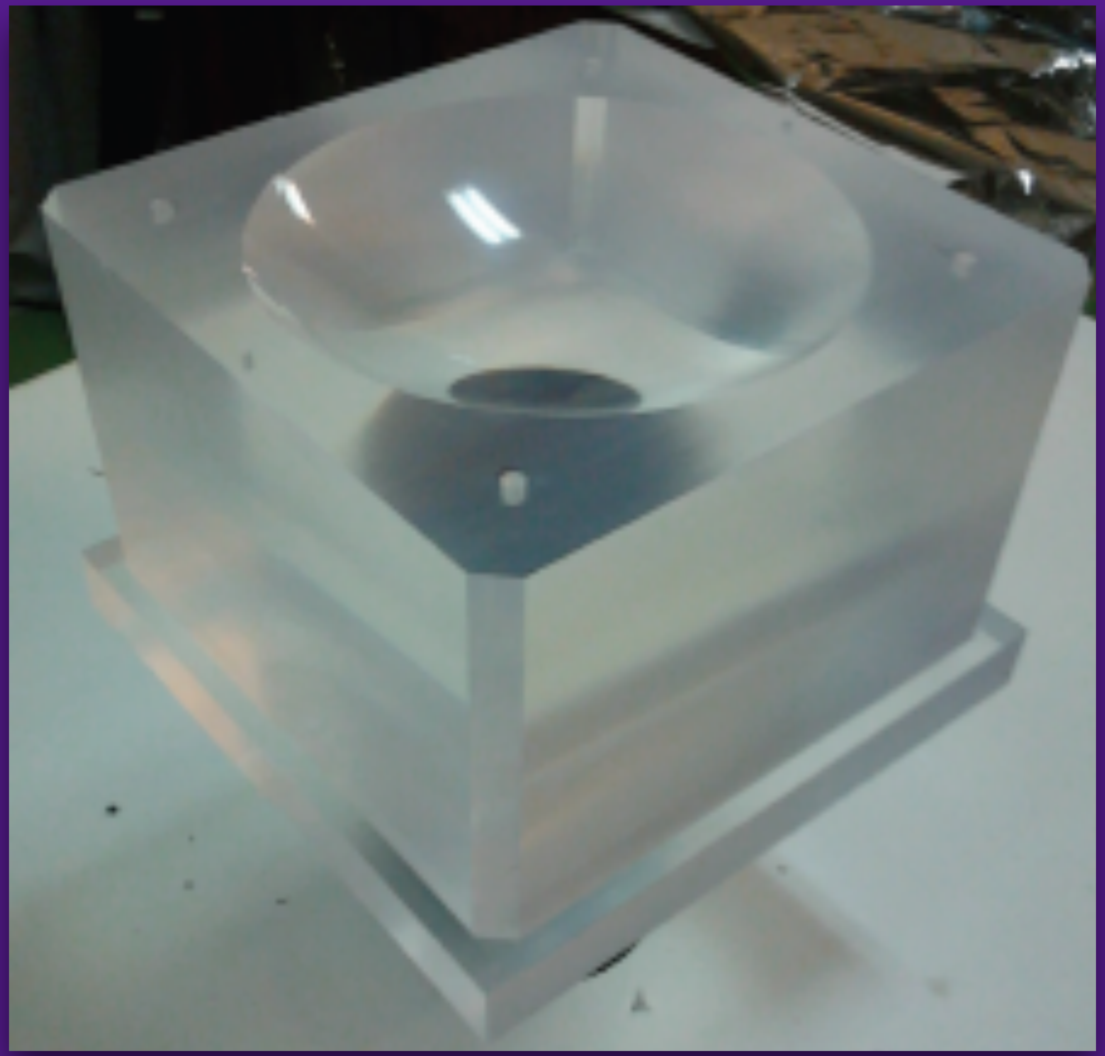

- 440 8” radiopure PMTs (plus 5” NEMO-3 PMTs)
- Improved photocathode quantum efficiency
- Directly coupled to polystyrene scintillator (no light guide) *(Nucl.Inst.Meth. A 868 98-108)*

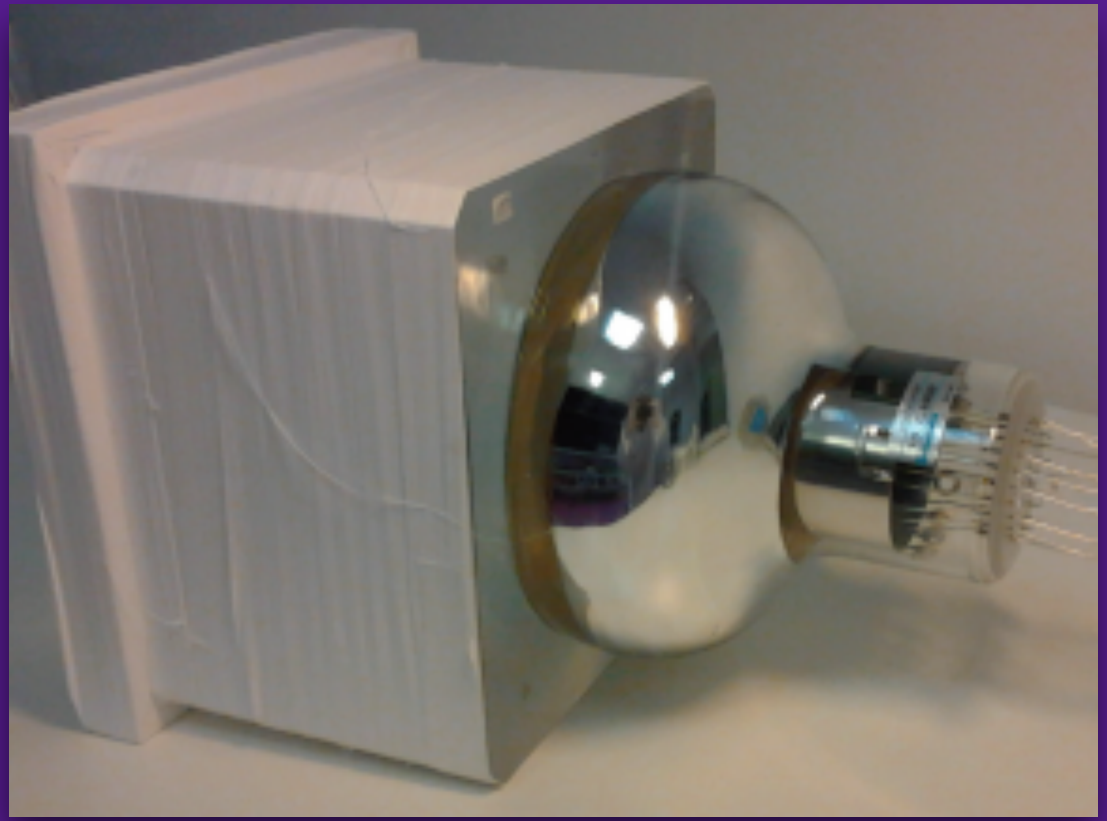

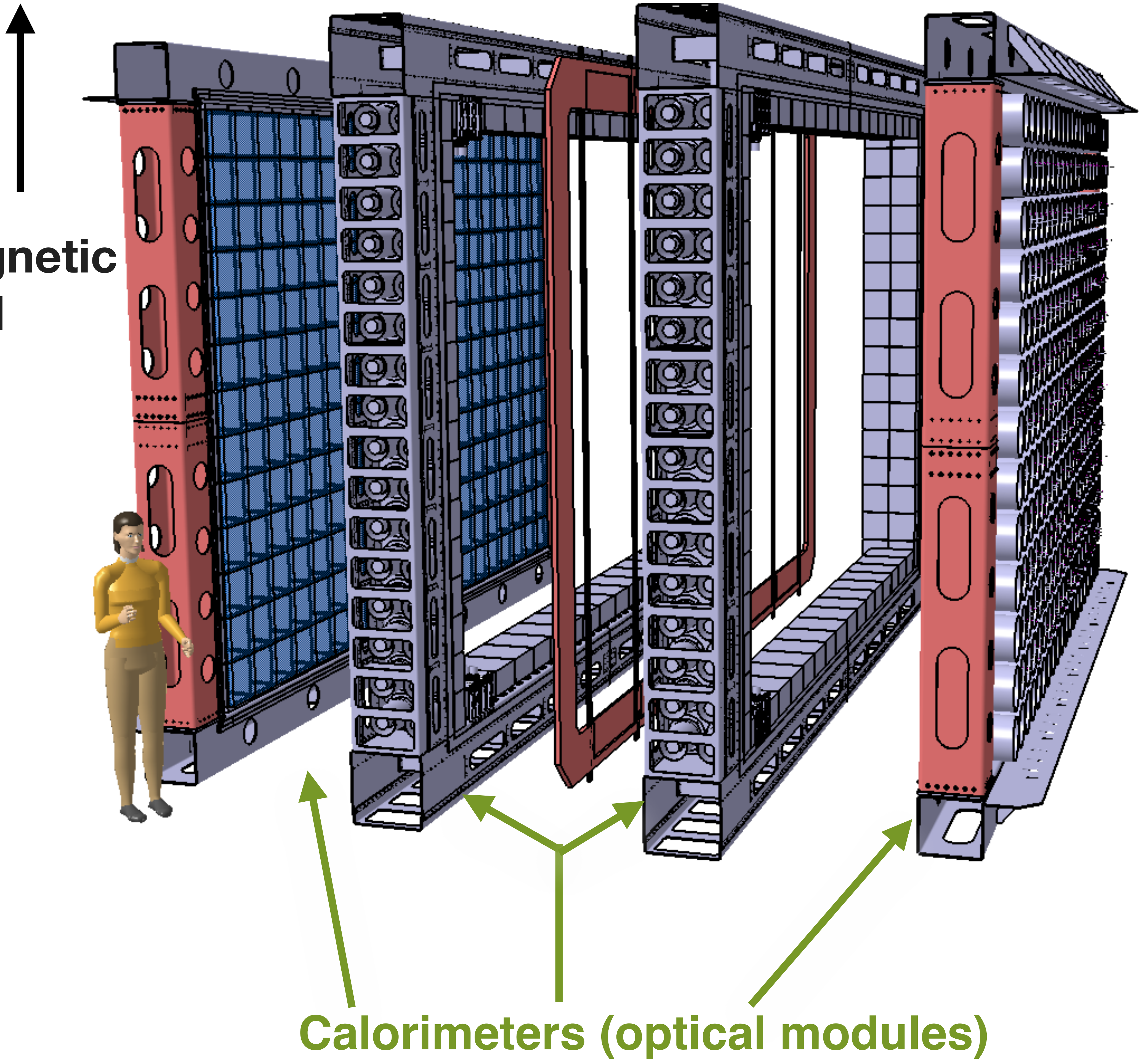

Now at LSM: SuperNEMO Demonstrator

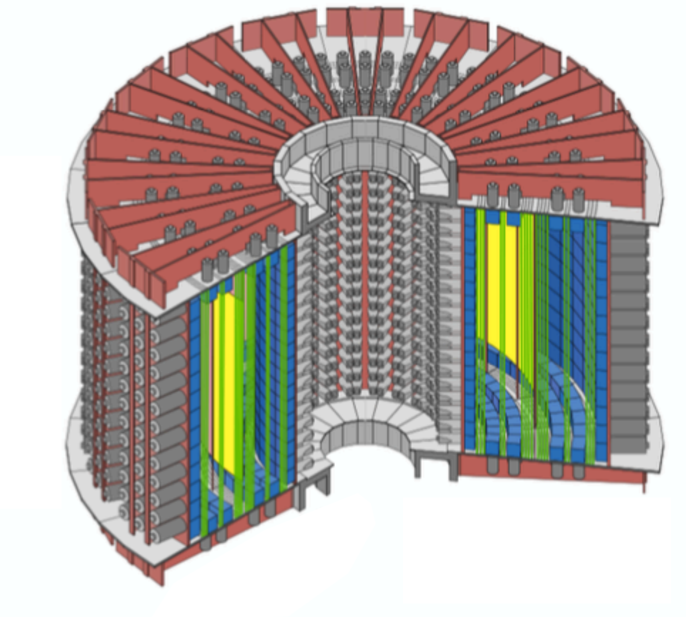

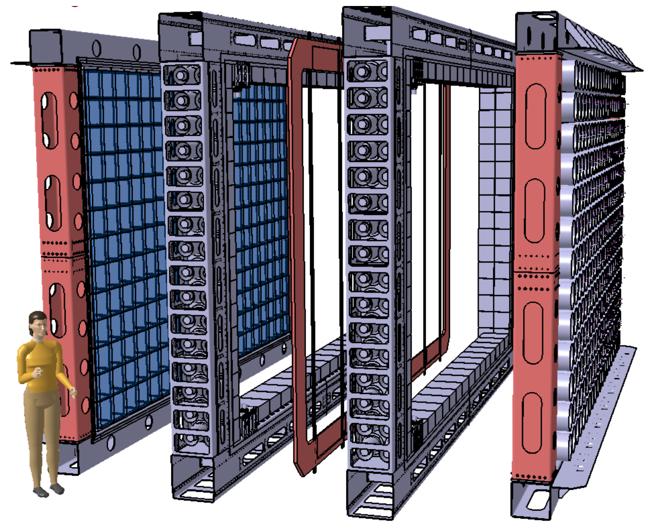

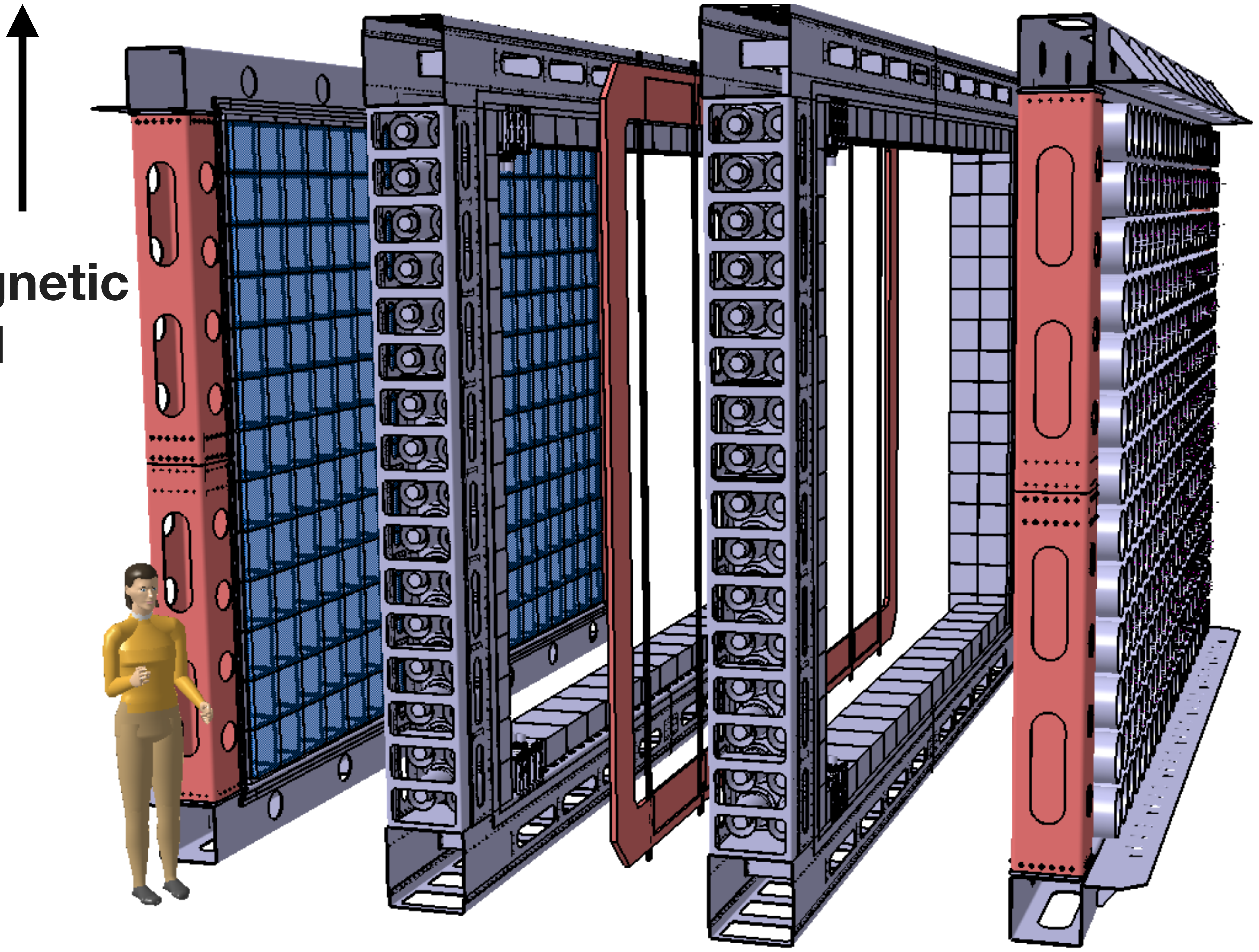

	NEMO-3	SuperNEMO demonstrator
Mass [kg] (main isotopes)	7 (^{100}Mo)	6.3 (^{82}Se)
$T^{2\nu}_{1/2}$ [y]	6.8 x 10^{18}	9.4 x 10^{19}
Energy resolution		
FWHM at 1 MeV	15 %	8 %
FWHM at 3 MeV	8 %	4 %
Source radiopurity		
A(^{208}Tl)	$\sim 100\ \mu$Bq/kg	$< 2\ \mu$Bq/kg
A(^{214}Bi)	$< 300\ \mu$Bq/kg	$< 10\ \mu$Bq/kg
Level of radon A(^{222}Rn)	~ 5.0 mBq/m^3	< 0.15 mBq/m^3
Sensitivity after 5 (2.5) y data taking	$T^{0\nu}_{1/2} > 10^{24}$ y	$T^{0\nu}_{1/2} > 6 \times 10^{24}$ y

$T_{1/2}^{0\nu} > 6 \times 10^{24}$ years

Now at LSM: SuperNEMO Demonstrator

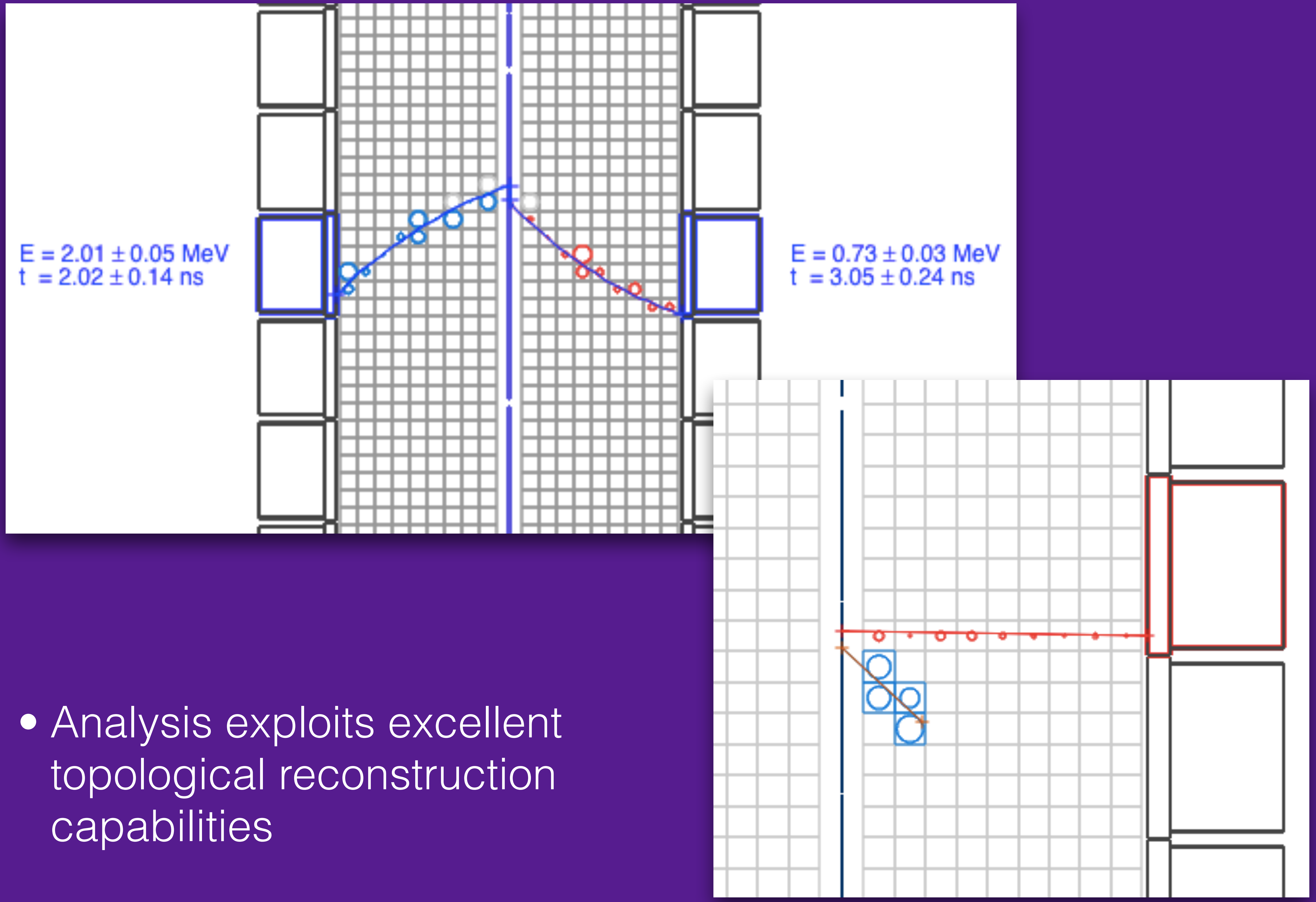

- Analysis exploits excellent topological reconstruction capabilities

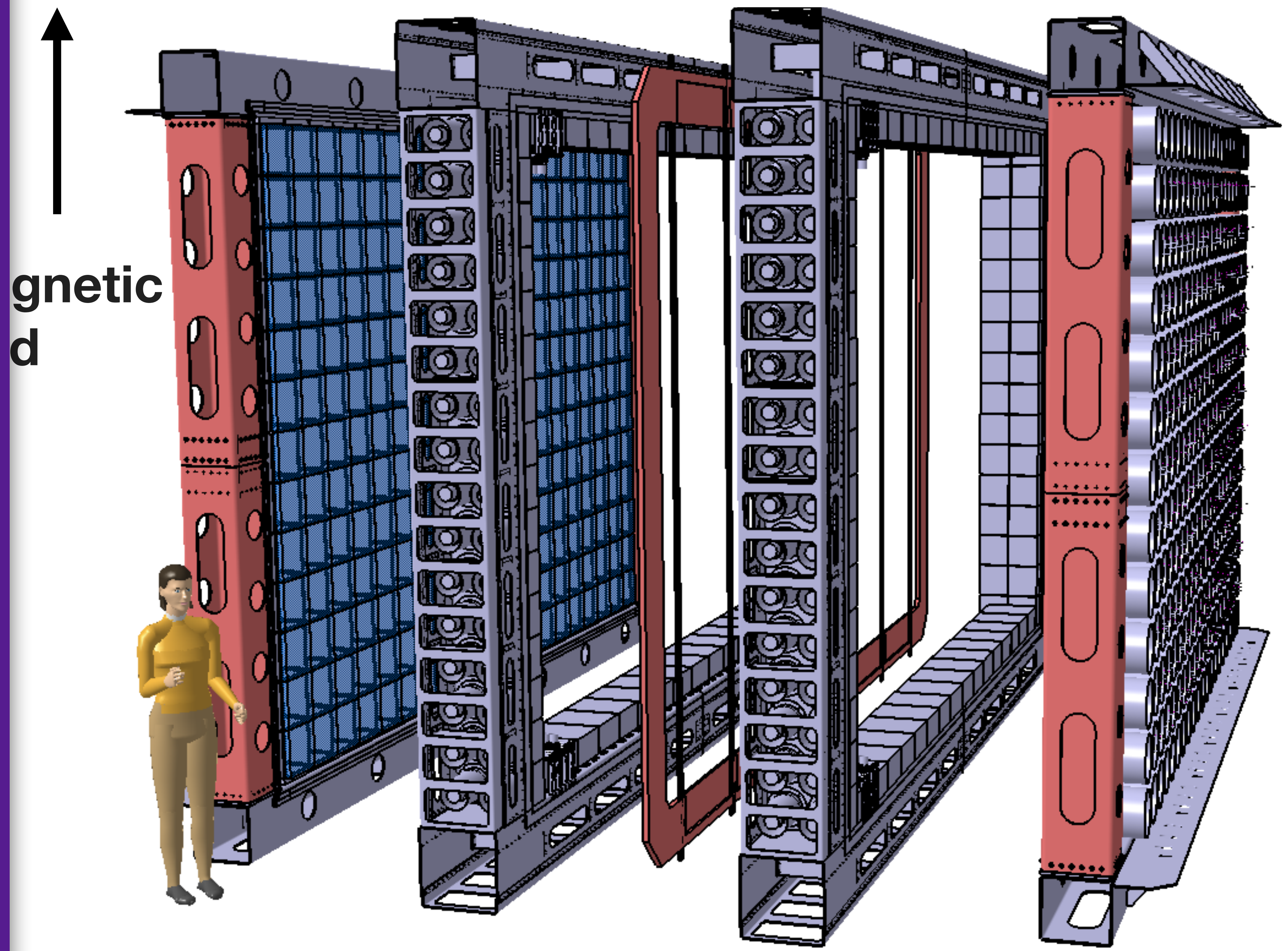

$T_{1/2}^{0\nu}$ > 6 x 10^{24} years

SuperNEMO picture gallery

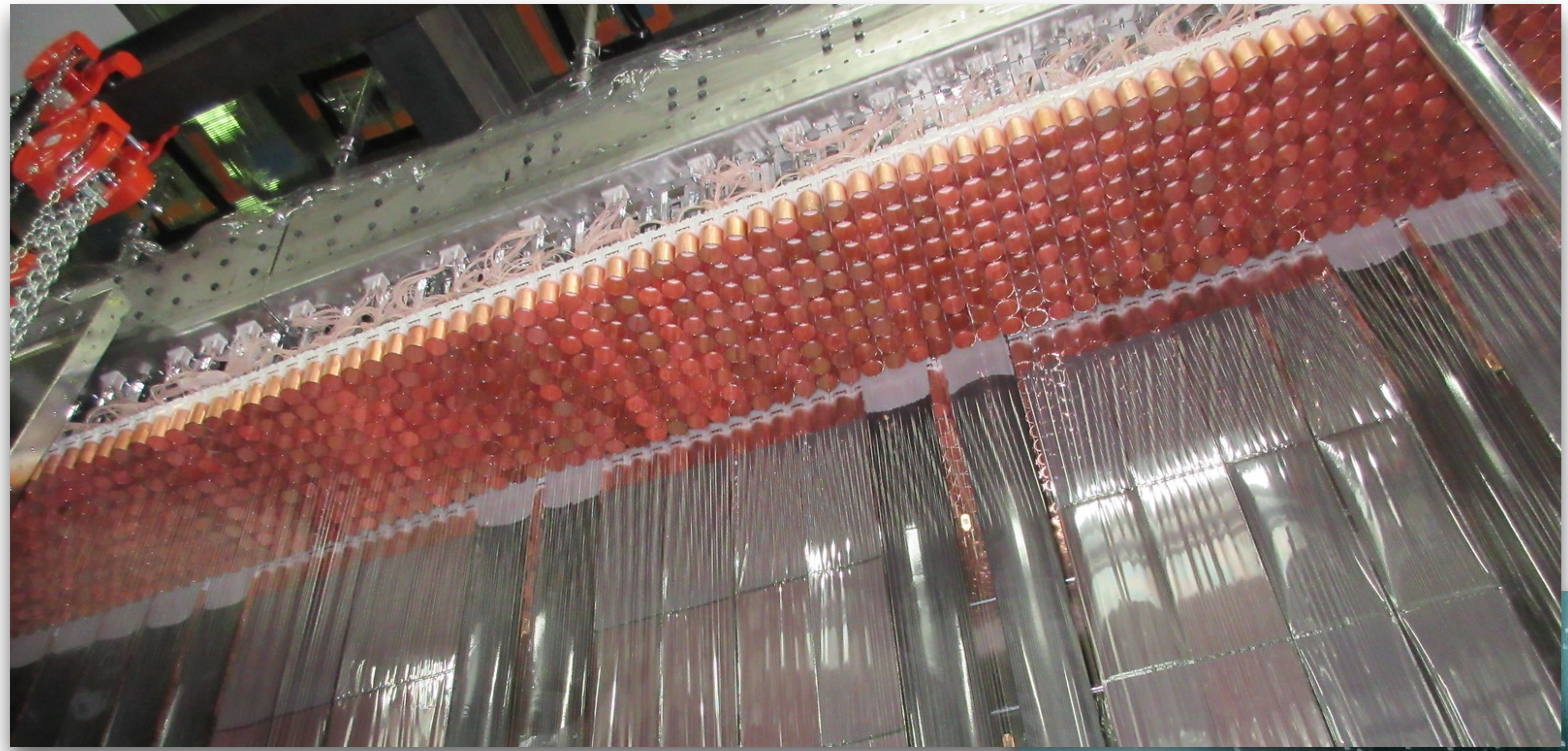

Source foils through the tracker

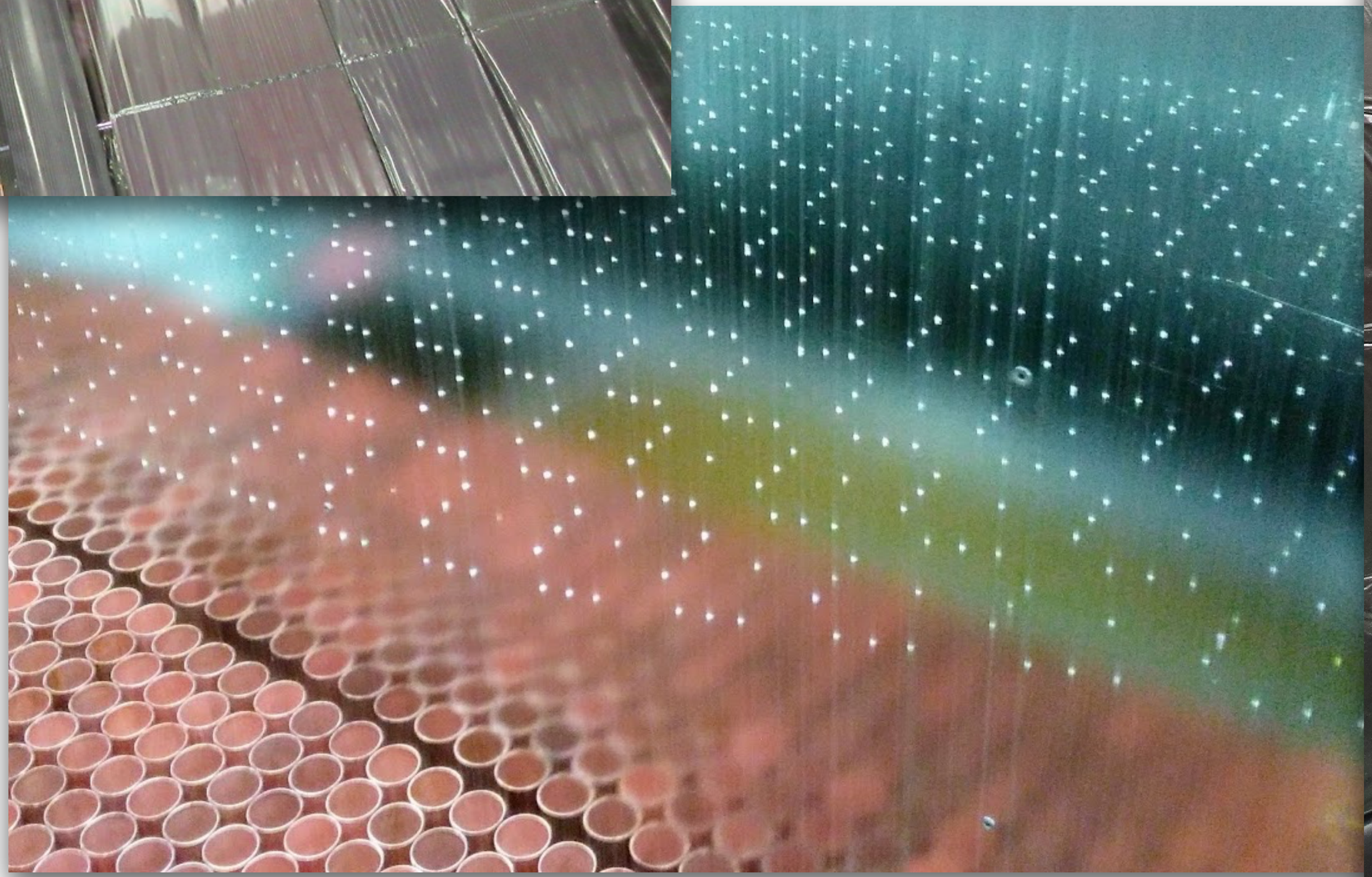

Tracker wire pattern

Calorimeter through the tracker

SuperNEMO physics goals

$0\nu\beta\beta$: $T_{1/2} > 6 \times 10^{24}$ years; $\langle m_\nu \rangle < 160\text{-}400$ meV

SuperNEMO physics goals

$0\nu\beta\beta$: $T_{1/2} > 6 \times 10^{24}$ years; $\langle m_\nu \rangle <$ 160-400 meV

Exotic $0\nu\beta\beta$ mechanisms

Lorentz invariance violation test

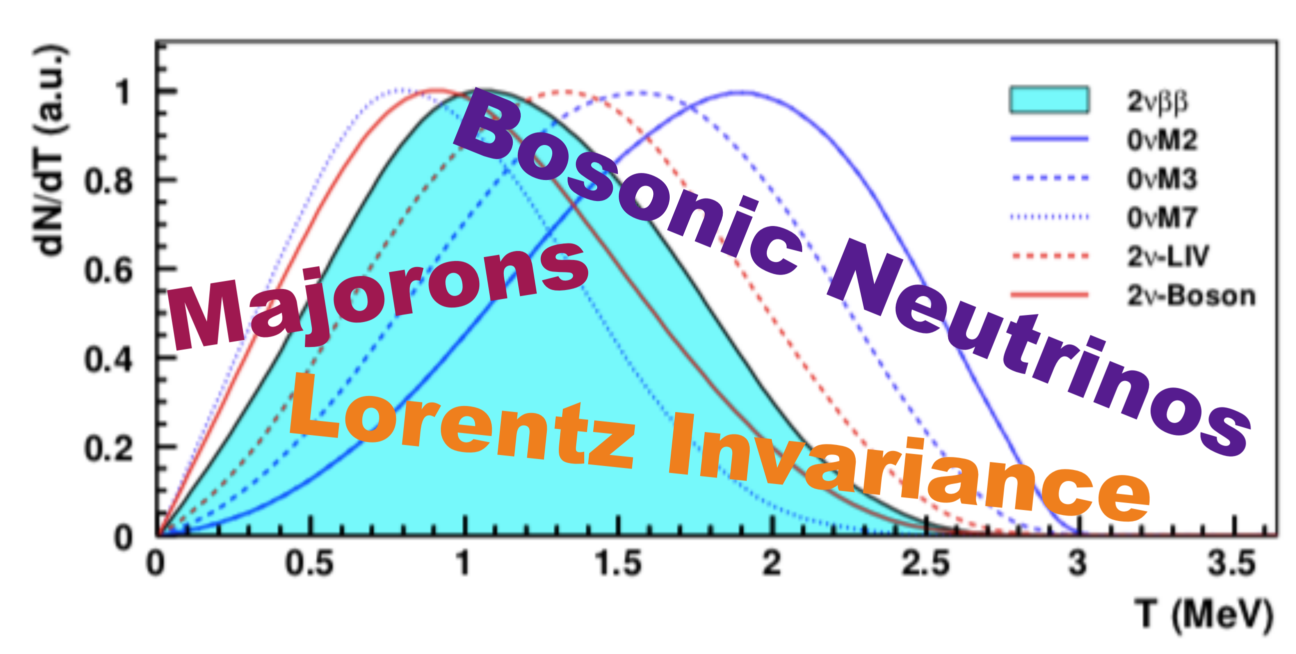

Extend NEMO-3's measurements

SuperNEMO physics goals

$0\nu\beta\beta$: $T_{1/2} > 6 \times 10^{24}$ years; $\langle m_\nu \rangle < 160\text{-}400$ meV

Exotic $0\nu\beta\beta$ mechanisms

Lorentz invariance violation test

$2\nu\beta\beta$: SSD/HSD discrimination at 5σ level

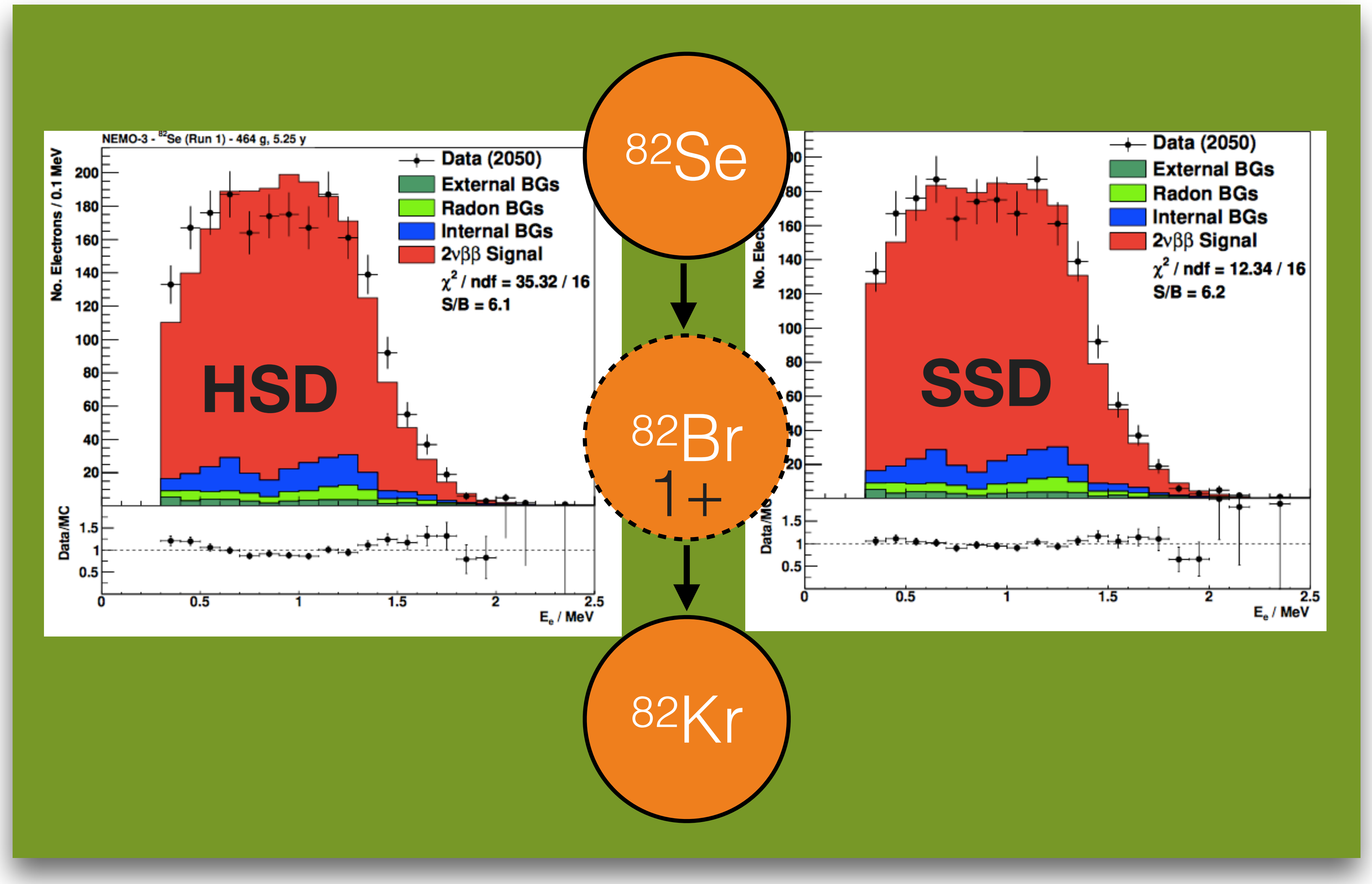

0νββ: $T_{1/2}$ > 6 x 10^{24} years; ⟨$m_ν$⟩ < 160-400 meV

Exotic 0νββ mechanisms

Lorentz invariance violation test

2νββ: SSD/HSD discrimination at 5σ level

Probe nuclear physics by investigating g_A

- Axial-vector coupling constant g_A is **quenched** in heavy nuclei

- **2νββ rate** proportional to g_A^4

$$\left(T_{1/2}^{2\nu}\right)^{-1} = \left(g_A^{\mathrm{eff}}\right)^4 \left|M_{GT}^{2\nu}\right|^2 G^{2\nu}$$

- New KamLAND-Zen paper investigates this quenching https://arxiv.org/pdf/1901.03871.pdf

Precision measurement of the ^{136}Xe two-neutrino $\beta\beta$ spectrum in KamLAND-Zen and its impact on the quenching of nuclear matrix elements

Gando,[1] Y. Gando,[1] T. Hachiya,[1] M. Ha Minh,[1] S. Hayashida,[1] Y. Honda,[1] K. Hosokawa,[1] H. Ikeda,[1] K. Inoue,[1,] . Ishidoshiro,[1] Y. Kamei,[1] K. Kamizawa,[1] T. Kinoshita,[1] M. Koga,[1,2] S. Matsuda,[1] T. Mitsui,[1] K. Nakamura,[1,2] Ono,[1] N. Ota,[1] S. Otsuka,[1] H. Ozaki,[1] Y. Shibukawa,[1] I. Shimizu,[1] Y. Shirahata,[1] J. Shirai,[1] T. Sato,[1] K. Soma,

- NEMO's topological capabilities mean it could do even **better**!

SuperNEMO physics goals

$0\nu\beta\beta$: $T_{1/2} > 6 \times 10^{24}$ years; $\langle m_\nu \rangle <$ 160-400 meV

Exotic $0\nu\beta\beta$ mechanisms

Lorentz invariance violation test

$2\nu\beta\beta$: SSD/HSD discrimination at 5σ level

Probe nuclear physics by investigating g_A

Alternative isotopes: ^{150}Nd and ^{96}Zr

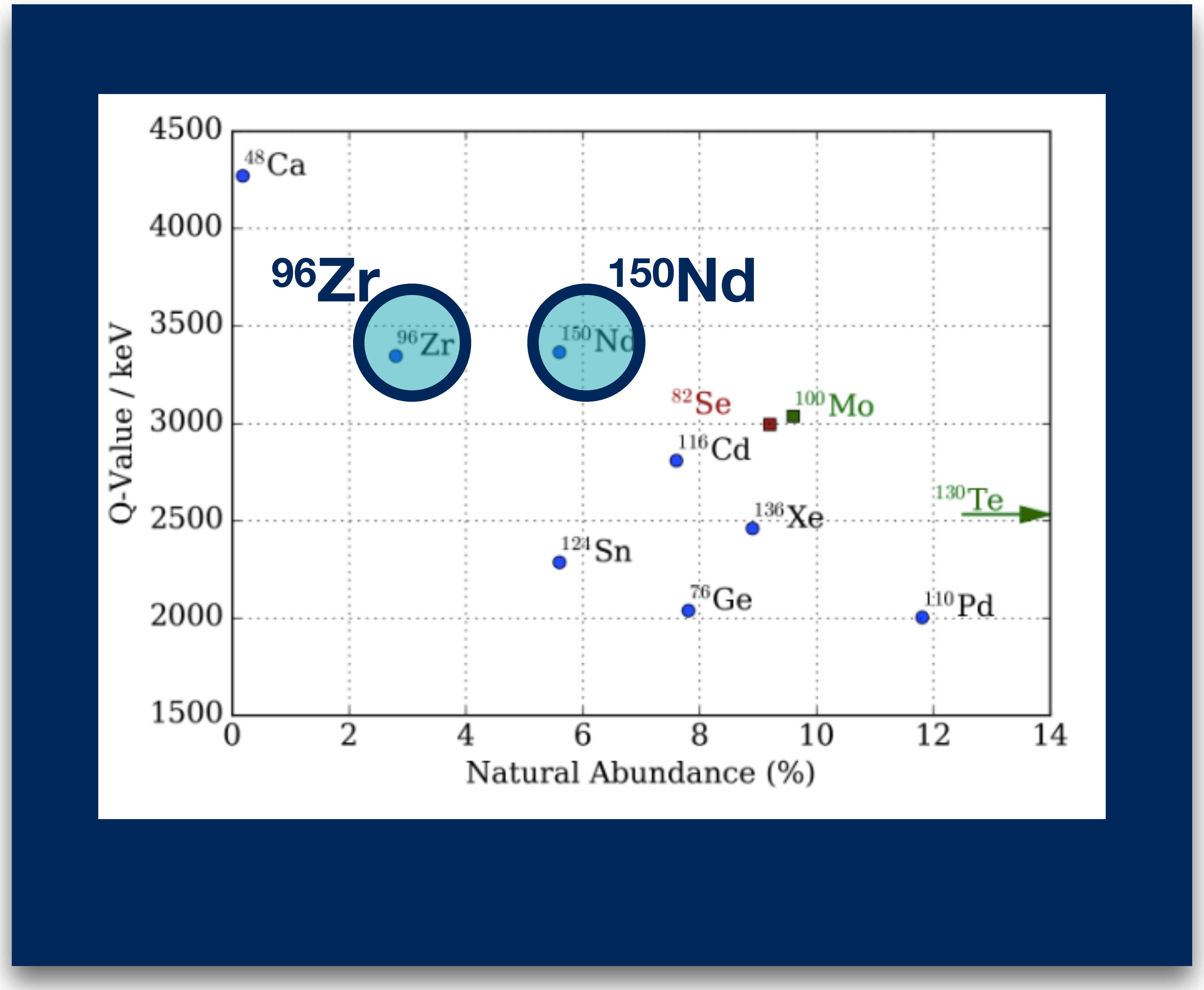

SuperNEMO physics goals

$0\nu\beta\beta$: $T_{1/2} > 6 \times 10^{24}$ years; $\langle m_\nu \rangle < 160\text{-}400$ meV

Exotic $0\nu\beta\beta$ mechanisms

Lorentz invariance violation test

$2\nu\beta\beta$: SSD/HSD discrimination at 5σ level

Probe nuclear physics by investigating g_A

Alternative isotopes: ^{150}Nd and ^{96}Zr

$0\nu4\beta$: for ^{150}Nd

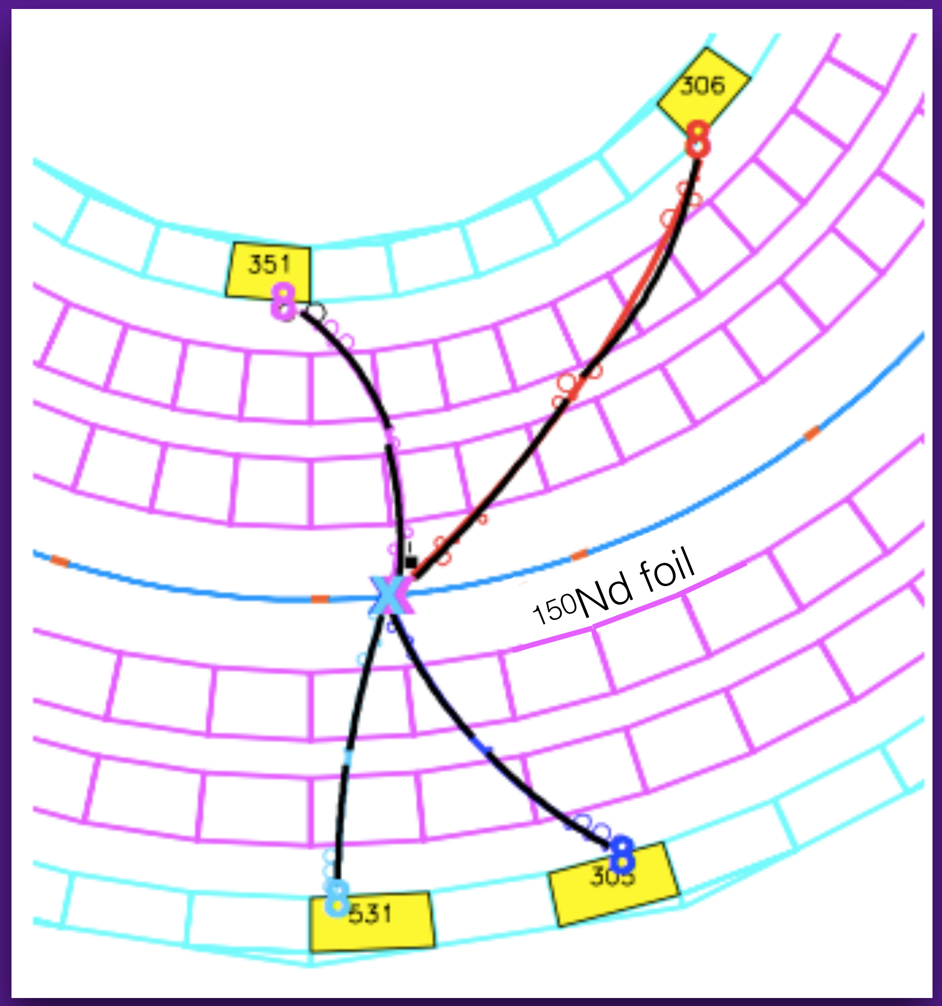

NEMO-3 placed limit on lepton number-violating process, which could affect even Dirac neutrinos

Phys. Rev. Lett. 119, 041801

SuperNEMO physics goals

$0\nu\beta\beta$: $T_{1/2} > 6 \times 10^{24}$ years; $\langle m_\nu \rangle < 160\text{-}400$ meV

Exotic $0\nu\beta\beta$ mechanisms

Lorentz invariance violation test

$2\nu\beta\beta$: SSD/HSD discrimination at 5σ level

Probe nuclear physics by investigating g_A

Alternative isotopes: ^{150}Nd and ^{96}Zr

$0\nu4\beta$: for ^{150}Nd

plus proof of concept for…

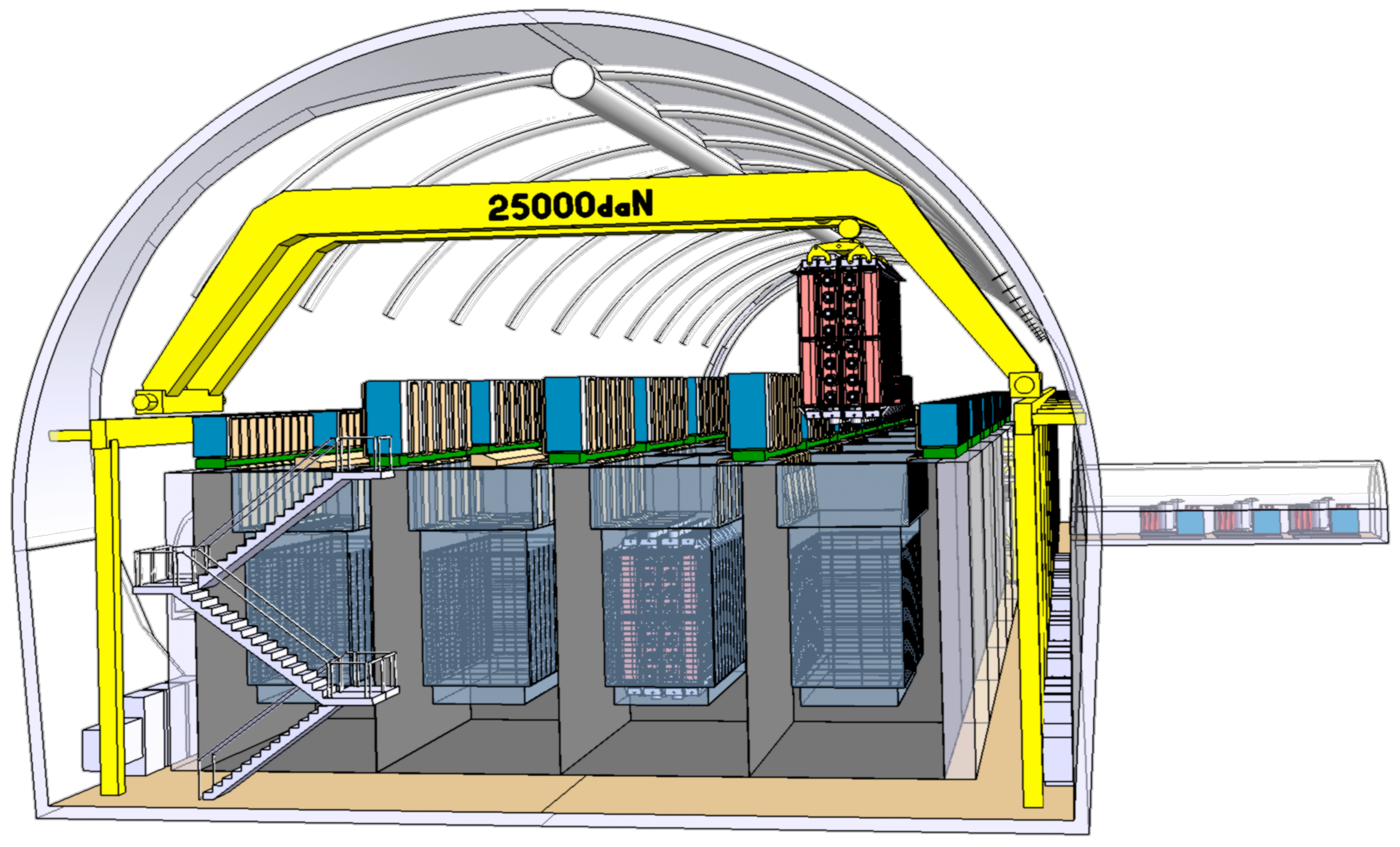

Full SuperNEMO

- **Modular** design allows easy scaling up
- 20 modules x 5 years (500 kg year) gives sensitivity comparable or better than current **leading experiments**
- Best technique to understand more about **$0\nu\beta\beta$ mechanism** in the event of discovery

Look to the future…

Next-generation 0νββ searches

Bayesian probability density fit by D'Agostini, Benato & Detwiler: Phys. Rev. D 96, 053001 (2017)

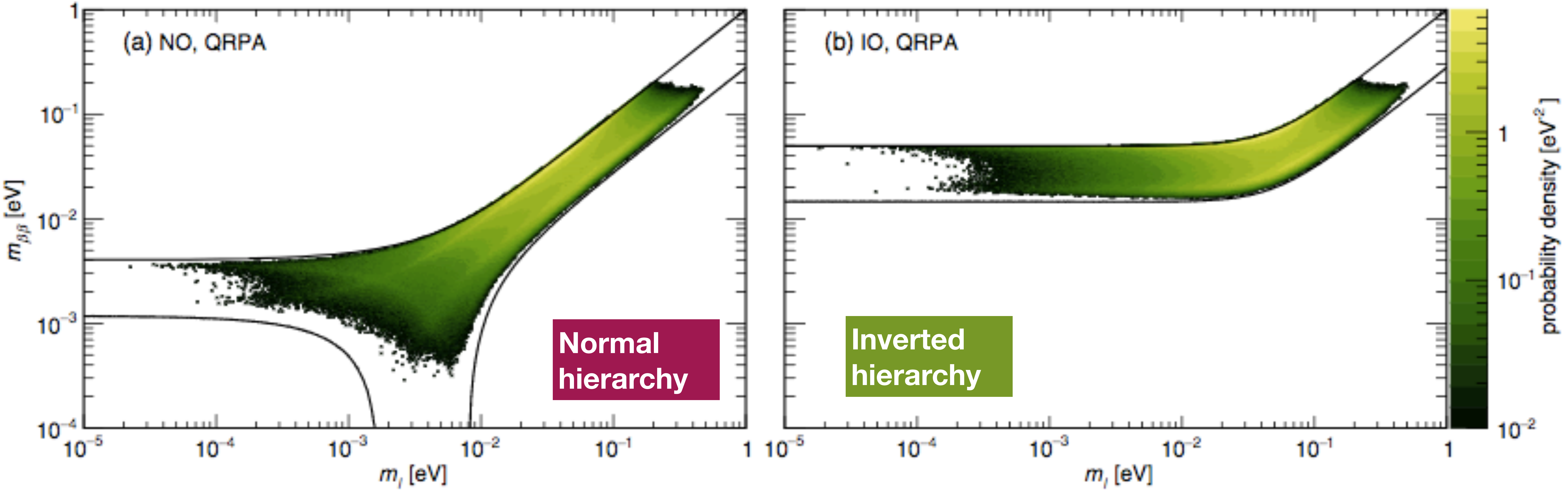

Known parameters:

- Mass splittings $\Delta m^2_{12}, \Delta m^2_{13}$ (NO) or Δm^2_{13} (IO)
- Mixing angles θ_{12}, θ_{13}

Thrown from a flat prior:

- Majorana phases α_1, α_2
- CP violating phase δ

Thrown from a logarithmic prior:

- Sum of neutrino masses $\sum$ (upper limit from cosmology)

Next-generation 0νββ searches

Bayesian probability density fit by D'Agostini, Benato & Detwiler: Phys. Rev. D 96, 053001 (2017)

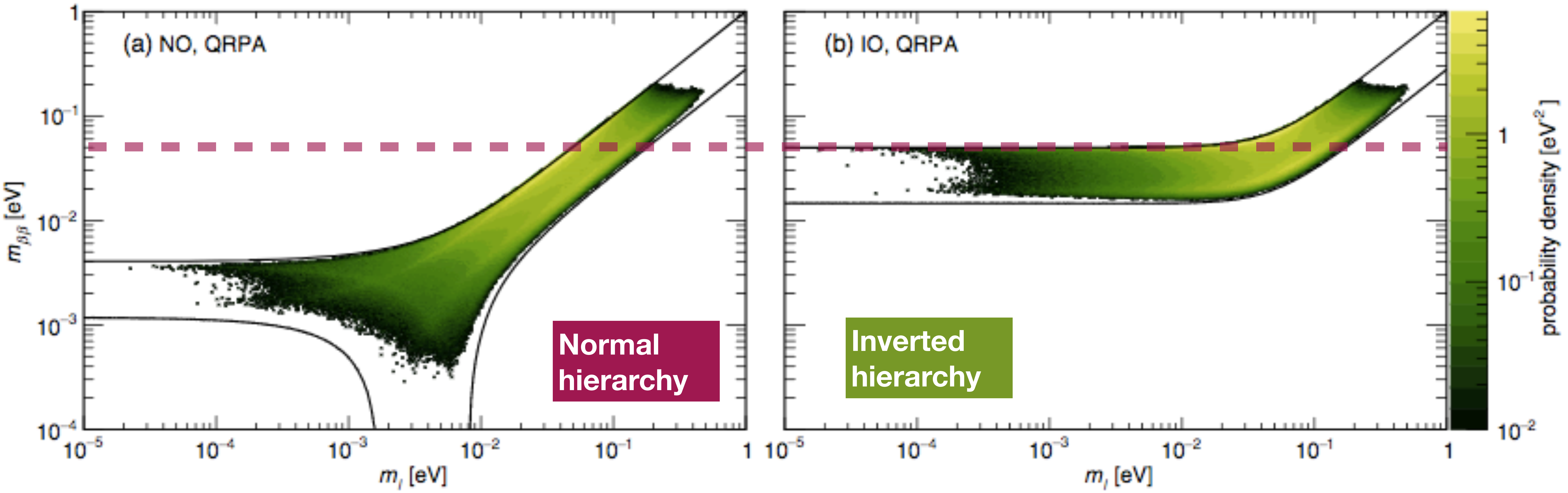

- Current experiments probe the **degenerate** regime

Next-generation 0νββ searches

Bayesian probability density fit by D'Agostini, Benato & Detwiler: Phys. Rev. D 96, 053001 (2017)

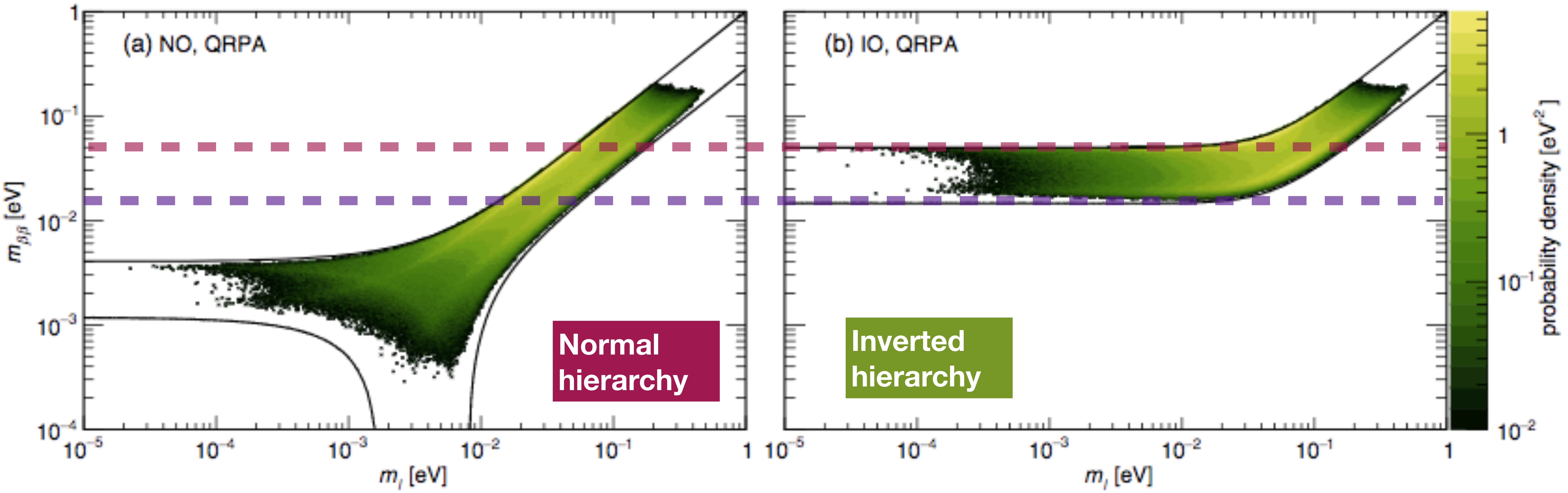

- Current experiments probe the **degenerate** regime
- Next-generation will cover **full inverted hierarchy** region

Next-generation 0νββ searches

Bayesian probability density fit by D'Agostini, Benato & Detwiler: Phys. Rev. D 96, 053001 (2017)

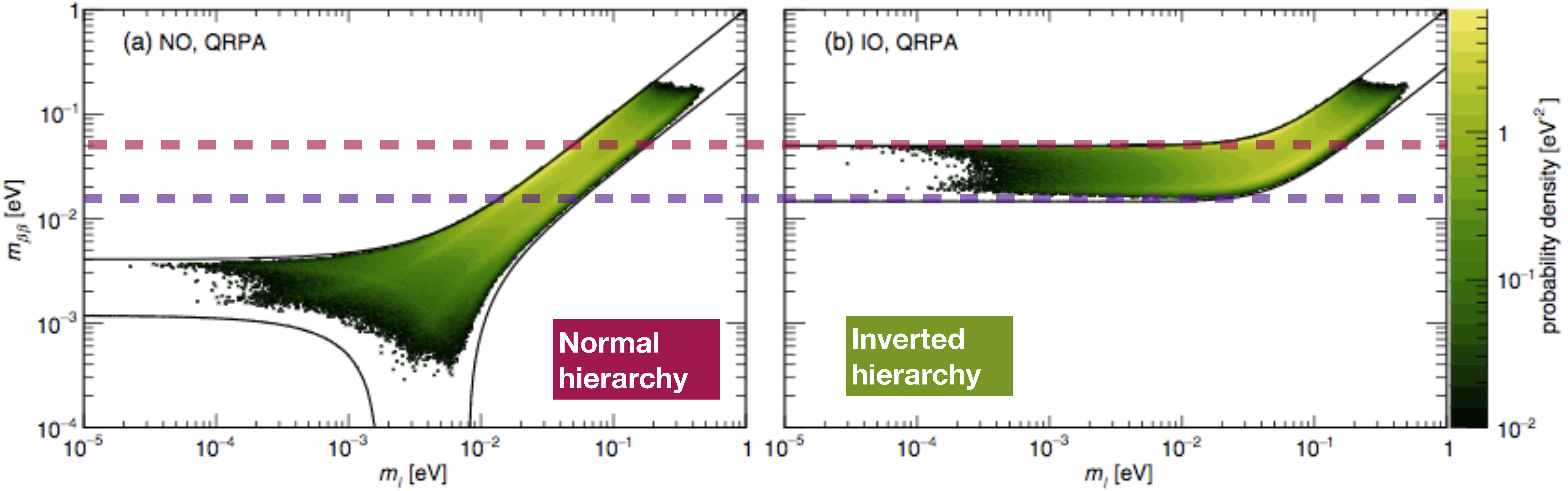

- Current experiments probe the **degenerate** regime
- Next-generation will cover **full inverted hierarchy** region
- When likelihood density is considered, this mass range also covers more than **50% of normal hierarchy** probability

Will the next generation find it?

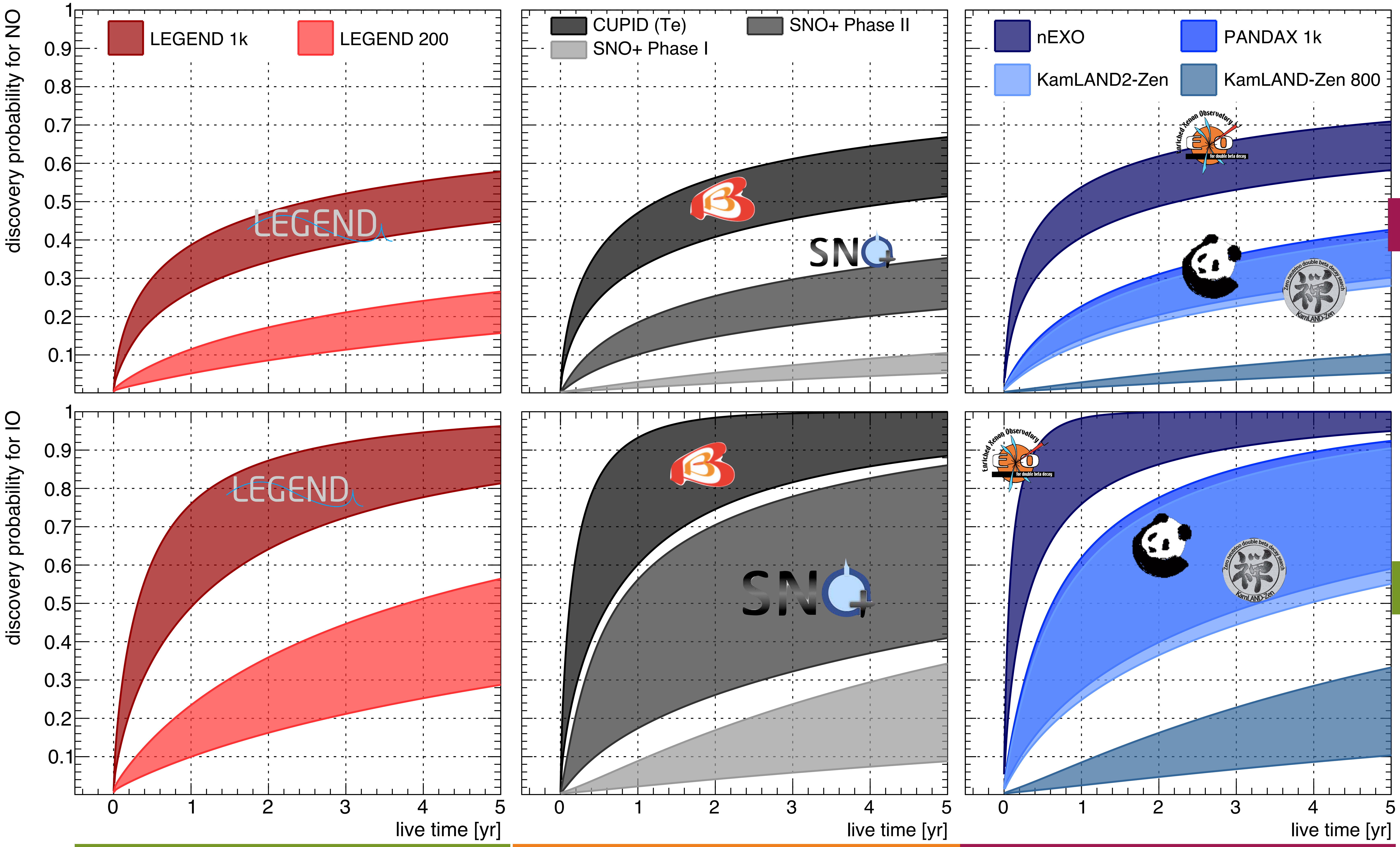

Normal hierarchy

Inverted hierarchy

^{76}Ge | ^{130}Te | ^{136}Xe

Phys. Rev. D 96, 053001 (2017)

Postcards from double-beta land

Did you spot the pictures?

CUORE

Did you spot the pictures?

CUORE GERDA

Did you spot the pictures?

CUORE

GERDA

SuperNEMO

Did you spot the pictures?

CUORE GERDA SuperNEMO KamLAND-Zen

Did you spot the pictures?

CUORE GERDA SuperNEMO KamLAND-Zen SNO+

Did you spot the pictures?